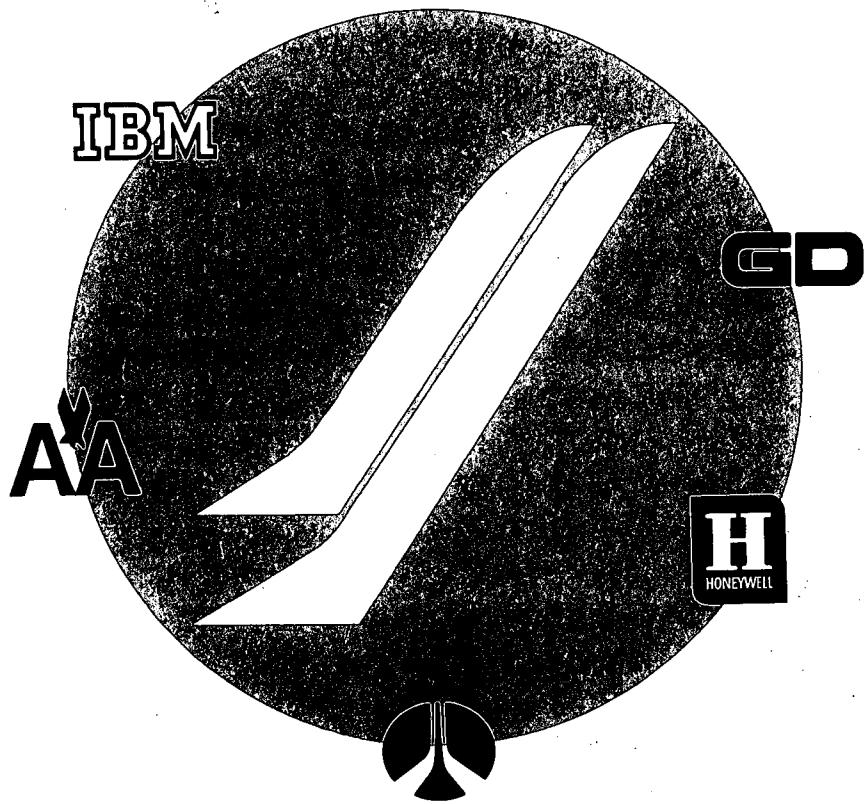


CR - 128670
NTIS \$25.00

Space Shuttle Program

MSC-03321



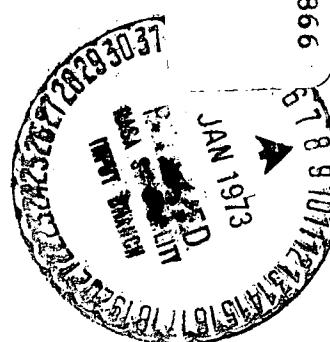
Reproduced by
**NATIONAL TECHNICAL
INFORMATION SERVICE**
U.S. Department of Commerce
Springfield, VA. 22151

(NASA-CR-128670) EXPENDABLE SECOND STAGE
REUSABLE SPACE SHUTTLE BOOSTER. VOLUME
2: TECHNICAL SUMMARY. BOOK 1:
EXPENDABLE SECOND (North American Rockwell
Corp.) 25 Jun. 1971 460 p CSCL 22B

G3/31

Unclassified
50790

N73-14866



Phase B Final Report Expendable Second Stage Reusable Space Shuttle Booster

Volume II. Technical Summary

Book 1. Expendable Second Stage/Reusable Booster System Definition

Contract NAS9-10960, Exhibit B
DRL MSFC-DRL-221, DRL Line Item 6
DRD MA-078-U2
SD 71-140-2
25 June 1971



SD 71-140-2
(MSC-03321)

25 June 1971

PHASE B FINAL REPORT
EXPENDABLE SECOND STAGE
REUSABLE SPACE SHUTTLE BOOSTER

Volume II
Technical Summary

Book 1

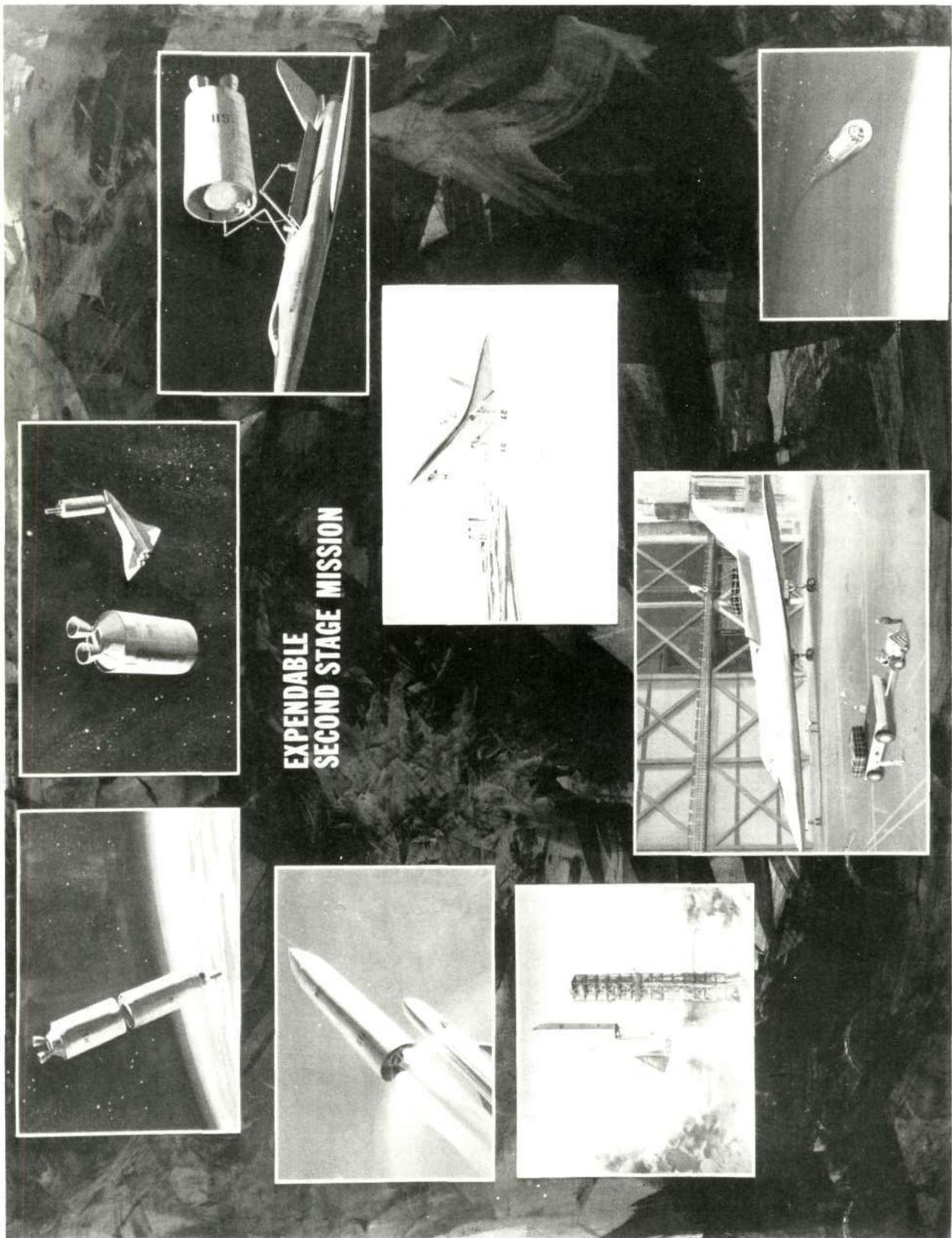
Expendable Second Stage/Reusable Booster System Definition

Contract NAS9-10960, Exhibit B
DRL MSC-DRL-221, DRL Line Item 6
DRD MA-078-U2

Approved by



B. Hello
Vice President and General Manager
Space Shuttle Program





FOREWORD

The Space Shuttle Phase B studies are directed toward the definition of an economical space transportation system. In addition to the missions which can be satisfied with the shuttle payload capability, the National Aeronautics and Space Administration has missions planned that require space vehicles to place payloads in excess of 100,000 pounds in earth orbit. To satisfy this requirement, a cost-effective multimission space shuttle system with large lift capability is needed. Such a system would utilize a reusable shuttle booster and an expendable second stage. The expendable second stage would be complementary to the space shuttle system and impose minimum impact on the reusable booster.

To evaluate the expendable second stage concept, a two-phase study was authorized by NASA. Phase A efforts, which ended in December 1970, concentrated on performance, configuration, and basic aerodynamic considerations. Basic trade studies were carried out on a relatively large number of configurations. At the conclusion of Phase A, the contractor proposed a single configuration. Phase B commenced on 1 February 1971, based on the recommended system. Whereas a large number of payload configurations were considered in the initial phase, Phase B was begun with specific emphasis placed on three representative payload configurations. The entire Phase B activity has been directed toward handling the three representative payload configurations in the most acceptable manner with the selected expendable second stage, and toward the design of the subsystems of the expendable second stage. Results of this activity are reported in this 12-volume Phase B final report. This is Volume II, Technical Summary.

Volume I	Executive Summary	SD 71-140-1
Volume II	Technical Summary	SD 71-140-2
Volume III	Wind Tunnel Test Data	SD 71-140-3
Volume IV	Detail Mass Properties Data	SD 71-140-4
Volume V	Operations and Resources	SD 71-140-5
Volume VI	Interface Control Drawings	SD 71-140-6
Volume VII	Preliminary Design Drawings	SD 71-140-7
Volume VIII	Preliminary CEI Specification - Part 1	SD 71-140-8
Volume IX	Preliminary System Specification	SD 71-140-9
Volume X	Technology Requirements	SD 71-140-10
Volume XI	Cost and Schedule Estimates	SD 71-140-11
Volume XII	Design Data Book	SD 71-140-12



Volume II, Technical Summary, is divided into three books:

Book 1 Expendable Second Stage/Reusable Booster System
Definition

Book 2 Expendable Second Stage Vehicle Definition

Book 3 Booster Vehicle Modifications and Ground Systems
Definition.

This book is intended to be used together with the other books of Volume II. Book 1 contains basic data on mission/system requirements, performance, trajectories, aerodynamics, stability and control, loads, heating, and acoustic environment. Book 2 is devoted to the definition of the selected expendable second stage, its subsystems, and overall ESS operation. Book 3 covers the definition of the ESS/booster separation system, modifications required on the reusable booster for ESS/payload flight, and the ground systems needed to operate the ESS complementary with the space shuttle.



CONTENTS

Section		Page
1.0	INTRODUCTION AND STUDY OBJECTIVES	1-1
2.0	STUDY APPROACH	2-1
3.0	MISSION, SYSTEM, AND PROGRAM REQUIREMENTS	3-1
	3.1 Integrated System Requirements	3-1
	3.1.1 Mission Requirements	3-1
	3.1.2 System Requirements	3-2
	3.1.3 Desired System Characteristics	3-6
	3.1.4 Criteria and Assumptions	3-10
	3.2 ESS Vehicle Requirements	3-20
4.0	SYSTEM/PROGRAM DEFINITION	4-1
	4.1 System Elements	4-1
	4.1.1 Expendable Second Stage	4-1
	4.1.2 Main Propulsion Engine—Space Shuttle Orbiter Engine	4-1
	4.1.3 Booster	4-1
	4.1.4 Operations	4-2
	4.2 System Operations	4-2
5.0	INTEGRATED VEHICLE CHARACTERISTICS AND ENVIRONMENT	5-1
	5.1 Physical Characteristics	5-1
	5.1.1 General Arrangement	5-1
	5.1.2 Mass Properties	5-1
	5.1.3 Booster/ESS Interfaces	5-5
	5.2 Performance and Flight Characteristics	5-9
	5.2.1 Payload Capability	5-9
	5.2.2 Trajectory Characteristics and Flight Environment	5-19
	5.2.3 Aborts and Contingency Missions	5-259
	5.3 Orbital Operations and Deorbit	5-268
	5.3.1 Rendezvous/Safing	5-268
	5.3.2 Recovery of Components	5-268
	5.3.3 Deorbit	5-269
	5.4 System Safety	5-299
	5.4.1 Methods of Approach and Assumptions	5-299
	5.4.2 Areas Requiring Further Effort—Separation System	5-304



Section	Page
APPENDIXES	
A. COST/DESIGN PERFORMANCE MANAGEMENT FOR ESS PHASE B STUDY	A-1
B. IMPACT OF UTILIZING ESS ON BOOSTER FOR EXTERNAL HYDROGEN TANK STUDY	B-1
C. DELIVERY OF PROPELLANTS TO ORBIT	C-1
D. SINGLE-ENGINE ESS PERFORMANCE ANALYSIS	D-1
E. EFFECTS OF FIXED EXPANSION RATIO NOZZLE	E-1
F. TRAJECTORY DATA—SELECTED SYSTEM	F-1
G. LOW-LOAD TRAJECTORY/PERFORMANCE EFFECTS	G-1



ILLUSTRATIONS

Figure	Page
1-1 Expendable Second-Stage Payloads	1-3
1-2 Study Phases	1-4
2-1 Study Approach and Logic, Phase A	2-2
2-2 Study Approach and Logic, Phase B	2-2
2-3 Expendable Second Stage on a Reusable Space Shuttle Booster MPS-02	2-3
3-1 Payload Description Form, Nuclear Stage	3-3
3-2 Payload Description Form, Space Tug	3-4
3-3 Payload Description Form, Space Station (MDAC)	3-5
4-1 Design Reference Mission Profile	4-3
5-1 Basic Configuration, B-9U/ESS Booster	5-3
5-2 Booster/ESS Interface Drawing	5-7
5-3 Performance Capability of Baseline ESS System	5-11
5-4 Off-Loading for Low-Energy Missions	5-12
5-5 ESS Performance to High Altitude Circular Orbits	5-13
5-6 ESS Performance to High Altitude Elliptical Orbits	5-14
5-7 Comparison of Third Stages for ESS Equatorial Synchronous Missions	5-16
5-8 Nominal Ascent Trajectory for Space Station Payload	5-20
5-9 Nominal Ascent Trajectory for Space Tug Payload	5-22
5-10 Nominal Ascent Trajectory for RNS Payload	5-24
5-11 Separation Trajectory-Staging of ESS With MDAC Space Station Payload (Two ESS Engines Operative - BECO at 0.2 Second)	5-27
5-12 Thrust Scheduling, Normal Staging of ESS With MDAC Space Station Payload	5-28
5-13 Separation Trajectory, Staging of ESS With MDAC Space Station Payload (Two ESS Engines Operative)	5-29
5-14 Separation System Link Loads, Normal Staging of ESS With MDAC Space Station Payload (BECO at 0.2 Second)	5-30



Figure		Page
5-15	Separation System Link Loads, Normal Staging of ESS With MDAC Space Station Payload (BECO at 0.1 Second)	5-31
5-16	Separation Trajectory, Staging of ESS With MDAC Space Station Payload (One ESS Engine Operative)	5-32
5-17	Thrust Scheduling, Staging of ESS With MDAC Space Station Payload (One ESS Engine Operative)	5-33
5-18	Booster Entry Profile and Entry Corridor	5-34
5-19	Booster Entry, RNS Payload Mission	5-36
5-20	Booster Entry, Space Tug Payload Mission	5-41
5-21	Booster Entry, Space Station Payload Mission	5-46
5-22	Cruise Trimmed Lift/Drag Characteristics	5-50
5-23	Aerodynamic Data-Integrated System Boost Configuration (B-9U/RNS) Forebody Axial Force Coefficient Versus Mach Number	5-54
5-24	Aerodynamic Data-Integrated System Boost Configuration (B-9U/MDAC) Forebody Axial Force Coefficient Versus Mach Number	5-55
5-25	Aerodynamic Data-Integrated System Boost Configuration (B-9U/Space Tug) Forebody Axial Force Coefficient Versus Mach Number	5-56
5-26	Aerodynamic Data-Integrated System Boost Configuration (B-9U/RNS) Attitude Versus Base Axial Force	5-57
5-27	Aerodynamic Data-Integrated System Boost Configuration (B-9U/RNS) Normal Force Coefficient Curve Slope Versus Mach Number	5-58
5-28	Aerodynamic Data-Integrated System Boost Configuration (B-9U/MDAC) Normal Force Coefficient Curve Slope Versus Mach Number	5-59
5-29	Aerodynamic Data-Integrated System Boost Configuration (B-9U/Space Tug) Normal Force Coefficient Curve Slope Versus Mach Number	5-60
5-30	Aerodynamic Data-Integrated System Boost Configuration (B-9U/RNS) Zero Angle-of-Attack Pitching Moment Coefficient Versus Mach Number	5-61



Figure		Page
5-31	Aerodynamic Data-Integrated System Boost Configuration (B-9U/MDAC) Zero Angle-of-Attack Pitching Moment Coefficient Versus Mach Number	5-62
5-32	Aerodynamic Data-Integrated System Boost Configuration (B-9U/Space Tug) Zero Angle-of-Attack Pitching Moment Coefficient Versus Mach Number	5-63
5-33	Aerodynamic Data-Integrated System Boost Configuration (B-9U/RNS) Side Force Coefficient Curve Slope Versus Mach Number	5-64
5-34	Aerodynamic Data-Integrated System Boost Configuration (B-9U/MDAC) Side Force Coefficient Curve Slope Versus Mach Number	5-65
5-35	Aerodynamic Data-Integrated System Boost Configuration (B-9U/Space Tug) Side Force Coefficient Curve Slope Versus Mach Number	5-66
5-36	Aerodynamic Data-Integrated System Boost Configuration, Yaw Aerodynamic Center Versus Mach Number	5-67
5-37	Aerodynamic Data-Integrated System Boost Configuration (B-9U/Space Tug) Rolling Moment Coefficient Curve Slope Versus Mach Number	5-68
5-38	Aerodynamic Data-Integrated System Boost Configuration (B-9U/MDAC) Rolling Moment Coefficient Curve Slope Versus Mach Number	5-69
5-39	Distribution of Local Normal Force Coefficient for RNS	5-71
5-40	Distribution of Local Normal Force Coefficient for RNS	5-72
5-41	Distribution of Local Axial Force Coefficient for RNS	5-73
5-42	Distribution of Local Side Force Coefficient for RNS	5-74
5-43	Distribution of Local Normal Force Coefficient for RNS	5-75
5-44	Distribution of Local Axial Force Coefficient for RNS	5-76
5-45	Distribution of Local Side Force Coefficient for RNS	5-77
5-46	Distribution of Local Normal Force Coefficient Slope for MDAC	5-78
5-47	Distribution of Local Normal Force Coefficient for MDAC	5-79
5-48	Distribution of Local Axial Force Coefficient for MDAC	5-80



Figure		Page
5-49	Distribution of Local Side Force Coefficient for MDAC	5-81
5-50	Distribution of Local Normal Force Coefficient Slope for MDAC	5-82
5-51	Distribution of Docking Ports Normal Force Coefficient	5-83
5-52	Distribution of Local Axial Force Coefficient for MDAC	5-84
5-53	Distribution of Local Side Force Coefficient for MDAC.	5-85
5-54	Distribution of Local Normal Force Coefficient for Space Tug	5-86
5-55	Distribution of Local Normal Force Coefficient at $\alpha = 0$ Degrees for Space Tug	5-87
5-56	Distribution of Local Axial Force Coefficient for Space Tug	5-88
5-57	Distribution of Local Side Force Coefficient for Space Tug	5-89
5-58	Distribution of Local Normal Force Coefficient for Space Tug	5-90
5-59	Distribution of Local Axial Force Coefficient for Space Tug	5-91
5-60	Distribution of Local Side Force Coefficient for Space Tug	5-92
5-61	Booster Engine Arrangement and TVC Requirements .	5-93
5-62	Design Winds	5-95
5-63	Boost Phase Control System	5-96
5-64	Control Logic	5-97
5-65	ESS Low q Ascent Trajectories	5-100
5-66	Effect of Variation in Nominal Trajectory on Max q α Gust at h = 36,000 Feet	5-101
5-67	Space Station Head/Tail Wind Trajectory Data (Wind Gust at Max q Altitude)	5-103
5-68	RNS Head/Tail Wind Trajectory Data (Wind Gust at Max q Altitude)	5-104
5-69	Space Tug Head/Tail Wind Trajectory Data (Wind Gust at Max q Altitude)	5-105
5-70	αq Summary, Wind Gust at Max q Altitude	5-106
5-71	Space Station Crosswind Trajectory Data (Wind Gust at Max q Altitude)	5-107
5-72	RNS Crosswind Trajectory Data (Wind Gust at Max q Altitude)	5-108



Figure		Page
5-73	Space Tug Crosswind Trajectory Data (Wind Gust at Max q Altitude)	5-109
5-74	β_q Summary, Wind Gust at Max q Altitude	5-110
5-75	Booster/ESS Space Station Gimbal Requirements Due to CG Travel, Nominal	5-112
5-76	Launch Pad Arrangements	5-116
5-77	B-9U/ESS/RNS Launch Drift Pitch Plane Wind	5-118
5-78	B-9U/ESS/RNS Launch Drift Yaw Plane Wind	5-119
5-79	ESS Vehicle Configuration, Coordinate Axes, and Propulsion Subsystems Used for Flight Control	5-120
5-80	ESS Flight Control System Block Diagram	5-122
5-81	Three-Axis Attitude Control With TVC From Main Engines	5-123
5-82	Three-Axis Attitude Control With ACPS	5-125
5-83	Pitch Attitude Control System and Control Equations, ESS With Space Station Payload	5-126
5-84	Moment of Inertia and Center-of-Gravity Variations Ascent to Orbit (ESS With Space Station Payload)	5-127
5-85	Pitch Axis Root Locus Plot at 10 Seconds After Staging (ESS With Space Station Payload)	5-128
5-86	Pitch Axis Root Locus Plot at 125 Seconds After Staging (ESS With Space Station Payload)	5-129
5-87	Pitch Axis Root Locus Plot at 250 Seconds After Staging ESS With Space Station Payload	5-130
5-88	Constant Rate and Position Gains Which Assure That Damping Ratio is Between 0.4 and 0.7 for Ascent ESS With Space Station Payload	5-131
5-89	Pitch Closed Loop Frequency Response 10 Seconds After Staging ESS With Space Station Payload	5-133
5-90	Pitch Closed Loop Frequency Response 125 Seconds After Staging ESS With Space Station Payload	5-134
5-91	Pitch Closed Loop Frequency Response 250 Seconds After Staging ESS With Space Station Payload	5-135
5-92	Pitch Axis "Tail Wags Dog" Zero, ESS With Space Station Payload	5-136
5-93	ESS 6 DOF Controlled Trajectory for Ascent to Orbit, Nominal Trajectory With Space Station Payload	5-138
5-94	ESS 6 DOF Controlled Trajectory for Ascent to Orbit, Nominal Trajectory With Space Station Payload (Pitch)	5-139
5-95	ESS 6 DOF Controlled Trajectory for Ascent to Orbit, Nominal Trajectory With Space Station Payload (Yaw)	5-140



Figure		Page
5-96	ESS 6 DOF Controlled Trajectory for Ascent to Orbit, Nominal Trajectory With Space Station Payload (Roll)	5-141
5-97	MPS Engine Angle Definitions (Yaw Plane)	5-143
5-98	MPS Engine Deflection for Yaw Axis Static Trim (One Orbiter Engine Inoperative)	5-145
5-99	Required Engine Deflection for Controlling Yaw Axis Dynamic Transient	5-146
5-100	Yaw Axis Engine Deflection Requirement Versus Cant Angle for ESS + Space Tug (One MPS Engine Inoperative)	5-148
5-101	Yaw Axis Engine Deflection Requirement Versus Cant Angle for ESS + MDAC Space Station (One MPS Engine Inoperative)	5-149
5-102	Yaw Axis Engine Deflection Requirement Versus Cant Angle for ESS/RNS Vehicle (One MPS Engine Inoperative)	5-150
5-103	Summary of MPS Engine Deflection Requirement Versus Cant Angle (One MPS Engine Inoperative)	5-152
5-104	Vehicle Payload Penalty Versus MPS Engine Cant Angle	5-153
5-105	Maximum Roll Attitude and Roll Rate Following Arrest of 2 Deg/Sec Pitchup Maneuver and Initiation of -0.2 Deg/Sec Pitch Over	5-156
5-106	6 DOF Controlled Trajectory for Ascent to Orbit, Separation Transient, One Main Engine Inoperative, Space Station Payload	5-158
5-107	6 DOF Controlled Trajectory for Ascent to Orbit, Separation Transient, One Main Engine Inoperative, Space Station Payload	5-159
5-108	ESS 6 DOF Controlled Trajectory for Ascent to Orbit, Separation Transient, One Main Engine Inoperative, Space Station Payload	5-160
5-109	OMS Engine Angle Definitions (Pitch Plane)	5-161
5-110	Pitch Engine Deflection From Static Trim (One OMS Engine Inoperative)	5-163
5-111	OMS Engine Deflection for Pitch Axis Static Trim as a Function of CG Position (One OMS Engine Inoperative)	5-164
5-112	OMS Engine Deflection for Controlling Pitch Axis Dynamic Transient (One OMS Engine Inoperative)	5-165



Figure		Page
5-113	Pitch Axis Engine Deflection Requirement Versus Cant Angle, ESS/Space Tug (One OMS Engine Inoperative)	5-168
5-114	Pitch Axis Engine Deflection Requirement Versus Cant Angle, ESS/Space Station (One OMS Engine Inoperative)	5-169
5-115	Pitch Axis Engine Deflection Requirement Versus Cant Angle, ESS/RNS (One OMS Engine Inoperative)	5-170
5-116	Summary of OMS Engine Deflection Requirements Versus Cant Angle Orbital ΔV Maneuvers (One OMS Engine Inoperative)	5-172
5-117	Vehicle Payload Loss Versus OMS Engine Cant Angle	5-173
5-118	Summary of OMS Engine Deflection Requirement Versus Cant Angle Orbital ΔV Maneuvers Plus ESS Deorbit (One OMS Engine Inoperative)	5-174
5-119	ACPS Requirement for Pitch Axis Control During Single OMS Engine ESS Deorbit	5-178
5-120	Number of Pitch ACPS Jets Required for Pitch Trim (Deorbit Condition With One OMS Engine Inoperative)	5-180
5-121	Number of Roll Jets Required for Roll Trim (Deorbit Condition With One OMS Engine Inoperative)	5-181
5-122	Booster Airload Distribution, ESS/RNS Payload, Maximum α_q Headwind	5-184
5-123	Booster Airload Distribution, ESS/RNS Payload, Maximum α_q Tailwind	5-185
5-124	Booster Airload Distribution, ESS/RNS Payload, Maximum β_q Launch (Pitch Plane)	5-186
5-125	Booster Airload Distribution, ESS/RNS Payload, Maximum β_q Launch (Yaw Plane)	5-187
5-126	Booster Airload Distribution, ESS/Space Station Payload, Maximum α_q Headwind	5-188
5-127	Booster Airload Distribution, ESS/Space Station Payload, Maximum α_q Tailwind	5-189
5-128	Booster Airload Distribution, ESS/Space Station Payload, Maximum α_q Launch (Pitch Plane)	5-190
5-129	Booster Airload Distribution, ESS/Space Station Payload, Maximum β_q Launch (Yaw Plane)	5-191
5-130	Booster Airload Distribution, ESS/Space Tug Payload, Maximum α_q Headwind	5-192
5-131	Booster Airload Distribution, ESS/Space Tug Payload, Maximum α_q Tailwind	5-193
5-132	Booster Airload Distribution, ESS/Space Tug Payload, Maximum β_q Launch (Pitch Plane)	5-194



Figure		Page
5-133	Booster Airload Distribution, ESS/Space Tug Payload, Maximum βq Launch (Yaw Plane)	5-195
5-134	Interconnect Loads Comparison	5-198
5-135	Internal Loads, Top Centerline (RNS Payload)	5-200
5-136	Internal Loads, Side (RNS Payload)	5-201
5-137	Internal Loads, Bottom Centerline (RNS Payload)	5-202
5-138	Internal Loads, Top Centerline (Space Station Payload)	5-203
5-139	Internal Loads, Side (Space Station Payload)	5-204
5-140	Internal Loads, Bottom Centerline (Space Station Payload)	5-205
5-141	Internal Loads, Top Centerline (Space Tug Payload)	5-206
5-142	Internal Loads, Side (Space Tug Payload)	5-207
5-143	Internal Loads, Bottom Centerline	5-208
5-144	Design Attachment Loads (Nuclear Stage)	5-209
5-145	Design Attachment Loads (MDAC Stage)	5-210
5-146	Design Attachment Loads (Space Tug)	5-211
5-147	ESS/Nuclear Stage Effect on Bulkheads	5-212
5-148	ESS/Space Station Effect on Bulkheads	5-213
5-149	ESS/Space Tug Effect on Bulkheads	5-214
5-150	Trajectory Comparison	5-216
5-151	MDAC Space Station/Booster Interaction	5-218
5-152	Space Tug/Booster Interaction	5-219
5-153	Peak Wall Temperature Difference Due to Change in Trajectory	5-223
5-154	Comparison of Ascent Trajectories Studies	5-225
5-155	Booster Top Centerline Locations Investigated	5-227
5-156	Aerodynamic Heating Factor for Area Around Mated Attachment Strut	5-228
5-157	Booster Upper Surface Skin Temperature	5-229
5-158	Orbital Heat Transfer	5-235
5-159	ESS Base Region Geometry	5-236
5-160	Isomach Times for Nozzle Retracted	5-237
5-161	Isomach Times for Nozzle Extended	5-238
5-162	ESS Base Region Convective Heating Rates, APS LO ₂ Tank	5-240
5-163	ESS Base Region Convective Heating Rates, Base Heat Shield	5-241
5-164	ESS Base Region Convective Heating Rates, Shuttle Orbiter Engine Shroud	5-242
5-165	ESS Base Region Convective Heating Rates, OMS Engine Support Structure	5-243



Figure		Page
5-166	ESS Base Region Radiative Heat Rates	5-244
5-167	ACPS/ESS Schematic	5-245
5-168	ESS/ACPS Engine Exhaust Plume Isomachs	5-247
5-169	ACPS Plume Impingement Pressures, Air Stream Deflector	5-248
5-170	ACPS Plume Impingement Pressures, Roll Engine/ESS Surface	5-249
5-171	ACPS Plume Impingement Pressures to ESS Surface	5-250
5-172	ACPS Plume Impingement Heating, Air Stream Deflector	5-251
5-173	ACPS Plume Impingement Heating to ESS Surface	5-252
5-174	ACPS Plume Impingement Heating to ESS Surface	5-253
5-175	Booster Temperature When Used With the ESS	5-254
5-176	Launch Acoustic Environment (on Pad)	5-256
5-177	Launch Acoustic Environment (on Pad), 1/3-Octave Band Sound Pressure Levels	5-257
5-178	Aerodynamic Pseudo-Noise	5-258
5-179	Vibration Spectra	5-260
5-180	Variation in Reserve Propellant Requirements for Mission Completion With One Engine Failed at Ignition	5-266
5-181	One Engine-Out Performance for Baselines	5-267
5-182	Structural Arrangement, Mid-Body	5-271
5-183	Expendable Second Stage Recoverable Hardware From Horizontal/Vertical Engine Orientation	5-273
5-184	Manipulator Installation, SSV Orbiter Configuration 161C	5-275
5-185	Payload Retention, SSV Orbiter Model 161C(A)	5-277
5-186	Cargo Transfer Tunnel Installation, SSV Orbiter Configuration 161C	5-279
5-187	Orbit Trace for 55-Degree, 270-NM Orbit	5-282
5-188	ESS Impact for Various Velocity Increments and Orbital Altitudes	5-283
5-189	Locus of Footprint Length Due to ΔV Perturbation	5-284
5-190	Effect of Angle of Attack on ESS Impact Range	5-286
5-191	ESS Deorbit Profiles	5-287
5-192	Ballistic Parameter Values for Spheres of Various Radii and Composition	5-289
5-193	Debris Footprint Resulting From ESS Vehicle Breakup	5-290
5-194	Impact Range Versus Ballistic Parameter	5-290
5-195	ESS 1520-NM Impact Areas	5-293
5-196	Minimum Velocity Required to Deorbit and Escape From Circular Orbit	5-297
5-197	Gross Hazards Analysis	5-300

Preceding page blank



TABLES

Table		Page
5-1	Configuration Weight Summary 5-2
5-2	Performance Characteristics of Third-Stage Candidates 5-17
5-3	Frequency at Liftoff 5-98
5-4	Head/Tail Wind Gimbal Requirements 5-111
5-5	Cross-Wind Gimbal Requirements 5-114
5-6	Aerodynamic Force Summary 5-117
5-7	ESS Flight Control Requirements 5-154
5-8	ESS Engine Cant-Angle and Deflection Requirements .	. 5-175
5-9	B-9U/ESS Critical Flight Conditions 5-183
5-10	Heat Transfer Factors 5-232
5-11	Peak Temperatures on Booster Top Surface During Ascent 5-233
5-12	Shuttle Payload Assessment for Recovery 5-270
5-13	ESS Deorbit Footprint 5-292
5-14	Effect of Engine Failures on ESS Deorbit 5-295
5-15	ESS Preliminary (Gross) Hazard Identification 5-305

PRECEDING PAGE BLANK NOT FILMED



1.0 INTRODUCTION AND STUDY OBJECTIVES

A space shuttle system utilizing a reusable booster and orbiter that can transport persons and cargo to low earth orbit and return the crew/ passengers and cargo safely to earth is being evaluated through preliminary design/development (Phase B) study. Future space exploration and operations will be greatly enhanced through the basic economic efficiency which will evolve through development of such a space logistics system. The shuttle system presently is being designed to handle payloads up to approximately 65,000 pounds. The cargo bay into which these payloads must fit is cylindrical and is 60 feet long and 15 feet in diameter. Whereas most of the total projected payload spectrum for the decade of the 1980's can be handled by the shuttle, a significant number of payloads have been defined which are much larger and heavier than can be placed in orbit by the booster/orbiter combination.

To supplement the shuttle capability, a space system using an expendable second stage (ESS) with a reusable space shuttle booster has been under investigation for the past nine months of the Phase B Shuttle Study. The prime objective of this supplemental study has been to determine the feasibility, cost effectiveness, and preliminary design of such a system which is to be suitable for a wide variety of advanced space missions beginning in the last half of CY 1979. The results of the study will be available for comparison with results of past studies of all-expendable systems for launching the same types of large, heavy payloads.

On 14 September 1970, NASA authorized the Phase A/B Study for an Expendable Second Stage on a Reusable Space Shuttle Booster, as Exhibit B to Contract NAS9-10960. Supplementary study during Phase A, on a modified Saturn S-II, as a candidate expendable second stage, was authorized by Change Order 1980 to Contract NAS7-200. During Phase B, which commenced on 1 February 1971, supplementary study was defined by Task Authorization 5 to Contract NAS7-200. Beginning in March 1971, additional supplementary or related technical effort by the IBM Corporation, on guidance, navigation, and control for the ESS was authorized by NASA. Appropriate results of this effort are utilized in this report. The entire final report is organized in accordance with Contract NAS9-10960, DRL MSFC-DRL-221, Line Item 6, and DRD MA-078-U2, dated 28 August 1970. The document is submitted by North American Rockwell Corporation through its Space Division and contains results of design, performance, and resource studies performed during the Phase B portion of the contract.



As previously indicated, the study was divided into two sequential phases, Phase A and Phase B. The Phase A work was concentrated on such aspects as performance, configuration, and basic aerodynamic considerations to provide the foundation for a proposed single configuration for analysis in the Phase B portion. Phase A required analysis and definition of space shuttle systems with an optimized expendable second stage (1) utilizing existing hardware, (2) space shuttle engines with 400,000 pounds of thrust*, and (3) new hardware or (4) combination of existing and new hardware. Further, the definitions of systems with minimum modified S-II stages and minimum modified S-IVB stages were included.

The study depth was to be sufficient to permit a decision by the NASA on whether to proceed with a particular approach or to eliminate all concepts from further consideration. To accomplish this objective, consideration was given to the following:

1. The defined payload spectrum
2. The required operational characteristics
3. Identification of any modifications and the extent of penalties (if any) in payload and performance required to employ the reusable booster with the selected expendable second stage (but without incorporation into the Phase B Space Shuttle System Study).
4. Research, design, test and evaluation, production, and operational costs.
5. Identification of cost/performance/mission effectiveness.

The contractor recommended that an ESS derived from the Saturn S-II be investigated in the Phase B portion of the study.

The recommended ESS main propulsion system featured two space shuttle orbiter engines and its liquid hydrogen tank was shortened by 99 inches. The results of the Phase A study were reported in December 1970 in the interim final report (Phase A only), SD 70-607. A summary of these results is included in Volume I, Executive Summary, of this report.

*The thrust level for Phase B was increased to 550,000 pounds at sea level.



This volume of the final report, Volume II, Technical Summary, covers the selected expendable second stage/reusable booster system and consists of the following:

1. Study objectives
2. Mission/system requirements
3. Study approach
4. System and flight characteristics and environment
5. Analyses and design data generated during the Phase B study

On 1 February 1971, a technical directive was received from NASA that indicated for the remaining portions of the Phase B Study emphasis should be placed on the short S-II stage with two space shuttle engines. Further, to facilitate an in-depth study up to mid-June 1971, baseline payloads should be consolidated into three. The specific payloads are indicated in Figure 1-1, along with the candidate payload spectrum for the Phase B study. Other ground rules to be used in Phase B were defined in an updated study control document dated 1 February 1971 and are included in Section 2.0. The overall study phasing is summarized in Figure 1-2.

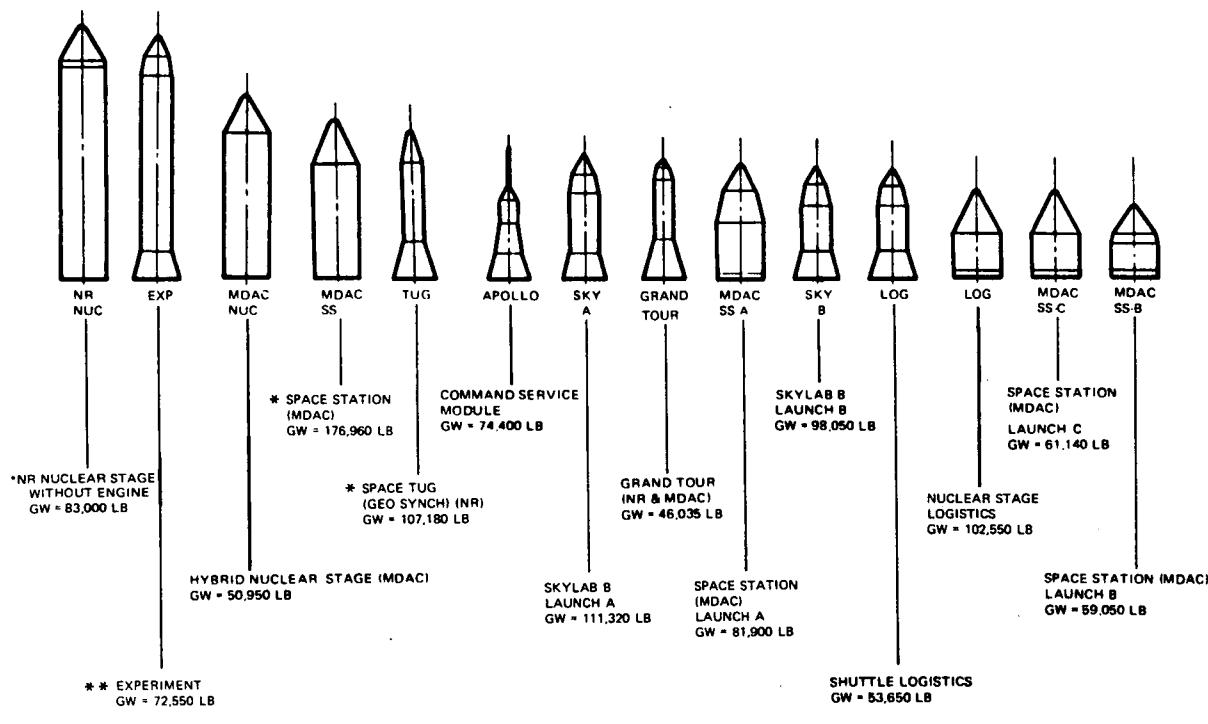


Figure 1-1. Expendable Second-Stage Payloads

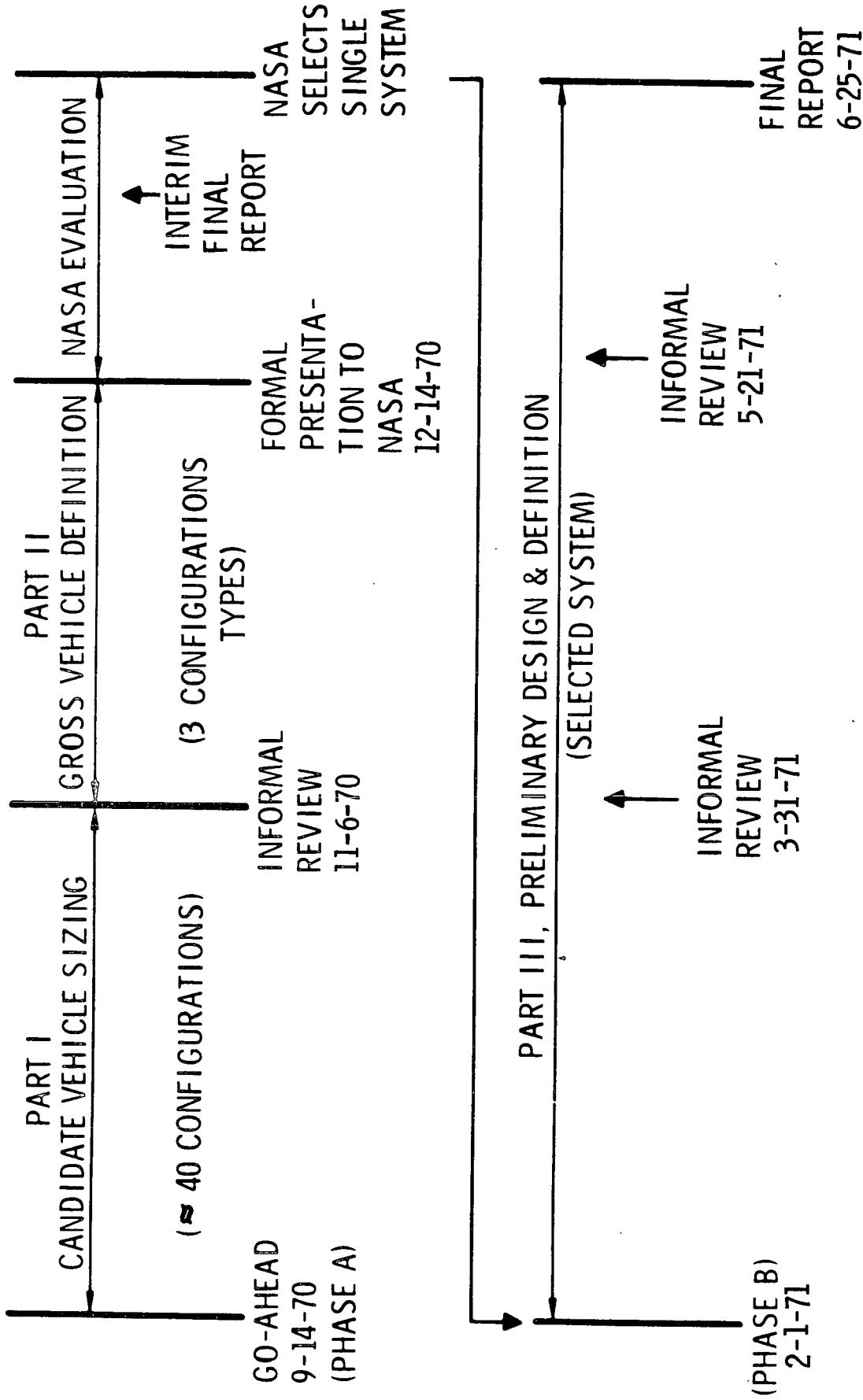


Figure 1-2. Study Phases



2.0 STUDY APPROACH

Figures 2-1 and 2-2 illustrate the study approach and logic used throughout the study.

During the Phase B portion of this study, the technical approach leading to the selected system emphasized the use of the most up-to-date information on the shuttle baseline booster configuration along with an ESS which contained subsystems best meeting the requirements for the ESS missions and payloads. Early in the Phase B activity, the shuttle baseline booster was identified as a vehicle containing 12 550,000-pound thrust space shuttle engines. The selected ESS concept (short S-II stage with two space shuttle engines), combined with the booster, was quickly determined to have more than adequate payload performance to meet all the NASA-defined requirements. However, minimization of structural effect on the reusable booster is a requirement. Hence, primary attention was directed toward this goal, and the three specified payloads were analyzed to cover the anticipated payload spectrum requirements.

The basic approach was to create flight trajectories which would meet the requirements for each payload, and still yield only minimal effects on the booster. The nominal (no-wind) trajectories that evolved permitted control and loads investigations to proceed, including wind effects. Also, since de-orbit of the spent ESS structure is a requirement, along with the necessity for safing the ESS after reaching orbit, the requirement exists to minimize unused residual propellants which otherwise would remain in the ESS if normal propellant loading is associated with a bulky but relatively lightweight payload. The technical approach adopted took these factors into account.

The ESS design approach relative to the several subsystems was balanced between the maximum use of existing qualified subsystems and/or elements; and selective use of shuttle-developed components which will perform similar functions. Also, since growth potential is desirable providing no significant penalties are incurred, the thrust structure arrangement selected in a separate study on the Chemical Interorbital Shuttle (NAS7-200, Change Order 2021) was utilized.

The Phase B study task schedule as carried out through the final report submittal is shown in Figure 2-3.

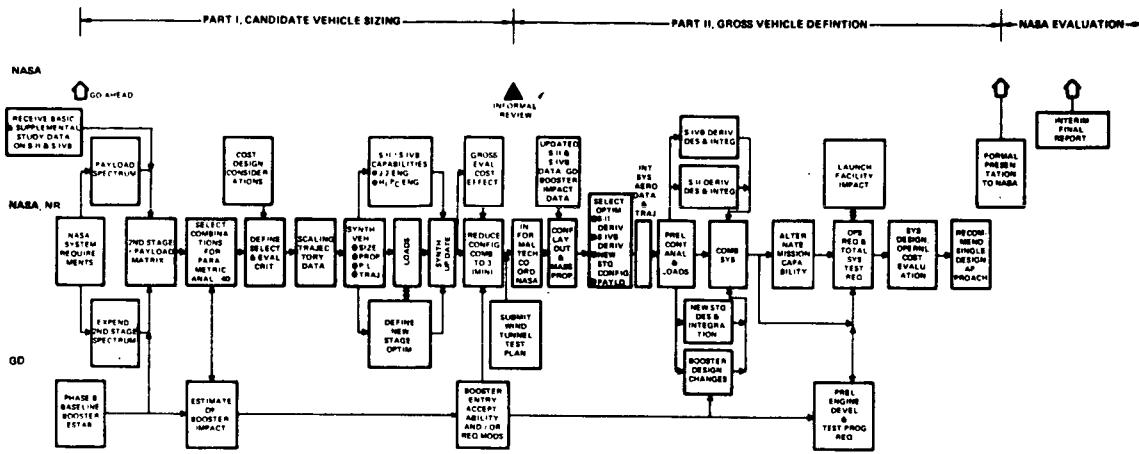


Figure 2-1. Study Approach and Logic, Phase A

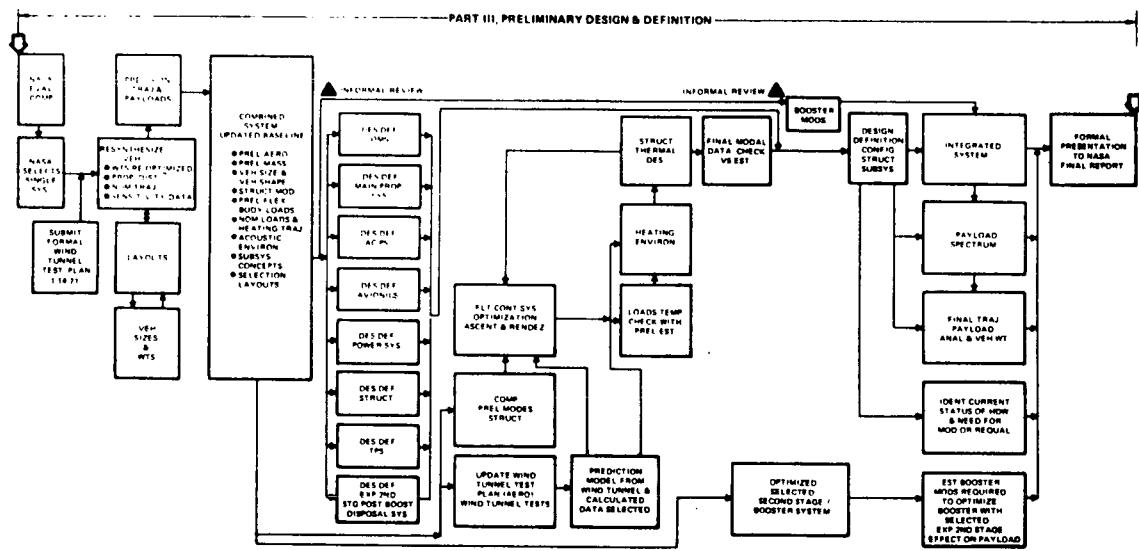


Figure 2-2. Study Approach and Logic, Phase B



PHASE B STUDY SCHEDULE

2 OF 2		TASK	SOW	1971																							
5	12	19	26	5	12	19	26	2	9	16	23	30	7	14	21	28	4	11	18	25	2	9	16	23	30		
MAIN PROPULSION SYS	4.3.1.1	DEFINE REQMTS																									
ATTITUDE CONT PROPL SYS	4.3.1.2	DEFINE REQMTS																									
ORBIT MANEUVERING SYS	4.3.1.3	DEFINE REQMTS																									
CRYO TANKAGE SYS	4.3.1.5	DEFINE REQMTS																									
ELECTRO - MECH & INTEG AVION	4.3.2	STAGE CRYO TANK SYS DEFINED																									
POWER SYS	4.3.6	DEFINE REQMTS																									
LAUNCH SYS INTERFACES	4.3.8	INTERFACE DEFINITION																									
VEHICLE DESIGN INTEGRATION	4.4																										
PRELIMINARY DESIGN DRAWINGS	4.4																										
INTERFACE DEF & CONT DOCUM	4.4																										
CEI SPEC'S PART I	4.4																										
SYSTEM SPECS	4.4	W/T MODEL DWG RELEASE	✓																								
CONFIG PRELIM VERIFICATION	4.5																										
SUPPORTING RESEARCH & TECH	4.6																										
PROGRAM COST & SCH EST PLAN	4.7.7	PROGRAM SCHEDULE ANALYSIS	✓																								
PREPARE FINAL REPORT	5.7																										
COST CONSID IN DESIGN	5.8	COST/DESIGN PLAN	✓																								

8.0.1.1

Figure 2-3. Expendable Second Stage on a Reusable Space Shuttle Booster MPS-02 (Sheet 1 of 2)

PHASE B STUDY SCHEDULE

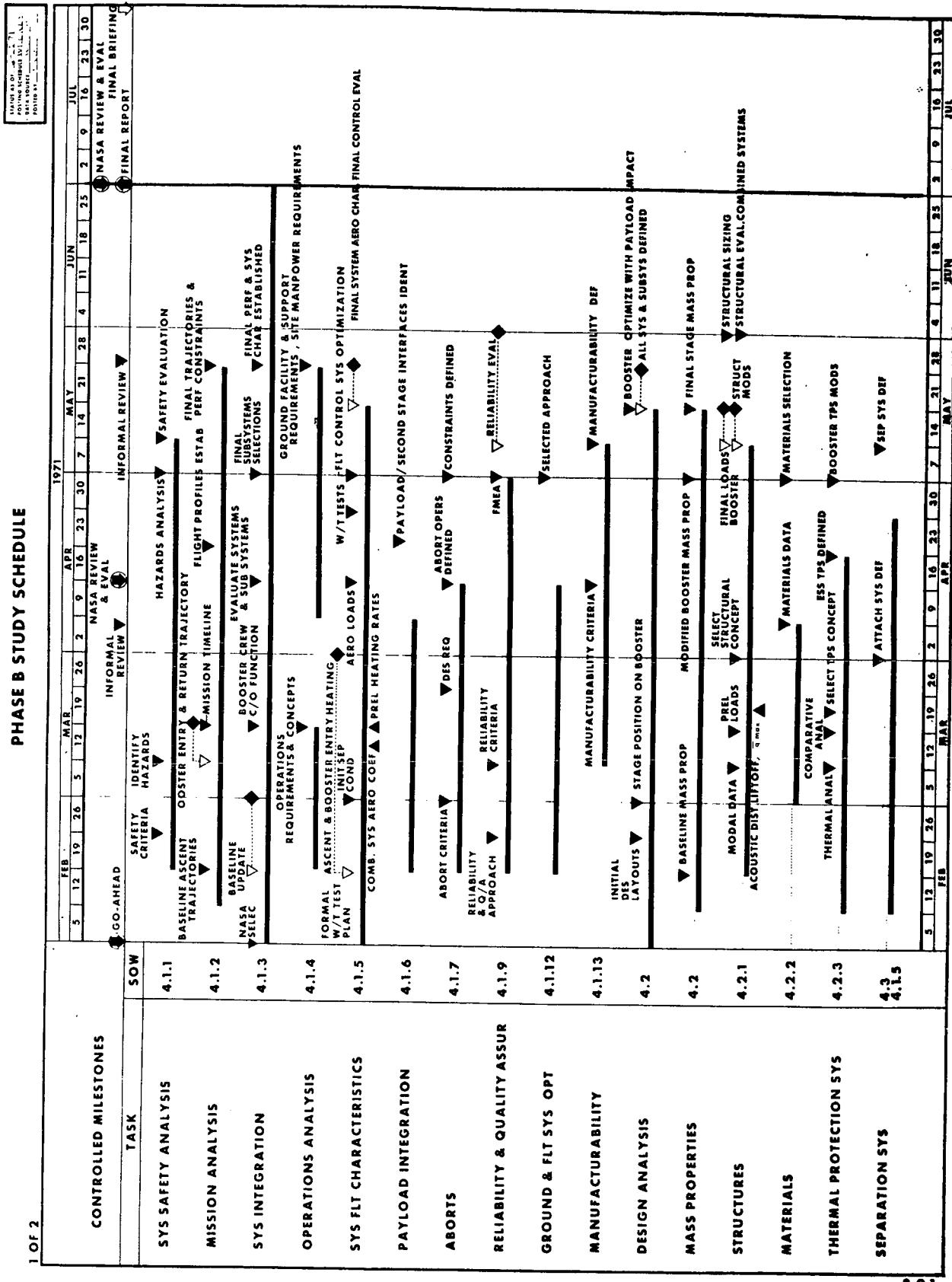


Figure 2-3. Expendable Second Stage on a Reusable Space Shuttle Booster MPS-02 (Sheet 2 of 2)



3.0 MISSION, SYSTEM, AND PROGRAM REQUIREMENTS

Specific requirements for the mission and system were provided by NASA in the Study Control Document. Also, desired program, vehicle, and operational characteristics were provided by NASA. These requirements and characteristics are enumerated here along with contractor interpretations and clarifications where appropriate. It is noted that certain items related to the mechanics of conducting the study have been removed from this listing and the remaining items have been renumbered accordingly. In addition, certain criteria derived from the above and from design and operational characteristics of the vehicles are listed.

3.1 INTEGRATED SYSTEM REQUIREMENTS

3.1.1 Mission Requirements

The following mission requirements were provided by the NASA as nominal conditions for expendable second stage on a reusable space shuttle booster baseline. In instances where the Space Division made an interpretation or clarification of these requirements, the interpretation/clarification is indented below the NASA requirement.

1. Mission duration: Maximum time from ground launch through deorbit burn shall be 24 hours.
2. Design reference mission: The reference mission to be used in designing the expendable second stage on a reusable space shuttle booster is a logistic supply of maximum payloads into the design reference orbit.

The MDAC space station is assumed to represent the maximum payload requirement for the study (Item 4 below). Growth potential is also covered to a limited extent.

3. Design reference orbit: The reference orbit to be used in designing an expendable second stage on a space shuttle booster shall be a 270-nautical-mile circular orbit, with a 55-degree inclination. For purpose of performance calculation, the vehicle shall be considered to be launched from a latitude of 28.5 degrees north.

Launch site assumed to be KSC. See 3.1.3 under Operational Characteristics, Item 1.



4. Payloads per Section VII of this document: For this study, detail control and load analyses were limited to the following three representative payload configurations:
 1. Nuclear stage or experiment module (the NR ESS study concentrated on the nuclear stage)
 2. Space tug, geosynchronous mission
 3. Space station (MDAC)—single launch configuration

These payload configurations are shown in Figures 3-1, 3-2, and 3-3.

3.1.2 System Requirements

The following characteristics were provided by NASA as baseline system requirements. In instances where SD had interpretations or clarifications of these requirements they are indented beneath the requirement.

1. The rocket engines used for this study shall be the J-2 and RL-10 engines (with modifications as required identified by the contractor) and the space shuttle high performance engine as identified in drawing 13M15000 space shuttle vehicle/engine 550K(SL) Interface Control Document.

A 10,000 pound thrust OMS engine evolved from the Shuttle Phase B Study. Therefore, it was added as a candidate for the orbit maneuvering system. Per TD 503 the Phase B Study was carried out on a short S-II stage with two (2) space shuttle engines.

2. The safety factor shall be 1.4.
3. Designs that compromise the booster to the extent that would preclude its use with the orbiter will not be considered and the load carrying capability of booster primary structure shall not be exceeded.
4. This Statement of Work will not duplicate the present Phase B space shuttle contract.
5. Minimum modification definition is "using present stage tankage."



PAYLOAD DESIGNATION: NUCLEAR STAGE - WITHOUT ENGINE (NR)											
WEIGHT CHARACTERISTICS:											
<table border="1"> <thead> <tr> <th>ITEM</th> <th>DESIGNATION</th> <th>WEIGHT, LB</th> </tr> </thead> <tbody> <tr> <td>NOSE FAIRING NUCLEAR STAGE INTERSTAGE</td> <td>NR SHAPE NR HYBRID</td> <td>5,500 60,000 17,500</td> </tr> <tr> <td>TOTAL</td> <td></td> <td>83,000</td> </tr> </tbody> </table>			ITEM	DESIGNATION	WEIGHT, LB	NOSE FAIRING NUCLEAR STAGE INTERSTAGE	NR SHAPE NR HYBRID	5,500 60,000 17,500	TOTAL		83,000
ITEM	DESIGNATION	WEIGHT, LB									
NOSE FAIRING NUCLEAR STAGE INTERSTAGE	NR SHAPE NR HYBRID	5,500 60,000 17,500									
TOTAL		83,000									
$I \text{ PITCH/YAW} = 5.051 \times 10^6 \text{ SLUG FT}^2$ C. G. = 935 IN.											
INJECTION ORBIT:											
<table border="1"> <thead> <tr> <th>PERIGEE, N. MI.</th> <th>APOGEE, N. MI.</th> <th>INCLINATION, DEG.</th> </tr> </thead> <tbody> <tr> <td>260</td> <td>260</td> <td>31.5</td> </tr> </tbody> </table>			PERIGEE, N. MI.	APOGEE, N. MI.	INCLINATION, DEG.	260	260	31.5			
PERIGEE, N. MI.	APOGEE, N. MI.	INCLINATION, DEG.									
260	260	31.5									
COMMENTS:											
1. STATION "O" AT FIELD JOINT. 396 FLD JOINT											
DATA SOURCE:											
NERVA REFERENCE DATA (FULL ENGINE FLOW), S-130-CP-090290-F1-PREL, AEROJET NUCLEAR SYSTEMS, APRIL 1970.											

Figure 3 - 1. Payload Description Form, Nuclear Stage



PAYLOAD DESIGNATION: SPACE TUG (GEOSYNCHRONOUS MISSION) - NR																
WEIGHT CHARACTERISTICS:																
<table border="1"> <thead> <tr> <th>ITEM</th> <th>DESIGNATION</th> <th>WEIGHT, LB</th> </tr> </thead> <tbody> <tr> <td>STAGE</td> <td>SPACE TUG + PROPELLANTS</td> <td>92,180</td> </tr> <tr> <td>PAYOUT</td> <td></td> <td>10,000</td> </tr> <tr> <td>SHROUD</td> <td></td> <td>5,000</td> </tr> <tr> <td>TOTAL</td> <td></td> <td>107,180</td> </tr> </tbody> </table>		ITEM	DESIGNATION	WEIGHT, LB	STAGE	SPACE TUG + PROPELLANTS	92,180	PAYOUT		10,000	SHROUD		5,000	TOTAL		107,180
ITEM	DESIGNATION	WEIGHT, LB														
STAGE	SPACE TUG + PROPELLANTS	92,180														
PAYOUT		10,000														
SHROUD		5,000														
TOTAL		107,180														
$I_{PITCH/YAW} = 770,880 \text{ SLUG} - \text{FT}^2$ $C.G. = 286.7 \text{ IN.}$																
INJECTION ORBIT:																
<table border="1"> <thead> <tr> <th>PERIGEE, N. MI.</th> <th>APOGEE, N. MI.</th> <th>INCLINATION, DEG.</th> </tr> </thead> <tbody> <tr> <td>100</td> <td>100</td> <td>28.5</td> </tr> </tbody> </table>		PERIGEE, N. MI.	APOGEE, N. MI.	INCLINATION, DEG.	100	100	28.5									
PERIGEE, N. MI.	APOGEE, N. MI.	INCLINATION, DEG.														
100	100	28.5														
COMMENTS:																
<ol style="list-style-type: none"> 1. THE SPACE TUG CAN DELIVER THE PAYLOAD TO SYNCHRONOUS ORBIT FROM LEO. 2. AS AN EXPENDABLE STAGE CAPABILITY TO SYNCHRONOUS ORBIT IS 40,000 POUNDS. 3. STATION "O" IS AT THE ENGINE EXIT PLANE. 																
DATA SOURCE:																
<ol style="list-style-type: none"> 1. NR SPACE TUG STUDY. 																

Figure 3-2. Payload Description Form, Space Tug

PAYLOAD DESIGNATION: SPACE STATION (MDAC)		SINGLE LAUNCH CONFIGURATION
WEIGHT CHARACTERISTICS:		
ITEM	DESIGNATION	WEIGHT, LB
NOSE FAIRING	NONE	1,140
SPACE STATION	CORE & ARTIFICIAL GRAVITY MODULES	175,820
TOTAL		176,960
I PITCH/YAW = 5.1×10^6 SLUG - FT ²		C. G. = 500 IN.
INJECTION ORBIT:		
PERIGEE, N. MI.	APOGEE, N. MI.	INCLINATION, DEG.
270	270	55
COMMENTS:		
<p>1. SPACE STATION SHOWN IS A CONFIGURATION EMPLOYING ARTIFICIAL GRAVITY.</p> <p>2. CORE MODULE HAS 4 DECKS. ARTIFICIAL GRAVITY MODULE PROVIDES 2 ADDITIONAL DECKS.</p> <p>3. MODULES ARE JOINED BY A TELESCOPING TUNNEL.</p>		
DATA SOURCE:		
<p>1. "SPACE STATION DEFINITION" VOLUMES IV AND VIII, MDAC REPORT NO. MDC-G0605, JULY, 1970.</p> <p>2. "SPACE STATION - MASS PROPERTIES DATA" MDAC REPORT NO. MDC-G0640, AUGUST, 1970</p>		

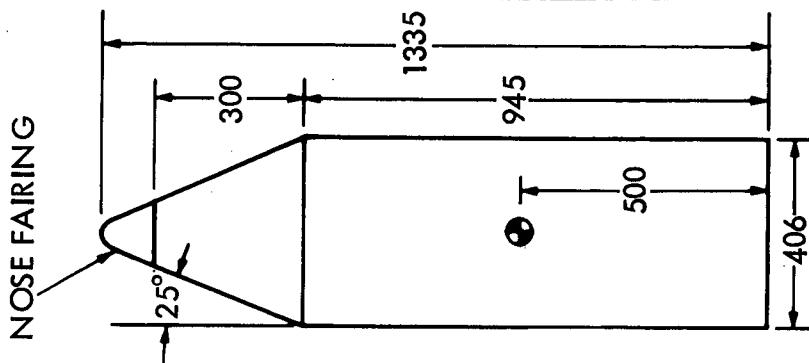


Figure 3-3. Payload Description Form, Space Station (MDAC)



6. Definition of the reusable booster will be limited to description of modification to the baseline developed in the Space Shuttle Phase B contract activity.
7. The reusable space shuttle booster configuration used for this study shall be current with Phase B shuttle progress. Prior to the final report, the contractor shall establish a cut-off date establishing the latest booster configuration that was possible to consider in this study. This configuration and date shall be identified in the final report.

The Phase B shuttle baseline booster configuration is designated as the GDC B-9U, dated March 15, 1971. This configuration is current as of the date of this final report, and has been used with the selected ESS for all data in the main body of these documents.

8. For this study, the gimbal angle shall be ± 10 degrees for the booster engines.
9. Structural modifications to the booster shall be kept to a minimum.

3.1.3 Desired System Characteristics

The desired characteristics listed below were provided by the NASA. For convenience, the following tabulation of characteristics has been grouped under three headings: program characteristics, vehicle characteristics, and operational characteristics. It is noted that each item applies to the total system. In cases where SD made interpretations or clarifications, these are listed below the NASA characteristics and are indented.

Program Characteristics

1. Cost will be reported using the design reference mission and should not include payload cost. A communication satellite system is assumed to be available and shall not be costed in the program.
2. The calendar year 1972 will be used as the materials technological base.
3. IOC baseline is the last half of 1979.
4. Flexibility shall be maintained to incorporate technology advancements and alternate missions.



5. Launch rates will be 2 per year from ten years using the Space Shuttle operational time frame. Cost estimates shall be developed for 2 launches per year for ten years.
6. Maximum consideration will be given to the use of existing hardware concepts and in determining cost.
7. Selection of the expendable second stage components will be based principally on demonstrated technology.
8. Advanced components technology may be considered for component selection where improvements are clearly capable of development, including ground qualification prior to 1977.
9. Applicable data (provided by NASA where necessary) from current programs and from previous and concurrent studies will be utilized to the greatest extent possible. The sources of such data will be identified in all reports and presentations.

See statement in Section 1.0.

10. Cost will be based on 1970 dollars with no inflationary factors added.
11. The current production status of hardware and the need for modification and/or requalification of hardware may represent major program impacts. Such impacts and their effects will be assessed.
12. No flight test stages are to be considered as RDT&E.

Vehicle Characteristics

1. All subsystems except primary structure and pressure vessels shall be designed to fail operational after the failure of the most critical component and to fail safe for crew survival after the second failure. Electronic systems shall be designed to fail operational after failure of the two most critical components and to fail safe for crew survival after the third failure. Existing subsystems that do not meet this criteria shall be identified. These criteria may be revised by technical directives for design of new subsystems where improvements in cost and effectiveness would result. The FO/FO/FS criteria will be observed for all new avionics equipment designs, subject to item-by-item waiver. Existing avionics equipments which do not conform to FO/FO/FS criteria may be selected to provide cost-effective design solutions



providing the hardware selection consistently maintains at least Saturn/Apollo reliability standards. Candidate hardware selections will be reviewed to assure desired system safety characteristics, especially with respect to stage operation in the vicinity of the booster. Avionics subsystems retained from the S-II, S-IVB, and IU are judged generally acceptable, but the need for reliability improvements will be considered. Recommended avionics modifications will be identified to enable cost impact evaluation. The FO/FS criteria will be observed for all new subsystems proposed for the S-II and S-IVB expendable second stages, subject to item-by-item waiver. Existing S-II and S-IVB subsystems excepting the primary propulsion system, primary structures and pressure vessels will be reviewed for FO/FS compliance and alternate approaches will be identified. Subsystem modifications which significantly improve booster/ESS launch success will be identified. Mechanical subsystems, such as rendezvous propulsion modules, derived from existing hardware other than Saturn/Apollo vehicles, will at least meet Saturn/Apollo safety/reliability standards. Emphasis will be placed on booster safety particularly during stage separations and abort.

During mated flight with the reusable shuttle booster, Technical Directive No. 2560, "Redundancy/Fault Tolerance Criteria for Orbiter/Booster Electronic Systems", dated 1-21-71, has been assumed to apply.

2. The hardware modifications and performance effects for synchronous orbit and deorbit capability shall be identified.
3. In systems where redundancy is needed, the expendable second stage systems shall be developed to provide redundant full mission capability and shall avoid minimum requirements, minimum performance backup system concepts. All existing stage subsystems will not be redesigned for added redundancy but new or modified stage systems will consider redundancy to enhance full mission capability. Significant reliability improvements obtainable by incorporating redundant elements will be identified.
4. The hardware modifications and performance effect for close rendezvous with a passive target to the following limits shall be identified:

11 ± 10 miles
±15 feet per second velocity



The bulk of the design analysis was conducted prior to removal of rendezvous as a baseline requirement (5 May 1971). (Refer to Technical Directive 506.)

5. To the extent feasible, the impact of utilizing the selected expendable second stage with the booster selected for the orbiter external hydrogen tank study shall be identified.

(Refer to TD 506)

6. The expendable second stage on a reusable space shuttle booster system shall provide for safe mission termination in the event major malfunctions occur during prelaunch preparation and subsequent to liftoff. The desired safe mission termination capabilities should allow for crew egress prior to liftoff and for separation of expendable second stage from booster following liftoff.
7. Multiple redundancy system techniques that minimize or eliminate system transients caused by system component failures shall be adopted.
8. The expendable second stage shall be designed for maximum on-board control, using on-board and ground capabilities as appropriate to maximize operational flexibility and minimize ground mission operations consistent with low cost. ESS dependence on ground mission support should not exceed that available for the Shuttle vehicles.
9. Guidance and navigation functions shall be performed on-board, using ground and other navigation aids when appropriate.

Operational Characteristics

1. All launches will be from KSC/ETR.
2. The vehicle trajectory load factors shall not exceed 3 g for manned mission and 4 g for unmanned missions after staging.
3. All-azimuth launch capability.

Hardware jettisoning during ascent is not permitted.

4. The expendable second stage shall have minimal checkout requirements at the launch pad.



5. Use of specialized facilities (i. e., clean room, altitude chamber, etc.) shall be minimized.
6. A variety of self-sustaining payload types shall be included in the payload integration. In general, payloads should be loaded prior to moving to the launch pad (safe aborts for manned payloads shall be the responsibility of the payload system).
7. The expendable second stage on a reusable space shuttle booster shall be designed to liftoff within a four-hour launch window for all launch azimuths.
8. Systems sensitivity to weather conditions during checkout and launch shall be minimized.
9. Service lines at launch pad should be minimal preferably only for the main propulsion systems propellants.
10. Maximum use of existing standards for the selection, design, packaging, and integration of hardware should be employed, consistent with program operational requirements.
11. The expendable second stage shall be safed during orbit and will not present a hazard to other orbital elements and payloads.
12. For the launch configuration, ground launch wind criteria shall be that given in TMX-53872, Terrestrial Environment (climatic) criteria guidelines for use in Space Vehicle Development, 1969 Revision, and TMX-53957, "Space Environment Guidelines for Use in Space Vehicle Development, 1969 Revision".
13. The expendable second stage shall be capable of accomplishing deorbit.

3.1.4 Criteria and Assumptions

This section lists criteria, rationale, and assumptions used in developing the ESS system described in this report. They fall in two categories; NASA-supplied and contractor-developed.

NASA-Supplied Criteria and Assumptions

An orbiter will be available subsequent to ESS payload delivery and prior to deorbit, at no cost to the ESS, for the purpose of removing selected ESS components and returning them to earth.



Contractor-Developed Criteria and Assumptions

General

1. The system will be designed functionally to complete the mission after sustaining loss of one main propulsion engine and one orbit maneuvering engine. However, in some failure cases, the performance capability will not permit mission completion.
2. The ESS will be designed for positive separation from the payload.
3. The system will be designed to provide the same degree of safety to the booster and its crew as the shuttle provides.
4. The ESS element will be compatible with the chemical inter-orbital shuttle (CIS) study design (Contract NAS7-200, Change Order 2021) in those areas where such compatibility does not seriously compromise the ESS design.

Reliability, Quality, and Safety Criteria. The purpose of this section is to identify reliability, quality, and safety criteria to be considered in the design of the expendable second stage. Booster design is not a subject of these criteria, except in those instances where substitution of the expendable second stage for the orbiter introduces new requirements and/or modifications to the booster.

These criteria, for the most part, were based on criteria for shuttle design. Therefore, there may be criteria identified which cannot be met employing a reasonable derivative of S-II. The items listed here supplement the basic requirements listed in Paragraphs 3.2.1, 3.2.2, and 3.2.3.

1. Alternate means of performing a necessary function shall be separated physically as much as practically possible, such that both (two or more) functions will not be lost due to a single event.
2. Malfunction or inadvertent operation of vehicle electrical, electronic, or mechanical equipment caused by exposure to conducting or nonconducting debris or foreign material floating in a gravity-free state shall be prevented by the following:
 - a. Electrical circuitry shall be designed and fabricated to prevent unwanted current paths being produced by such debris.
 - b. Critical mechanical items shall be provided with debris-proof covers or containers, while critical electrical items shall be provided with suitable containers, potting, or epoxy coating.



- c. Filters, strainers, or traps shall be provided in all moving-fluid systems to trap residual debris in a manner that will eliminate it as a threat to critical mechanical or electrical components. In installation wherein flow reversal may occur, filters or strainers shall be installed on both sides of critical components.
- 3. Subsystem or component failures shall not propagate sequentially; all equipment shall be designed to fail safe.
- 4. Inadvertent activation of critical systems shall be inhibited by design of systems or protective devices.
- 5. The design of vehicle subsystems incorporating redundancies shall include a means of verifying satisfactory operation of each redundant path.
- 6. All critical systems or circuits whose malfunction could result in unsafe or potentially hazardous situations or in early mission termination shall be monitored. Automatic flight vehicle control systems that are critical to booster or payload crew safety shall be provided with the capability for manual override.
- 7. Failure modes that result in hardware being classed as Criticality I (hardware whose failure in a credible mode could cause loss of personnel) shall be provided redundant means of failure detection plus either a third means of detection or a means of failure verification. Failure verification may be accomplished by verification of the detection equipment.
- 8. The expendable second stage should meet the safety requirements established by the Air Force Eastern Test Range (AFETRM 127-1) or the Air Force Western Test Range (AFWTRM 127-1) if appropriate. Waivers or deviations to these requirements must be identified and justified.
- 9. The system should be designed such that a failure in either vehicle will not propagate to the other.
- 10. The expendable stage design shall include the following considerations to ensure the highest practical level of cleanliness:
 - a. Inaccessible areas where debris and foreign material can become lodged, trapped, or hidden shall be avoided.



- b. Protective covers shall be provided to prevent entrance of debris into inaccessible areas. Where appropriate, these protective covers may be designed for ground operations only and may be removed for flight.
- 11. Space vehicle (booster and expendable second stage) subsystems will be designed with the capability to return the entire system to a safe condition in event of a hold at any time during test or launch countdown.
- 12. Provision shall be made, so that emergency situations, with the exception of those due to primary structural failure, can be isolated and contained or controlled.
- 13. The launch window shall be constrained to current range safety requirements. Special emphasis will be directed toward the elimination of the possibility of any debris from the expendable second stage falling on populated areas.
- 14. Components that contain mercury will not be specified for use with systems or their testing, checkout, handling, or maintenance equipment.
- 15. The destruct system used for the expendable second stage shall be designed to allow sufficient time for safe separation of the expendable stage from the booster before destruct.
- 16. In addition to built-in redundancy and multiple line replaceable units, alternate modes of operation are acceptable to fulfill redundancy requirements when their use does not create the need for additional hardware.
- 17. Design and operations required to implement in-space recovery of ESS components with the shuttle orbiter will be designed to minimize hazards to the orbiter and its crew.
- 18. Deorbit will be accomplished so that exposure of personnel and property to hazards is minimized.

Fluid Subsystems. The items listed here apply to fluid subsystems.

- 1. Vehicle fluid systems and their servicing equipment shall be designed to permit complete flushing and draining. The following conditions shall be satisfied as a minimum:
 - a. The system shall be free from dead-ended piping or passages through which flushing fluid cannot be made to flow.
 - b. Drain ports shall be located at the low points in the system.
- 2. Positive measures shall be taken to prevent incorrect installation of fluid line components whose function is dependent on direction of flow.



- a. Where feasible, the design of these fluid line components shall incorporate end fitting or connections whose dimensions or configuration will not permit incorrect installation or servicing.
 - b. The direction of flow shall be clearly indicated with permanent markings on the exterior of components and parts and every six feet on fluid lines.
 - c. Subsystem media shall be identified by anodizing or other permanent color coding on the exterior of the fluid lines/fittings.
3. Servicing and test ports not required to function in flight shall be designed to preclude leakage in flight. If caps are used, the material shall be compatible with the applicable subsystem media and the expected environment.
 4. Stainless steel tubing and fittings, such as L's, T's, and couplings, shall be joined by brazing or welding, except where mechanical disconnects are required for replacement or servicing, or where components would be adversely affected by brazing or welding.
 5. Fluids that can produce toxic fumes shall not be used in systems if a substitute with equivalent performance exists. When no satisfactory substitute for the fluid exists, tests shall be performed to assure that the total leakage is less than the concentration that would result in a level of toxicity which would impair safety.
 6. Service points for fluid systems, including those for filling, draining, purging, or bleeding, shall be accessibly located.
 7. Potentially explosive containers, such as high pressure vessel and volatile gas storage containers, shall be isolated one from the other. Such containers will be provided special pressure relief valves or vents.
 8. Venting, drainage, and hazardous fluid disposal provisions shall be designed into structural compartments for the safe elimination of hazardous products and so located to prevent drainage or vented fluids from reentering the vehicle.
 9. Means of reducing hazards caused by stored propellants shall be provided as a safety measure.
 10. Those systems that must have fuel and oxidizer tanks with common structural interfaces will be capable of being leak-checked independently of each other. During the leak checks, only the tank and surface being checked will be pressurized, with the other tank and surface held in an unpressurized condition.



11. Automatic protective equipment shall be incorporated in vehicle cryogenic systems to sense the onset of ullage pressure drop during the initial period of cryogenic loading. Pressure level drops that could result in system failure (collapsing of tanks or tubing) shall be controlled by protective devices.
12. Means of isolation shall be provided for liquid and gas systems, so as to not inadvertently result in liquid or gas leaks to the ECS.
13. Bypass circuits used during checkout shall not override system pressurization relief mechanisms.
14. The ignition and flammability characteristics of onboard combustible fluids shall be compatible with mission temperature profiles.

Structural/Mechanical Subsystems. The following items apply to structural/mechanical subsystems.

1. Structures designed only for positive pressure shall have provisions to prevent inadvertent depressurization.
2. Flight vehicles shall be structurally divided into compartments or zones that are classified according to the types of systems or equipment housed therein and that can be structurally or environmentally isolated from the remainder of the vehicle.
3. Structure and equipment shall be designed to prevent thermal paths from high-temperature areas to hazardous vehicle areas.
4. Provisions shall be incorporated to prevent damage to propulsion system components due to aerodynamic or engine-induced heating.
5. The separation mechanism utilized must provide positive separation of the expendable second stage under any credible condition in such a manner as not to incur damage to the booster.

Electrical/Avionics. The following items apply to the electrical and avionics subsystems.

1. Redundant electrical circuits shall not be routed through the same connector. Also, redundant connectors or paths for electrical wiring shall be so located that an event which damages one line is not likely to damage another.



2. No materials shall be used for wire insulation, ties, identification marks, and protective covering on wiring that will generate toxic fumes in a concentration sufficient to impair personnel safety when exposed to a short circuit resulting in the melting of a single wire at a single point of highest resistance.
3. The equipment shall be designed to contain the minimum number of test points required to ascertain satisfactory performance of all primary and redundant circuits. These test points shall permit normal planned subsystem checkout tests without disconnecting connectors that are normally connected in flight. Isolation between test/monitor points and internal circuits shall be such that misapplication of ± 28 vdc to any test/monitor point shall not degrade the equipment.
4. Electrical circuits shall not be routed through adjacent pins of an electrical connector if a short circuit between them would constitute a single failure that would cause loss of the booster crew.
5. Electrical circuits that are to be disconnected or cut in the normal course of mission events (e. g., vehicle separation) shall be protected against short circuiting or compromising of other circuits during the remaining phases of the mission.
6. Connectors shall be designed to prevent the possibility of mismating.
7. Vehicle electrical systems will be shielded from lightning and lightning-induced transients through proper bonding techniques to metallic vehicle structure.

Materials. The following items apply to materials selection.

1. Titanium, magnesium, lead, or any of their alloys shall not be used where exposed to liquid oxygen nor where exposed to gaseous oxygen exceeding two atmospheres of absolute pressure.
2. The risk of galvanic corrosion in flight vehicles shall be minimized by consideration of relative electrical potential (E. M. F.) in the selection and application of metals. Metals that differ in potential by more than 0.25 volts shall not be used in direct contact when exposed to a common electrolyte such as the atmosphere.
3. Materials used in the expendable second stage shall be selected with ignition, flammability, toxicity, expansion, contraction, and



shock sensitivity characteristics that do not present potential hazards due to use in the intended environment.

4. Zinc or cadmium plating shall not be used on the expendable second stage.
5. Insulation and other materials will be compatible with the fluid within the fluid systems to avoid hazards in the event of leaks. The materials will be nonwicking and should not react with moisture, propellants, or other agents to produce corrosive, toxic, flammable, noxious, or otherwise undesirable byproducts.

Ground Support Equipment Safety. The following items apply to ground support equipment (GSE).

1. Where maintenance of a fluid pressure by ground support equipment is critical to prevent major damage to an ESS component such as a propellant tank, the design of the ground support equipment shall not permit the pressurant source to be used simultaneously to supply fluid flow for other purposes such as purging and flushing. The GSE shall be designed such that recovery from failures of the pressurant source can be accomplished without damage to the ESS component.
2. GSE pressure systems will be designed for a minimum factor of 4 (4 x maximum operating pressure).
3. If GSE equipment cannot be designed to prevent critical hazards due to a structural or mechanical component failure, fail-safe features as a structural shear section or frangible element will be incorporated to restrict failure to a predetermined point where it will not cause secondary hazards. The design of GSE equipment which during operation, transmits mechanical loads to ESS should be avoided.
4. The purge capability for ground inerting of propellant systems will encompass the inerting of the propellant system, from source through vent exhaust. This includes all systems and monitoring lines whose surface has been wetted by the medium being purged in either the liquid or gas phase.
5. All nozzles and vents shall be protected from entrance of rain, debris, or other contaminants prior to launch. Protective covers shall be designed to be readily removable during the countdown prior to launch and shall be designed so that removal can be accomplished without risk of dumping accumulated debris into the



the nozzle, vents, or damaging nozzle radiation coatings. Wherever feasible, the covers should be designed so that failure to remove the cover will not cause failure of the system.

6. GSE for use with the ESS shall be designed with automatic protection from overpressure created in line segments by lockup pressures isolated between system valving.
7. GSE containing ignition sources shall be sealed and purged continuously when located in an area containing flammable gases or fluids.
8. GSE shall contain current limiting devices to preclude hazardous overcurrents from damaging ESS systems.
9. Emergency procedures shall be developed for all safety critical GSE, which covers emergency shutdown and backout/safing procedures.
10. GSE subsystems shall be designed such that component failures do not propagate sequentially.
11. Inadvertent activation of critical systems shall be inhibited by design of the GSE systems and/or protective devices.
12. Provide a specific location(s) and fittings for the attachment of a grounding cable to the ESS. If necessary, provide additional fittings or means for grounding the ESS where mated to the shuttle booster.
13. All GSE tools, fixtures, workstands, and servicing units that are affected by orientation of the vehicle, must be designed with horizontal, mated, and erected positions of the vehicle considered in the GSE design concept.
14. Include hazardous gas detection system in all ground areas and in the ESS compartments which might be exposed or collect hazardous gas fumes. Provide automatic means to signal appropriate station where corrective action can be taken.
15. Design the ESS inerting and safing systems GSE so that they may be rapidly and safely operated by operations personnel.



Facilities Safety. The following items apply to design of facilities.

1. Propellant disposal provisions such as a burn stack, burn pond, or controlled burners shall be used to safely dispose of excess propellants or vented gas.
2. There shall be no facilities valves between the ESS tank vents and the propellant disposal system which could block or otherwise obstruct the venting of the ESS tanks.
3. Facilities vent and disposal systems shall not have backpressures which are in excess of the system being vented into the system.
4. The vent stack outlet shall be located downwind from the building, inhabited areas, etc., to a point where the separation distance will provide safe conditions under the most severe local weather conditions.
5. Burn-stacks shall be equipped with flame arresters to prevent flame propagation into the system.
6. All burn-type installations shall be equipped with an automatic pilot ignition system.
7. Cryogenic tankage shall be provided with a means for monitoring the ullage pressure, during initial loading, by automatic protective equipment or by qualified personnel who have pressurization controls immediately available to them to prevent tank implosion.
8. A tank outlet shutoff valve which can be remotely activated will be installed at the cryogenic tank outlet for safing the tank in the event of line rupture.
9. Provide relief provisions in each section of a system where a cold propellant or gas entrapment can occur.
10. The cryogenic facility system shall be capable of being drained, flushed, purged, and inerted.
11. All cryogenic facilities systems shall be grounded and electrically bonded.
12. Provisions shall be made during installation to allow for "working" of piping systems at cryogenic temperatures.



13. A continual means for detection of hydrogen leaks and a warning system shall be included in the facility.
14. The facility shall have fire detection, warning, and fire water management system capable of extinguishing or containing a hydrogen fire.
15. A means for properly grounding storage tanks, lines, GSE, and facility against static electricity and/or lightning strikes shall be provided to meet the national electrical code requirements.
16. Hydrocarbon materials will not be used for road surfaces or expansion joints in liquid oxygen handling, use, or storage areas.
17. Backup and emergency power will be provided for use, if needed, during propellant loading/offloading in case of primary power failure.

3.2 ESS VEHICLE REQUIREMENTS

ESS vehicle requirements and criteria are included in Volume VIII, Preliminary CEI Specification, Part I. Subsystem requirements for the ESS are presented in Book 2 under the appropriate subsystem.



4.0 SYSTEM/PROGRAM DEFINITION

An operable system is composed of all the hardware, software, facilities, personnel, and consummables required to operate the hardware for the purpose of meeting mission and program objectives, including traffic requirements. The quantities of each of these items are a function of the program to be completed.

4.1 SYSTEM ELEMENTS

The expendable second stage on a reusable shuttle booster system elements are as shown on the work breakdown structure (WBS) at Level 3. The elements and quantities of those elements for the proposed program are as follows:

4.1.1 Expendable Second Stage

This stage (vehicle) is defined in detail in Book 2 of this volume. Since the basic stage structure is expendable and 20 missions are desired, 20 of these vehicles are necessary to meet the program requirements.

4.1.2 Main Propulsion Engine (ESS)—Space Shuttle Orbiter Engine

These engines are the ones required by the ESS, and they are listed as a separate element since NASA will contract for and provide them separately. The engines are to be installed in such a way that they may be recovered in orbit by the orbiter for later reuse. Therefore, it has been concluded that three sets (six engines) plus spare parts for the refurbishments should adequately provide for the ESS program. Since these engines are the same as those used by the space shuttle orbiter, and since they have a life of about ten hours each, they might conceivably be space shuttle used engines.

4.1.3 Booster

The booster is defined in the space shuttle study. It requires only minimum modification, as discussed in Book 3 of this volume. The basic space shuttle program requires four of these boosters. The traffic rate (two flights per year) for the ESS does not require that all four of the boosters be modified, but for the sake of flexibility, all boosters are assumed to be modified (and costs are associated with modifying all four vehicles).



In addition to the flight vehicle (booster), this element includes booster specific support equipment (handling, servicing, checkout, training, etc.).

4.1.4 Operations

The facilities, support equipment, and personnel required to perform all phases of the operation of the vehicle system, at the flight rate and the duration of the program, are discussed in Volume V of this report. Those facilities (maintenance and repair, landing and recovery, safing, etc.) required by the booster and/or the orbiter are discussed in SD 71-104-2, and are not repeated herein.

4.2 SYSTEM OPERATIONS

Functional flow block diagrams are provided in Volume 5, Section I, and show that the ESS is compatible with, and complementary to, the basic space shuttle system. The ESS requires the use of the space shuttle booster (to act as the first stage of a two-stage vehicle system) and its required support equipment and facilities. The cost of the ESS on a reusable shuttle booster system has been reduced by assuming that a space shuttle orbiter is available, after it has completed its up-mission and is still in space, for rendezvous and docking with the ESS for the purpose of removing (recovering) the ESS high value components. These recovered components would be refurbished and reused in subsequent ESS flights. Thus the ESS must provide for docking by the orbiter and for easy removal (minimum EVA) of those components.

Figure 4-1 illustrates the basic operations in the design reference mission profile. The ESS on a reusable shuttle booster (RSB) is launched from Kennedy Space Center (KSC); staging occurs; the ESS injects into orbit; the orbit is circularized; the ESS payload is deployed; a space shuttle orbiter performs rendezvous and docking with the ESS; the orbiter removes ESS components and separates from the ESS; at the appropriate times, the ESS and orbiter perform deorbit; the ESS disintegrates and some portions impact the earth; the orbiter returns to the operational site; following separation from the ESS, the RSB reenters and flies back to the operational site.

After the orbiter returns to the operational site, the recovered ESS components are removed, refurbished, and installed in the next ESS to be prepared for flight. Of course, the orbiter is also serviced for subsequent space shuttle flights.

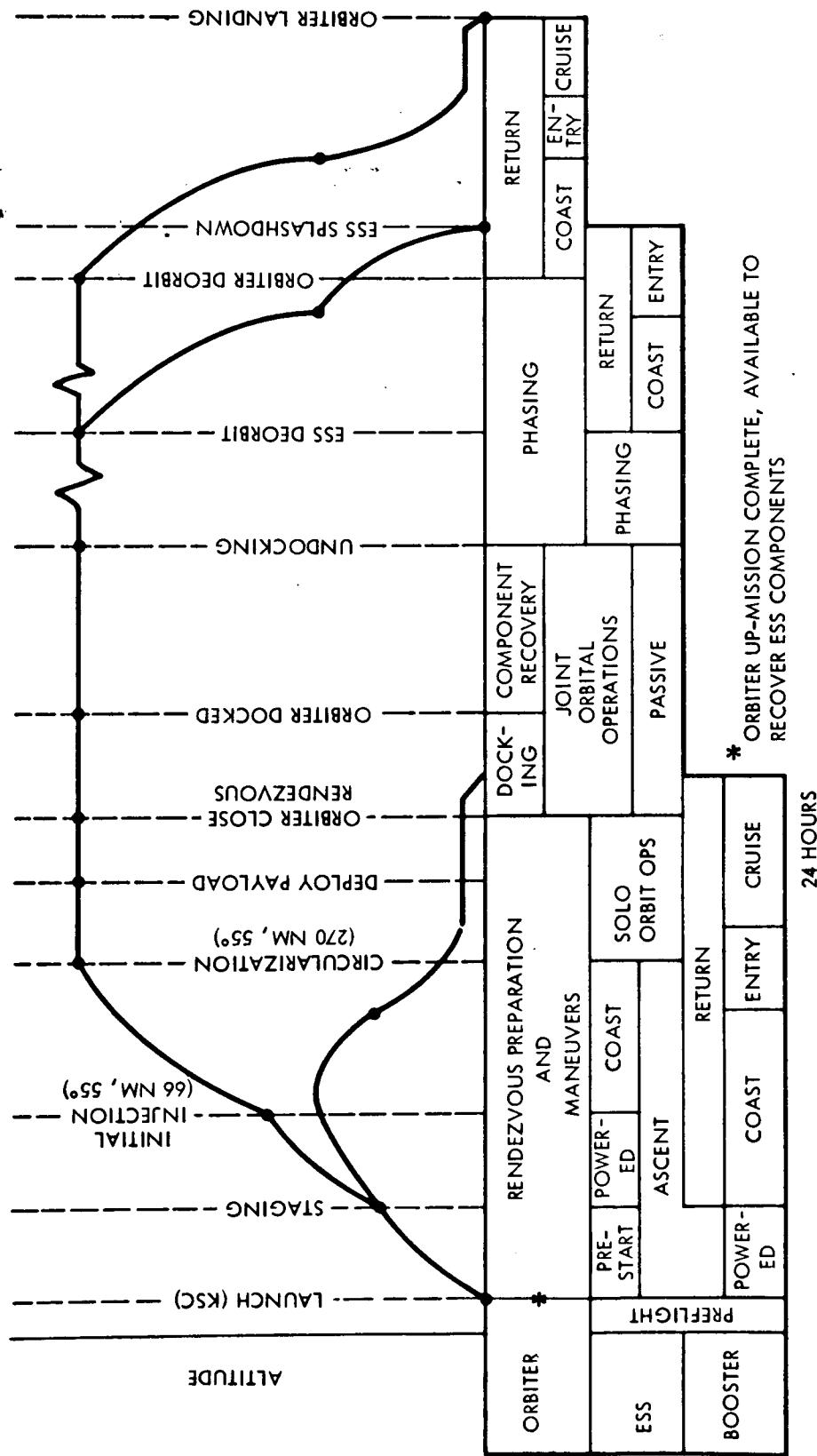


Figure 4-1. Design Reference Mission Profile



After the booster returns to the operational site, it is also refurbished for subsequent ESS or space shuttle flights. Booster flight preparation and refurbishment due to ESS flights are charged (costed) to the ESS system. The support by the orbiter is not charged to the ESS system since the flight preparation and refurbishment were for space shuttle operations.

After KSC receipt of the ESS, normal operations will be inspection, installation of the reusable components, checkout, servicing, and handling before the launch and flight operations.

Ground support for flight operations for the ESS will not exceed that required for the basic space shuttle.

Operations relative to the ESS payloads are considered beyond the scope of this study; thus, there is little mention of direct operations with the payloads.



5.0 INTEGRATED VEHICLE CHARACTERISTICS AND ENVIRONMENT

5.1 PHYSICAL CHARACTERISTICS

The integrated vehicle consists of an expendable second stage (ESS) mated to a delta-winged booster (B-9U as described by Space Shuttle Phase B final reports, dated 26 March 1971). The characteristics of these vehicles are described here by general arrangement, mass properties of the overall vehicles, and booster-to-ESS interfaces.

5.1.1 General Arrangement

The general arrangement of the integrated vehicles is depicted in Figure 5-1. The ESS is positioned approximately 2.8 feet above the booster. The ESS vehicles carried by the booster are:

1. An ESS combined with an RNS (nuclear stage) payload,
2. An ESS combined with a MDAC space station payload, and
3. An ESS combined with a space tug.

Launch of the integrated vehicles is similar to that of the baseline booster/orbiter systems.

5.1.2 Mass Properties

Mass properties were estimated for three expendable second stage systems. These data were then combined with similar data estimated for the B-9U space shuttle booster, resulting in mass properties of the total space vehicle system. Mass properties data were then used as parameters for structural loads, performance trajectories, and stability and control analysis. A weight statement, presenting the summarized weight breakdown of three space vehicles, is included as Table 5-1. The mass properties of each ESS system presented include a specific payload and its appropriate installation provisions. Mass properties data for these payloads are referenced in Section VII of the study control document.

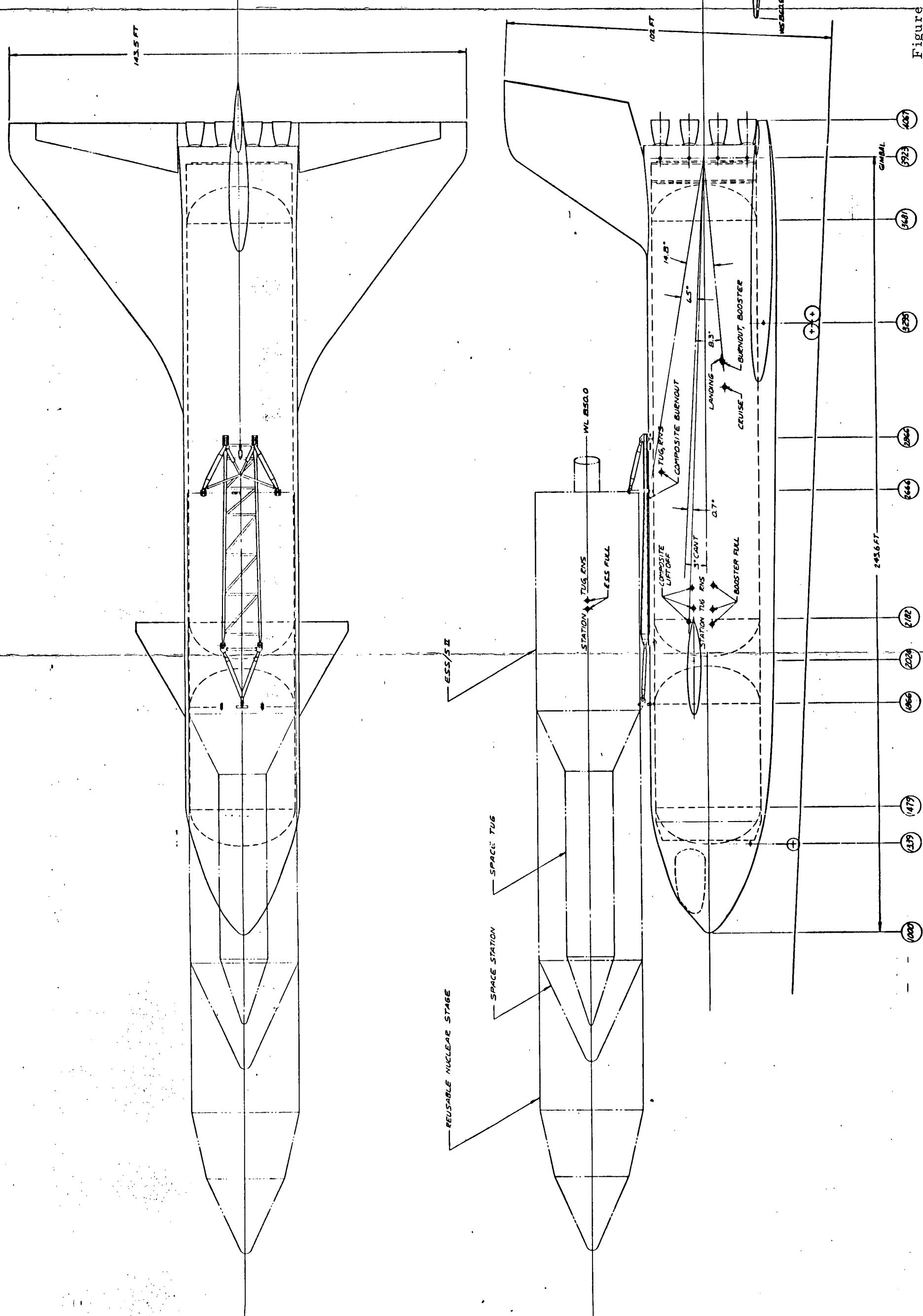
Table 5-1. Configuration Weight Summary

Configuration	MDAC SS	RNS	Tug
Item	B-9U	ESS	B-9U
Dry weight	643,117	96,936	643,117
Personnel	476	476	476
Payload	176,960		
Payload adapter		83,000	
Residual fluids	11,476	11,476	11,476
Payload margin	5,965	5,965	5,965
	5,330	9,314	9,413
Inert weight	655,069	655,069	655,069
Reserve fluids	6,659	10,480	10,487
Inflight losses	20,802	20,802	83
Propellant ascent	3,382,307	2,749,260	2,941,395
Propellant cruise	143,786	143,786	143,786
Propellant man/ACS	1,500	1,500	1,500
Stage total weight	4,203,464	3,570,417	3,762,552
Spacecraft GLOW	5,195,464	4,222,117	4,517,437





NOTES
1. B-9U/ESS CONFIGURATION SAME AS B-9U
ON TC 2040 EXCEPT AS SHOWN.
2. FOR LINES SEE TC 2040.
3. FOR B-9U INDICATED PROFILE SEE TC 2040.





5.1.3 Booster/ESS Interfaces

The prime booster/ESS physical interfaces are the structural mating/separation link and the communications hardline link.

The booster mating/separation subsystem will support the ESS in the mated position during transport, erection, launch, and ascent. The physical interfaces are similar to those of the shuttle and consist of four attachment links with the forward links incorporating the communications hardlines as depicted in Figure 5-2. During mated flight, loads applied by the ESS to the booster are transmitted through the mating/separation interface. A description of the separation system is presented below.

Communications between the booster and ESS at the interfaces will consist of three hardline data links for (FO/FS) redundancy. Each link will be separate from the others, including individual terminating connectors, and will consist of two twisted wire pairs with each pair shielded. The booster-ESS separation sequence will be able to be actuated automatically through the data interchange channel in any one of the communications links. Input data from the booster and/or ESS buses will be integrated by the booster computer which will provide separation sequence signals. The communications interface for booster-orbiter and booster-ESS is similar, the difference being in the voice link which is inoperative for ESS missions.

The separation system is summarized in this section with more details in Book 3.

Separation System Requirements

1. The mating/separation subsystem shall be capable of withstanding all loads imposed during ground operations and mated flight.
2. The system shall provide safe operation during normal staging with one or two ESS engines operating and with two ESS engines operating and two booster engines inoperative.
3. The separation mechanism shall have FO/FO capability. For purposes of interpreting the redundancy requirements, the primary load paths through the links, joints, pivots, and bearings of the stage interconnect structure and separation system are considered primary structure.
4. Operation of the separation system shall not produce any debris (including explosive residue) which could damage the booster or ESS.



5. The system shall provide independent separation control from both ESS and booster, which does not rely on crew management.

General

Separation of the ESS from the booster is accomplished in a manner similar to that used to separate the orbiter from the booster. Booster thrust is used to accelerate the ESS transversely from the booster. Forces for the transverse separation are transmitted by the rotating links located at the fore and aft linkage attach points on the structural adapter shown in Figure 5-2. The structural adapter is supported by the same structural hard points provided for the orbiter/booster mating/separation system — that is, fittings located on the two major forward and the two major aft bulkheads. Forces are transmitted to the ESS through linkage attach points provided.

Forward Linkage Arrangement

The forward linkage arrangement resembles the aft linkage arrangement of the baseline booster/orbiter separation system. A rotatable A-frame expansion compensator functions as on the baseline system by accommodating forward/aft structural/thermal deformations between the ESS and the adapter. Axial loads are not transmitted by the expansion compensator until the separation maneuver is started. The vertical links react vertical loads, and the lateral restraint—the spherical end of which nests in a socket-like fitting in the ESS—reacts side loads until the separation maneuver is effected. Vertical and lateral links attach to the existing linkage attach points on the booster.

As in the shuttle system, spherical bearings are used at the pinned joints to facilitate installation and to compensate for structural deflections and provide relative motion.

A snubber/retract actuator is provided to snub and retract the rotating A-frame link to a faired position after separation has been completed.

Aft Linkage Arrangement

The aft linkage arrangement consists of vertical links that react vertical loads only, the lateral restraint number that reacts side loads only, and rotating links. The vertical and side restraint members attach to the same lugs provided for the baseline orbiter/booster separation system. The aft rotating links, however, pivot about lugs which are integral to the fixed

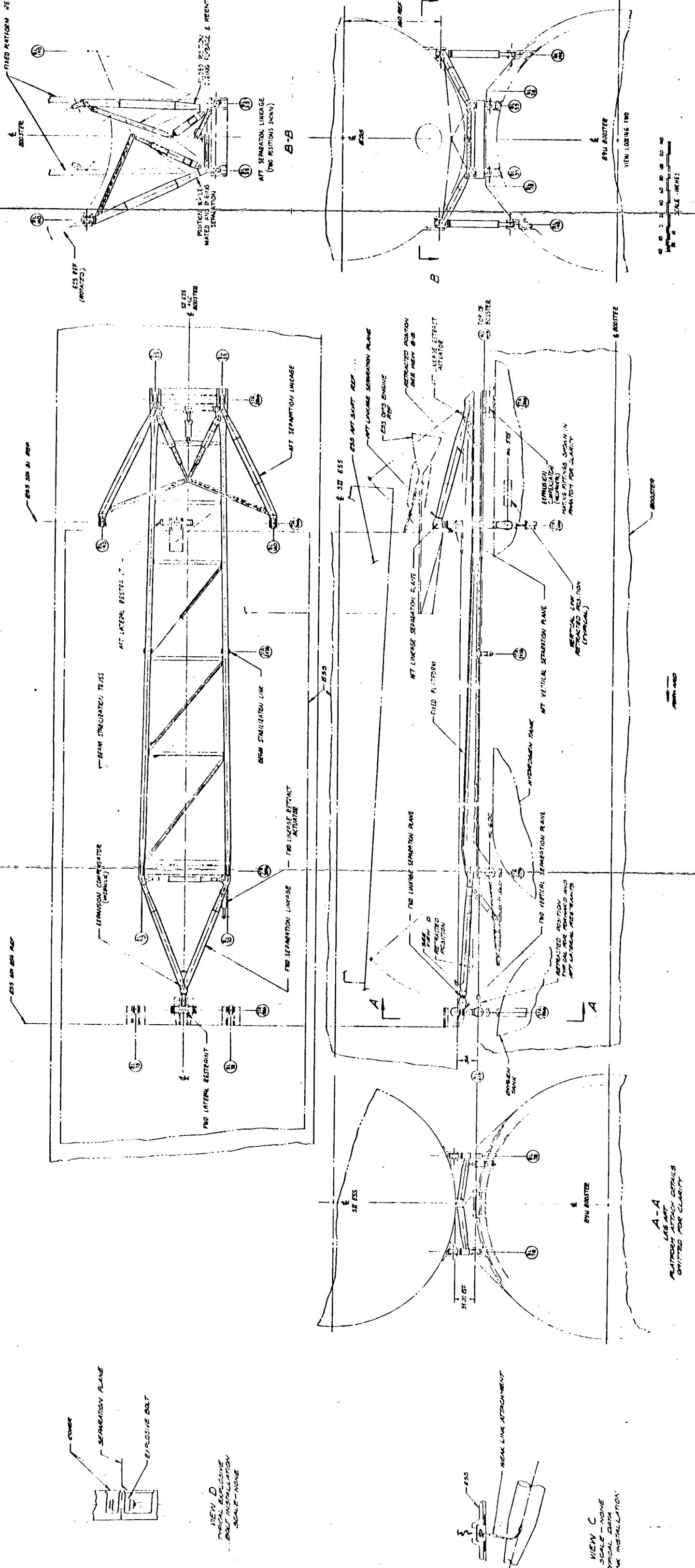


Figure 5-2. Booster/ESS Interface Drawing

FOLDOUT FRAME

◎ 人物

EOLDOUT FRAME

SD 71-140-2



platform. Also, as for the forward links, the aft rotating links are snubbed and retracted after separation has been completed. In addition, the aft links are made to fold inward to facilitate protection of those elements during reentry and to reduce drag during the flyback phase. Spherical bearings are provided at critical points to facilitate installation alignment and to compensate for structural deflections.

5.2 PERFORMANCE AND FLIGHT CHARACTERISTICS

This section presents the overall performance capabilities of the ESS system, along with trajectory data and flight environment associated with the missions investigated. Nominal trajectories are given for the three specified payload cases. Aerodynamic data were calculated for the three configurations to provide a basis for stability and control analyses, and also for distributed air load evaluations.

Mated flight presents the greatest stability and control, as well as airloads problems for the system. Control characteristics also are covered for the ESS after separation. Booster entry is similar to the shuttle baseline condition. Considerable attention is given to loads because they are critical during boost relative to the minimization of effects on the reusable booster. Thermal effects are estimated and are found not to be critical except that a few local areas require special attention. Aborts and/or contingency missions are described briefly.

5.2.1 Payload Capability

This section presents launch vehicle performance as related to the three specified payloads for which substantive design analyses were conducted. Also parametric data are presented which show the performance of the vehicle for other missions of interest.

Specified Payloads

The three payloads for which the vehicle was specifically designed are the space station, space tug, and reusable nuclear shuttle. Of these, the space station is by far the heaviest, and its orbit requires the largest energy expenditure for launch from KSC. Its launch therefore was used as the basis for vehicle sizing. The two lighter payloads with their corresponding lower energy orbits are accommodated by off-loading the system so that ballast, either inert or unused residual propellant, is not required. For post-separation safing, large propellant residuals are not desirable, and hence, have been eliminated. Therefore, the launch configuration varies only to the extent that the payload configuration is different and the stage



propellant loads are different. The propellant loadings were derived assuming a fixed booster delta V. This rationale minimizes the variance in staging conditions.

Combined system mass properties are given in Volume IV for the three payloads.

It is noted that the vehicle was sized to provide a small payload margin (5330 pounds) above the space station mission requirement and that a 9314-pound margin is provided for the space tug and a 9413 pound margin for the reusable nuclear stage payloads. Also with the latter two payloads, the propellant loadings were sized to provide for completion of the specified mission with only one ESS main engine operative.

Generalized Payload Capability

This section presents parametrically the payload capability of the vehicle. The data shown are within the performance constraints of the system but, in some cases, involve requirements which have not been incorporated into the selected system design, e.g., restart of the ESS main propulsion system. Except for cases specifically identified, the results are based on the liftoff weight and ESS/payload gross weight compatible with the design.

Figure 5-3 shows the variation in payload with orbital inclination for orbit altitudes from 100 nm to 270 nm. Deorbit after delivery of the payload is assumed, and except for inclinations of less than 28.5 degrees, space recovery of ESS components by the shuttle is also assumed. It should be noted that for inclinations less than 28.5 degrees, restart of the main propulsion system is required to execute the in-orbit plane change.

Figure 5-4 shows the variation in stage propellant loadings for payloads less than maximum. Loadings are shown which permit completion of the nominal mission after having incurred an ESS main engine failure at staging. Also shown are loadings which do not permit that capability. The mated ascent trajectories for these cases all reflect the low attachment loads rationale discussed under the previous heading, "Specified Payloads."

Figures 5-5 and 5-6 show the potential of the vehicle to perform relatively high energy missions. Figure 5-5 shows its capability to high circular orbit. Three cases are illustrated: (1) neither component recovery nor deorbit is executed, (2) deorbit is executed but component recovery is not, and (3) both are executed. The profile for establishing the orbits

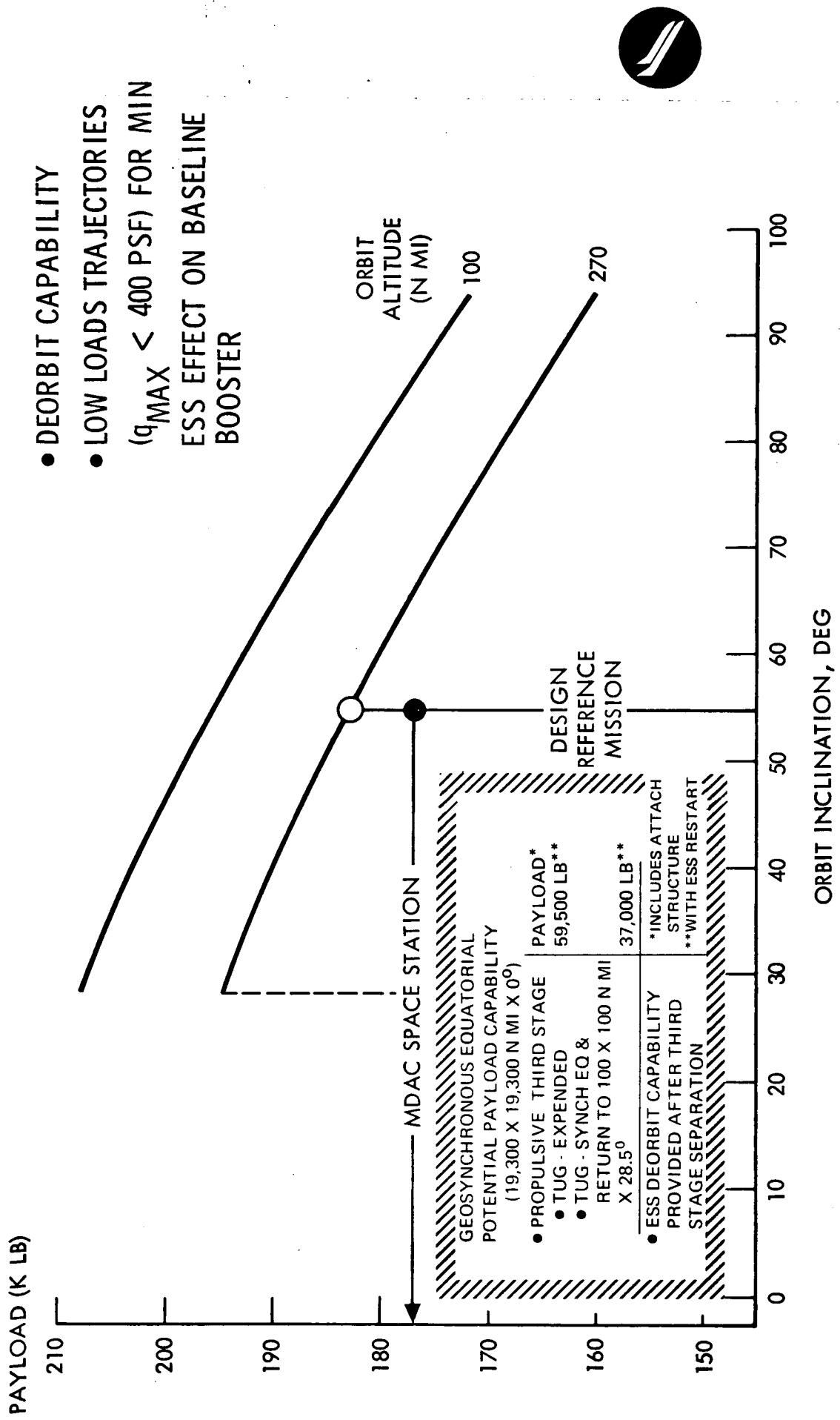


Figure 5-3. Performance Capability of Baseline ESS System

- LOADING PERMITS MISSION COMPLETION
- WITH ESS ENGINE FAILURE AT STAGING
- NO ENGINE OUT CAPABILITY

- DEORBIT
- FIXED BOOSTER ΔV
- DRM WITH MDAC SS AERO

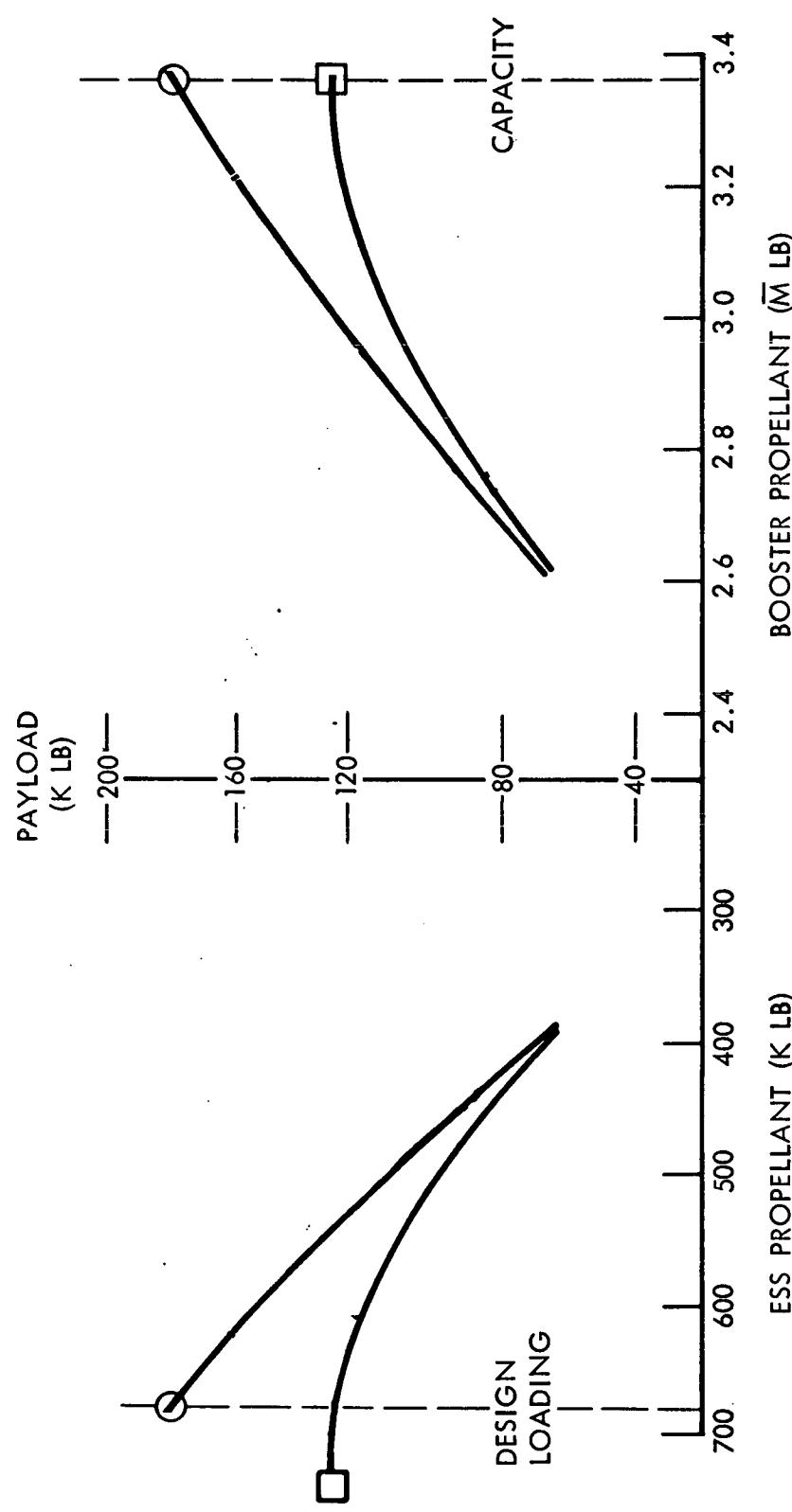


Figure 5-4. Off-Loading for Low-Energy Missions (Minimum Residuals)

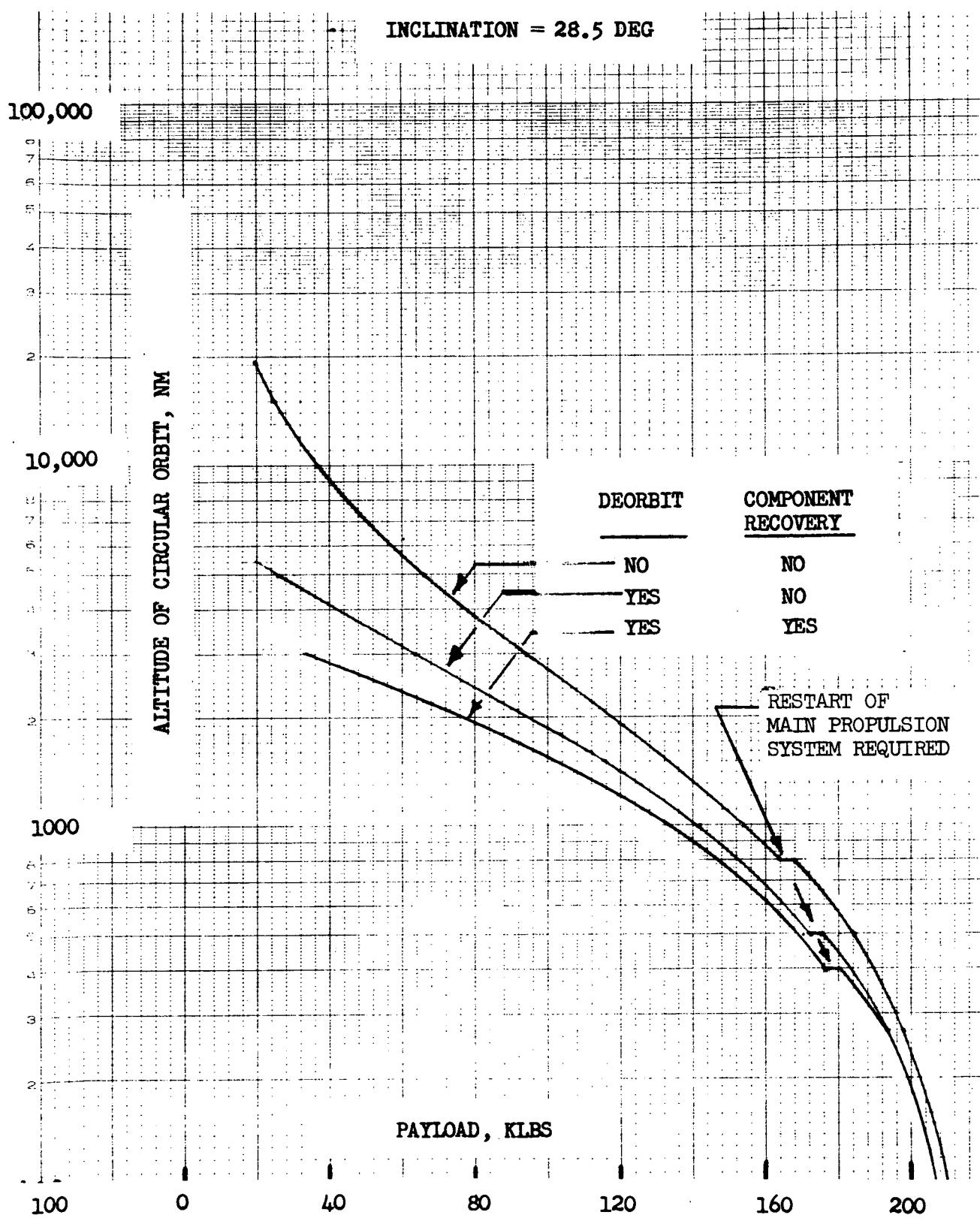


Figure 5-5. ESS Performance to High-Altitude Circular Orbits



PERIGEE ALTITUDE = 66 NM
INCLINATION = 28.5 DEG

100,000

10,000

1000

APOGEE ALTITUDE, NM

PAYOUT, KLBS

100

0

40

80

120

160

200

DEORBIT

COMPONENT
RECOVERY

NO
YES
YES

NO
NO
YES

RESTART OF MAIN PROPULSION
SYSTEM REQUIRED

Figure 5-6. ESS Performance to High-Altitude Elliptical Orbits



employs supercircular burnout at 66 nm (400,000 ft), establishing an elliptical orbit with a 66-nm perigee and apogee of the specified orbit altitude, followed by circularization at apogee. In case 3, after delivery of the payload to the specified orbit, the ESS maneuvers down to a 270-nm orbit where component recovery by the shuttle is accomplished. Deorbit with the ESS OMS follows. Note the approximate points where restart of the main propulsion system becomes necessary.

Figure 5-6 shows similar data for elliptical orbits. Supercircular burnout is also assumed for these cases. Therefore, restart of the main propulsion system is not required except for relatively high apogee orbits when component recovery by the shuttle is required. Note that the perigee of these orbits is located at burnout of the ESS or roughly 700 nm down-range of the launch site.

Equatorial Geosynchronous Missions

A cursory performance analysis was conducted to determine the capability of the system to perform the equatorial geosynchronous mission both with and without the assistance of a third stage (or third stages). This mission requires the main propulsion system of the ESS to be restartable.

Figure 5-7 shows some typical results. It is seen that without a third stage, the payload capability is trivial. The addition of a third stage improves it dramatically. The performance characteristics used for the third stages are representative and are listed in Table 5-2. Payloads ranging from 45,000 to 55,000 pounds can be expected from an expendable Centaur-derived system while payloads above 55,000 pounds can be expected assuming an expendable tug or OOS. If the tug or orbit-to-orbit shuttle (OOS) is used and it is to be recovered, over 35,000 pounds can be launched.

Booster Optimization With Selected ESS

A prime objective of this study was to provide a booster that had the capability of accomplishing the shuttle and the ESS missions with minimum compromise to the shuttle missions. Specifically, the effects on the booster structure were minimized since an increase in booster structural weights would either require an increase in booster size to satisfy the shuttle missions or it would be necessary to accept a corresponding reduction in the vehicle payload delivery capability. To assure minimum booster impact, the ESS payload weights were limited to the maximum specified payload. The ascent trajectories were shaped to minimize dynamic pressure, and the maximum axial acceleration at booster burnout was limited, for the space station use, to 2.06 g's.

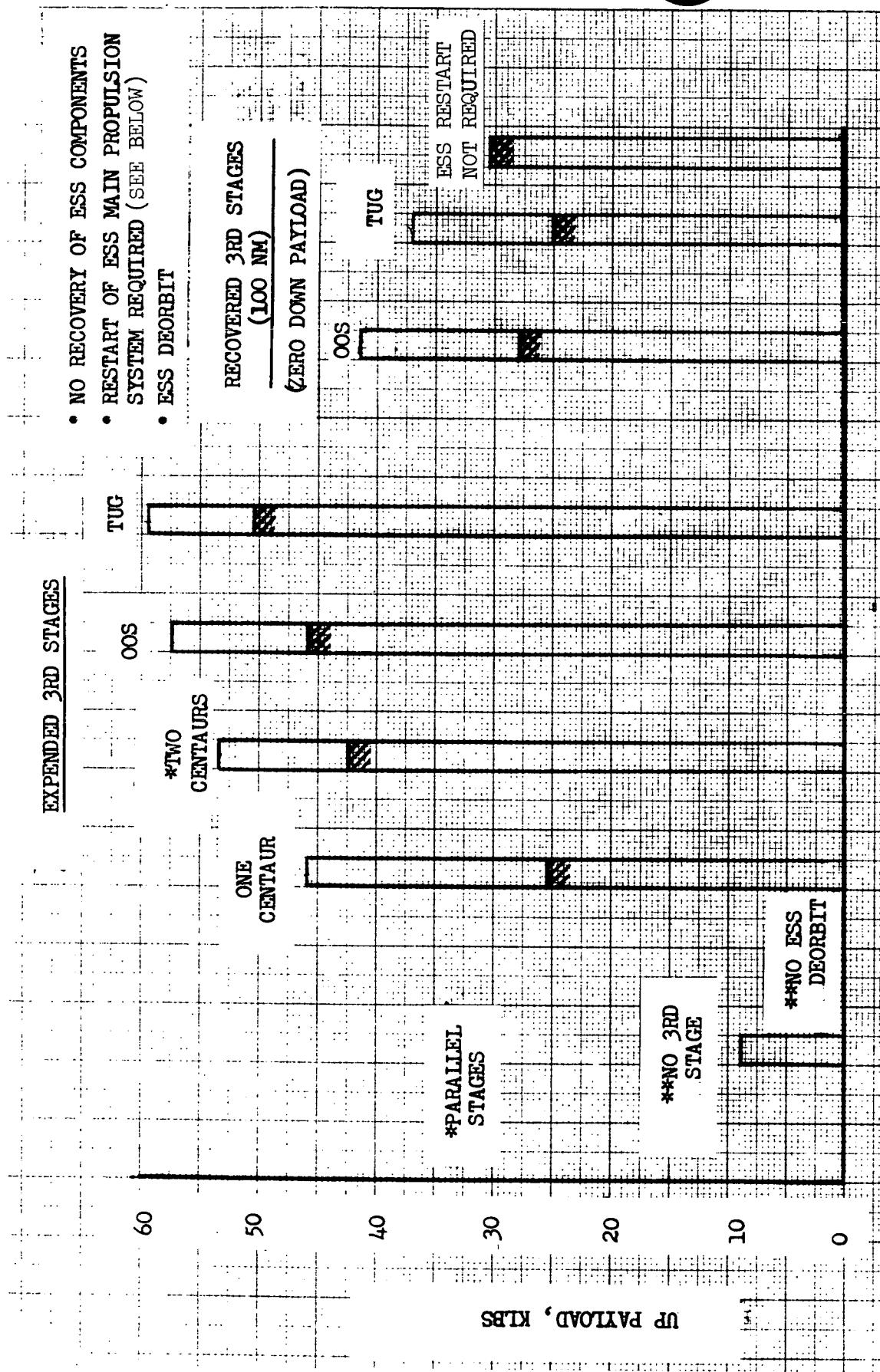


Figure 5-7. Comparison of Third Stages for ESS Equatorial Synchronous Missions



Table 5-2. Performance Characteristics of Third-Stage Candidates

Stage*	Centaur	Space Tug	OOS**
Gross weight, lb	(34,500)	(90,900)	(73,870)
Usable propellant, lb	30,000	80,000	65,000
Burnout weight, lb	4,500	10,900	8,870
Mass fraction (δ_B)	0.87	0.88	0.88
Specific impulse, sec	444	462	462
Adapters and interconnecting structure	Zero	Zero	Zero

*For performance trends only; all values typical of type
**Orbit-to-orbit shuttle (USAF)

Section 3.0, Statement of Work, Item 6, states "Identify any modifications and extent of penalties (if any) in payload and performance required to optimize the booster with the selected expendable second stage, but do not incorporate in the Phase B Space Shuttle system study."

Performance calculations indicate that approximately a 250,000-lb payload can be placed in the design reference orbit (270 nm, 55°) by the selected ESS (fully loaded) on the B-9U booster.

A cursory analysis was conducted, based on extrapolation of data developed during this study, to develop an estimate of the impact on the booster of providing an ESS system based on the prime objective of achieving maximum payload performance. The basic differences in the trajectories and control requirements, comparing a philosophy which minimizes booster impact to one which maximizes performance, are as follows.



Item	Low-Q Trajectory	Optimum Performance Trajectory
Payload	Space station	Space station
Gross weight	992,000 lb	1,150,000 lb
Max g	2.06g	3.0g
Max F _x	2,239,000 lb	3,450,000 lb
αq	+1500, -2900 psf deg	± 2800 psf deg
βq	± 1600 psf deg	± 2400 psf deg

The use of the optimum performance trajectory would have the following effects on the booster:

1. On the pad: to withstand one-hour ground winds, the strength of the hydrogen tank skins and thrust section holddown structure would have to be increased.
2. At maximum βq : the forward ESS support bulkhead and adjacent skins would require beef-up.
3. At maximum αq : the aft hydrogen tank skins would be affected, the lower tank section being more critical than the upper section.
4. At maximum thrust: the aft ESS support bulkhead and adjacent skins would be affected.
5. Thermal protection system: the thermal protection system as defined for the shuttle booster is satisfactory when used for ESS mission and flying the low-q trajectories. With the maximum performance trajectory, the temperatures on the upper surface of the body would exceed design temperatures during ascent. This would require the addition of a removable carbon phenolic ablator panel for the ESS missions.

The estimated weight penalties for the above changes are as follows:

1. Body structure: 12,000 to 15,000 pounds
2. Carbon phenolic ablator: 2500 to 3000 pounds



5.2.2 Trajectory Characteristics and Flight Environment

This section describes the ascent trajectories and resulting flight environment from liftoff to termination of ESS main propulsion system operation. The three specified payloads are treated separately as required.

Nominal Trajectories

Mated System and ESS Ascent. The objective of launch trajectory design was to produce a trajectory which would minimize variations in shuttle design and would also satisfy the mission requirements. The shapes and mass distributions of the ESS and the specified payloads were found to produce higher booster attachment loads than were permitted by the booster design if the baseline shuttle rationale was used for trajectory derivation. Therefore, it was necessary to employ load reduction techniques during mated flight to minimize structural effect on the reusable booster.

As discussed earlier under "Specified Payloads," the space tug and reusable nuclear stage launches were made with off-loaded stages. Except for this, the rationale used to derive the trajectories for the three payloads was the same. Engine throttling and steering were used to reduce the dynamic pressure and the acceleration.

The trajectories are initiated with an acceleration of approximately 1.3 g's (similar to shuttle). After clearing the launch tower, the engines are throttled to a level commensurate with a liftoff acceleration of 1.2 g's. This throttle setting is maintained until passing through the maximum dynamic pressure region. The vehicle follows a nearly vertical trajectory until shortly before maximum dynamic pressure is reached. The vehicle attitude is then changed so that the angle of attack is -2 degrees through the maximum dynamic pressure region. After passing through this region, the angle of attack is changed to -8 degrees and held constant to staging. The transition from -2 degrees to -8 degrees is made subject to the constraint that the product of dynamic pressure and angle of attack not exceed 800 psf deg. After passing this region, throttling is employed to limit the acceleration to a level compatible with 50-percent throttling at booster burnout.

Following staging, the ESS follows an optimum trajectory to insertion at 66 nm (400,000 ft) into a 66-nm by 100-nm elliptical orbit. Throttling is employed to limit the acceleration to 4 g's during this portion of the flight.

Figures 5-8, 5-9, and 5-10 depict typical trajectory parameters for the space station, space tug, and reusable nuclear stage payloads respectively.

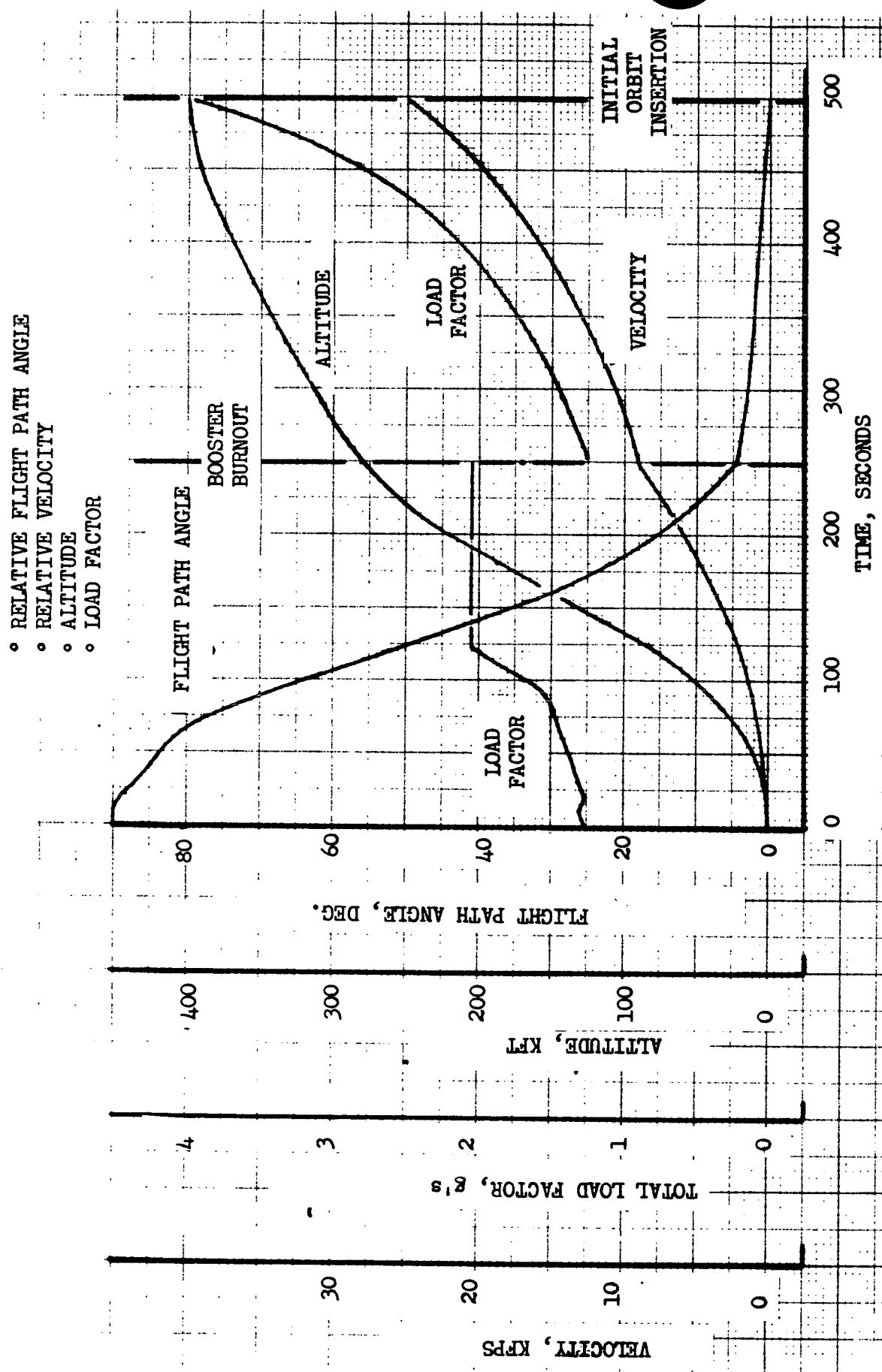


Figure 5-8. Nominal Ascent Trajectory for Space Station Payload (Sheet 1 of 2)

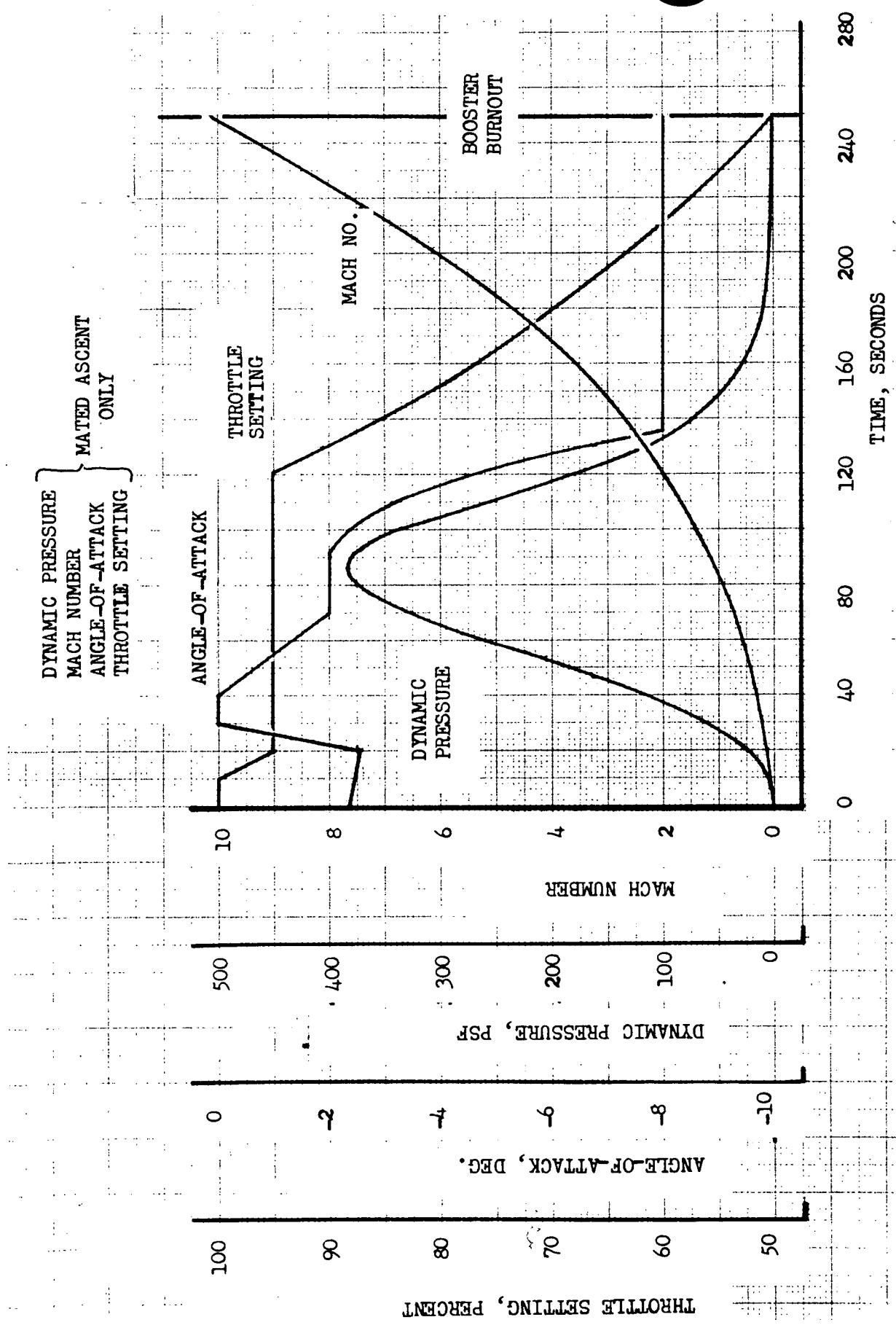


Figure 5-8. Nominal Ascent Trajectory for Space Station Payload (Sheet 2 of 2)

- RELATIVE FLIGHT PATH ANGLE
- RELATIVE VELOCITY
- ALTITUDE
- LOAD FACTOR

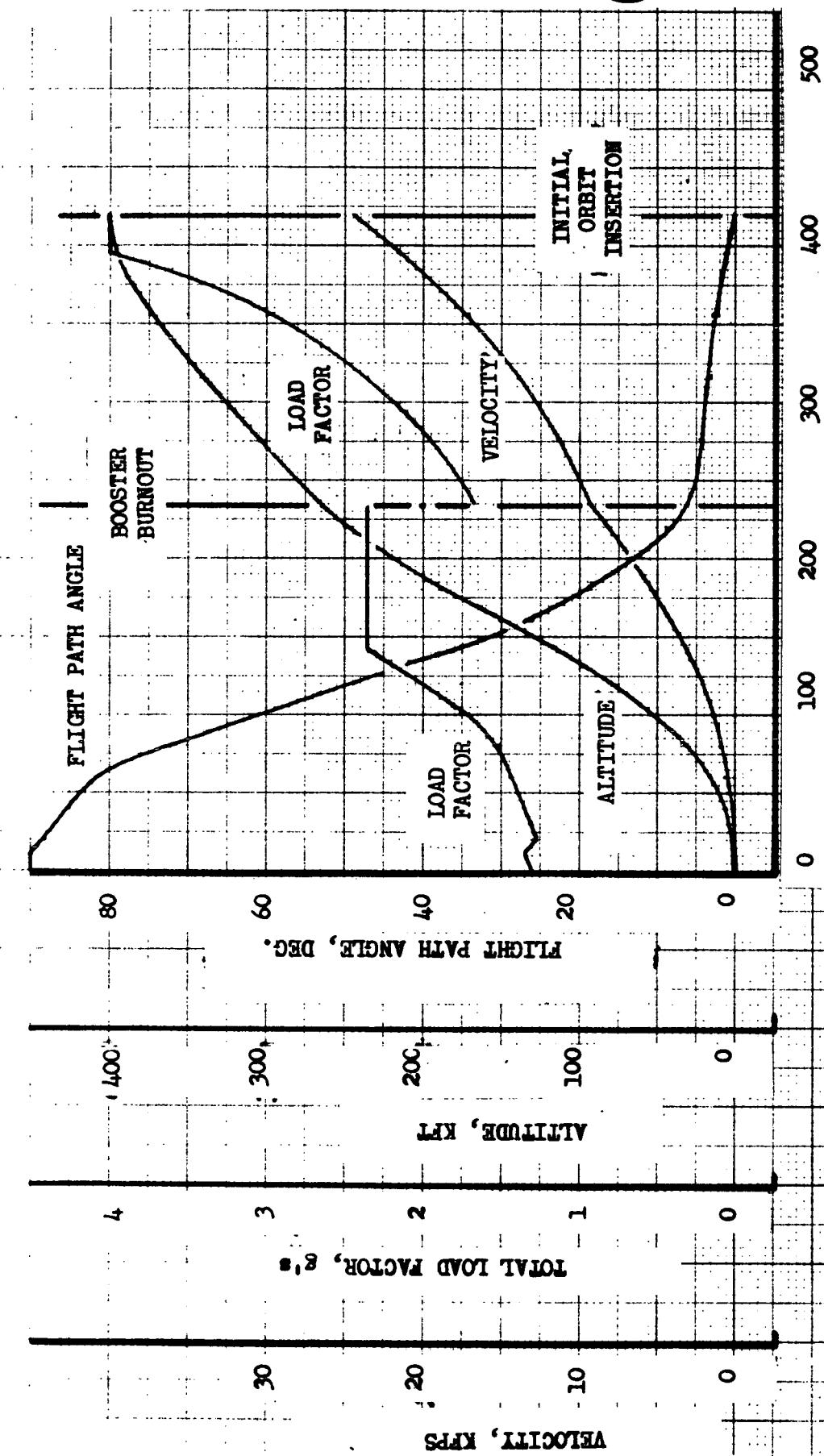


Figure 5-9. Nominal Ascent Trajectory for Space Tug Payload (Sheet 1 of 2)

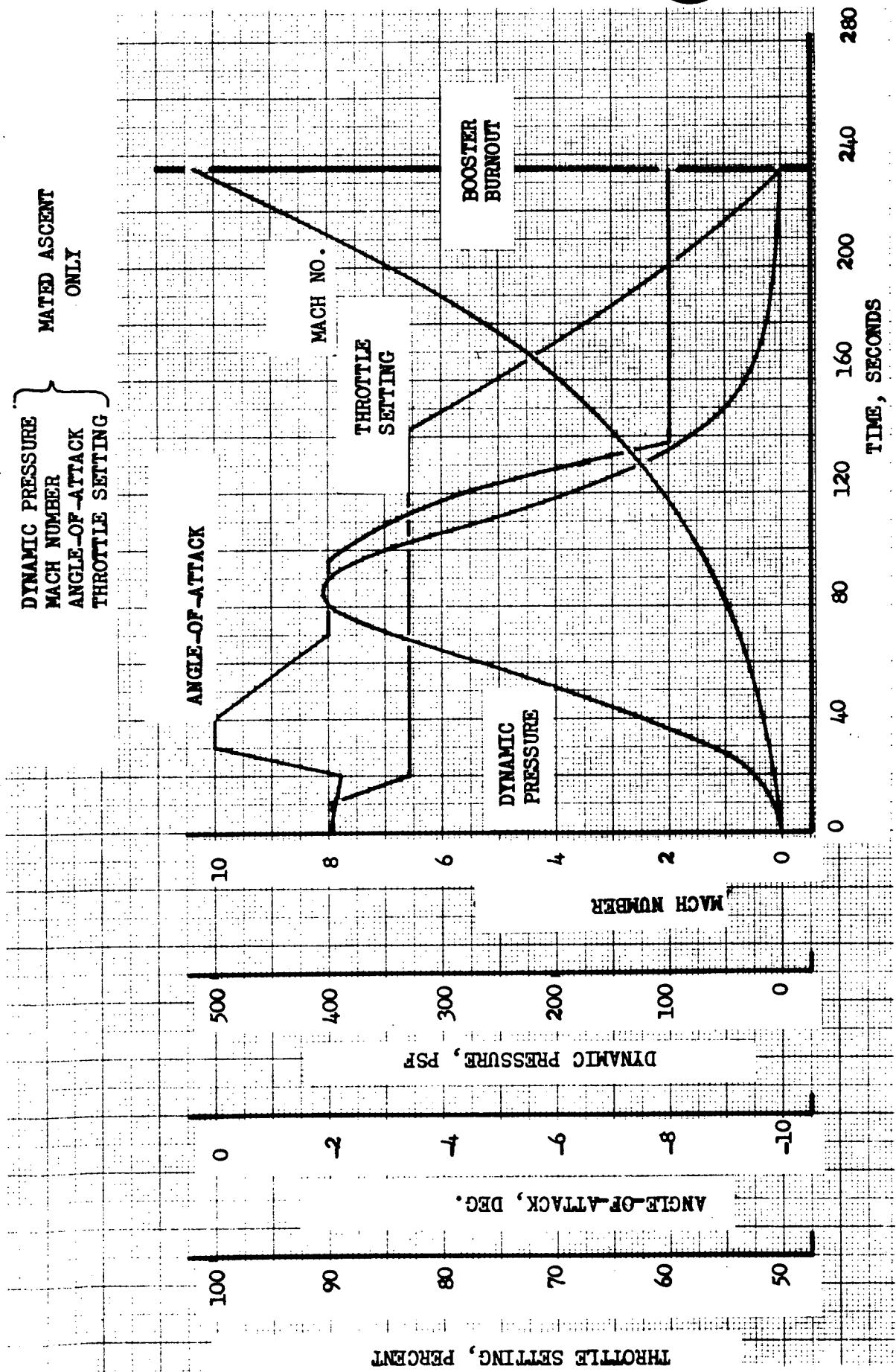


Figure 5-9. Nominal Ascent Trajectory for Space Tug Payload (Sheet 2 of 2)

- RELATIVE FLIGHT PATH ANGLE
- RELATIVE VELOCITY
- ALTITUDE
- LOAD FACTOR

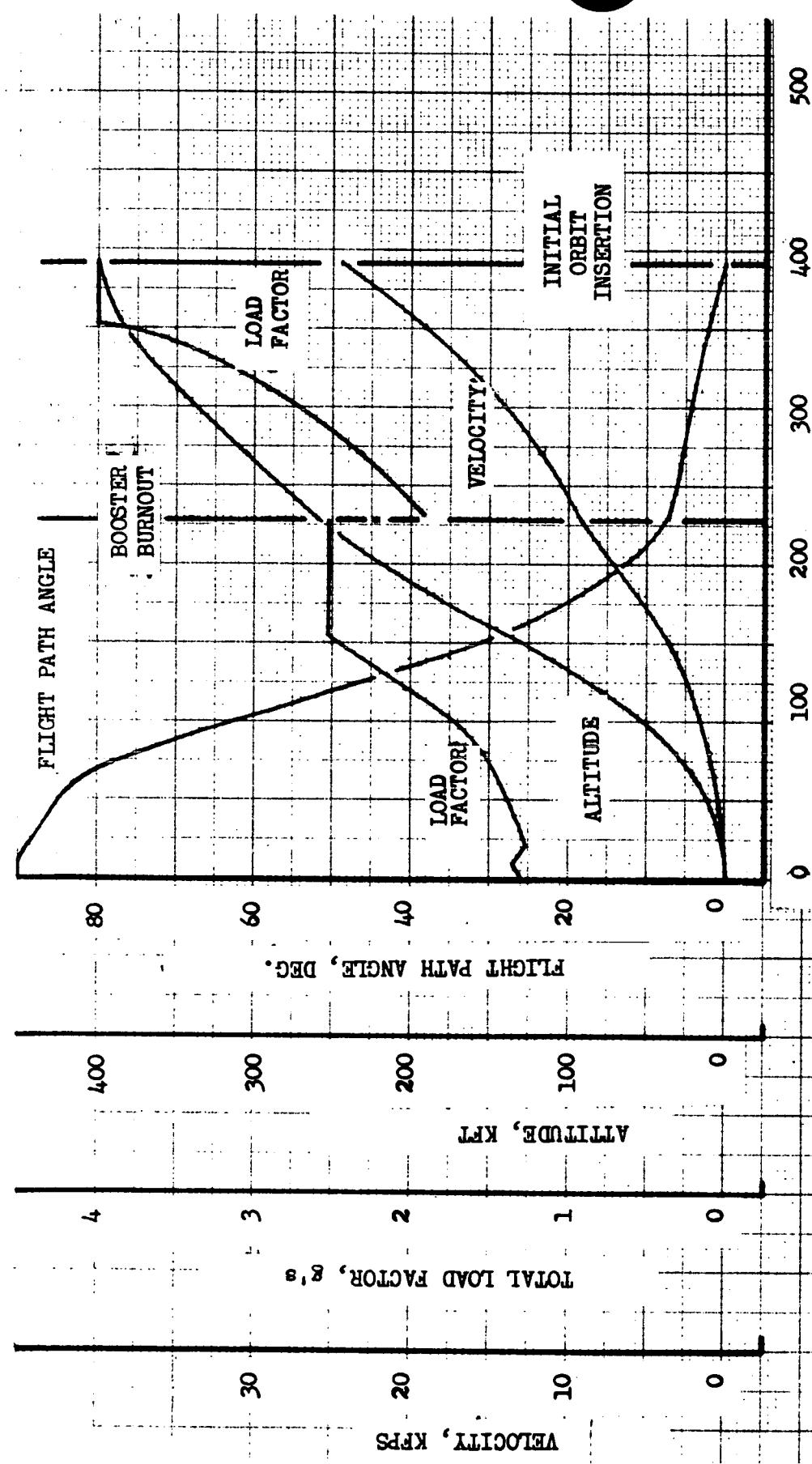


Figure 5-10. Nominal Ascent Trajectory for RNS Payload (Sheet 1 of 2)

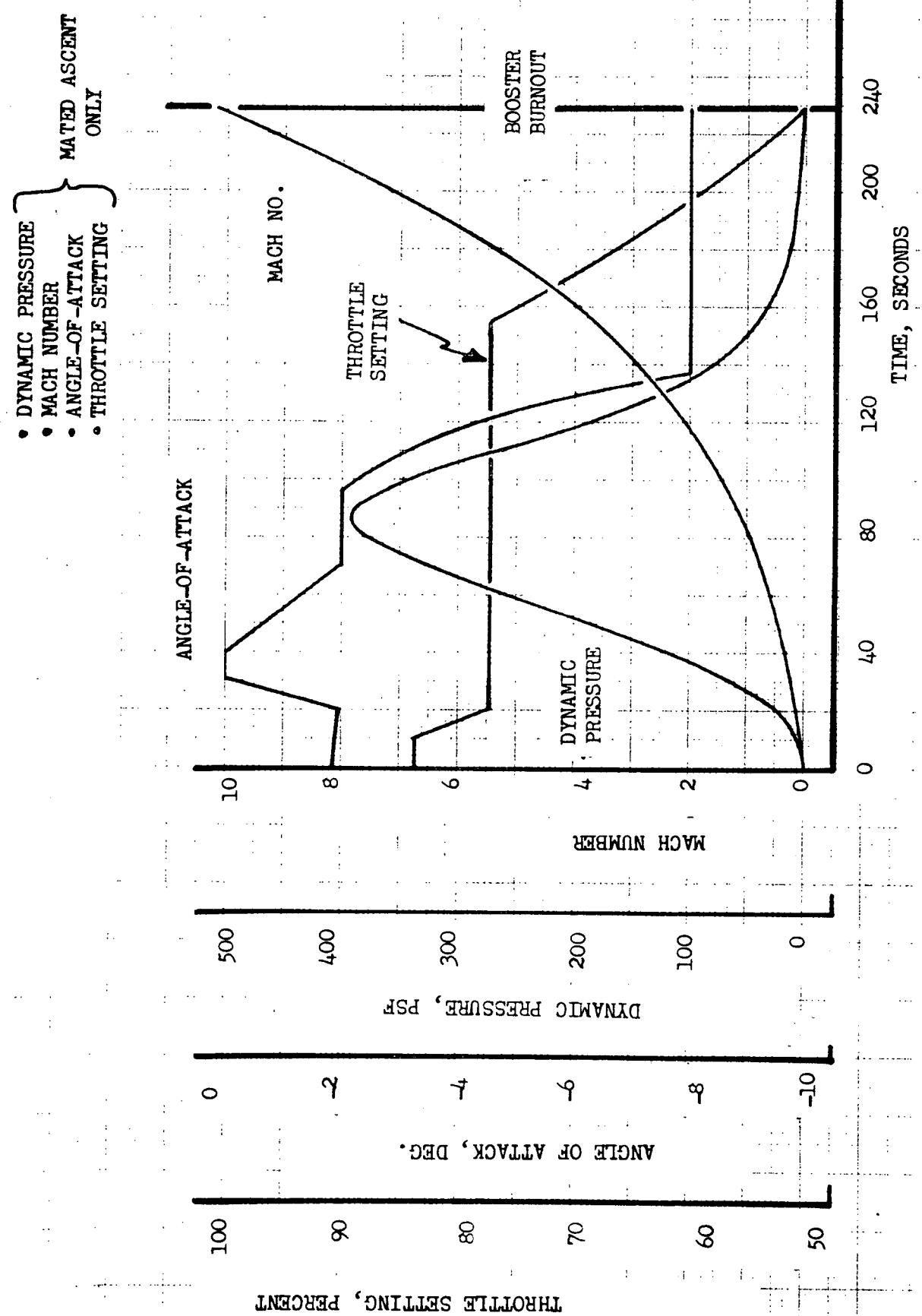


Figure 5-10. Nominal Ascent Trajectory for RNS Payload (Sheet 2 of 2)



It is noted that the above discussion and results are based on a trajectory/performance iteration conducted after the bulk of the design analyses were completed. The design analyses were based on an earlier set of trajectories (Appendix TBD) which were derived from a slightly different rationale. The variations in vehicle design factors due to small differences in the trajectories are believed to be negligible.

Separation Operational Sequence. Booster and ESS thrust scheduling is sequenced with relation to release of the disconnects. A signal from the booster LO₂ depletion sensor initiates—as in the baseline system—throttling of booster engines to 50-percent thrust, and concurrently, the ESS engines are started. However, the rate of change of booster thrust prior to the 50 percent thrust throttle ratio will be small since the booster thrust levels are limited to values slightly greater than 50 percent during the final boost phase. When the ESS engines are at 50-percent thrust, the explosive bolts in the four vertical links are fired, thus releasing vertical restraint on the ESS. At the same time, the expansion compensator in the forward rotating frame is caused to lock, and 0.10 second later, booster engine cutoff occurs. After the vertical links are broken, the booster accelerates longitudinally relative to the ESS. When this occurs, the rotating links provide the transverse ESS acceleration. After a 0.75-second delay, the explosive bolts restraining the ESS to the rotating links are fired, freeing the ESS from the booster. Immediately upon ESS release, the snubber/retractor actuators are activated to return and lock the rotating links to their faired positions. In addition, the aft link members are drawn inward by actuators.

The control of all sequencing functions necessary for accomplishing separation and maintaining control of both the ESS and booster is accomplished by software in the main computer. This includes thrust scheduling, release timing, link retraction, guidance, engine gimbaling, and attitude control propulsion system (ACPS).

Typical separation trajectories are shown in Figures 5-11 through 5-17, and a detailed description of the separation subsystem is given in Book 3, Booster/ESS Separation Subsystem.

Booster Entry and Flyback. Booster entry trajectories for three ESS configurations (nuclear stage, space tug, and space station) have been generated and are described in this section.

The booster entry mode is a supersonic gradual transition. The angle-of-attack characteristics of this type of entry are shown as a function of Mach Number, along with the entry corridor, in Figure 5-18. Pitch and bank angle scheduling are used to minimize the flyback distance to the landing site with a 4.0-g load factor constraint.

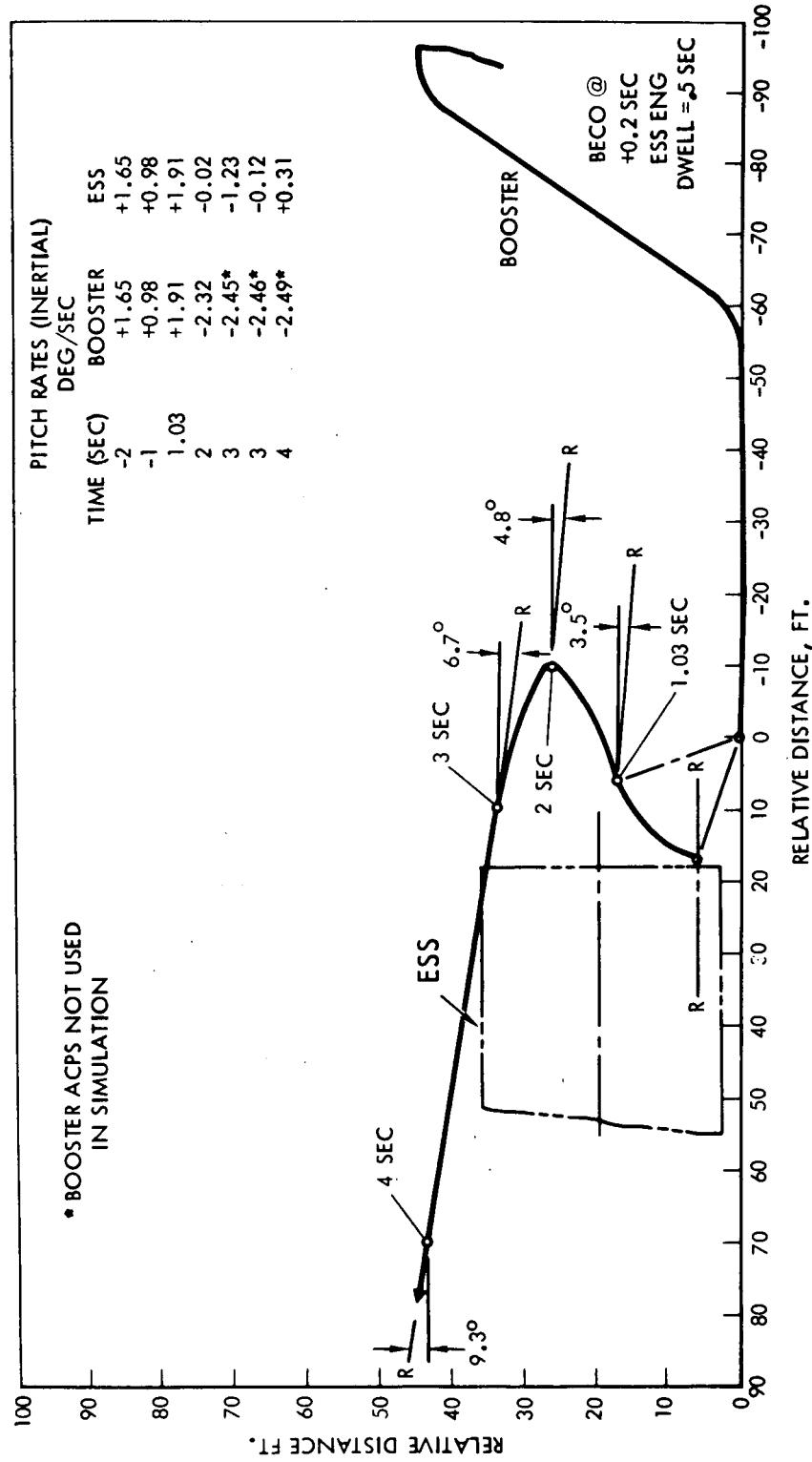


Figure 5-11. Separation Trajectory-Staging of ESS With MDAC Space Station Payload
(Two ESS Engines Operative-BECO at 0.2 Second)

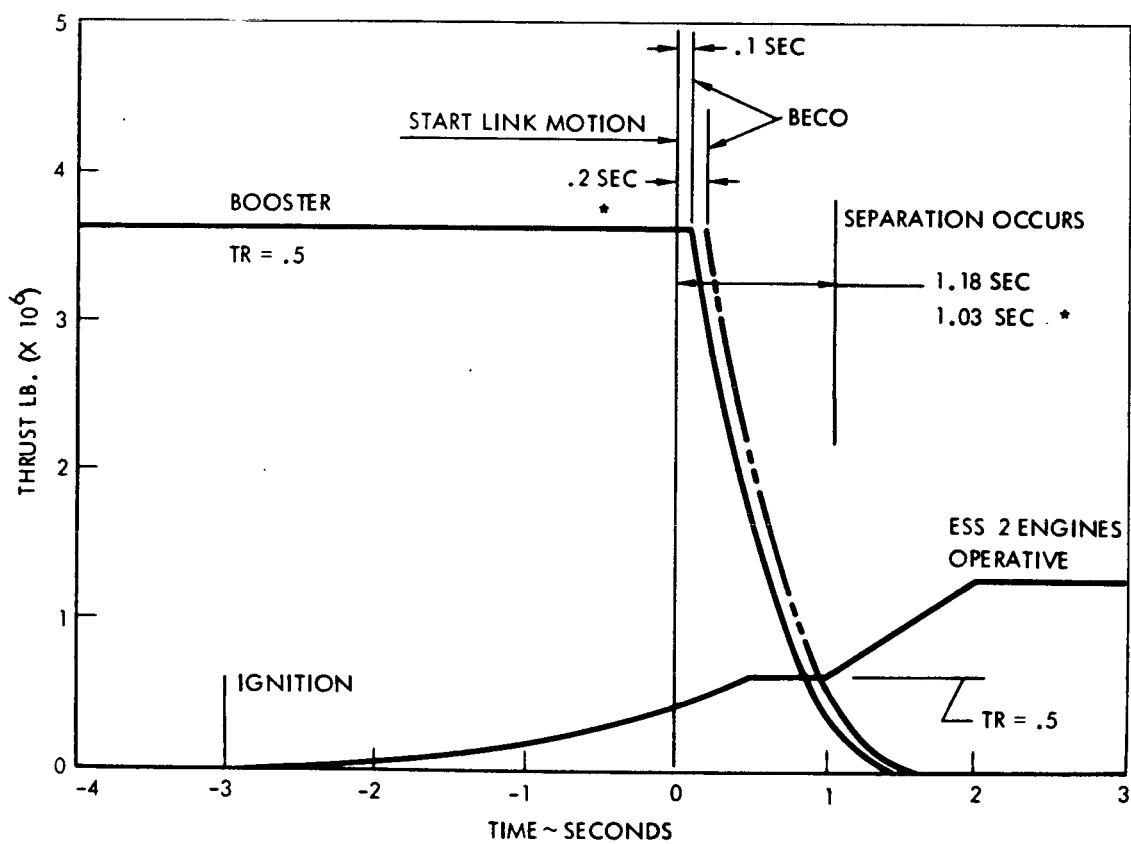


Figure 5-12. Thrust Scheduling, Normal Staging of ESS With MDAC Space Station Payload

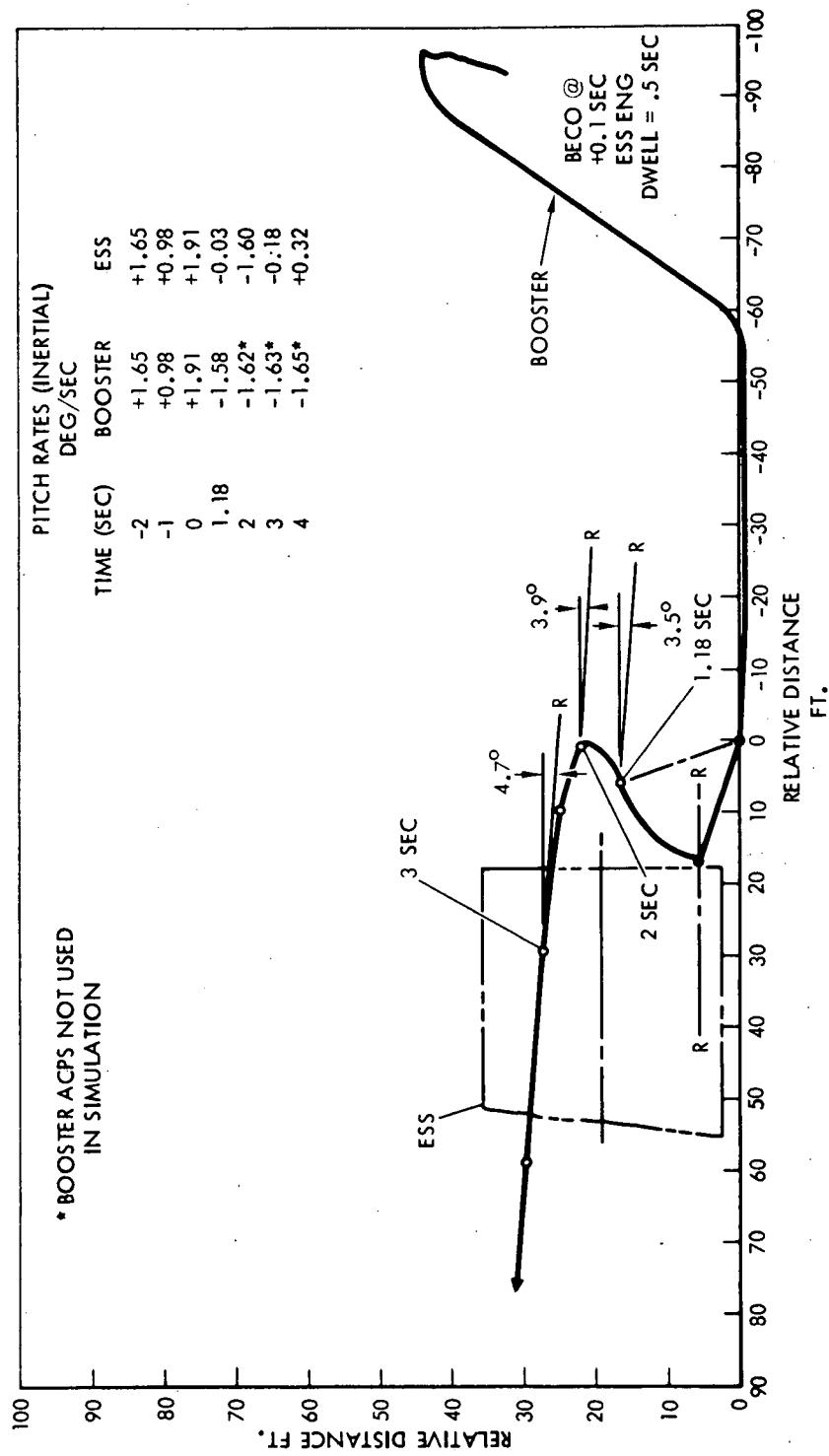


Figure 5-13. Separation Trajectory, Staging of ESS With MDAC Space Station Payload (Two ESS Engines Operative)

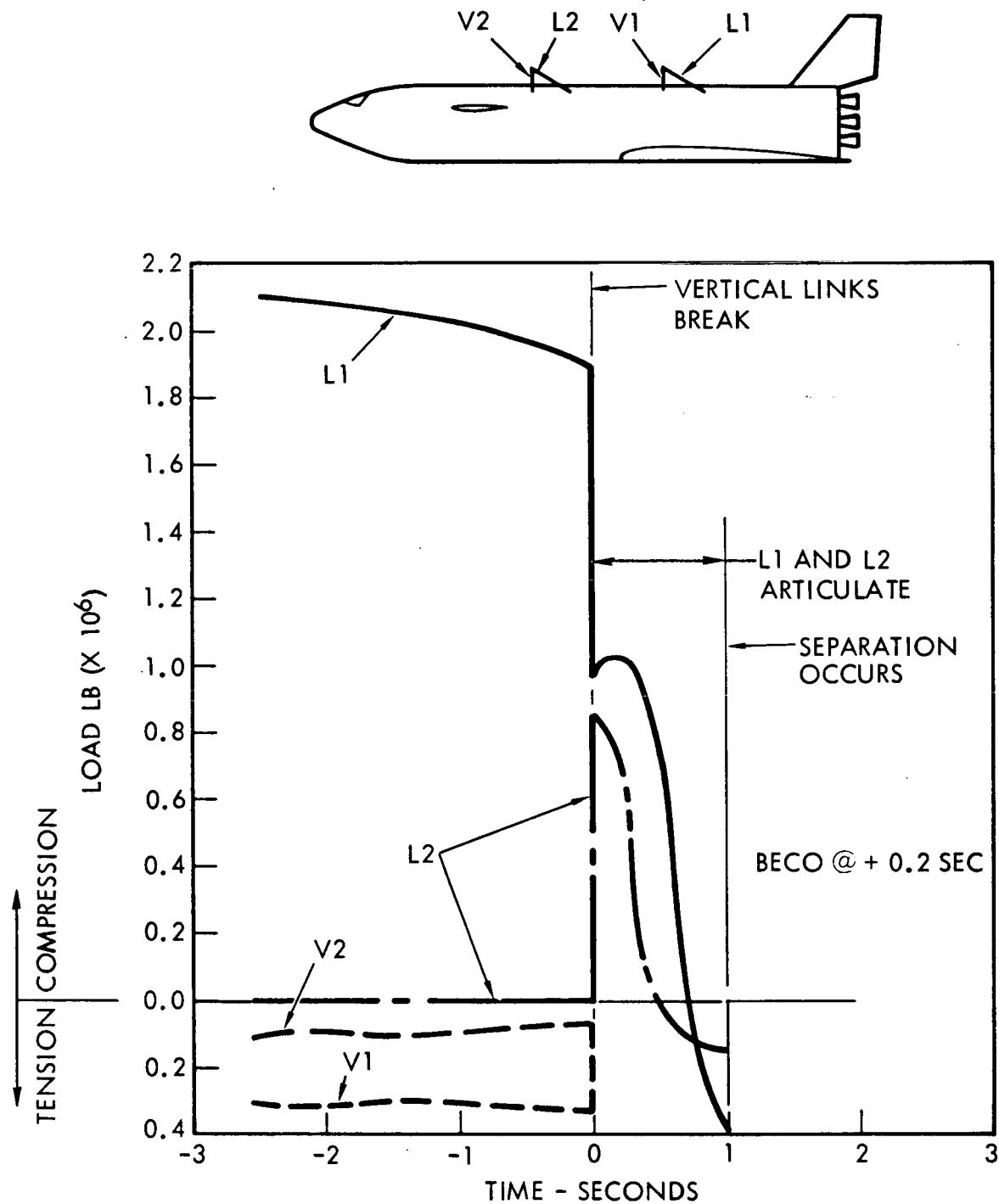


Figure 5-14. Separation System Link Loads, Normal Staging of ESS With MDAC Space Station Payload (BECO at 0.2 Second)

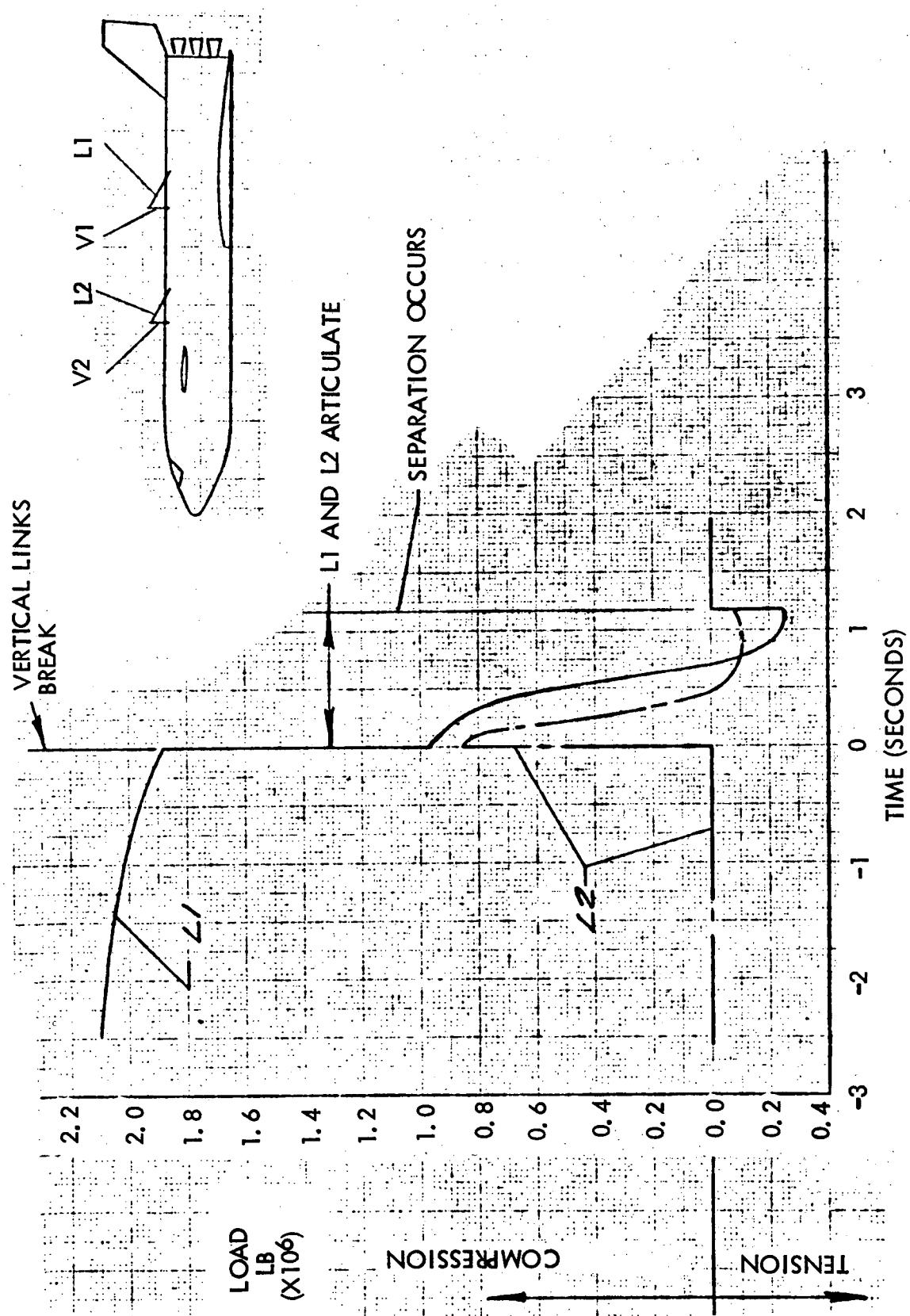


Figure 5-15. Separation System Link Loads, Normal Staging of ESS with MDAC
Space Station Payload (BECO at 0.1 Second)

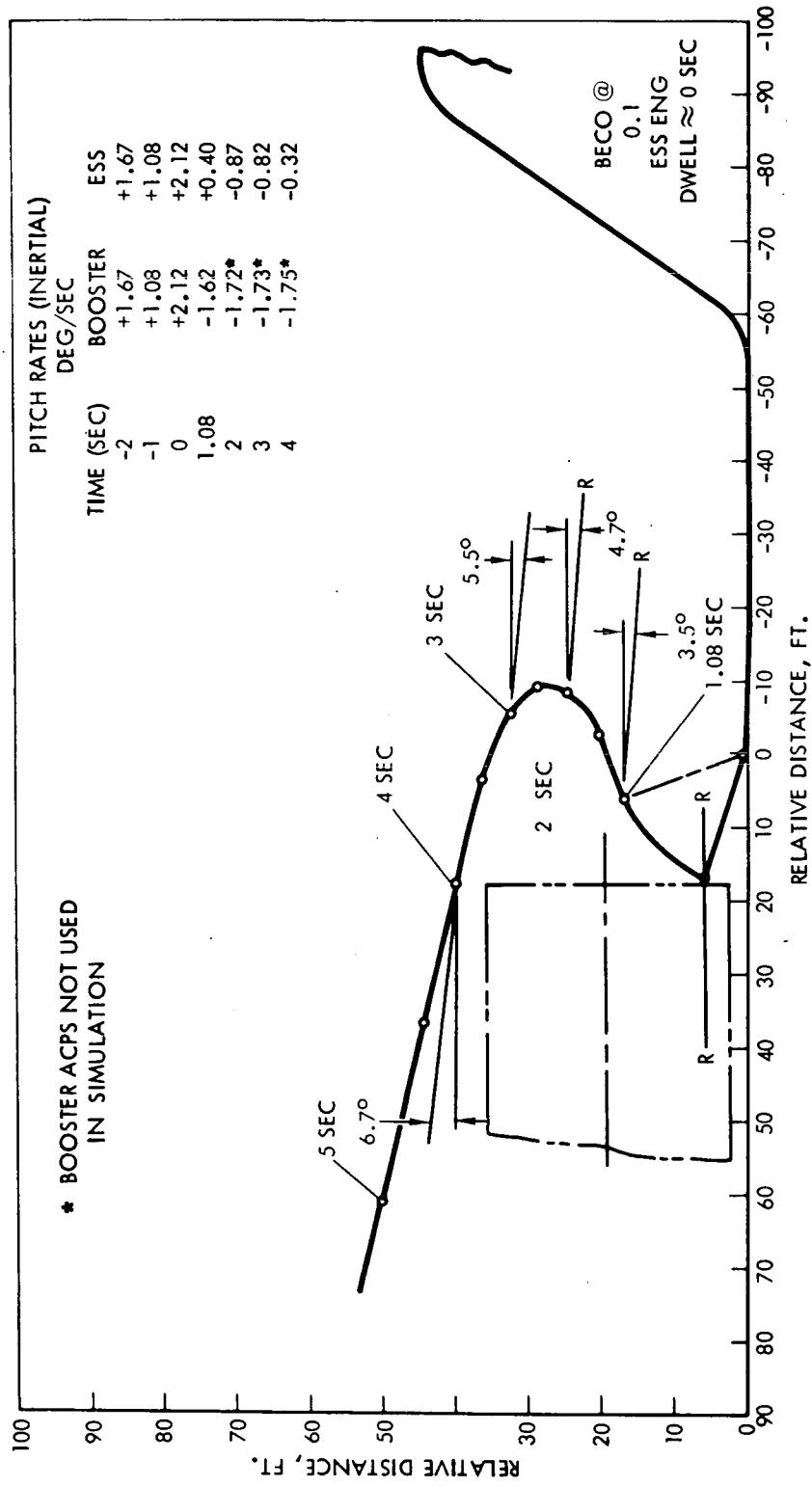


Figure 5-16. Separation Trajectory, Staging of ESS With MDAC Space Station Payload (One ESS Engine Operative).

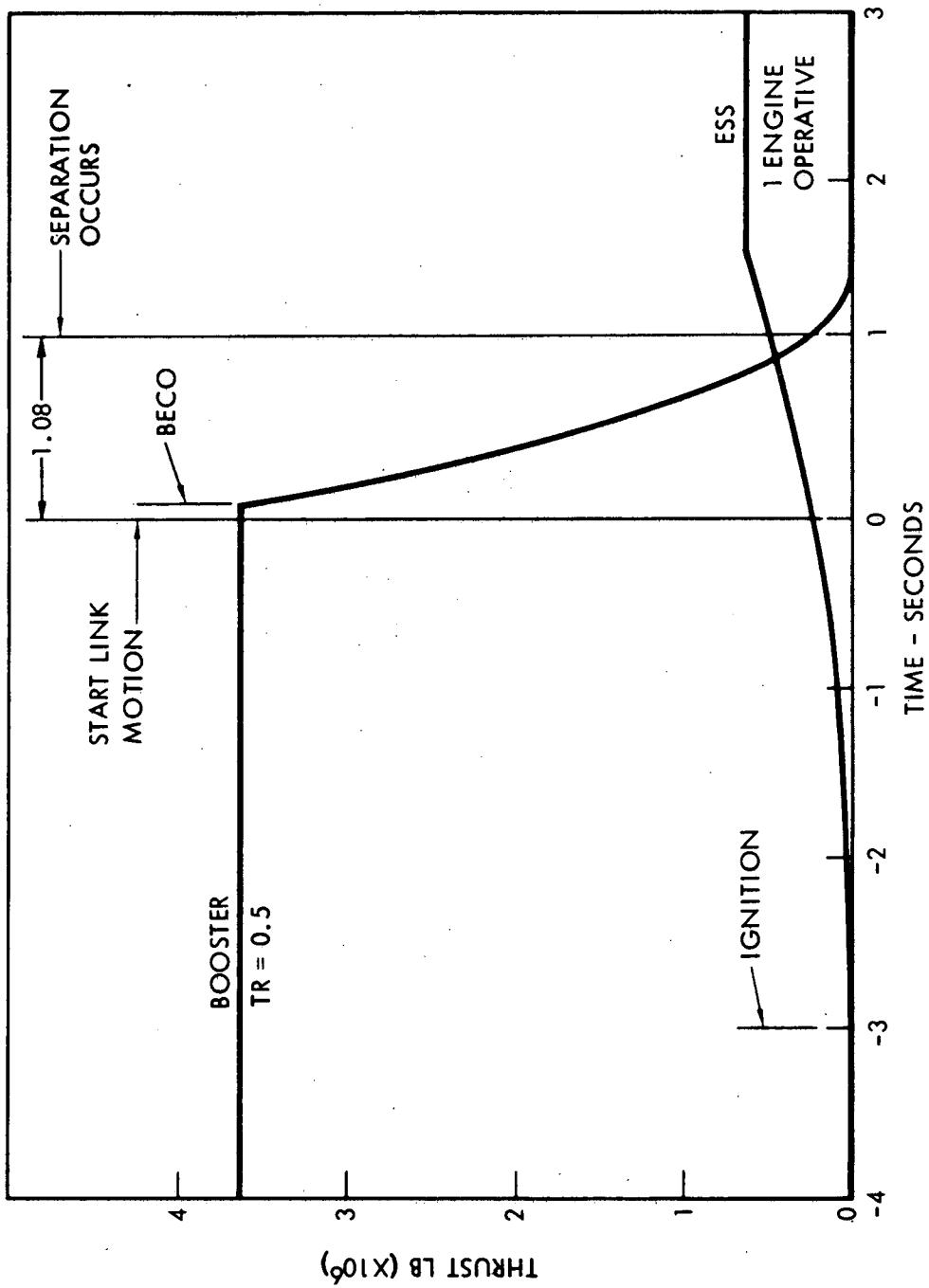


Figure 5-17. Thrust Scheduling, Staging of ESS With MDAC Space Station Payload
(One ESS Engine Operative)

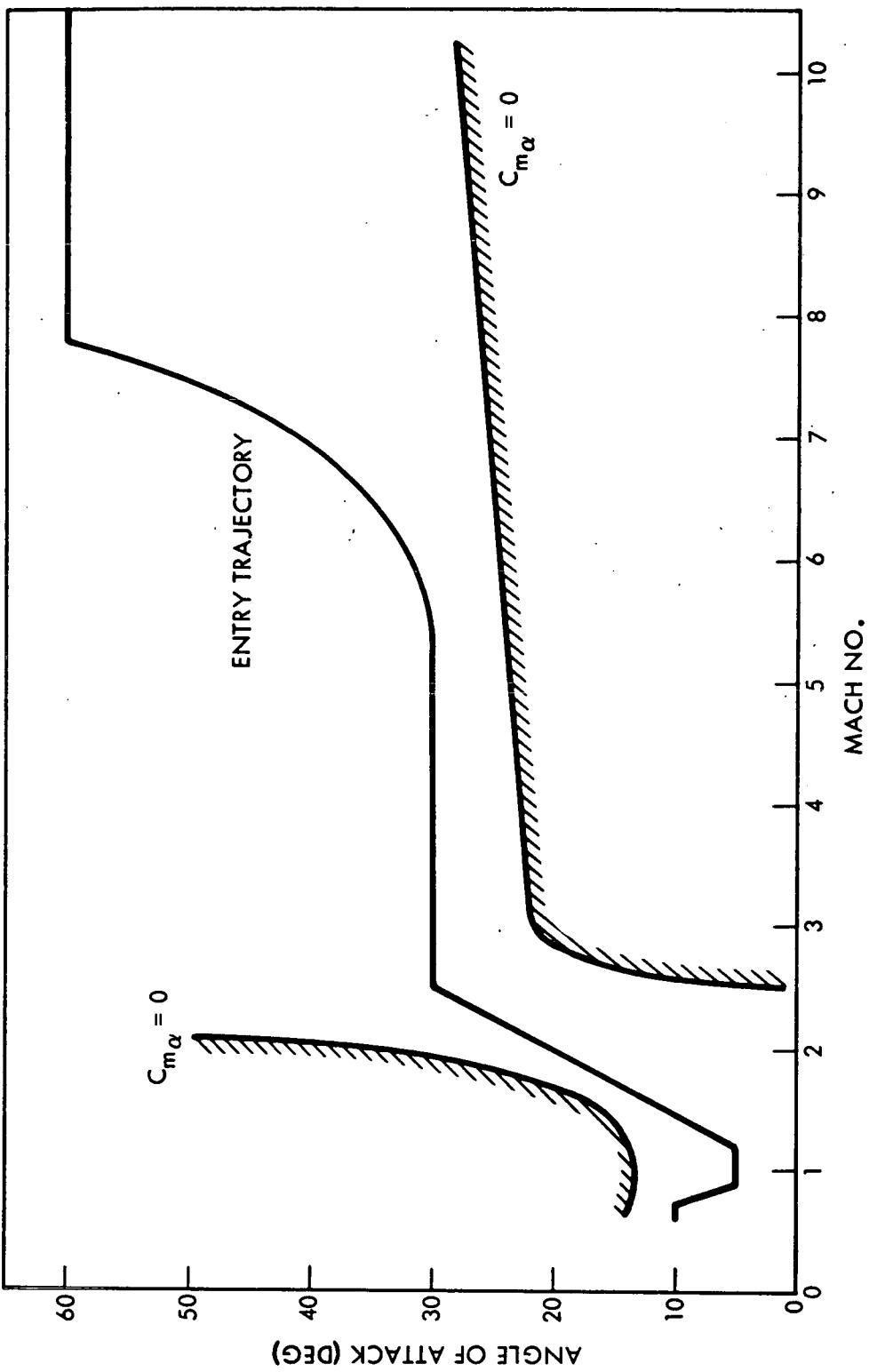


Figure 5-18. Booster Entry Profile and Entry Corridor



The staging conditions for the three ESS missions (and the space shuttle polar orbit mission) are:

Configuration	Velocity (fps)	Altitude (ft)	Gamma (deg)	Range (nm)
Nuclear stage	8048	251,695	10.8	72.7
Space tug	10,059	251,529	3.3	113.7
Space station	9044	278,509	4.7	110.7
(Space shuttle)	(10,824)	(244,784)	(5.6)	(116.1)

Following staging, the booster pitches to 60 degree angle of attack and banks to a specified bank angle. This attitude is maintained until a load factor of 4.0 g's is reached. Starting at this point, the angle of attack is modulated downwards so that 4.0 g's is not exceeded. The bank angle is chosen so that the lowest angle of attack during this pitch modulation maneuver is limited to 30 degrees. A peak dynamic pressure occurs at this point. The bank angle is then increased to 75 degrees and held there until the vehicle has completed a 180 degree turnaround. Angle of attack is held at 30 degrees until Mach 2.5 when the booster starts to pitch down for its passage through the transonic regime. The entry phase is considered terminated when the 20,000-ft altitude level is reached. At that point the flyback distance to the landing site is measured. Time histories of significant flight conditions during booster entry for the nuclear stage, space tug, and space station configurations are shown in Figures 5-19, 5-20, and 5-21, respectively.

The additional frontal area due to the installation of the structural separation/mating adapter will increase the cruise drag of the B-9U booster, thereby increasing the rate of fuel consumption during flyback cruise. This additional drag lowers the B-9U cruise lift-to-drag ratio from 5.80 to 5.47 as Figure 5-22 indicates. With no change in fuel capacity, it is determined that the additional drag caused increased fuel consumption that will reduce the flyback capability approximately 22 nm. The entry trajectories for the ESS and the various payloads all result in flyback distance requirements that are significantly less than those for shuttle, as shown below. The added drag, therefore, does not penalize the ESS mission.

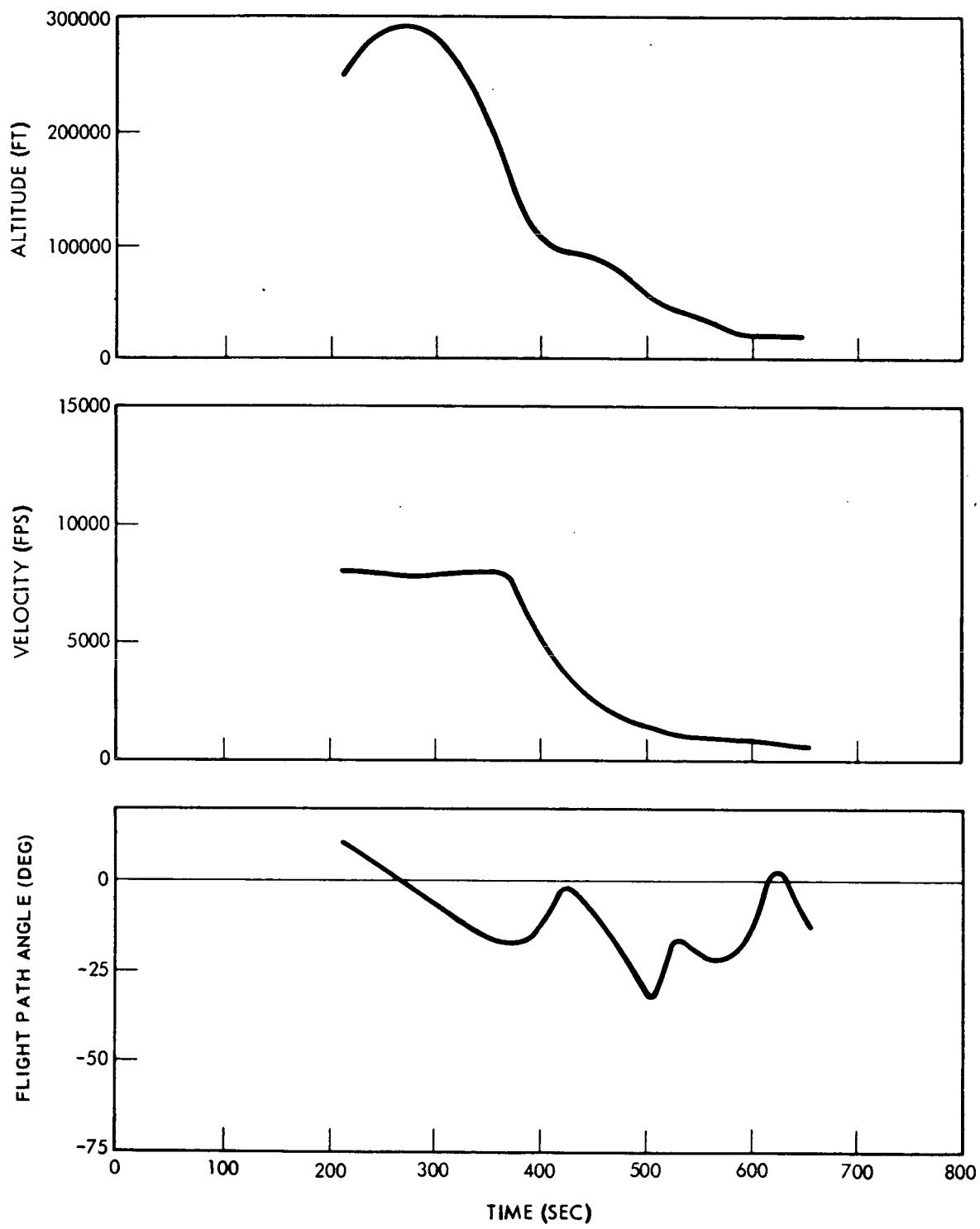


Figure 5-19. Booster Entry, RNS Payload Mission (Sheet 1 of 5)

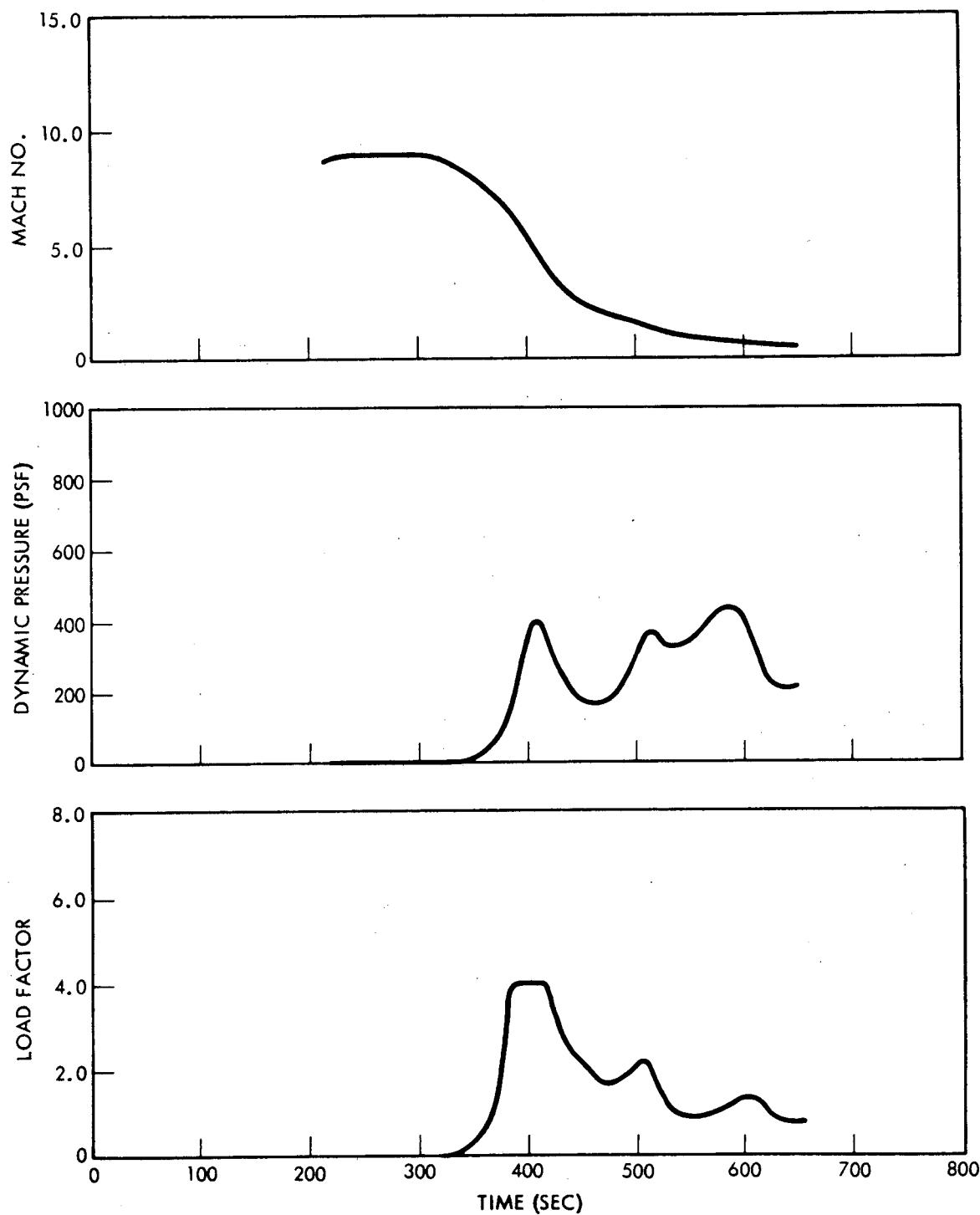


Figure 5-19. Booster Entry, RNS Payload Mission (Sheet 2 of 5)

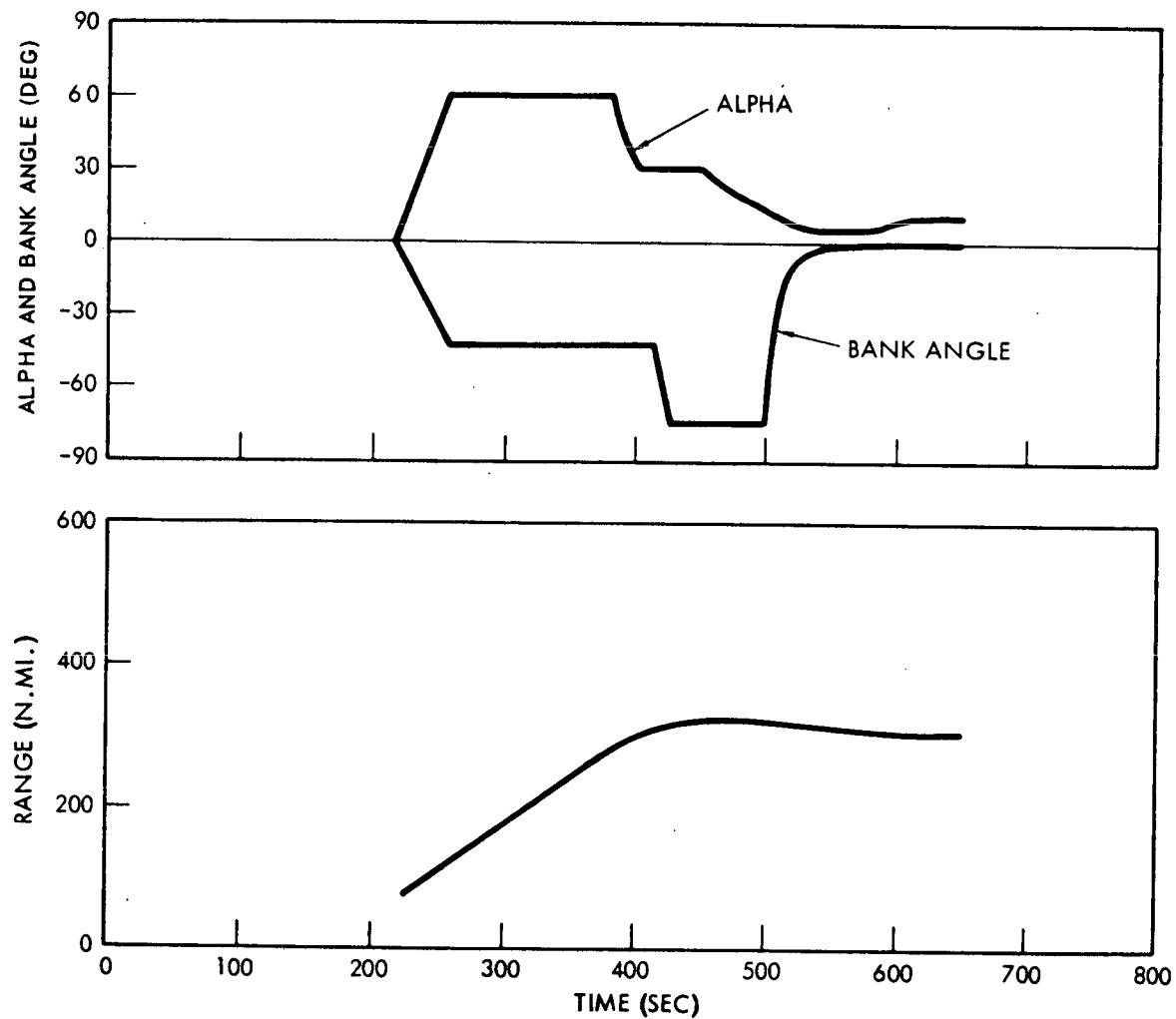


Figure 5-19. Booster Entry, RNS Payload Mission (Sheet 3 of 5)

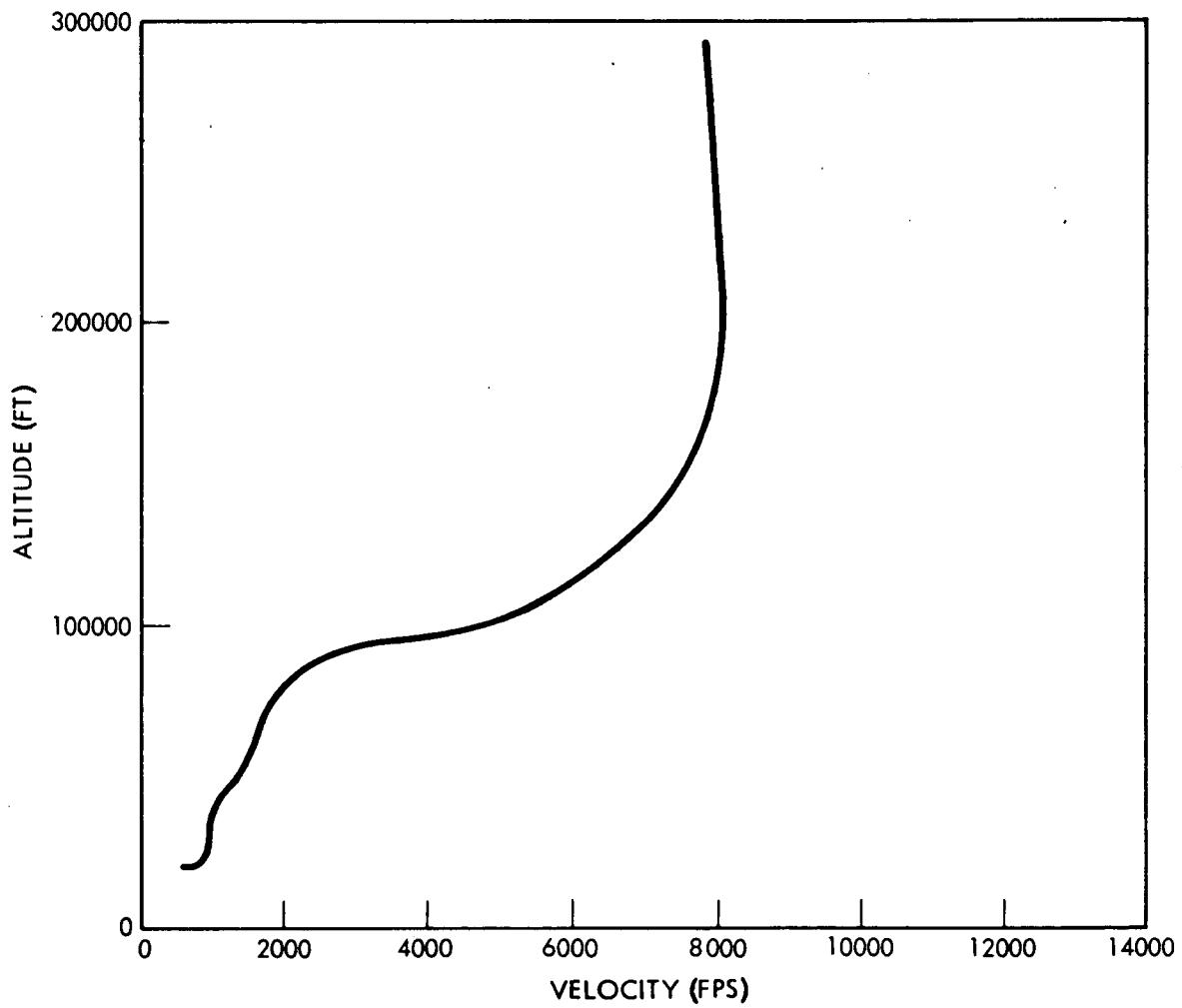


Figure 5-19. Booster Entry, RNS Payload Mission (Sheet 4 of 5)

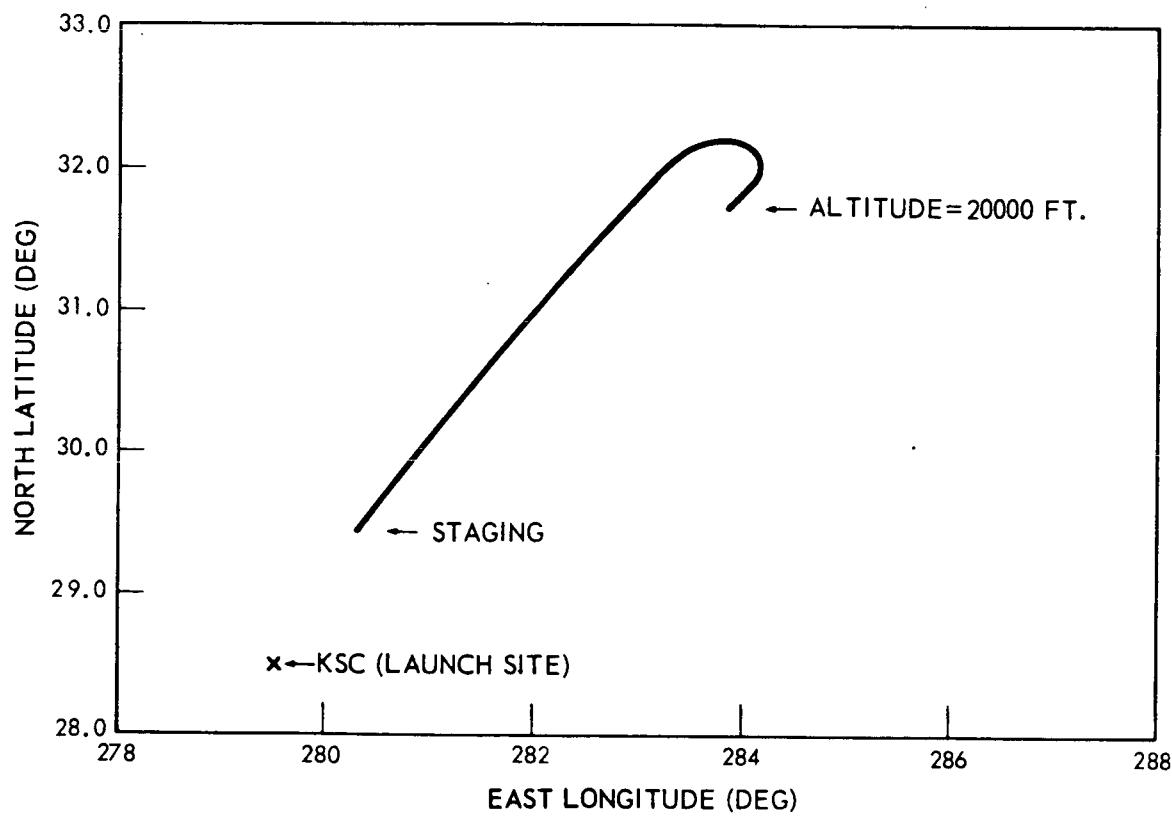


Figure 5-19. Booster Entry, RNS Payload Mission (Sheet 5 of 5)

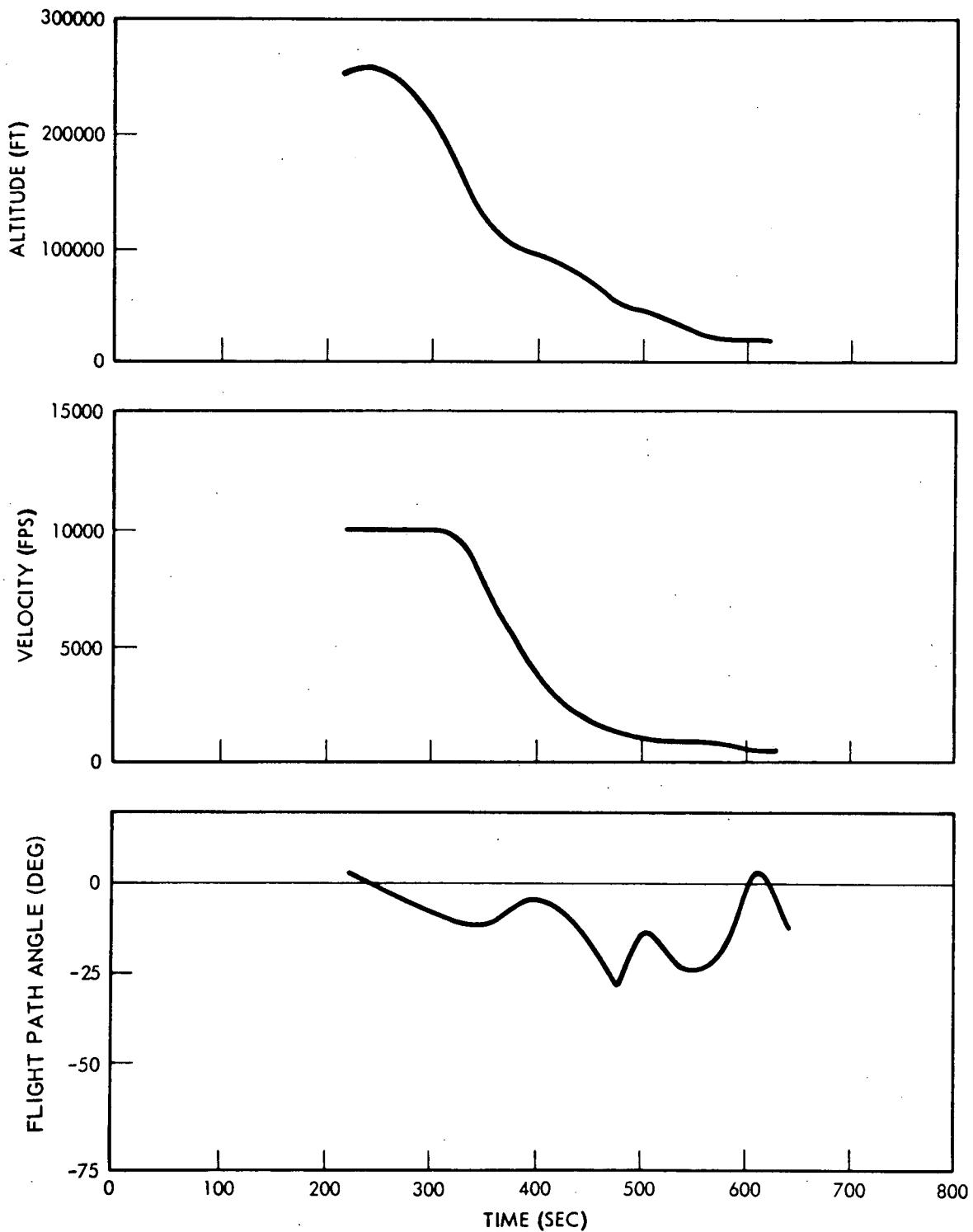


Figure 5-20. Booster Entry, Space Tug Payload Mission (Sheet 1 of 5)

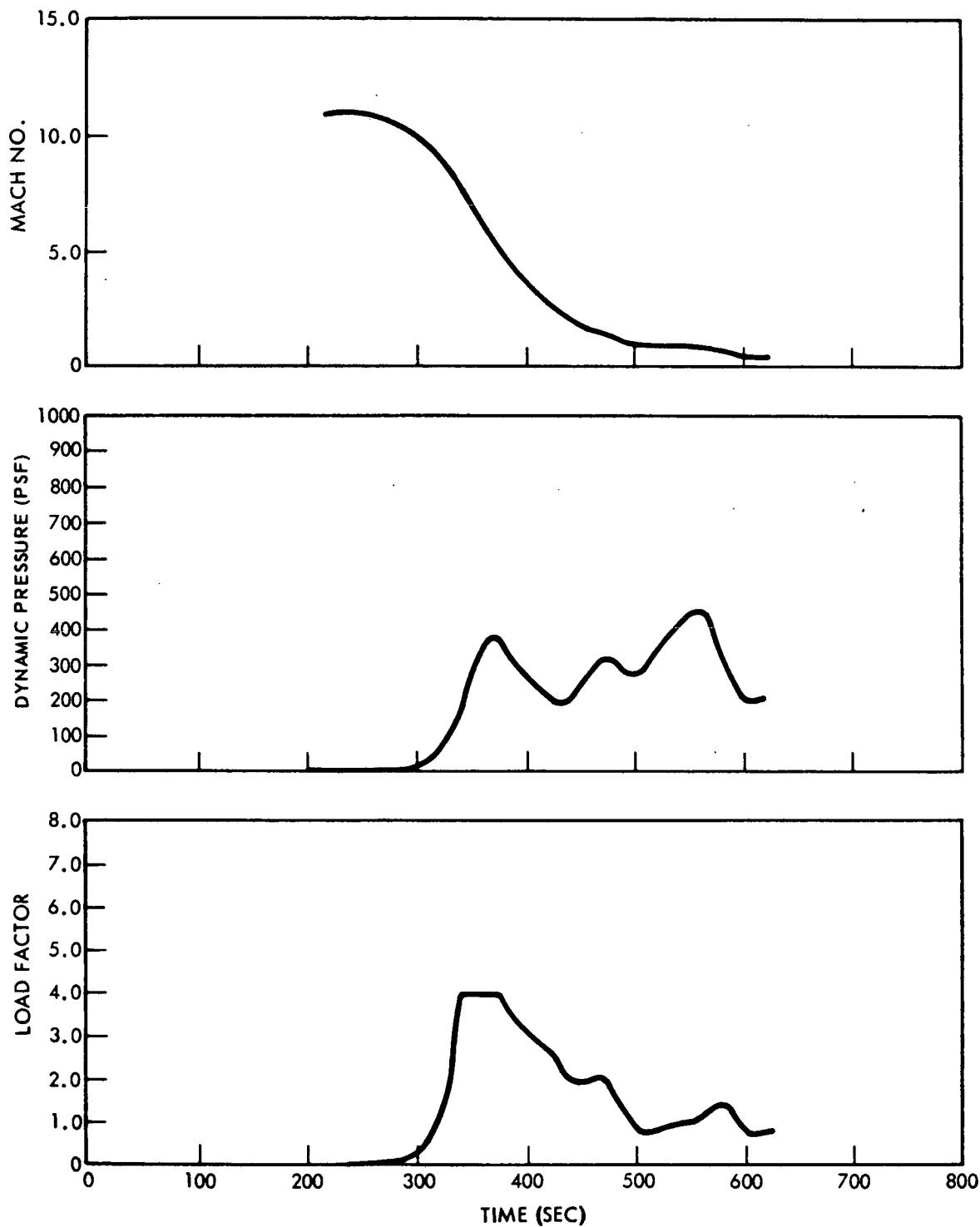


Figure 5-20. Booster Entry, Space Tug Payload Mission (Sheet 2 of 5)

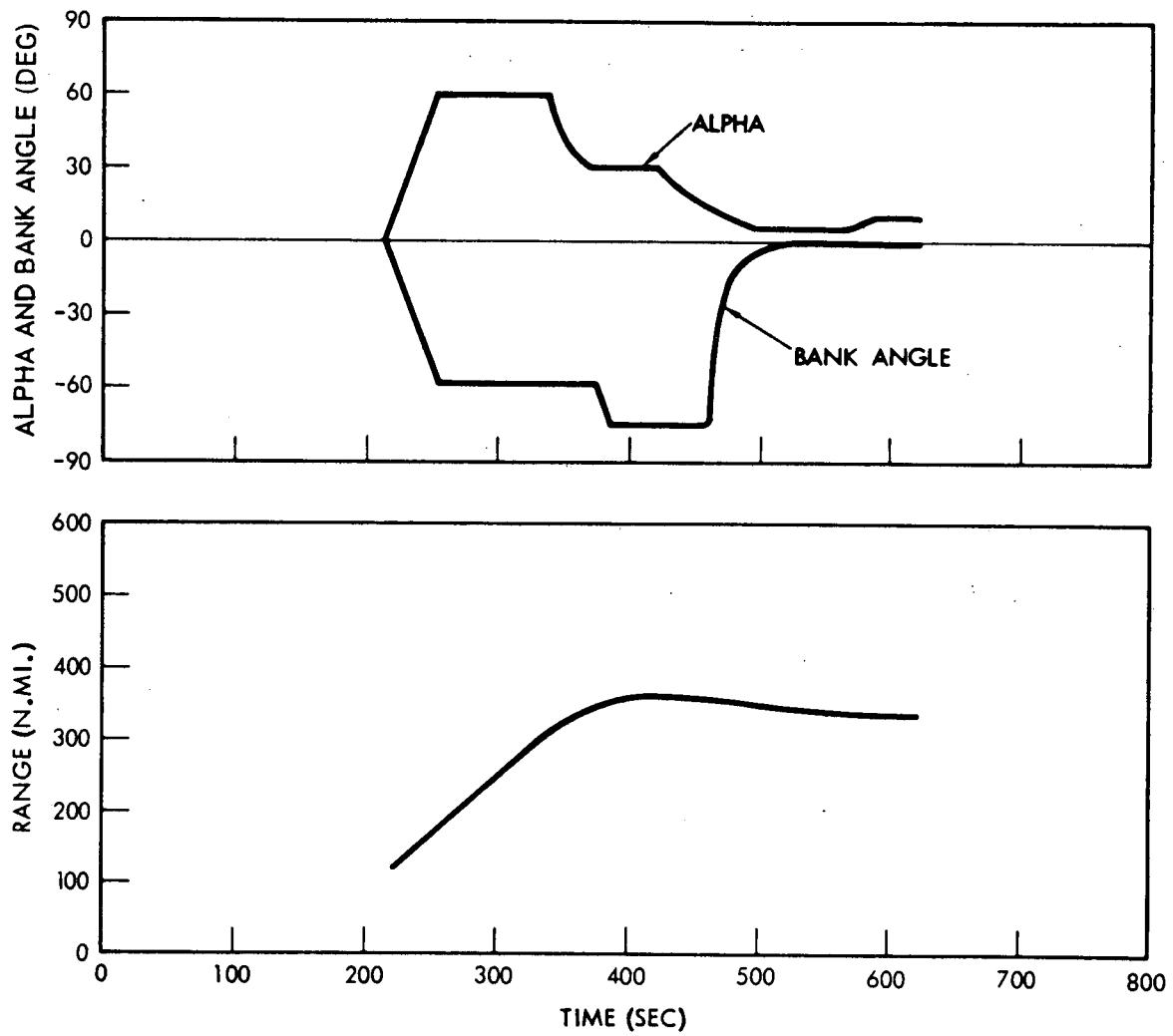


Figure 5-20. Booster Entry, Space Tug Payload Mission (Sheet 3 of 5)

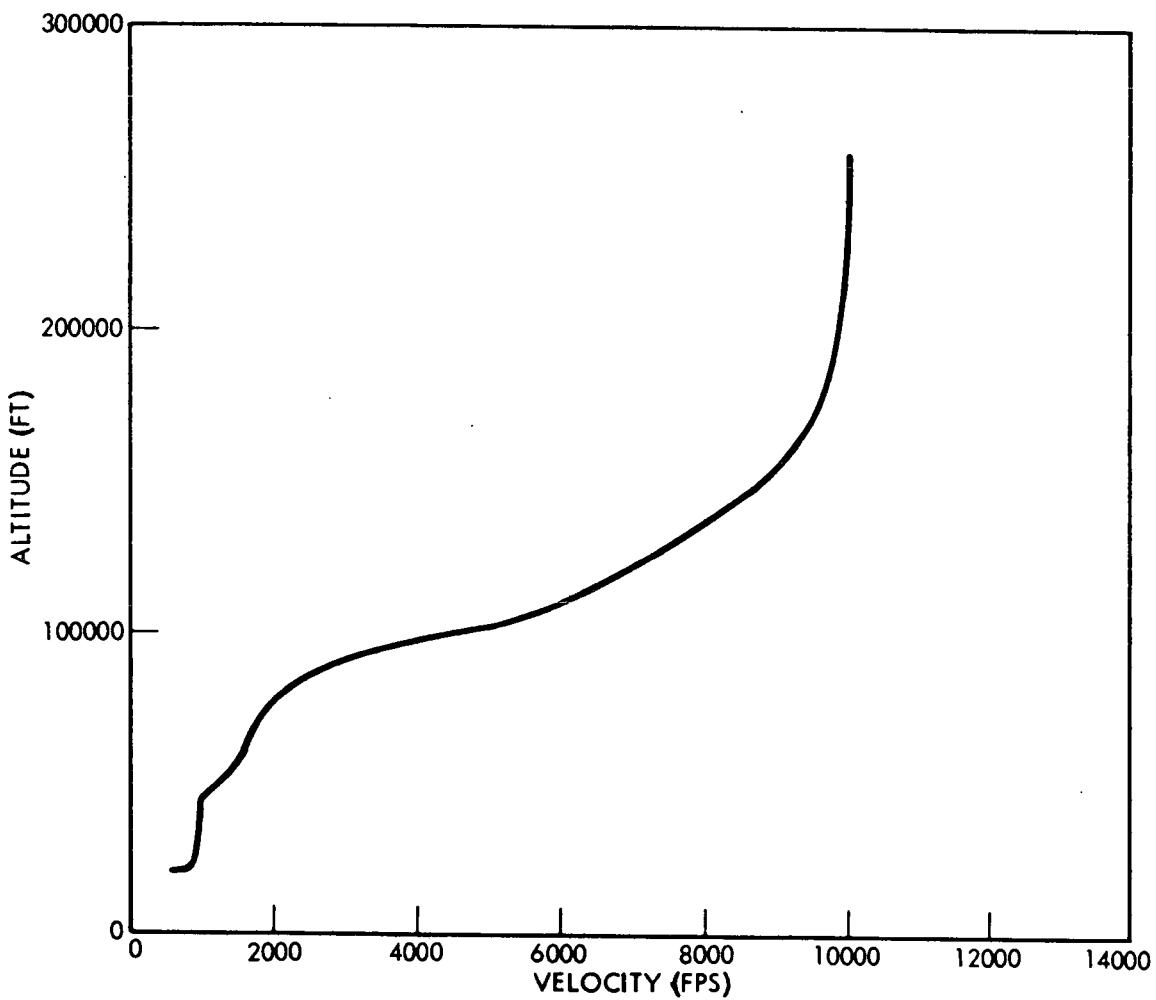


Figure 5-20. Booster Entry, Space Tug Payload Mission (Sheet 4 of 5)

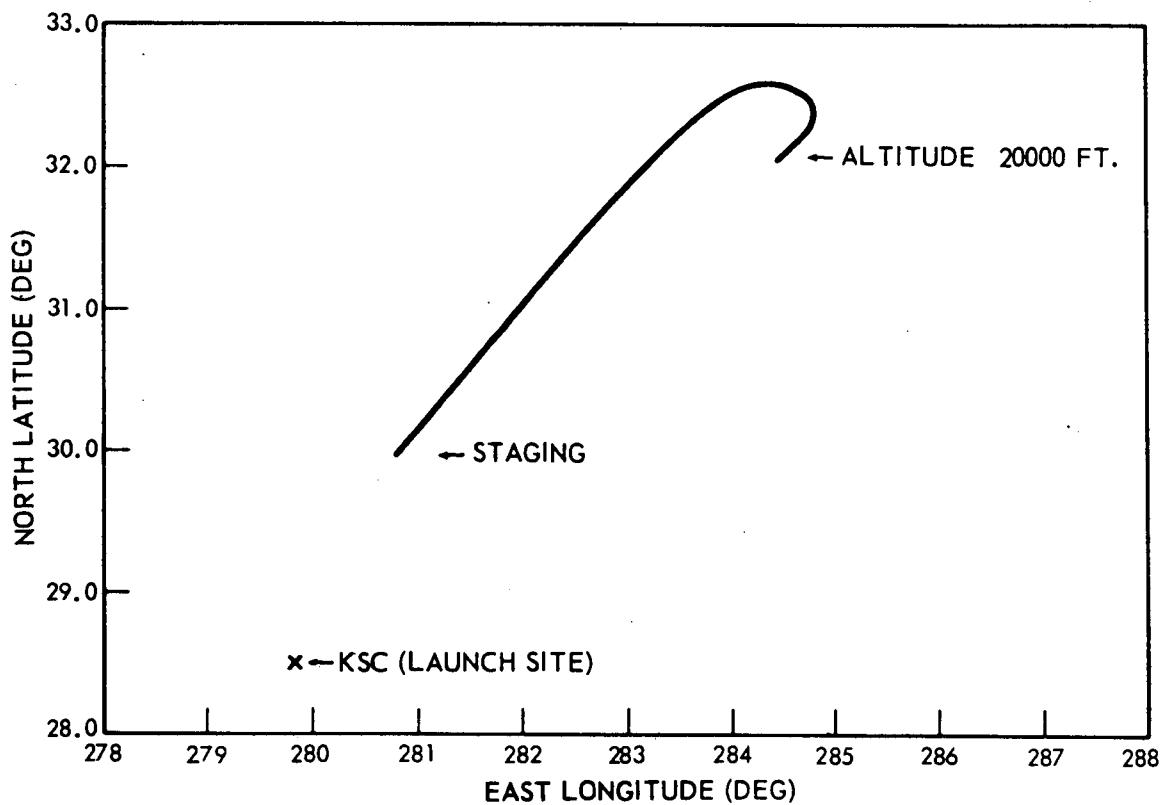


Figure 5-20. Booster Entry, Space Tug Payload Mission (Sheet 5 of 5)

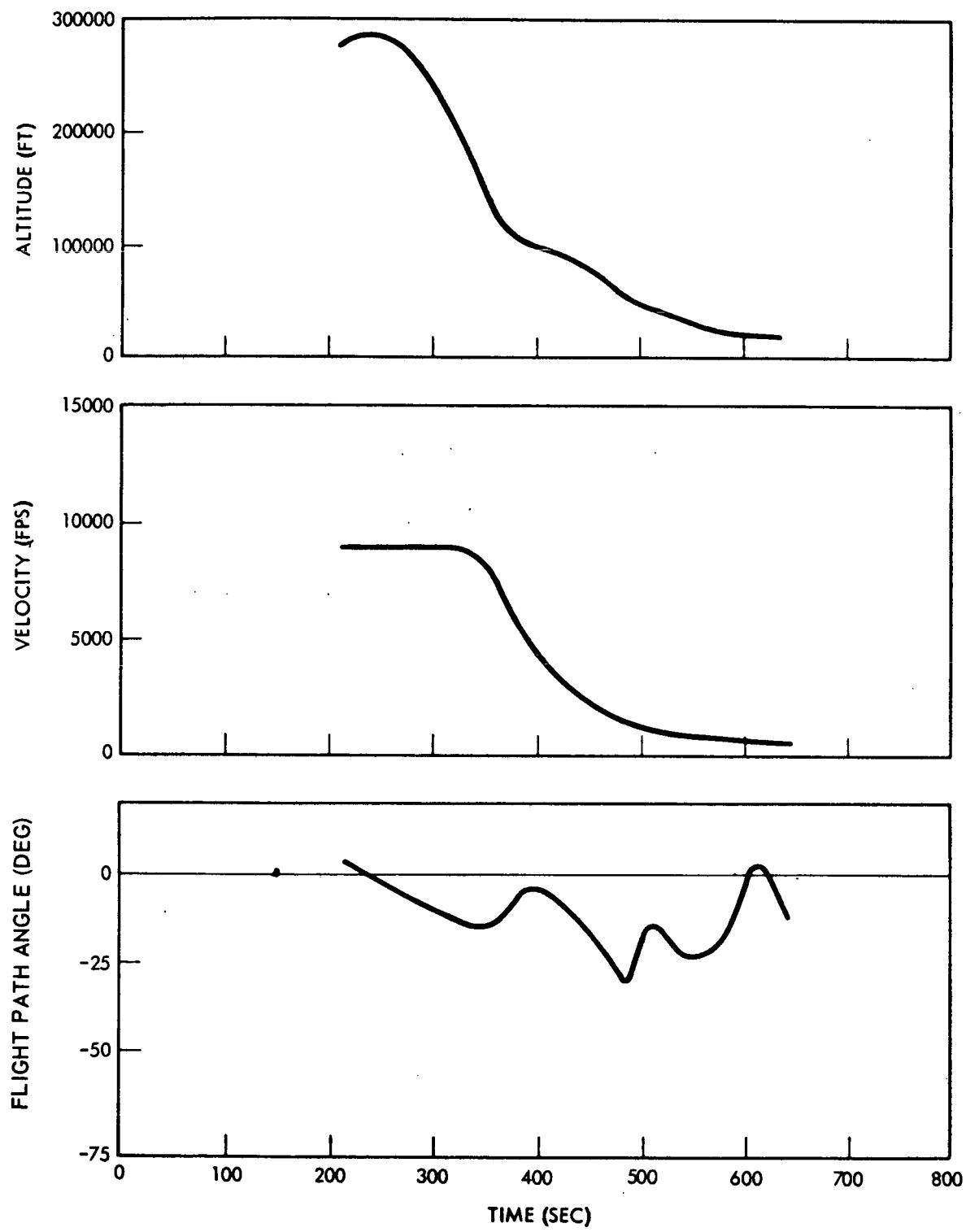


Figure 5-21. Booster Entry, Space Station Payload Mission (Sheet 1 of 5)

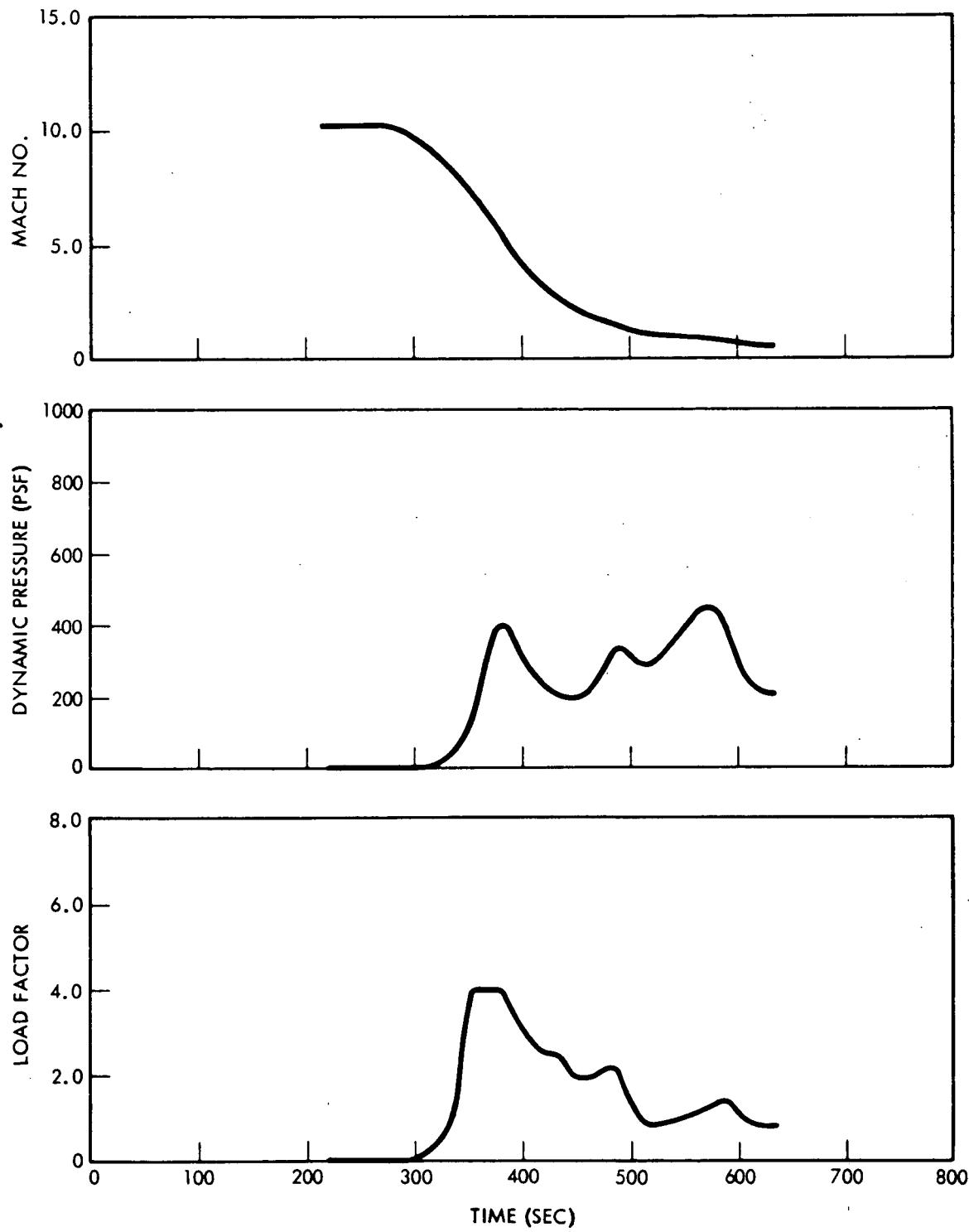


Figure 5-21. Booster Entry, Space Station Payload Mission (Sheet 2 of 5)

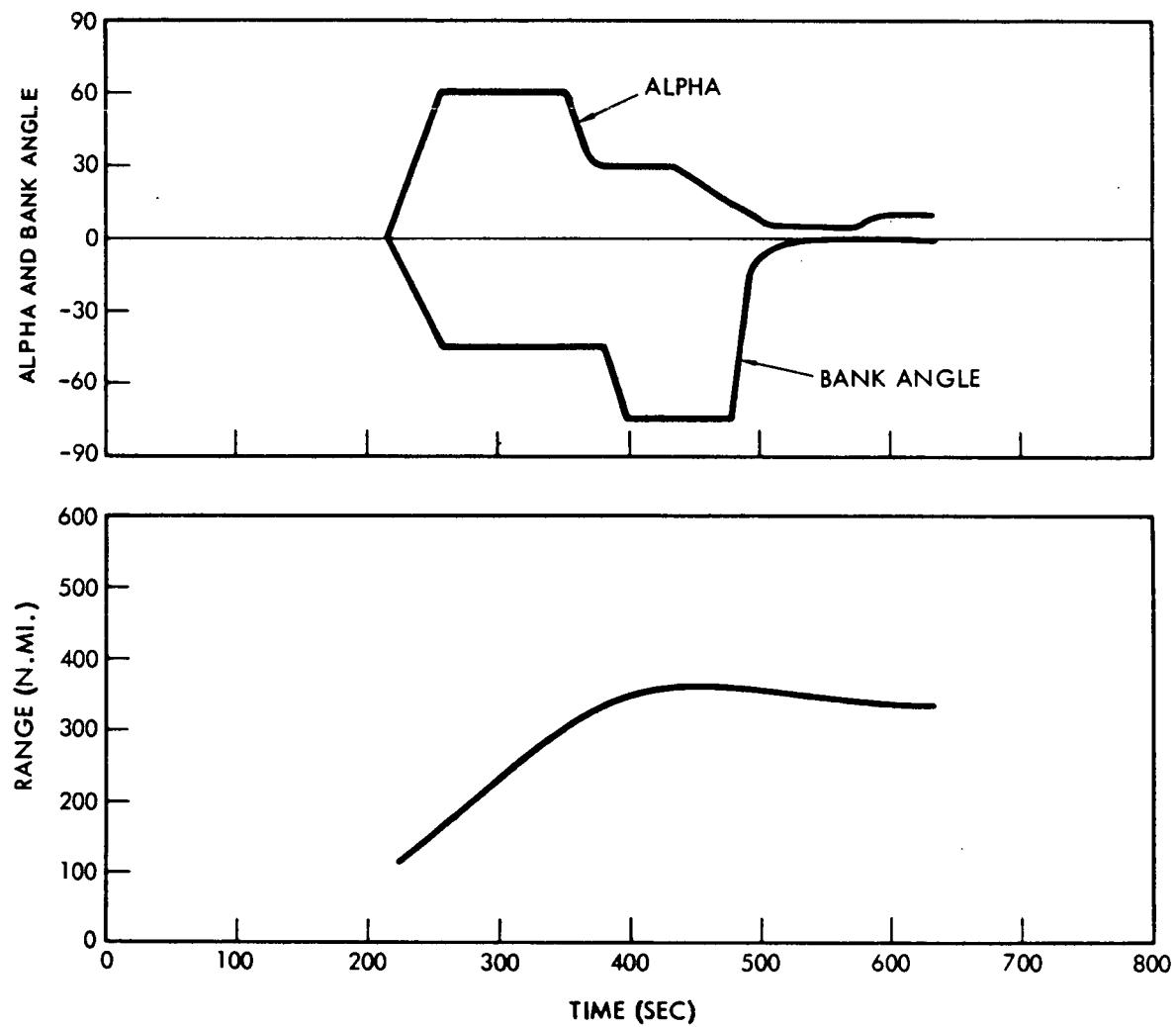


Figure 5-21. Booster Entry, Space Station Payload Mission (Sheet 3 of 5)

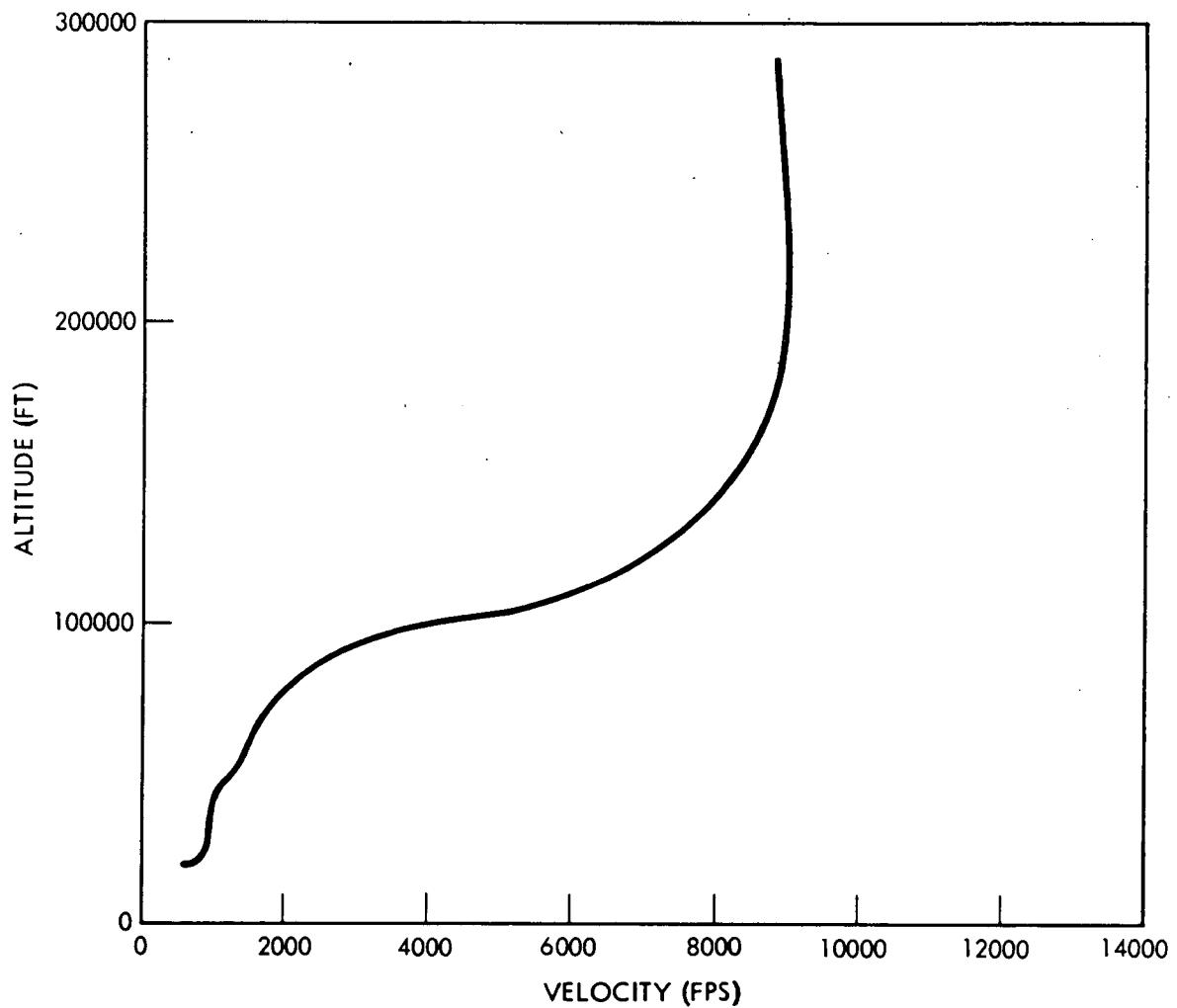


Figure 5-21. Booster Entry, Space Station Payload Mission (Sheet 4 of 5)

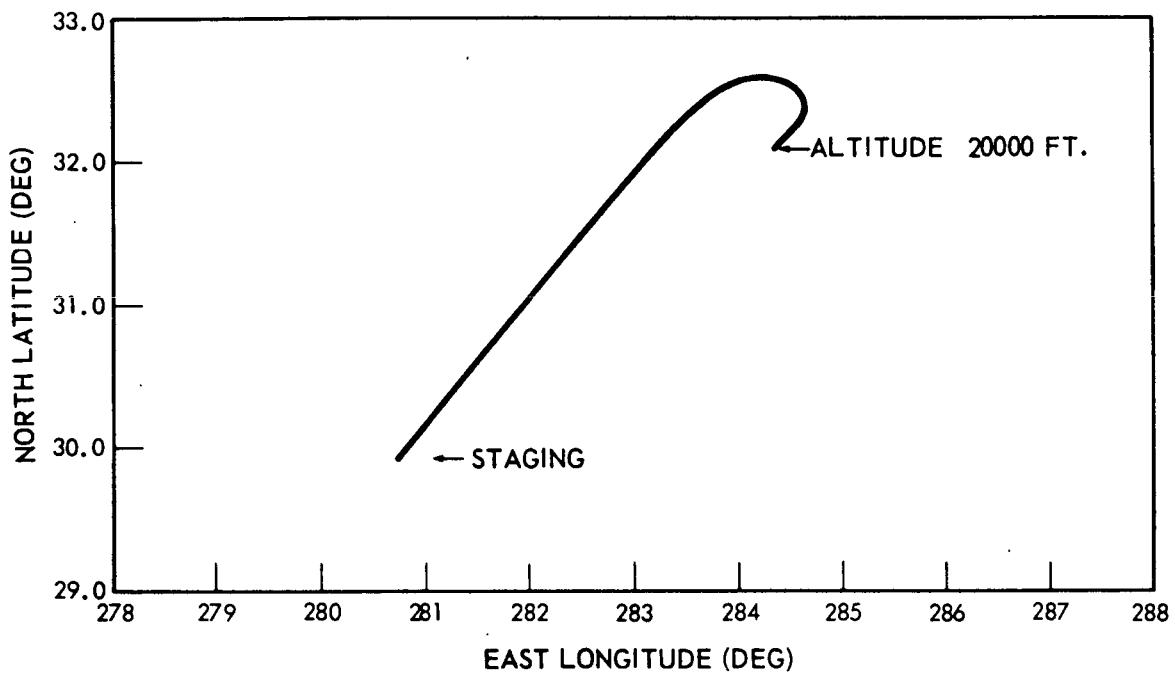


Figure 5-21. Booster Entry, Space Station Payload Mission (Sheet 5 of 5)

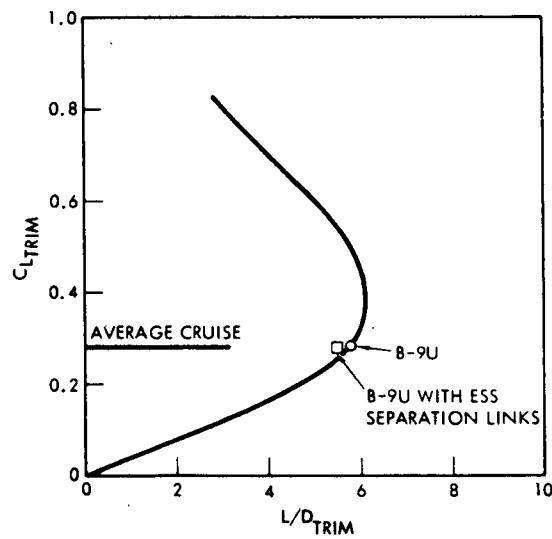


Figure 5-22. Cruise Trimmed Lift/Drag Characteristics



Flyback fuel requirements are calculated for the return cruise starting at 20,000-ft altitude and terminating at landing. The fuel requirements are for twelve cruise engines operating in still air and include allowances for descent, cruise, go-around at landing site, reserves, and landing. Because of extra drag associated with the ESS configurations, cruise specific range is about 5 percent lower than that of the space shuttle booster. However, the fuel requirement for all three ESS boosters are less than that for the shuttle booster.

Configuration	Flyback Distance (nm)	Flyback Fuel (lb)
Nuclear stage	301	94,000
Space tug	335	115,200
Space station	336	115,500
(Space shuttle)	399	129,815

With one engine inoperative and 95 percentile ETR headwinds and no reserve or go-around fuel, the requirements are as follows:

Configuration	Flyback Fuel
Nuclear stage	107,000
Space tug	120,000
Space station	120,000
Space shuttle	144,000



Aerodynamics—Mated Ascent

Predicted Aerodynamic Coefficients. Isolated aerodynamic data for the three ESS/payload configurations were based on a combination of wind tunnel results and theoretical analyses presented in the following documents.

1. NASA/MSFC Standard Nose Shape Wind Tunnel Test Report. Report R-AERO-AD-66-31 (1966).
2. R. L. Hamner, and A. D. Leff, Linear Aerodynamic Loads on Cone-Cylinders at Mach Numbers From 0.7 to 2.0, NASA CR-413 (March 1966).
3. S. F. Hoerner. Fluid-Dynamic Drag, published by the author, Midland Park, N. Y. (1965).
4. USAF Stability and Control DATCOM. Flight Control Division, Air Force Flight Dynamics Laboratory (revised July 1963).
5. S-II Aerodynamic Loads Data Manual II. North American Rockwell Corporation, Space Division, Report SID 63-498 (revised June 15, 1966).
6. J. N. Nielson. Missile Aerodynamics, New York: McGraw-Hill Book Co., Inc. (1960).

Predictions for the ESS/RNS configuration with its biconic nose shape were based on test data presented in Reference(1) above. Predictions for the ESS/MDAC and ESS/space tug were based primarily on data presented in Reference (2) supplemented with results from References (3) through (6). The aerodynamic effects of the protuberances on the ESS vehicle and the docking ports on the MDAC payload were theoretically estimated using material in References (2) through (6) as a guide. The ESS protuberances were assumed identical to current Saturn S-II design permitting direct use of data presented in Reference (5).

Flow interference effects for the ESS/payload in the presence of the booster were obtained by extrapolating experimental data for the space shuttle configuration from tests ARC 66-505 and ARC-66-511 conducted at NASA/Ames Research Center to the present design configurations. These tests were conducted with a dual force balance providing insight into the relative interference effects due to the presence of each body on the other when in the mated launch configuration. The tests also provide information on the effect of relative booster/orbiter location (i. e., nose position) on flow interference phenomena.



The aerodynamic data for the booster, both as an isolated body and body in the presence of ESS/payload were determined by General Dynamics/Convair. These data were primarily based on wind tunnel data for a body similar in design to the GD/B-9U booster. Component buildup test results were used where necessary to modify the aerodynamic characteristics to account for differences between the wind tunnel model and B-9U booster.

The predicted aerodynamic data for the integrated launch configuration (i.e., booster and ESS/payload) were obtained by combining the data for the booster with interference with the data for the ESS/payload with interference. These results are plotted in Figure 5-23 through 5-38 over the Mach number range. The reference dimensions shown in the plots are applicable to the present B-9U design configuration and represent the following:

S_{REF} — Theoretical total wing plan area

\bar{c} — Mean aerodynamic chord (MAC)

b_{REF} — Theoretical total wing span

Pitch and yaw moment coefficients are referenced to the booster nose position and rolling moment is referenced to the booster centerline. The total axial aerodynamic force for the launch configuration is obtained by combining the forebody axial force data with the "power on" base thrust data which are a function of altitude.

Experimentally Derived Aerodynamic Coefficients. Data points for $M = 1.2$ and $M = 3.0$ based on wind tunnel test TWT-489, conducted at NASA/MSFC, are presented in Figures 5-23 through 5-38 for comparison with the theoretical predictions discussed in the previous section. The booster model consisted of a 0.0035-scale version of the B-9U wing and a 0.0031-scale model of the B-9U body. The ESS/payload models were built to a 0.0031 scale for consistency with the booster model body size. No provision was made for simulating the MDAC docking ports and ESS protuberances. Thus, the basic test data were corrected for this difference in scale factor and further modified to include a theoretical estimate of protuberance and docking port effects. Test results for lateral/directional aerodynamic coefficients for the ESS/RNS and ESS/space tug were not available for comparison with the theoretical predictions.

The primary reason for the overestimation of forebody $C_A(\alpha = 0 \text{ deg})$ at $M = 1.2$ for the three payload configurations is due to an overprediction of the isolated booster data. The other large difference between predicted

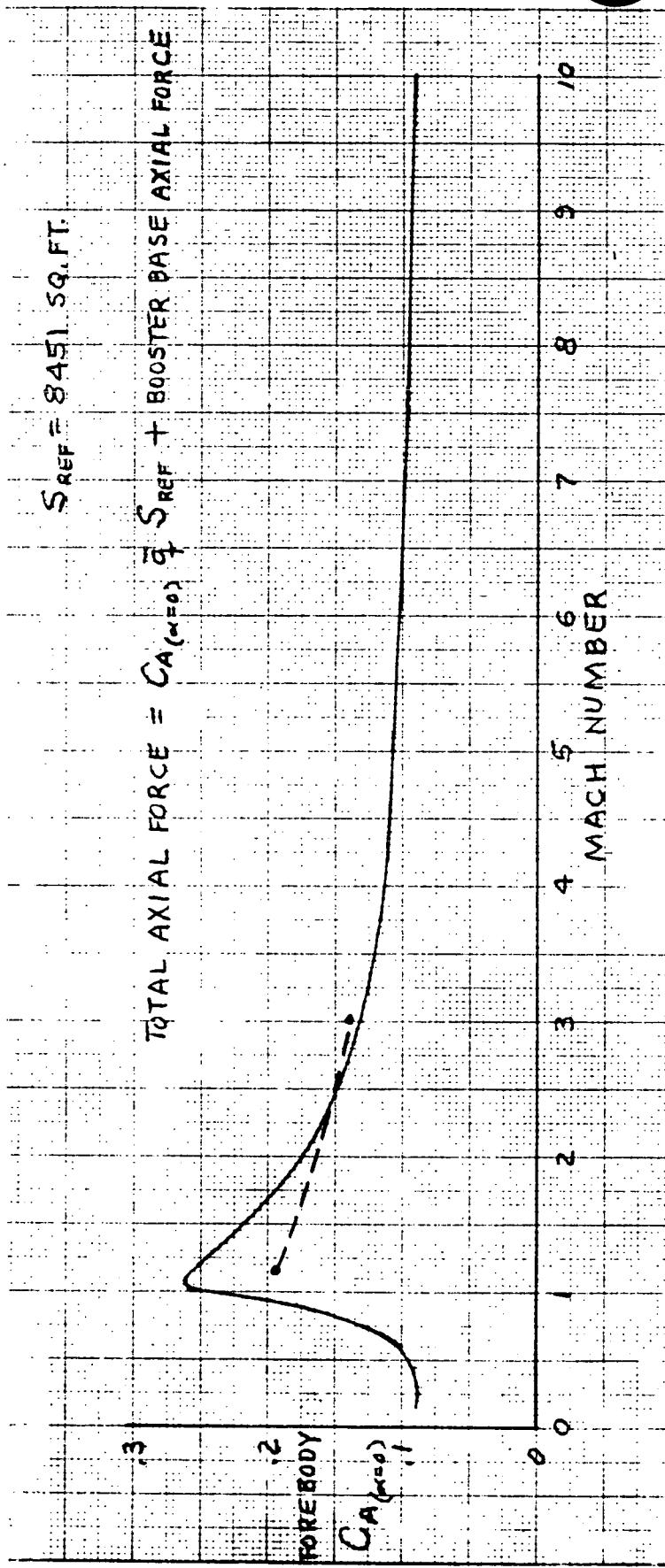


Figure 5-23. Aerodynamic Data-Integrated System Boost Configuration (B-9U/RNS)
 Forebody Axial Force Coefficient Versus Mach Number

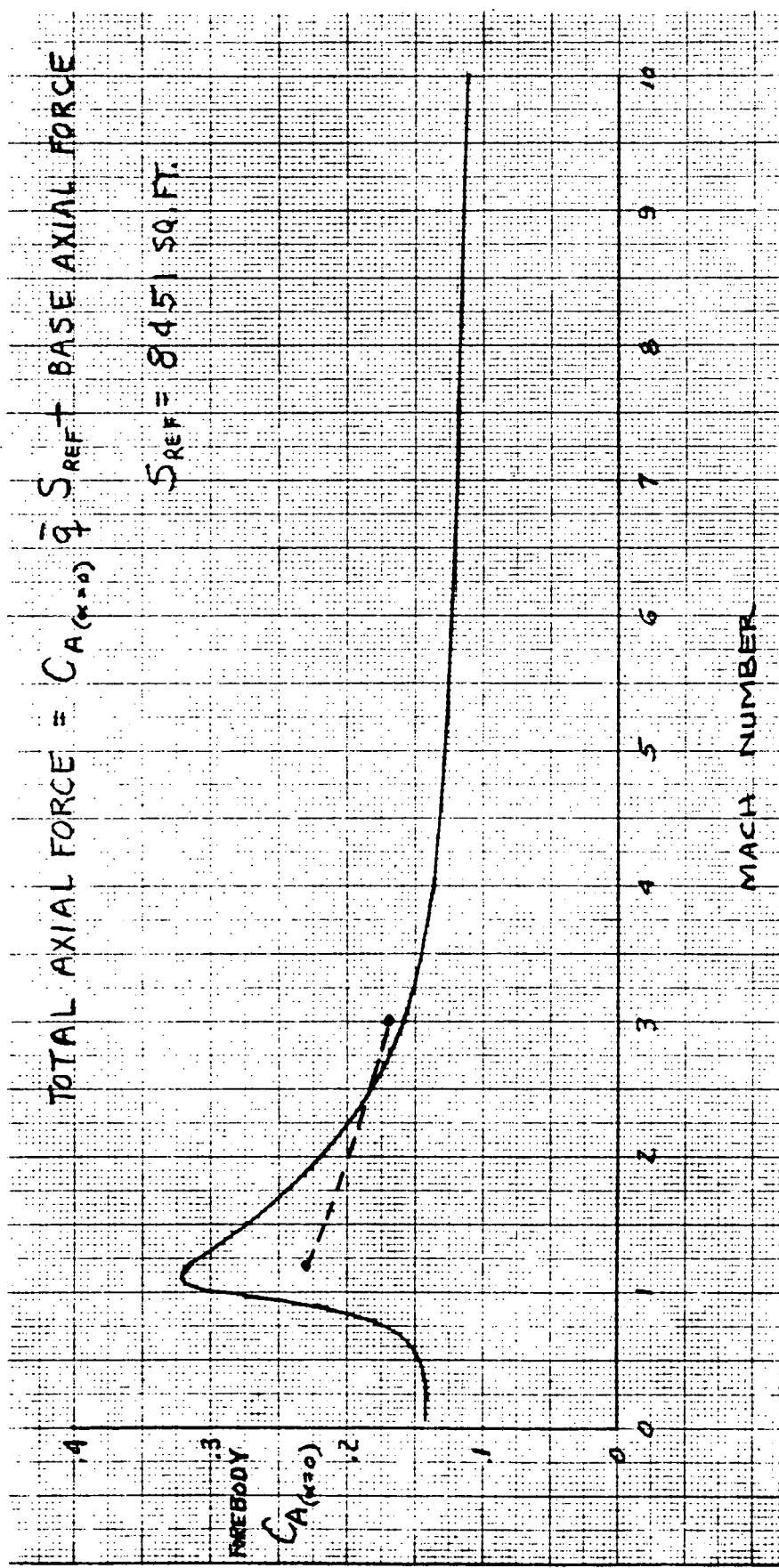


Figure 5-24. Aerodynamic Data-Integrated System Boost Configuration (B-9U/MDAC)
Forebody Axial Force Coefficient Versus Mach Number

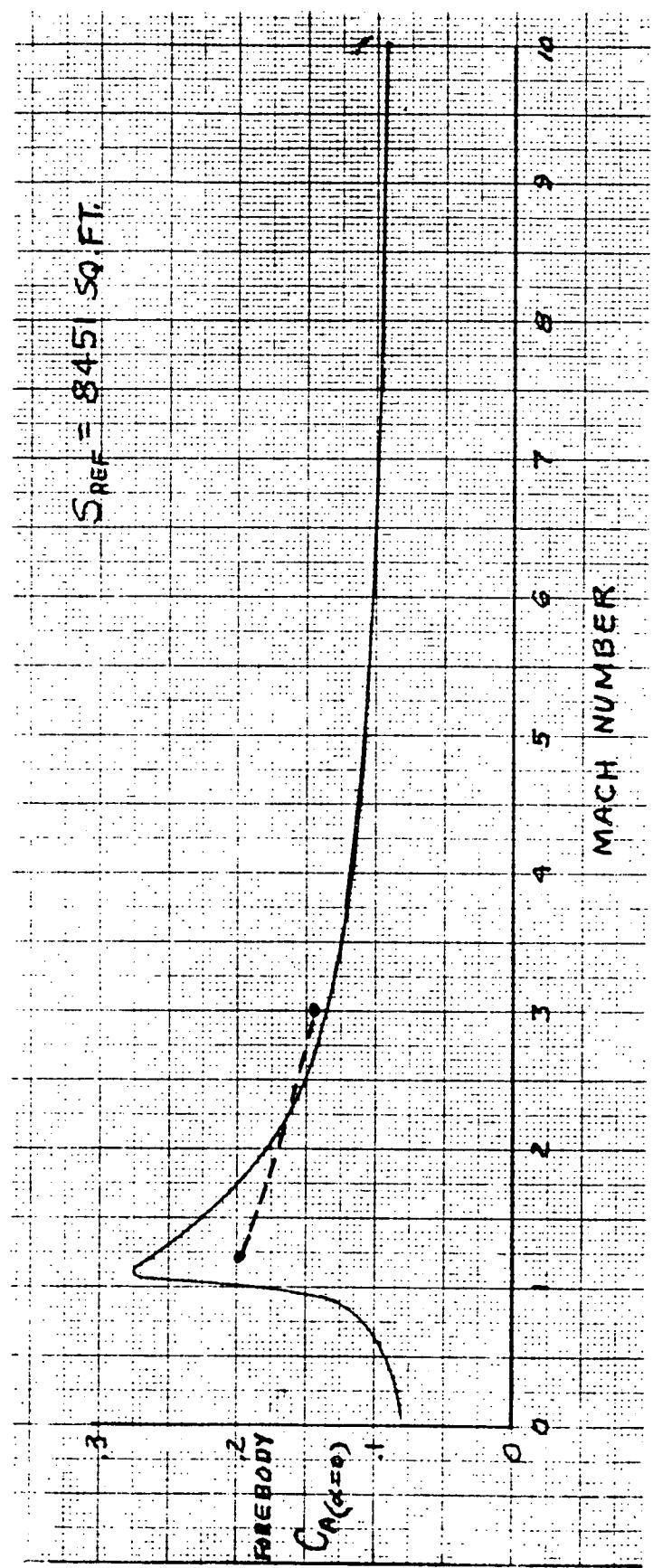


Figure 5-25. Aerodynamic Data - Integrated System Boost Configuration (B-9U/Space Tug)
Forebody Axial Force Coefficient Versus Mach Number

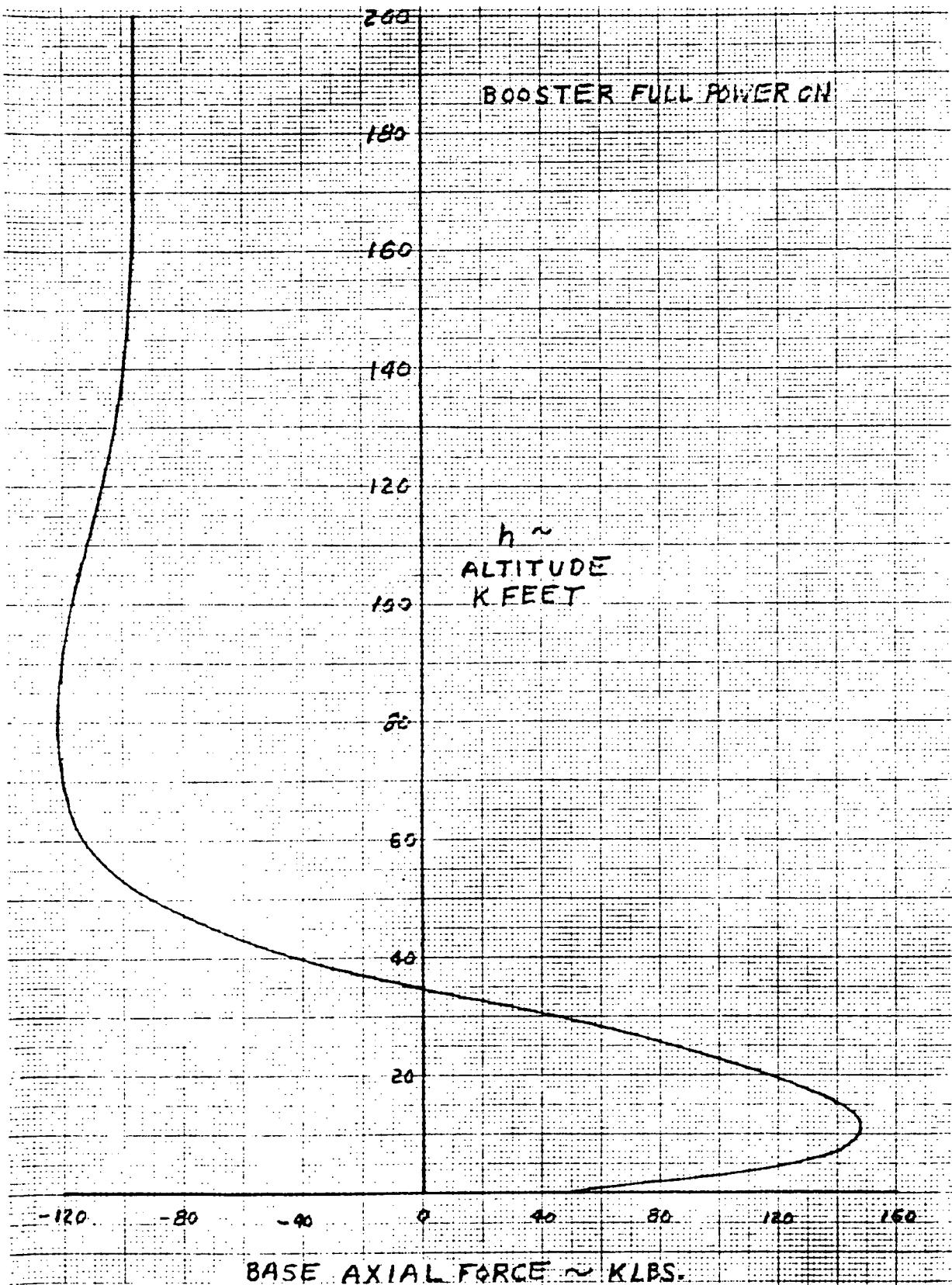


Figure 5-26. Aerodynamic Data-Integrated System Boost Configuration
(B-9U/RNS) Attitude Versus Base Axial Force

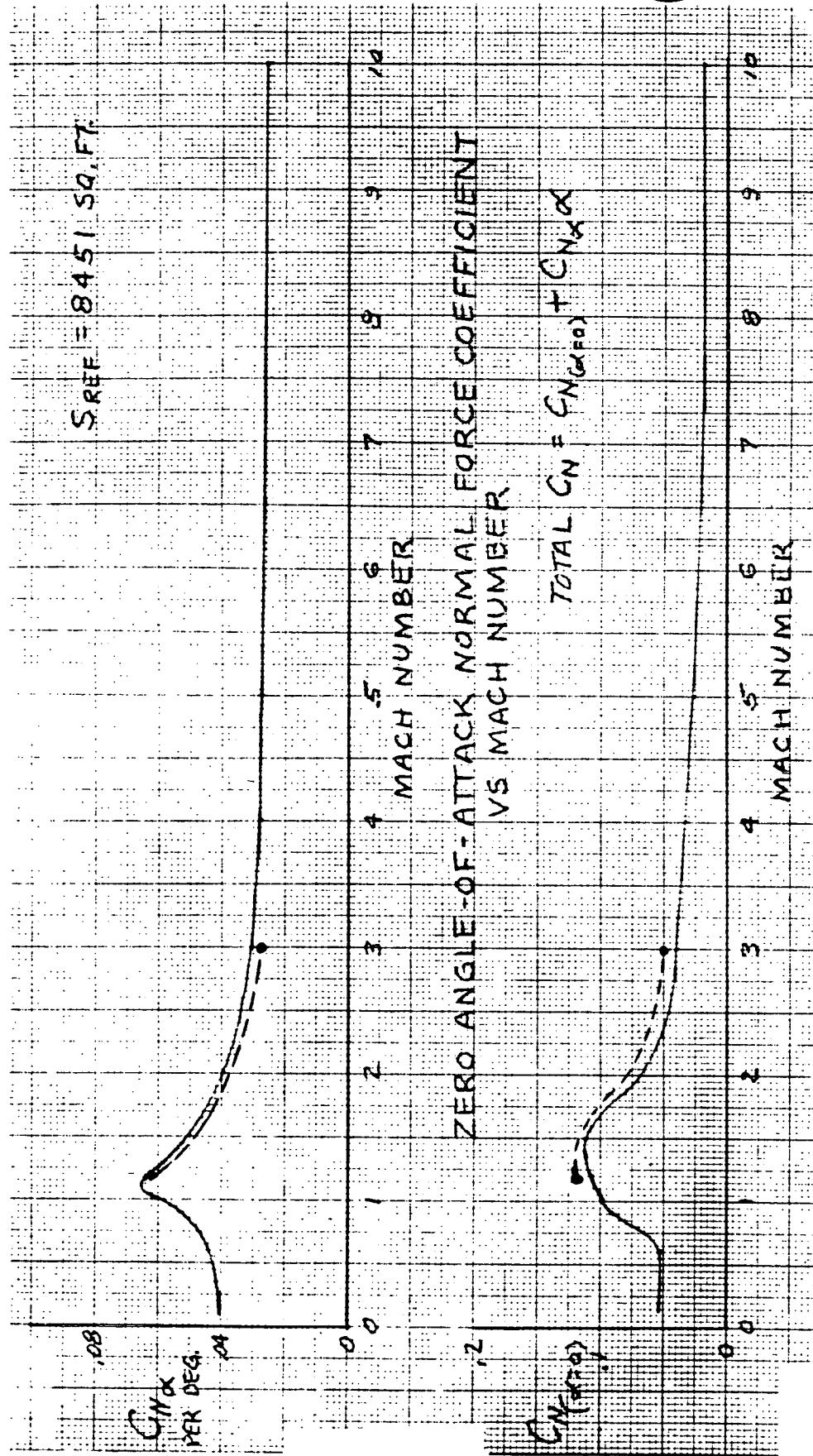


Figure 5-27. Aerodynamic Data-Integrated System Boost Configuration (B-9U/RNS)
Normal Force Coefficient Curve Slope Versus Mach Number

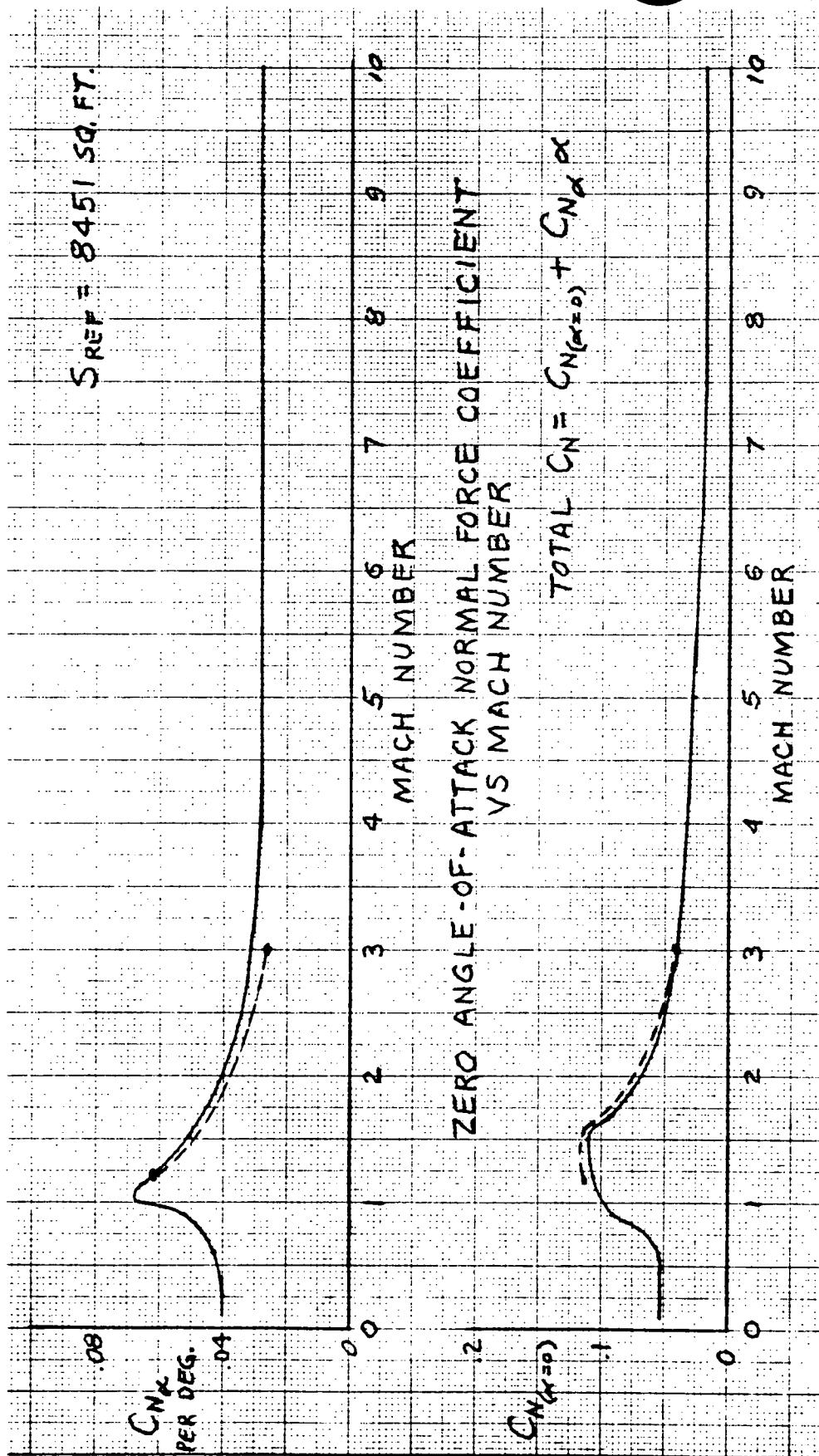


Figure 5-28. Aerodynamic Data - Integrated System Boost Configuration (B-9U/MDAC)
Normal Force Coefficient Curve Slope Versus Mach Number

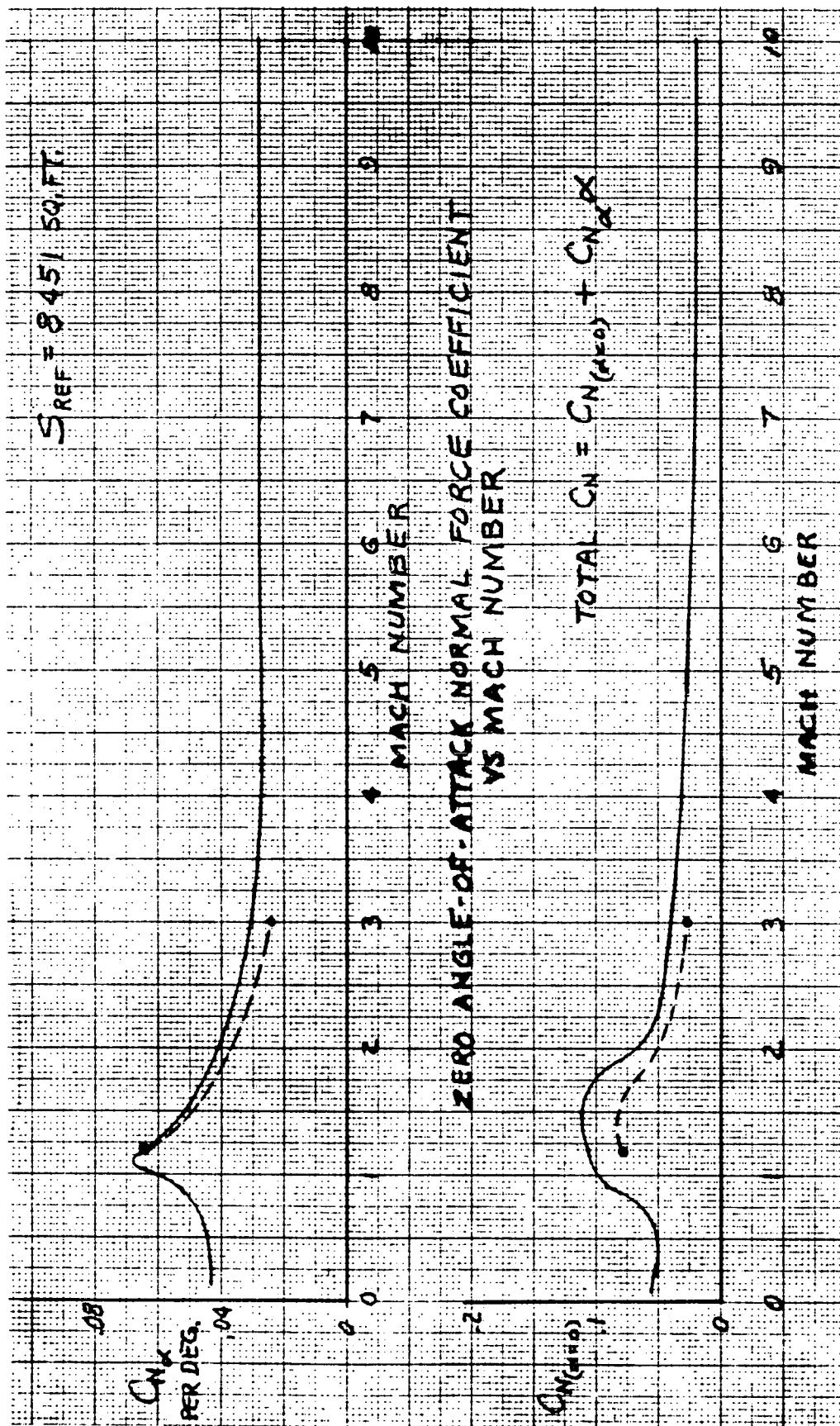


Figure 5-29. Aerodynamic Data-Integrated System Boost Configuration (B-9U/Space Tug)
 Normal Force Coefficient Curve Slope Versus Mach Number

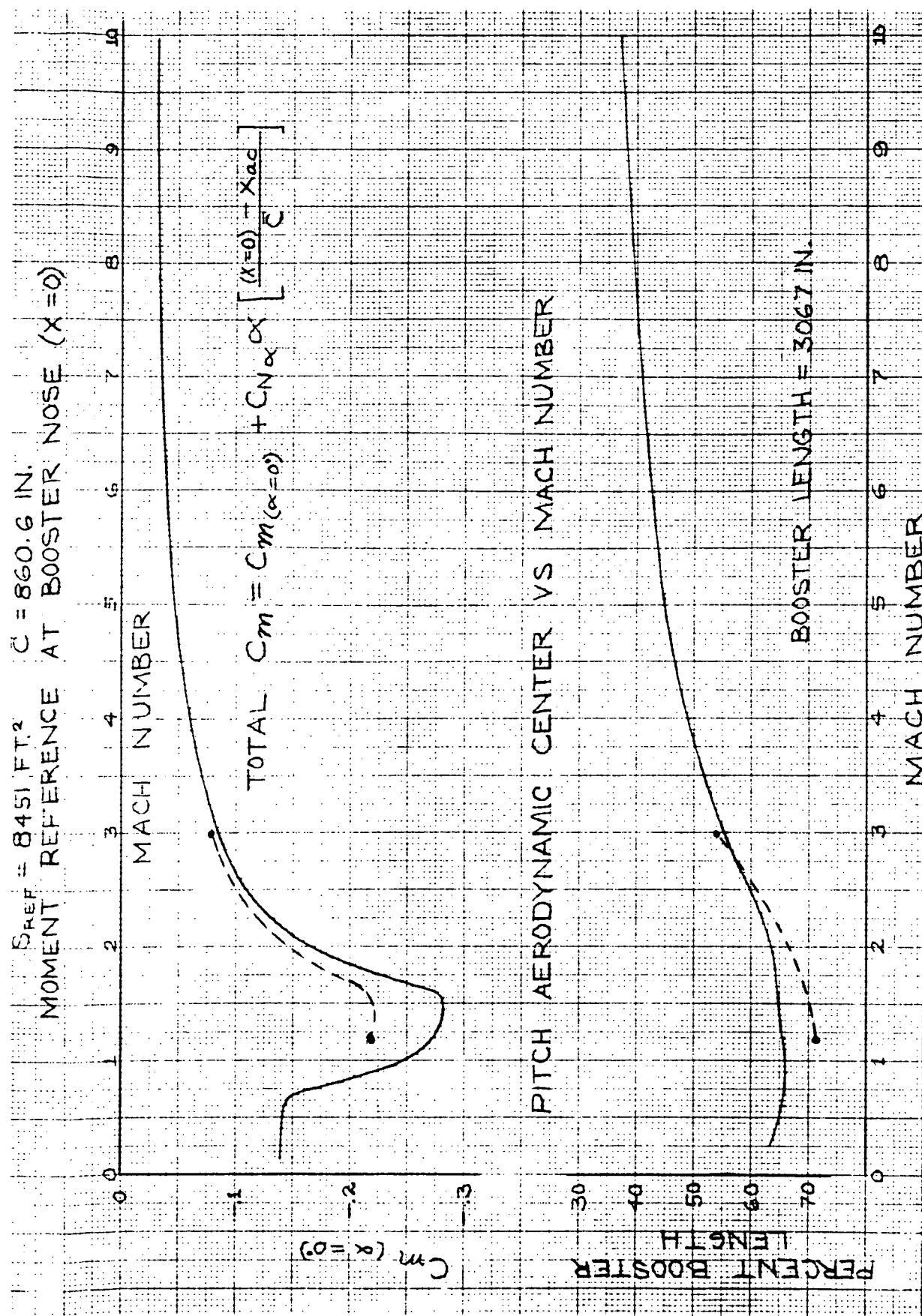


Figure 5-30. Aerodynamic Data-Integrated System Boost Configuration (B-9U/RNS)
Zero Angle-of-Attack Pitching Moment Coefficient Versus Mach Number

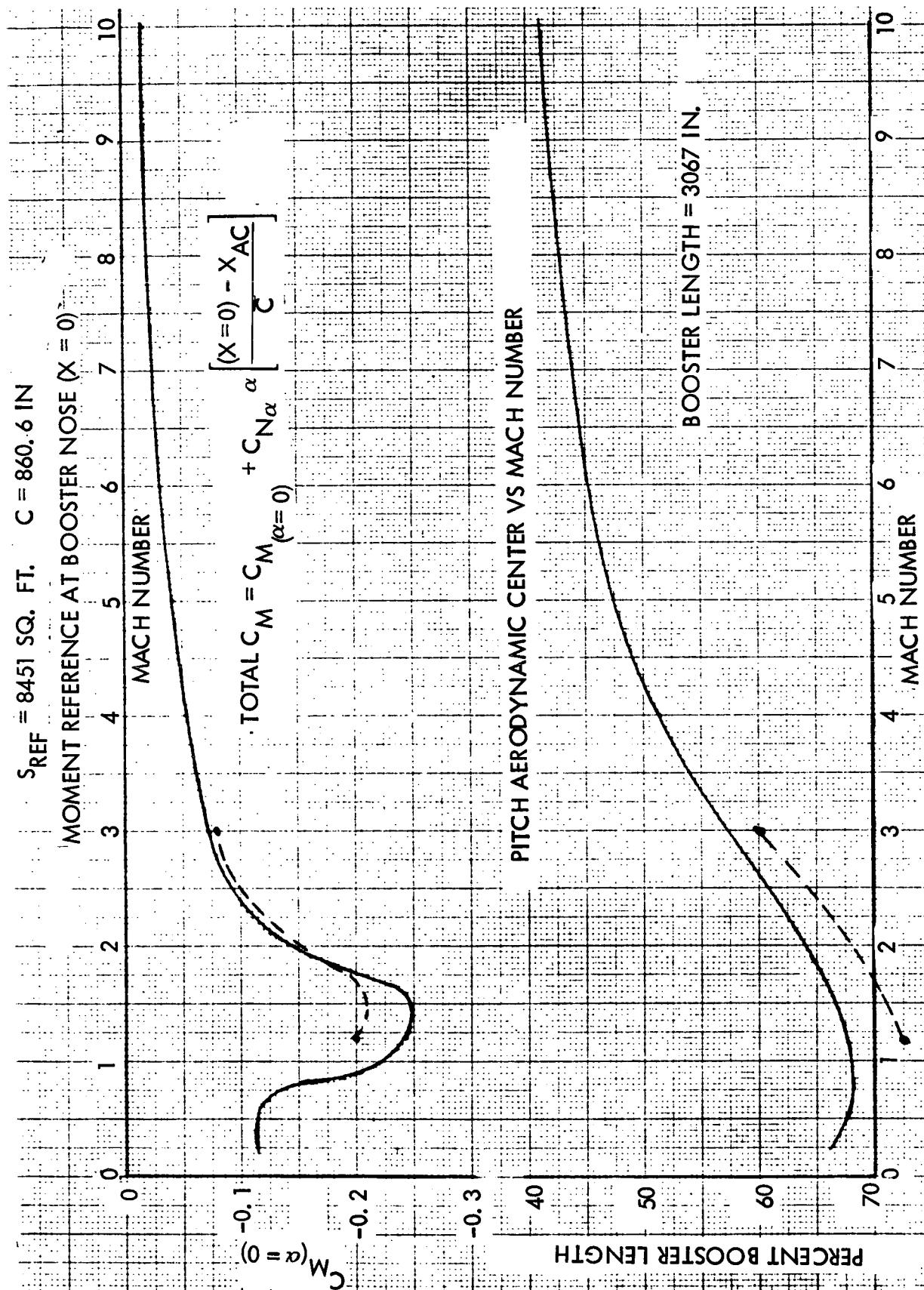


Figure 5-31. Aerodynamic Data-Integrated System Boost Configuration (B-9U/MDAC) Zero Angle-of-Attack Pitching Moment Coefficient Moment Reference at Booster Nose ($X = 0$) Versus Mach Number

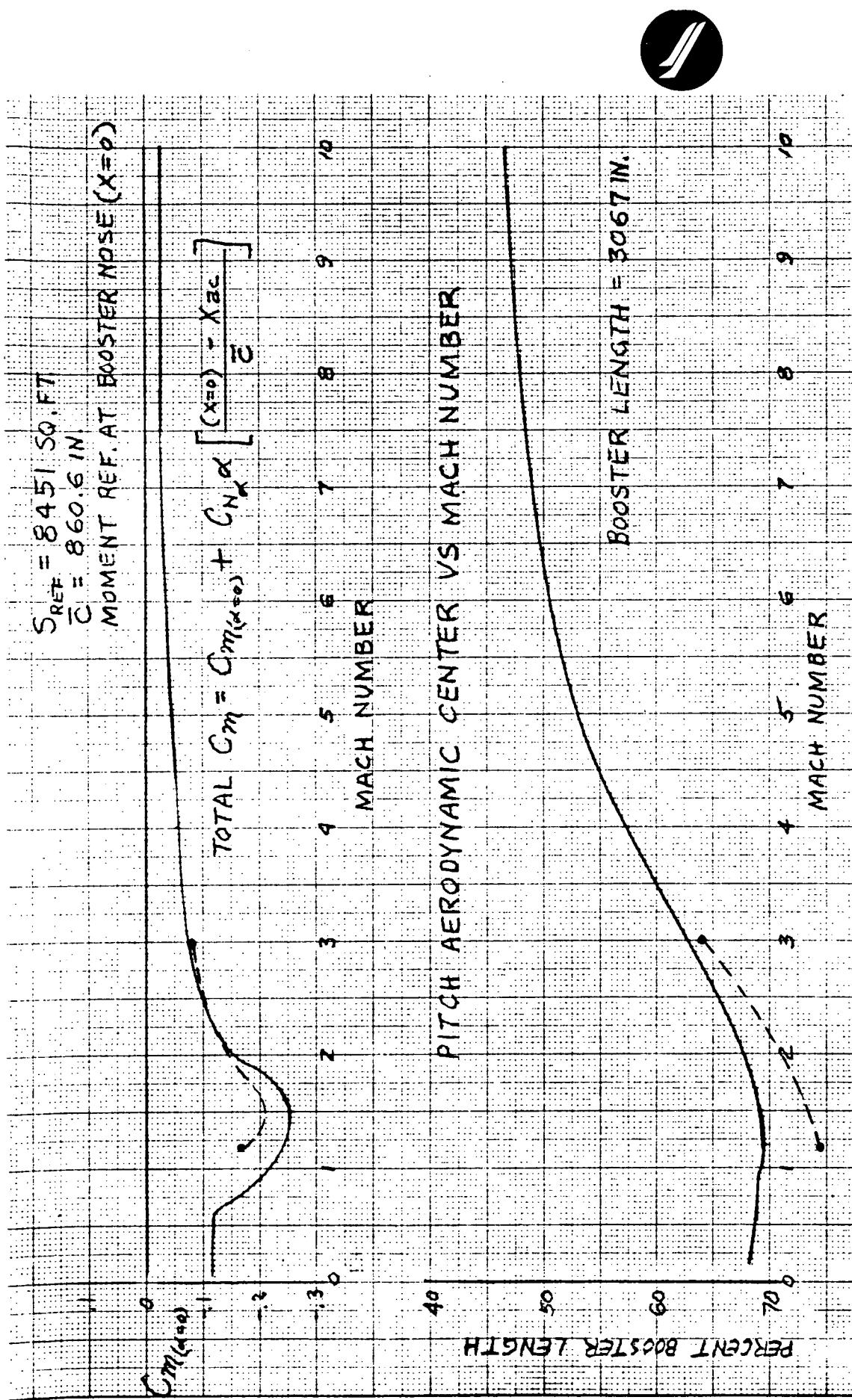


Figure 5-32. Aerodynamic Data-Integrated System Boost Configuration (B-9U/Space Tug)
Zero Angle-of-Attack Pitching Moment Coefficient Versus Mach Number

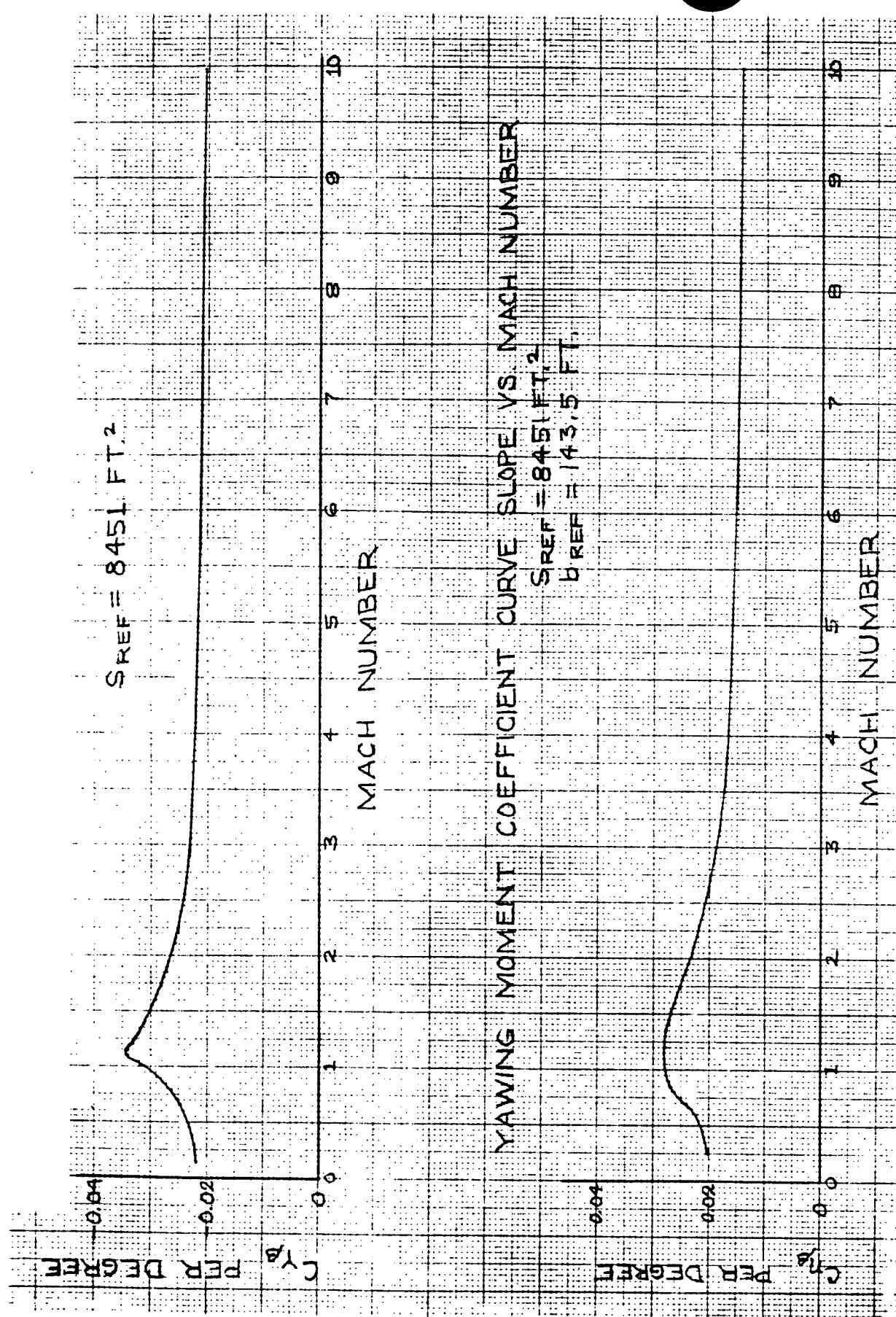


Figure 5-33. Aerodynamic Data-Integrated System Boost Configuration (B-9U/RNS)
Side Force Coefficient Curve Slope Versus Mach Number

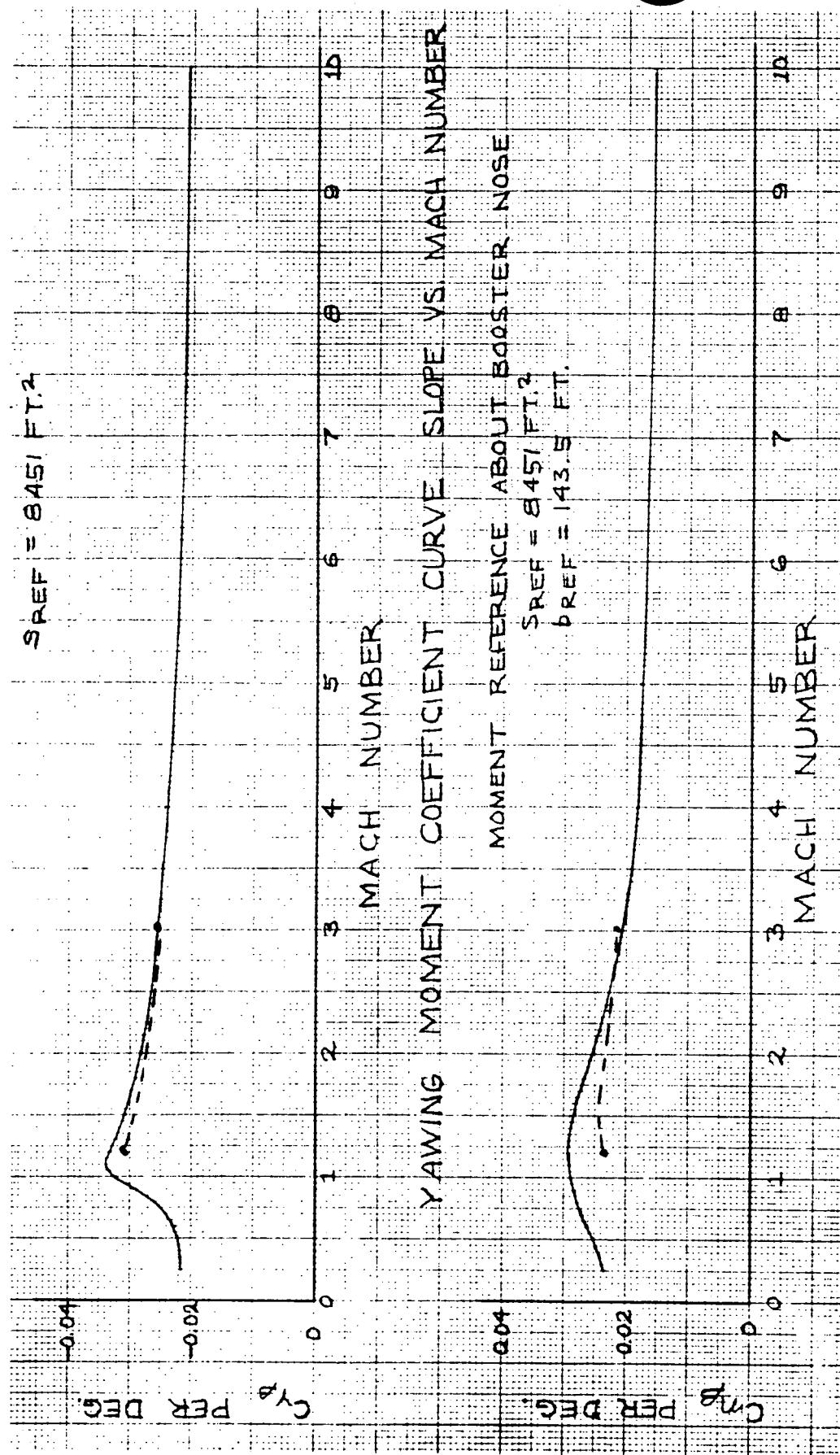


Figure 5-34. Aerodynamic Data-Integrated System Boost Configuration (B-9U/MDAC)
Side Force Coefficient Curve Slope Versus Mach Number

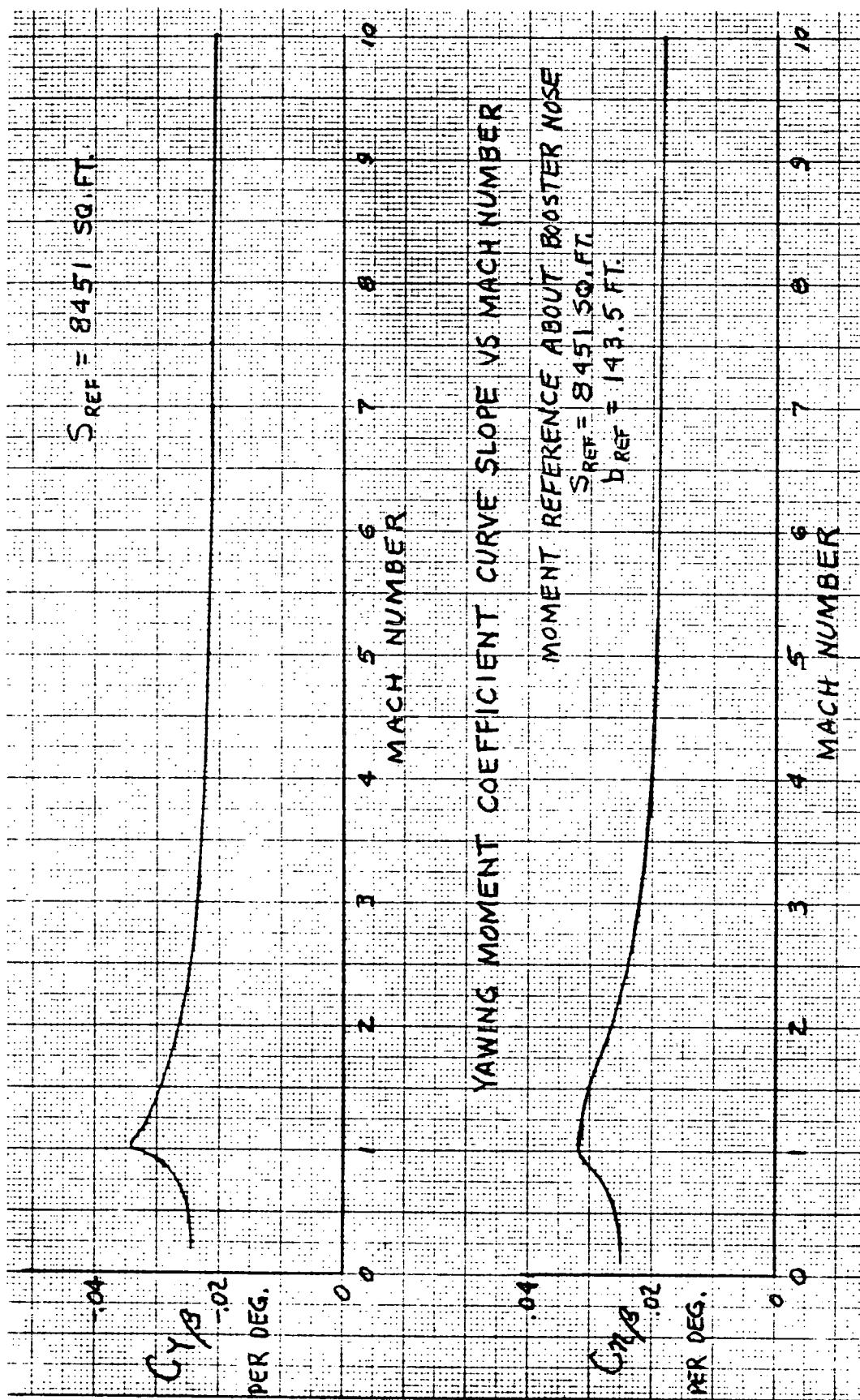


Figure 5-35. Aerodynamic Data-Integrated System Boost Configuration (B-9U/Space Tug)
Side Force Coefficient Curve Slope Versus Mach Number

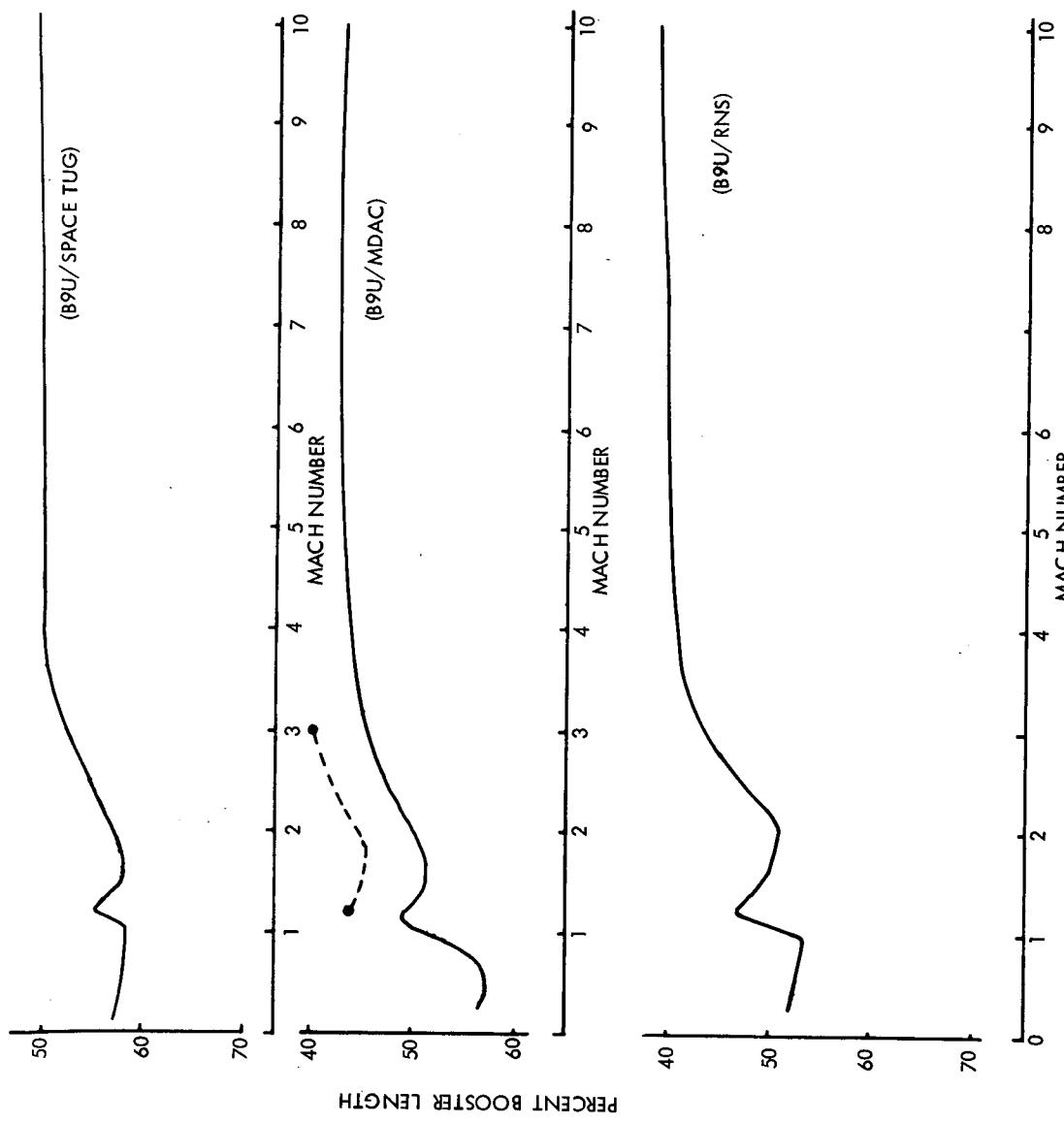


Figure 5-36. Aerodynamic Data-Integrated System Boost Configuration,
Yaw Aerodynamic Center Versus Mach Number

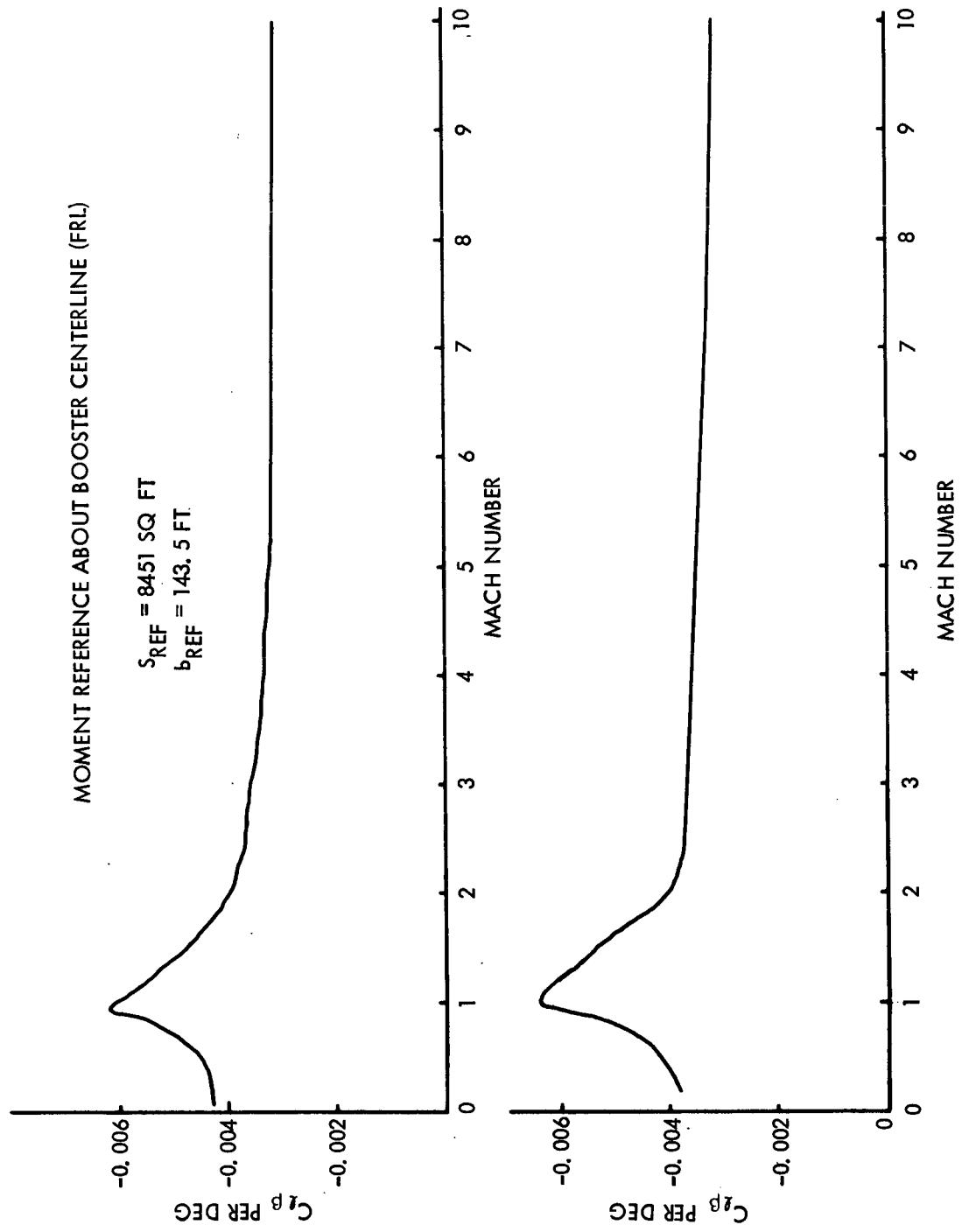


Figure 5-37. Aerodynamic Data-Integrated System Boost Configuration (B-9U/Space Tug) Rolling Moment Coefficient Curve Slope Versus Mach Number

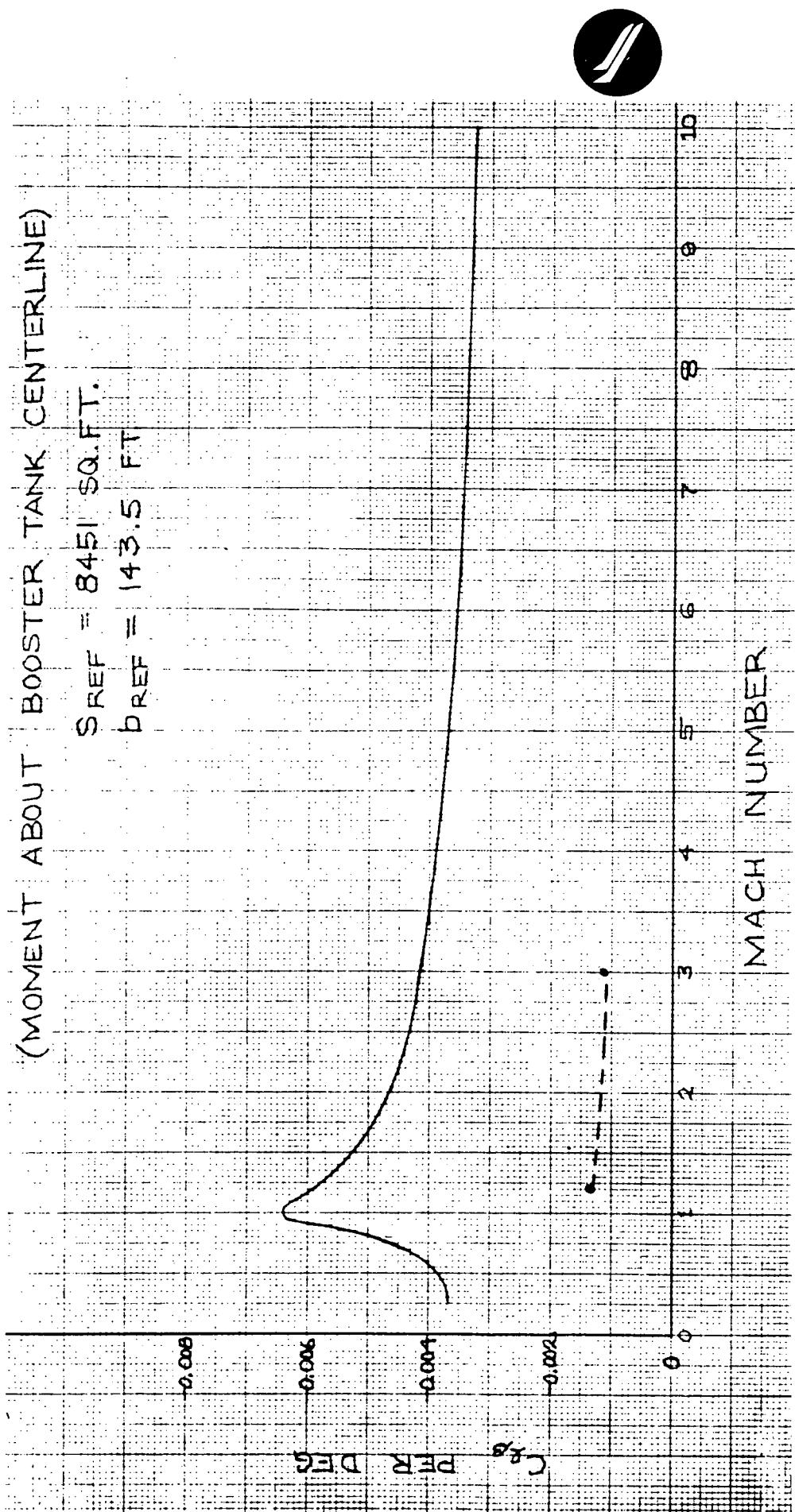


Figure 5-38. Aerodynamic Data-Integrated System Boost Configuration (B-9U/MDAC)
Rolling Moment Coefficient Curve Slope Versus Mach Number



and experimental results occurs in the rolling moment curve slope where again the predicted values overestimate the actual situation. The lateral interference data supplied by General Dynamics for the B-9U booster indicated a reduction in booster rolling moment when "in the presence of" the ESS/payload. It appears that the applied correction for interference was insufficient and should have been increased to the point that the rolling moment curve slope for the booster "in the presence of" is represented as a positive rather than a negative contribution to the launch configuration data. This point is substantiated by recent wind tunnel test results of the space shuttle configuration (i. e., test ARC 66-548) conducted at NASA/ARC. The comparison of experimental and predicted results for the remaining aerodynamic coefficients show a reasonable correlation. The experimental data indicate an increase in stability over the predicted data for the pitch plane but a decrease in stability for the lateral plane.

Distributed Air Loads Coefficients. Figures 5-39 through 5-60 contain distributed air loads coefficient data utilized in the determination of mated ascent aerodynamic loads.

Stability and Control

Mated Ascent Control Analyses. The expendable second stage (ESS) launch vehicle, consisting of the shuttle booster with a modified S-II stage mounted in place of the reusable orbiter vehicle, was analyzed with the following S-II stage payloads:

1. Space station (MDAC configuration)
2. Space tug
3. Nuclear stage (RNS)

The controls study is aimed at verifying the feasibility of this launch vehicle concept and analyzing the ascent phase control problems which are different from those of the shuttle launch vehicle. The following sections contain the results and conclusions of the analyses that were conducted.

Study Ground Rules and Objectives. The overall objective was to minimize the impact of the ESS with its various payloads on the shuttle booster. Thus, the shuttle booster thrust vector control (TVC) system requirements, illustrated in Figure 5-61, must be adequate for the ESS launch vehicle. Also, all attitude stabilization and control system modifications required by the ESS launch vehicle are confined to the areas of system software and, possibly, input sensor locations.

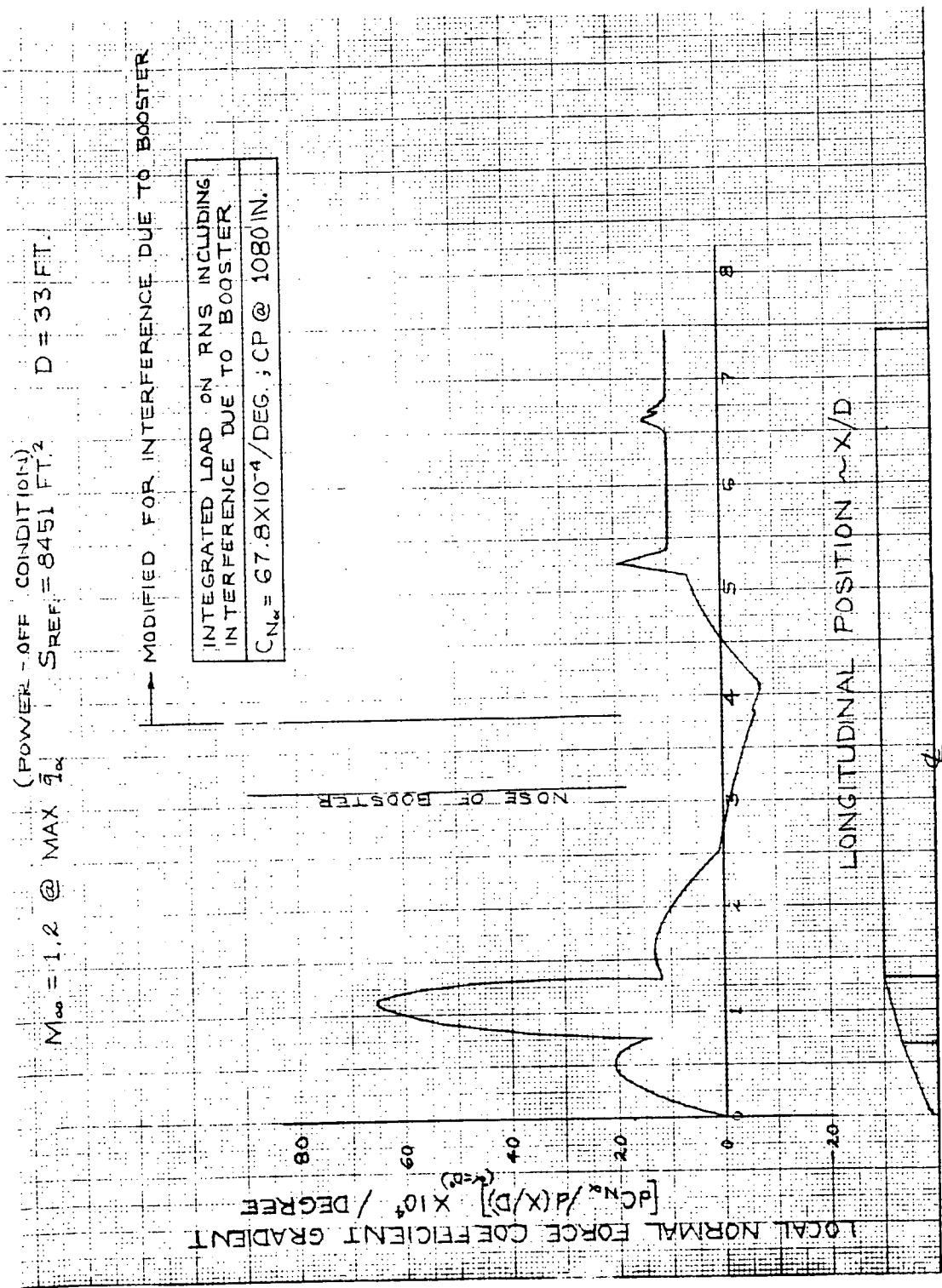


Figure 5-39. Distribution of Local Normal Force Coefficient for RNS

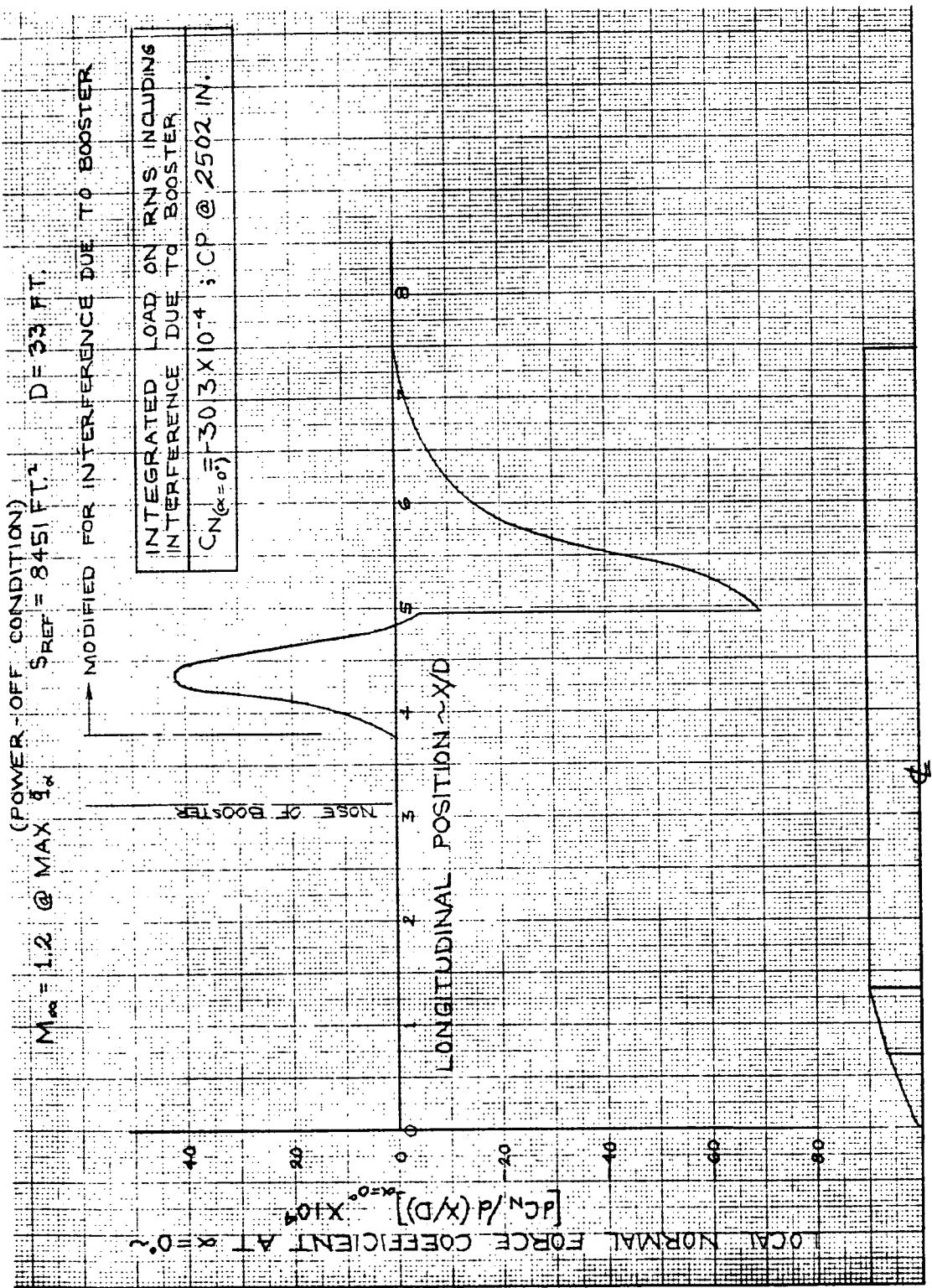


Figure 5-40. Distribution of Local Normal Force Coefficient for RNS

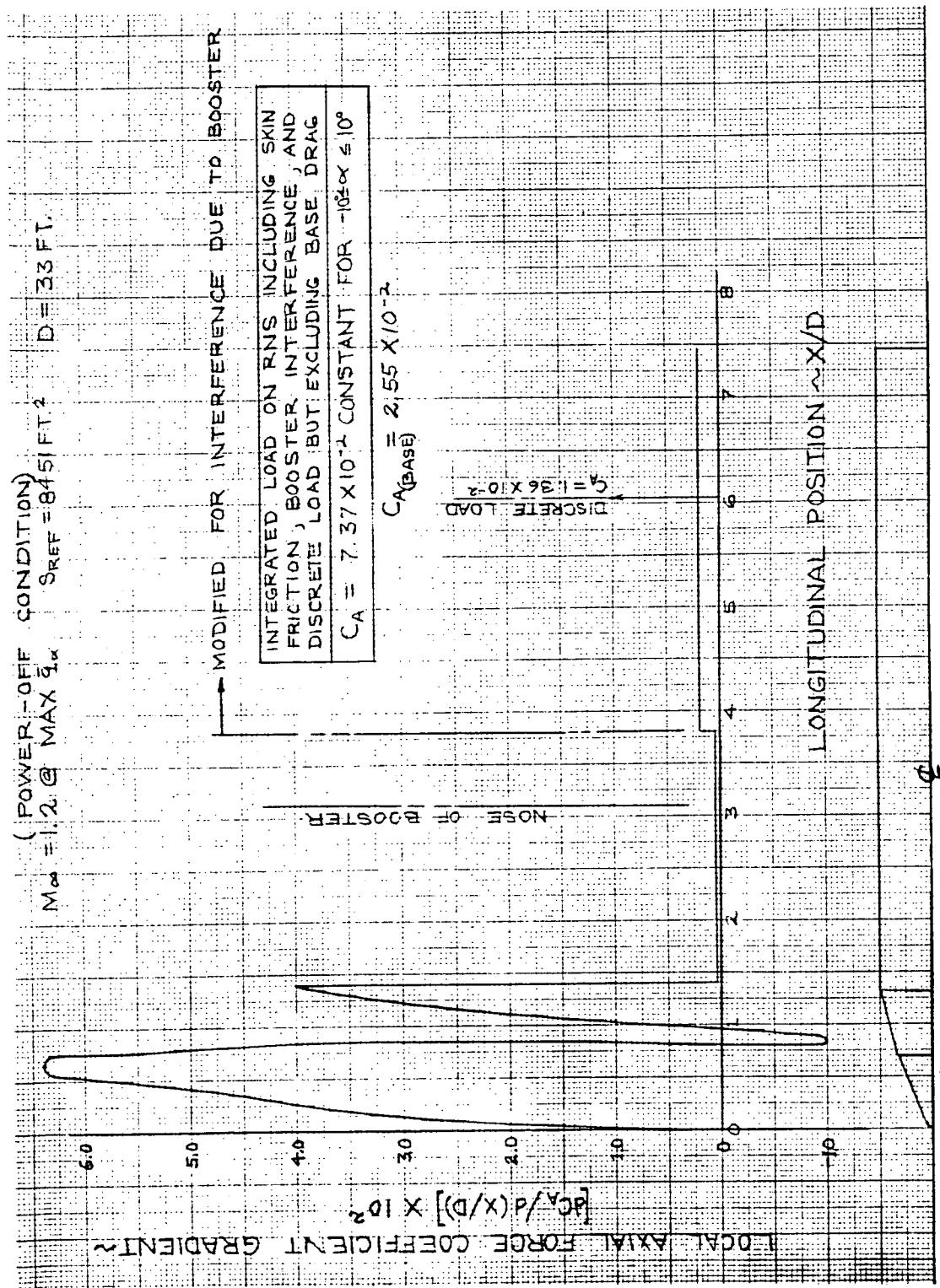


Figure 5-41. Distribution of Local Axial Force Coefficient for RNS

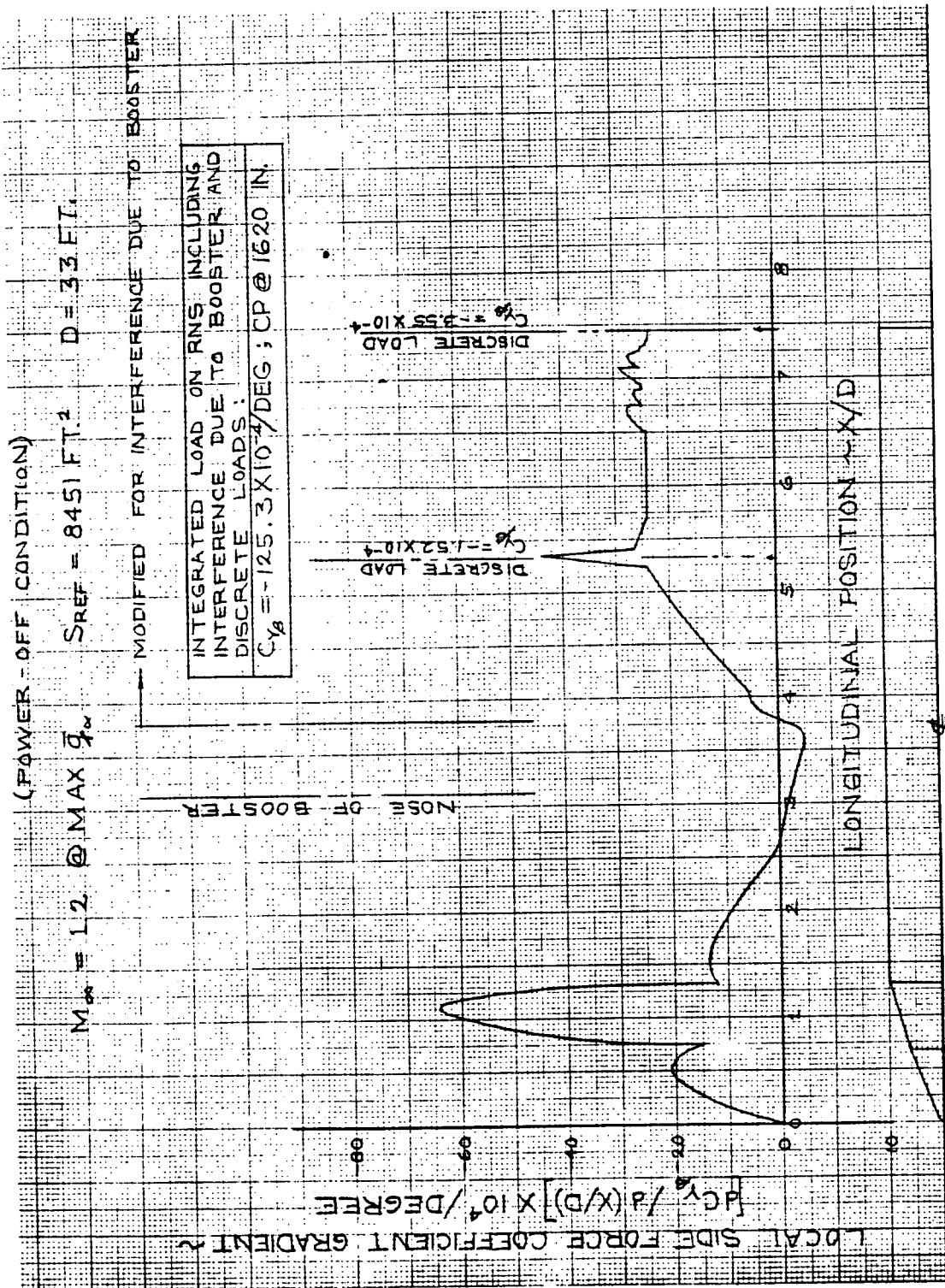


Figure 5-42. Distribution of Local Side Force Coefficient for RNS

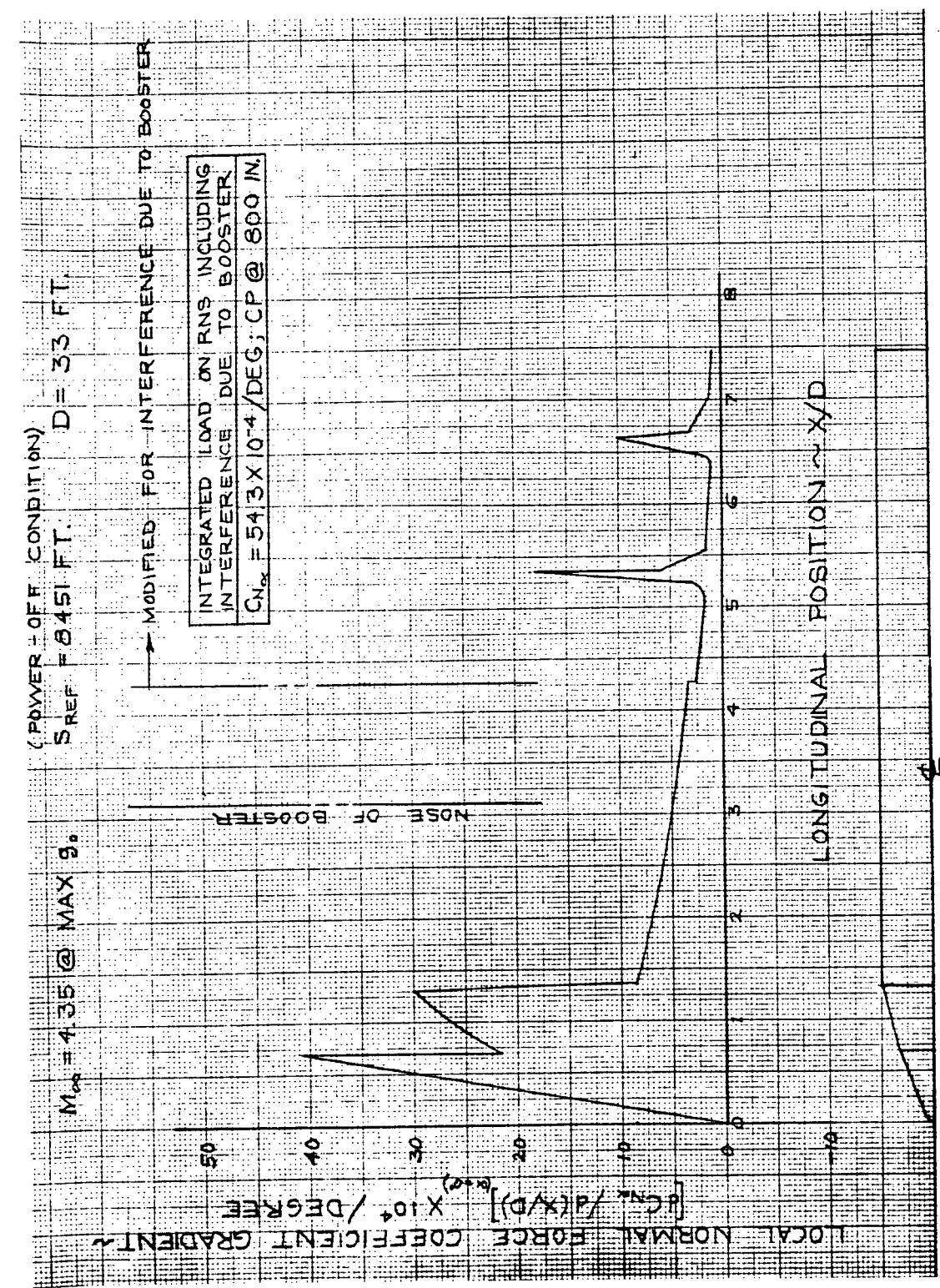


Figure 5-43. Distribution of Local Normal Force Coefficient for RNS

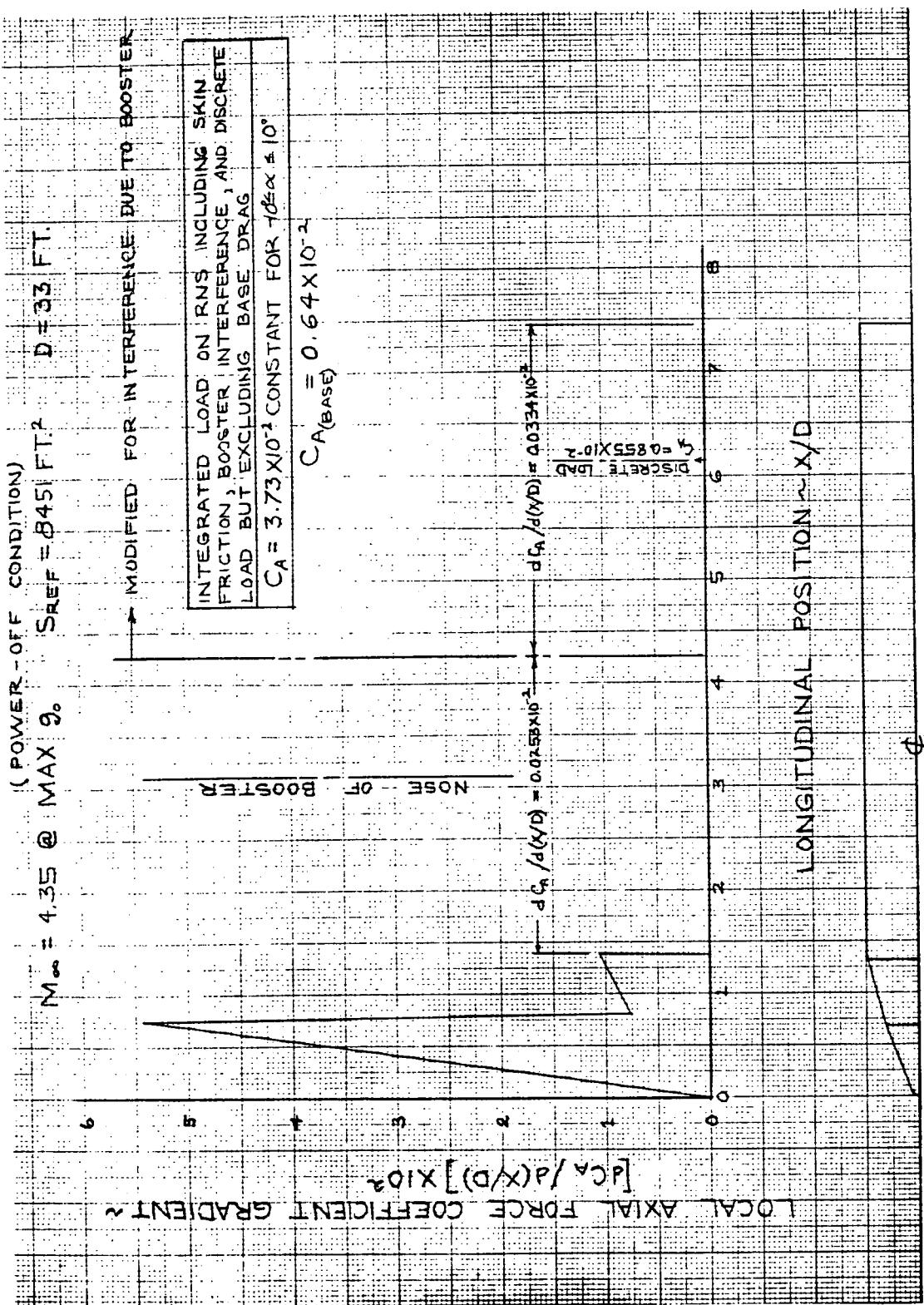


Figure 5-44. Distribution of Local Axial Force Coefficient for RNS

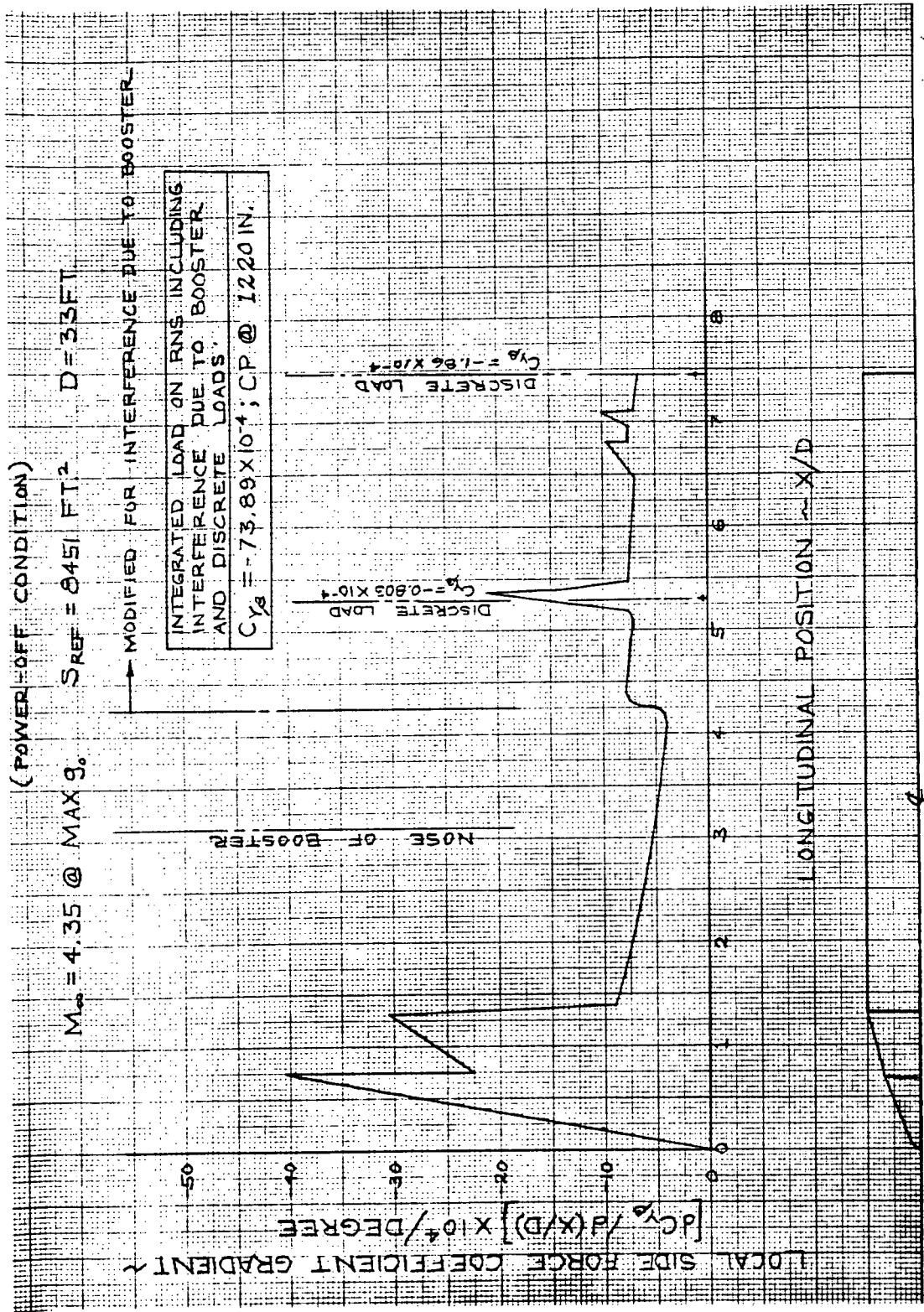


Figure 5-45. Distribution of Local Side Force Coefficient for RNS

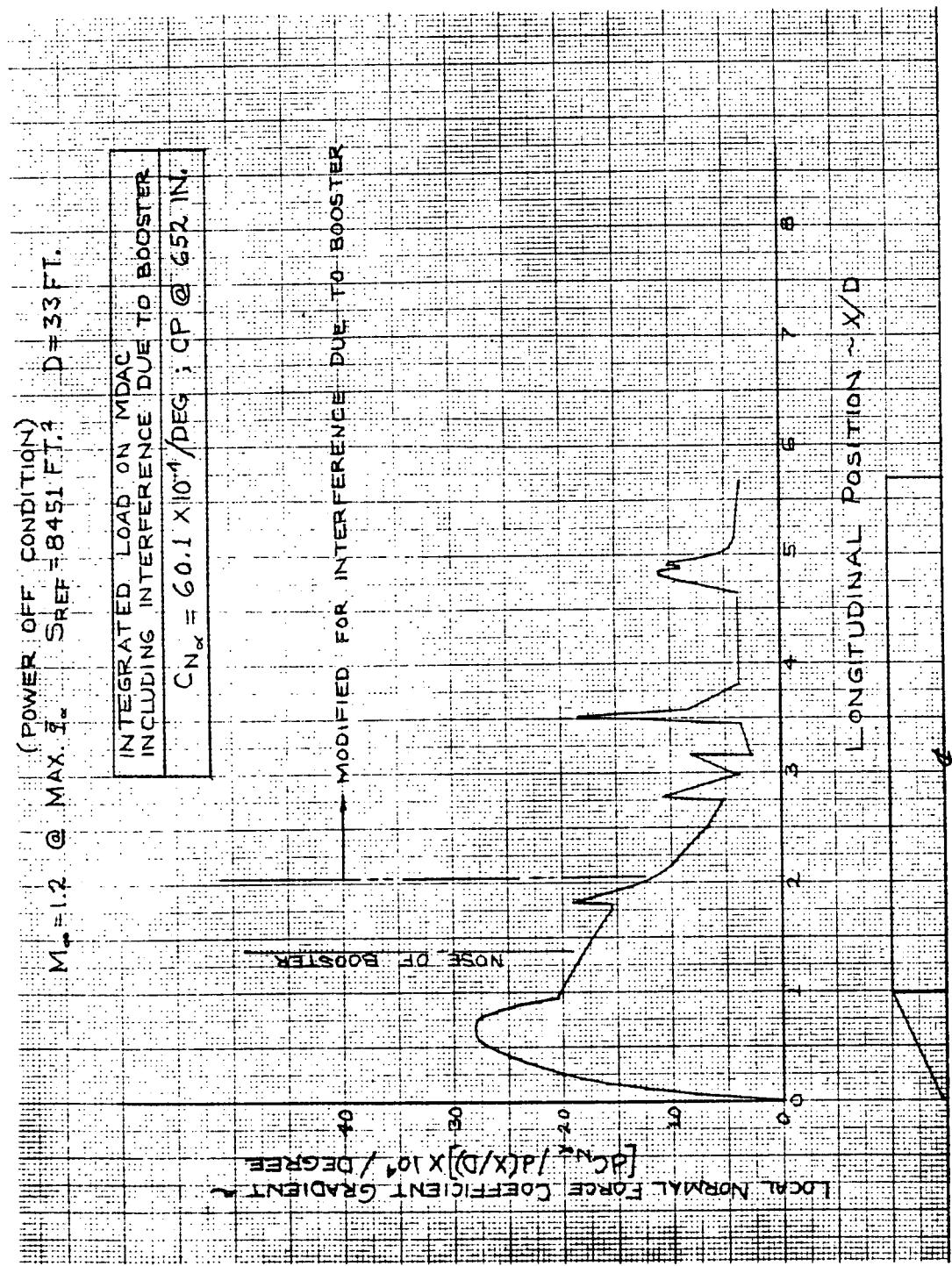


Figure 5-46. Distribution of Local Normal Force Coefficient Slope for MDAC

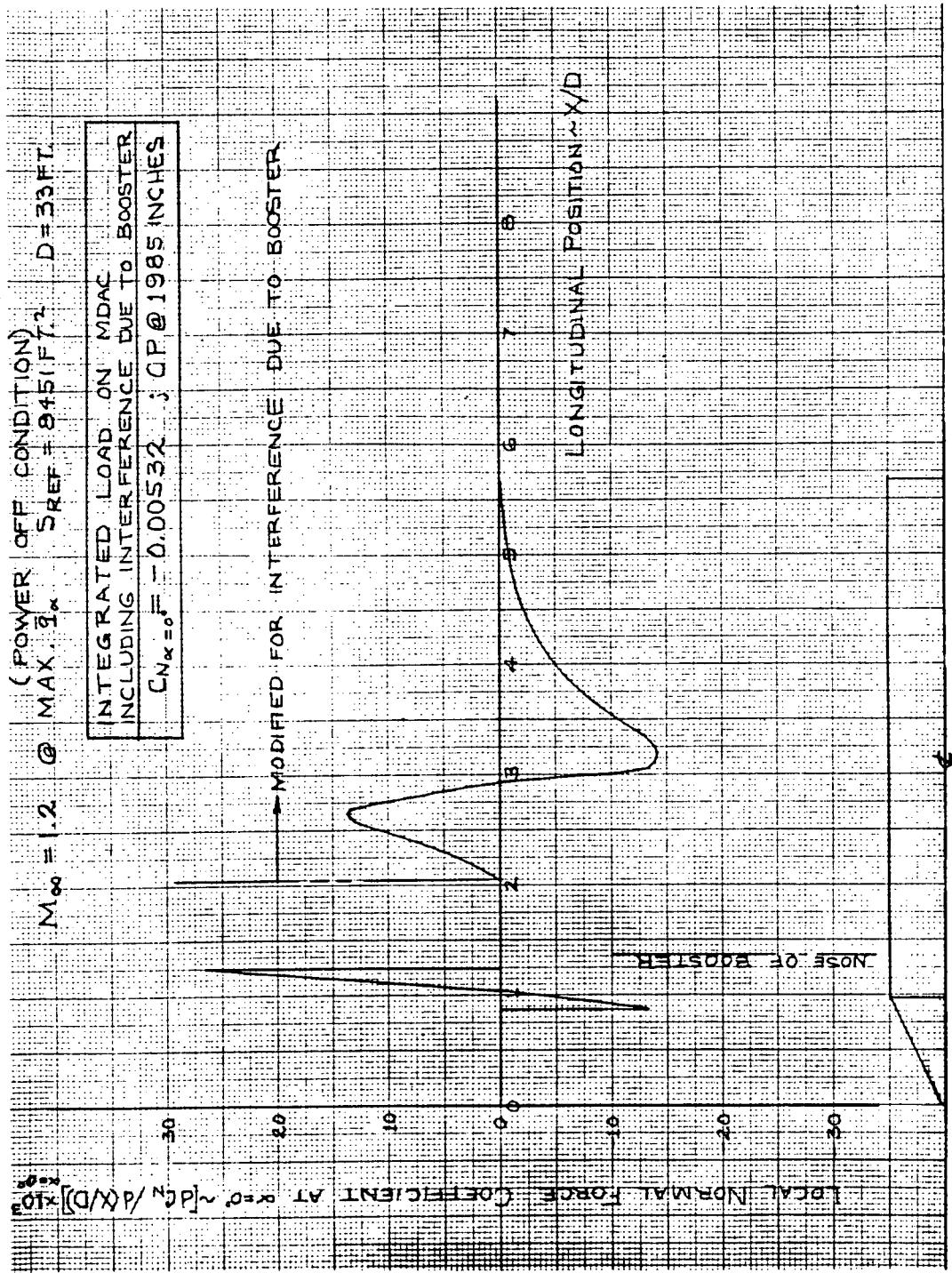


Figure 5-47. Distribution of Local Normal Force Coefficient for MDAC

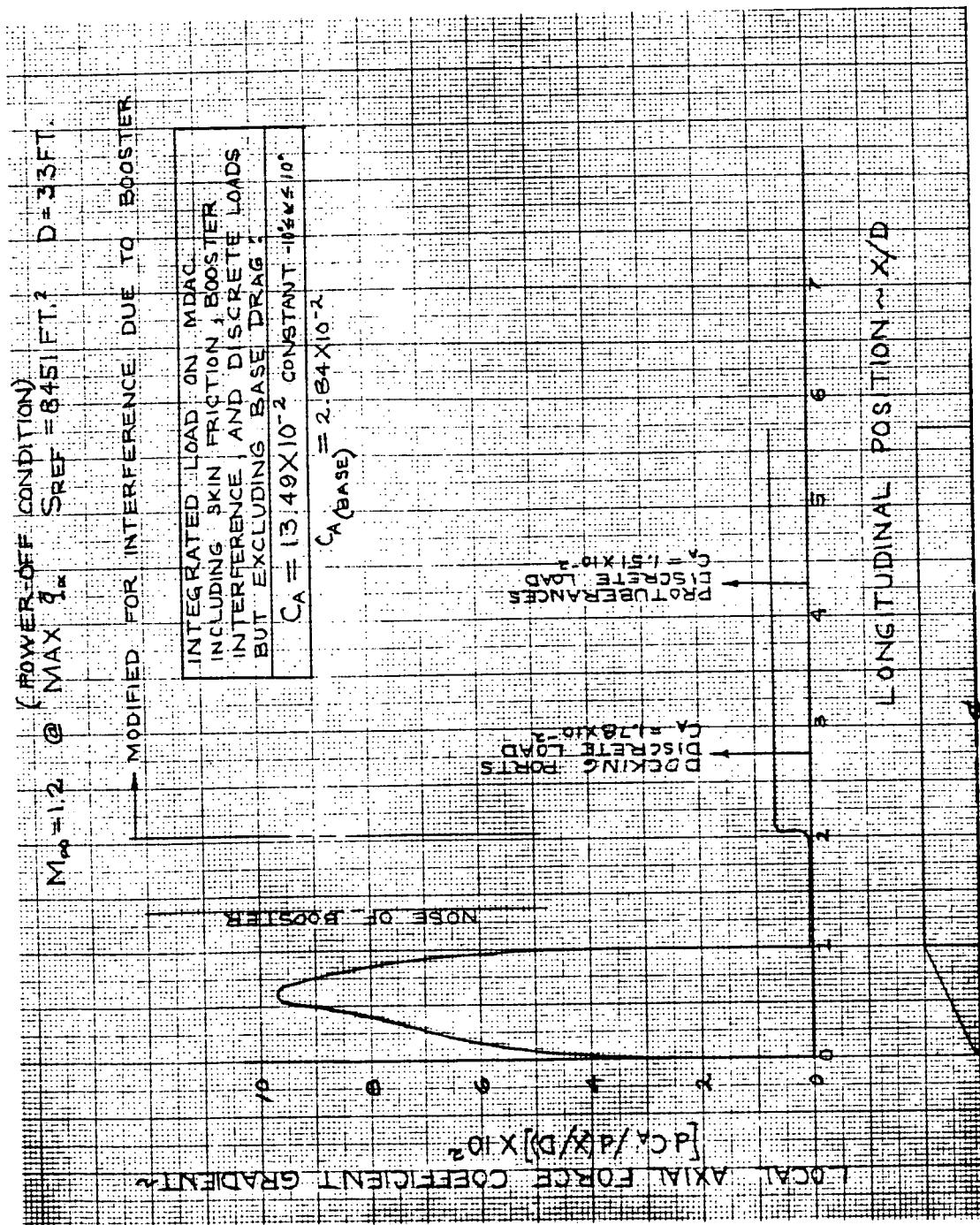


Figure 5-48. Distribution of Local Axial Force Coefficient for MDAC

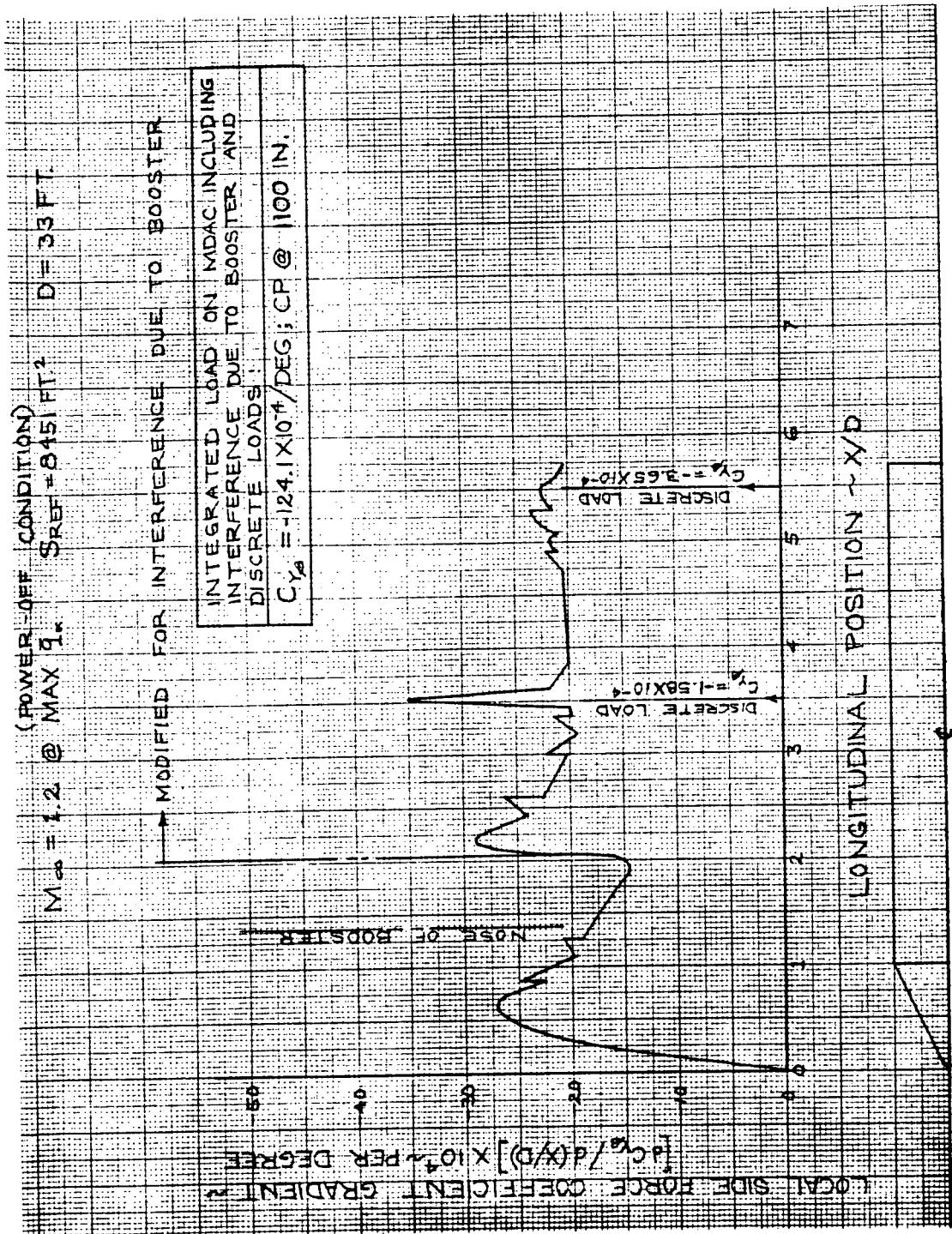


Figure 5-49. Distribution of Local Side Force Coefficient for MDAC

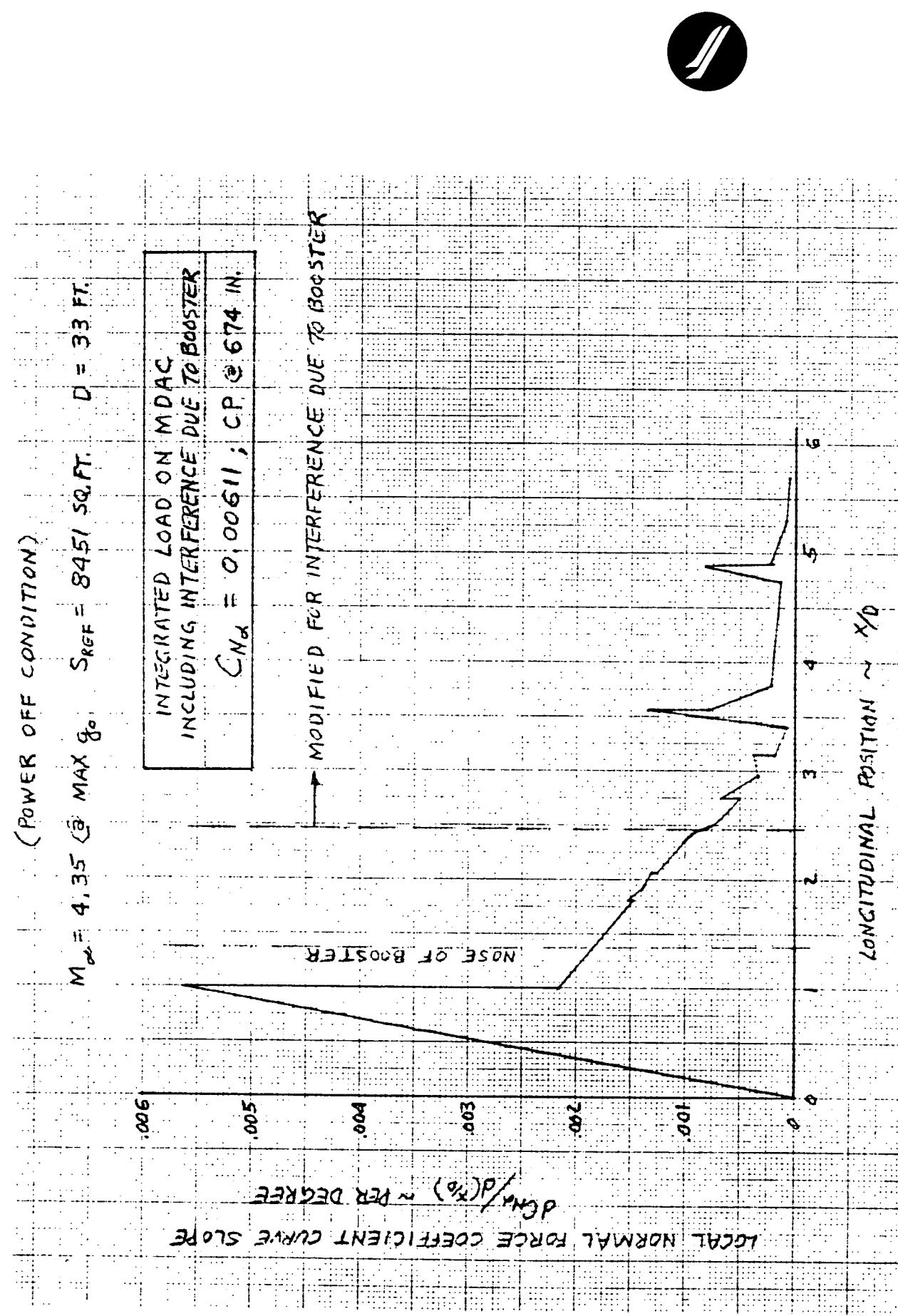


Figure 5-50. Distribution of Local Normal Force Coefficient Slope for MDAC

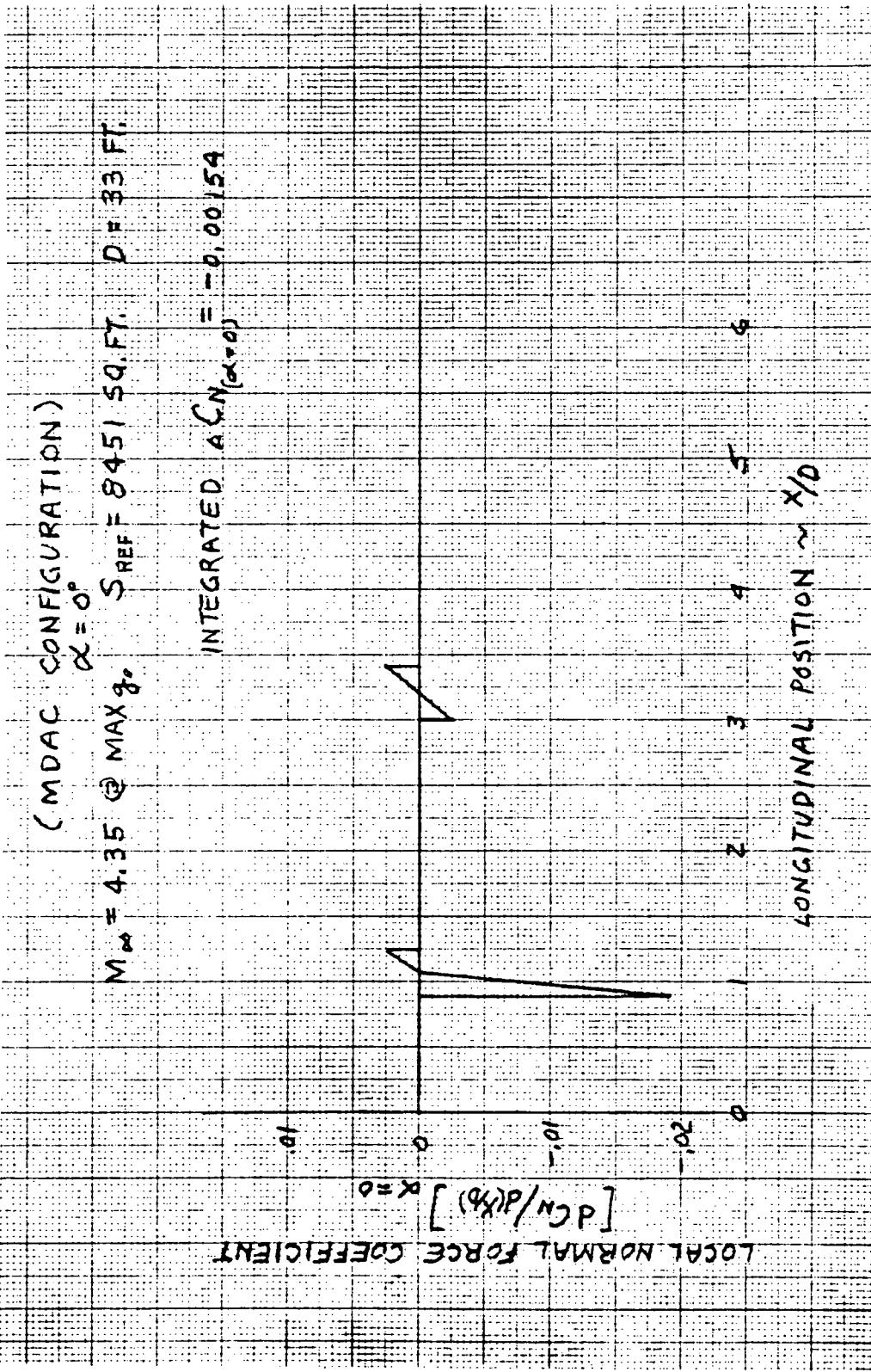


Figure 5-51. Distribution of Docking Ports Normal Force Coefficient

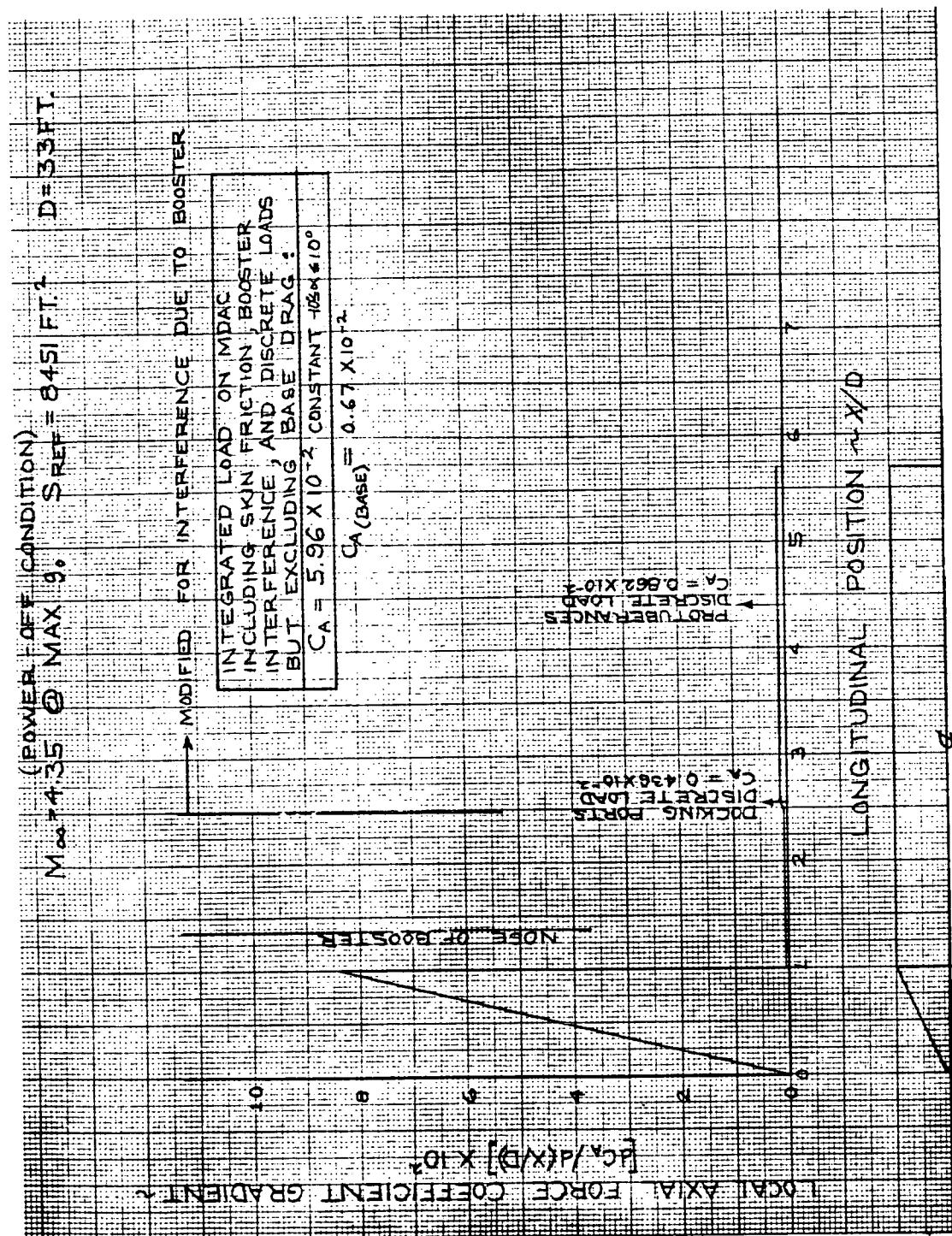


Figure 5-52. Distribution of Local Axial Force Coefficient for MDAC

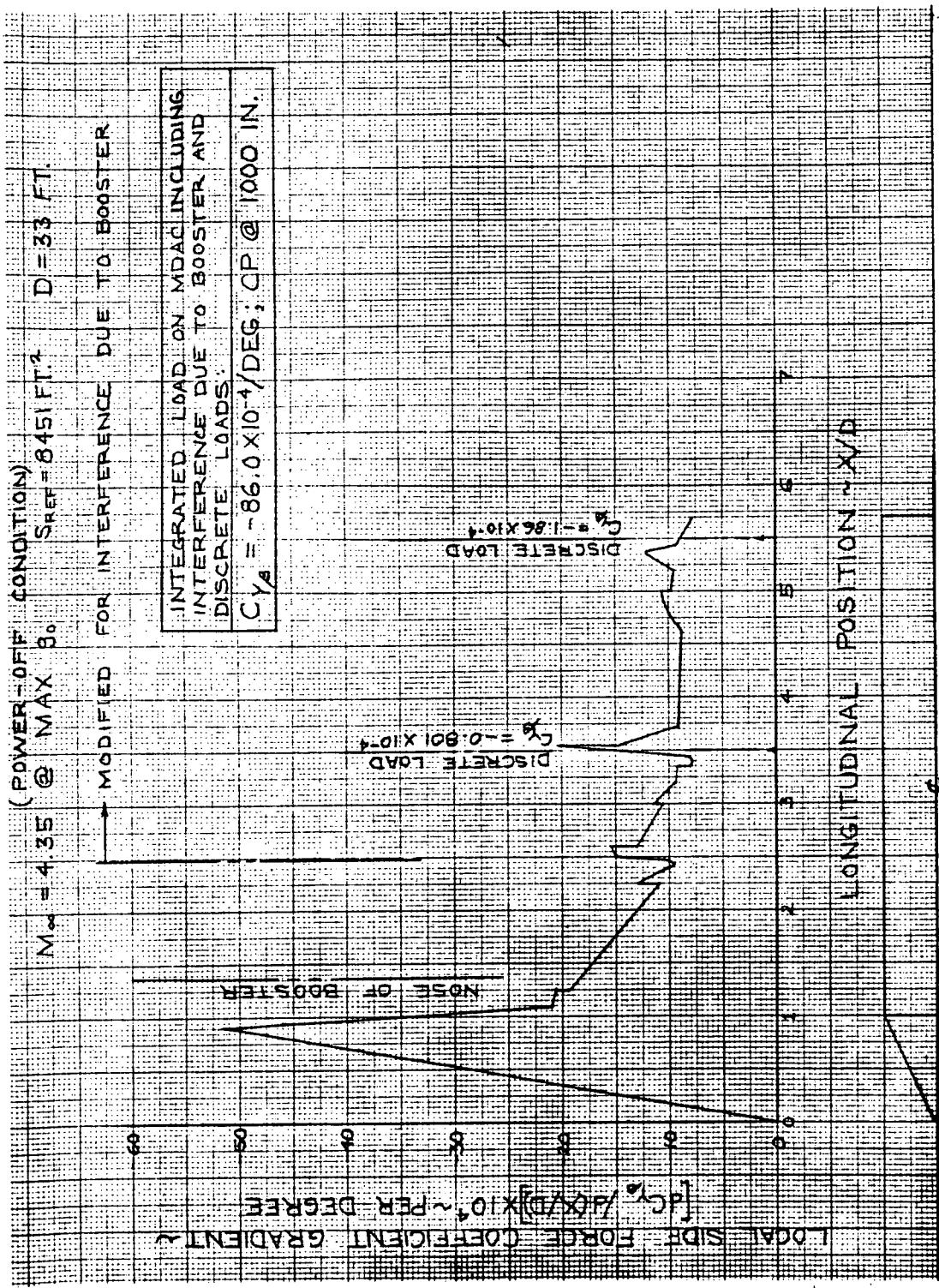


Figure 5-53. Distribution of Local Side Force Coefficient for MDAC

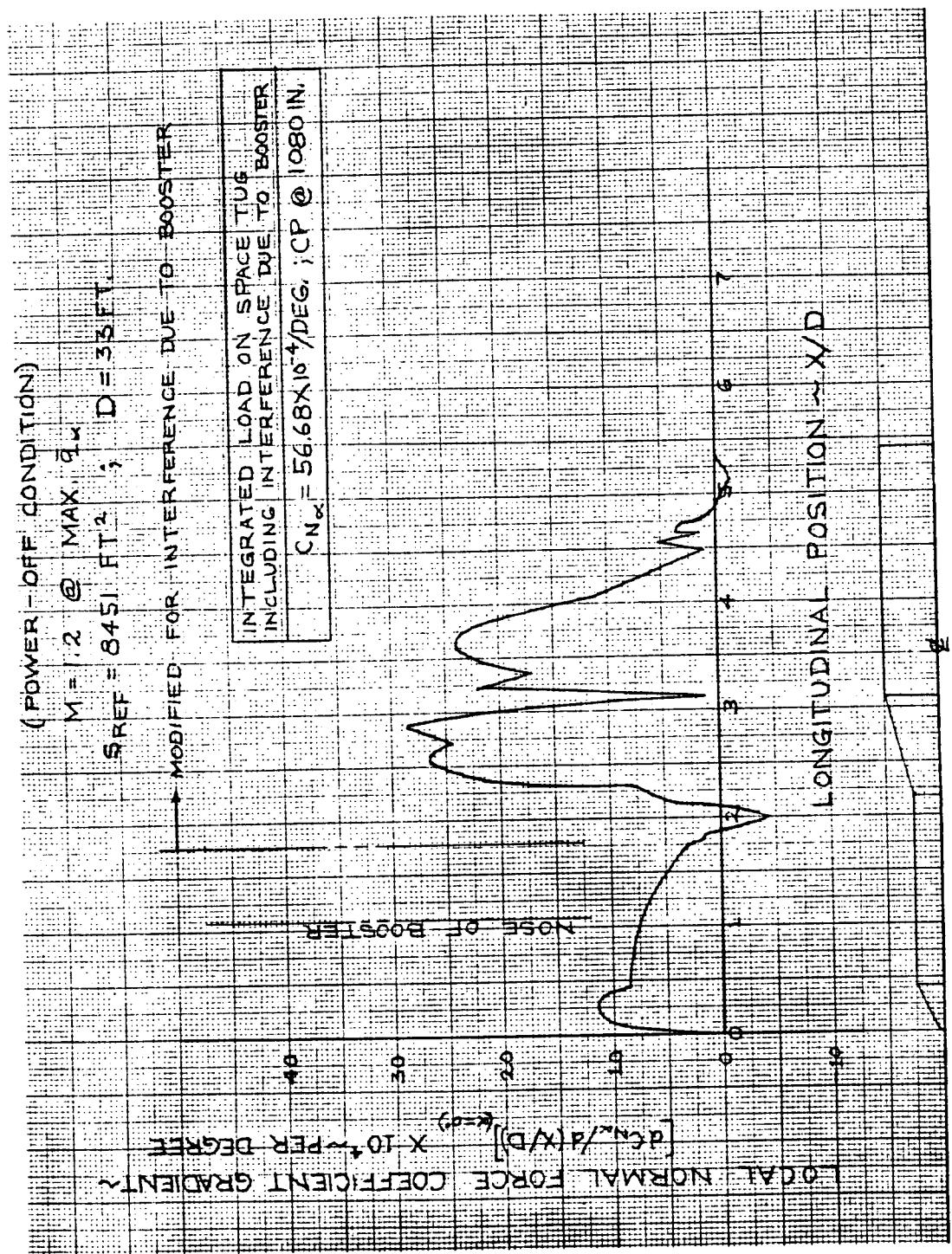


Figure 5-54. Distribution of Local Normal Force Coefficient for Space Tug.

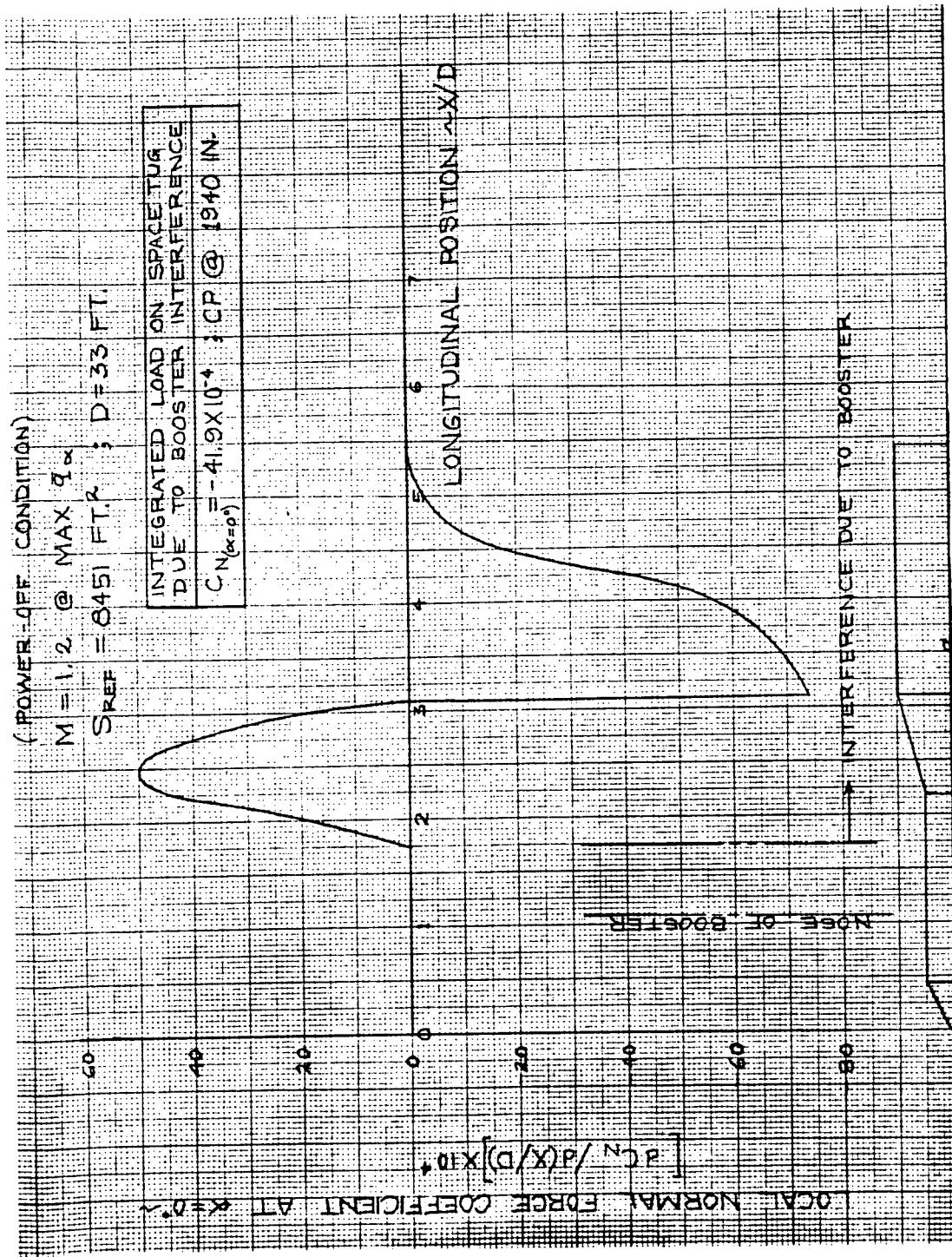


Figure 5-55. Distribution of Local Normal Force Coefficient
at $\alpha = 0$ Degrees for Space Tug

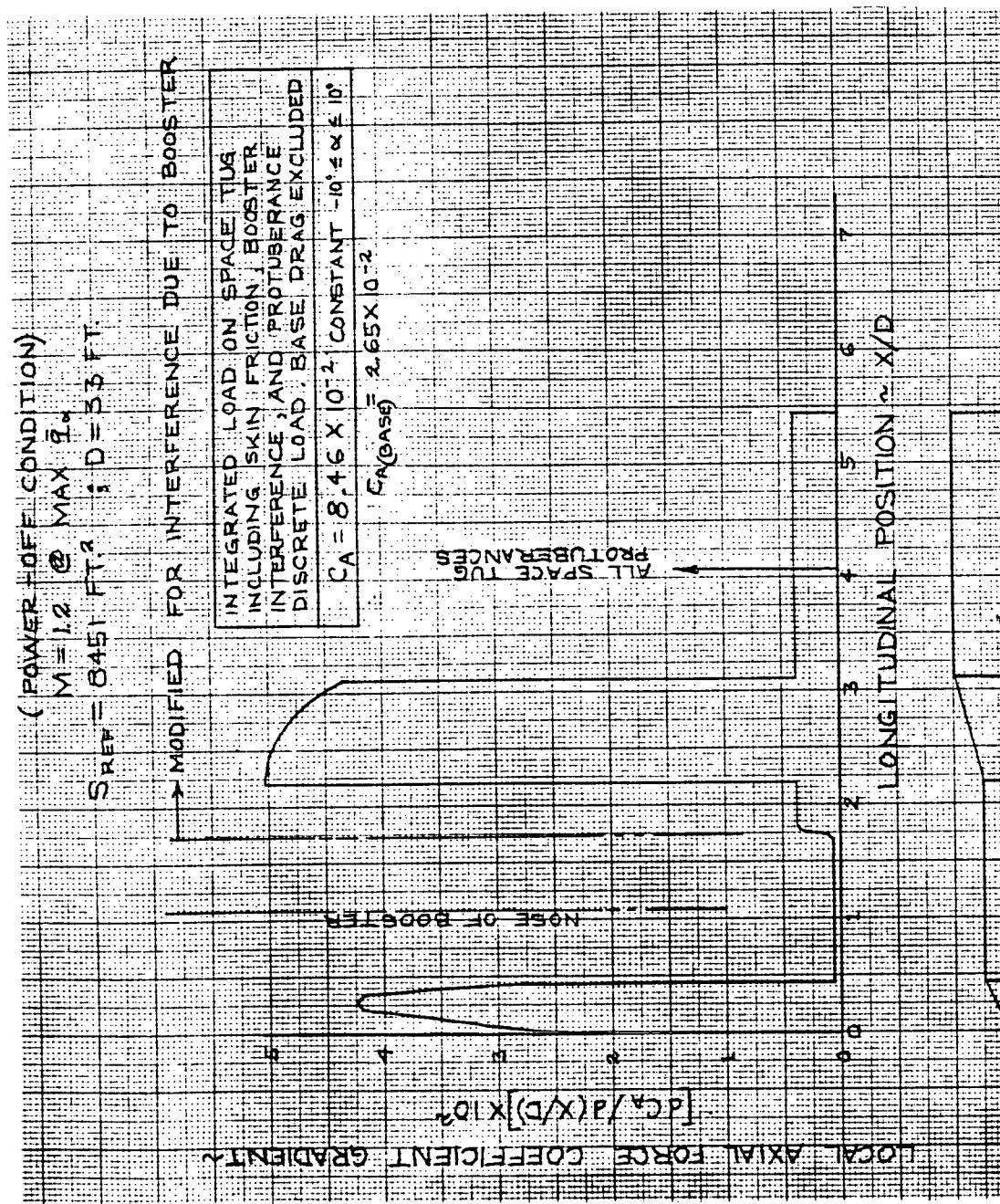


Figure 5-56. Distribution of Local Axial Force Coefficient for Space Tug

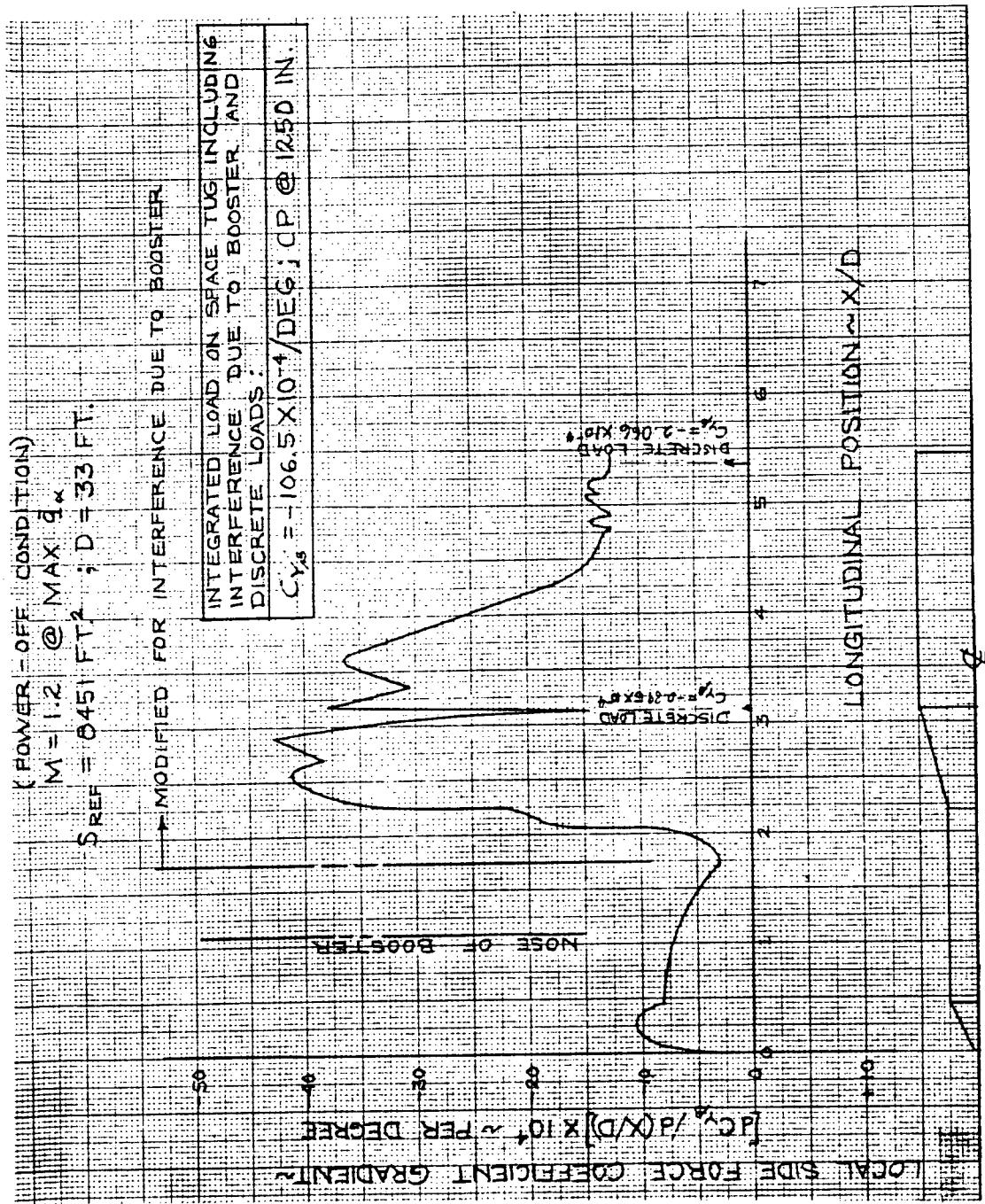


Figure 5-57. Distribution of Local Side Force Coefficient for Space Tug

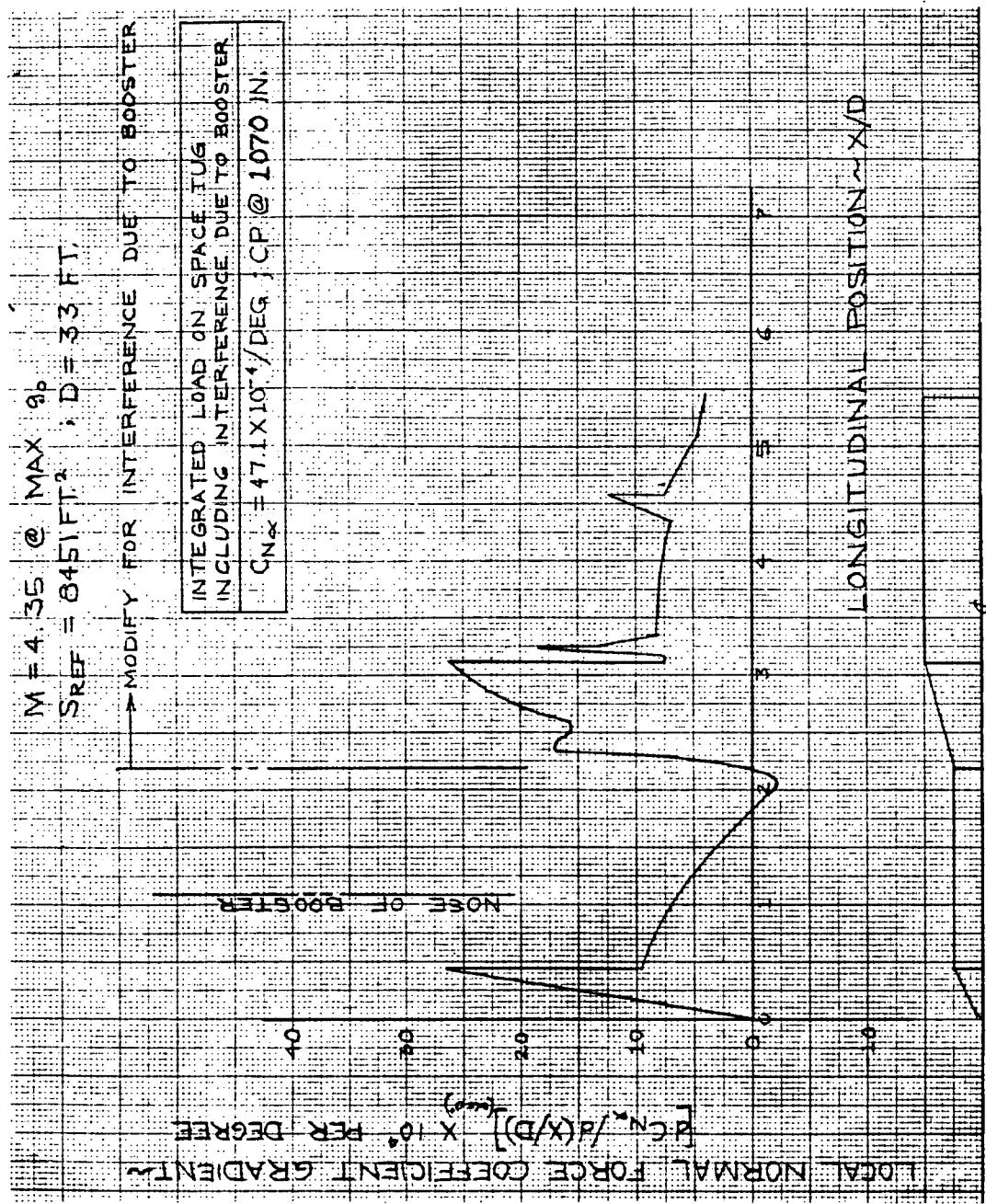


Figure 5-58. Distribution of Local Normal Force Coefficient for Space Tug

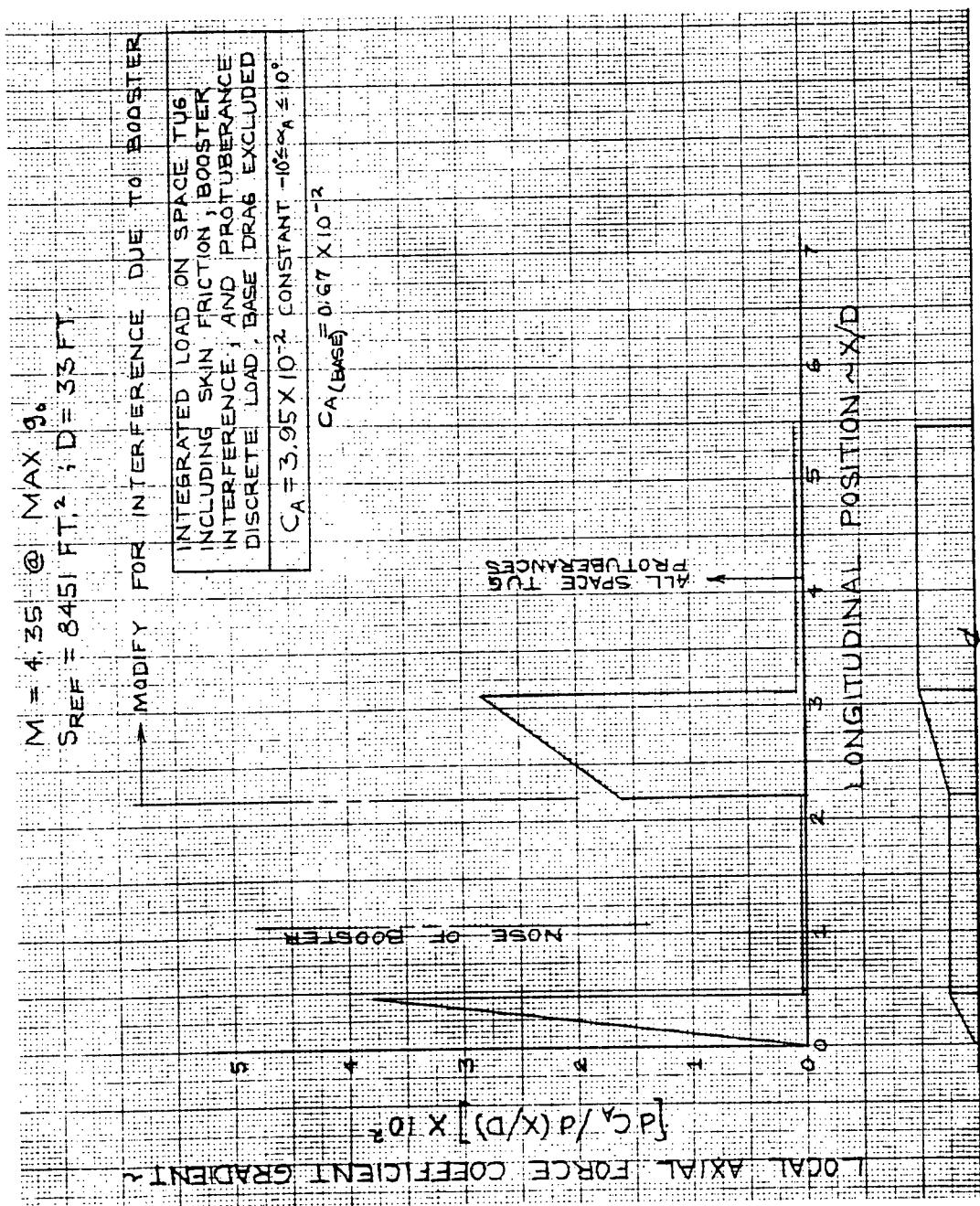


Figure 5-59. Distribution of Local Axial Force Coefficient for Space Tug

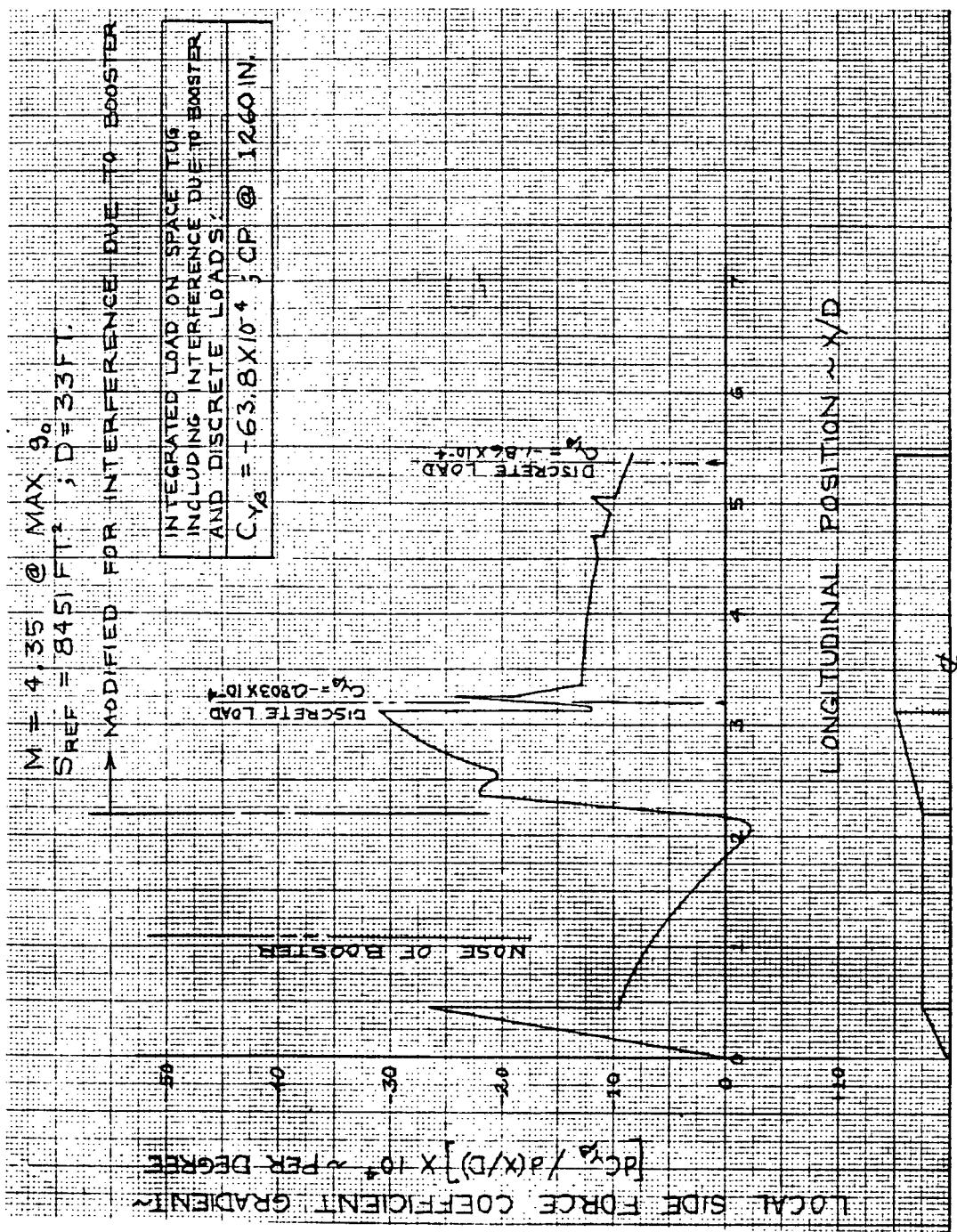


Figure 5-60. Distribution of Local Side Force Coefficient for Space Tug

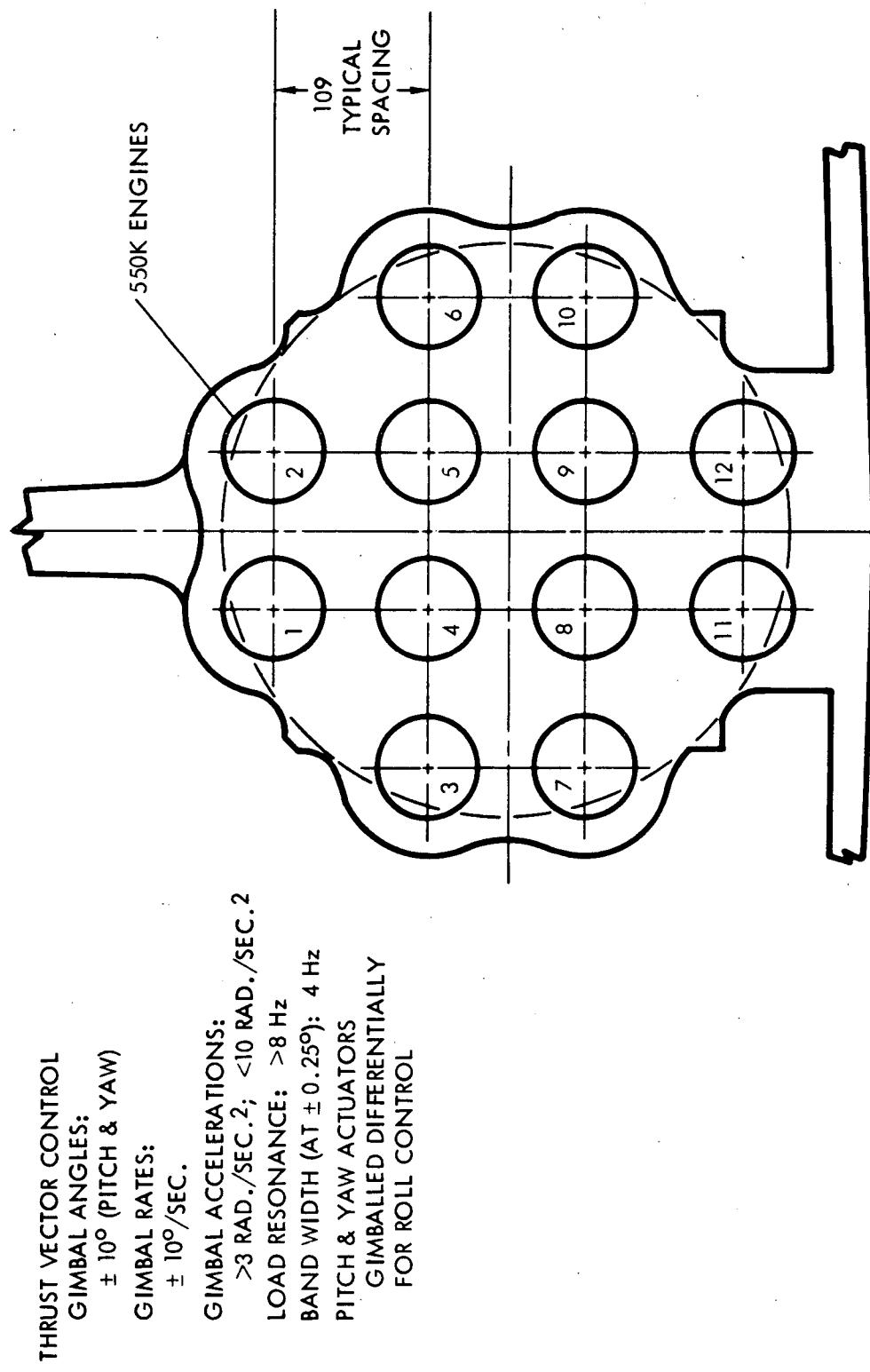


Figure 5-61. Booster Engine Arrangement and TVC Requirements



To minimize the amount of structural strengthening required in the area of the interstage attach points, aerodynamic loading limits were established which were less than those applicable to the shuttle launch vehicle. In particular, during the maximum dynamic pressure region of flight, these limits can be interpreted to constrain αq to be within +1500 and -2900 degrees psf, and βq within ± 1600 degrees psf. These constraints must be satisfied for the shuttle synthetic design wind conditions shown in Figure 5-62.

Both trajectory shaping and load relief techniques are to be employed as required to satisfy the αq and βq constraints. The use of load relief in the pitch control plane represents a modification (software only) to the shuttle booster attitude control system. However, the shuttle booster also utilizes load relief in the yaw plane, primarily to solve the yaw-roll aerodynamic coupling problem.

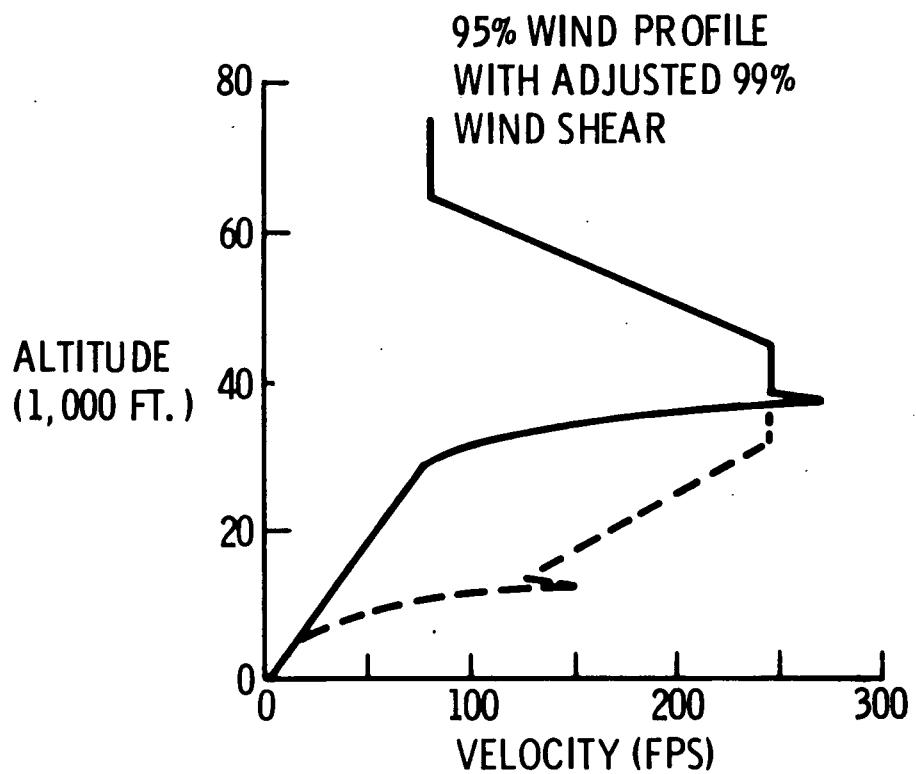
Booster Attitude Control System. A block diagram of the booster attitude control system is shown in Figure 5-63. Figure 5-64 illustrates the control logic that was used in this controls study.

In the pitch plane, load relief by gimbal limiting was studied for all three launch vehicle configurations with the limits shown in Figure 5-64. Limiting the attitude error signal to the same or slightly tighter limits than those applied to the commanded engine gimbal angle provides partial rate compensation during the limiting periods. This compensation is necessary to obtain satisfactory rigid body response characteristics and to provide phase stabilization for some vehicle parasitic modes. Angle-of-attack (normal accelerometer) feedback load relief was also studied for one of the RNS trajectories that was analyzed, but proper trajectory shaping precludes the need for this in pitch.

Angle of sideslip (lateral accelerometer) feedback load relief was studied for all three ESS configurations. The use of the elevon aerodynamic surfaces for roll control was also analyzed with the ratio of three degrees of commanded elevon deflection for each degree of commanded engine deflection.

These load relief systems are used only in the maximum dynamic pressure region of flight. For flight times beyond this region ($t > 100$ seconds), the aerodynamic loads are not large enough to require load relief.

The primary purpose of the ascent phase control simulations is to determine the control law and TVC deflections necessary to assure that the



MUST CONSIDER:
WIND FROM ANY DIRECTION WITH RESPECT TO PITCH PLANE,
DUE TO ALL-AZIMUTH LAUNCH

Figure 5-62. Design Winds

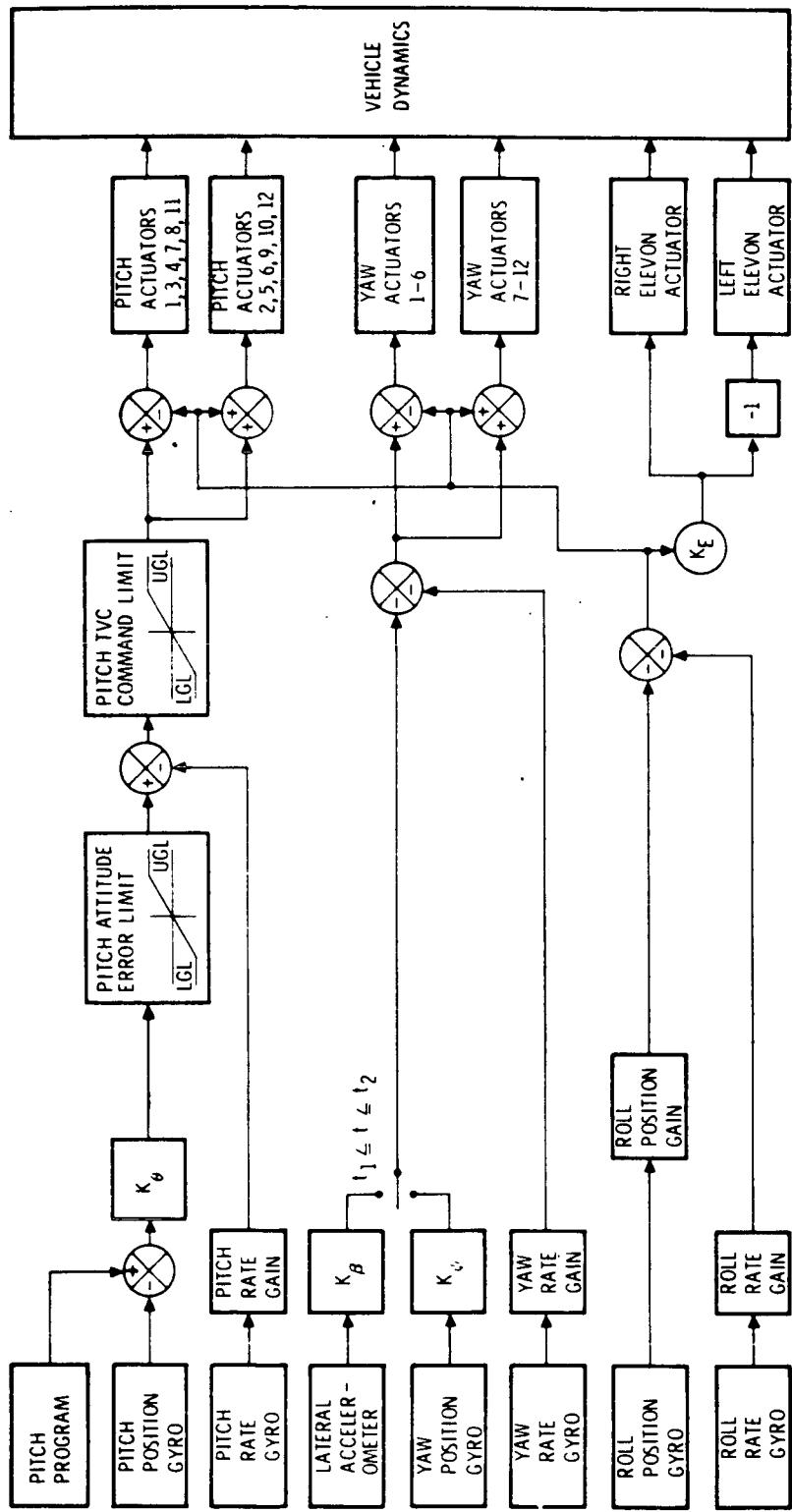


Figure 5-63. Boost Phase Control System

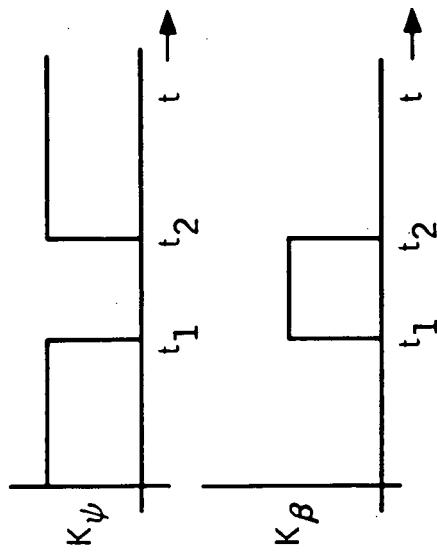
PITCH PLANE

GIMBAL LIMIT LOAD RELIEF

	RNS	SPACE STATION	SPACE TUG
UGL	2.5°	3.0°	3.0°
LGL	-2.5°	-2.5°	-3.0°
	ATTITUDE ERROR UPPER LIMIT		
UGL	TVC COMMAND UPPER LIMIT		
	ATTITUDE ERROR LOWER LIMIT		
LGL	TVC COMMAND LOWER LIMIT		

YAW/ROLL (ESS/ALL 3 PAYLOADS)

LOAD RELIEF



$t_1 = 62 \text{ SEC.}, t_2 = 100 \text{ SEC}$

ELEVONS FOR ROLL CONTROL

$K_E = 0 \text{ OR } K_E = 3.0$

Figure 5-64. Control Logic



vehicle can be controlled in the expected external environment (winds, etc.) and to control the expected internal environment (sloshing and bending), thus assuring that the vehicle has adequate control authority.

Stabilizing body bending and sloshing is accomplished in two ways. First, control loop gains are kept low. Second, appropriate filtering of sensor signals is required to control the phase shift in the closed-loop control system. The control-loop gain can be kept low so long as the vehicle is aerodynamically stable in pitch and yaw. Since configuration changes obviated any detailed sloshing or bending analysis early in the study, a decision was made to allow ± 0.4 -degree gimbal angle in pitch and in yaw for slosh suppression and ± 0.25 degree in each axis for bending suppression.

Primary concern during the ascent phase is the potential coupling between rigid body control, sloshing, and vehicle structural modes. For the B-9U/161C shuttle configuration, the frequencies are similar to the Saturn/Apollo as indicated by Table 5-3. Proper control should be possible with state-of-the-art control techniques.

Table 5-3. Frequency at Liftoff

Vehicle	Rigid Body (Hz)	Slosh (Hz)	Flexible Vehicle (Hz)
B-9U/161C	0.24	0.36	0.91
Saturn/Apollo	0.2	0.2	1.00
B-9U/ESS	0.24	0.35	0.75

Comparison with the B-9U/ESS shows the spread between rigid body and flexible vehicle modes remains sufficiently large. The sloshing mode is closer to the flexible vehicle mode but should not cause instability. If a problem did exist, the most probable solution would be to add several baffles near the top of the liquid oxygen tank thereby increasing the slosh mode damping.

Since the vehicle must continue to be operational after one main engine failure and fail safe after two engine failures, some allowance in the gimbal requirements must be made for this. Two engines failed with all others thrusting can cause the thrust vector of all others to be rotated about 1.4 degrees for trim of pitch or yaw gimbals. Similarly, by failing the thrust of one engine just before the peak wind shear and gust, the thrust of all other engines overshoots about 1.5 degrees (pitch or yaw) before returning to the static offset. It was decided that the allowance of ± 1.5 degrees for engine failure would cover both of these eventualities, and this was



utilized as an engine failure allowance. When these allowances are applied along with the center-of-gravity travel and the effects of winds, head, tail, or side as the case may be, a total control requirement can be generated. Therefore, the allowances for sloshing, bending, and engine-out capability used for shuttle B-9U booster/161C orbiter were considered applicable for B-9U booster/ESS.

Study Results — αq and βq Constraints.

1. Trajectory Design. To minimize αq and βq , nominal no wind trajectories were designed to have a low maximum dynamic pressure and to have a desired angle of attack (α) in the maximum dynamic pressure region of flight.

The dynamic pressure for the ESS trajectories is shown in Figure 5-65.

The effect of variation in the nominal trajectory angle of attack at maximum dynamic pressure on max αq under head wind/tail wind conditions is illustrated in Figure 5-66. It is immediately evident from the dashed curves that trajectory shaping is not adequate to satisfy the αq constraints, and some form of load relief is required. With gimbal limit-load relief, the solid curves indicate that these constraints can be satisfied for the space station and RNS vehicles by a nominal trajectory with an angle of attack at maximum dynamic pressure of about -2 degrees. It will be subsequently shown that the αq constraints are also satisfied for the space tug vehicle.

Some of the consequences of these trajectory designs are:

- a. Minimum T/W = 1.2 after clearing the tower
- b. 50 percent (maximum) throttling at the end of booster flight
- c. Off-loading ESS stage propellants

It should be noted here that as a result of the third consideration, launch vehicle stability considerations may dictate that a specially located slosh baffle(s) be placed in the ESS tank(s).

By using a six-degree-of-freedom rigid-body simulation, the launch vehicle response to the design wind conditions was obtained. Two representative wind conditions were studied. The first and most critical is a shear buildup and gust occurring at the vehicle's

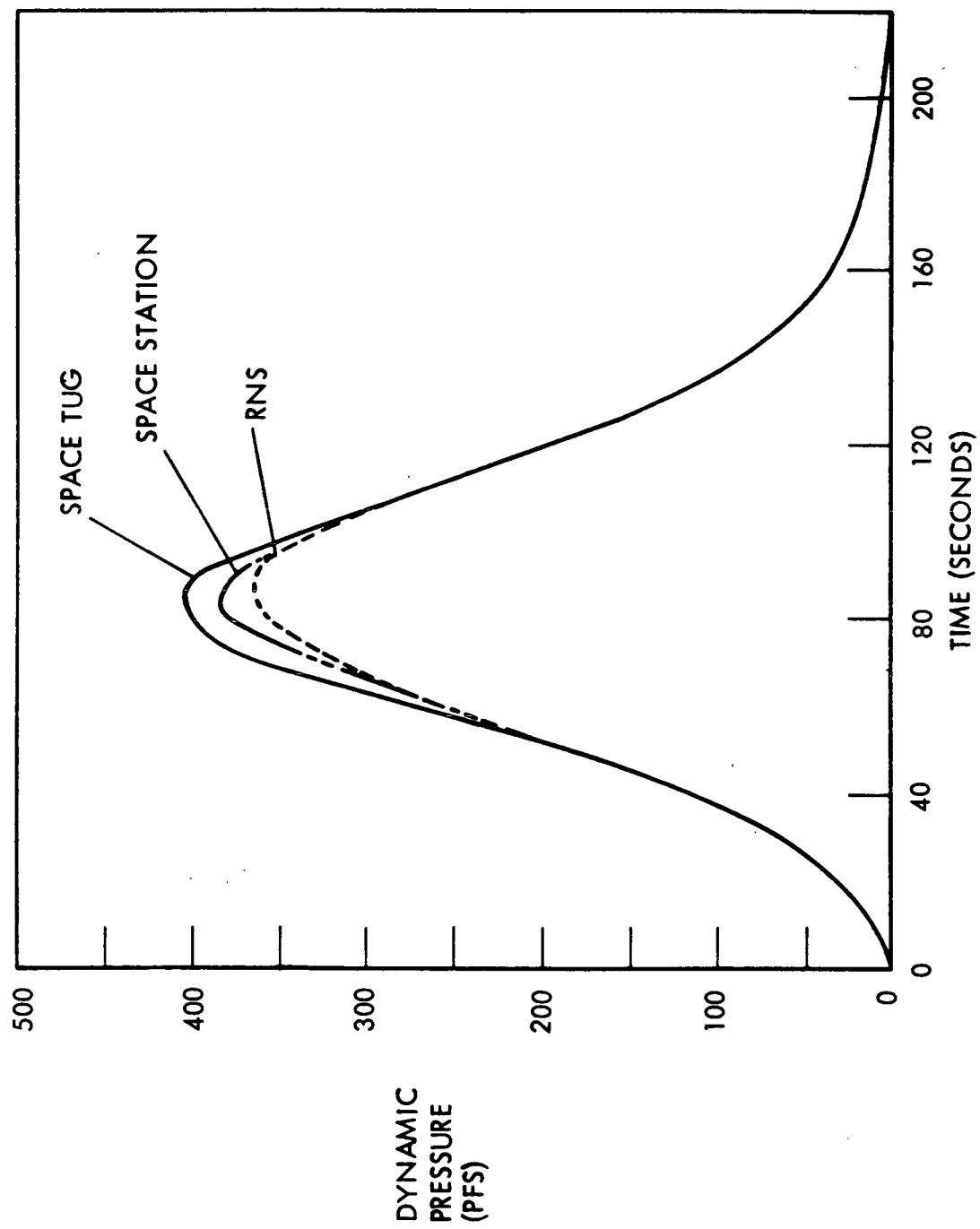


Figure 5-65. ESS Low q Ascent Trajectories

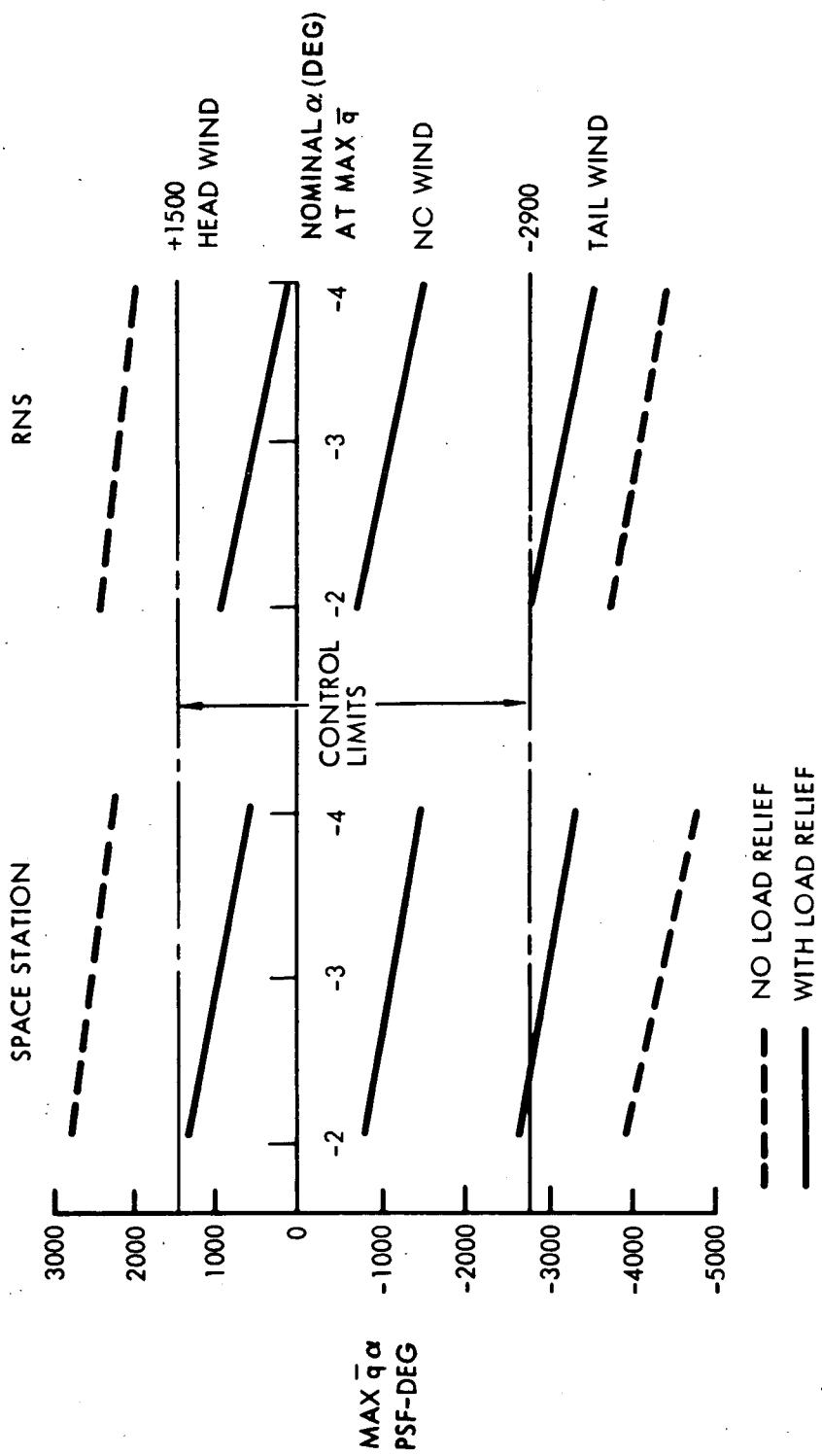


Figure 5-66. Effect of Variation in Nominal Trajectory on Max \bar{q}_α Gust at
 $h=36,000$ Feet



maximum dynamic pressure altitude (high-altitude head/tail winds and high-altitude cross winds). The second condition is a shear buildup and gust occurring at 10,000 feet (low-altitude winds).

2. High-Altitude Head/Tail Winds. The simulation head wind and tail wind trajectory data for each of the three launch vehicles is shown in Figures 5-67, 5-68, and 5-69. For each vehicle, the no-load relief case results in values of αq which exceed the +1500 and -2900 degrees-psf limits. However, with gimbal limit load relief, the peak values of αq are within these constraints for the space station, RNS and space tug vehicles.

For the gimbal limit-load relief cases, the gimbal limiting condition extends for about 5 to 10 seconds. These limiting times did not produce excessive trajectory dispersions.

Figure 5-70 summarizes the peak αq values for the head-wind and tail-wind conditions. It is clear that load relief is required to satisfy the αq constraints. It also appears that the nominal trajectory with a max q angle of attack near -2 degrees produces the desired negative αq bias in the maximum dynamic pressure region of flight.

3. High Altitude Cross Winds. The simulation cross wind trajectory data for each of the three launch vehicles is presented in Figures 5-71, 5-72, and 5-73. The no-load relief case exceeds the 1600 degrees-psf βq constraint by about a factor of three. Also, the large sideslip angles (approximately 12 degrees) result in excessive roll control moment requirements of 7 degrees of engine gimbal angle and 21 degrees of elevon surface deflection. This latter condition is produced by the high degree of aerodynamic yaw-roll coupling exhibited by these vehicles. Incorporating the β -feedback load relief system used in the shuttle booster results in peak values of βq within the constraint limits and roll control moment requirements within the capability of the TVC and elevon control systems.

Figure 5-74 summarizes the peak βq values for the cross-wind condition. The shuttle β -feedback load-relief system holds the peak βq values within the ± 1600 degrees-psf constraint.

4. Low Altitude Winds. At the lower altitudes and subsonic Mach numbers, the air loads are not as critical as they are at higher altitudes and transonic Mach numbers.

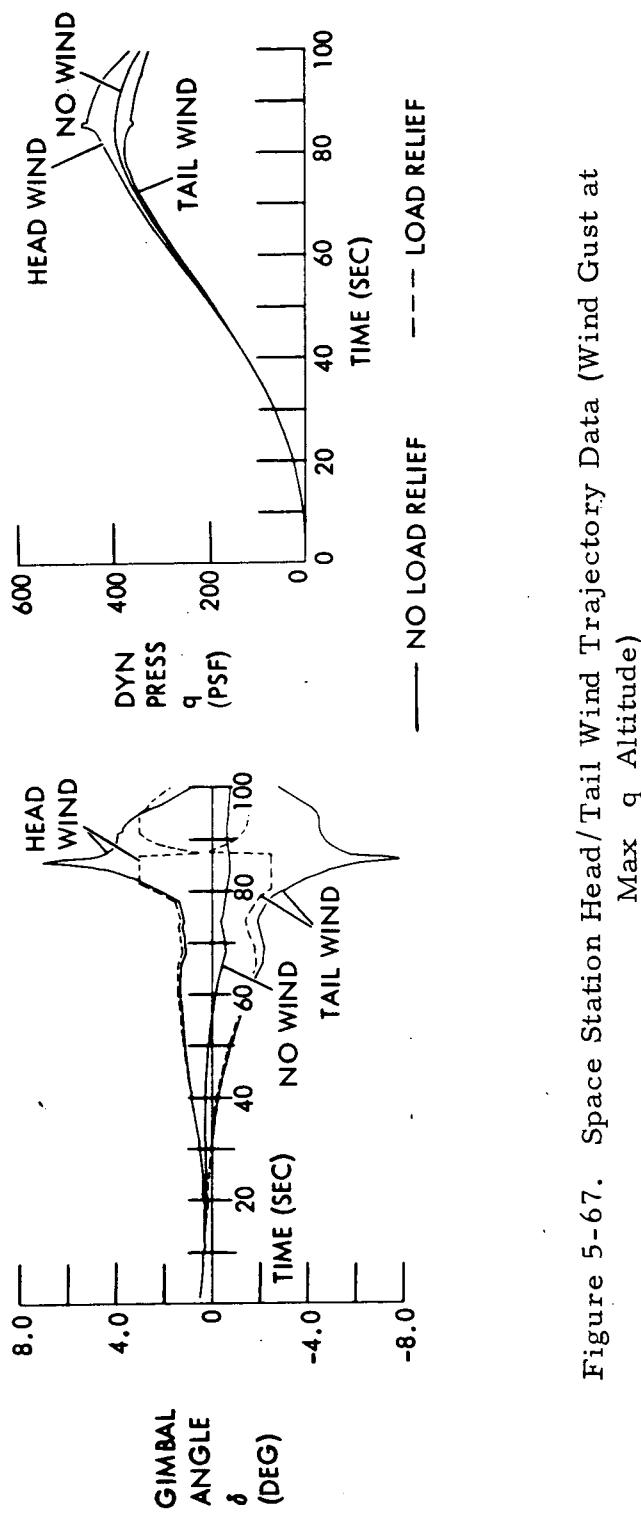
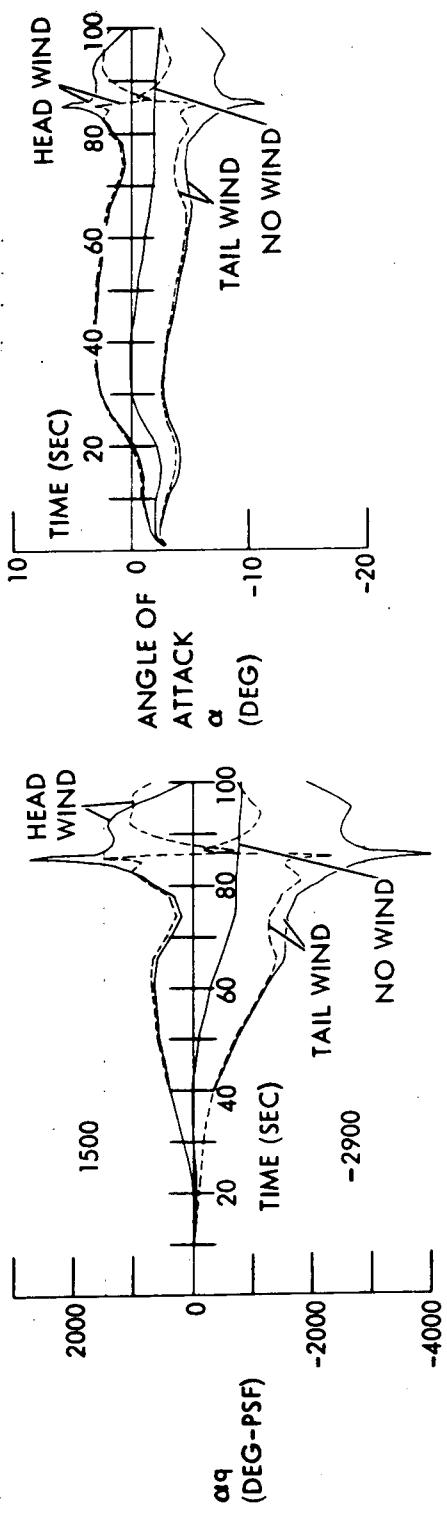


Figure 5-67. Space Station Head / Tail Wind Trajectory Data (Wind Gust at Max q Altitude)

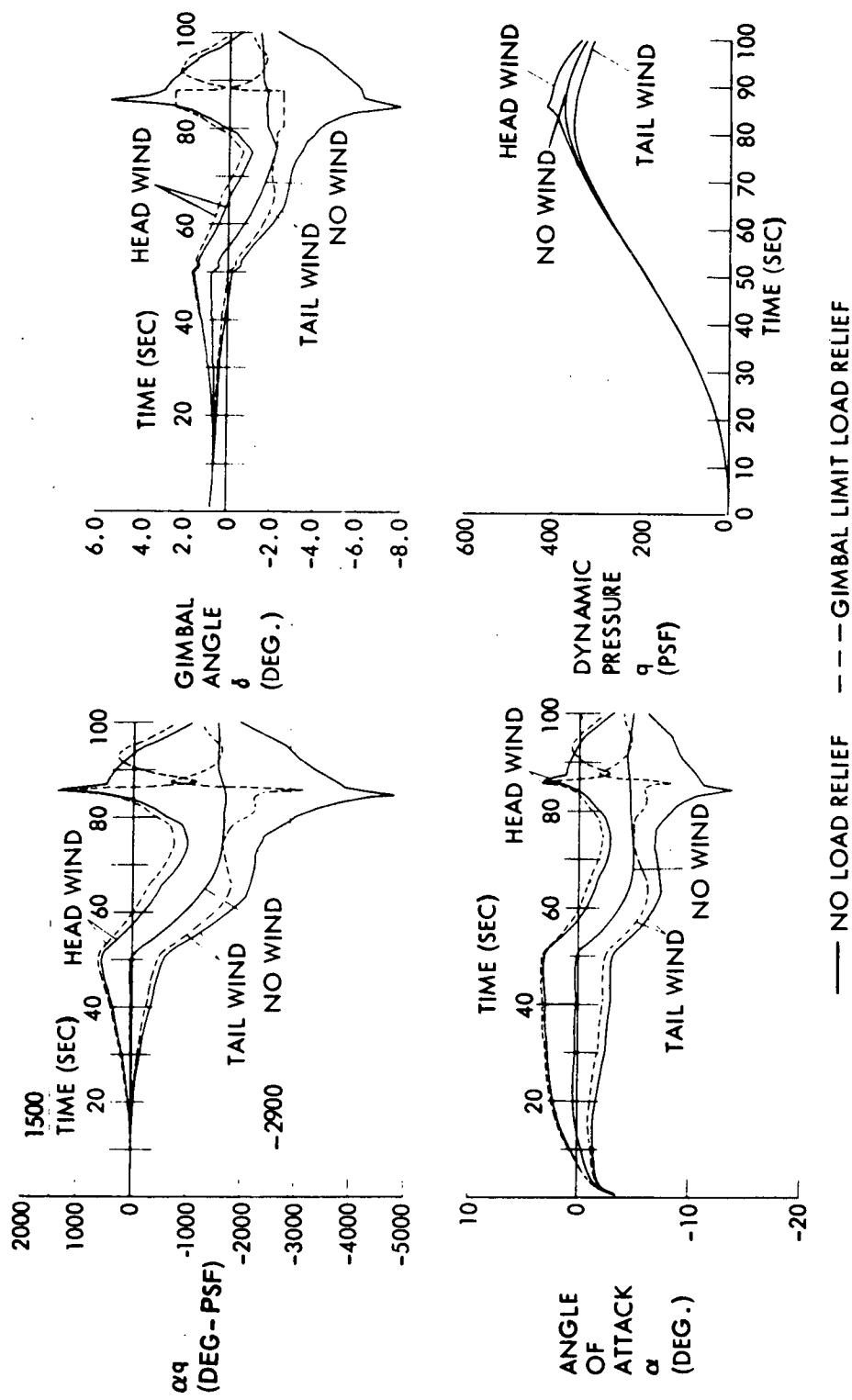


Figure 5-68. RNS Head/Tail Wind Trajectory Data (Wind Gust at Max q Altitude)

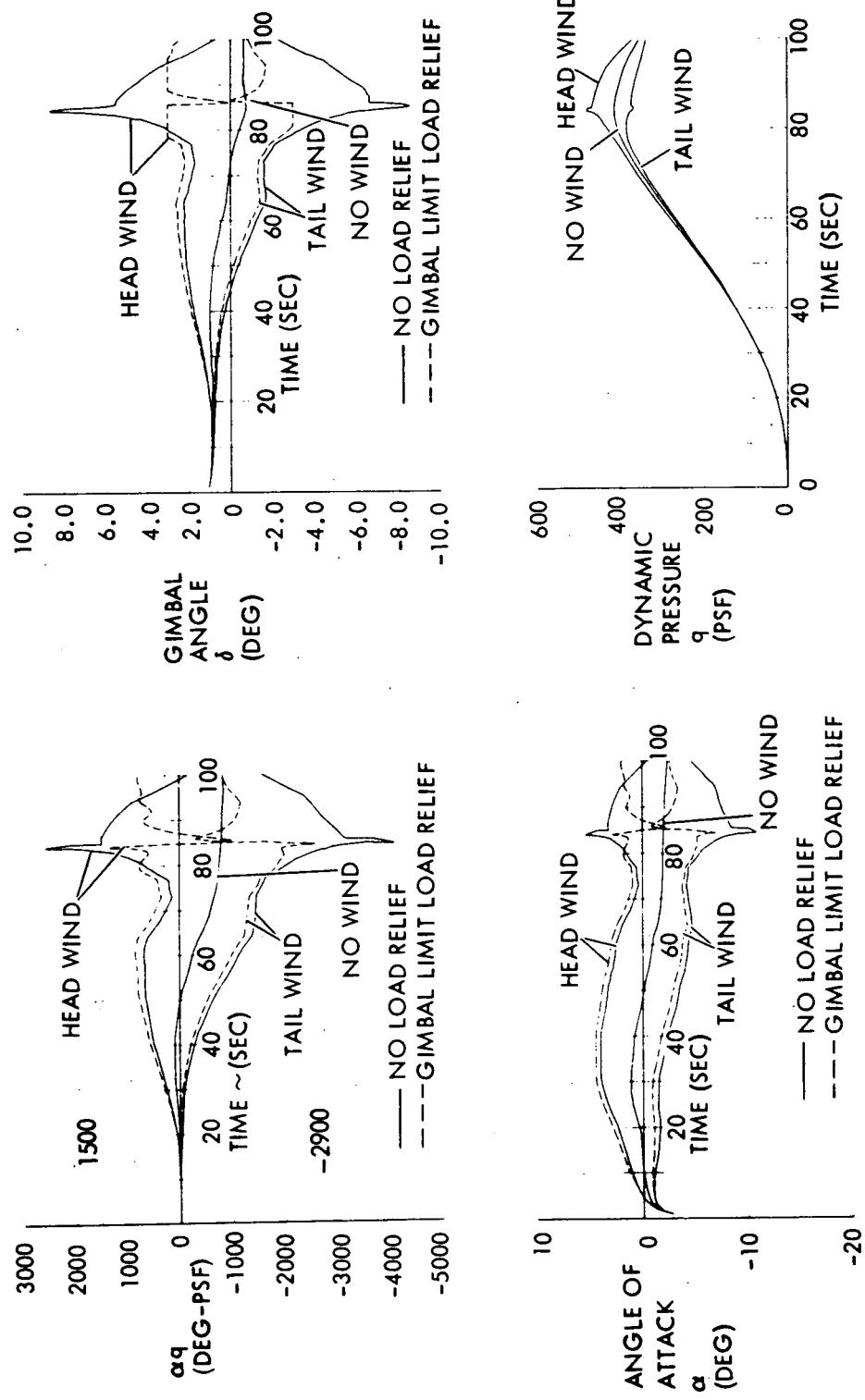


Figure 5-69. Space Tug Head / Tail Wind Trajectory Data (Wind Gust at Max q Altitude)
 — NO LOAD RELIEF
 - - - GIMBAL LIMIT LOAD RELIEF

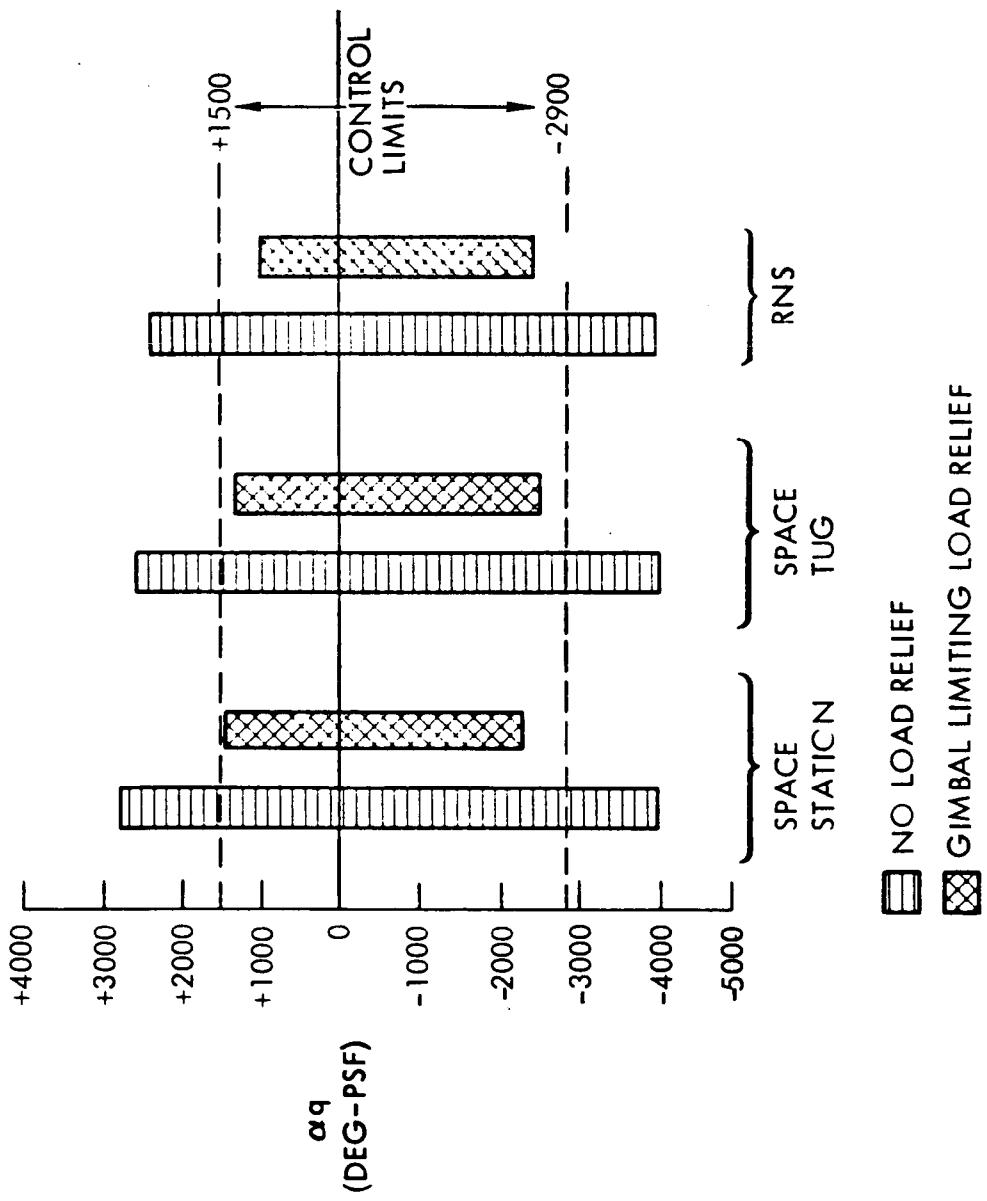


Figure 5-70. α_q Summary, Wind Gust at Max q Altitude

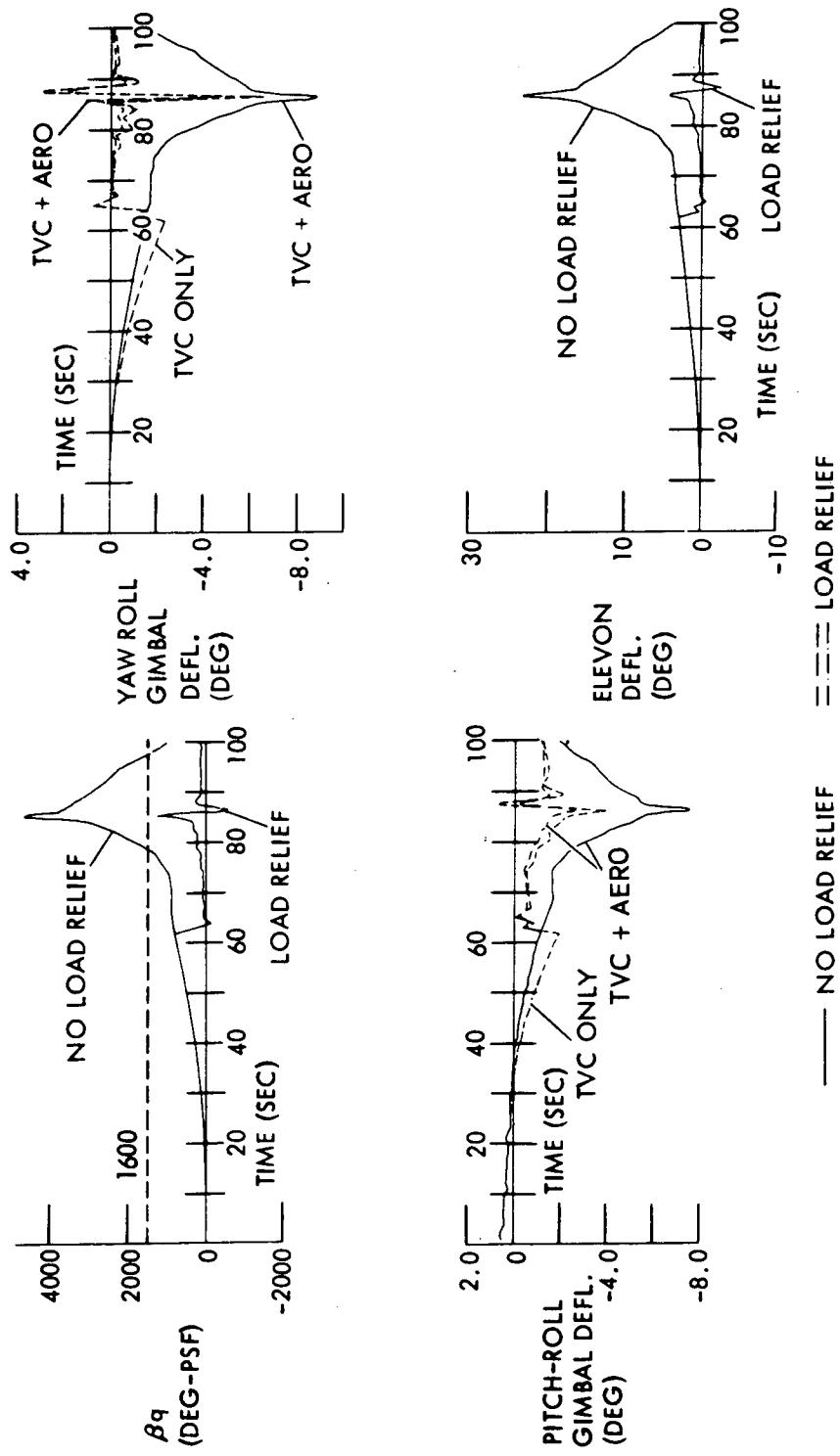


Figure 5-71. Space Station Crosswind Trajectory Data
(Wind Gust at Max q Altitude)

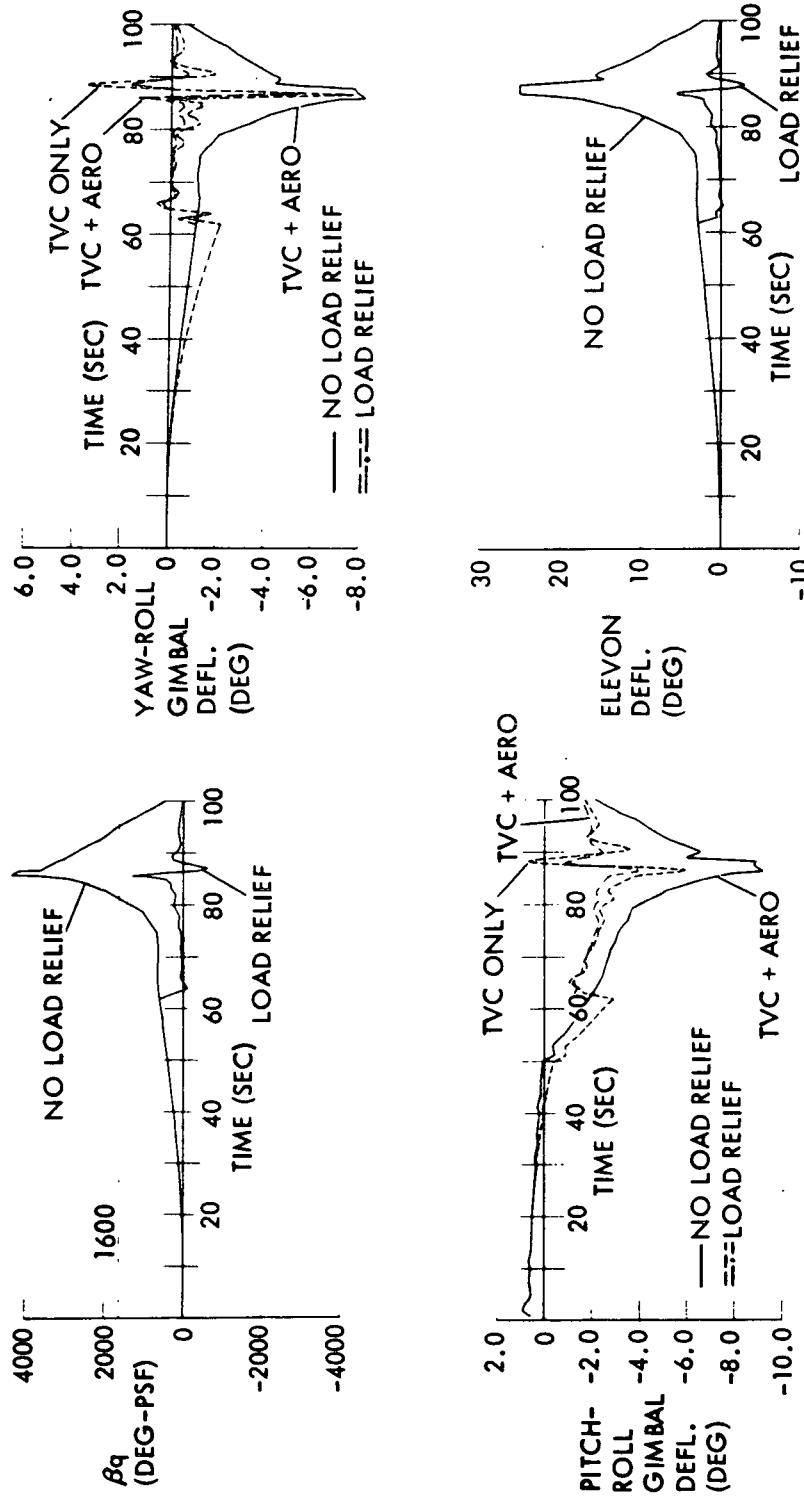


Figure 5-72. RNS Crosswind Trajectory Data (Wind Gust at Max q Altitude)

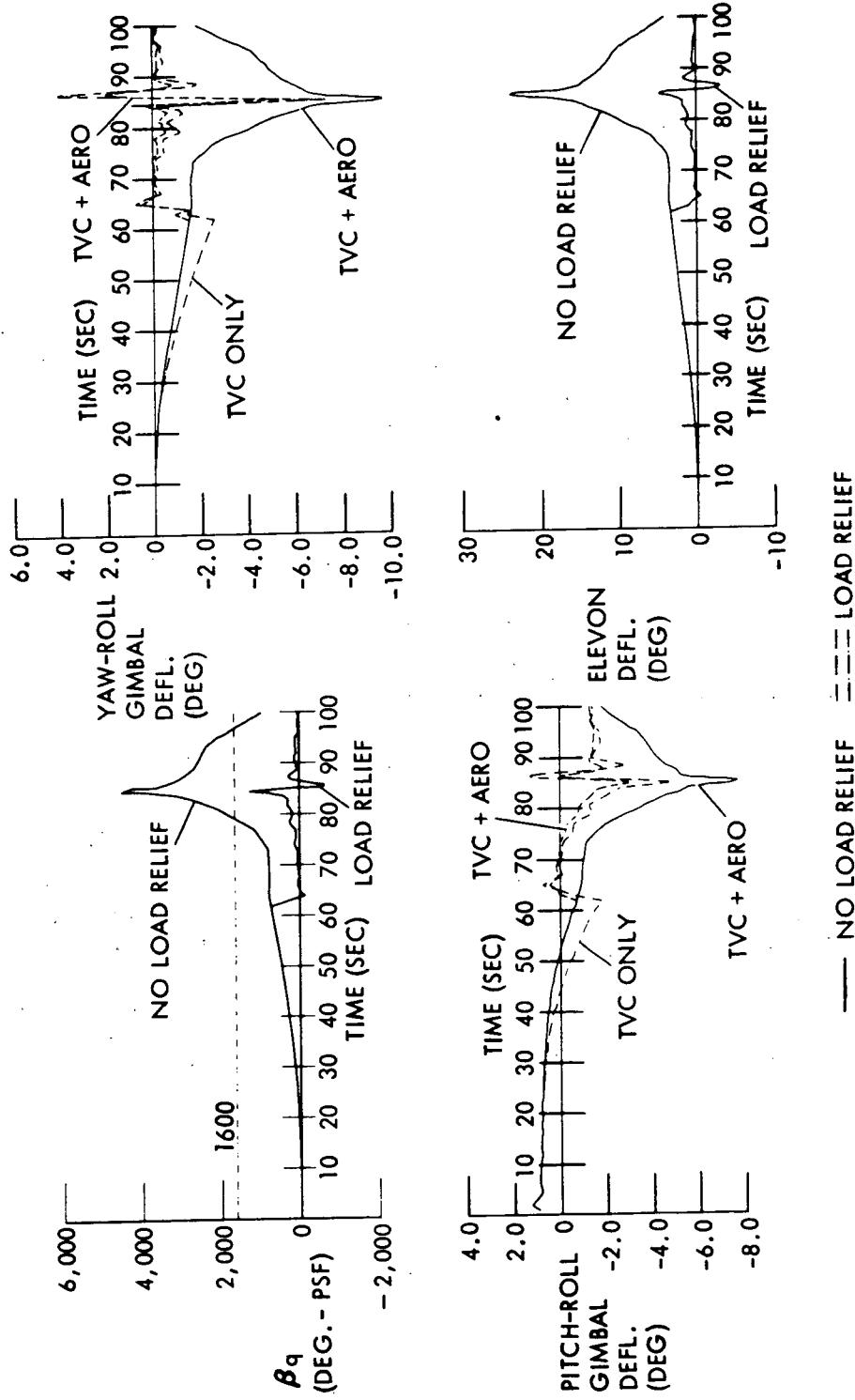


Figure 5-73. Space Tug Crosswind Trajectory Data (Wind Gust at Max β_q Altitude)

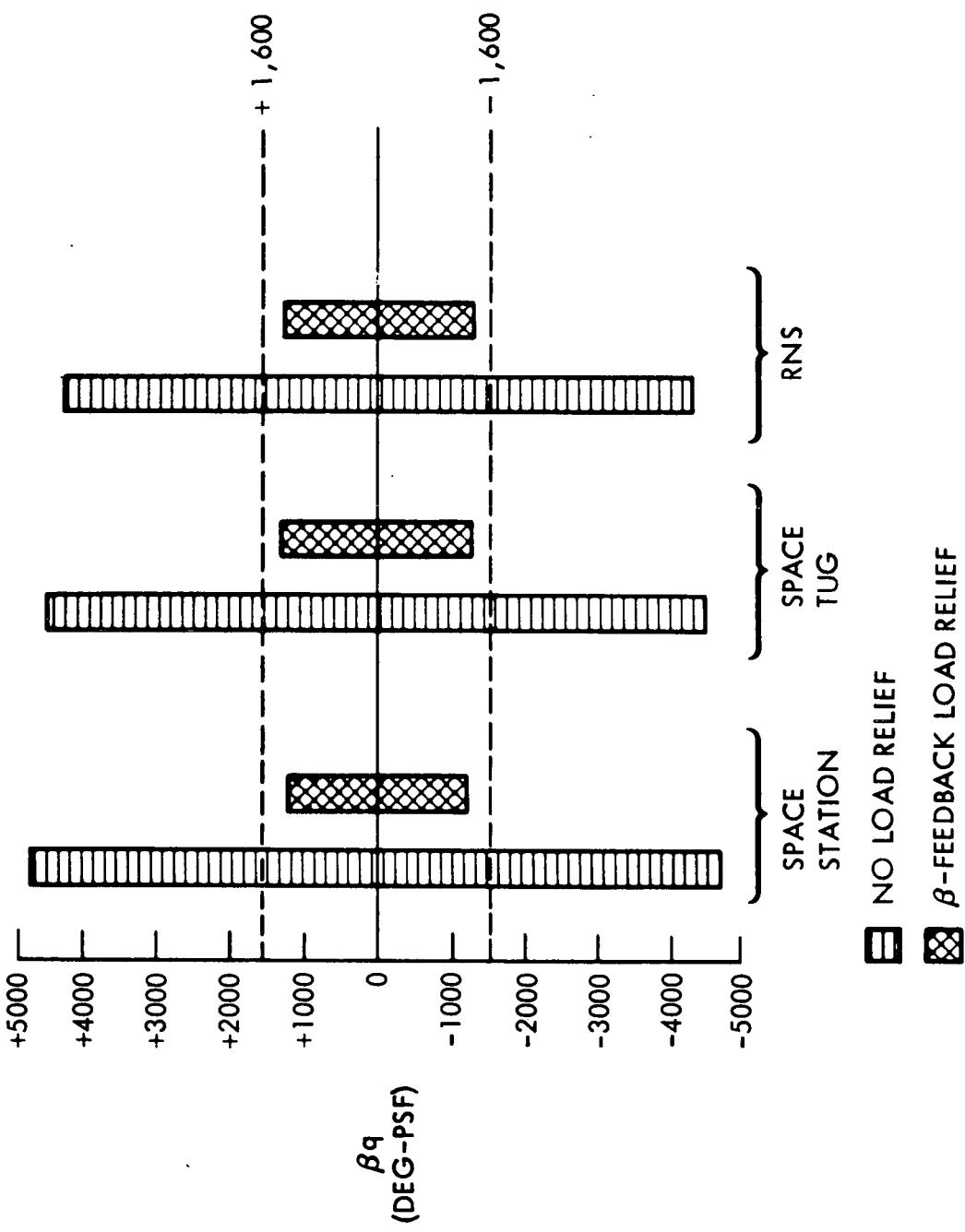


Figure 5-74. β_q Summary, Wind Gust at Max q Altitude



5. Gimbal Angle Requirements. The space station gimbal angle requirements due to motion of the center of gravity are shown in Figure 5-75. Also shown are the total angles for the space tug and RNS launch vehicles. These angles are well within the ± 10 -degree (total deflection range of 20 degrees) gimbal angle capability of the shuttle booster.

The head/tail wind gimbal requirements for the ESS launch vehicles are summarized in Table 5-4. The c. g. travel is listed as zero because it is included in the simulation wind data. The bending and sloshing entries are estimates for these vehicles, and the engine failure number includes dynamic response due to the loss of TVC of a single engine. The values

Table 5-4. Head/Tail Wind Gimbal Requirements
(Gust at Max Q Altitude)

	NO LOAD RELIEF	LOAD RELIEF
		GIMBAL LIMIT
\pm CG TRAVEL	0.0	0.0
\pm BENDING	0.25	0.25
\pm SLOSHING	0.40	0.40
\pm ENGINE FAIL	1.50	1.50
\pm WINDS (SPACE STATION)	7.10 7.90	3.00 2.50
TOTAL TVC DEFLECTION (DEGREES) SPACE STATION	19.3	9.8
SPACE TUG	21.5	10.3
RNS ($\alpha = -2^\circ$ TRAJ)	17.9	9.3
RNS ($\alpha = -4^\circ$ TRAJ)	17.7	9.3

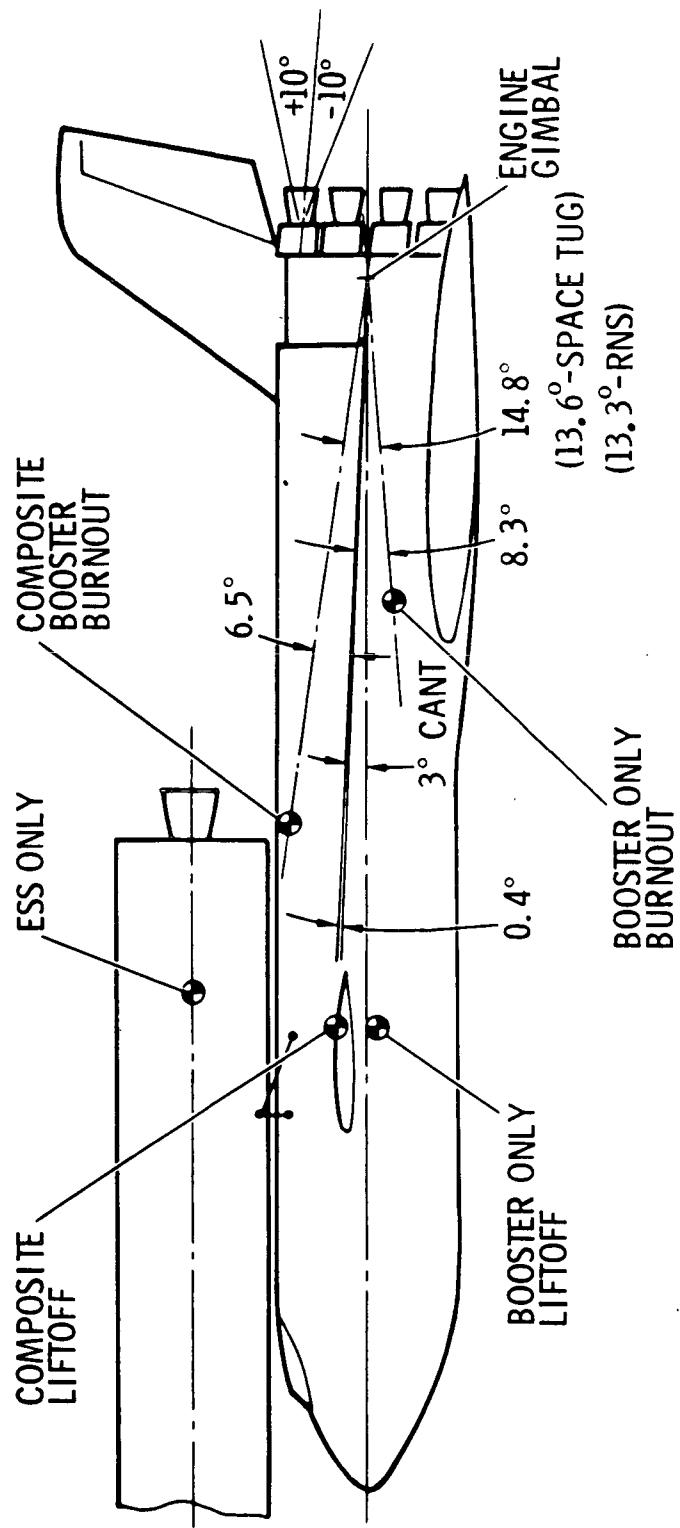


Figure 5-75. Booster/ESS Space Station Gimbal Requirements Due to CG Travel, Nominal



for the winds are taken from the simulation results previously shown with the space station vehicle results used as an example.

With no load relief, only the space tug vehicle exhibits requirements greater than the ± 10 -degree capability. With load relief, all ESS vehicle gimbal angle requirements are within ± 10 degrees.

Table 5-5 shows the cross-wind gimbal angle requirements and elevon deflections. The pitch and yaw control planes are shown because both the pitch actuators and yaw actuators are differentially deflected for roll control. Since the simulation assumes zero lateral c.g. offset, an estimate of $\pm 1/2$ degree is included in the yaw plane.

The large no-load relief TVC and elevon deflections are due to the roll control moment requirements. With the load relief system incorporated, the TVC and elevon deflections are acceptable. The use of the elevons can be eliminated, even for the space tug and RNS vehicles, by giving the pitch actuators more roll control authority.

6. Gimbal Limiting Performance Effect. The effect of gimbal limiting on vehicle performance was examined under contract NAS9-11191, Preliminary Investigation of Potential Value Loads Alleviation Control for Space Shuttle Vehicle. The results indicated a maximum of 3000 pounds additional booster propellant was required to account for dispersions resulting from winds and gimbal limiting. Results with winds but no gimbal limiting showed dispersions requiring 1500 pounds of booster propellant. Therefore, about 1500-pounds propellant penalty can be attributed to gimbal limiting. For the booster-orbiter configuration under study at that time, the equivalent payload loss was approximately 100 pounds.

To obtain approximate values for the ESS mission, the amount of propellant penalty due to gimbal limiting can be proportioned by the engine thrust capability of the two vehicles. This ratio is 550 to 415 and would increase the propellant penalty caused by gimbal limiting and trajectory dispersion to 2000 pounds.

Conclusion-Aerodynamic Flight. The angle of attack and angle of sideslip final results are within the α_q and β_q constraints, although some degradation from the results presented can be expected because of the simulation assumption of perfect α and β sensor data and the exclusion of propellant sloshing and body bending effects.



Table 5-5. Cross-Wind Gimbal Requirements (Gust at Max Q Altitude)

	YAW		PITCH	
	NO LOAD RELIEF ELEVONS	LOAD RELIEF ELEVONS	NO LOAD RELIEF ELEVONS	LOAD RELIEF ELEVONS
± CG TRAVEL	0.50	0.50	0.50	0.0
± BENDING	0.25	0.25	0.25	0.25
± SLOSHING	0.40	0.40	0.40	0.40
± ENGINE FAIL	1.50	1.50	1.50	1.50
+ WINDS (SPACE STATION)	8.70	5.00	6.50	7.50
-	8.70	5.00	6.50	7.50
TOTAL TVC DEFLECTION (DEGREES) SPACE STATION	22.7 _{±23}	15.3 _{±4}	18.3 -	19.3 -
SPACE TUG { ELEV. *	24.7 _{±24}	16.2 _{±5}	20.1 -	19.5 -
RNS { ELEVONS*	21.5 _{±25}	15.9 _{±5.5}	20.5 -	22.5 -

*ELEVONS USED DIFFERENTIALLY FOR ROLL CONTROL ONLY



The parameters αq and βq can be limited to acceptable values, from the standpoint of air loads in the maximum dynamic pressure region of flight, by

1. Designing trajectories with a low maximum q and a desired angle of attack at the time of maximum q ,
2. Incorporating a gimbal limiting control law into the vehicle pitch plane attitude control system, and
3. Utilizing the shuttle booster β -feedback load relief system.

The shuttle booster TVC and aero surface requirements are not impacted by the ESS configurations.

Launch Drift. A launch drift analysis was performed to ensure that the vehicle clears all obstructions in the launch area. The obstructions include the launch umbilical tower (LUT), the orbiter umbilical towers, the ESS umbilical tower, and the launcher pedestals. This worst-case analysis assumed any two engines inoperative and the design wind profile (17.7 meters/sec at an altitude of 18.3 meters) specified in NASA-TMS-53973. A drag coefficient of 1.2 was assumed. The remaining engines were assumed to be throttled to maintain 1.2 g's with a limit of nine-percent overthrust. Actually, for most payloads the T/W would be maintained at 1.3 until clearing the towers to minimize the drift problem. Critical points are the engine bells clearing the launcher pedestals, the booster body or vertical fin clearing the orbiter umbilical towers, the booster wing or body clearing the ESS umbilical tower, and the booster body and wing clearing the launch tower. The launch pad arrangement is shown in Figure 5-76.

Tailwinds tend to blow the integrated vehicle into the LUT while headwinds and sidewinds cause drift toward the orbiter umbilical towers. Sidewinds and quartering winds tend to cause drift into the ESS umbilical tower. Aerodynamic forces and moments in the pitch and yaw planes for the integrated vehicle are listed in Table 5-6. A full six-degree-of-freedom simulation of the vehicle motion was used to obtain the clearance envelopes. A closed-loop guidance technique was simulated whereby lateral motion of the center of gravity was fed to the pitch and yaw channels of the vehicle attitude control system so as to minimize lateral motion of the vehicle's aft end. This tends to maximize the clearance, but does leave the vehicle in a nonvertical attitude when the highest obstruction is cleared.

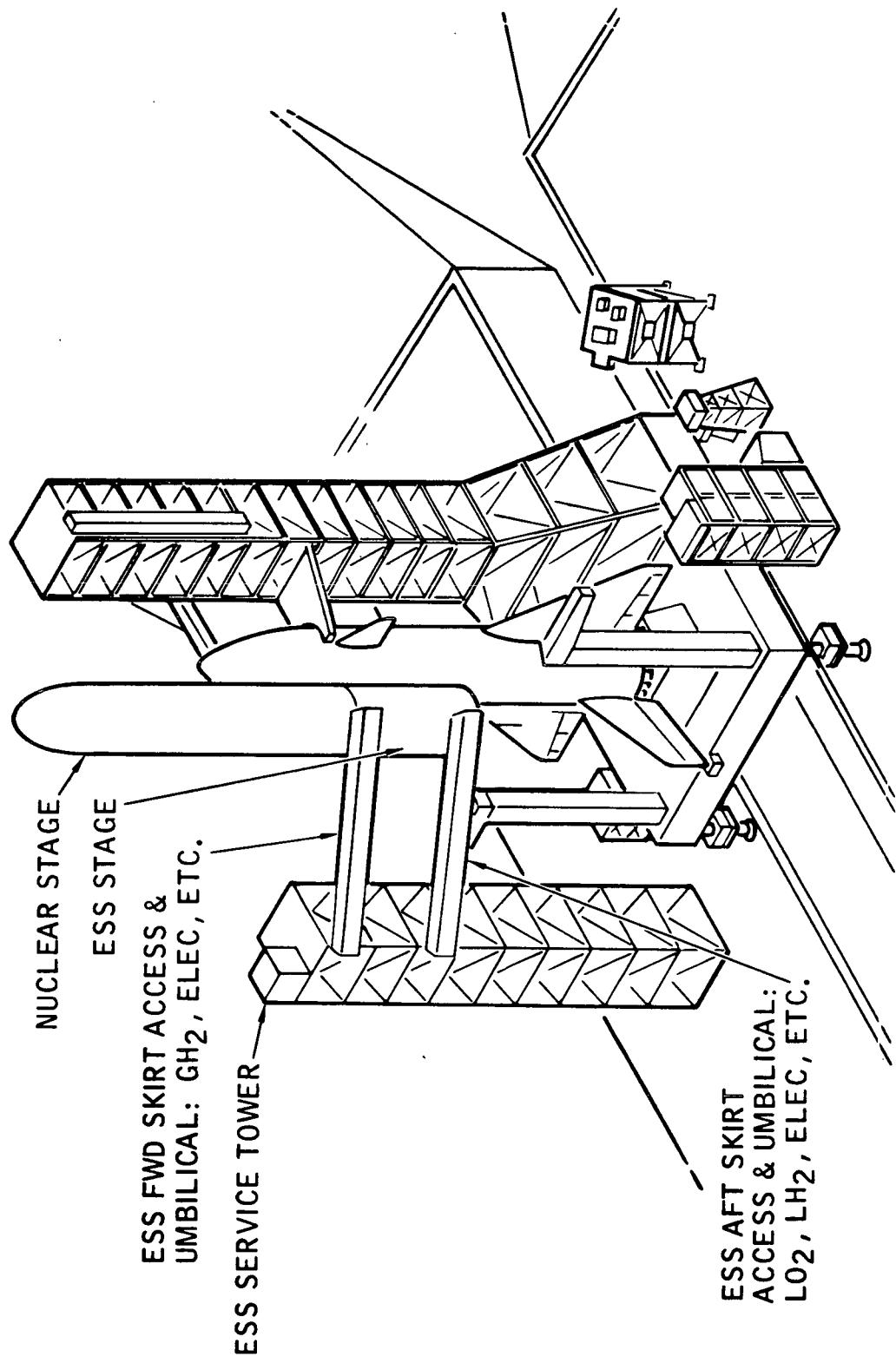


Figure 5-76. Launch Pad Arrangements



Table 5-6. Aerodynamic Force Summary

Plane	C. P. Station (in.)	CG Station (in.)	Aero Force (lb)
Pitch	2620	2190	139,700
Yaw	2334	2190	155,200

The vehicle center of gravity is offset from the booster centerline because of the ESS/payload location. Thus, to rise vertically in still air with all engines thrusting, the vehicle must be tipped off-vertical. By altering this tip angle and the ensuing attitude commands, it is possible to change this nominal, still-air path from vertical to any reasonable angle away from vertical. The ending out and wind-blown drift without guidance is essentially a straight path at some angle away from nominal. Thus, by tipping the vehicle the nominal design clearance envelopes can be biased to clear an obstruction in one direction at the expense of increased drift due to wind and engines out in the opposite direction. Figure 5-77 shows this techniques used to clear the LUT in a tailwind. Active guidance technique is also used to assure clearance of the launcher pedestals. Figure 5-78 illustrates the crosswind clearance envelope which shows that by using closed-loop guidance the vehicle clears the launcher pedestals, orbiter umbilical tower, the ESS umbilical tower.

Expendable Second Stage —Control System Analyses

General Description of System

The ESS is designed to boost large payloads into a 66 x 100-nm orbit, transfer to a 270-nm orbit and optionally can rendezvous with a target vehicle. The ESS is designed to operate with various payloads. Typical payloads are the MDAC space station, the reusable nuclear shuttle, and the space tug.

The ESS design, similar to space shuttle orbiter has three distinct types of propulsion systems (Figure 5-79): (1) The main propulsion system (MPS), which consists of two 632,000-pound shuttle orbiter main engines, (2) the orbital maneuvering system (OMS), which consists of two shuttle orbiter 10,000-pound thrust OMS engines, and (3) the attitude control propulsion system (ACPS), which includes 14 shuttle orbiter 2100-pound thrust ACPS engines.

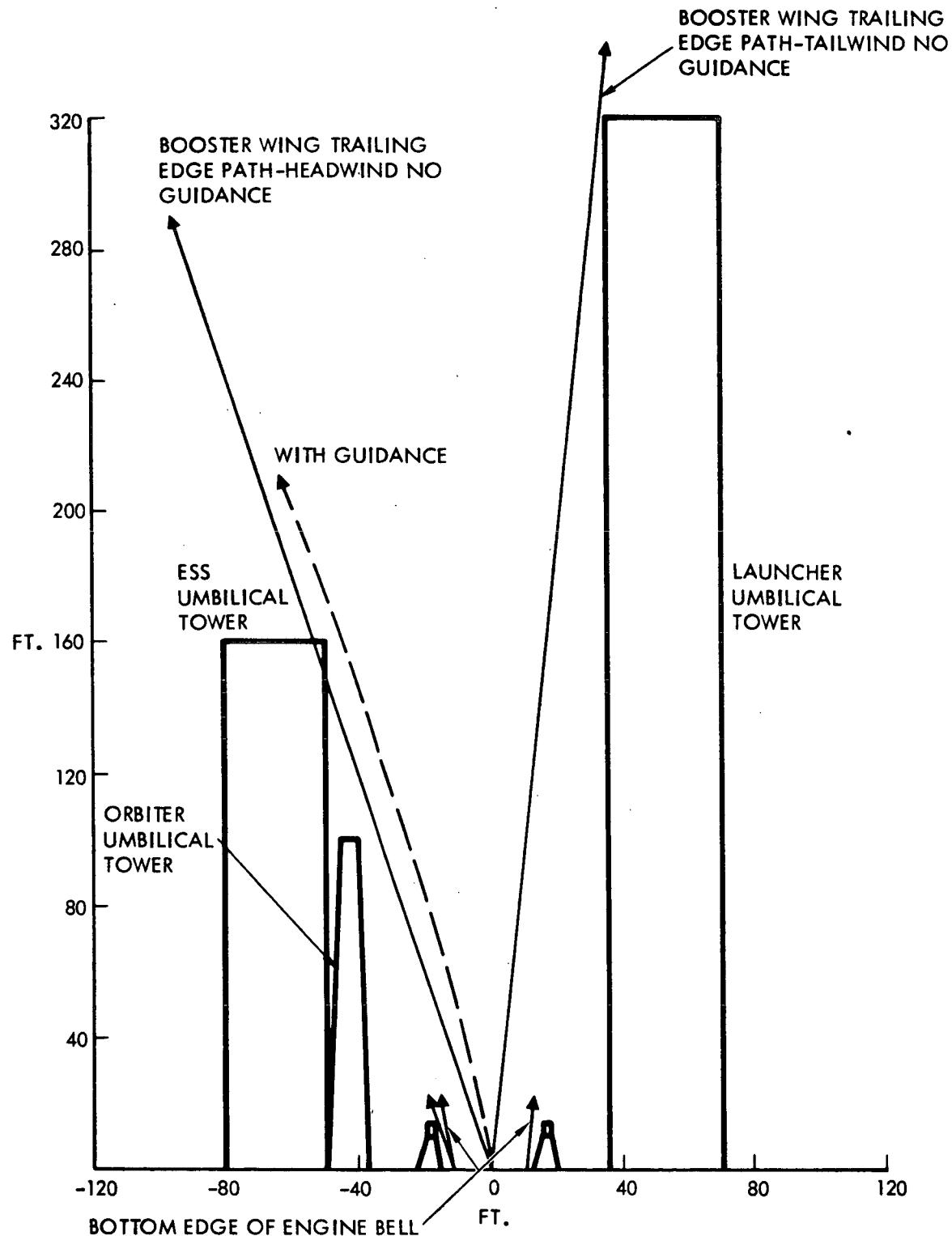


Figure 5-77. B-9U/ESS/RNS Launch Drift Pitch Plane Wind

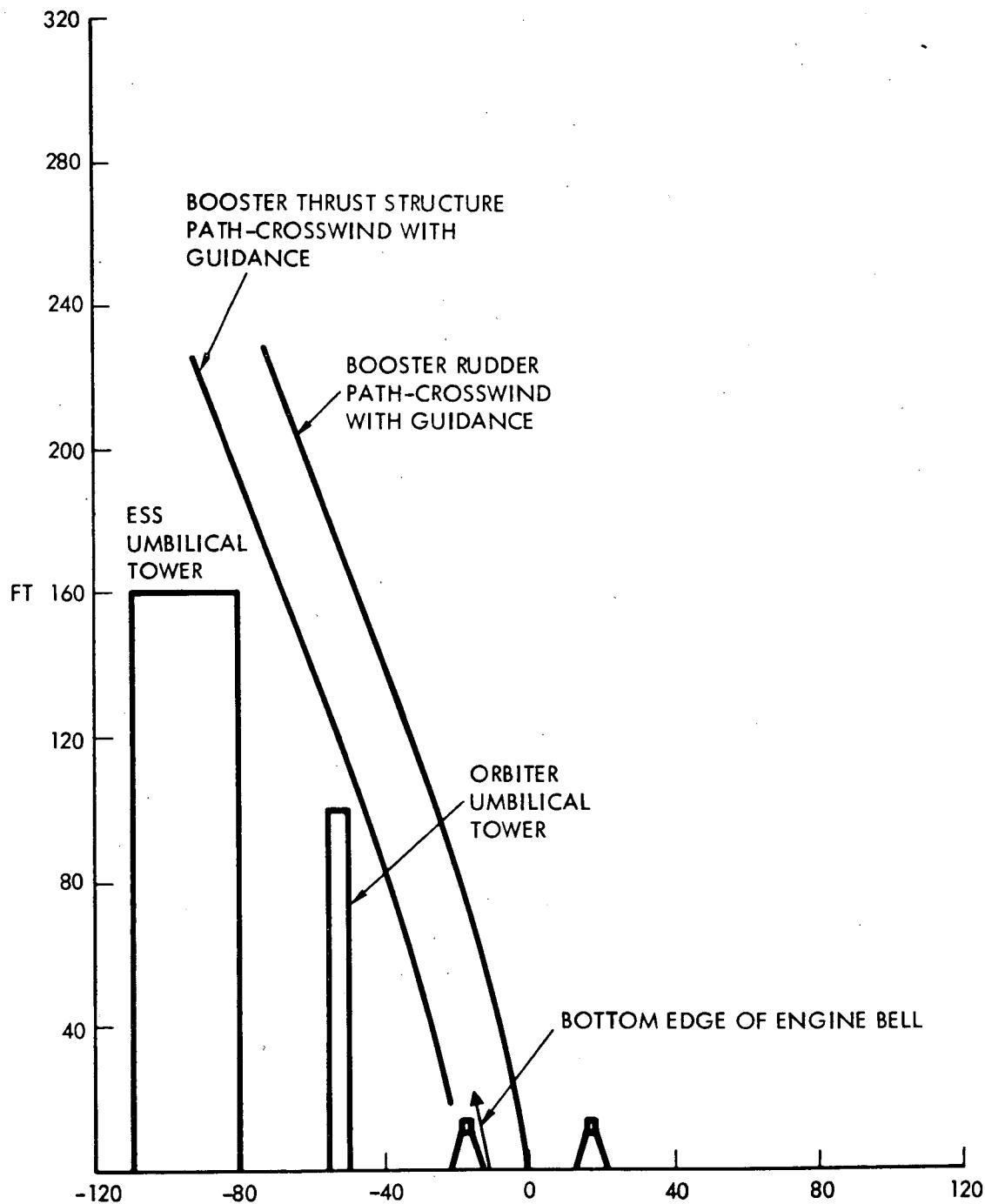


Figure 5-78. B-9U/ESS/RNS Launch Drift Yaw Plane Wind

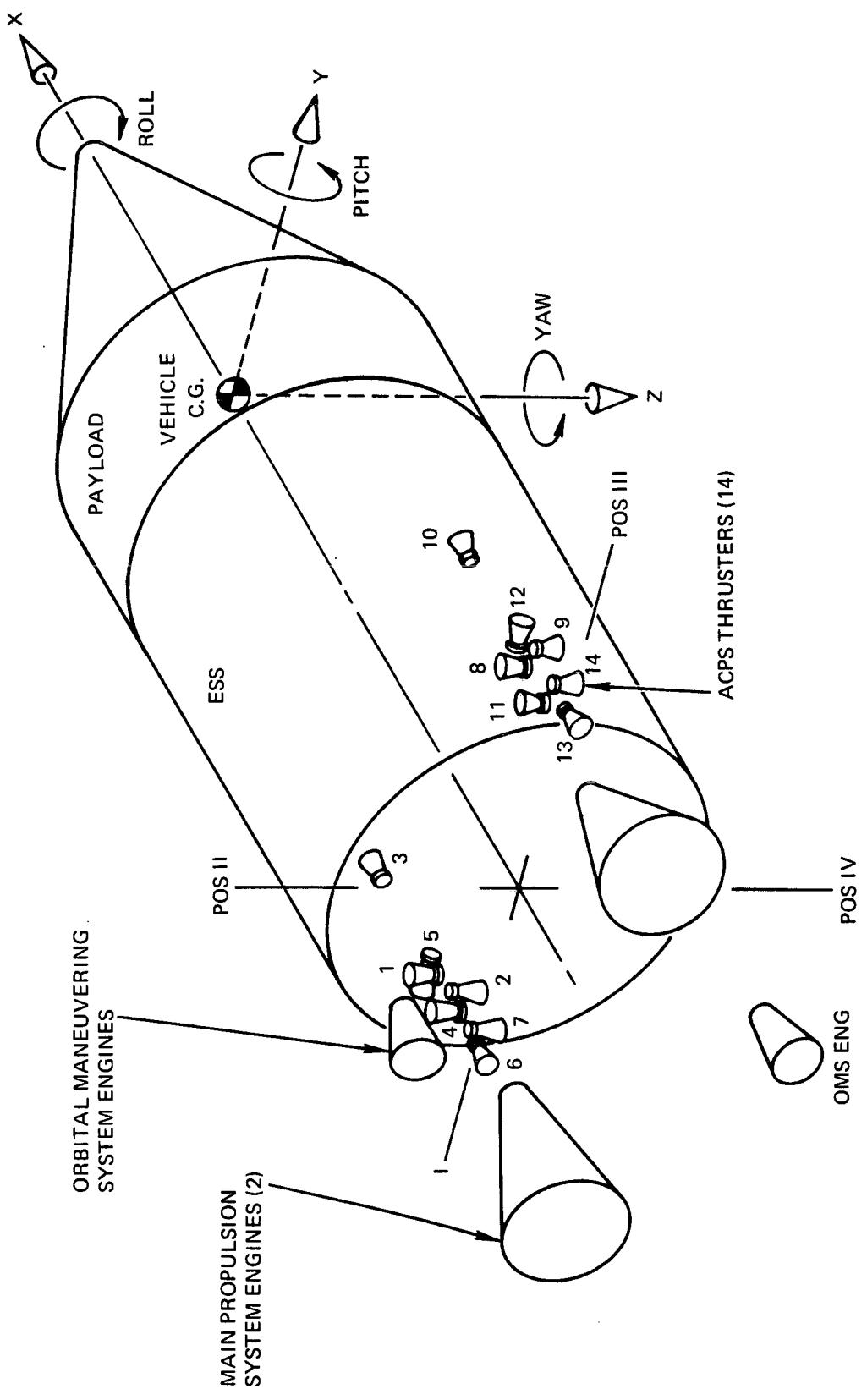


Figure 5-79. ESS Vehicle Configuration, Coordinate Axes, and Propulsion Subsystems Used for Flight Control



The flight control system consists of the mechanization and equipment required for vehicle control which is implemented through control of these engines. The manner in which these engines are used for control is similar to that used on the shuttle orbiter. The baseline ESS flight-control system concept is described as follows.

After staging, the ESS is operating with the MPS and the vehicle is controlled about three axes by thrust vector control (TVC) of the two MPS engines. The engines are gimbaled in pitch and yaw and the control logic is designed to provide three-axis control. The pitch gimbals of the two engines provide both pitch- and roll-axis control.

The OMS is used for orbit transfer and deorbit. The vehicle is controlled about all three axes similarly to the manner in which control is effected using MPS engines. However, because of the arrangement of OMS engines, the yaw gimbals are used for combined roll and yaw control.

If one main engine is inoperative, pitch and yaw control will be accomplished by TVC. Roll control is performed by ACPS jets. The same control concept is used for single-OMS-engine operation, if the vehicle is not in the deorbit mode. For ESS deorbit with one OMS engine operational, three-axis control will be provided by the ACPS jets.

The ACPS is employed for three-axis vehicle attitude control during orbital coast periods. The ACPS also provides the capability to perform critical separation, braking, docking maneuvers, and backup ESS deorbit if both OMS engines are not operative.

The ACPS is identified as a bang-bang type of control system as compared to the TVC of main and OMS engines which are proportional type systems.

A general block diagram (Figure 5-80) illustrates that body-mounted rate gyros and navigation platforms provide sensed information to a digital computing system. The digital computing system solves guidance equations, generates flight control commands, performs flight control filtering and logic, and finally, provides control of the vehicle through the required combination of TVC of main and OMS engines and ACPS.

Figure 5-81 illustrates the attitude control system feedback loops employed for TVC control of the main engines. The computation shown is performed in the central digital computing system. The control loops for

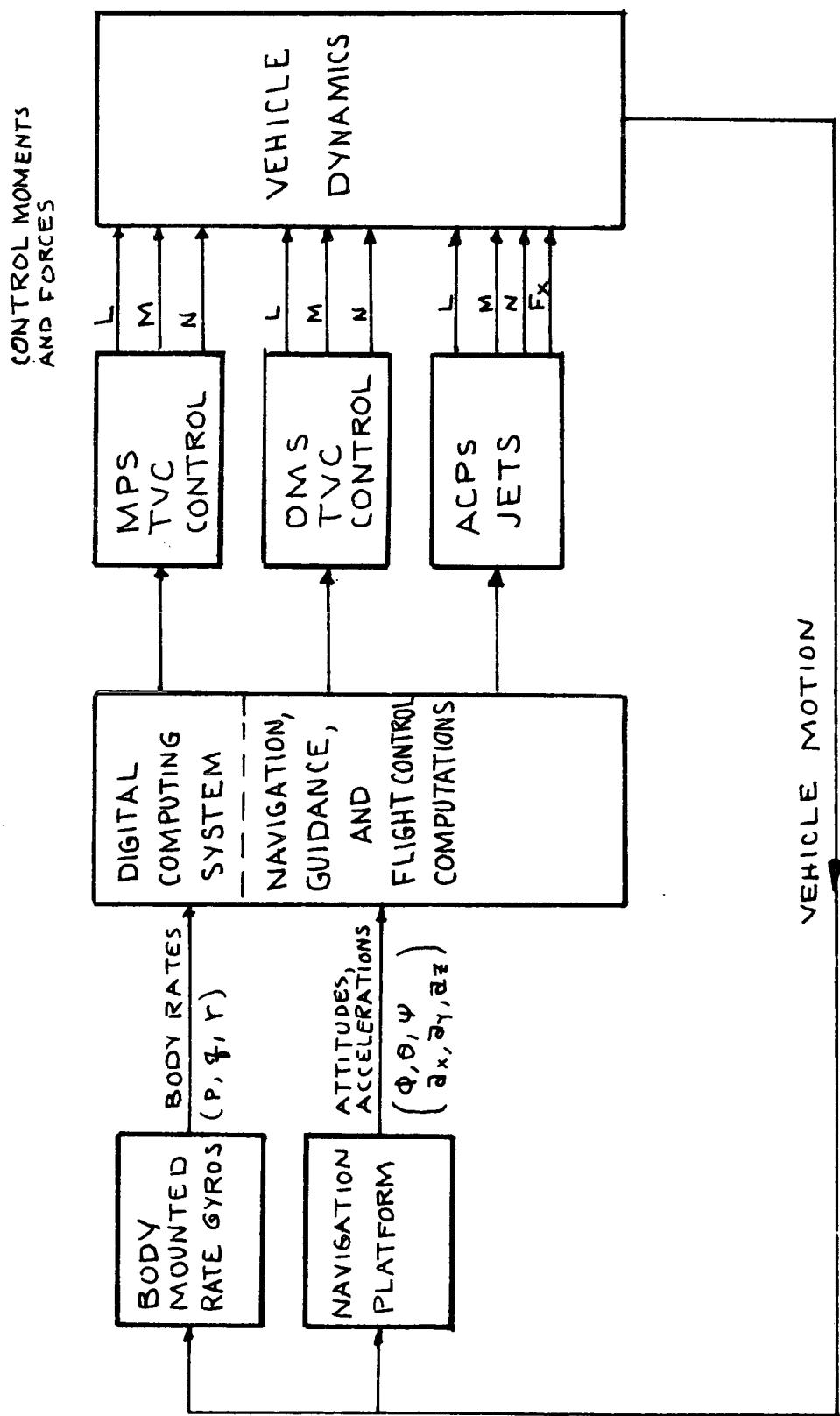


Figure 5-80. ESS Flight Control System Block Diagram

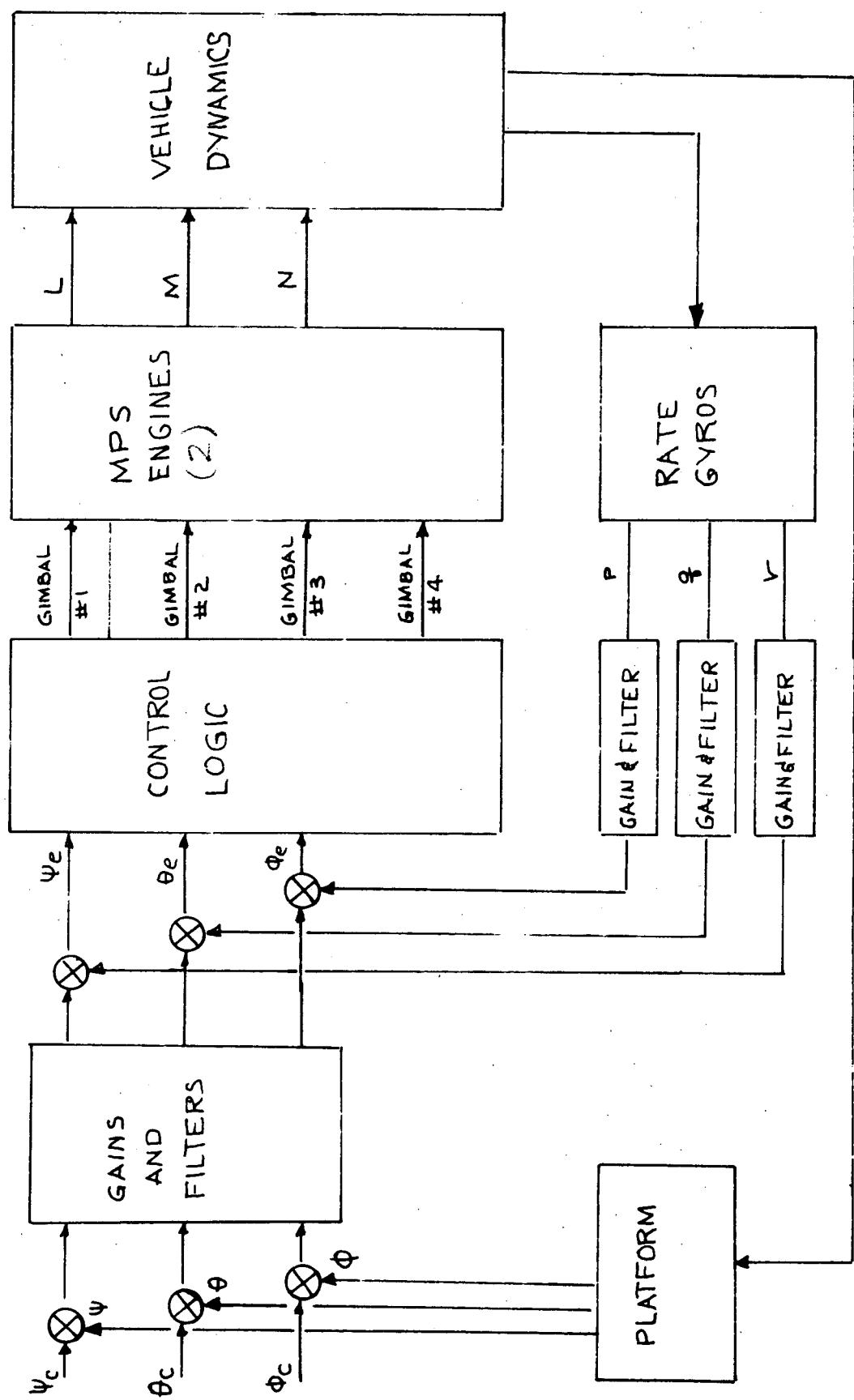


Figure 5-81. Three-Axis Attitude Control With TVC From Main Engines



attitude control using the OMS engines are similar, with the exception that for the OMS, the yaw gimbal (rather than the pitch gimbal) of the two OMS engines provides roll control.

Figure 5-82 illustrates the feedback loops employed in the attitude control system which uses ACPS jets. The control logic operates on the pitch, roll, and yaw errors ($\theta_\epsilon, \phi_\epsilon, \psi_\epsilon$) (which are generated in the manner shown) to determine whether to command each of the 14 jets to OFF or ON position. The computation and logic are performed within the central digital computing system.

The overall system is designed for FO/FS performance which is consistent with space shuttle philosophy. The detailed redundancy in the system is discussed in Book 2 of this report.

Subsequent paragraphs contain control system analyses performed which supports the control system configuration as described.

Attitude Control During Ascent.

1. Nominal System Operation. This section is concerned with control system analyses from staging through injection into orbit. As previously described, TVC deflection of the pitch and yaw gimbals are used to generate the control torques required for three-axis control. The analyses is discussed in two parts:
 - (1) selection of gains for good dynamic response throughout the trajectory, and (2) response to guidance commands to place the vehicle in near-optimum trajectory for injection into orbit.
- a. Gain Sensitivity Analysis. A pitch axis stability analysis was performed to establish preliminary values for attitude gain (a_θ) and rate gain (a_q).

The control system block diagram and corresponding characteristic equation are shown in Figure 5-83. The vehicle moment of inertia and center-of-gravity variations during ascent flight are shown in Figure 5-84 for the ESS with the MDAC space station as payload. Root locus plots are drawn to illustrate the effects of simultaneous variation of position and rate gain on rigid body natural frequency and damping ratio. The plots (Figures 5-85, 5-86, 5-87) represent three points along the ascent trajectory. As shown (Figures 5-85 through 5-88), attitude and position gains both adjusted to 0.6 units each, provide acceptable damping ratios throughout the trajectory of between 0.4 and 0.7. The corresponding

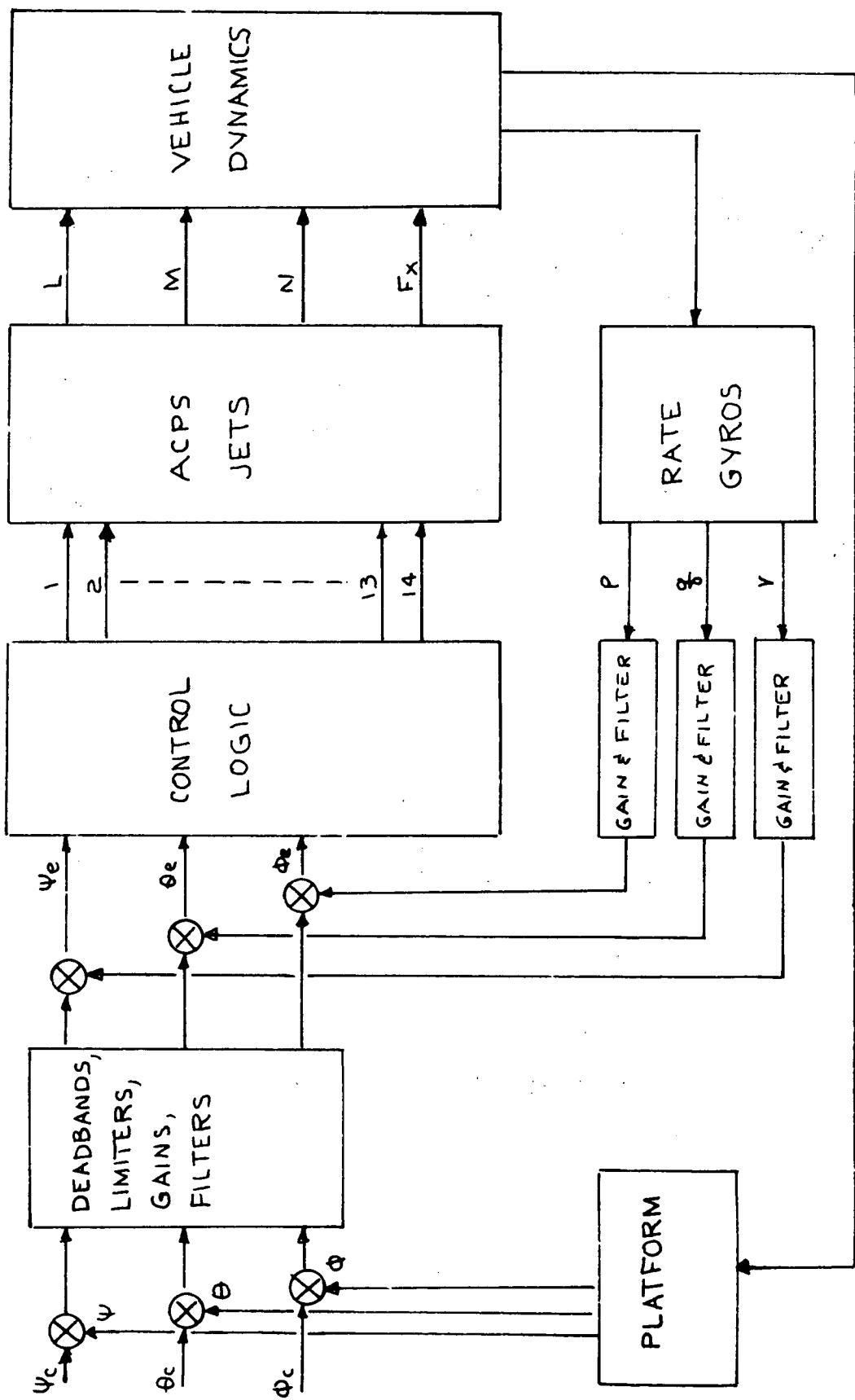
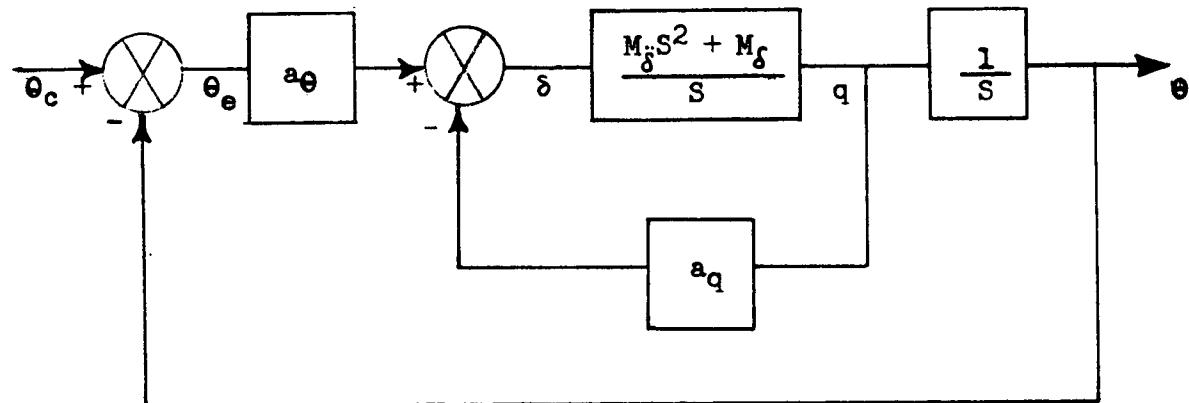


Figure 5-82. Three-Axis Attitude Control With ACPS



BLOCK DIAGRAM

$$\begin{array}{|c|c|c|} \hline
 S & -1 & 0 \\ \hline
 0 & -S & M_\delta S^2 + M_\delta \\ \hline
 a_\theta & a_q & 1 \\ \hline
 \end{array}
 \quad
 \left\{ \begin{array}{l} \theta \\ q \\ \delta \end{array} \right\}
 \quad
 \left\{ \begin{array}{l} 0 \\ 0 \\ a_\theta \end{array} \right\}_{\theta_c}$$

CHARACTERISTIC (MATRIX) EQUATION

*See Figure 5-93

Figure 5-83. Pitch Attitude Control System and Control Equations,
ESS With Space Station Payload

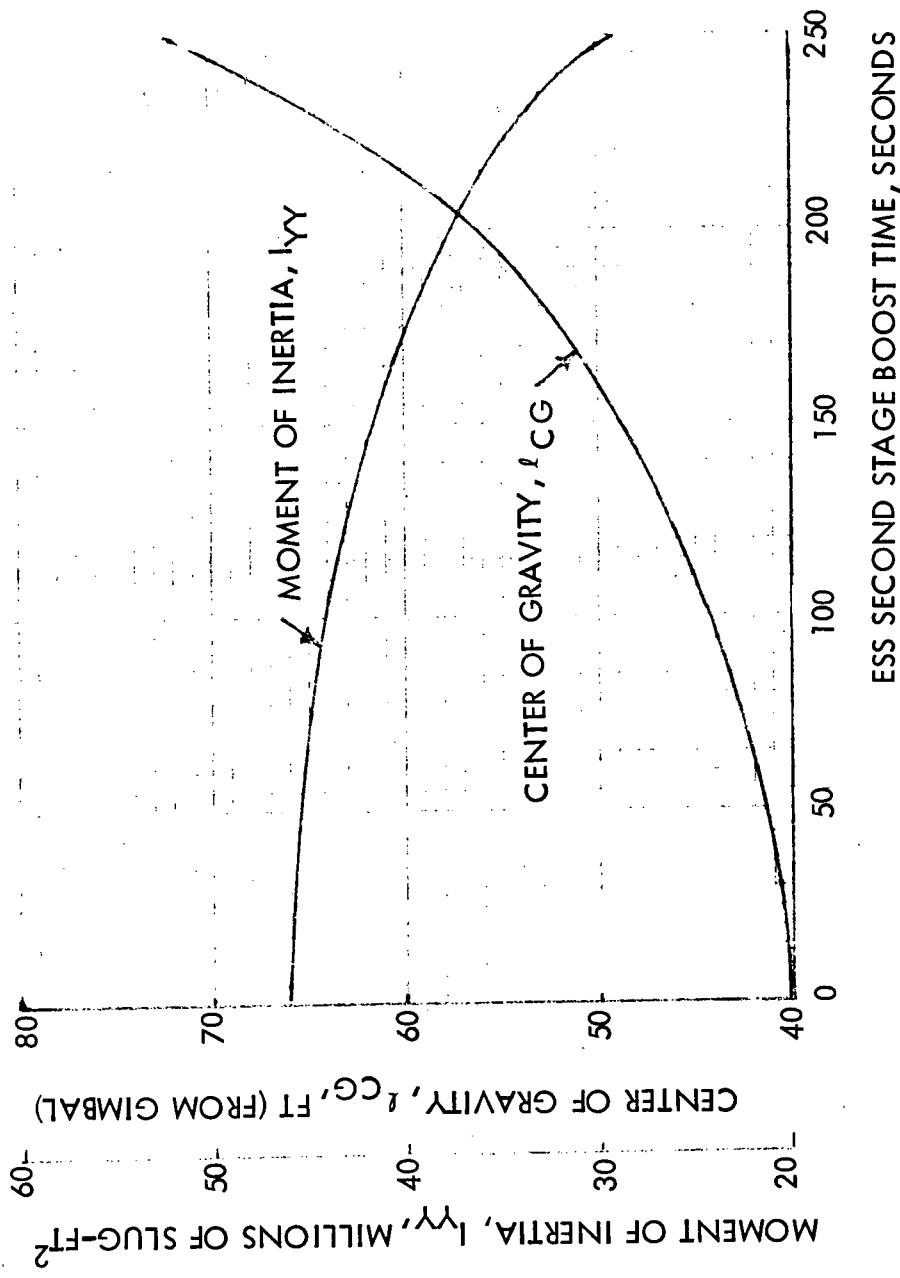


Figure 5-84. Moment of Inertia and Center-of-Gravity Variations Ascent to Orbit
(ESS With Space Station Payload)

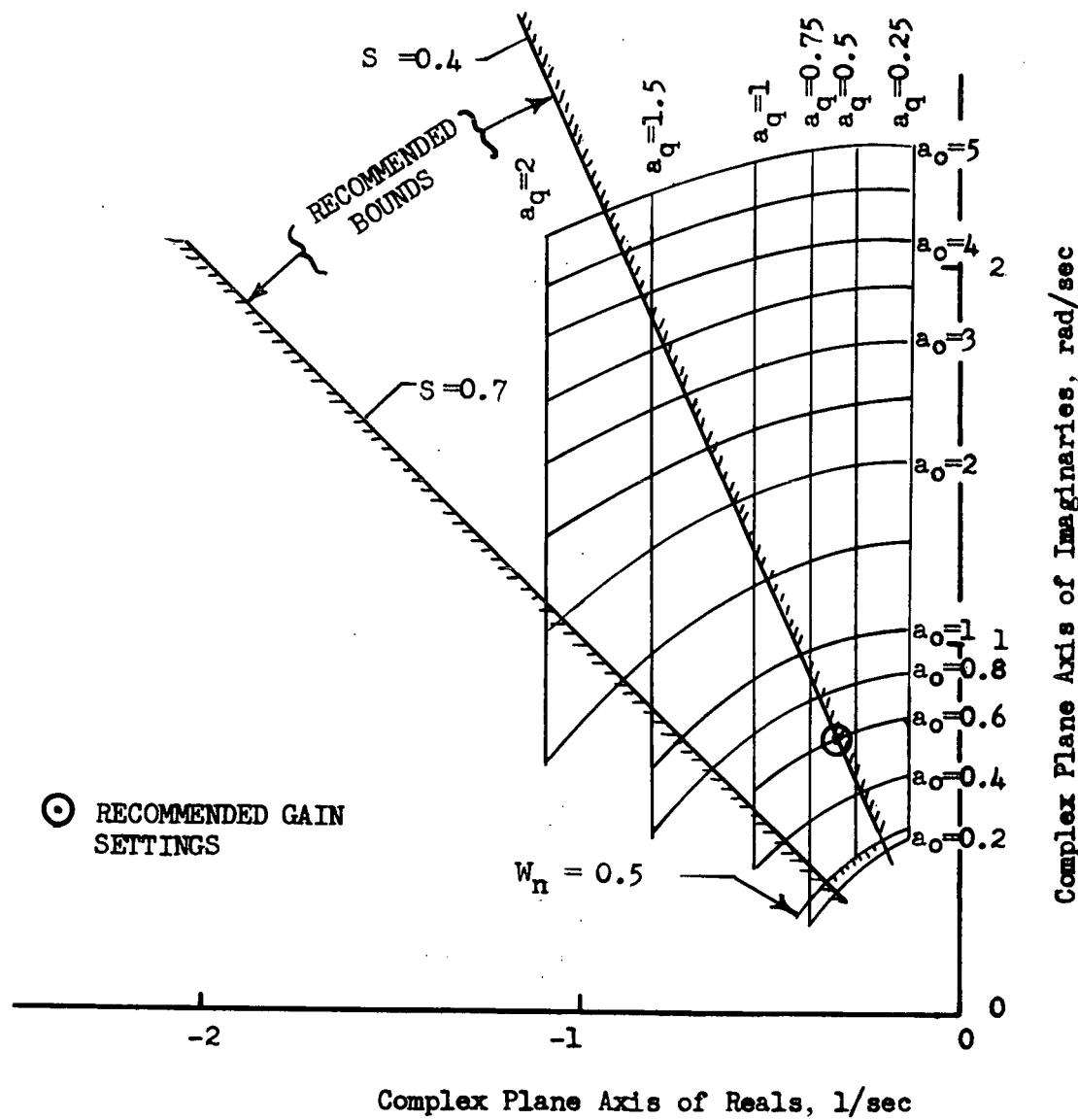


Figure 5-85. Pitch Axis Root Locus Plot at 10 Seconds After Staging
(ESS With Space Station Payload)

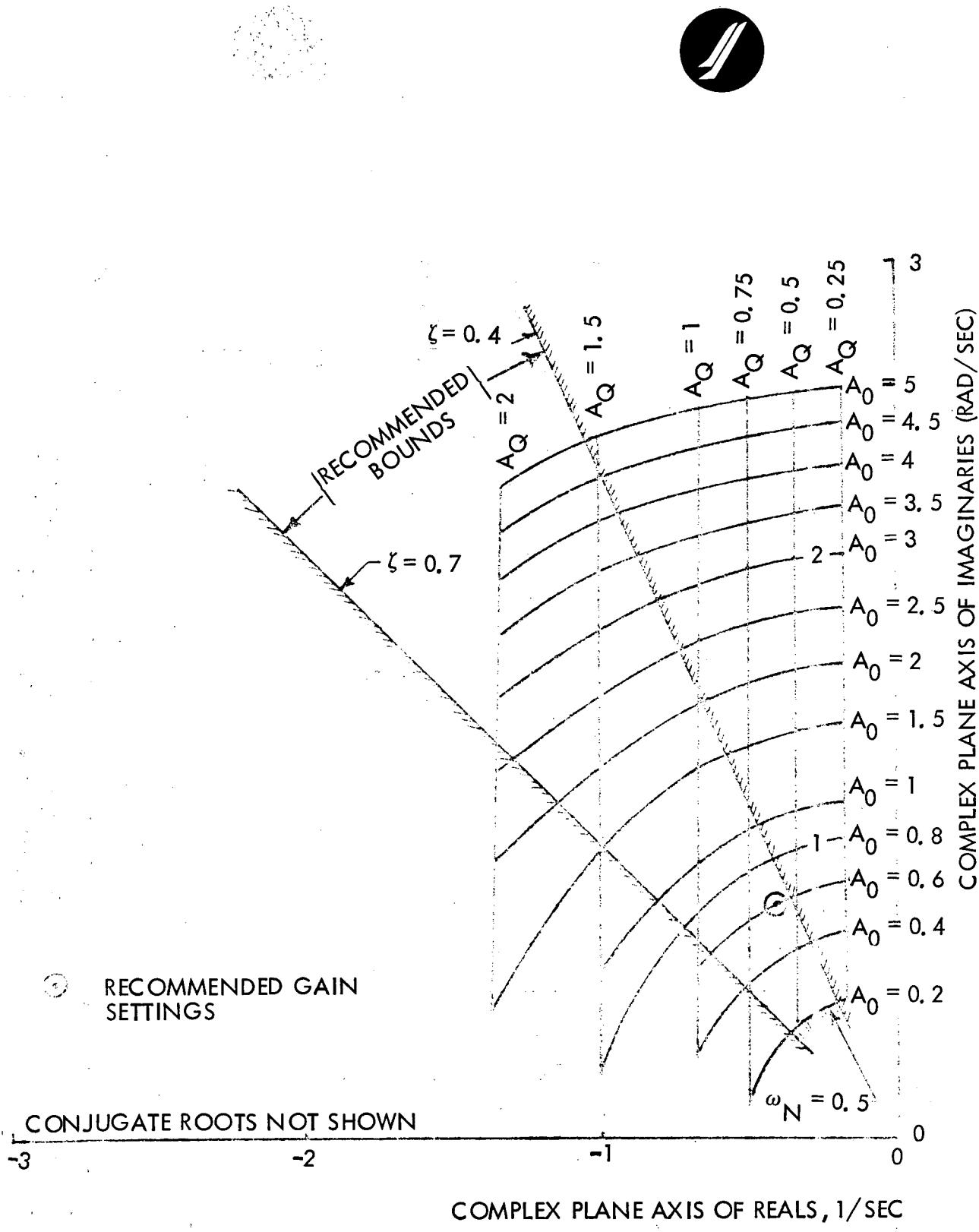


Figure 5-86. Pitch Axis Root Locus Plot at 125 Seconds After Staging
(ESS With Space Station Payload)

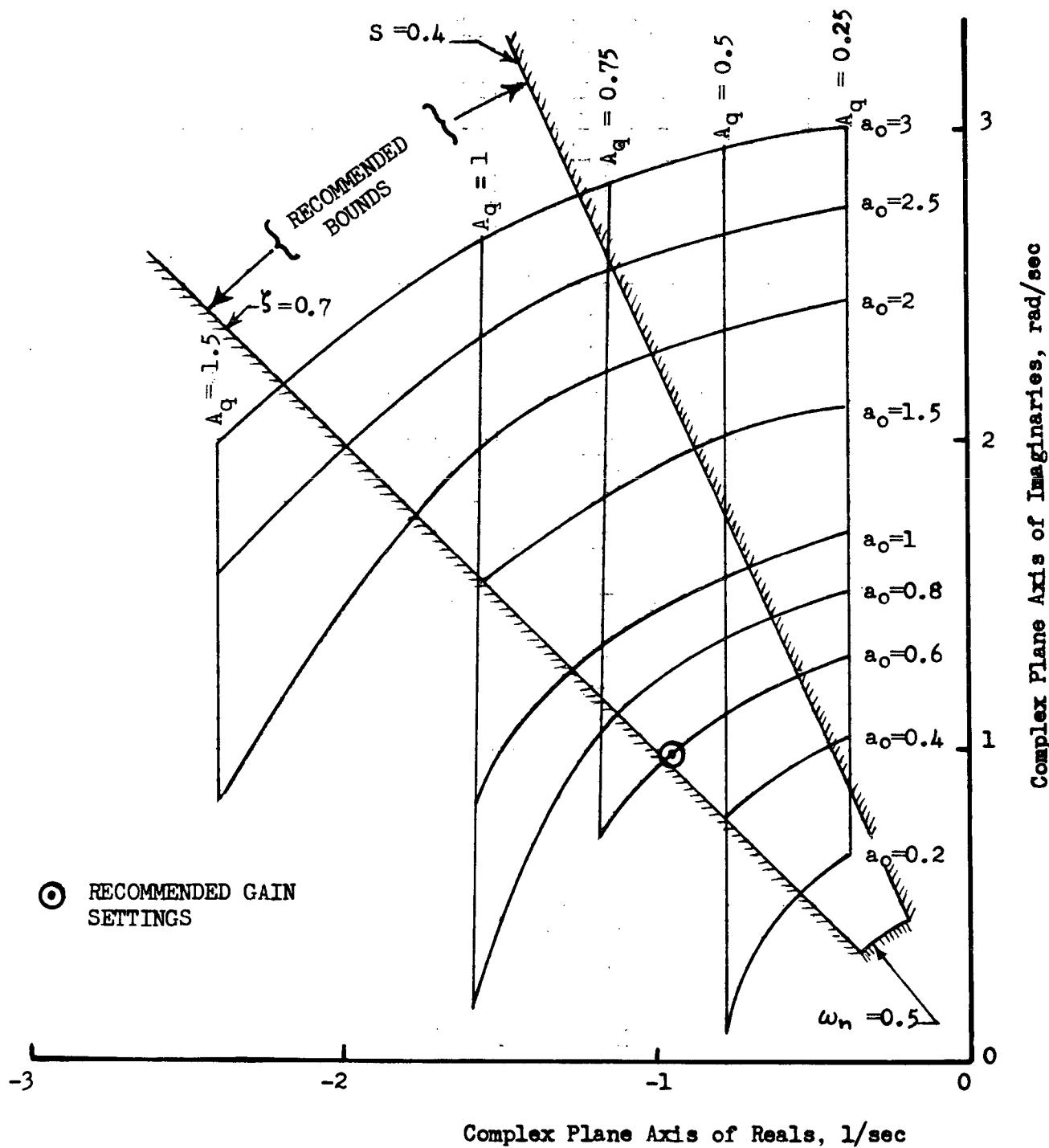


Figure 5-87. Pitch Axis Root Locus Plat at 250 Seconds After Staging ESS With Space Station Payload

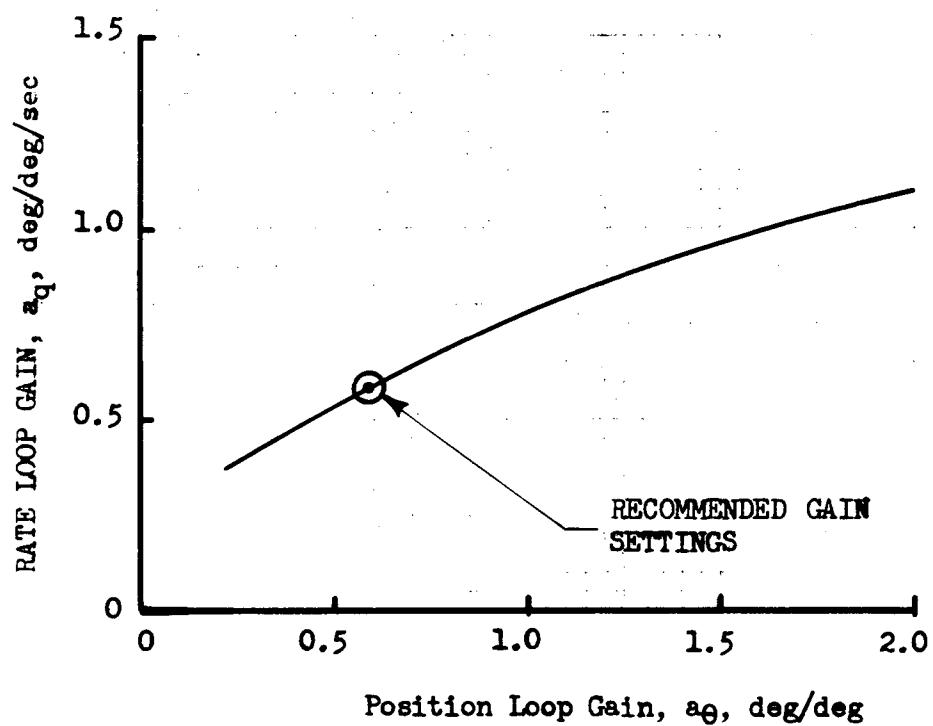


Figure 5-88. Constant Rate and Position Gains Which Assure That Damping Ratio is Between 0.4 and 0.7 for Ascent ESS With Space Station Payload



control system frequency (between 0.8 and 1.4 rad/sec) is below the anticipated slosh mode frequencies (of between 1.5 to 2.5 rad/sec). Since the attitude and rate gains may be constant through the ascent boost trajectory, the capability of switching gain levels during flight will not be required.

Closed-loop frequency response plots (Figures 5-89 through 5-91) to correspond with the flight times and recommended gain settings of the root locus plots, show the gain settings are acceptable. As shown, the phase shift is less than -180 degrees in those instances where the gain is at unity or greater, indicating the autopilot is stable with these values of gain. Also, the peak amplitude ratio is below 1.4, so damping ratio is assured of being greater than 0.4. The "tail-wags-dog" zero location is shown on the plots to indicate if engine inertia coupling will affect the control system. Since this zero is located more than a decade above the control system natural frequency, it will have no noticeable effect on rigid body vehicle dynamics. The calculations of this term are shown in Figure 5-92.

The yaw axis control system parameters are approximately the same as those of the pitch axis described below. Therefore, recommended settings for yaw attitude gain a_p is 0.6 deg/deg, and for yaw attitude rate gain a_r is 0.6 deg/deg/sec.

- b. Trajectory Control and Vehicle Dynamics. Initiation of orbital insertion guidance mode is assumed to start 10 seconds after booster/ESS separation. During this 10-second interval, the guidance command is in a hold attitude mode, and the vehicle is recovering from the disturbance conditions at separation. Vehicle body rates at separation, based on studies performed by General Dynamics, were assumed to be:

$$p_o = 4.6 \text{ deg/sec, roll rate}$$

$$q_o = 1.1 \text{ deg/sec, pitch rate}$$

$$r_o = -0.5 \text{ deg/sec, yaw rate}$$



$$\frac{\theta}{\theta_c} = \frac{(s^2 + (19.7)^2)}{(s+590)(s^2+2 \times 0.4 \times 0.81s + (0.81)^2)}$$

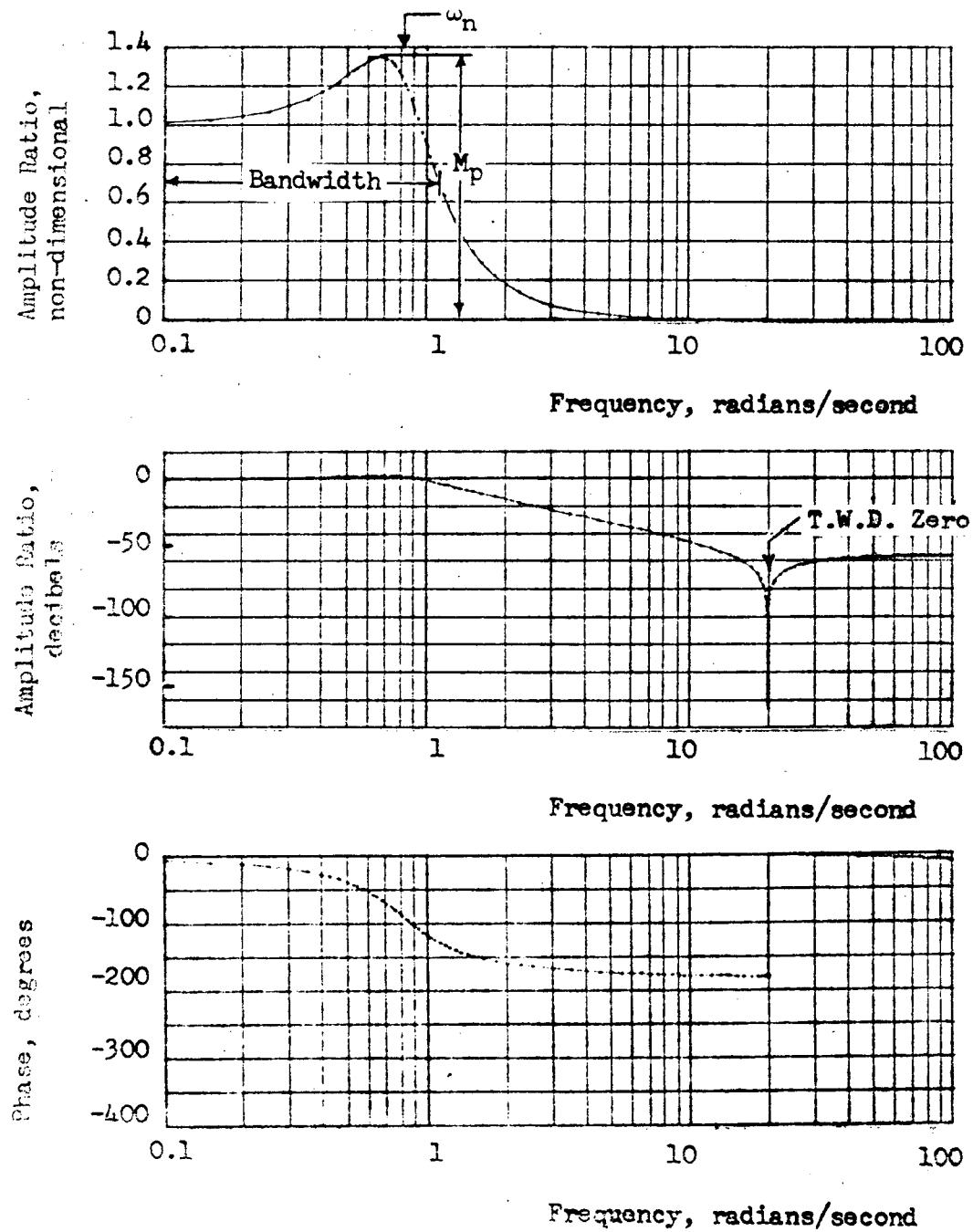


Figure 5-89. Pitch Closed Loop Frequency Response 10 Seconds After Staging ESS With Space Station Payload



$$\frac{\theta}{\theta_c} = \frac{(s^2 + (20)^2)}{(s+492)(s^2 + 2 \times 0.45 \times 0.9s + (0.9)^2)}$$

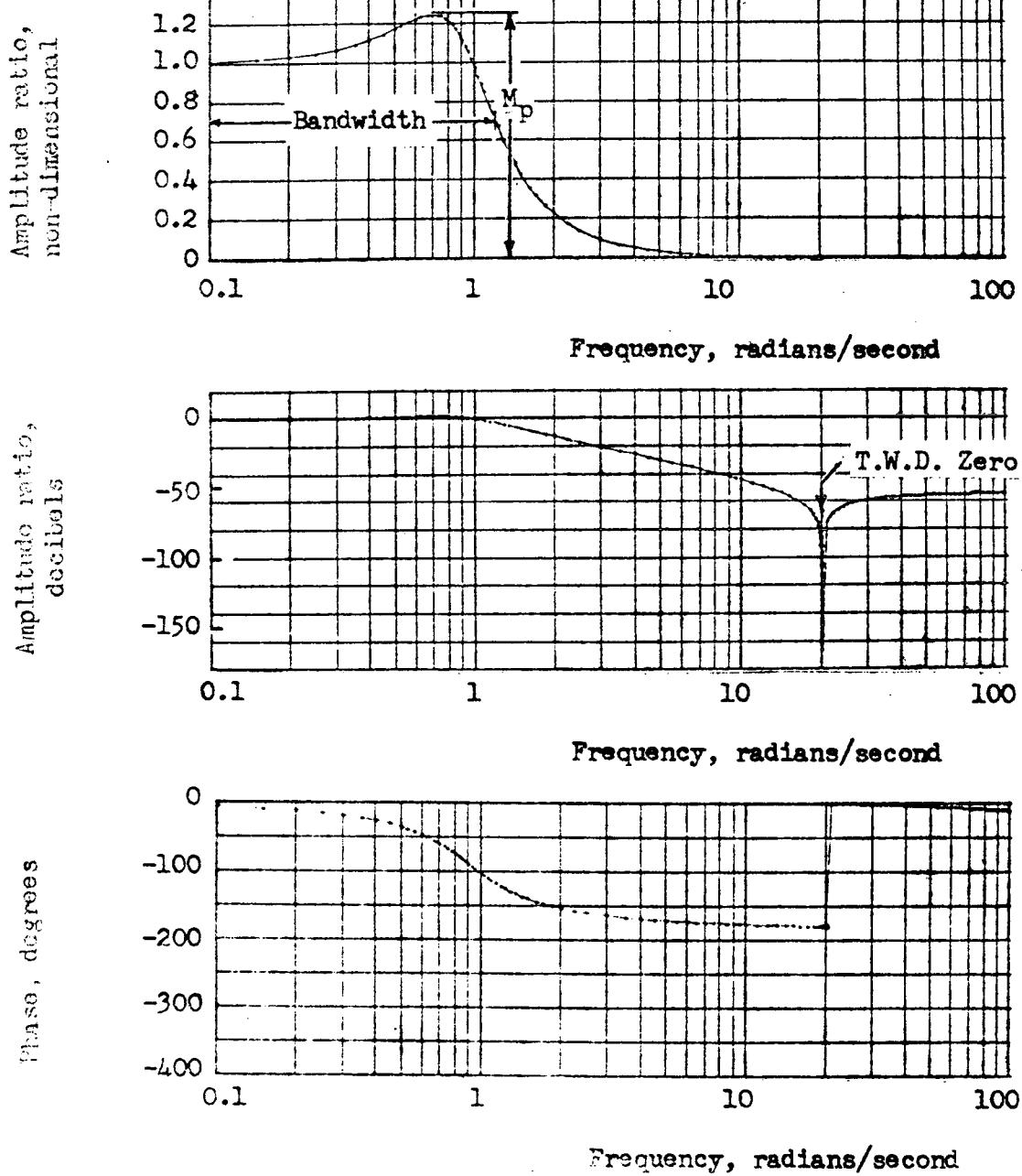


Figure 5-90. Pitch Closed Loop Frequency Response 125 Seconds After Staging ESS With Space Station Payload



$$\frac{\theta}{\theta_c} = \frac{(s^2 + (20.7)^2)}{(s+227)(s^2 + 2 \times 0.69 \times 1.4s + (1.4)^2)}$$

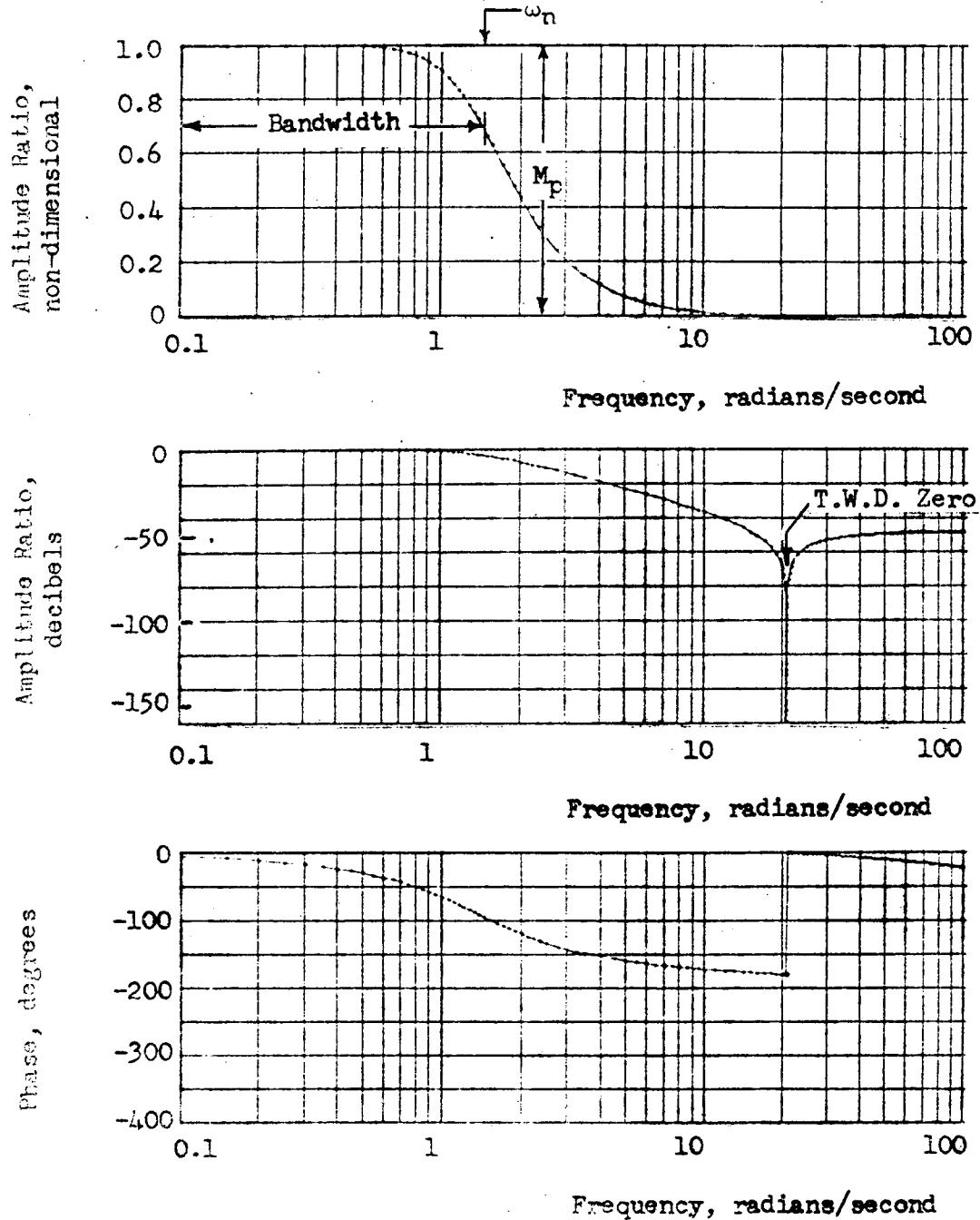


Figure 5-91. Pitch Closed Loop Frequency Response 250 Seconds After Staging ESS With Space Station Payload

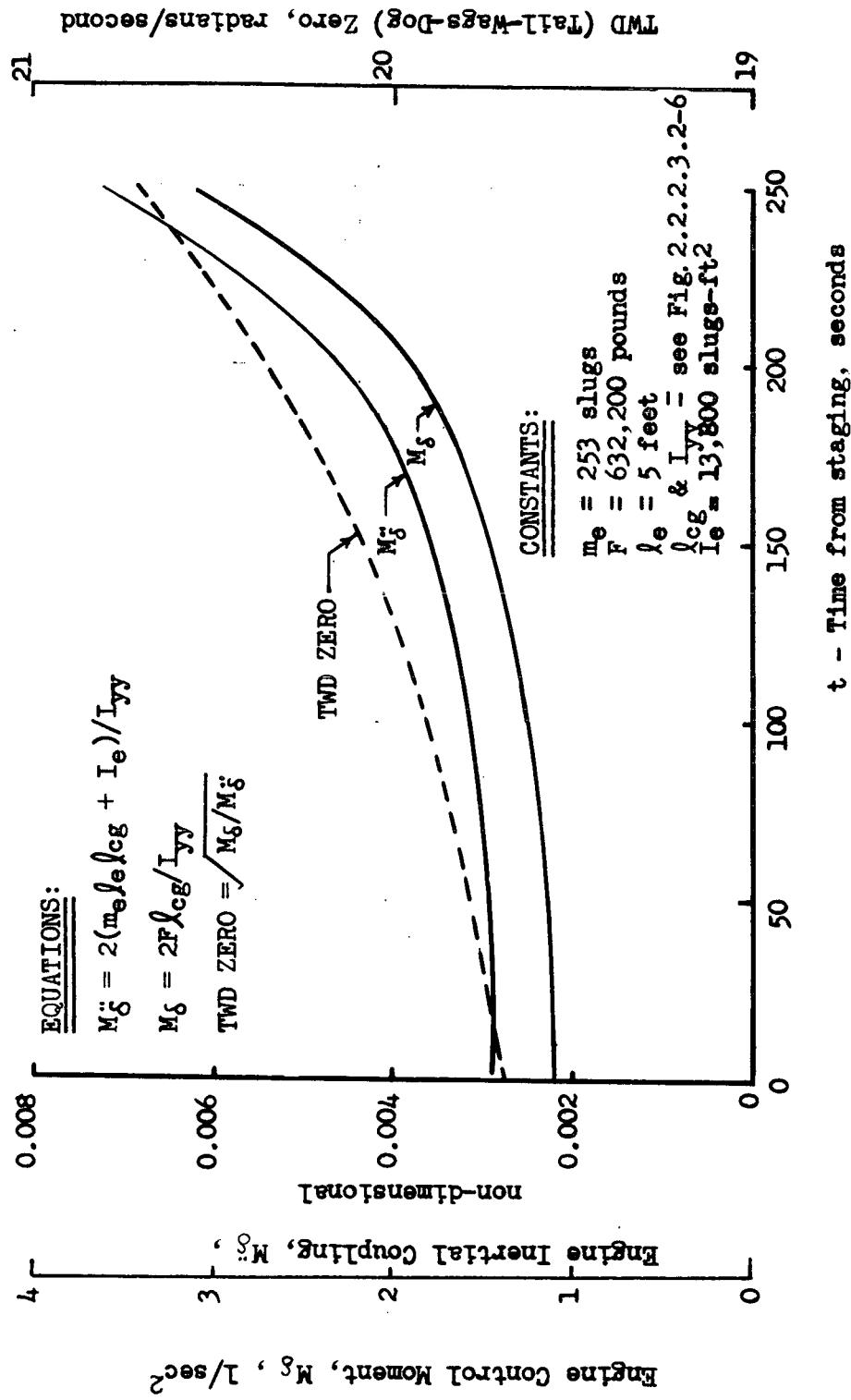


Figure 5-92. Pitch Axis "Tail Wags Dog" Zero, ESS With Space Station Payload



Following guidance initiation, the vehicle is commanded to pitch up at a 2 deg/sec rate until the vehicle attitude has reached 34 degrees. Thereafter, the vehicle pitches down at approximately 0.2 deg/sec until ESS burnout.

A 6-degree-of-freedom (DOF) digital control simulation, using the MDAC space station as the payload, was performed. For nominal separation with both ESS main engines operative, the results are shown in Figures 5-93 through 5-96. Figure 5-93 shows time history of pitch attitude and pitch attitude command. Figures 5-94 through 5-96 show attitude errors, vehicle body rates, and gimbal deflections. In general, the control system readily controlled the vehicle to the desired trajectory with good damping and with acceptable errors. Peak pitch and yaw gimbal deflections that occurred soon after separation were about 0.9 and 0.3 degrees, respectively.

2. One MPS Engine Inoperative. A critical aspect of TVC control for the main engines of ESS are the cant angles and TVC deflections required. Excessive cant angles and TVC deflections can impact vehicle performance and engine gimbaling requirements. Since the shuttle orbiter engines are being used, and have a gimbal deflection capability of ± 7 degrees for orbiter application, the ESS configuration will be established assuming no impact on orbiter engine design. A further consideration which has an appreciable impact on ESS design is a desirable inherent design capability that the ESS have a growth potential to a Chemical Interorbital Shuttle Mission. This condition for growth potential requires that the two main engines be widely spaced laterally as shown in Figure 5-79 to permit the addition of a docking adapter between the engines to provide for orbital mating for propellant loading.

For the one-engine-out condition, this wide lateral spacing of the engines has a major influence on the cant angle and of gimbal-angle requirements, and also on the magnitude of control axes coupling through the remaining engine.

The one-engine-out condition is critical with respect to yaw cant angle and yaw gimbaling in that the remaining engine must be toed in sufficiently to track the vehicle center of gravity (c. g.). A second critical aspect of the one-engine-out condition is that when the pitch gimbal is used for pitch control a large roll moment is generated.

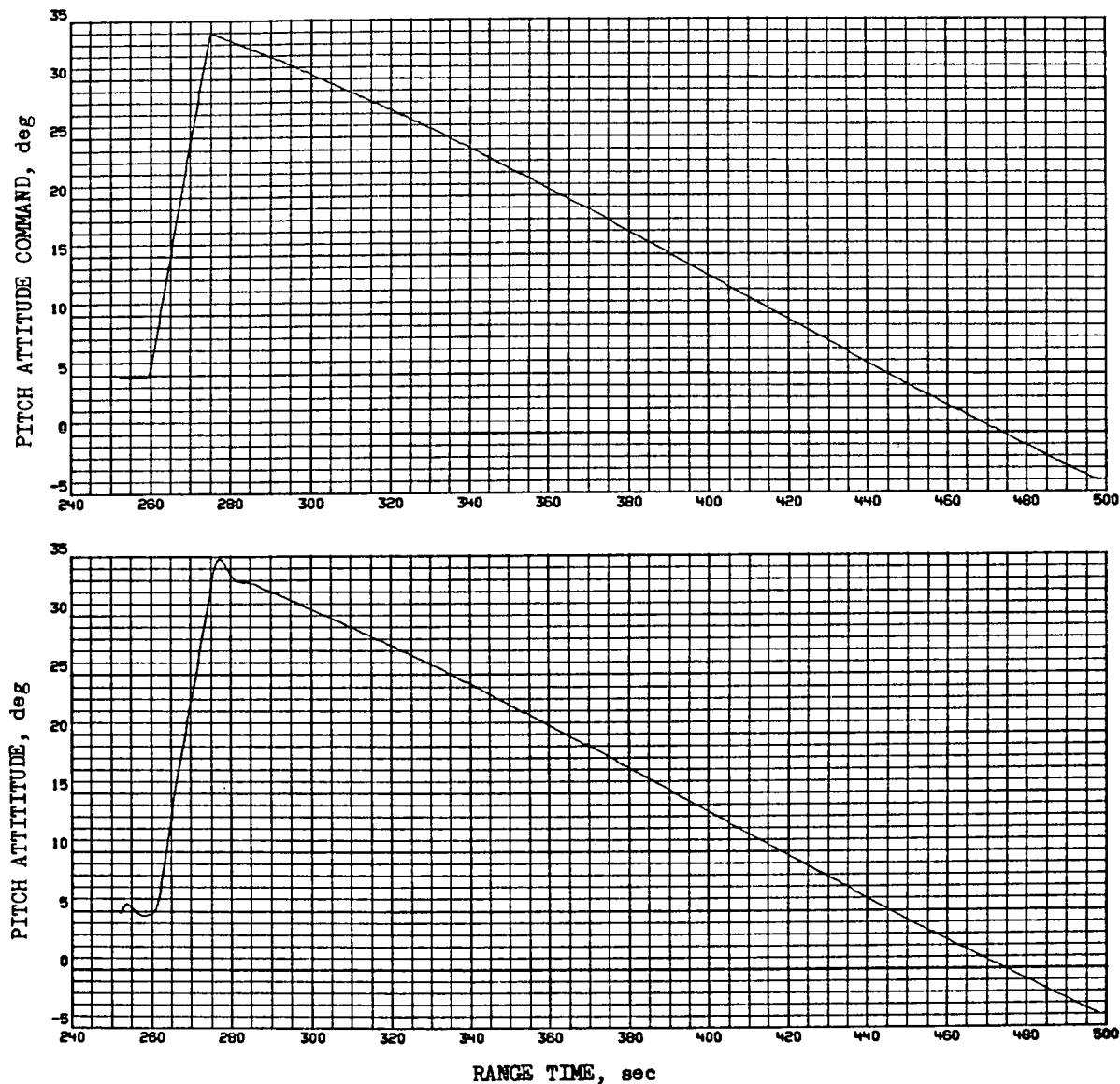


Figure 5-93. ESS 6 DOF Controlled Trajectory for Ascent
to Orbit, Nominal Trajectory With Space Station Payload

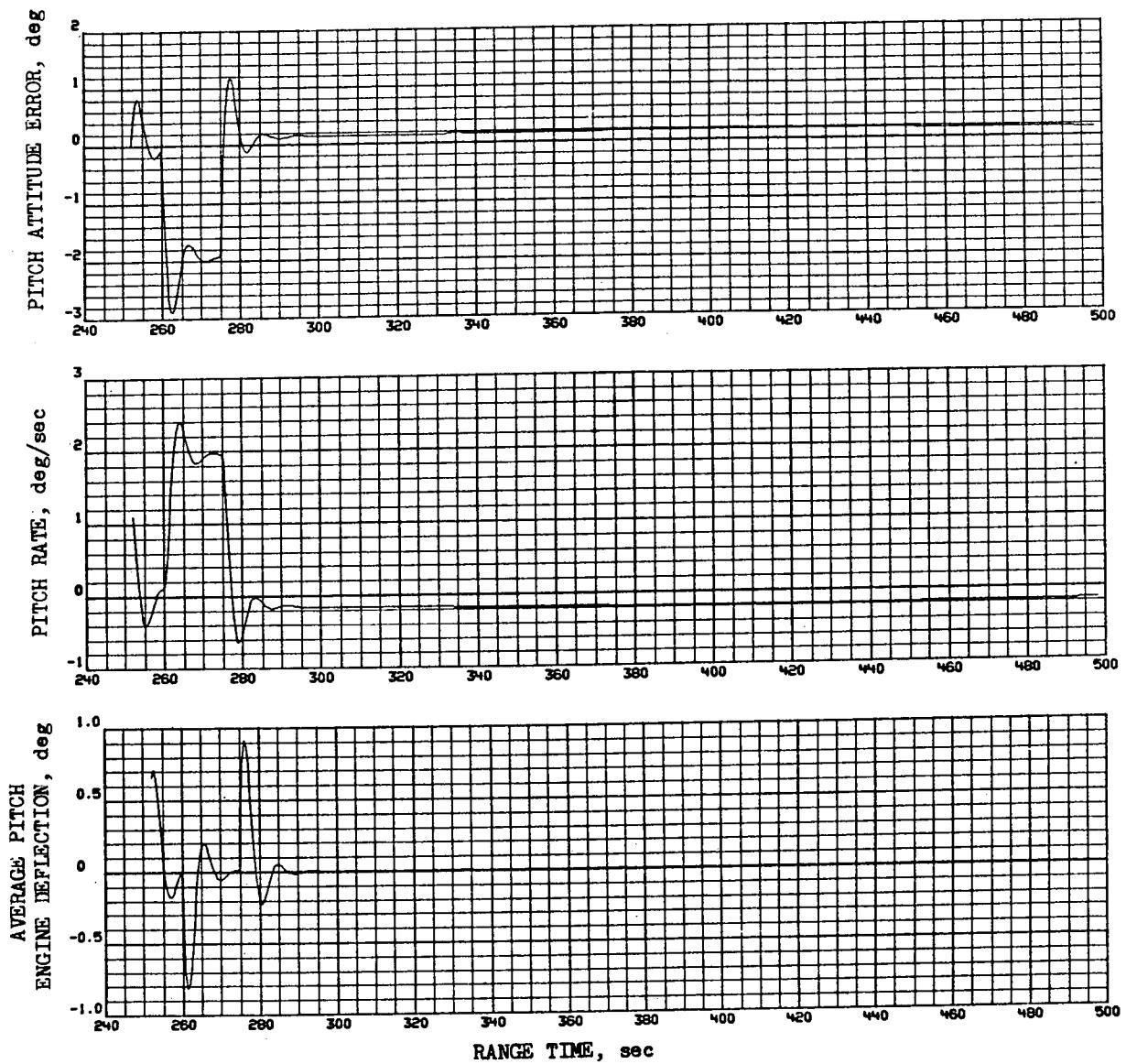


Figure 5-94. ESS 6 DOF Controlled Trajectory for Ascent
to Orbit, Nominal Trajectory With Space Station Payload
(Pitch)

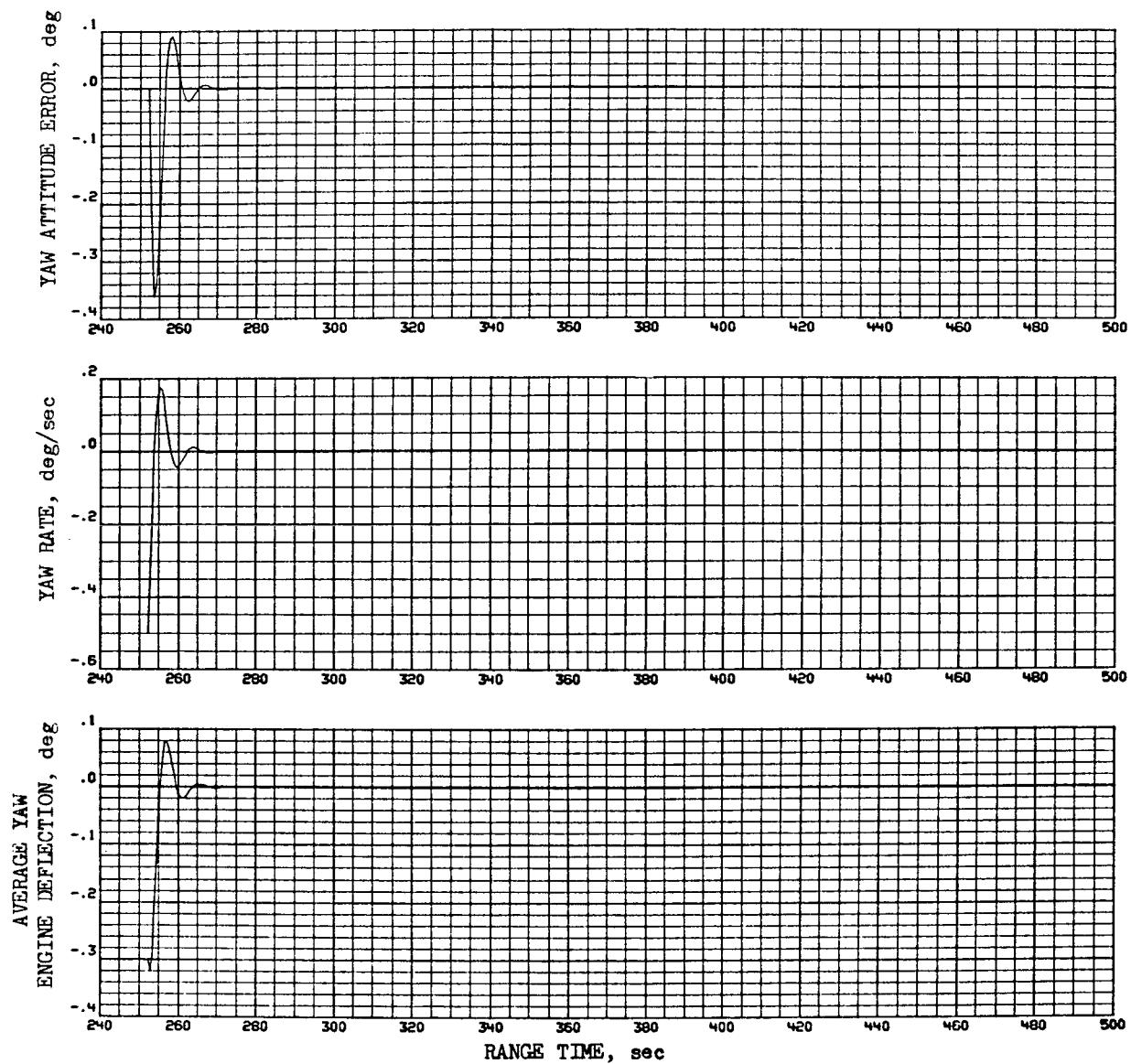


Figure 5-95. ESS 6 DOF Controlled Trajectory for Ascent
to Orbit, Nominal Trajectory With Space Station Payload
(Yaw)

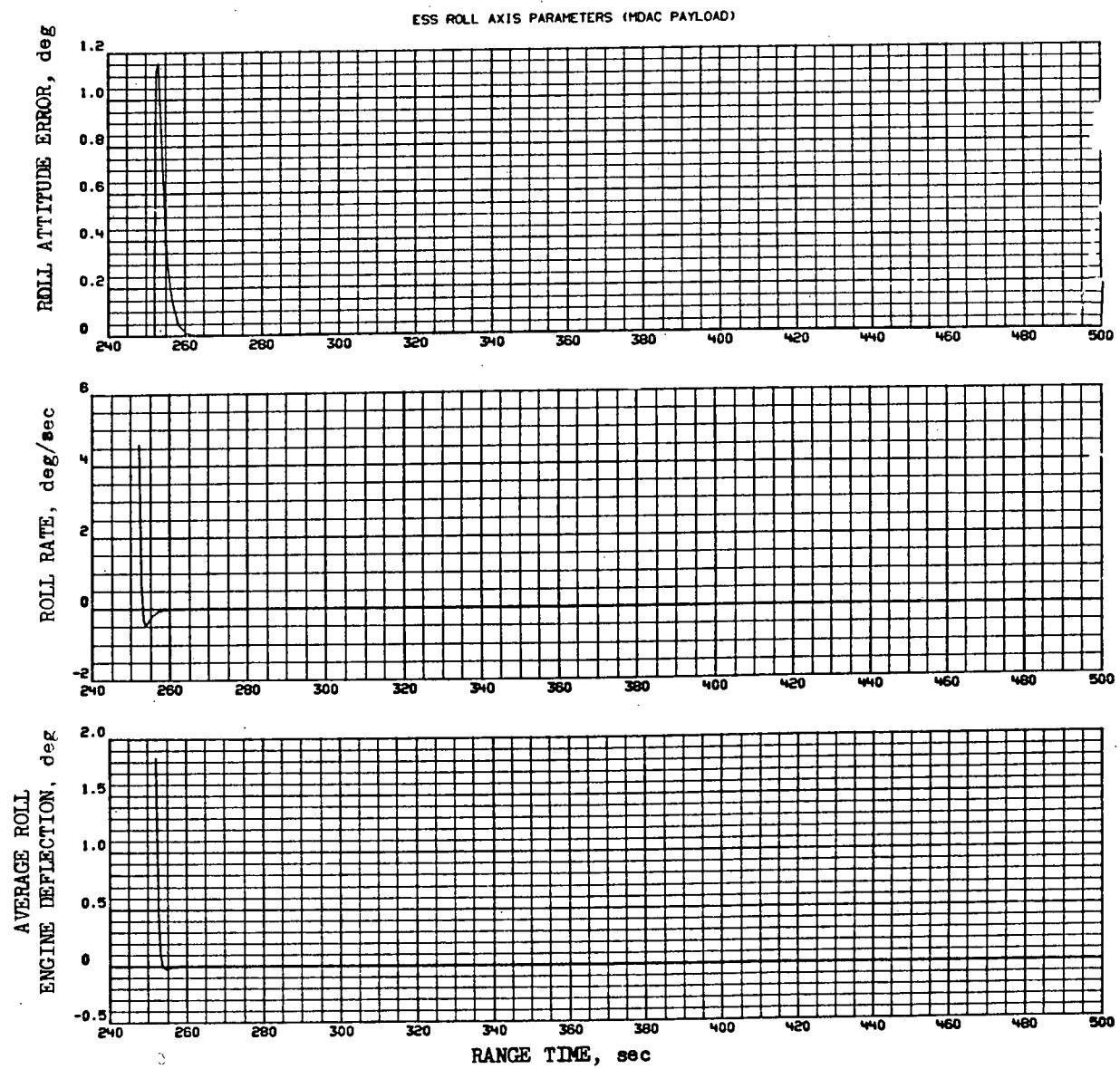


Figure 5-96. ESS 6 DOF Controlled Trajectory for Ascent to Orbit, Nominal Trajectory With Space Station Payload (Roll)



The analysis as presented here thus investigates cant- and gimbal-angle requirements with one engine out, determines the impact of cant- and gimbal-angle deflections on payload to orbit, and determines ACPS requirements for roll control.

- a. MPS Cant and Gimbal Angle Requirements. This section presents an analysis to determine the MPS engine cant-angle and deflection requirements. Also shown are the effects of engine cant angle on vehicle payload.

The ESS-plus-payload vehicle configuration, coordinate system, and MPS engine deflection angles are defined in Figure 5-97. The MPS engines are gimballed about the pitch and yaw vehicle-body axes for thrust-vector control. The design maximum deflection in each of these axes is ± 7 degrees. The MPS engines are oriented such that a total of ± 10 -degree TVC is available in pitch and yaw. An engine deflection of ± 7 degrees is used as the design maximum in one axis. The remaining three degrees are required for control in the other axis. The engines are also canted outboard in the yaw plane at installation to provide adequate yaw-axis control in the event of one engine failure. The cant angle points the thrust vector through an average center-of-gravity location which minimizes the upset moment when an engine fails.

This study is to determine the cant-angle and maximum-deflection requirements for the MPS engines with various payloads. In particular, the study questions are as follows:

- (1) What is the recommended engine cant angle (δ_{CT}) for each ESS-plus-payload vehicle configuration?
- (2) With the recommended cant angle, is the design maximum deflection of ± 7 degrees adequate for flight control?
- (3) If this ± 7 degree design maximum is not adequate, what maximum deflection (δ_{max}) is required?
- (4) What is the vehicle payload penalty resulting from the required cant angle?

The techniques for calculations of engine-deflection requirements and vehicle payload penalties as functions of cant angle are summarized below. In the calculations of δ_{max} , one of the MPS engines is assumed to be inoperative.



DEFINITIONS:
 δ_{CT} = ENGINE CANT ANGLE (YAW AXIS ONLY)
 δ = GIMBAL ENGINE DEFLECTION

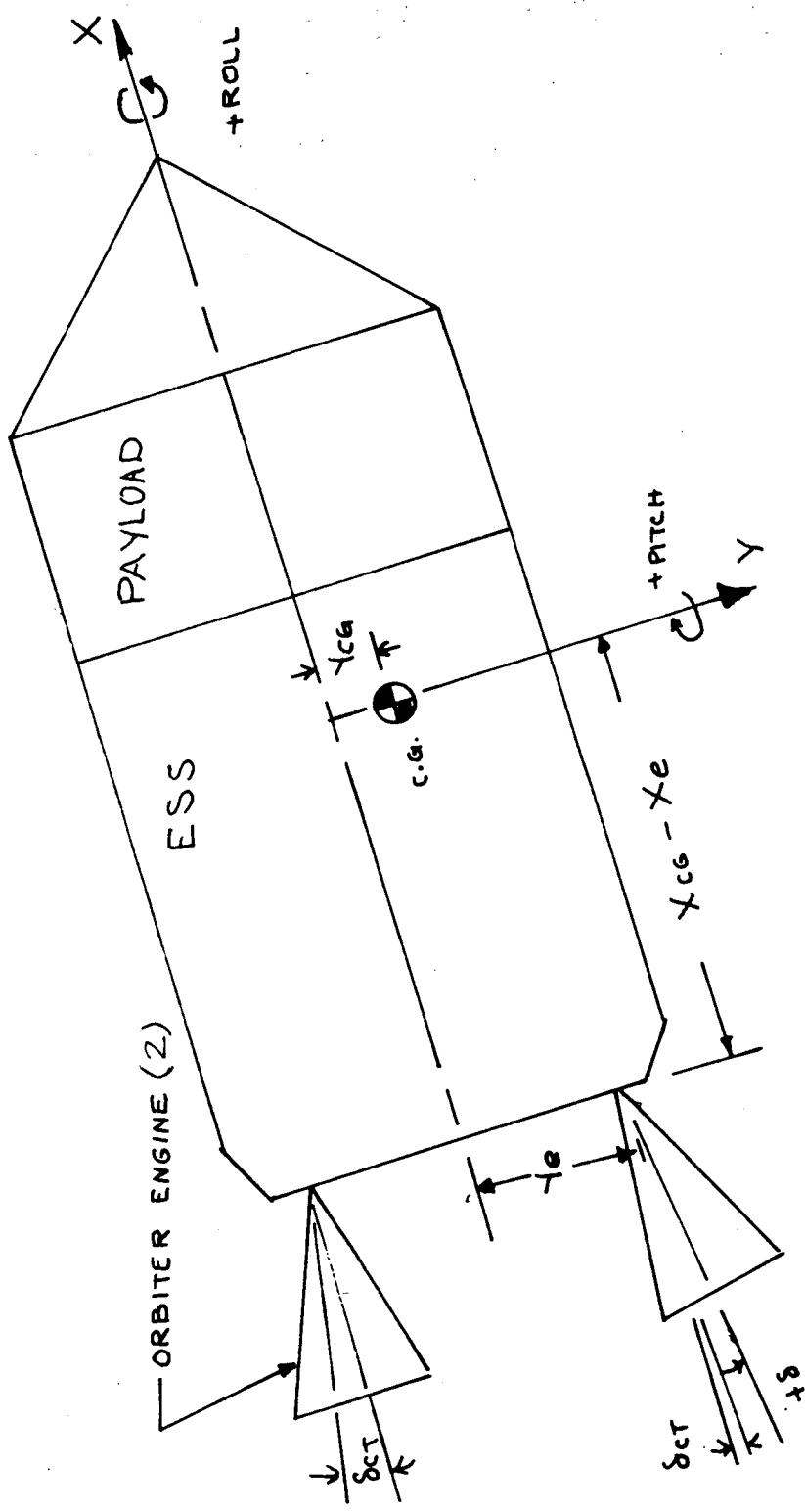


Figure 5-97. MPS Engine Angle Definitions (Yaw Plane)



- (1) Engine Deflection Requirement. The yaw-axis engine deflection requirement (δ_{max}) for each ESS vehicle with a payload is determined by the following steps.
- (a) Calculate engine deflection δ_s (with respect to vehicle centerline) required for yaw-axis static trim:

$$\delta_s = 57.3 \left(\frac{Y_e - Y_{cg}}{X_{cg} - X_e} \right) \text{ degrees}$$

The results are plotted in Figure 5-98. The extreme data points noted in Figure 5-98 are used for the calculations of (δ_{max}).

- (b) Calculate engine deflection δ_D (with respect to vehicle center line) required for yaw-axis control dynamic response.

$$\delta_D = \left(\frac{I_{zz} \dot{r}}{NF (X_{cg} - X_e)} \right) \text{ degrees}$$

N = number of control engines

F = 632,000-pound thrust per engine

\dot{r} = design angular acceleration

The results are plotted in Figure 5-99. Dynamic deflection requirements were selected based on a recommended design angular acceleration of 1 deg/sec².

- (c) Calculate the maximum engine deflection (δ_{max}) as function of cant angle (δ_{CT}) at the beginning and the end of engine thrusting.

$$\delta_{\text{max}} (\text{beginning burn}) = (1 + 0.25)$$

$$\times (\delta_{D1} + \delta_{S1} - \delta_{CT})$$

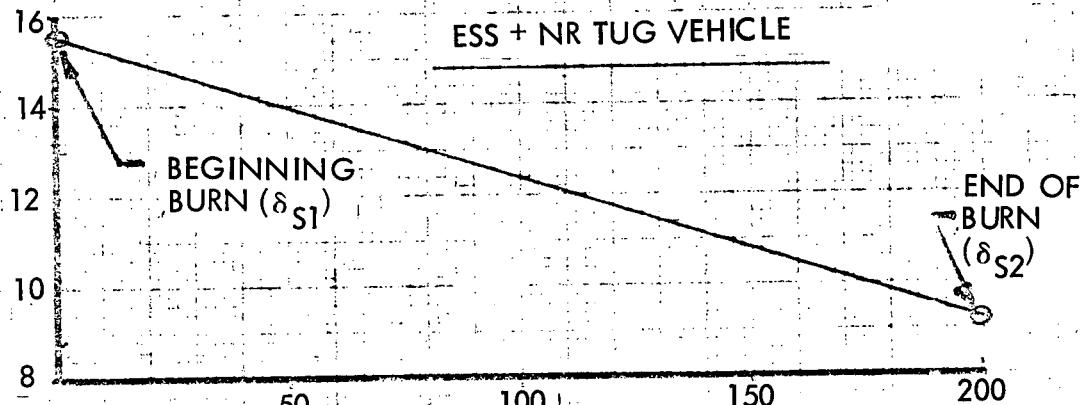
$$\delta_{\text{max}} (\text{end of burn}) = (1 + 0.25)$$

$$\times (-\delta_{D2} + \delta_{S2} - \delta_{CT})$$

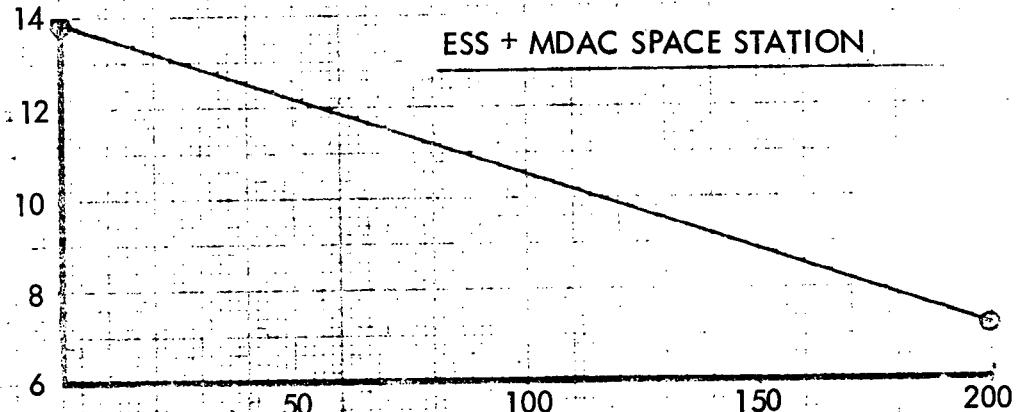
ENGINE DEFLECTION FOR STATIC TRIM, δ_S (DEGREES)

DATA POINTS USED FOR
CALCULATION OF δ_{MAX}

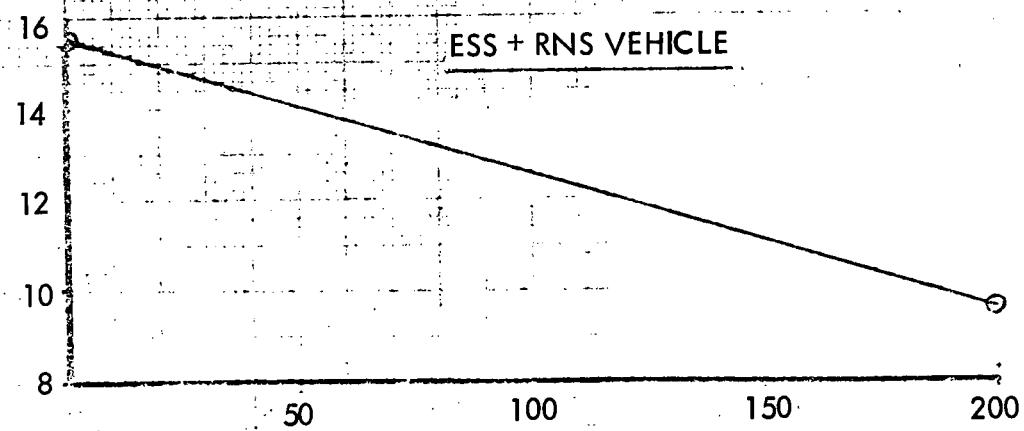
ESS + NR TUG VEHICLE



ESS + MDAC SPACE STATION



ESS + RNS VEHICLE



ESS FLIGHT TIME (SECONDS)

Figure 5-98. MPS Engine Deflection for Yaw Axis Static Trim (One Orbiter Engine Inoperative)

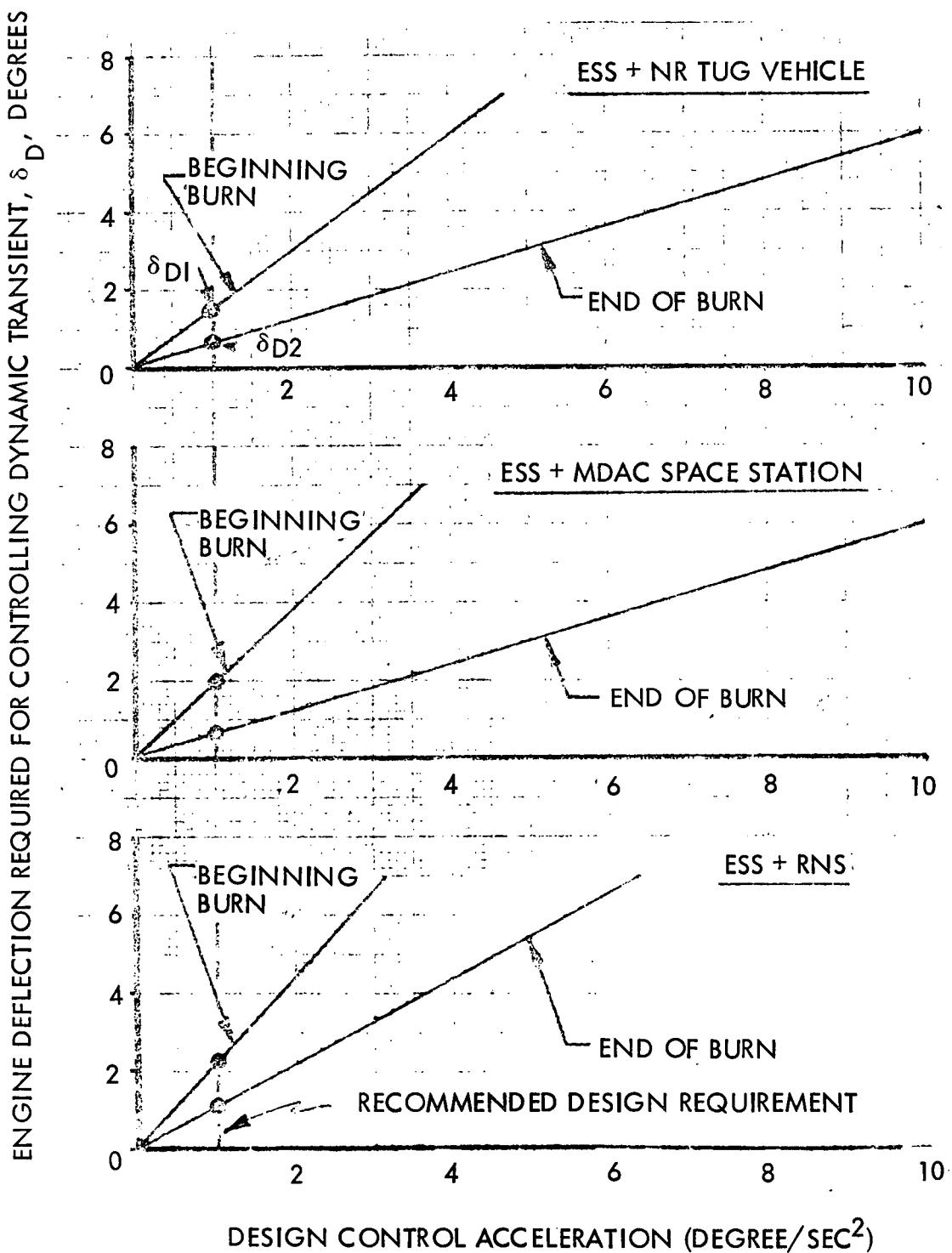


Figure 5-99. Required Engine Deflection for Controlling Yaw Axis Dynamic Transient



Where δ_S and δ_D are obtained from Figures 5-98 and 5-99. (See the noted data points in these figures.) A 25-percent design safety factor is added to the curves covering uncertainties such as thrust mis-alignments and other design tolerances. The results of this calculation are plotted in Figures 5-100 through 5-102.

The pitch-axis engine deflection requirements are calculated by the similar equations:

- (a) Engine deflection for pitch axis static trim.

$$\delta_S = 57.3 \left(\frac{Z_e - X_{cg}}{X_{cg} - X_e} \right) \text{ degrees}$$

$$\approx 57.3 \left(\frac{-Z_{cg}}{X_{cg} - X_e} \right), \text{ since } Z_e = 0$$

(Note that the engines are mounted on the Y axis.)

With the assumption that the maximum Z_{cg} variance is 4 inches*, the maximum value of δ_S is 0.6 degrees at beginning burn and is 0.3 degrees at end of burn. The angle δ_S is with respect to the vehicle centerline.

- (b) Engine deflection for controlling the pitch-axis dynamic transient.

$$\delta_D = \left(\frac{I_{yy}}{NF(X_{cg} - X_e)} \right) \dot{q} \text{ degrees}$$

Since $I_{yy} = I_{zz}$, the engine deflection for controlling the pitch-axis dynamic transient is approximately the same as that of the yaw axis (see Figure 5-100). The angle δ_D is with respect to the vehicle centerline.

* Recommended design value

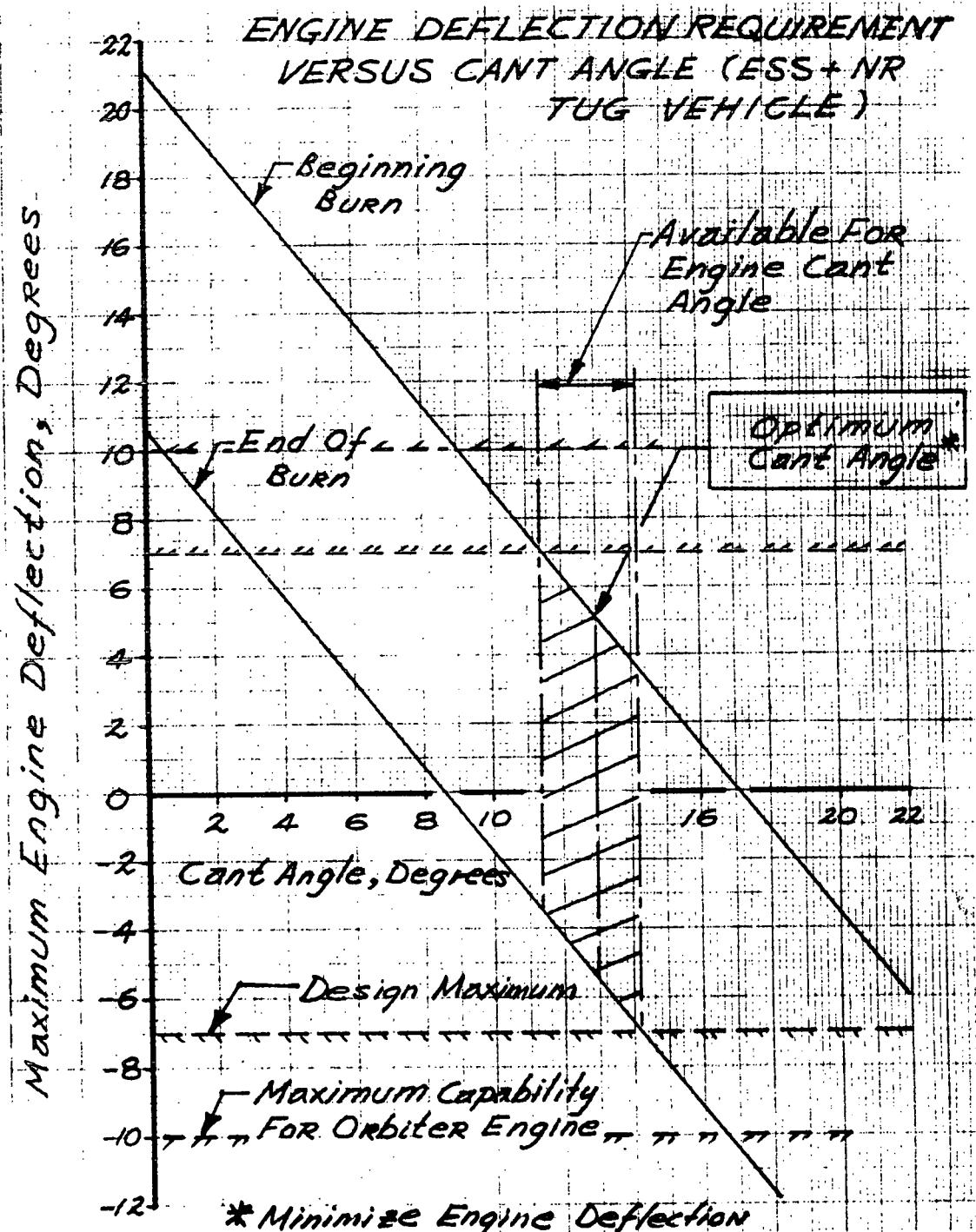


Figure 5-100. Yaw Axis Engine Deflection Requirement
Versus Cant Angle for ESS + Space Tug
(One MPS Engine Inoperative)



ENGINE DEFLECTION REQUIREMENT
VERSUS CANT ANGLE (ESS
+ MDAC SPACE STATION VEHICLE)

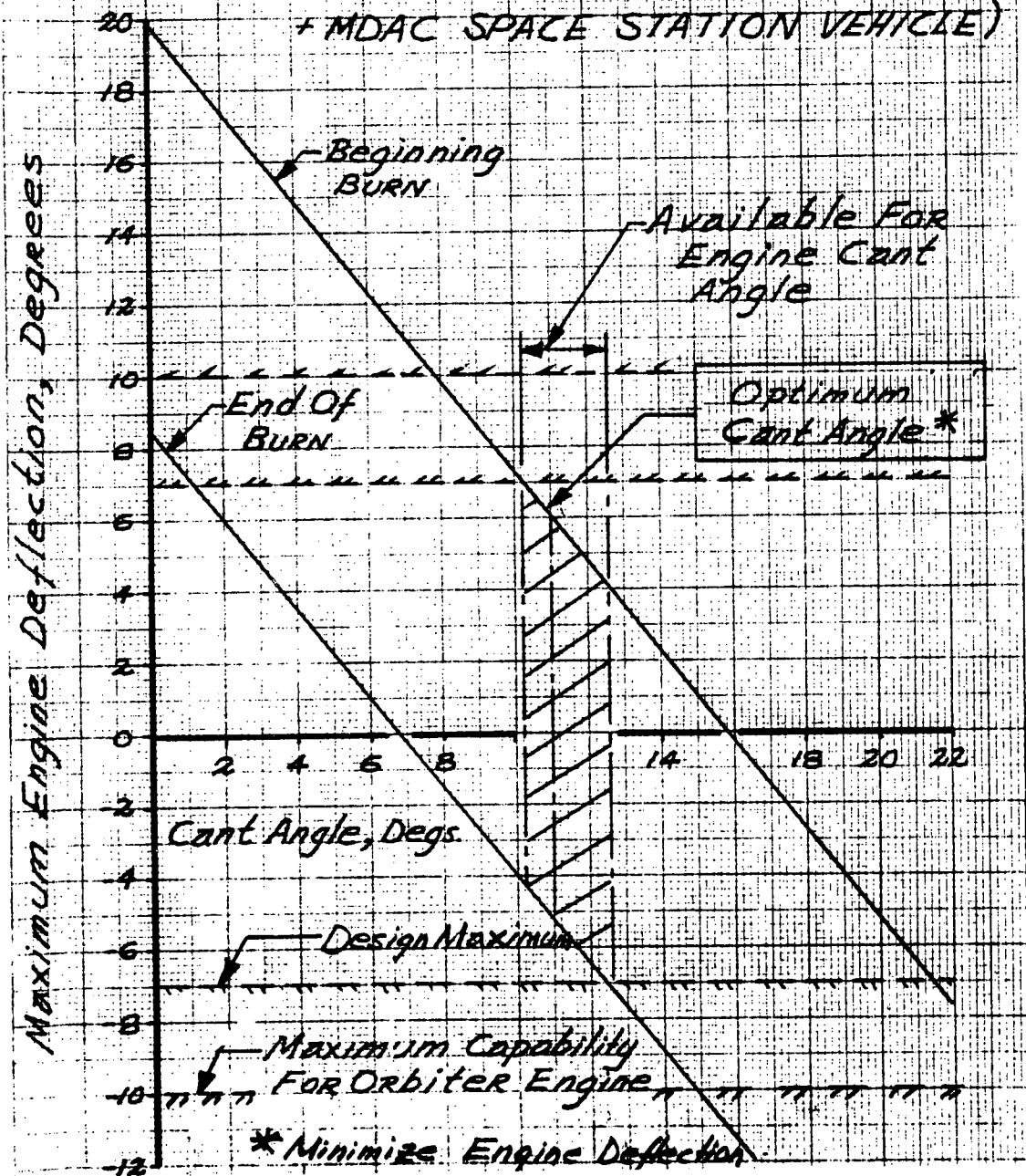


Figure 5-101. Yaw Axis Engine Deflection Requirement
Versus Cant Angle for ESS + MDAC Space Station
(One MPS Engine Inoperative)

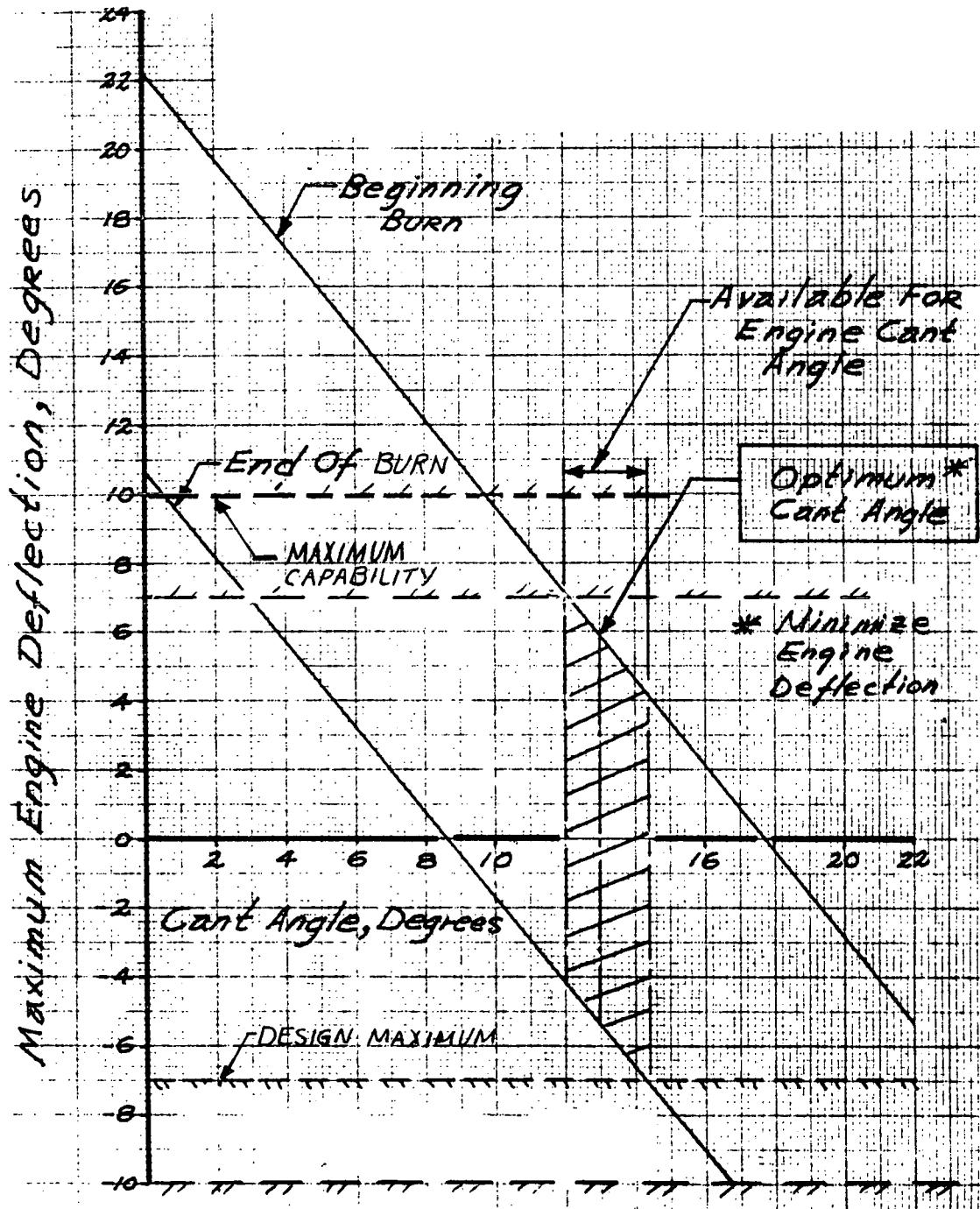


Figure 5-102. Yaw Axis Engine Deflection Requirement
Versus Cant Angle for ESS/RNS Vehicle
(One MPS Engine Inoperative)



(c) Maximum pitch axis engine deflection

$$\delta_{\max} (\text{beginning burn}) = 1.25 (\delta_{D1} + \delta_{S1})$$

$$\delta_{\max} (\text{end of burn}) = 1.25 (-\delta_{D2} + \delta_{S2})$$

The maximum values of δ_{S1} and δ_{S2} are 0.6 degrees and 0.3 degrees. From Figure 5-100, the maximum values of δ_{D1} and δ_{D2} at the recommended design acceleration are 2.2 degrees and 1.1 degrees. The maximum values of pitch-axis deflection at the beginning and end of burn are, therefore, 3.5 degrees and 1.8 degrees, respectively.

- (2) Vehicle Payload Penalty. The vehicle payload penalty (ΔW) as function of engine cant angle (δ_{CT}) is calculated by the following equation:

$$W = W_f \left[1 - \left(\frac{W_o}{W_f} \right) \left(\frac{W_f}{W_o} \right)^{1/\cos \delta_{CT}} \right]$$

Where W_o and W_f are the initial and final vehicle weights when the cant angle is zero.

From the above calculations, it can be seen that the maximum pitch-axis deflections are smaller than those of the yaw axis. For this reason, the maximum yaw-axis deflection is used to establish the engine-deflection requirements for both the pitch and yaw axes.

The engine deflection requirements (plus or minus δ_{\max}) as function of cant angle are plotted in Figure 5-103 whereas the vehicle payload penalty as function of MPS engine cant angle is plotted in Figure 5-104. These $|\delta_{\max}|$ characteristics are constructed by taking the maximum absolute values of the upper and lower curves (begin and end of burn) as shown in Figures 5-100 through 5-102.

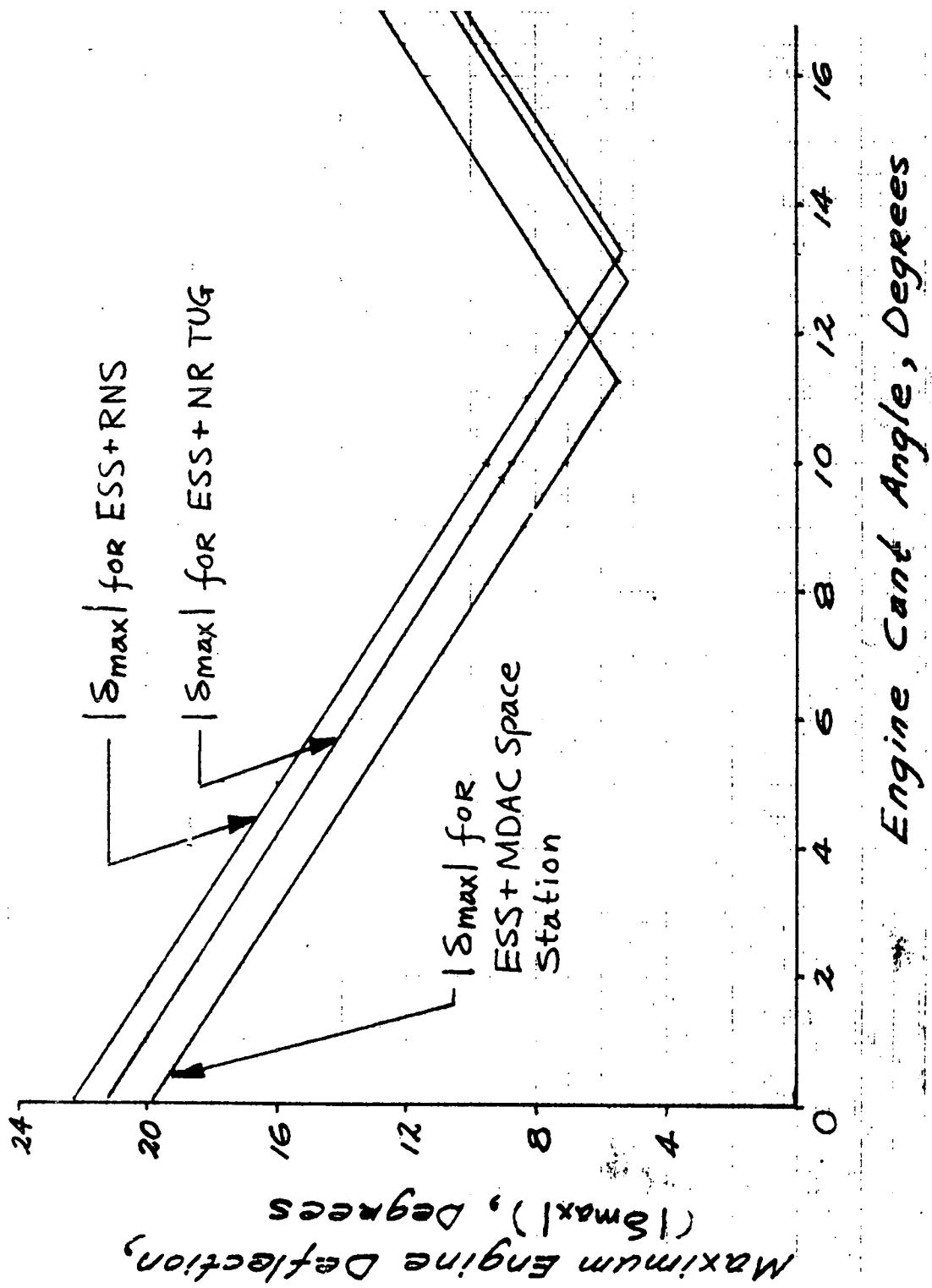


Figure 5-103. Summary of MPS Engine Deflection Requirement Versus Cant Angle
(One MPS Engine Inoperative)

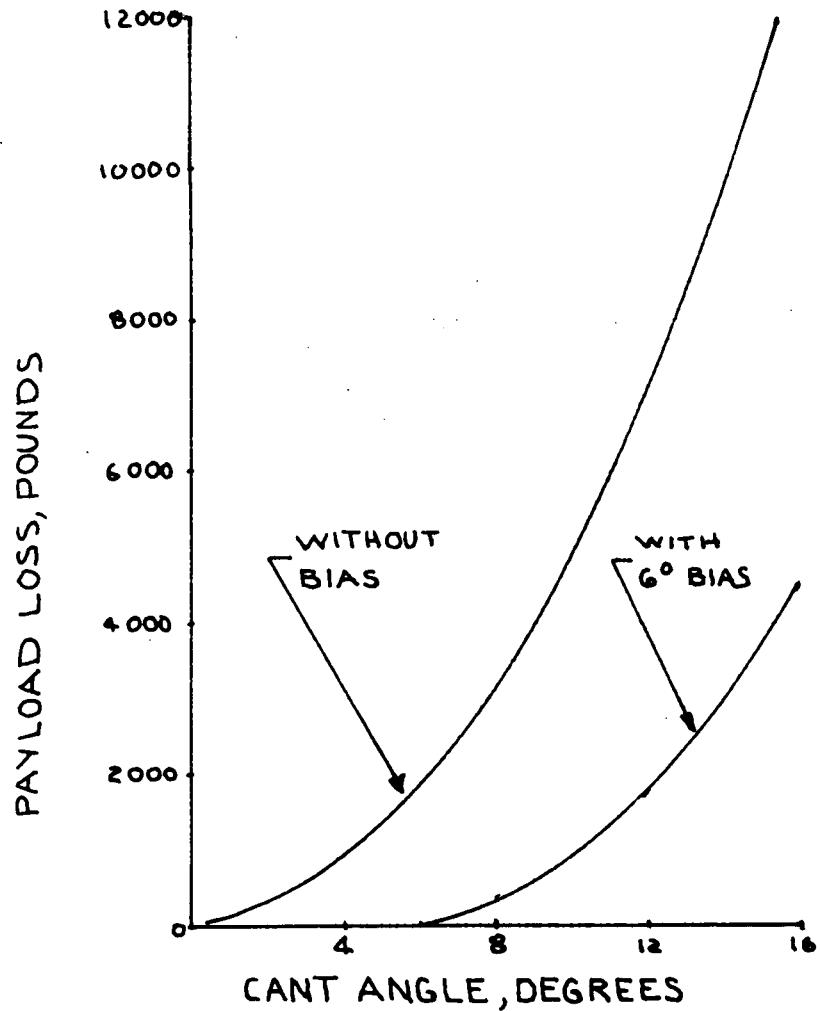


Figure 5-104. Vehicle Payload Penalty Versus MPS Engine
Cant Angle



Three important indications should be noted in Figure 5-103. First, the required gimbal deflection is a minimum for a particular cant angle. Second, there is no acceptable cant angle if the engine-deflection capability falls below 5.5 degrees. Third, the engine cant angle need not be greater than 13 degrees. With these indications and the ± 10 -degree limiting capability of the MPS engine, the possible combinations of cant-angle and maximum-deflection requirements are tabulated in Table 5-7 for comparison.

Table 5-7. ESS Flight Control Requirements

Maximum Engine Deflection Requirement (degrees)	Engine Cant-Angle Requirement (degrees)		
	MDAC Space Station	NR RNS	NR Tug
± 6	11	13	13
± 7	10	12	12
± 8	9	11	11
± 9	9	11	10
± 10	8	10	9

The main conclusion is that the design maximum engine deflection of ± 7 degrees is adequate for pitch- and yaw-axis control with one engine out provided the required engine cant angles are as follows.

Vehicle Configuration	Minimum Engine (Cant Angle (deg))
ESS + MDAC space station	10
ESS + NR RNS	12
ESS + NR tug	12



The vehicle payload penalties corresponding to these required cant angles range from 4800 to 7000 pounds (or 1.6 to 2.3 percent of the in-orbit ESS-plus-payload vehicle weight) if no engine-deflection bias is provided. This payload penalty can be reduced to 2000 pounds if the engine-deflection angle is biased by using a control signal to deflect the engine six degrees in the opposite direction to the cant angle during normal thrusting.

For the sake of design commonality, the recommended cant angle for all ESS vehicle configurations examined is 12 degrees.

- b. Roll Control in the Event of Single MPS Engine Failure. The attitude control propulsion system (ACPS) is used for ESS roll control in the event of one MPS failure. To determine the number of ACPS jets required for roll control, a 6-DOF simulation study was performed. The assumption used in this one-engine-out simulation study is the same as those of the nominal case discussed above. The results are plotted in Figure 5-105.

Figure 5-105 shows the maximum roll rate and attitude resulting from different numbers of jets and payload configurations. Three zones of acceptability are shown for maximum roll attitude. The 30-to-45-degree attitude range represents questionable acceptability based upon possible amplifier saturation. (The amplifier saturation level for the Saturn V is 15 deg and for the ESS higher values were assumed.) The effects of saturation are not considered hard limits as the vehicle is expected to remain stable and controlled. The three zones on the figures are thus stated as acceptable, and probably not acceptable. With four or less jets, the maximum roll attitude would probably not be acceptable or at least questionably acceptable. With eight jets or more, the maximum roll attitude is acceptable for all three payloads.

Figure 5-105 also shows that the maximum roll rate is relatively insensitive to the number of jets that are used. The maximum rates are less than 30 deg/sec, which implies 0.4-g radial acceleration at a radius of 16 feet. It requires 81-deg/sec roll rate for 1-g radial acceleration which might be considered as an upper limit for structural reasons. Thus, the predicted maximum rates are acceptable on this basis. Based on these results, eight jets have been selected for roll control to satisfy the one-MPS-out requirement.

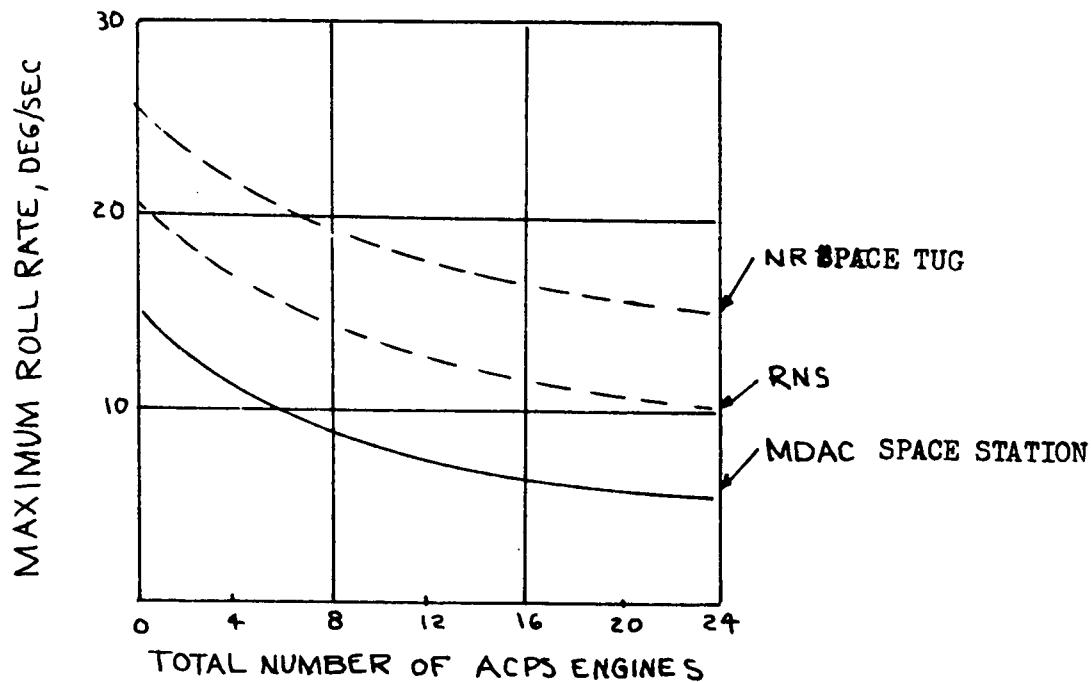
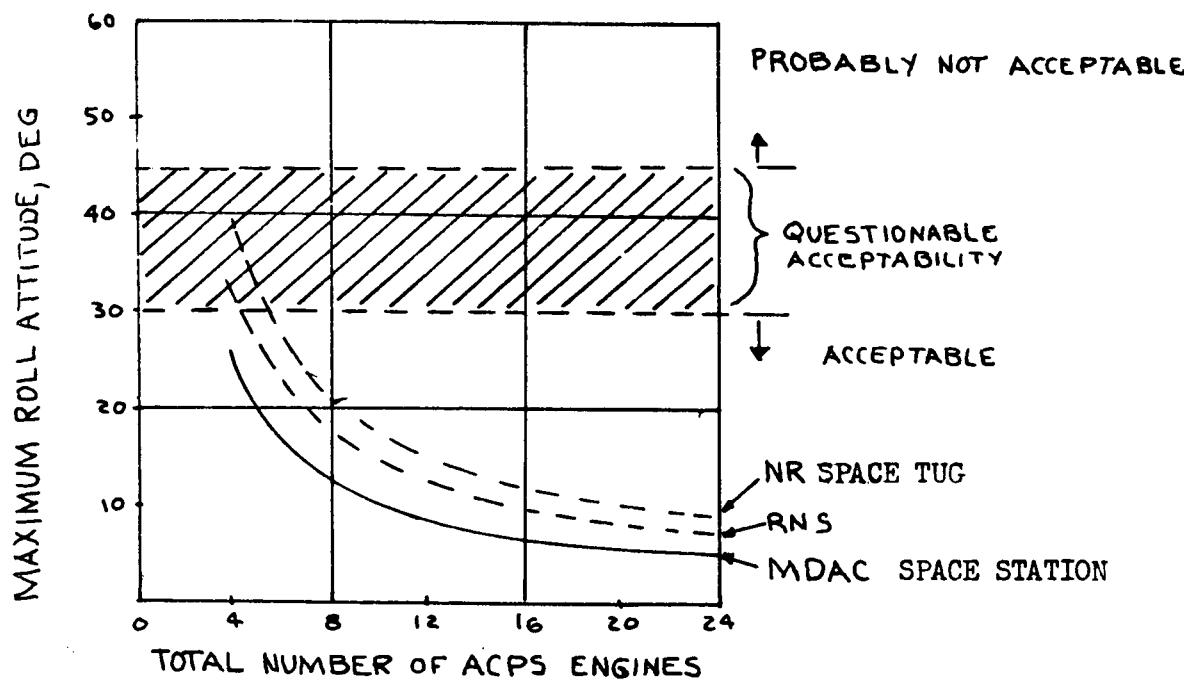


Figure 5-105. Maximum Roll Attitude and Roll Rate Following Arrest of 2 Deg/Sec Pitchup Maneuver and Initiation of -0.2 Deg/Sec Pitch Over



With the eight jets for roll control, the vehicle dynamics and MPS-engine deflection obtained from the simulation are shown in Figures 5-106 through 5-108. Figure 5-106 shows that the maximum pitch engine deflection is 1.5 degrees following arrest of the 2-deg/sec pitch-up maneuver. This deflection induces a roll moment and large roll dynamics. The roll dynamics that result from the orbiter engine deflection and the ACPS are shown in Figure 5-107. The maximum roll attitude error and roll rate are 13 degrees and 9 deg/sec, respectively.

The yaw-axis parameters are shown in Figure 5-108. The attitude error and average yaw-engine deflection change throughout the entire flight. This change is caused by the c. g. moving forward.

The results of this simulation study confirm that a total number of eight orbiter jets (with 2100-pound thrust each) is adequate for roll control during MPS operation with one engine out.

Attitude Control During Orbital Operations and ESS Deorbit. During nominal orbital and deorbit operations, three-axis attitude control is provided either by thrust vector control (TVC) of the OMS engines or by ON-OFF operation of the ACPS engines. The ACPS is also used to aid the OMS TVC if one, or both, OMS engines is not operative. An analyses is presented here of the gimbal- and cant-angle requirements of the OMS engines, and of the payload penalty resulting from OMS cant-angle deflection. An analysis is also presented of ACPS requirements with one OMS engine operative.

1. OMS Engine Cant-Angle and Deflection Requirements. This section presents the engine cant-angle and deflection requirements for the orbital maneuvering system (OMS) during the ESS orbital and deorbit ΔV maneuvers with one OMS operational. It also shows the effect of engine cant angle on vehicle payload penalty.

The ESS-plus-payload vehicle configuration, coordinate system, and OMS engine deflection angles are defined in Figure 5-109. The OMS engines are used for orbital ΔV maneuvers (such as orbit circulation, orbit phasing, and rendezvous) and deorbit. The total propellant for the OMS control operations is about 23,000 pounds of which 3,000 pounds are reserved for ESS deorbit.

The OMS engines are gimballed (with equal deflection capability) about the pitch and yaw vehicle-body axes for thrust-vector control.

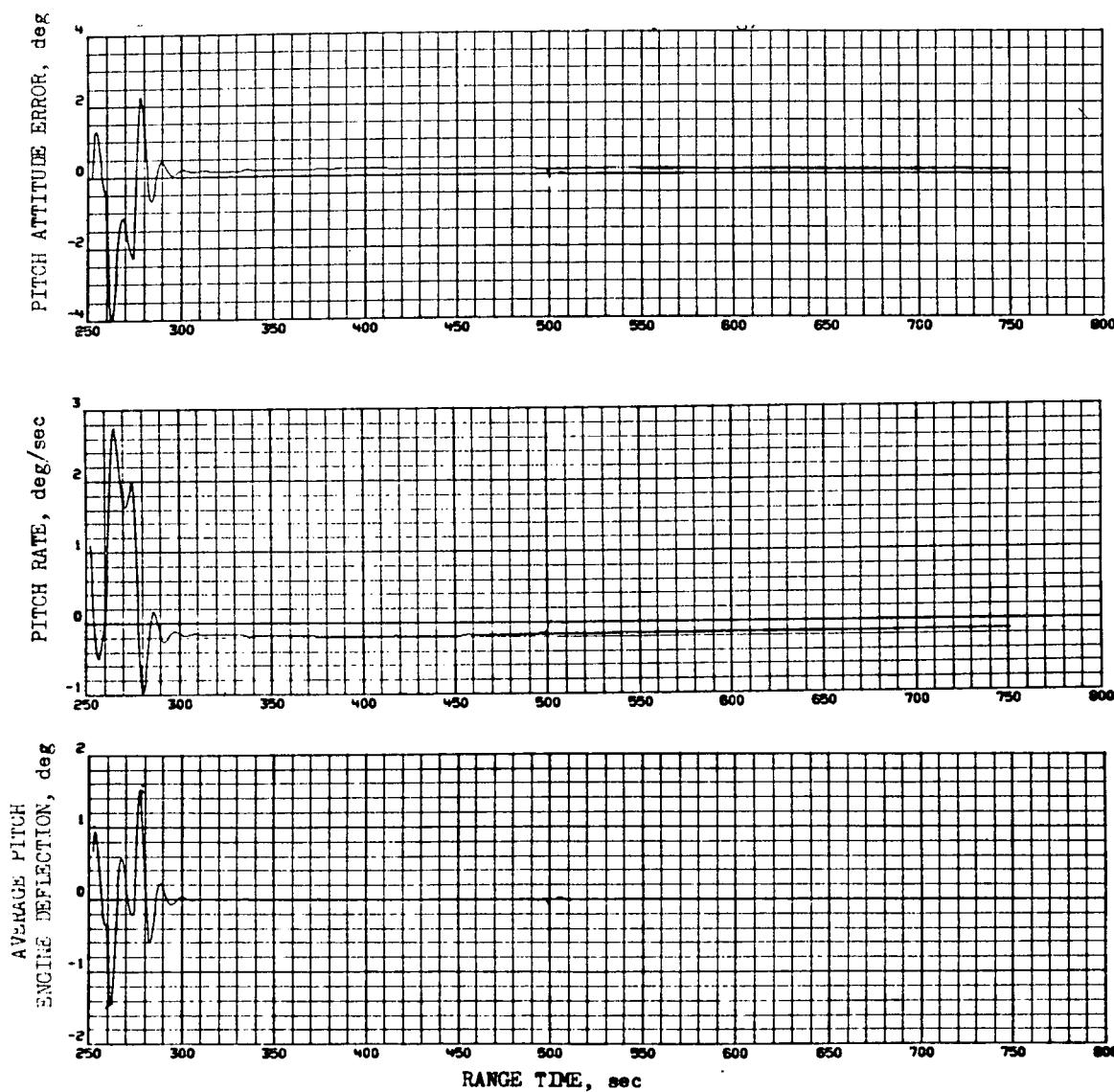


Figure 5-106. 6 DOF Controlled Trajectory for Ascent to Orbit,
Separation Transient, One Main Engine Inoperative,
Space Station Payload

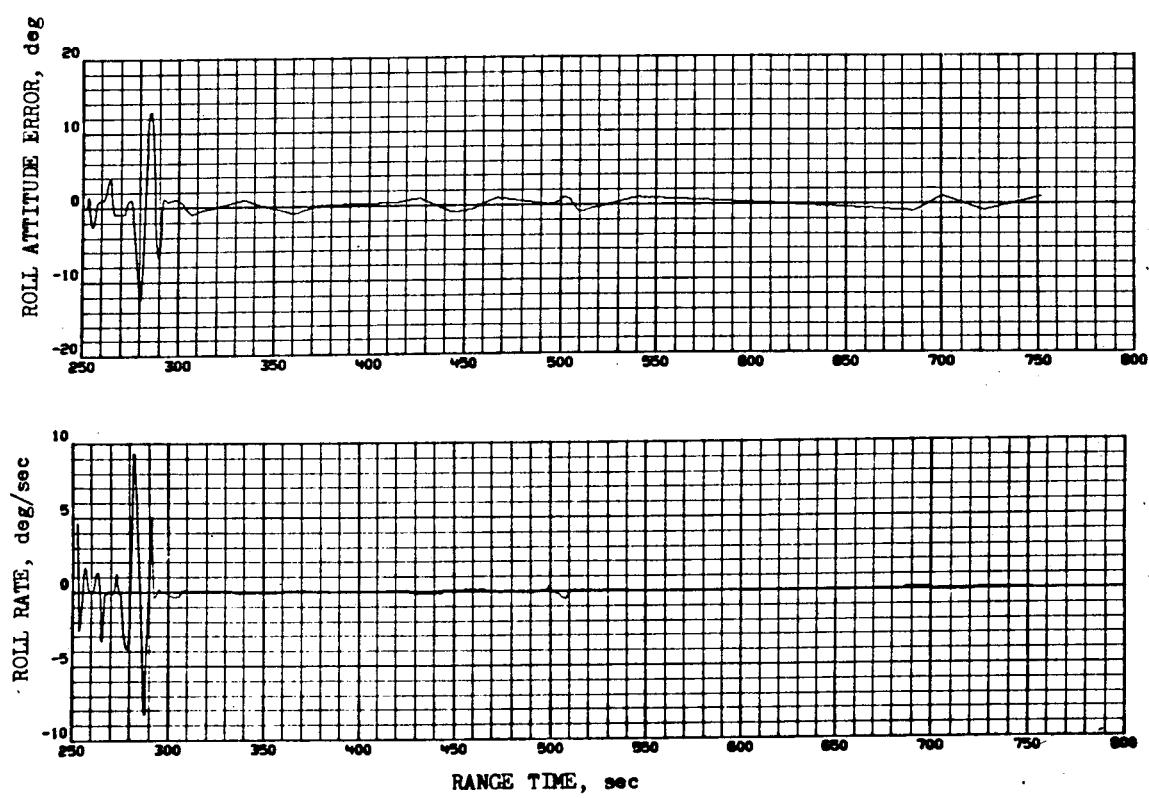


Figure 5-107. 6 DOF Controlled Trajectory for Ascent to Orbit,
Separation Transient, One Main Engine Inoperative,
Space Station Payload

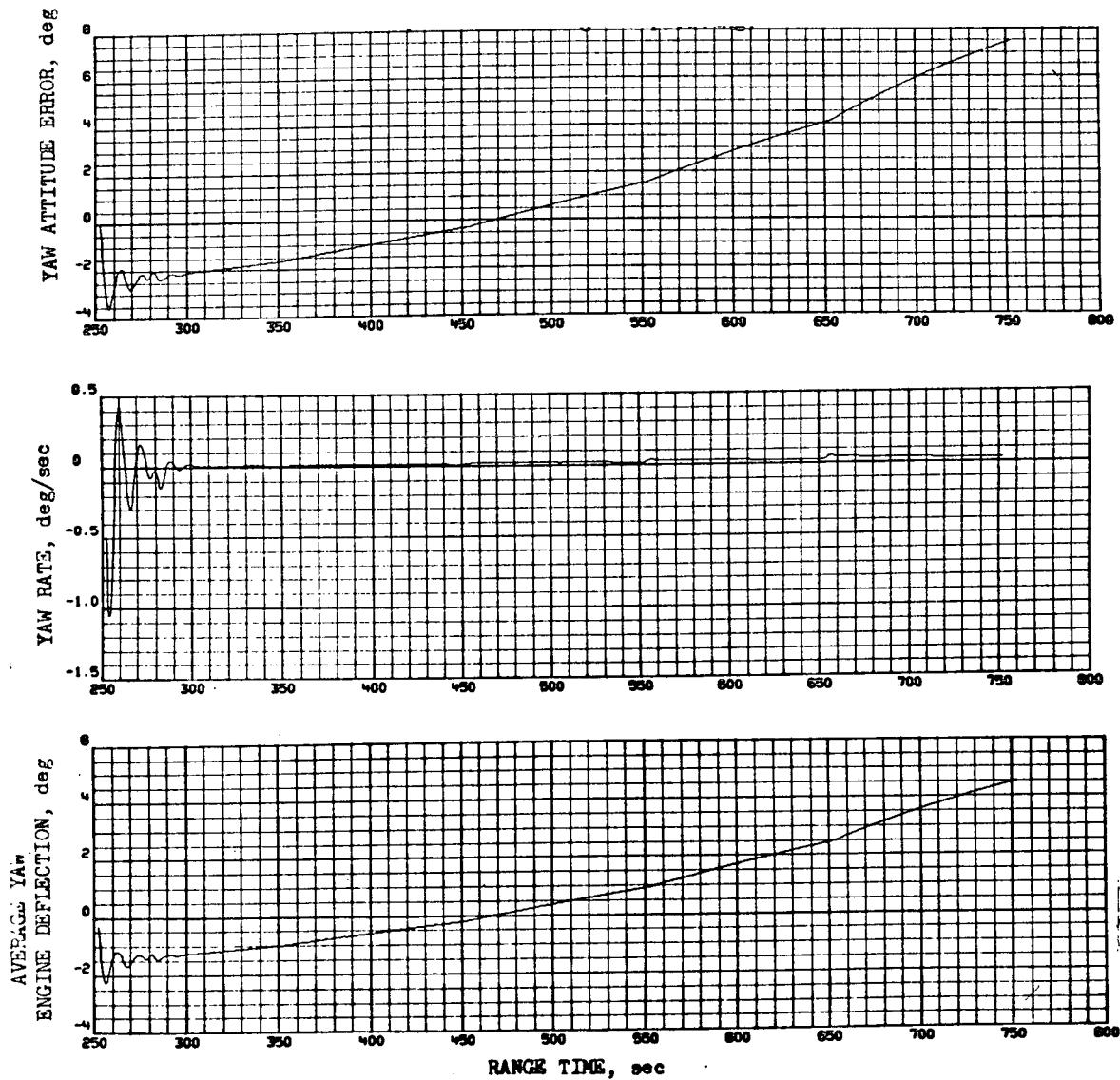


Figure 5-108. ESS 6 DOF Controlled Trajectory for Ascent
to Orbit, Separation Transient, One Main Engine
Inoperative, Space Station Payload

DEFINITIONS :
 δ_{ct} = OMS ENGINE CANT ANGLE
 ς = GIMBAL ENGINE DEFLECTION

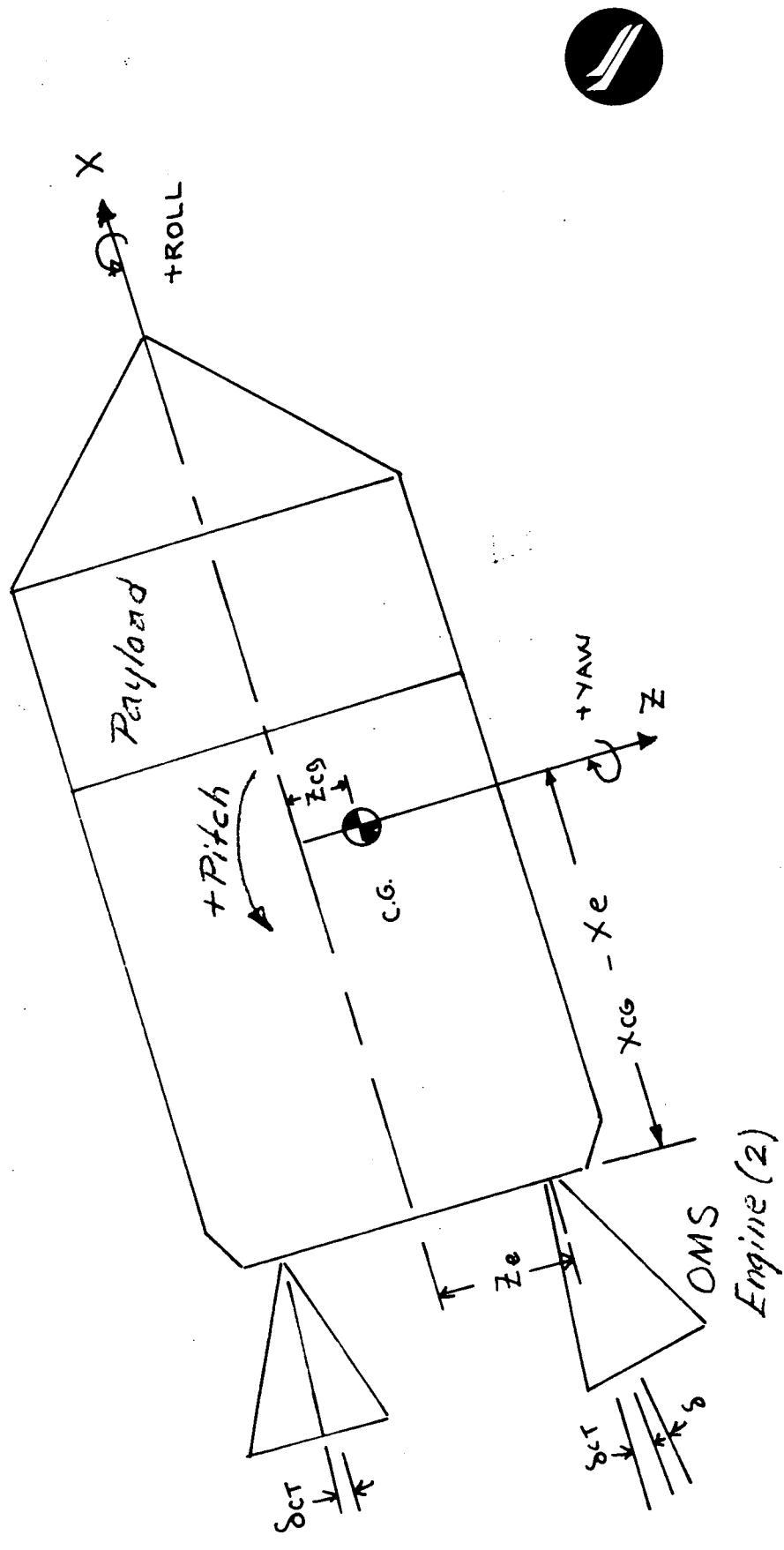


Figure 5-109. OMS Engine Angle Definitions (Pitch Plane)



- (1) Calculate engine deflection δ_s (with respect to vehicle centerline) for pitch-axis static trim:

$$\delta_s = 57.3 \left(\frac{Z_e - Z_{cg}}{X_{cg} - X_e} \right) \text{ degrees}$$

The results are plotted in Figure 5-110. The noted data points are used for δ_{max} calculation. The general characteristics for static-trim engine deflection versus vehicle X_{cg} location are also determined and are plotted in Figure 5-111.

- (2) Calculate engine deflection δ_D (with respect to vehicle center line) for controlling pitch-axis dynamic transient.

$$\delta_D = \left(\frac{I_{yy} \dot{q}}{NF(X_{cg} - X_e)} \right) \text{ degrees}$$

N = number of control engines

F = 10,000-pound thrust per engine

\dot{q} = design angular acceleration

The results are plotted in Figure 5-112. In this figure, an important remark should be noted. In a previous section, an acceleration level of 1.0 deg/sec^2 was used for the MPS. If 1.0 deg/sec^2 is used for the OMS, the δ_D angle can be as much as 50 degrees, which is not practical. For this reason, an arbitrary acceleration level of 0.05 deg/sec^2 is chosen as design basis. Further analysis is needed to verify the adequacy of this acceleration level. (An alternative method for pitch and yaw control is to use reaction jets.)

- (3) Calculate the maximum engine deflection (δ_{max}) as a function of cant angle (δ_{CT}).

$$\delta_{max} (\text{OMS propellant full}) = 1.25 (\delta_{D1} + \delta_{S1} - \delta_{CT})$$

$$\begin{aligned} \delta_{max} (\text{OMS propellant at 3000 lbs}) &= 1.25 (-\delta_{D2} + \delta_{S2} - \delta_{CT}) \end{aligned}$$



○ Data Points Used For
Calculation Of δ_{max}

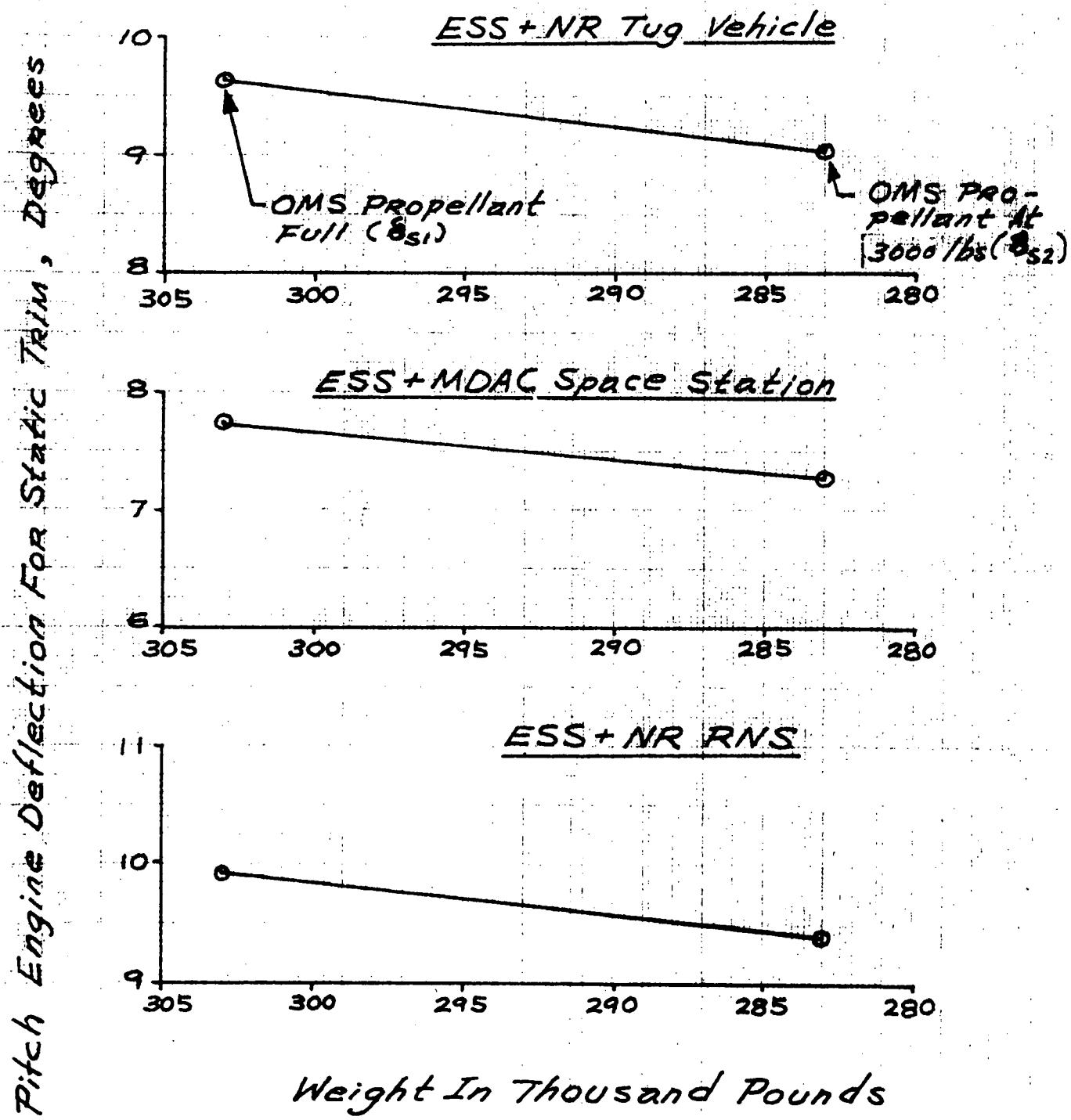


Figure 5-110. Pitch Engine Deflection From Static Trim
(One OMS Engine Inoperative)

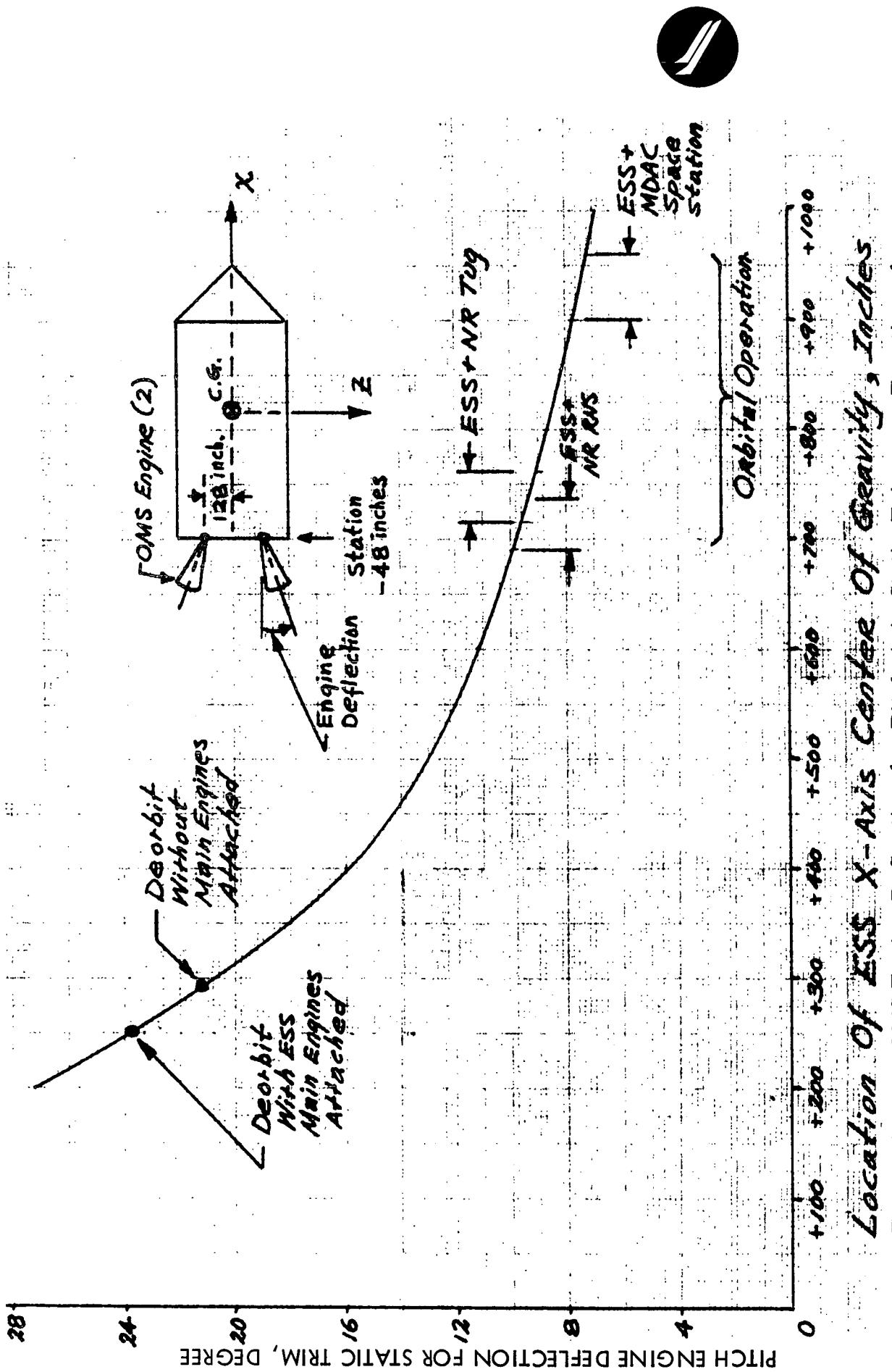


Figure 5-111. OMS Engine Deflection for Pitch Axis Static Trim as a Function of CG Position (One OMS Engine Inoperative)

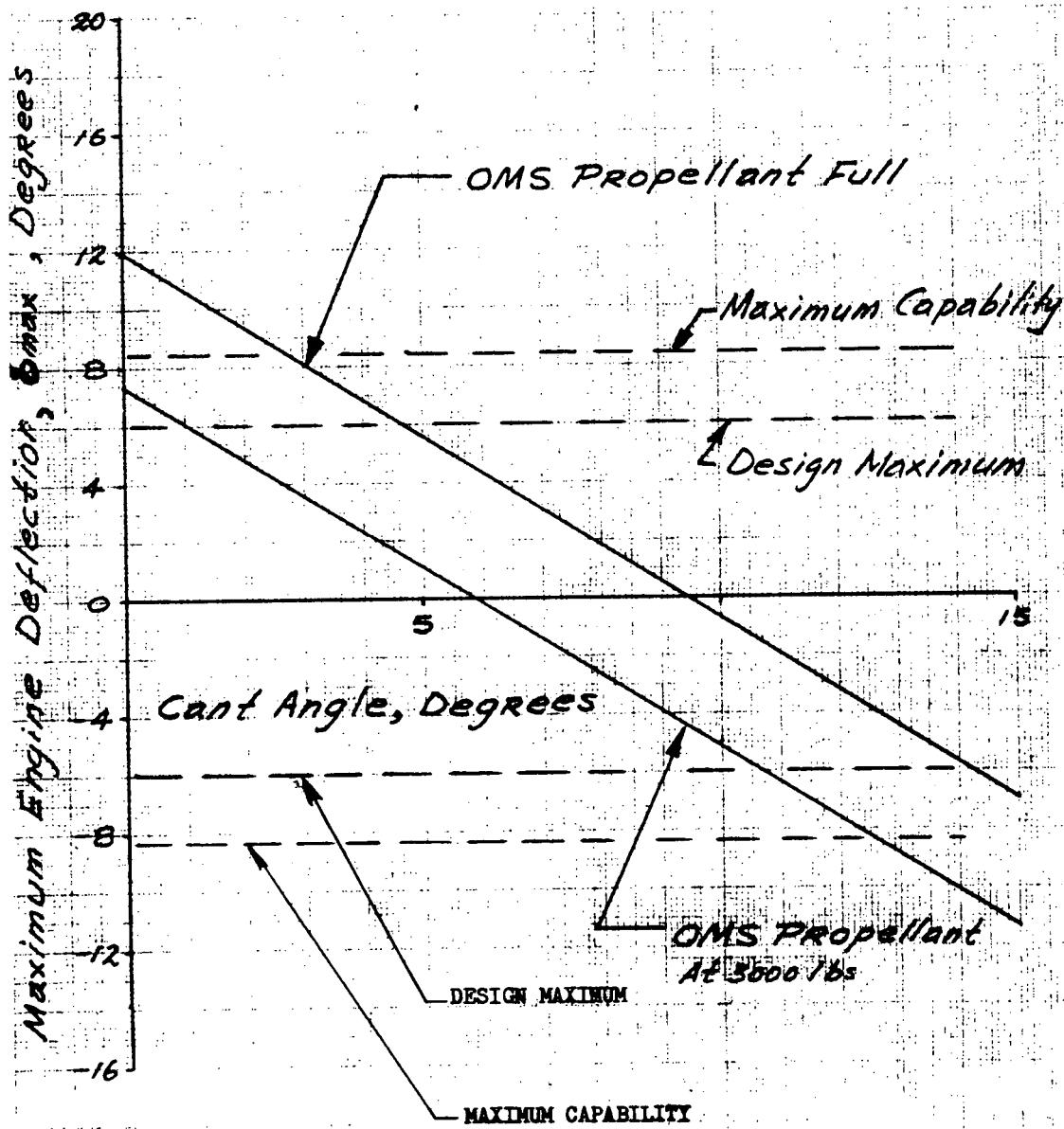


Figure 5-112. OMS Engine Deflection for Controlling Pitch Axis Dynamic Transient (One OMS Engine Inoperative)



These engines are also canted (before launch) to provide adequate pitch-axis control if there is one engine failure. The cant angles are measured on the X-Z plane and are δ_{CT} degrees outboard.

The problem of this study is to determine the OMS engine cant-angle and deflection requirements for the following conditions:

Study Case	Assumptions
1	One OMS engine has failed. The remaining OMS engine is required to provide thrust-vector control for orbital ΔV maneuvers.
2	Same as Study Case 1, except that single-engine thrust vector control is also required for ESS deorbit.

In particular, the study questions are as follows:

- a. What is the recommended engine cant angle (δ_{CT}) for all payload vehicle configurations?
- b. With this recommended cant angle, is the design maximum (δ_{max}) of ± 6 -degrees adequate for pitch yaw-axis control? (The OMS engines are oriented such that a total of ± 8.4 TVC is available in pitch and yaw.)
- c. What is the vehicle payload penalty because of the required engine cant angle?

The calculations of engine deflections and vehicle payload penalties for Study Case 1 (single-OMS-engine orbital ΔV maneuvers) are summarized below. The calculations for Study Case 2 (orbital ΔV maneuvers and ESS deorbit) are not presented but are similar to those of Case 1.

a. Engine Deflection Requirement

The pitch-axis engine deflection requirement (δ_{max}) for each ESS plus payload vehicle is determined by the following steps.



Where δ_S and δ_D are obtained from Figures 5-110 and 5-112. (See the noted data points in these figures.) The 25-percent safety factor is added to cover uncertainties such as thrust misalignments and other design tolerances. The results of this calculation are plotted in Figures 5-113 through 5-115.

The yaw-axis engine deflection can be calculated by the similar equation as follows:

- (1) Engine deflection for yaw-axis static trim.

$$\begin{aligned}\delta_S &= 57.3 \left(\frac{Y_e - Y_{cg}}{X_{cg} - X_e} \right) \text{ degrees} \\ &\approx 57.3 \left(\frac{-Y_{cg}}{X_{cg} - X_e} \right), \text{ since } Y_e \approx 0\end{aligned}$$

(Note that the OMS engines are mounted on the Z axis.)

With the assumption that the maximum Y-axis c. g. offset 4 inches, the maximum values of δ_{S1} and δ_{S2} are 0.3 degrees and 0.29 degrees.

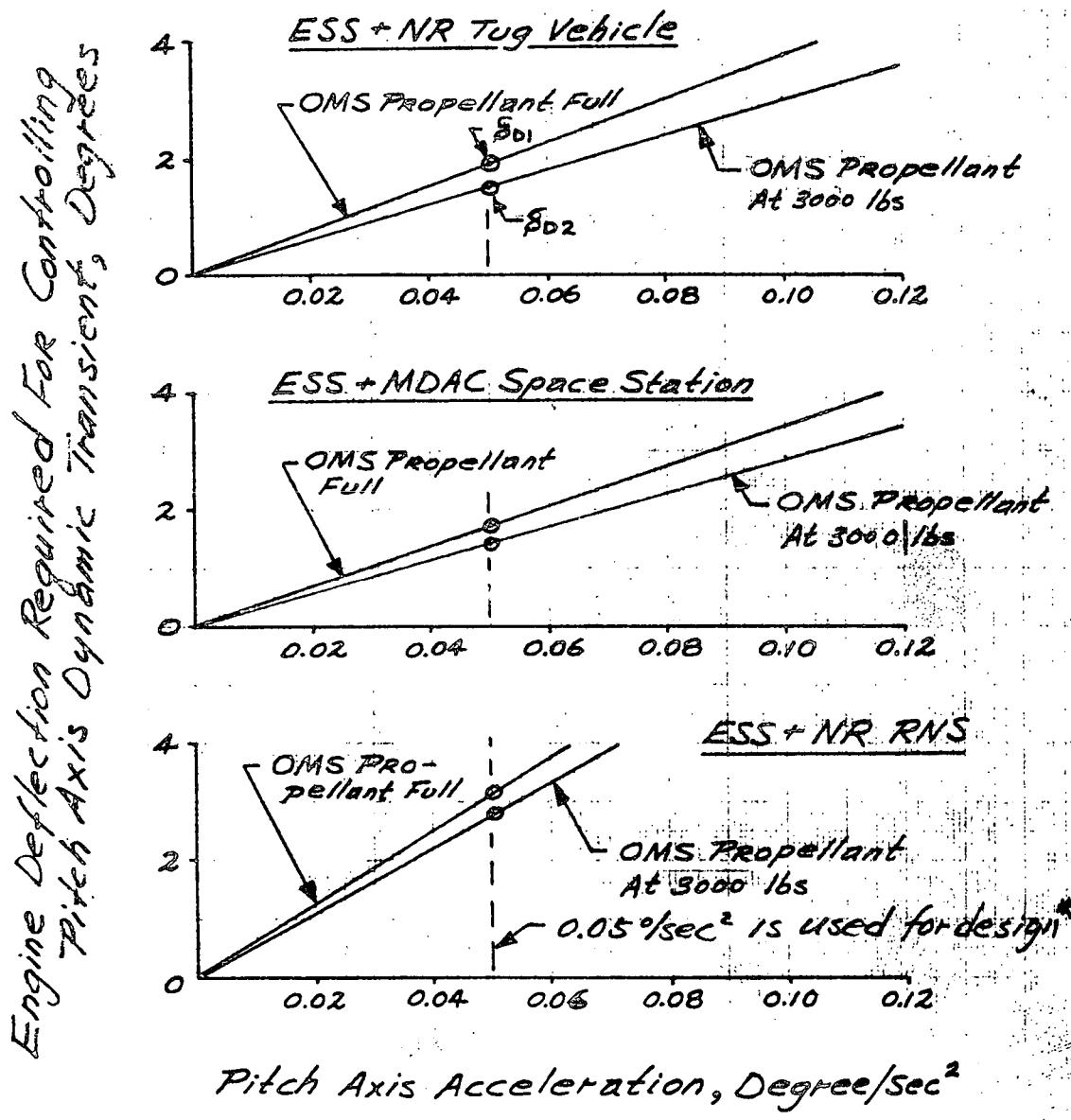
- (2) Engine deflection for controlling yaw-axis dynamic transient:

$$\delta_D = \left[\frac{I_{zz} \dot{r}}{NF (X_{cg} - X_e)} \right] \text{ degrees}$$

Since $I_{zz} \approx I_{yy}$, the engine deflection for controlling the yaw-axis dynamic transient is approximately the same as that for the pitch axis (see Figure 5-112). The worst-case δ_{D1} and δ_{D2} are 3.1 degrees and 2.8 degrees.

- (3) Maximum yaw-axis engine deflection (worst-case)

$$\begin{aligned}\delta_{\max} (\text{OMS propellant full}) &= 1.25 (\delta_{D1} + \delta_{S1}) \\ &= 4.3 \text{ degrees}\end{aligned}$$



* This acceleration level departs from the design criterion of $1.0^\circ/\text{sec}^2$ because it is impractical to design the OMS at this level. Further analysis is needed to verify that $0.05^\circ/\text{sec}$ is adequate for OMS control

Figure 5-113. Pitch Axis Engine Deflection Requirement
Versus Cant Angle, ESS/Space Tug
(One OMS Engine Inoperative)

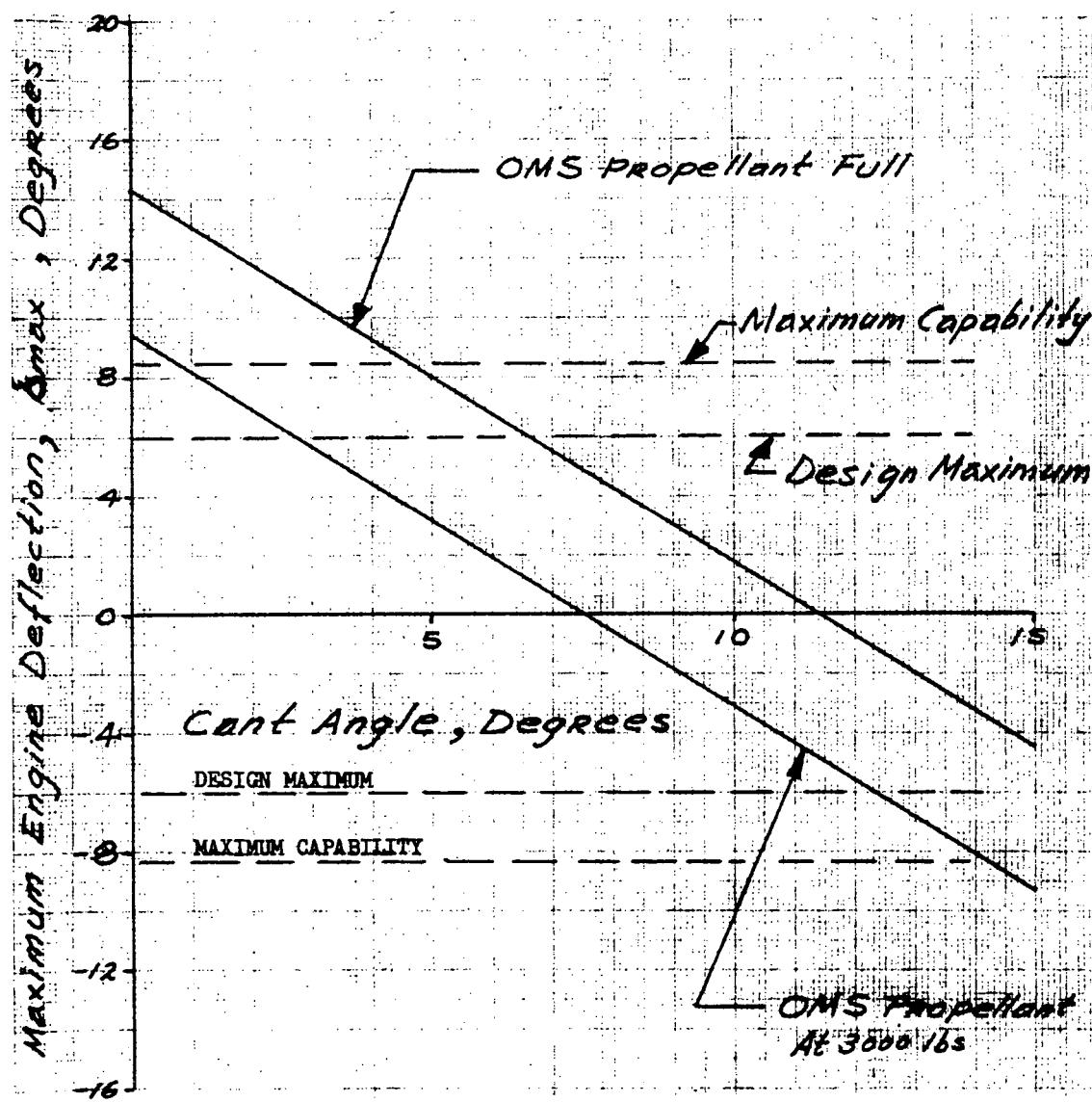


Figure 5-114. Pitch Axis Engine Deflection Requirement
Versus Cant Angle, ESS/Space Station
(One OMS Engine Inoperative)

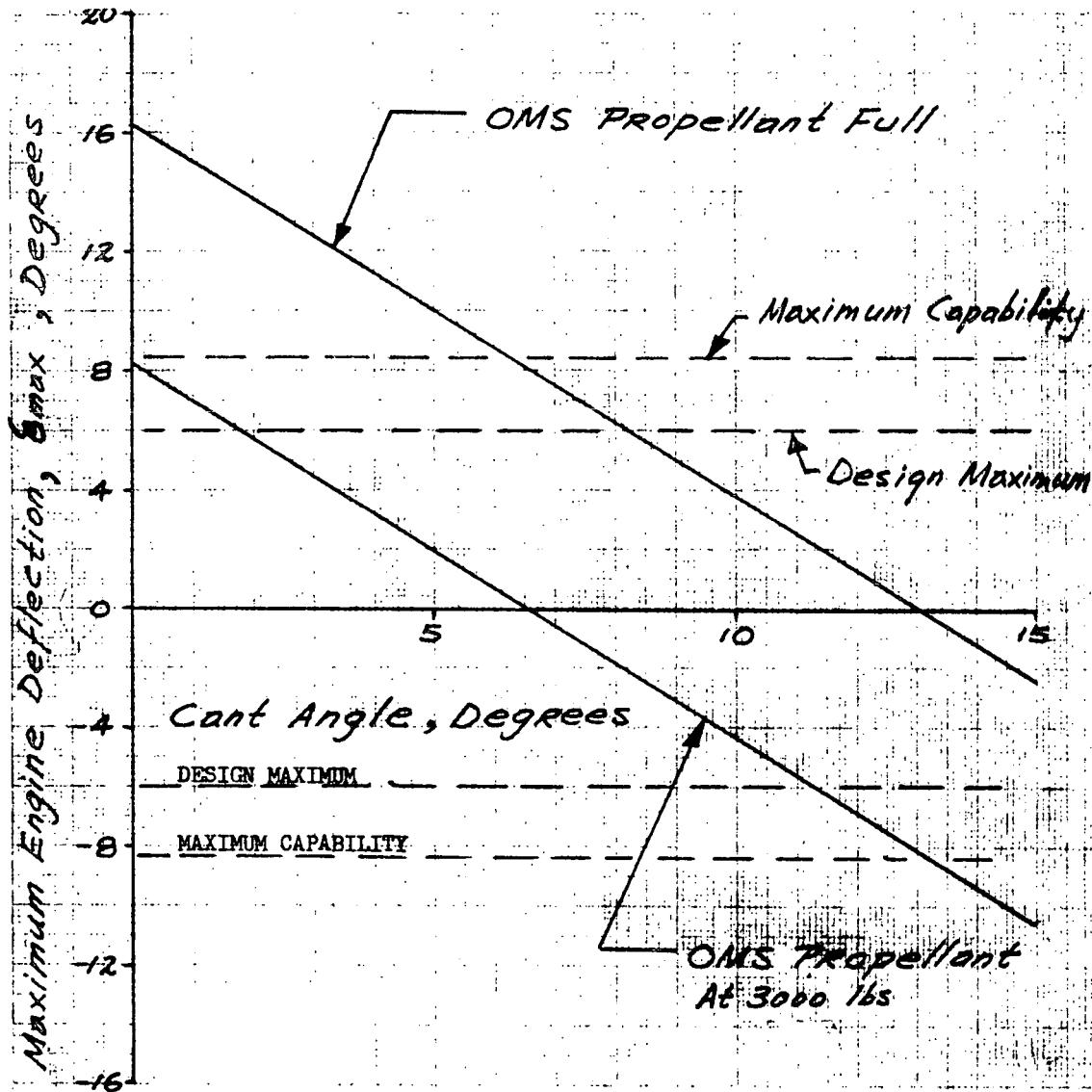


Figure 5-115. Pitch Axis Engine Deflection Requirement
Versus Cant Angle, ESS/RNS
(One OMS Engine Inoperative)



$$\begin{aligned}\delta_{\max} (\text{OMS propellant at 3000 lbs}) &= 1.25 (-\delta_{D2} + \delta_{S2}) \\ &= 3.1 \text{ degrees}\end{aligned}$$

b. Vehicle Payload Penalty

The vehicle payload penalty (ΔW) as a function of engine cant angle (δ_{CT}) is calculated by the following equation:

$$\Delta W = W_f \left[1 - \left(\frac{W_o}{W_f} \right) \left(\frac{W_f}{W_o} \right)^{1/\cos \delta_{CT}} \right]$$

where W_o and W_f are initial and final vehicle weights.

From the above calculations, it can be seen that the maximum pitch-axis engine deflection is greater than that of the yaw-axis. For this reason, the pitch-axis engine deflection is used to determine the engine deflection requirement for both the pitch and yaw axes.

The engine deflection requirements (plus or minus δ_{\max}) and the vehicle payload penalty as functions of cant angle for Study Case 1 (no deorbit) are plotted in Figure 5-116 and 5-117. These $|\delta_{\max}|$ characteristics are constructed by taking the maximum absolute values of the upper and lower curves (OMS propellant full and at 3000 pounds) as shown in Figures 5-113 through 5-115. In Figure 5-116 two important indications should be noted. First, there is no acceptable cant angle for design if the engine deflection capability falls below 4 degrees. Second, the engine cant angle need not be greater than 10 degrees. With these indications and the known deflection capability, the possible OMS engine requirements are tabulated in the upper portion of Table 5-8 for further evaluation.

If single-engine operation is required for orbital ΔV maneuvers and ESS-deorbit thrust vector control (Study Case 2), the characteristics of deflection requirements are plotted in Figure 5-118. Note that the engine deflection requirements for this study case are much greater than those of Figure 5-116.

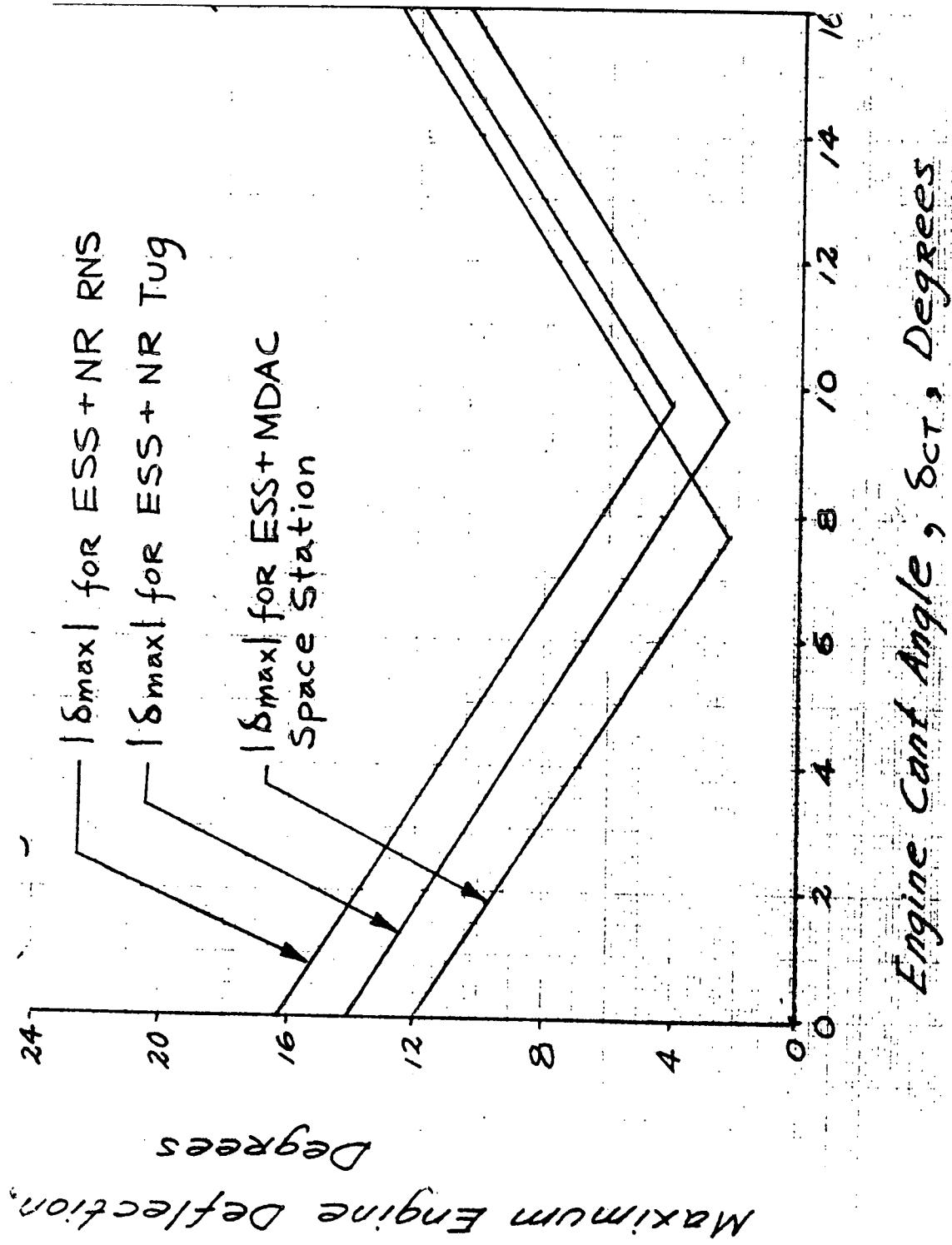


Figure 5-116. Summary of OMS Engine Deflection Requirements Versus Cant Angle
Orbital ΔV Maneuvers (One OMS Engine Inoperative)

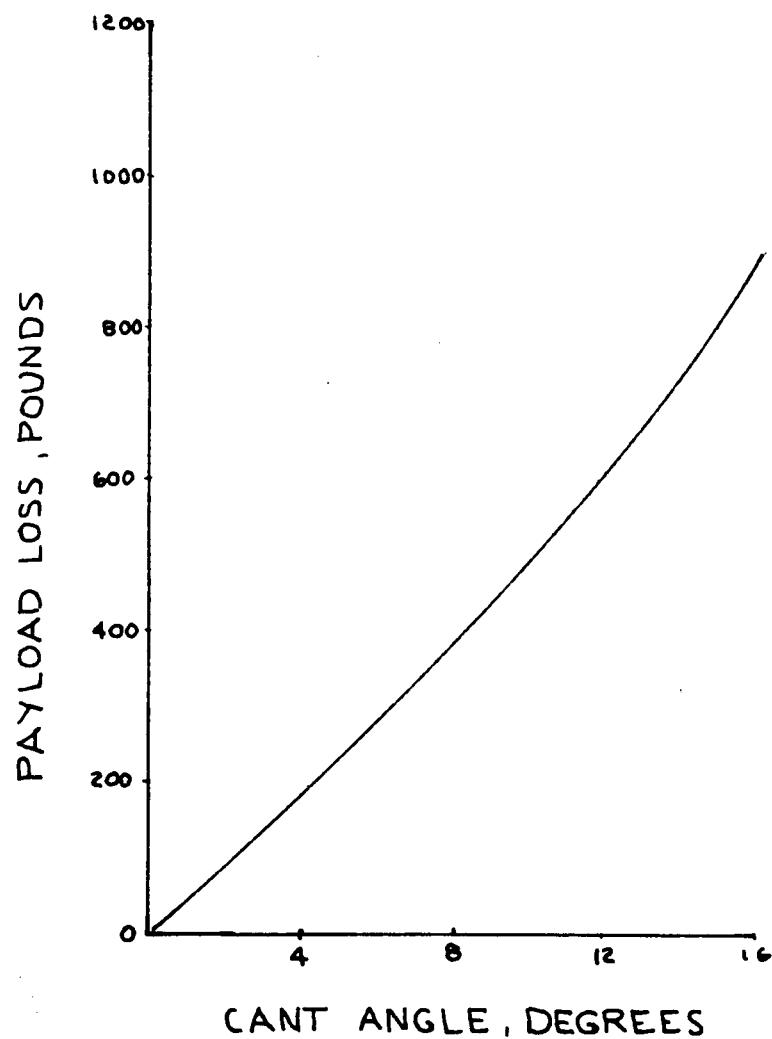
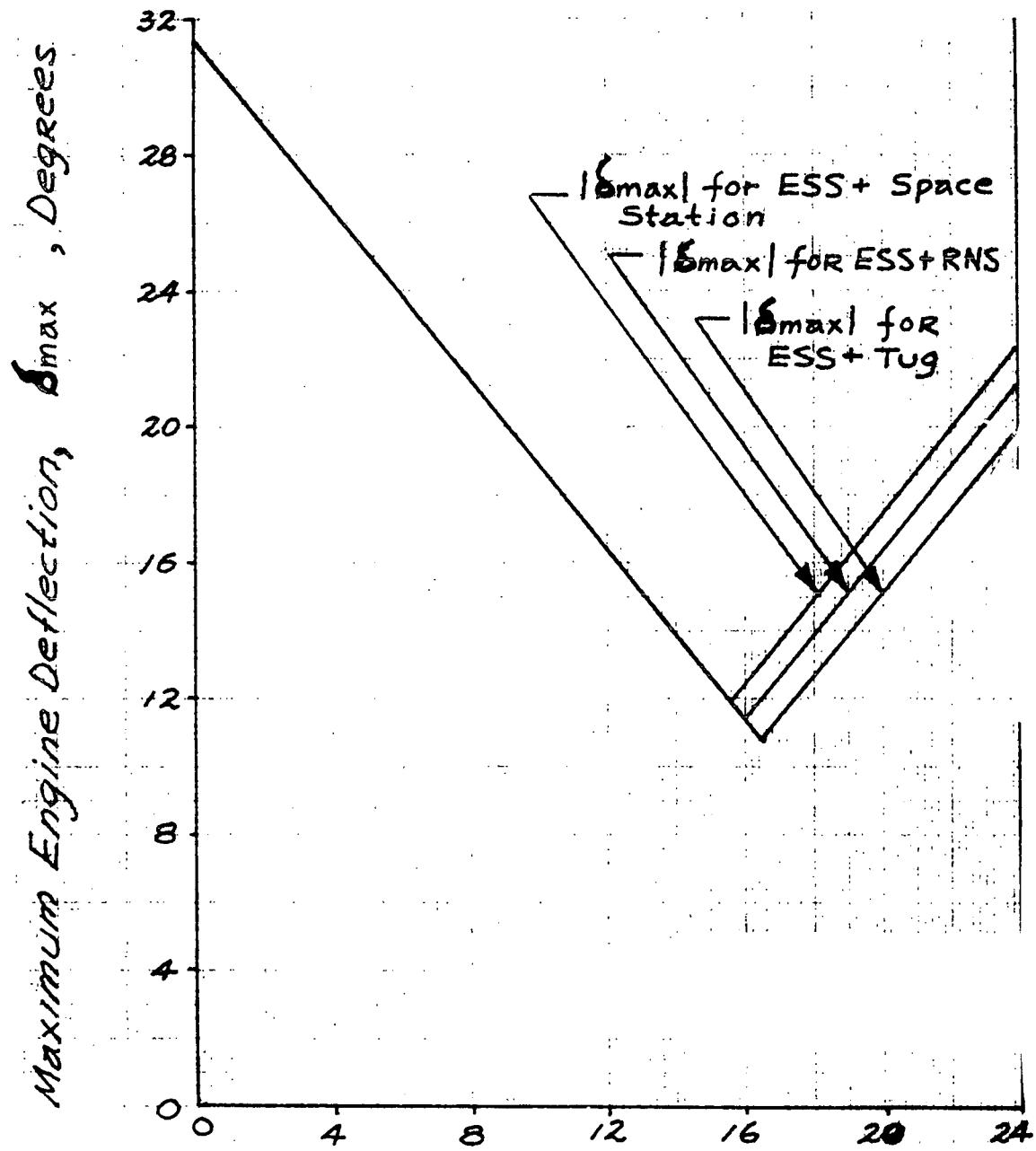


Figure 5-117. Vehicle Payload Loss Versus OMS Engine Cant Angle



Engine Cant Angle, δ_{cant} , Degrees

Figure 5-118. Summary of OMS Engine Deflection Requirement
Versus Cant Angle Orbital ΔV Maneuvers Plus
ESS Deorbit (One OMS Engine Inoperative)



Table 5-8. ESS Engine Cant-Angle and Deflection Requirements

Study Case	Assumptions	OMS Engine Requirements			
		Maximum Deflection (degrees)	Cant Angle (degrees)		
			ESS+NR Tug	ESS+MDAC Space Station	ESS+NR RNS
1	One OMS engine failed; remaining OMS engine required to provide thrust vector control for orbital ΔV maneuvers.	± 4	9	7	10
		± 5	8	6	9
		± 6	7	5	8
		± 7	6	4	7
2	Same as study Case 1, except that single-engine thrust vector control is required for ESS deorbit maneuver.	± 12	16	16	16
		± 14	14	14	14
		± 16	12	12	12
		± 18	11	11	11

This results from the removal of the payload before ESS deorbit. Without the payload attached, the X-axis vehicle center of gravity is much closer to the gimbal plane, thereby requiring larger engine deflection for static trim. A few data points of Figure 5-118 are also tabulated in Table 5-8 for comparison.

The results of this study show that the design maximum engine deflection of ± 6 degrees is capable of performing pitch-and-yaw attitude control during OMS orbital ΔV maneuvers, provided the acceleration level of 0.05 deg/sec^2 (see Figure 5-112) is acceptable for controlling the dynamic transient. The recommended cant angle for all vehicle payload configurations



is eight degrees. With single-OMS-engine used for ESS deorbit, the required cant angle is 16 degrees and the required maximum deflection is ± 12 degrees. In view of these large cant-angle and maximum-deflection requirements, the design for single-OMS-engine deorbit without additional attitude control does not appear to be practical, and is therefore not recommended. The ACPS will be used to provide three-axis attitude control during single-OMS-engine ESS deorbit.

2. Attitude Control Propulsion System Requirements. The important requirements for the attitude control propulsion system (ACPS) are jet location, thrust level, number of jets, and manner of using these jets for flight control.

The jets are located (as shown in Figure 5-79 to provide translation along the X-axis (vernier propulsion), and provide three-axis attitude control about the vehicle body axes. The jet modules are mounted in positions I and III for convenience and to avoid interference when the ESS is mounted on the shuttle booster. Forward-pointing jets are mounted separately ahead of the fuel feedlines to the MPS engines. The remaining nozzles are located aft of the fuel feedlines. This arrangement was convenient because it allows a single fairing at each position to cover the feedline and ACPS installation.

The number and size of jets needed for roll control during boost have been discussed earlier. This discussion is concerned only with ACPS requirements in orbit and deorbit. These requirements are determined principally during OMS operation with one OMS engine inoperative during deorbit. (For orbital operations, the ACPS requirements and performance have not been determined but are expected to be similar to those of shuttle orbiter.)

For orbital and deorbit control operations, the design in Figure 5-119 uses 14 jets with 2100-pound thrust each (shuttle orbiter jets). The use of these jets for flight control is summarized as follows:

a. Pitch axis

+ pitch: Jets 1, 4, 8, 11

- pitch: Jets 2, 7, 9, 14



Yaw axis

+ yaw: Jet 12

- yaw: Jet 5

(If one jet fails, used the X translation jets for yaw control)

Roll axis (sharing the pitch jets)

+ roll: Jets 2, 7, 8, 11

- roll: Jets 1, 4, 9, 14

b. X-axis translation

+ X: Jets 6 and 13

- X: Jets 3 and 10

The pitch and roll jet requirements are explained below. The requirements in other control axes are self-explanatory. (Note that the ACPS is designed to be operational with any one of its jets inoperative.)

The pitch-axis requirements are determined by the inoperative OMS engine case during ESS deorbit. In the previous section, it was shown that the cant angle and maximum deflection of the OMS engines are designed for orbital ΔV maneuvers only. For ESS deorbit, the OMS engine deflection is not able to point the thrust vector through the vehicle's center of gravity (see Figure 5-119). This results in an unbalanced pitch torque (M_u) as follows:

$$M_u = 10,000 \left[\frac{128}{12} \cos(\delta + \delta_{CT}) - \left(\frac{248 + 48}{12} \right) \sin(\delta + \delta_{CT}) \right]$$

$$= 43,800 \text{ ft-lb, if } \delta = 6 \text{ deg and } \delta_{CT} = 8 \text{ deg}$$

$$= 71,300 \text{ ft-lb, if } \delta = 0 \text{ deg and } \delta_{CT} = 8 \text{ deg}$$

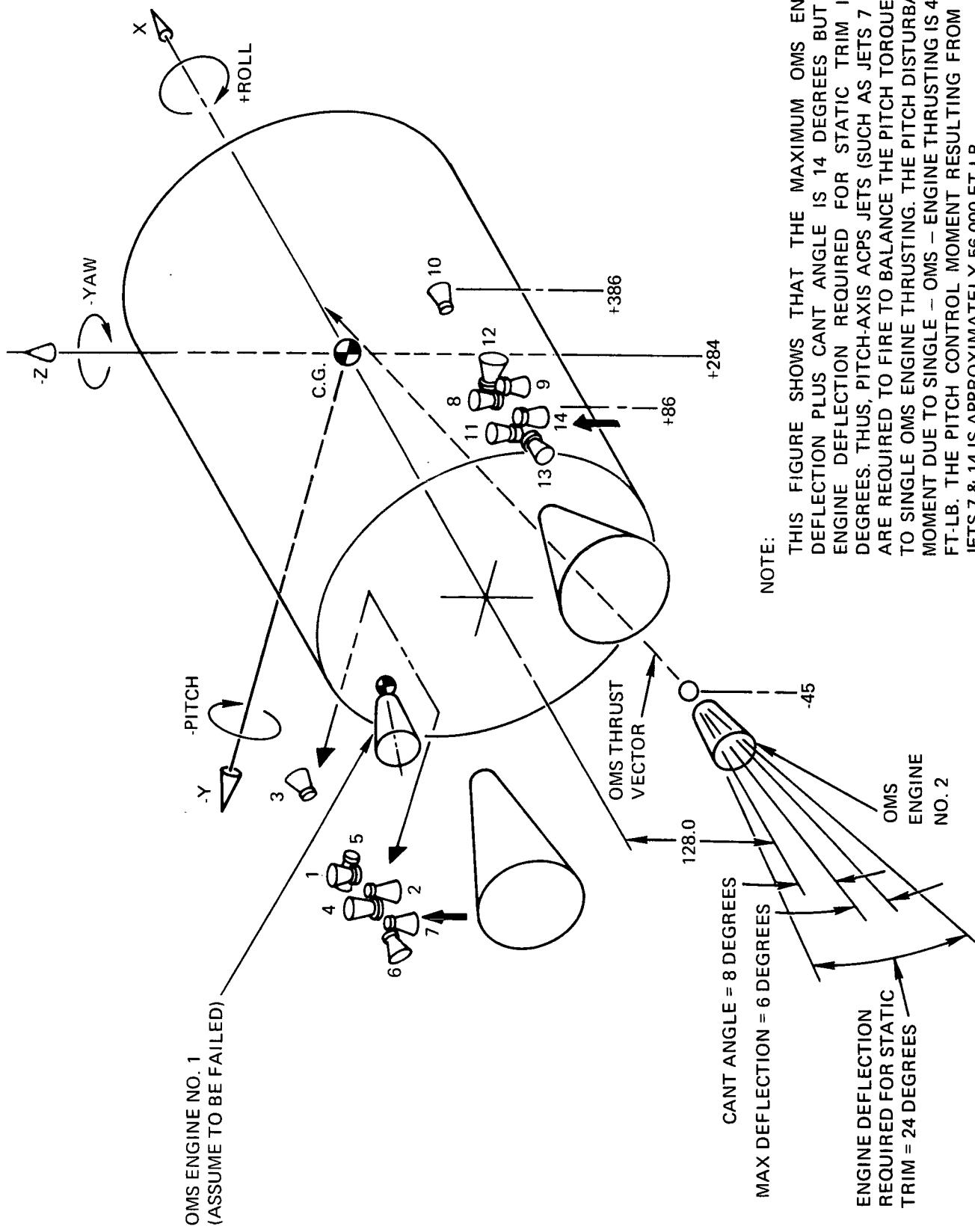


Figure 5-119. ACPS Requirement for Pitch Axis Control During Single OMS Engine ESS Deorbit



To balance this unbalanced torque (in each control direction), two 2100-pound pitch jets are adequate if the engines are deflected six degrees (see Figure 5-120). However, a total of eight jets is required to satisfy this pitch control with one jet inoperative.

Roll control requirements are shown in Figure 5-121. From Figure 5-121, it is seen that four 2100-pound thrusters will provide adequate roll control (two for positive and two for negative roll).

Conclusions and Recommendations. The study conclusions and recommendations for the ESS flight controls follow.

1. The main propulsion system can provide adequate pitch-and-yaw attitude control during ascent even with one MPS engine inoperative. To provide this capability with the ± 7 degree design maximum deflection of the MPS engines, a 12-degree outboard cant angle in the yaw plane is required. This will result in a 7000-pound payload penalty. However, this penalty can be reduced to approximately 2000 pounds by using a control signal to deflect the engines six degrees in the opposite direction to the cant angle during normal operation.
2. Eight 2100-pound orbiter reaction jets will provide roll control with one MPS engine inoperative.
3. A cant angle of eight degrees outboard is required to provide pitch control during OMS orbital operations with one engine failure. The design maximum engine deflection of ± 6 degrees is acceptable for attitude control.
4. For deorbit, it was determined to be impractical to provide an OMS engine cant angle that would allow attitude control with one engine not operating during the deorbit maneuver. Therefore, the ACPS is used for three-axis control.
5. For maneuvering and attitude control in orbit when the OMS is not operating, the attitude control propulsion system is utilized. This system also provides roll control during single OMS and MPS

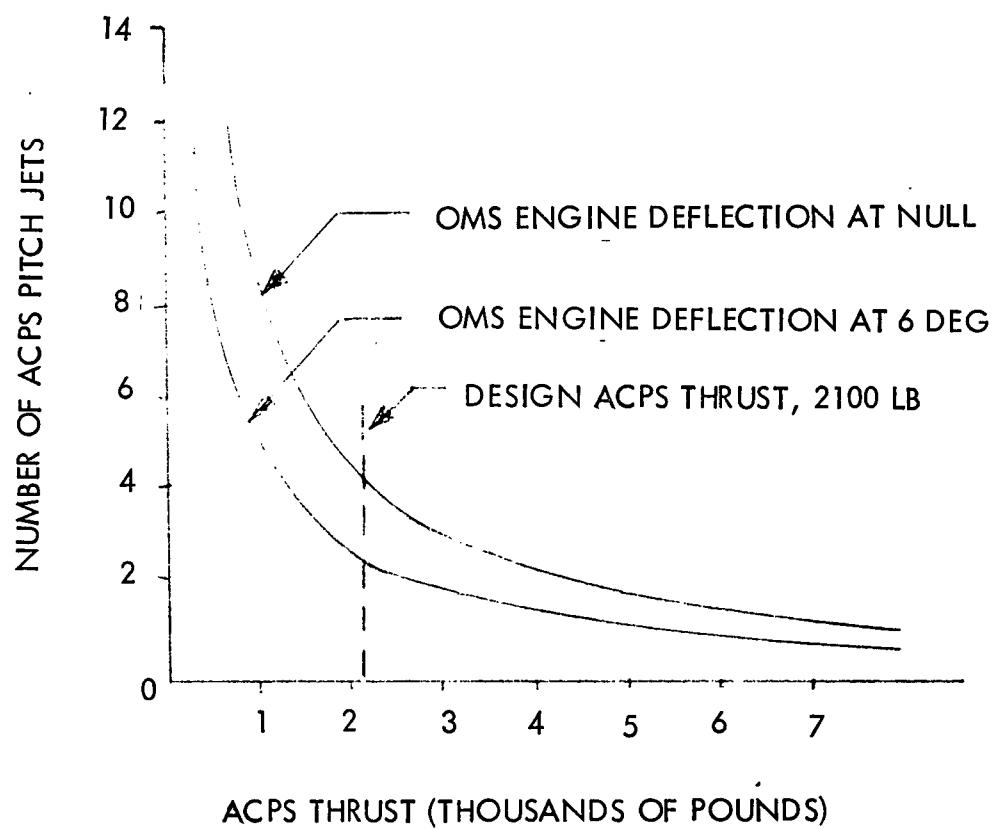


Figure 5-120. Number of Pitch ACPS Jets Required for Pitch Trim (Deorbit Condition with One OMS Engine Inoperative)

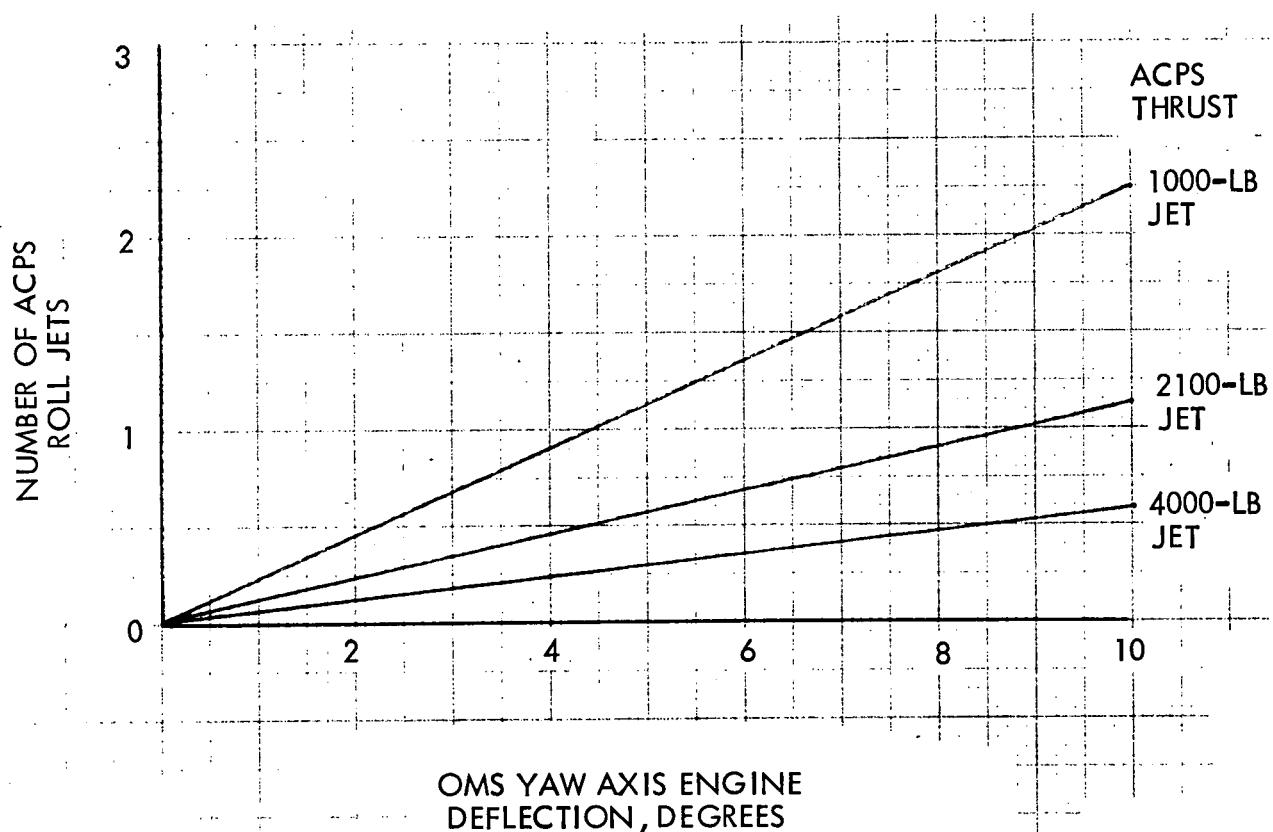


Figure 5-121. Number of Roll Jets Required for Roll Trim (Deorbit Condition with One OMS Engine Inoperative)



engine operation. The baseline ACPS design uses 14 2100-pound orbiter reaction jet nozzles as follows:

8 combined pitch-roll control nozzles
2 yaw control nozzles
4 combined vernier propulsion and yaw control nozzles
14 total

In summary, the results of these studies show that the baseline ESS flight control system can meet ESS mission flight control requirements.

Booster Entry and Flyback Control. The ESS staging conditions and minor modifications to the booster to accommodate the ESS result in booster entry and flyback control within the capability of the shuttle baseline booster.

Loads

Mated Ascent Aerodynamic Loads. This section summarizes the distributed aerodynamic loads data for the B-9U booster with three expendable second stage (ESS) payload configurations, referred to as B-9U/RNS, B-9U/MDAC, and B-9U/space tug. Data are presented for each of these configurations at maximum α_q and β_q launch flight conditions. These data maximize launch aerodynamic loads.

The data presented are based on B-9U booster reference dimensions:

$$S_{REF} = 8451 \text{ ft}^2 \quad - \text{theoretical wing planform area}$$

$$l_B = 255.6 \text{ ft} \quad - \text{booster length}$$

The maximum α_q and β_q flight conditions (Table 5-9) were obtained from preliminary launch trajectory data and will therefore differ from launch trajectory data presented above. These differences are not large enough to warrant reanalysis of the integrated system loads.

Figures 5-122 through 5-125 show the B-9U/RNS component loads for maximum α_q headwind, maximum α_q tailwind, and maximum β_q (pitch and yaw planes), respectively. Figures 5-126 through 5-129 and Figures 5-130 through 5-133 show the same sets of load distribution for the B-9U/MDAC space station and the B-9U/space tug, respectively.

These aerodynamic loads data show the B-9U booster body load distributions plus wing, canard, vertical tail, and ESS point loads. The body load distributions were obtained from ARC 66-509 (September 1970) wind tunnel pressure data. These pressure data were integrated and modified to



Table 5-9. B-9U/ESS Critical Flight Conditions

RNS	α_B	MACH	$q \sim \text{PSF}$	$\alpha q \sim ^\circ \text{PSF}$
Max. " αq " Headwind	3.5°	1.1	415	1453
Max. " αq " Tailwind	-7°	1.2	400	-2800
Max. " βq " Launch	-2°	1.2	400	-800
<u>MDAC</u>				
Max. " αq " Headwind	3.26°	1.1	460	1500
Max. " αq " Tailwind	-8.3°	1.1	350	-2900
Max. " βq " Launch	-2°	1.2	400	-800
<u>SPACE TUG</u>				
Max. " αq " Headwind	3.1°	1.1	484	1500
Max. " αq " Tailwind	-8°	1.1	363	-2900
Max. " βq " Launch	-2°	1.2	400	-800
	β	MACH	$q \sim \text{PSF}$	$\beta q \sim ^\circ \text{PSF}$
<u>MAX. "βq" LAUNCH</u>				
RNS	4°	1.2	400	1600
MDAC	4°	1.2	400	1600
Space Tug	4°	1.2	400	1600

to account for the B-9U configuration. The vertical and longitudinal stations (based on Z/ℓ_B and X/ℓ_B) of the point loads correspond to the component center of pressure. When tabulated, a positive " $(X/\ell_B)_{CP}$ " refers to the center of pressure forward of the booster nose.

The magnitude of the component loads and moments were determined from wind tunnel component buildup data. The wing, canard, and vertical tail loads are for exposed surfaces only and the body load distribution

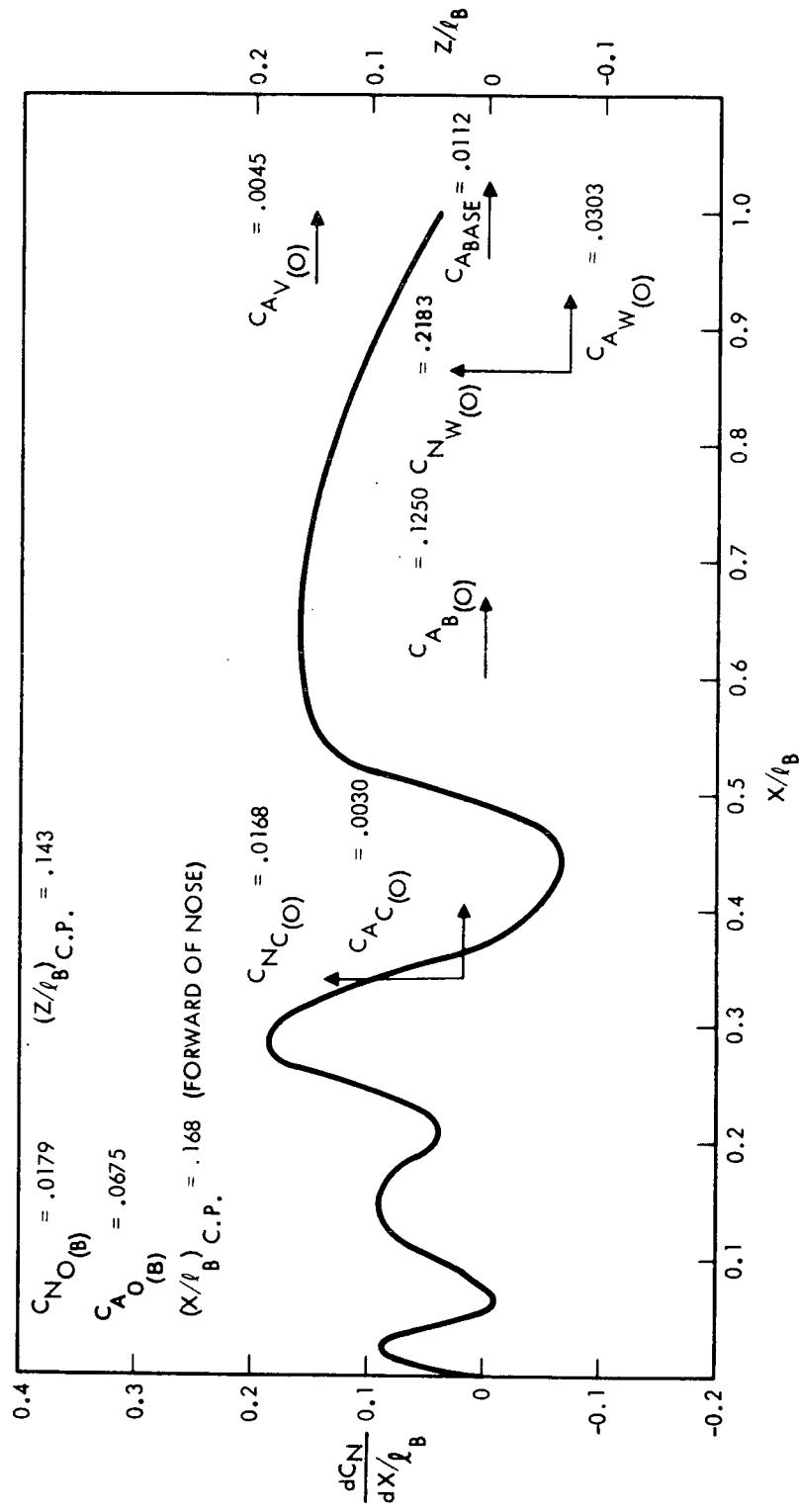


Figure 5-122. Booster Airload Distribution, ESS/RNS Payload,
Maximum α_q Headwind

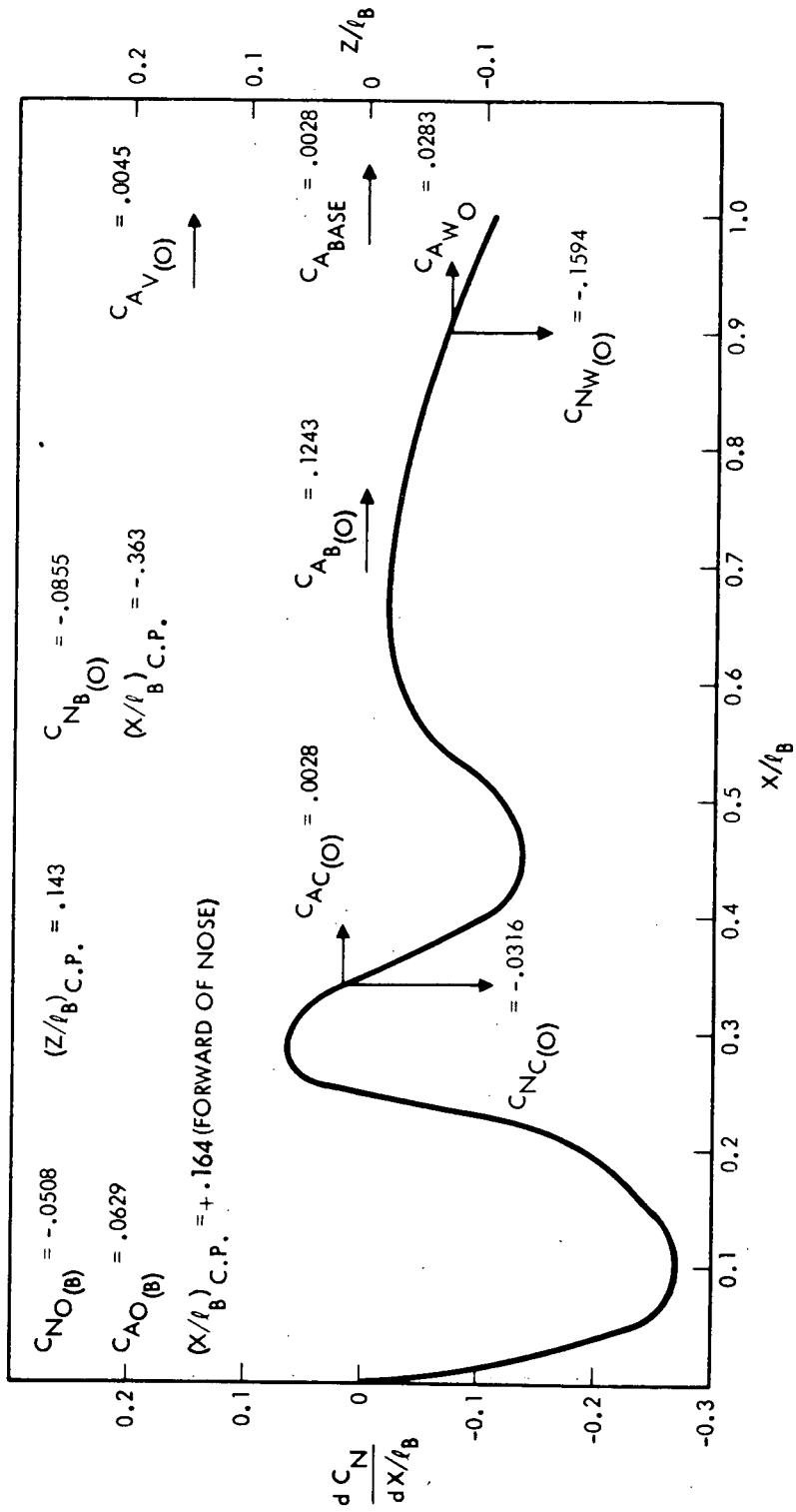
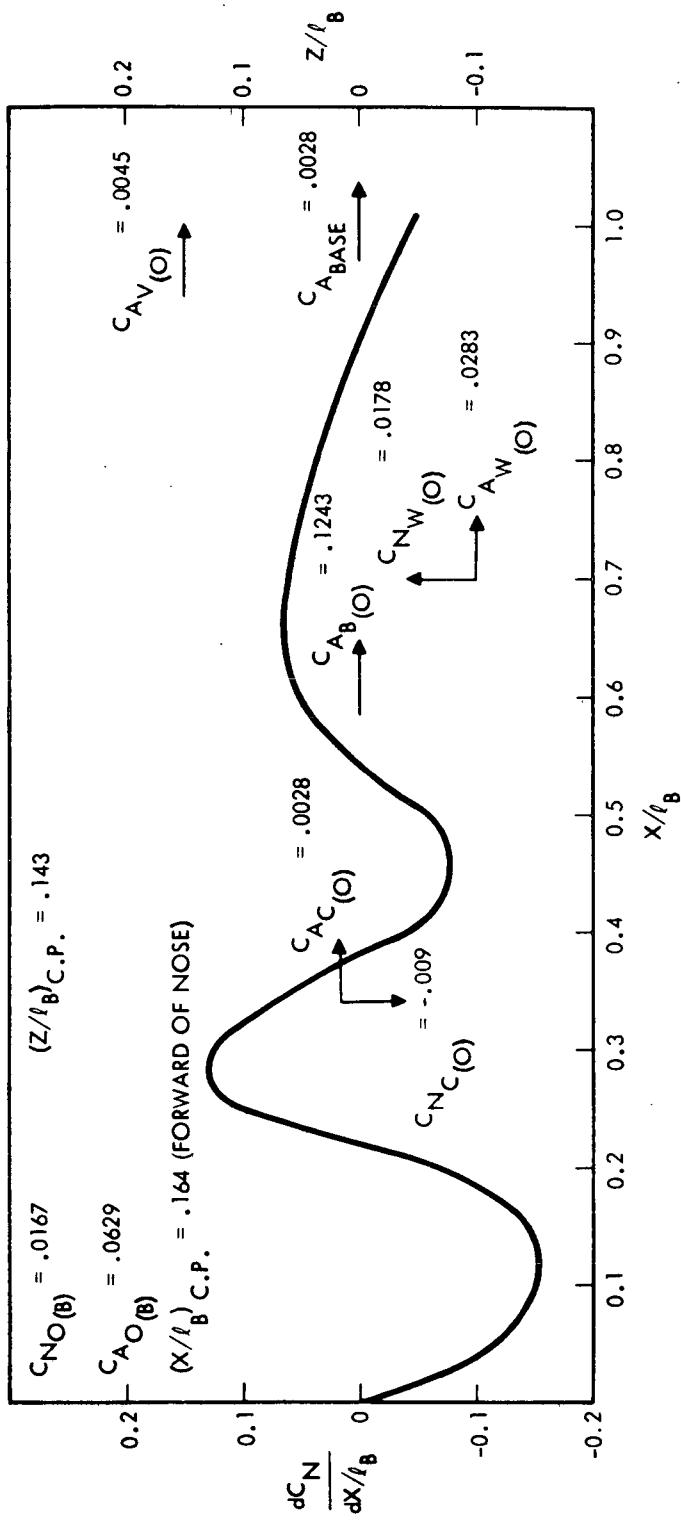


Figure 5-123. Booster Airload Distribution, ESS/RNS Payload,
Maximum αq Tailwind

Figure 5-124. Booster Airload Distribution, ESS/RNS Payload,
Maximum β_q Launch (Pitch Plane)



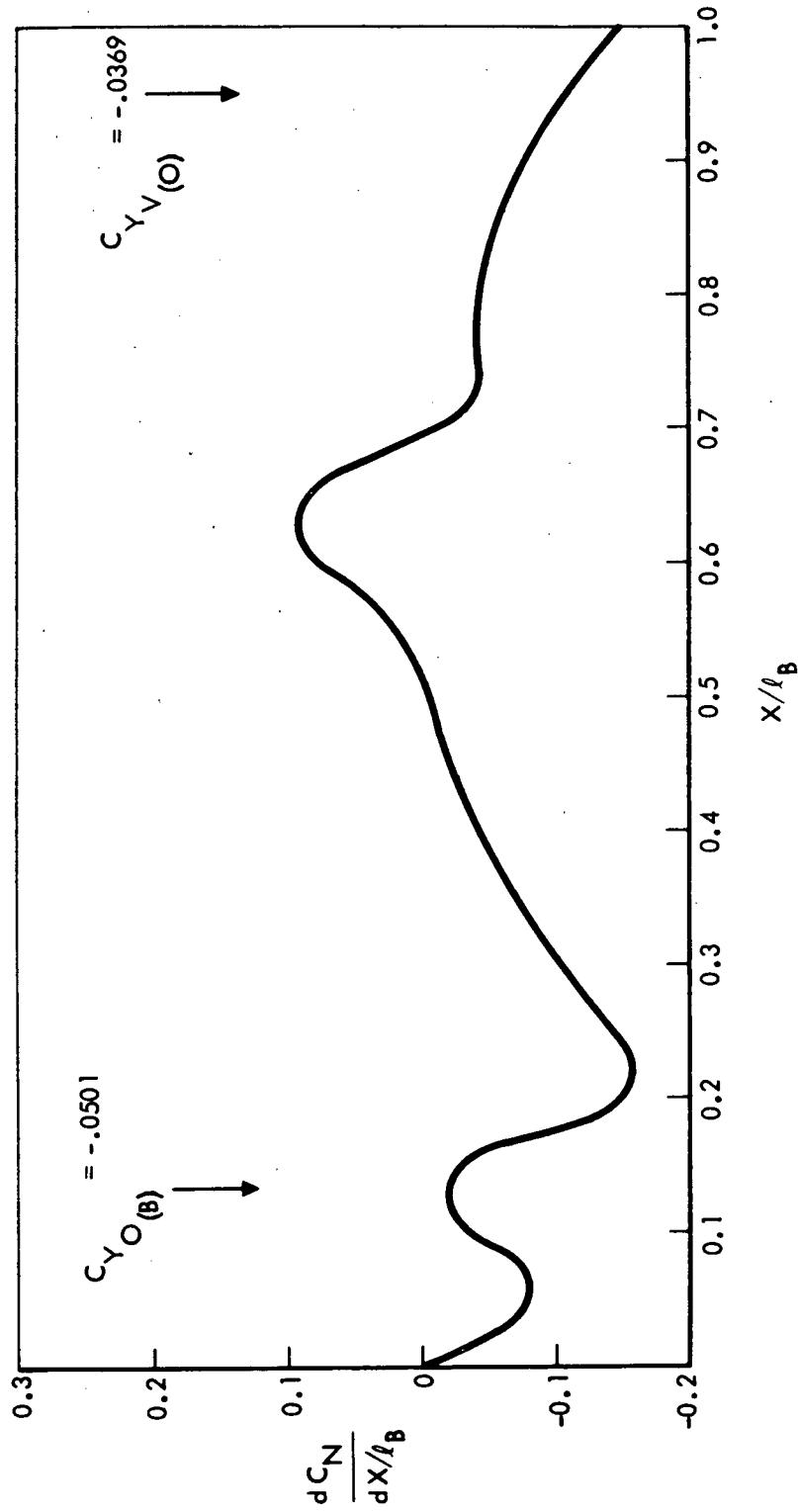


Figure 5-125. Booster Airload Distribution, ESS/RNS Payload,
Maximum βq Launch (Yaw Plane)

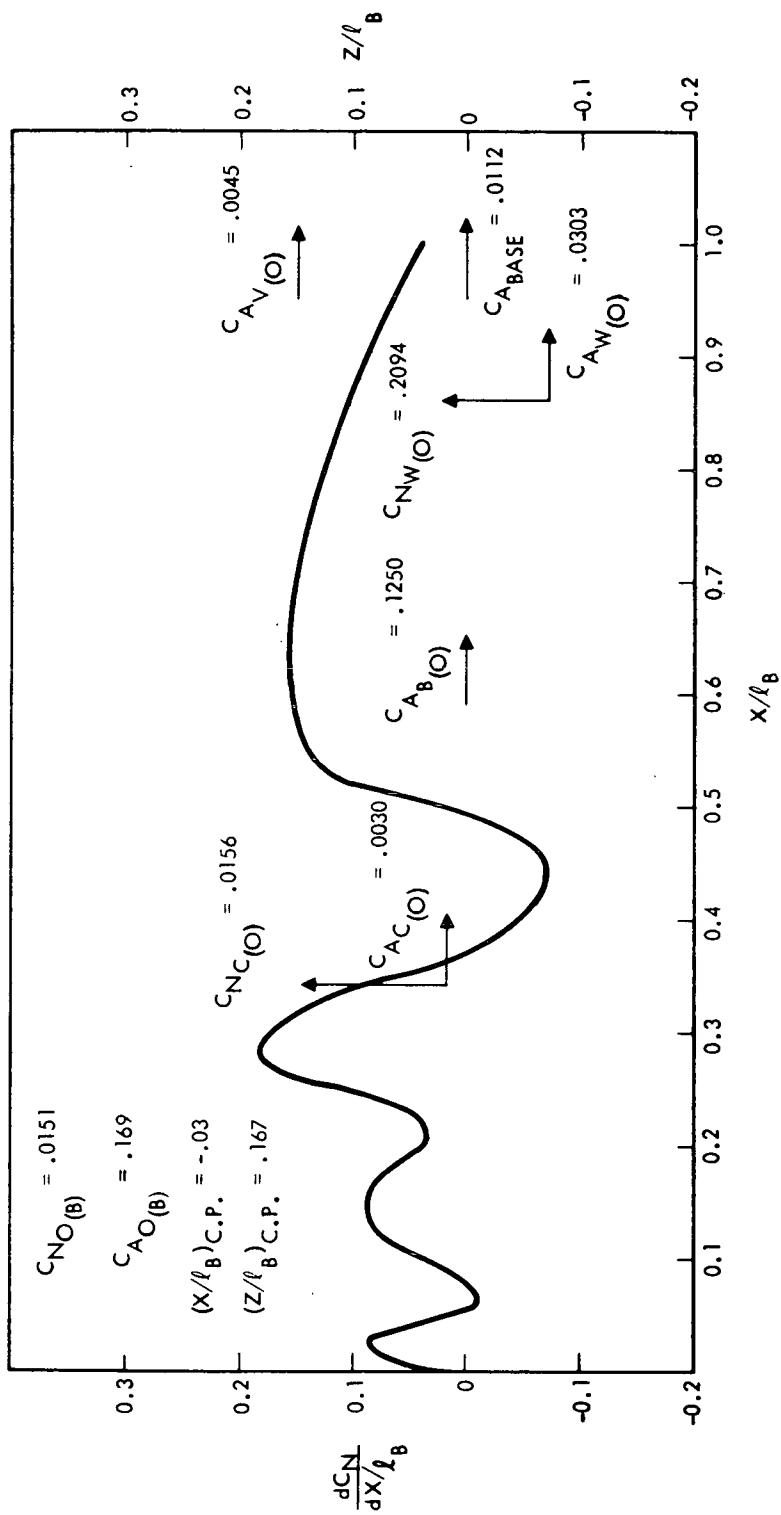


Figure 5-126. Booster Airload Distribution, ESS/Space Station Payload,
Maximum α q Headwind

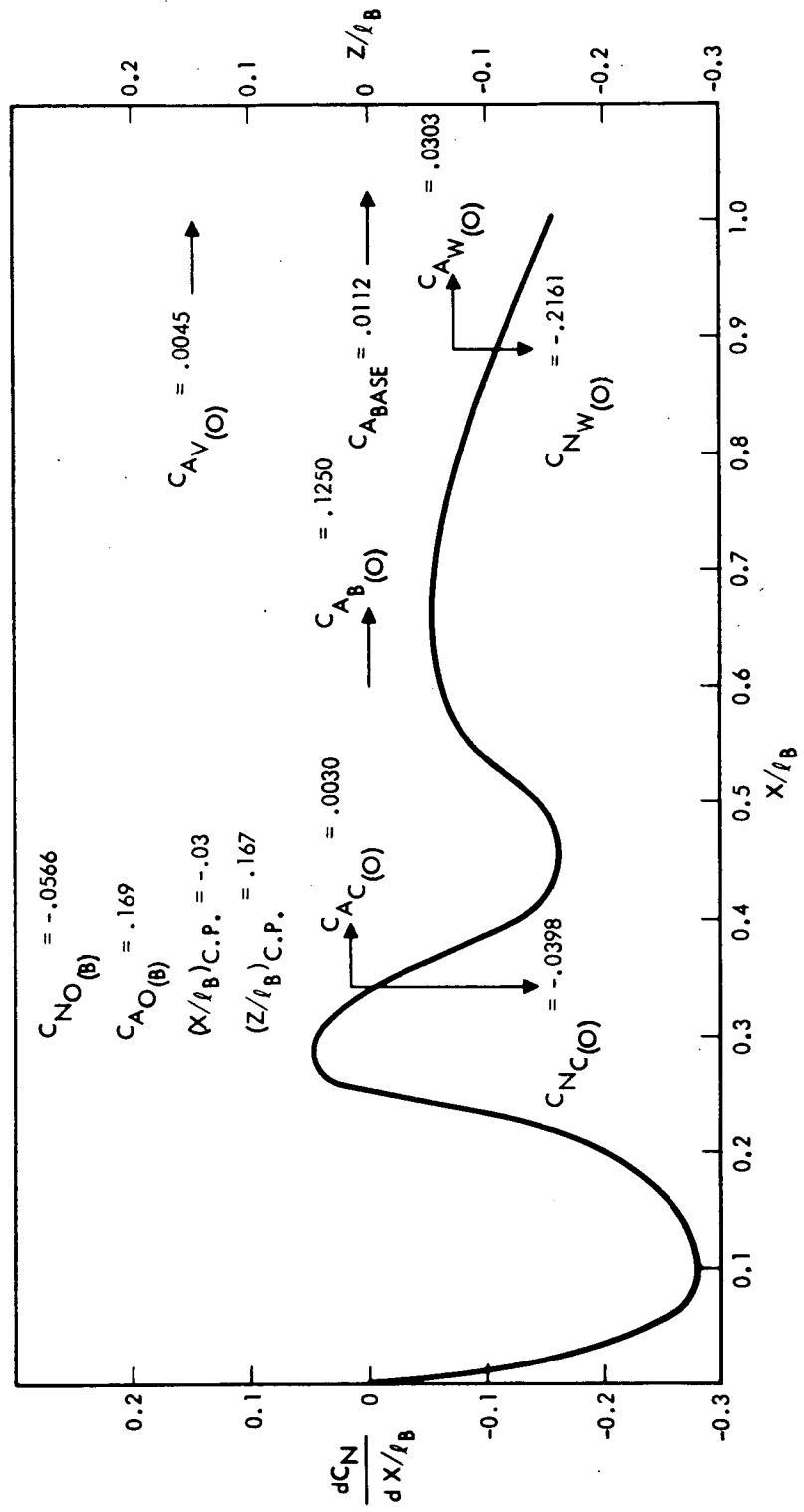


Figure 5-127. Booster Airload Distribution, ESS/Space Station Payload,
Maximum αq Tailwind

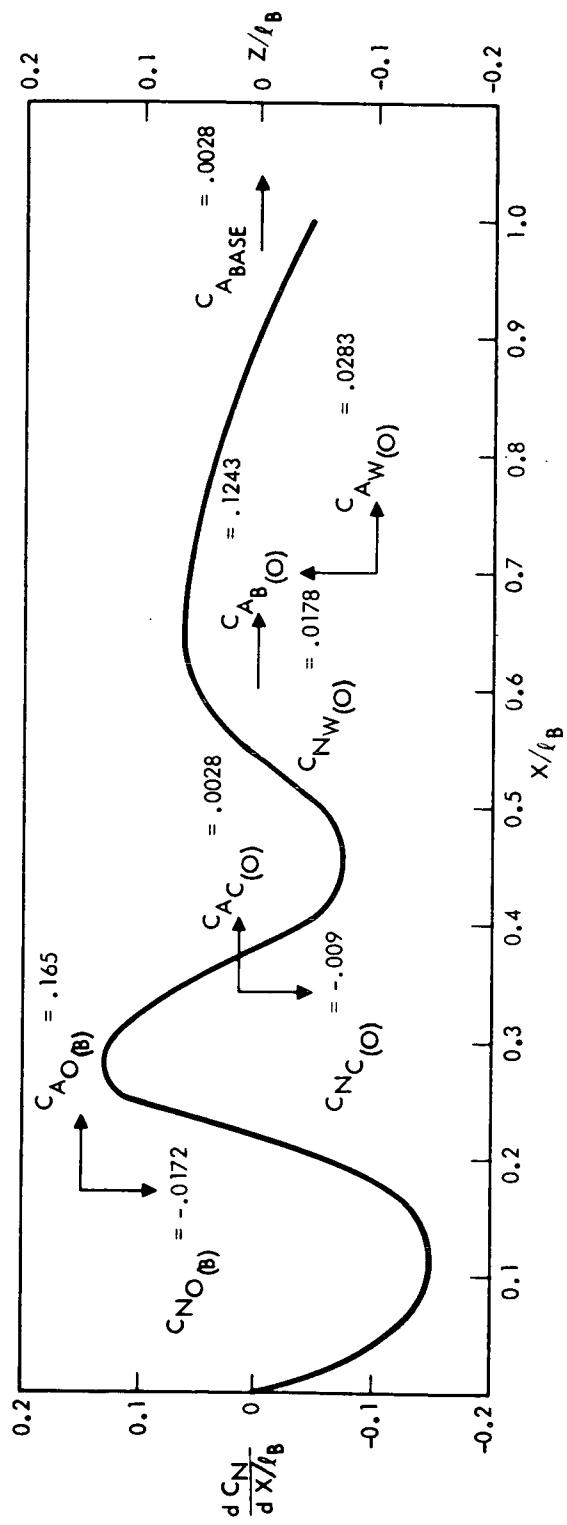


Figure 5-128. Booster Airload Distribution, ESS/Space Station Payload,
Maximum α_q Launch (Pitch Plane)

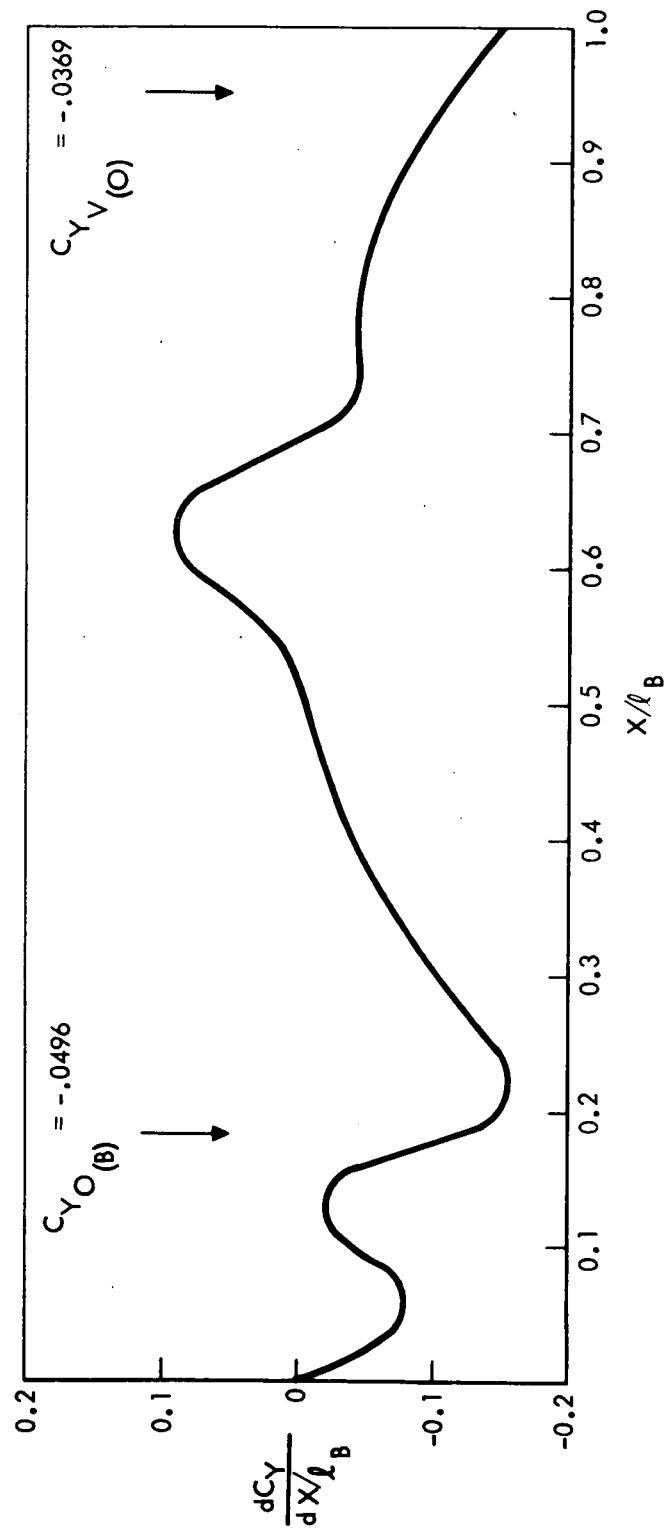


Figure 5-129. Booster Airload Distribution, ESS/Space Station Payload,
Maximum β_q Launch (Yaw Plane)

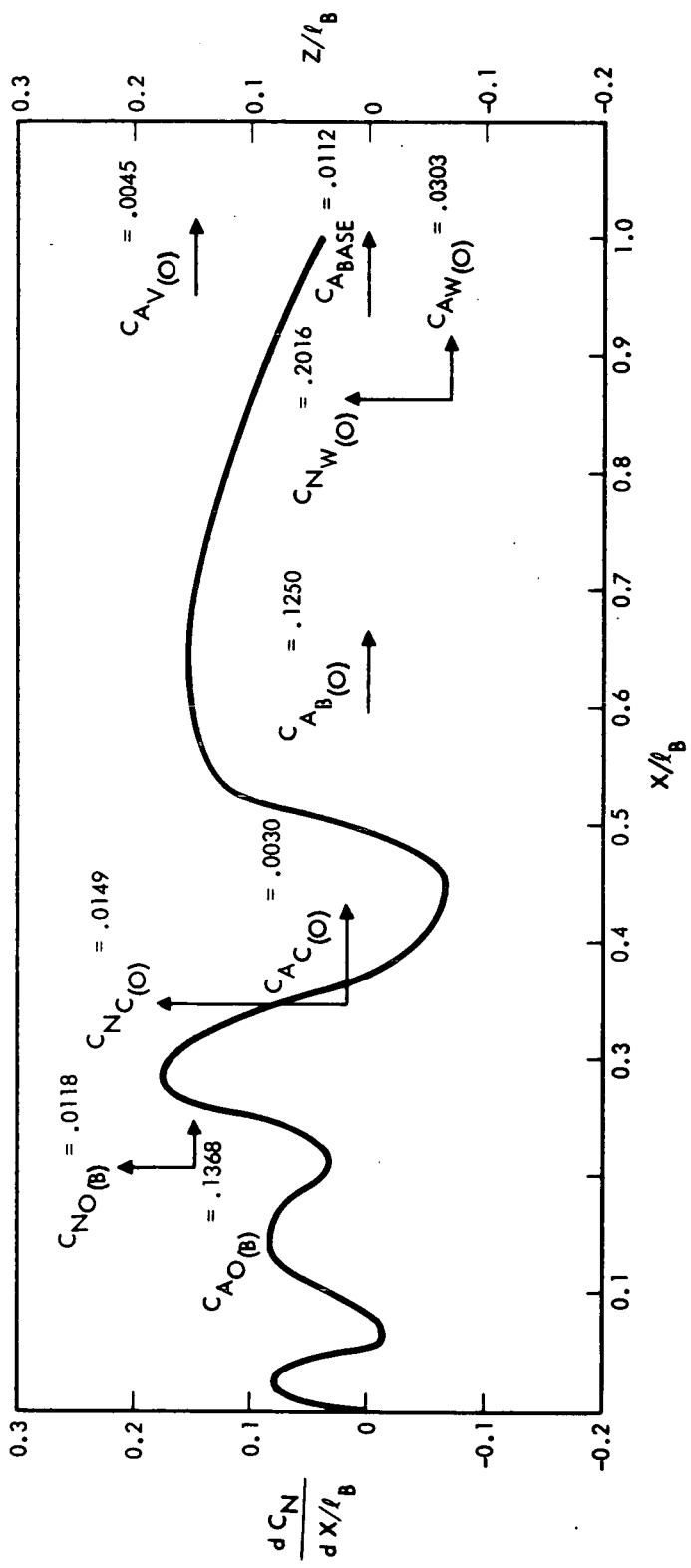


Figure 5-130. Booster Airload Distribution, ESS/Space Tug Payload,
Maximum αq Headwind

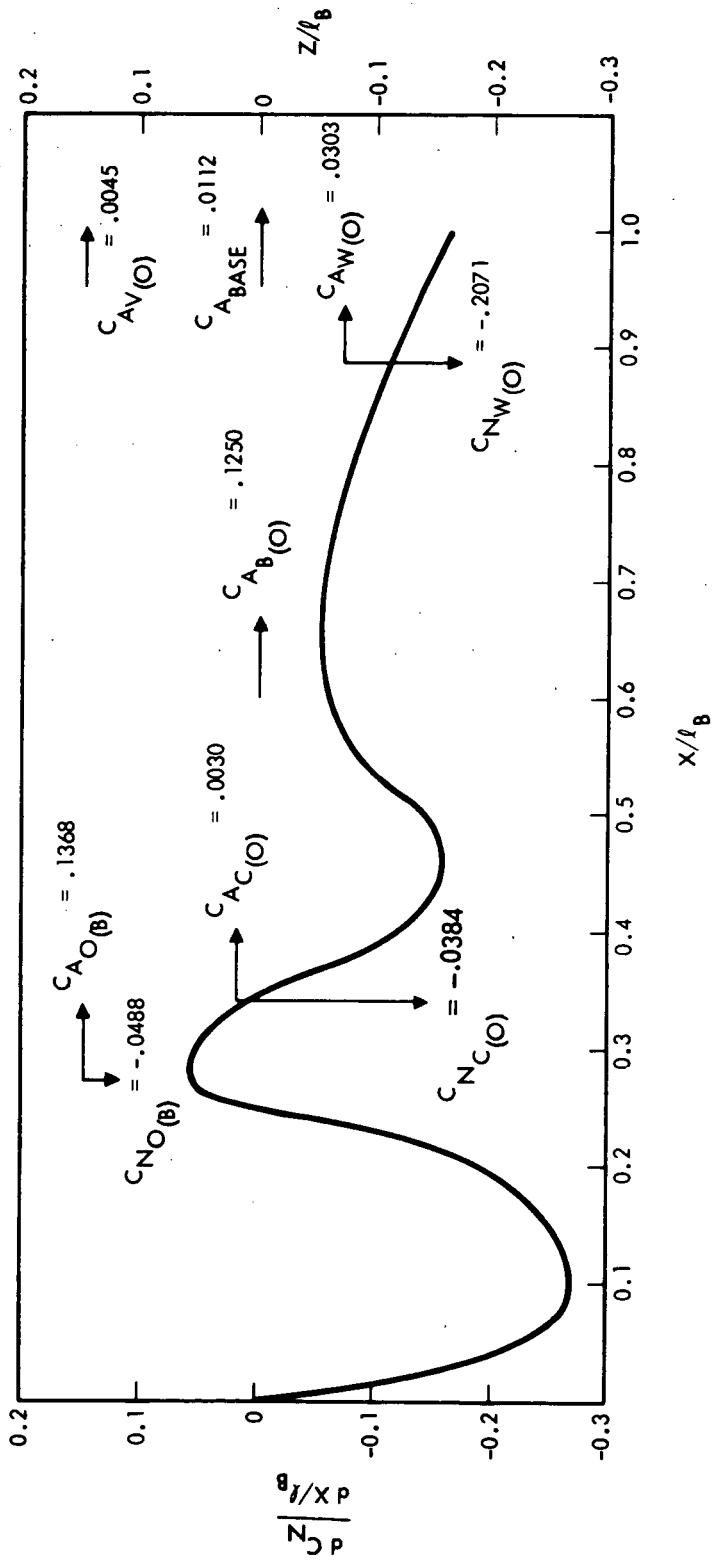


Figure 5-131. Booster Airload Distribution, ESS/Space Tug Payload,
Maximum α_q Tailwind

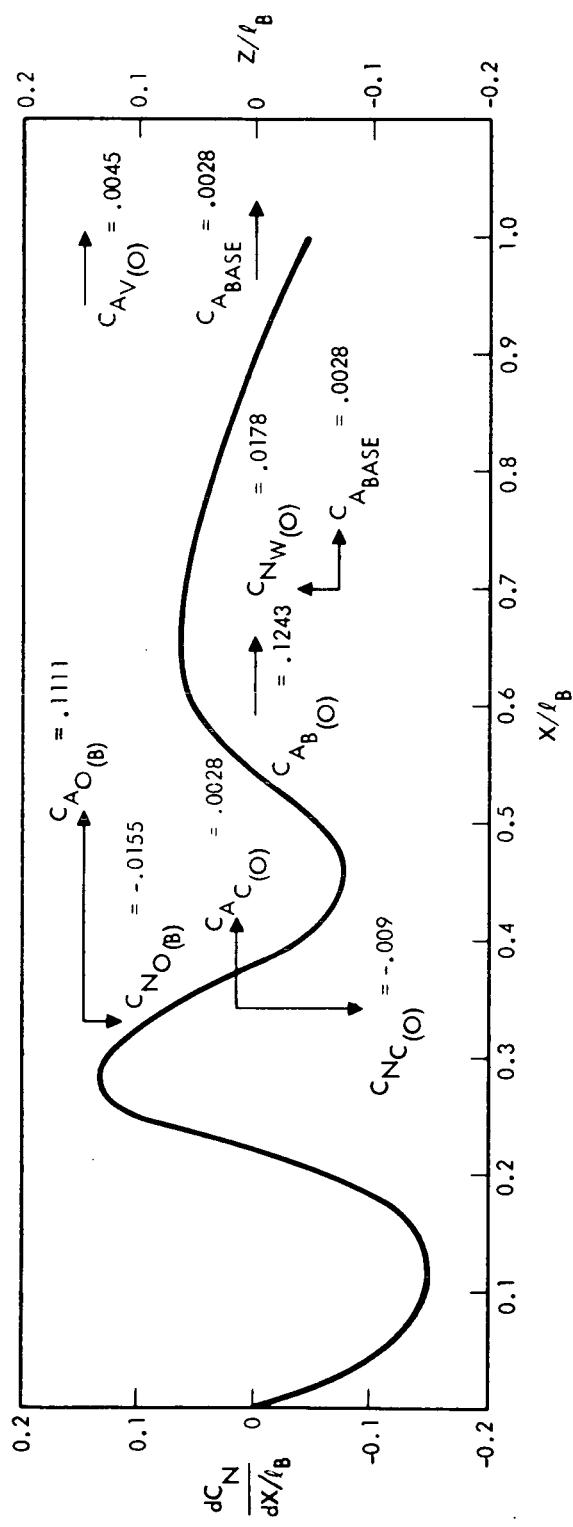


Figure 5-132. Booster Airload Distribution, ESS/Space Tug Payload,
Maximum βq Launch (Pitch Plane)

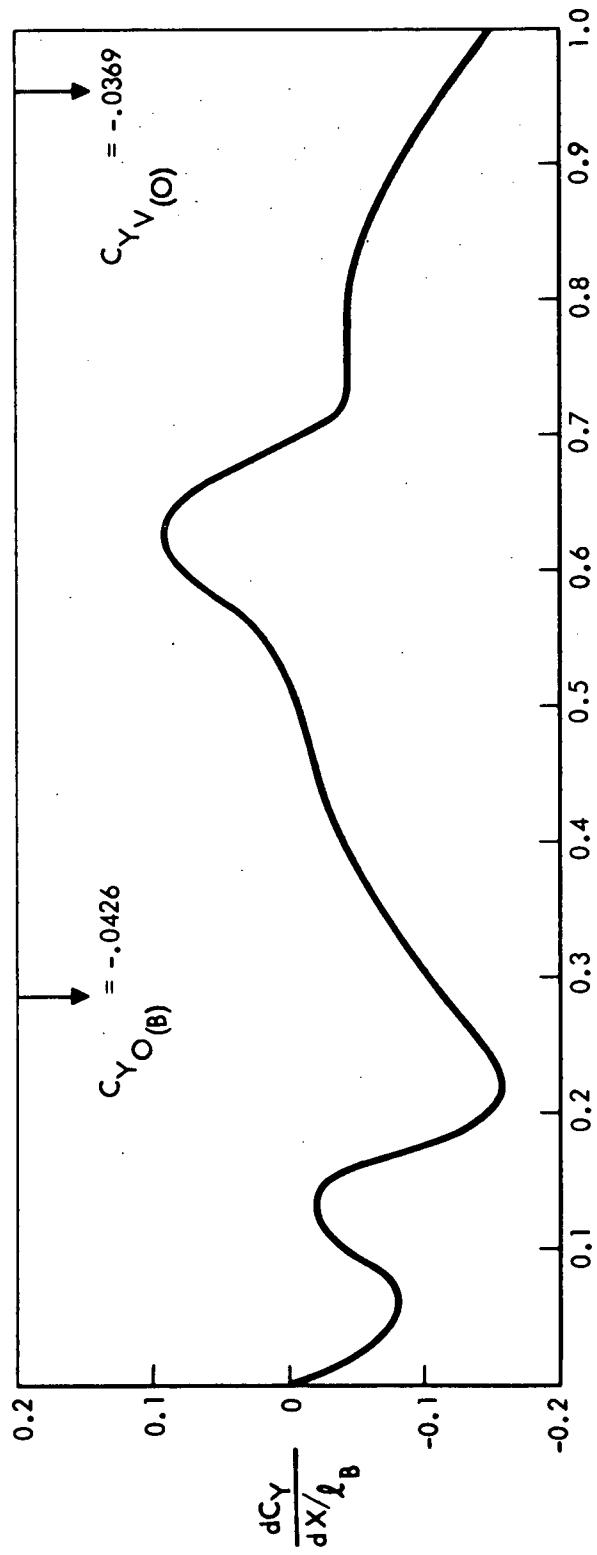


Figure 5-133. Booster Airload Distribution, ESS/Space Tug Payload,
Maximum β_q Launch (Yaw Plane)



includes wing carryover effects. Booster interference factors due to the presence of the ESS payloads were estimated as indicated above. All ESS loads are based on predictions in presence of the B-9U booster. Canard and elevon deflection were zero during launch. All component load distributions were balanced to obtain total integrated system loads.

The following symbols are used in Figures 5-122 through 5-133.

<u>Symbol</u>	<u>Definition</u>
C_A	axial force coefficient, axial force/ qS_{ref}
C_N	normal force coefficient, normal force/ qS_{ref}
C_Y	side force coefficient, side force/ qS_{ref}
ℓ_B	booster body length, ft
X	longitudinal body station, ft
Z	vertical body station, ft
q	dynamic pressure, lbs/ft ²
S_{ref}	wing reference area, ft ²
M	Mach number
$dC_N/dX/\ell_0$	booster body running load, normal
$dc_Y/dX/\ell_0$	booster body running load, side
α	angle of attack, booster reference line
β	angle of sideslip, booster reference line
<u>Subscripts</u>	
C. P.	center-of-pressure
B	booster body



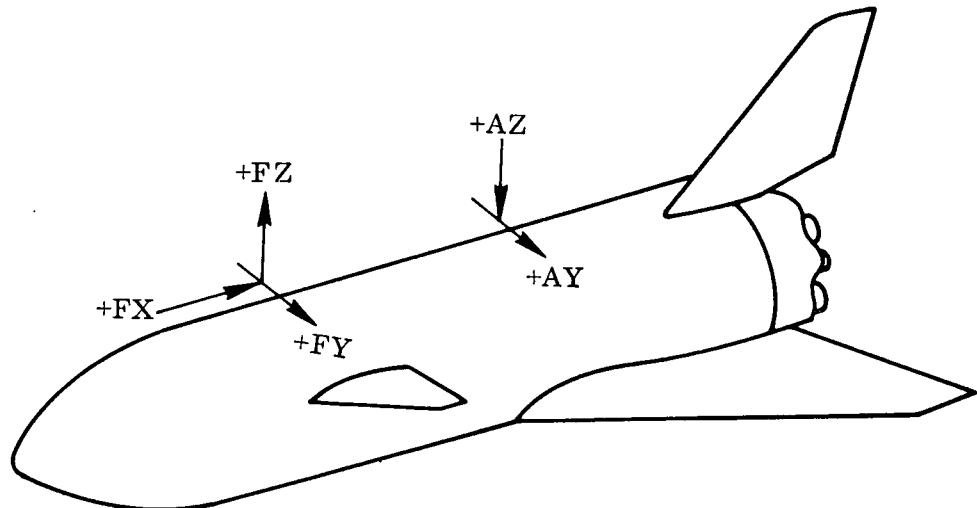
Subscripts (cont)

C	booster canard
O	orbiter
W	booster wing
V	booster vertical tail
(B)	in presence of booster
(O)	in presence of orbiter

Booster Body Design Loads. Before determining the final internal loads for the booster while it is mated to the ESS/RNS, ESS/MDAC Space Station and ESS/Space Tug, an initial excursion was run with the ESS/RNS payload. For this excursion a maximum performance trajectory was flown and the shuttle $q\alpha$ limits of $\pm 2800 \text{ (lb-deg)/ft}^2$ and $q\beta$ limits of $\pm 2500 \text{ (lb-deg)/ft}^2$ were observed. This approach resulted in high loads at the interconnect fittings. Figure 5-134 shows these loads and compares them to the shuttle booster fitting design loads. For the final loads analyses for the ESS and each of the three payloads, the following changes were made to insure minimum loads at the interconnect fittings during the critical high dynamic pressure flight regime:

1. Trajectory revisions were made to reduce the maximum dynamic pressure. This was achieved with a nominal compromise in performance as explained previously.
2. Maximum $q\alpha$ was reduced to the range of +1500 to -2900 $\text{lb-deg}/\text{ft}^2$. The -2900 value is the limit of the aft lower hydrogen tank structure and the total range of 4400 is a minimum control limit. The objective was to reduce the positive $q\alpha$ value to a minimum. Load relief in the pitch plane at maximum dynamic pressure was achieved through the use of gimbal limiting as described in above section on mated ascent control.
3. To minimize the effects of side loads in the region of maximum dynamic pressure, $q\beta_{\max}$ was reduced to $\pm 1600 \text{ (lb-deg)}\text{ft}^2$. This is also a minimum control limit. Load relief in the yaw plane was achieved by using a beta feedback loop, as on shuttle.

The effects of the above changes on the fittings loads, using the RNS payload are also shown in Figure 5-134. While these loads still exceed the shuttle booster design loads, they do represent achievable minimum loads. Another



REDUCTION

LOAD	BASELINE ($\times 10^3$)	ESS/RNS (23 MAR 71) ($\times 10^3$)	ESS/RNS (FINAL) ($\times 10^3$)
F_x (lb)	2825	2204	1818
F_y (lb) *	± 121	± 355	± 247
F_z (lb)	+ 195 - 151	+ 673 - 287	+ 426 - 495
A_y (lb) *	± 225	± 289	± 182
A_z (lb)	+ 842 - 254	± 860	+ 592 - 175

* MAX β_q CONDITION

Figure 5-134. Interconnect Loads Comparison



critical flight condition where shuttle booster design loads are exceeded is the point in the trajectory where the maximum vehicle axial acceleration is initially reached with propellant still remaining in the tank. This maximum "g" value was minimized by throttling to 50 percent thrust at burnout. Since this is the current design limit of the engine, no further relief could be achieved. The remainder of this section defines the booster internal loads, working to the trajectory and load relief constraints described above.

Internal loads consisting of axial and shear loads and bending and torsion moments were determined at 48 stations along the body length for 16 different load conditions. These booster internal loads were determined for the ESS/nuclear stage, ESS/MDAC stage and the ESS/space tug stage. Peak axial and tension load intensities were determined at 45-degree increments, starting at the bottom centerline, for each station location. In addition the loading condition causing the maximum load intensity was identified. The peak axial tension and compression ultimate load intensities are plotted versus booster station in Figures 5-135, 5-136, and 5-137 and for the ESS/nuclear stage, Figures 5-138, 5-139 and 5-140 for the ESS/MDAC stage and Figures 5-141, 5-142 and 5-143 for the ESS/space tug stage. All of these figures also contain a plot of the peak ultimate tension and compression load intensities versus booster station for the NR-161C Orbiter, as of March 26, 1971, for comparison. The areas where the maximum compression load intensities exceed the baseline have been shaded since they produce a weight increase. The areas where the tension intensities exceed the baseline have not been shaded since the booster has excess tension capability.

The interconnecting design attachment loads that are applied to the booster from the ESS/nuclear stage, ESS/MDAC stage and the ESS/space tug stage are shown in Figures 5-144, 5-145 and 5-146, respectively.

The bulkhead applied loads, as determined from the interconnecting loads, are shown in Figures 5-147, 5-148 and 5-149.

The 15-day ground wind conditions are not used in the booster body and bulkhead delta weight analysis based on the assumption that ground support equipment will be available to render these conditions not critical to the booster design.

The one-hour ground wind conditions produce load intensities that exceed the baseline capacity as shown in Figures 5-136, 5-138 and 5-139. These load intensities could be reduced to or below the baseline intensities by reducing the ground wind velocity profile to 80 percent of the present design value. This approximates 85 percentile NASA ETR peak one-hour ground winds.

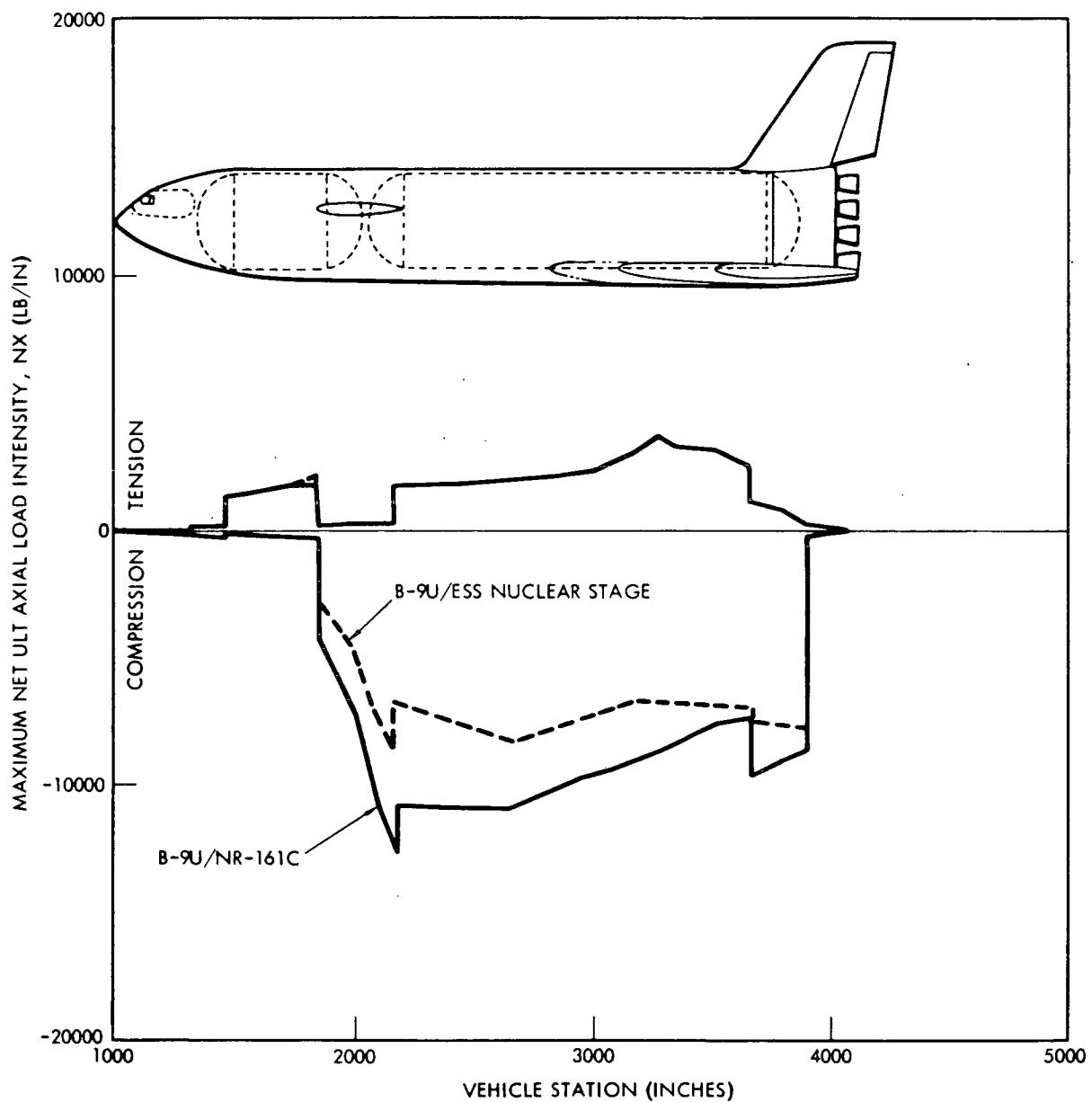


Figure 5-135. Internal Loads, Top Centerline
(RNS Payload)

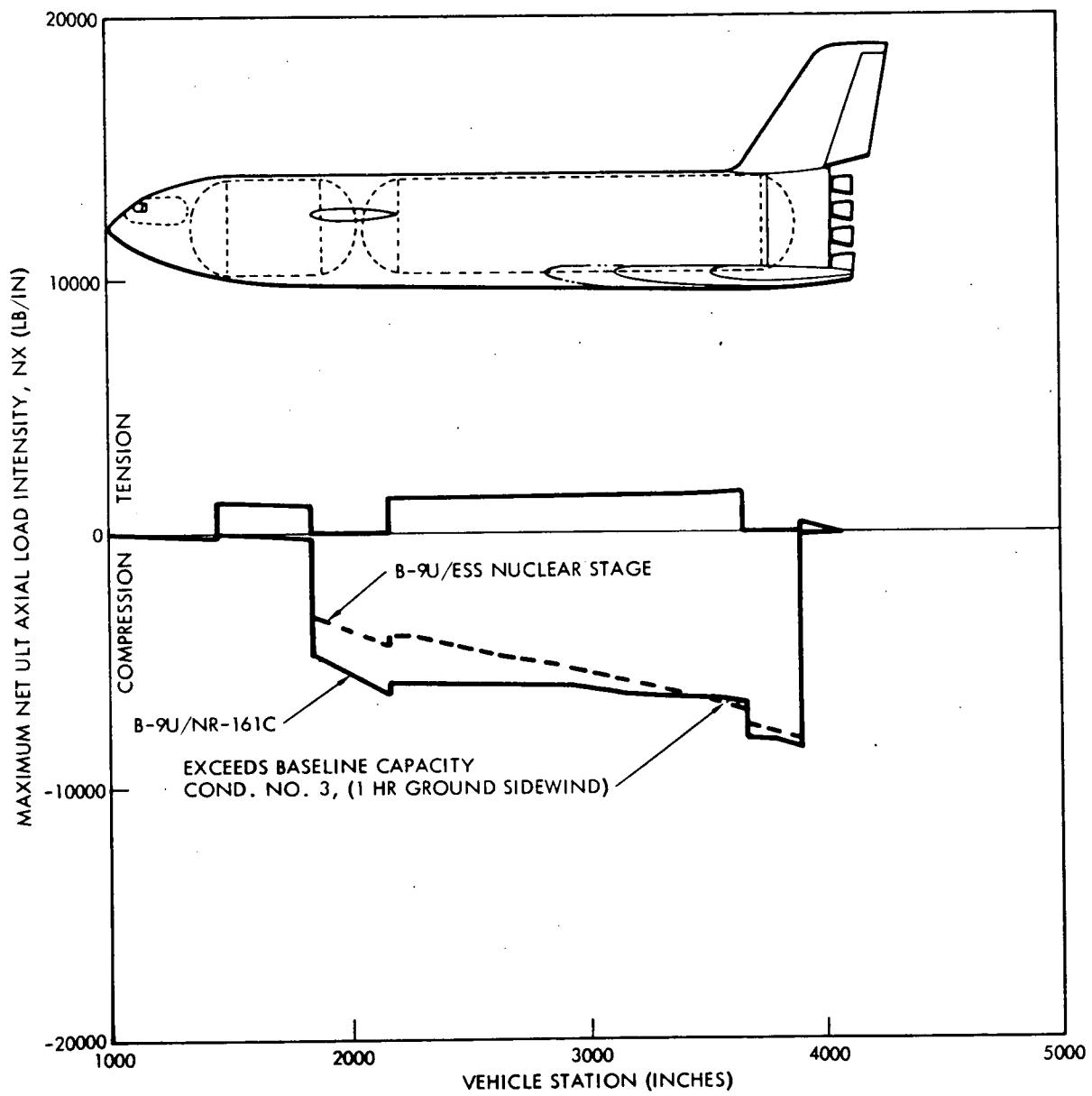


Figure 5-136. Internal Loads, Side (RNS Payload)

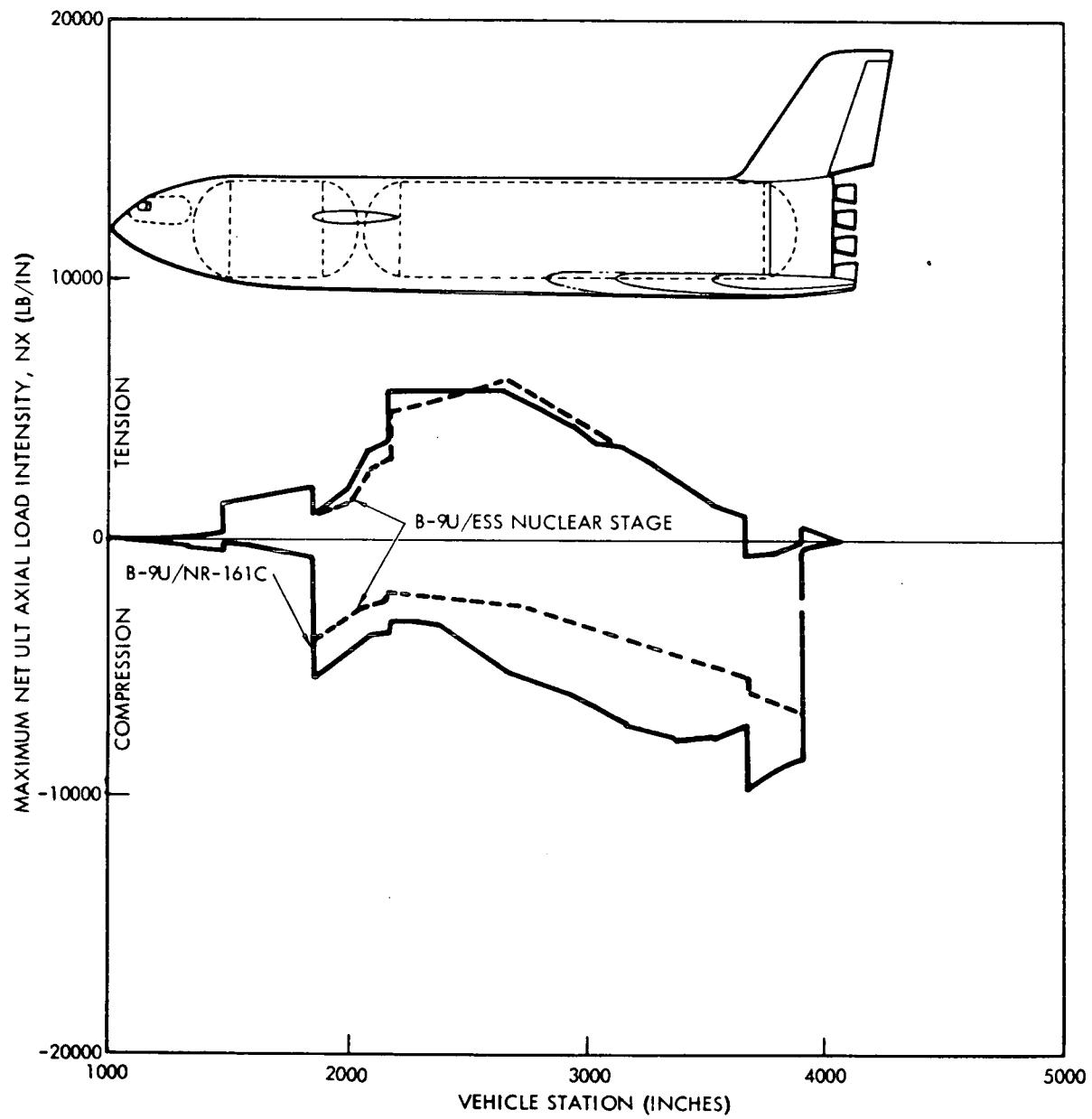


Figure 5-137. Internal Loads, Bottom Centerline
(RNS Payload)

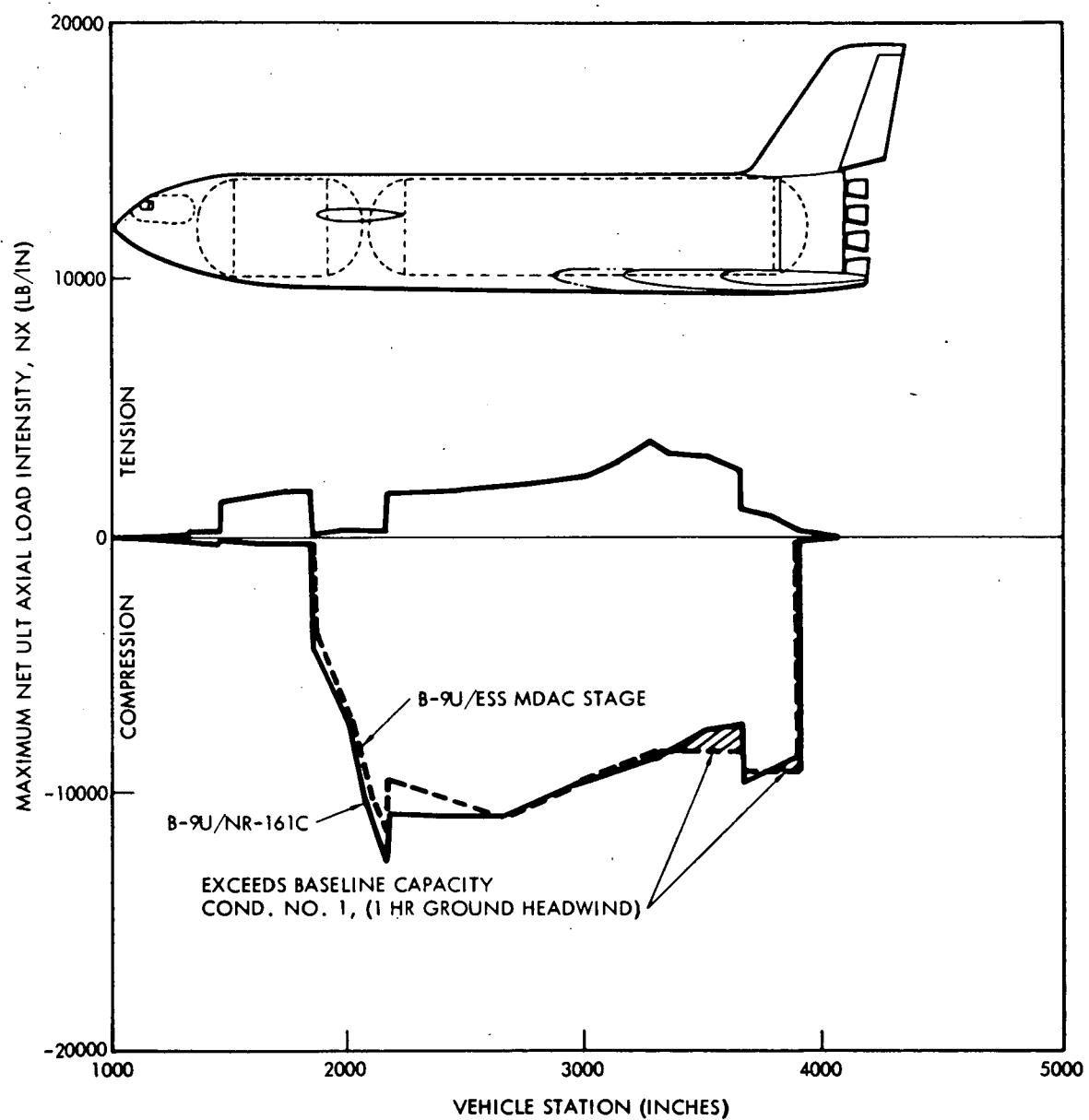


Figure 5-138. Internal Loads, Top Centerline
(Space Station Payload)

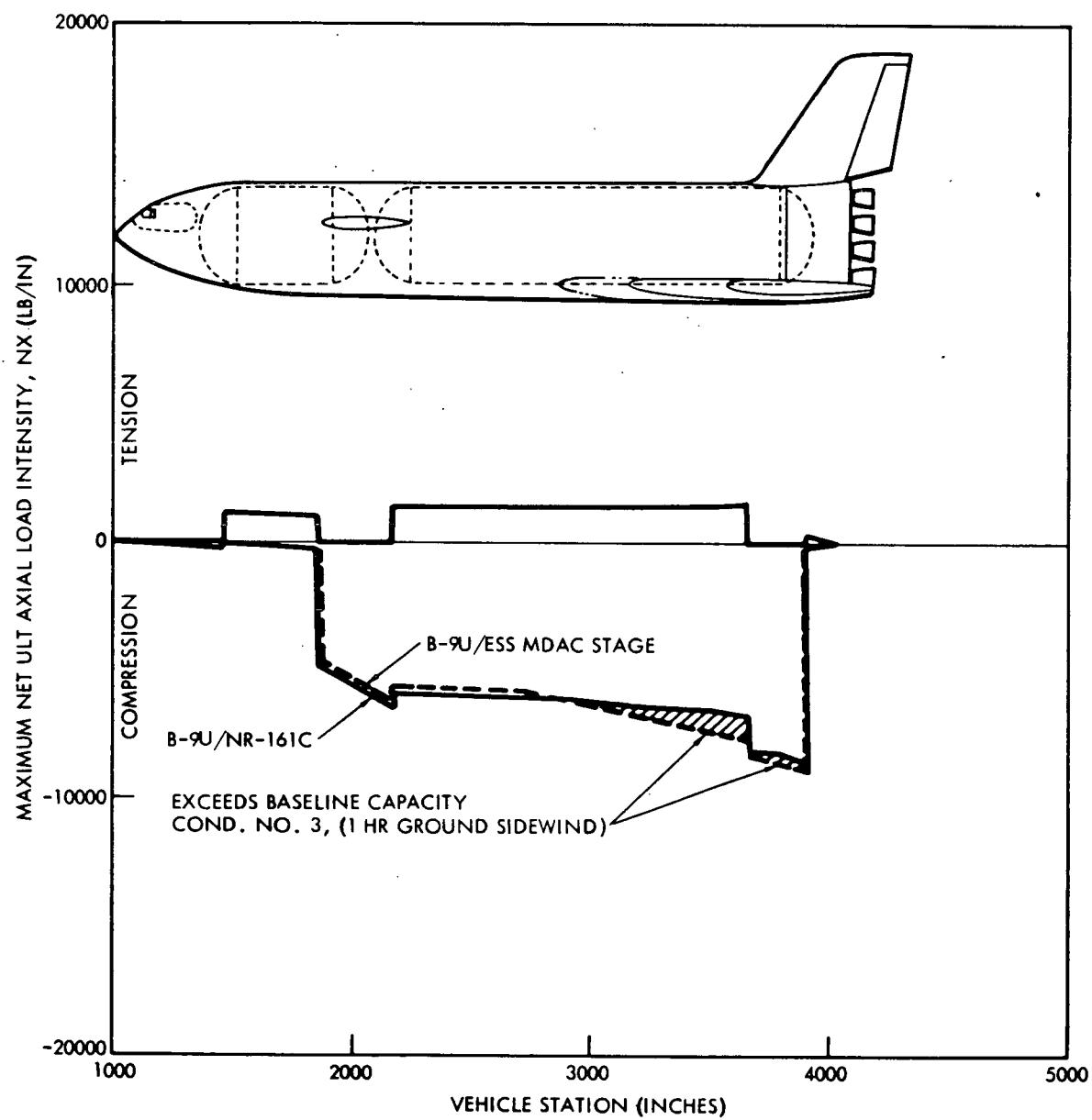


Figure 5-139. Internal Loads, Side
(Space Station Payload)

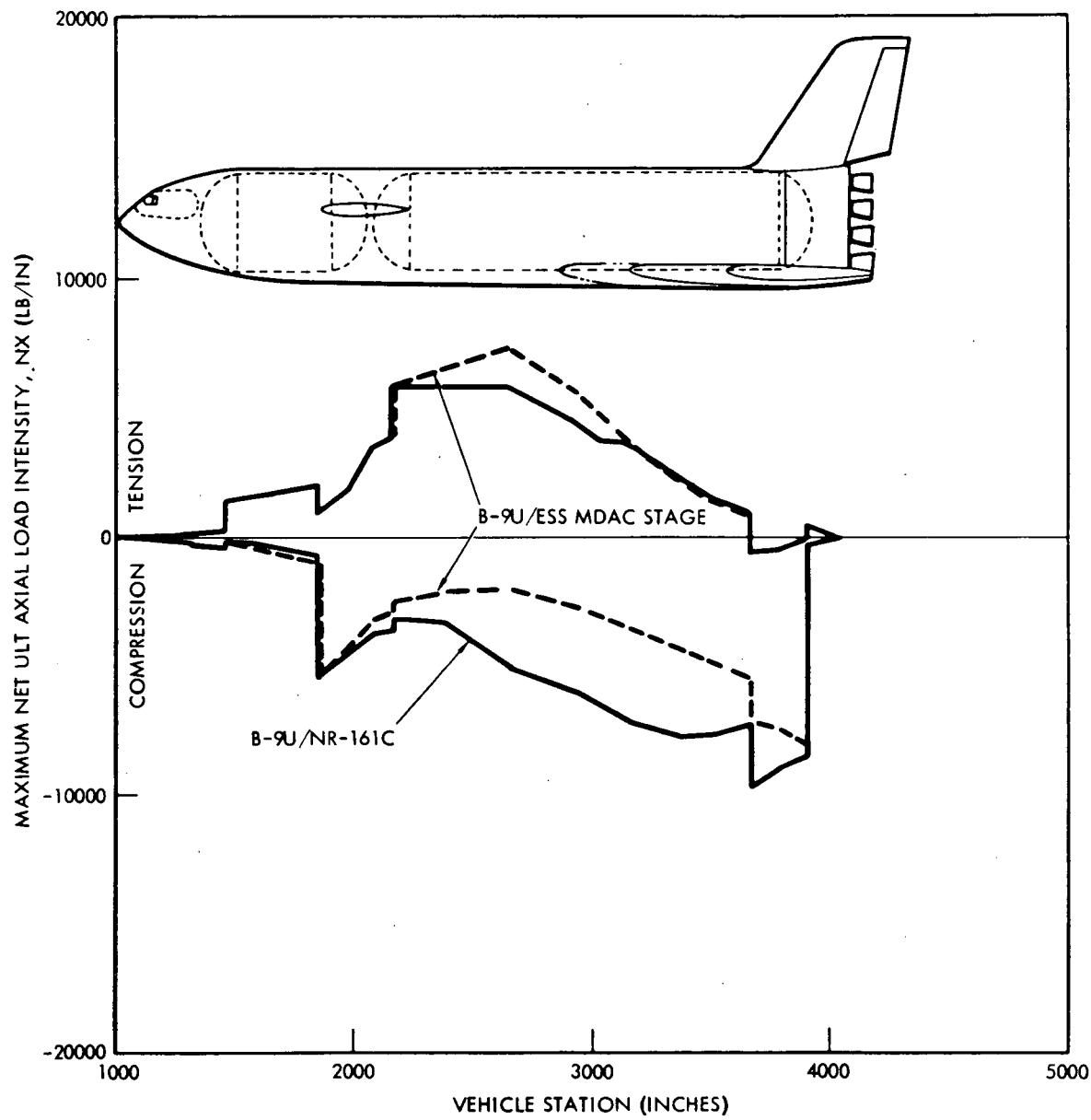


Figure 5-140. Internal Loads, Bottom Centerline
(Space Station Payload)

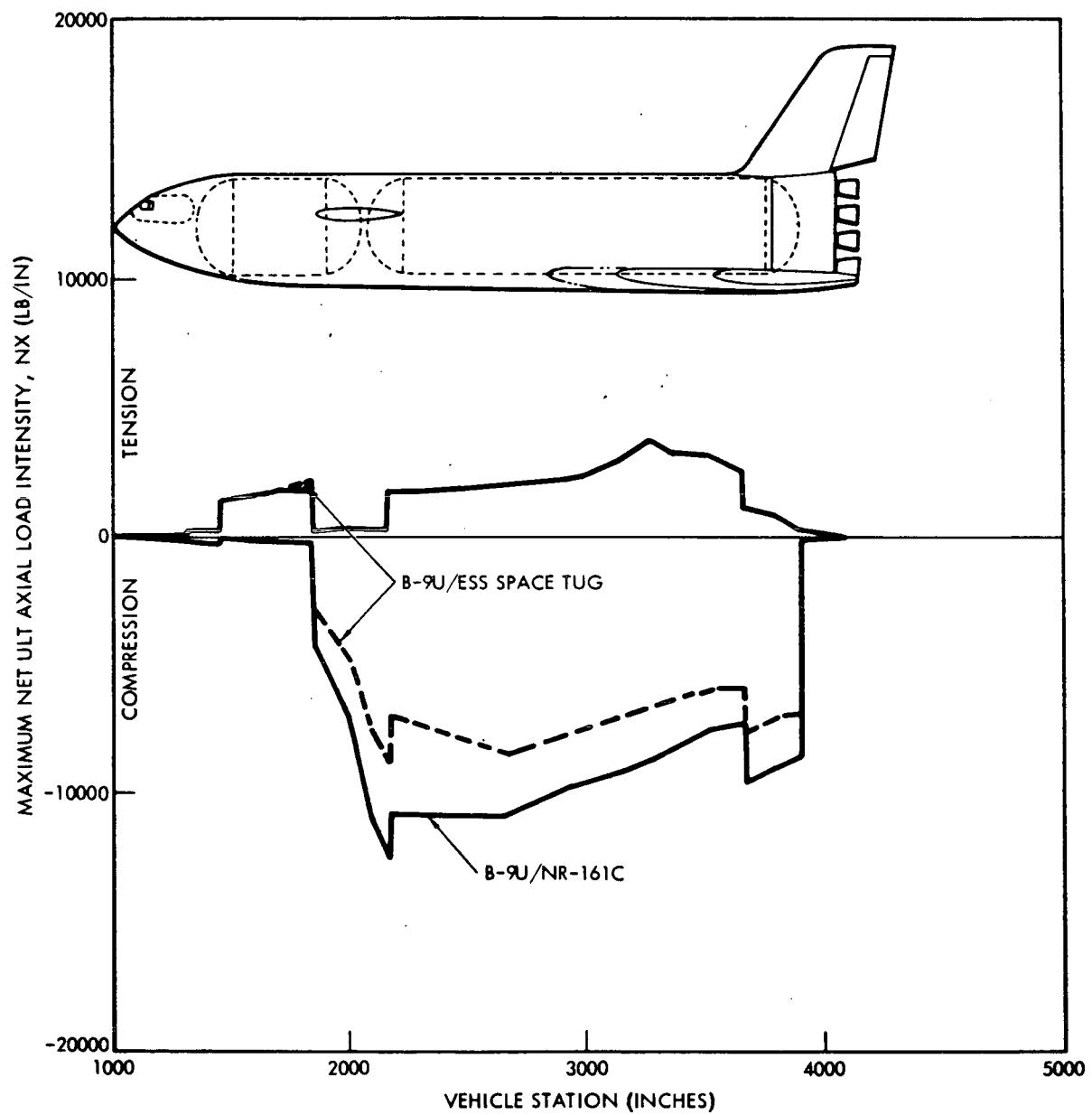


Figure 5-141. Internal Loads, Top Centerline
(Space Tug Payload)

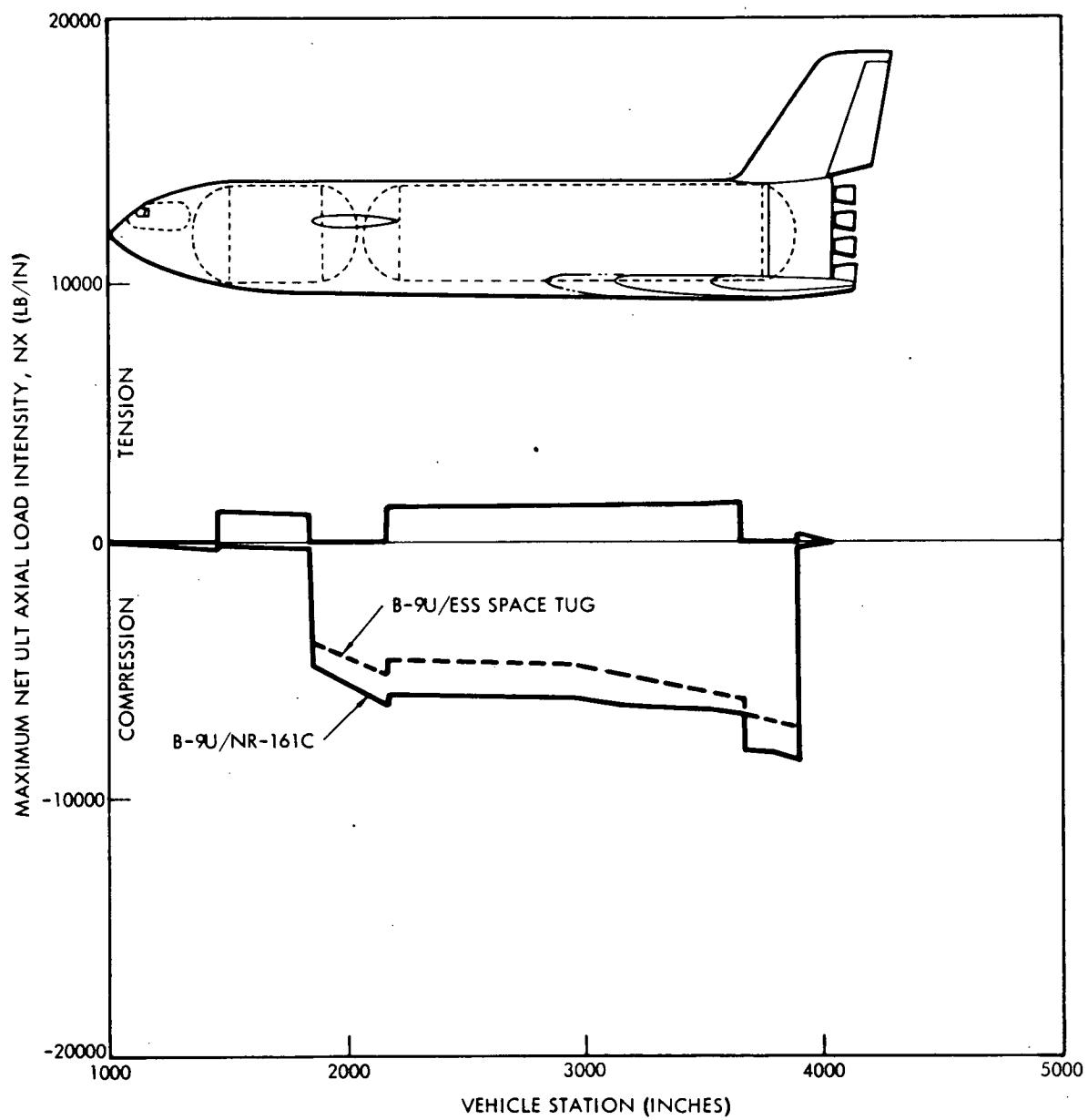


Figure 5-142. Internal Loads, Side (Space Tug Payload)

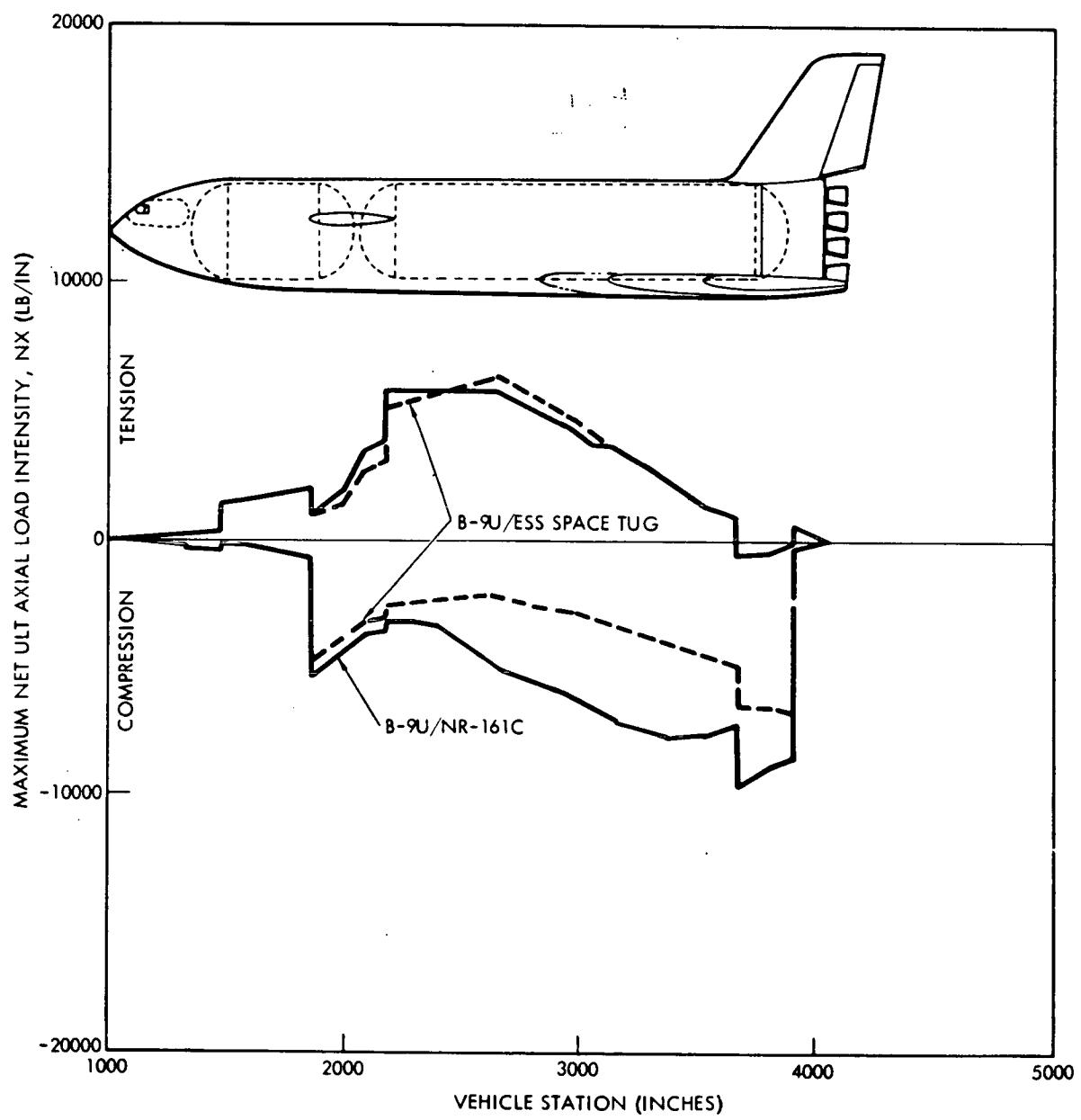
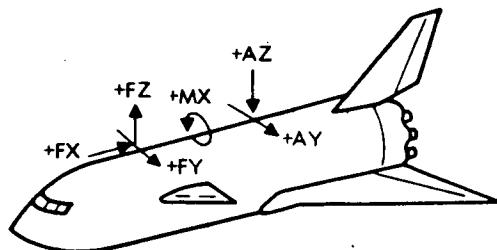


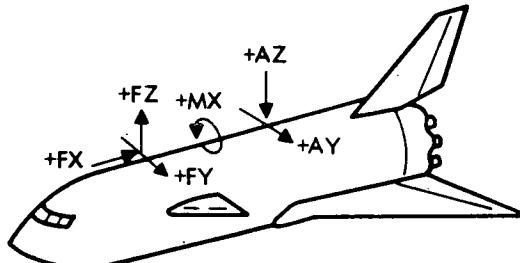
Figure 5-143. Internal Loads, Bottom Centerline (Space Tug Payload)



B-9U/ESS - NUCLEAR STAGE (LIMIT LOADS)

CONDITION	WIND	F_x ($\times 10^3$ lb)	F_y ($\times 10^3$ lb)	F_z ($\times 10^3$ lb)	A_y ($\times 10^3$ lb)	A_z ($\times 10^3$ lb)	M_x (10^6 in/lb)
TWO WEEK GROUND WINDS UNFUELED	HEAD TAIL SIDE	195 195 195	± 554	426 -495 48.7	∓ 230	289 -175 54.0	∓ 70.8
1 HOUR GROUND WINDS FUELED UNPRESSURIZED	HEAD TAIL SIDE	669 669 669	± 149	270 16.7 166	∓ 63.1	249 121 185	∓ 18.9
DYNAMIC LIFT OFF + 1 HOUR GROUND WINDS	HEAD TAIL SIDE	946 946 945	± 130	322 97.1 232	∓ 80.8	341 187 263	∓ 11.4
MAX. α -q	HEAD TAIL	1243 1237		409 -130		567 -124	
MAX. β -q	SIDE	1234	± 247	161	∓ 182	237	∓ 13.3
2.5g MAX. THRUST	-	1818		405		544	
BOOSTER BURNOUT	-	1797		343		592	

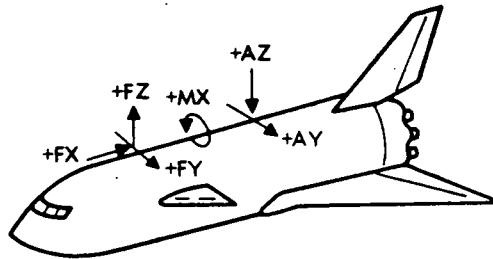
Figure 5-144. Design Attachment Loads (Nuclear Stage)



B-9U/ESS - MDAC STAGE (LIMIT LOADS)

CONDITION	WIND	F_x ($\times 10^3$ lb)	F_y ($\times 10^3$ lb)	F_z ($\times 10^3$ lb)	A_y ($\times 10^3$ lb)	A_z ($\times 10^3$ lb)	M_x (10^6 in/lb)
TWO WEEK GROUND WINDS UNFULED	HEAD TAIL SIDE	276 276 276		244 -286 68.8		165 -15.6 76.4	
1 HOUR GROUND WINDS FUELED UNPRESSURIZED	HEAD TAIL SIDE	991 991 991	± 354	293 148 245		297 247 272	∓ 15.44
DYNAMIC LIFT OFF + 1 HOUR GROUND WINDS	HEAD TAIL SIDE	1397 1397 1397		372 251 336	∓ 39.6	426 356 391	∓ 8.86
MAX. α -q	HEAD TAIL	2055 1964		508 203		744 255	
MAX. β -q	SIDE	1806	± 223	320	∓ 158.0	399	∓ 15.5
2.06g MAX. THRUST	-	2239		486		669	
BOOSTER BURNOUT	-	2217		377		746	

Figure 5-145. Design Attachment Loads (MDAC Stage)



B-9U/ESS - SPACE TUG (LIMIT LOADS)

CONDITION	WIND	F_x ($\times 10^3$ lb)	F_y ($\times 10^3$ lb)	F_z ($\times 10^3$ lb)	A_y ($\times 10^3$ lb)	A_z ($\times 10^3$ lb)	M_x (10^6 in/lb)
TWO WEEK GROUND WINDS UNFUED	HEAD TAIL SIDE	216 216 216		96.7 -108.0 52.6		82.9 56.9 58.5	± 33.3
1 HOUR GROUND WINDS FUELED UNPRESSURIZED	HEAD TAIL SIDE	691 691 691	± 44.2	184 128 172		197 190 191	± 9.17
DYNAMIC LIFT OFF + 1 HOUR GROUND WINDS	HEAD TAIL SIDE	975 974 974	± 34.2	274 204 241	± 9.81	283 262 269	± 5.23
MAX. α -q	HEAD TAIL	1506 1422		366 249		511 308	
MAX. β -q	SIDE	1389	± 125	302	± 38.8	393	± 18.65
2.47g MAX. THRUST	-	1874		423		556	
BOOSTER BURNOUT	-	1860		353		616	

Figure 5-146. Design Attachment Loads (Space Tug)

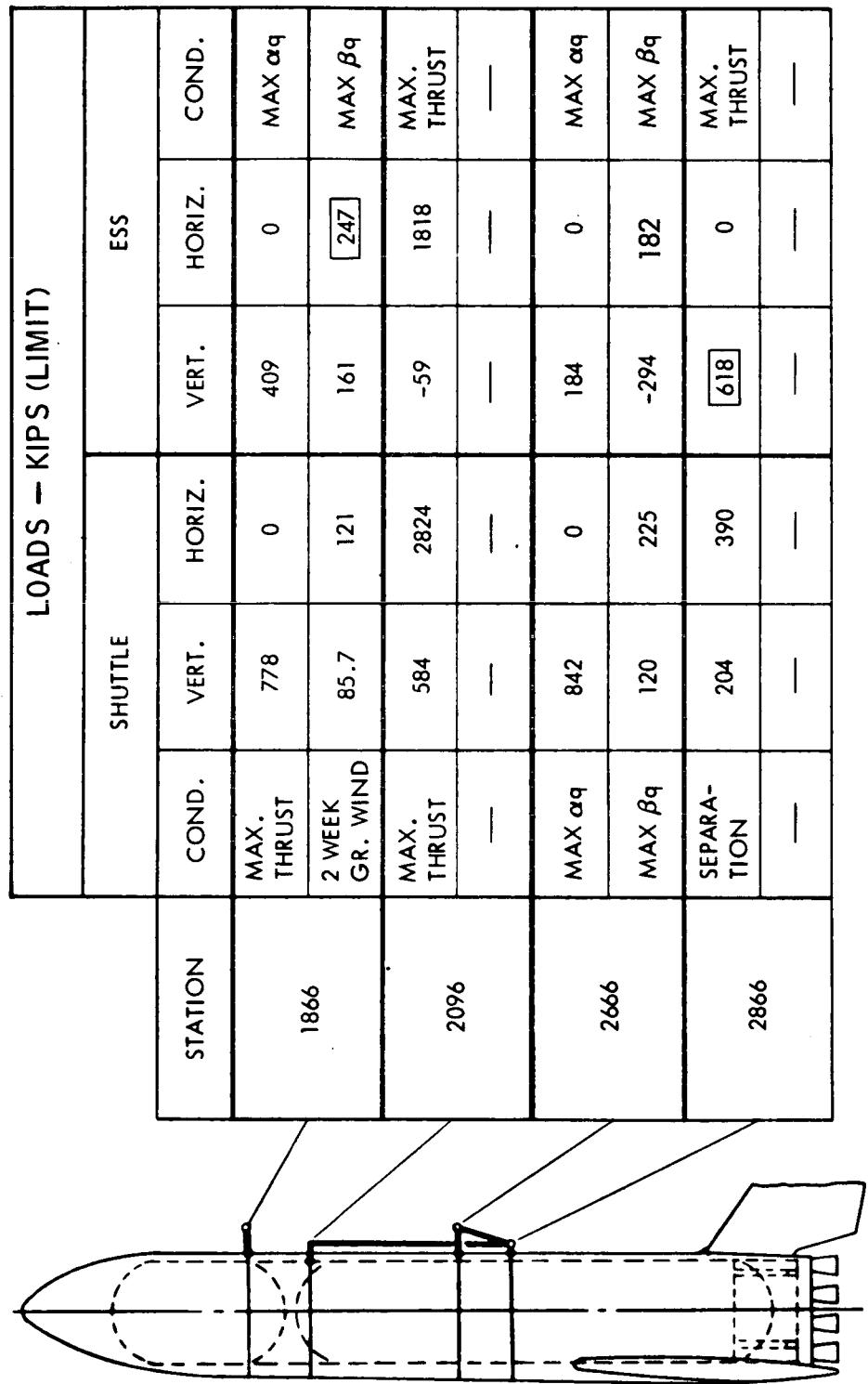


Figure 5-147. ESS Nuclear Stage Effect on Bulkheads

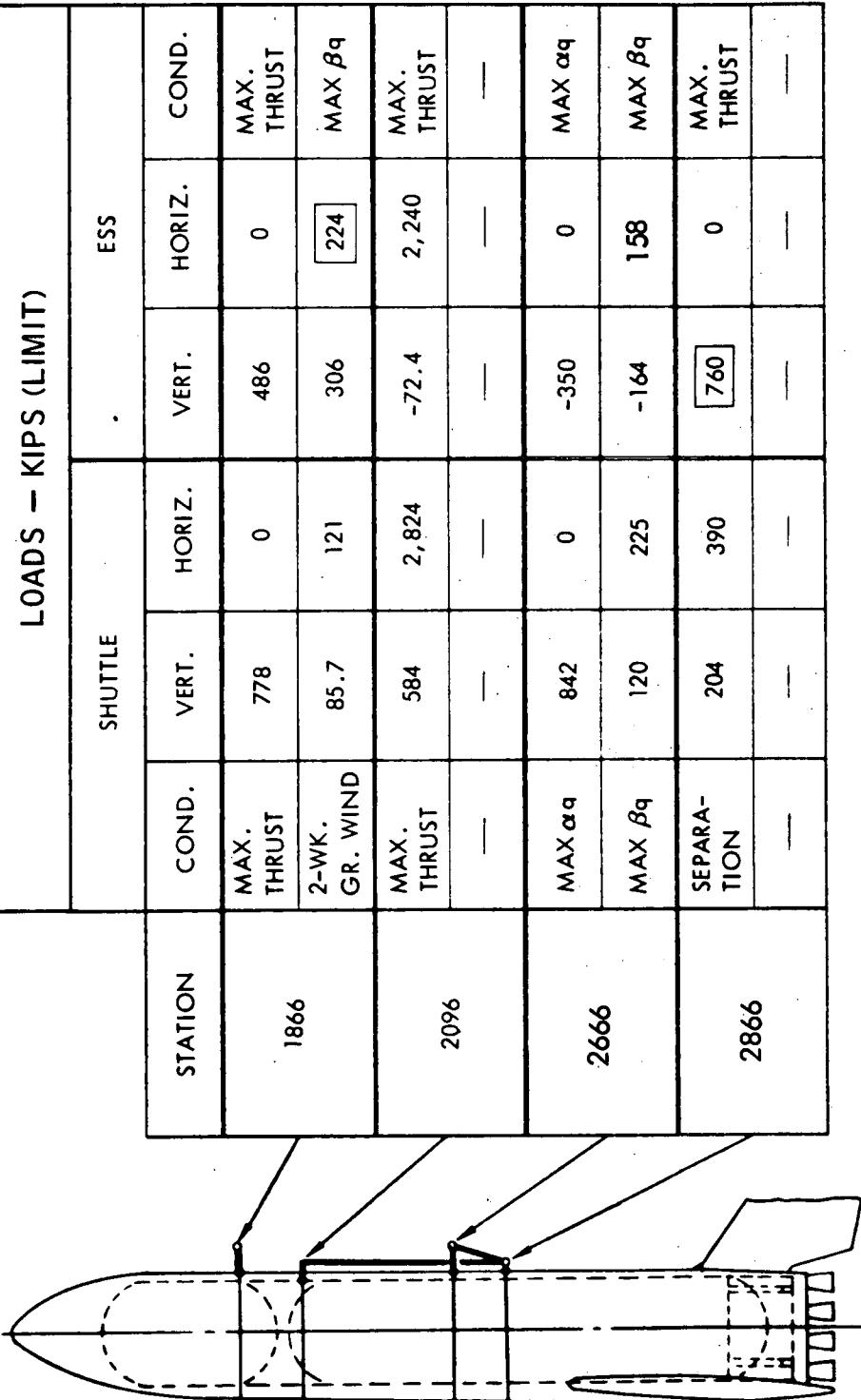


Figure 5-148. ESS/Space Station Effect on Bulkheads

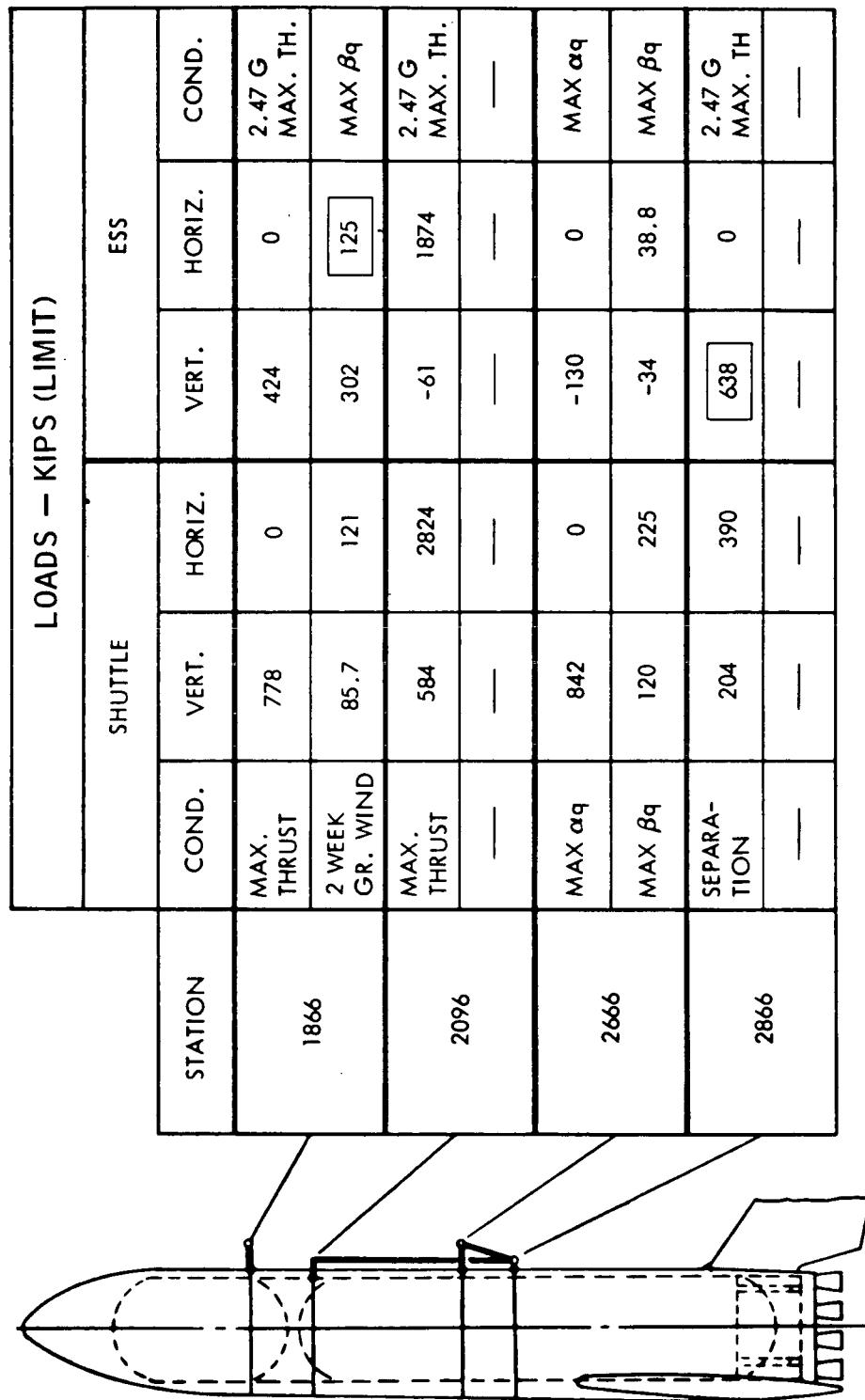


Figure 5-149. ESS/Space Tug Effect on Bulkheads



The effects on the booster for the loadings shown are given in Book 3.

ESS Loads. Applied loads to the ESS and effects therefrom are discussed in Book 2.

Booster Entry and Flyback Loads. Booster entry and flyback loads are within the baseline booster capability.

Thermal Environment

Mated Ascent Heating. This section presents the local heating rates on the ESS during ascent with the three following payloads configurations:

Reusable nuclear shuttle (ESS/RNS)

McDonnell-Douglas space station (ESS/MDAC)

North American Rockwell space tug (ESS/Space Tug)

The effect of the trajectory on the local heating rates has been analyzed and the results are also presented herein.

Vehicle Configuration, Trajectory, and Flow Regimes. The three selected payloads to be considered in the study are those previously described.

The launch trajectory used for the thermal environment (2/15/71 trajectory) is presented in Figure 5-150. The flight angle of attack varies slowly between $0 \leq \alpha \leq -2$. By analogy with the analysis performed on the shuttle/booster configuration, it is assumed that the flow is turbulent at $t = 0$ (takeoff) and becomes laminar at higher altitude. Transition is reached when, at a given location, the Reynolds number based on the momentum thickness is 150 times the local Mach number or

$$\frac{Re}{M_e}^{\theta} = 150$$

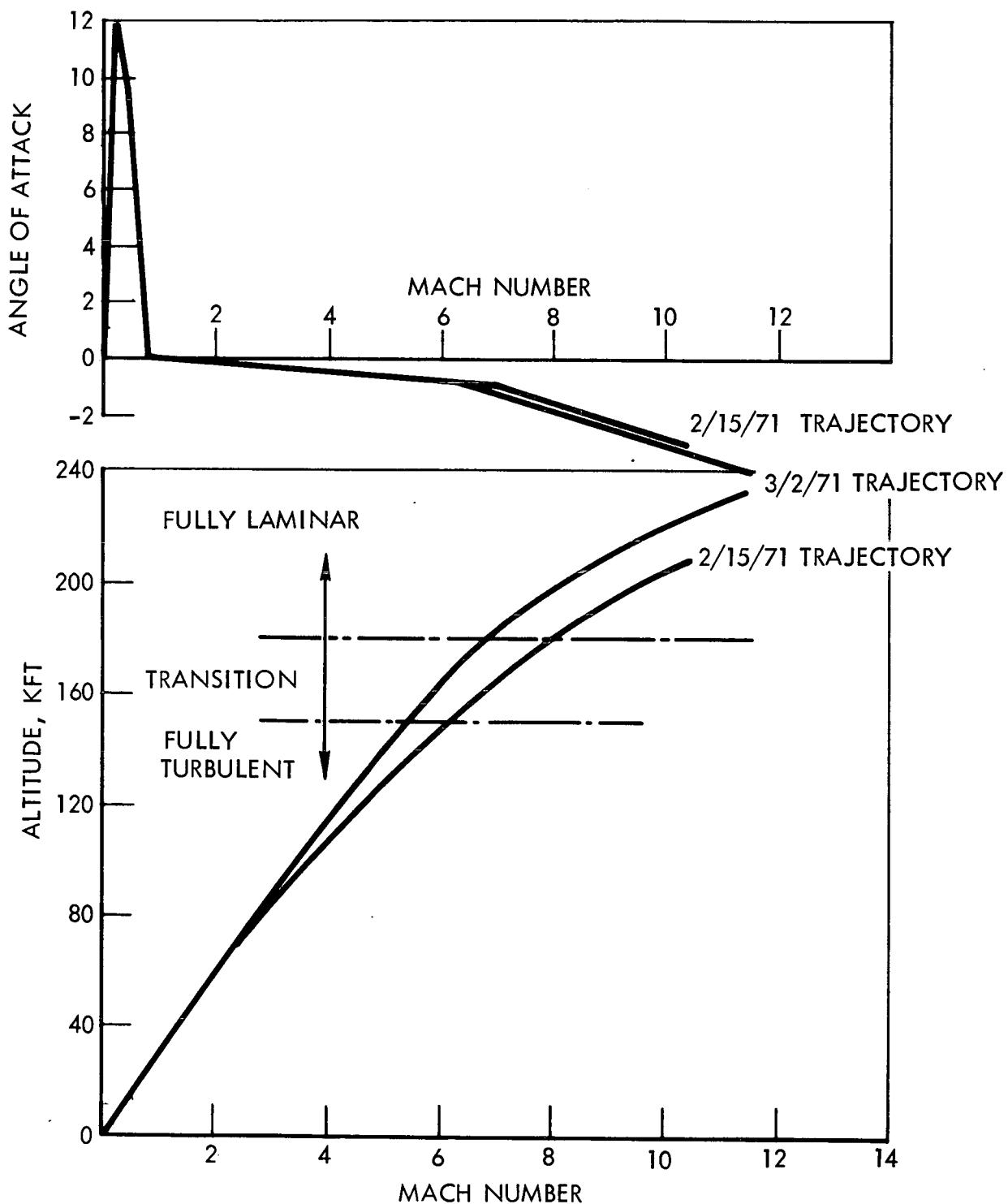


Figure 5-150. Trajectory Comparison



In the present analysis, it was assumed that the flow on the ESS remains fully turbulent as long as the transition point is still located on the ESS vehicle.

Determination of the Local Heating Rates. The determination of the local aerodynamic heating rates on the three payloads is not part of the present analysis. However, the influence of each payload on the ESS (protuberances) or on the booster (shock interaction, shock impingement) is of significant interest and has been investigated. In all analyses, it was assumed that the flight angle of attack was equal to zero. The results must not be extrapolated to cases where significant flight angles of attack ($\alpha > 5$ deg) exist.

Description of Space Shuttle Launch Heating Tests. Interference heating factors for the mated ESS/booster combination were based on the following two launch heating tests run as part of the NR Phase B Space Shuttle program.

1. NASA/ARC 3.5-ft HWT Test 107 (Reference 1), Conducted During the Period 28 September through 9 October 1970. Heat transfer data were obtained at a nominal Mach number of 7.4, a nominal total temperature of 1400 R and nominal Reynolds numbers of 0.7×10^6 and 3.5×10^6 per foot. Angles of attack of zero degrees and -5 degrees were investigated.
2. NASA/LRC UPWT Test 945 (Reference 2), Conducted During the Period from 13 through 22 January 1971. Heat transfer data were obtained by supersonic Mach numbers of 2.5 and 3.7 and at Reynolds numbers of 2.5×10^6 and 5×10^6 per foot. Angles of attack of zero degrees and -5 degrees were investigated.
3. NASA/MSFC 14 inch by 14 inch, Force and Moment tests conducted on the ESS/Shuttle Booster in April 1971. Although no heating data were measured, a typical shadowgraph obtained during this test illustrates the complex shock interference patterns between mated vehicles. Figure 5-151 shows the MDAC Space Station payload and Figure 5-152 the Space Tug payload.

Results

1. Aerodynamic Heating on the ESS with the Basic Payloads. The methods discussed in Volume XII for the analysis of the

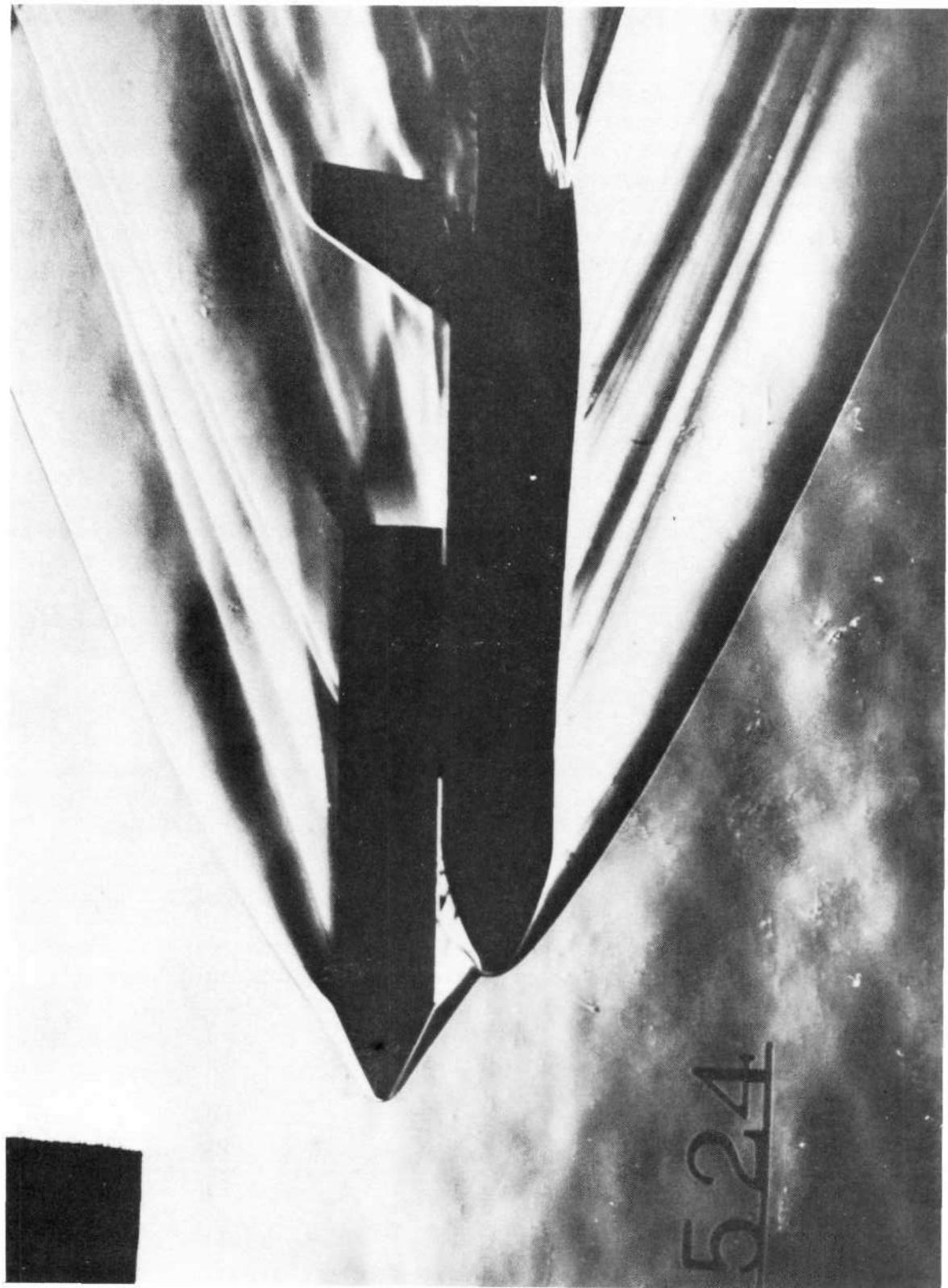


Figure 5-151. MDAC Space Station/Booster Interaction

5-218

SD 71-140-2

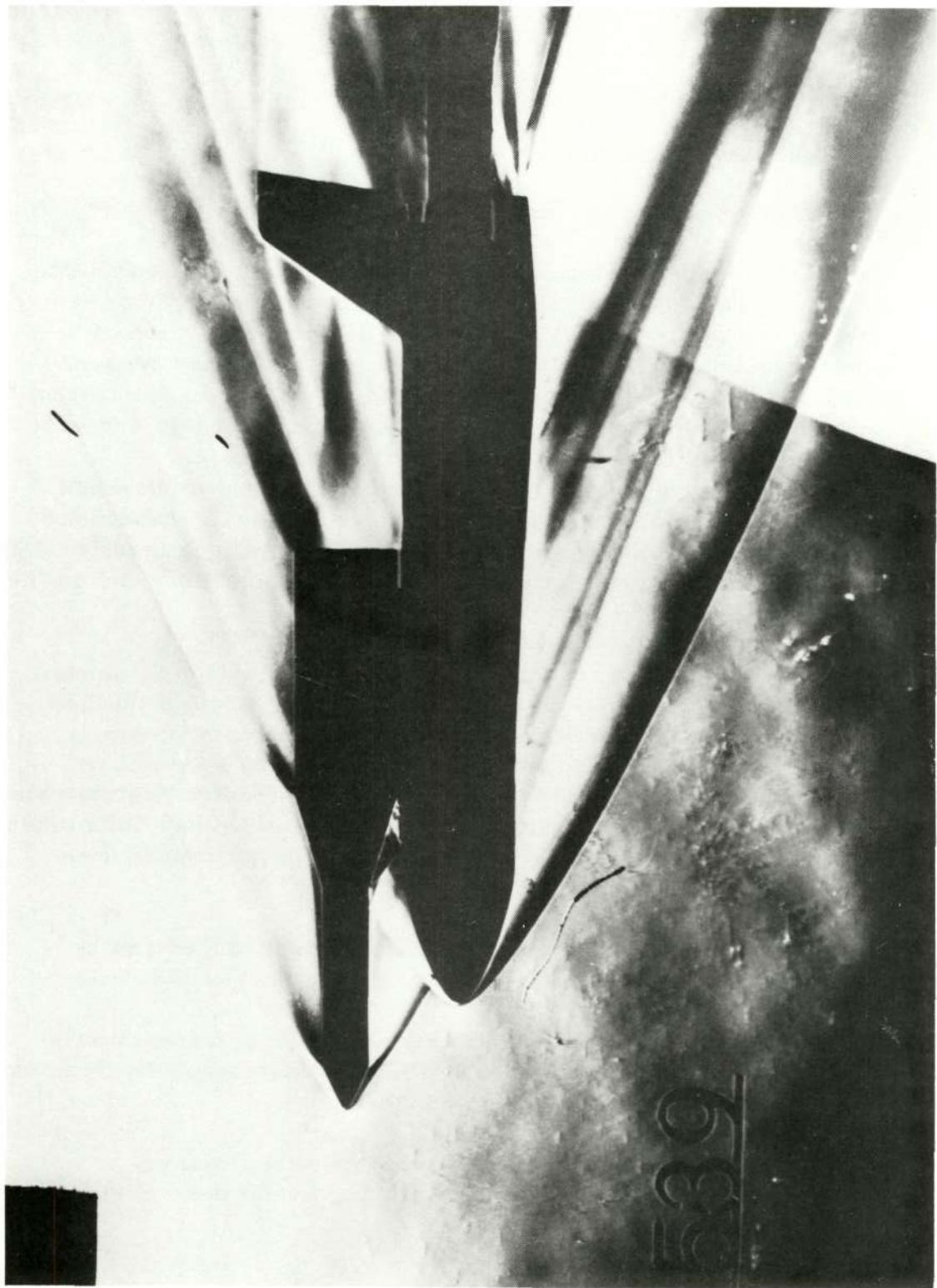


Figure 5-152. Space Tug/Booster Interaction

5-219

SD 71-140-2



aerodynamic heating have been applied to the three basic payloads. The results on the mated configurations are given as a function of time and include:

Film coefficient

Recovery temperature

Protuberance factor and interaction regions

The MDAC space station payload has large protuberances while the other payloads have none. The influence of these protuberances on the flow downstream will create a region of interaction heating that will be even amplified by the presence of the booster. The exact increase of heating due to the 12-foot docking ports has not been experimentally investigated and very few published data exist on such large protuberances. A conservative approach was then taken where the protuberance factor due to the docking port is increased by the protuberance factor due to the mated configuration. The approach leads to local heating rates that are 50 times greater than those obtained on the non-mated basic ESS.

The influence of the present attachment struts will, to a lesser extent, create a similar problem on the end section of the ESS. This is due to the interaction of the separation mechanism merging into the inviscid flow, generating shock waves that impinge on the surfaces, producing locally intensive heating rates. The same "protuberance style" approach as above has been taken during the investigation. However, the region of influence is smaller and decays rapidly.

The convective heating increase due to protuberances can be significantly reduced by the use of a fairing shroud that will:

Prevent the interaction from the MDAC space station protuberances to impinge on the ESS, but instead be diverted on the forebody of the fairing shroud.

Cover the strut attachment so that no shock will be introduced by the attachment sticking out in the undisturbed flow.

The preliminary design of such a device and its influence on the local aerodynamic heating is presented in a later section.



Shortly after the 15 February 1971 trajectory was computed, a more refined trajectory, dated 2 March 1971, was issued. These two trajectories are represented in Figure 5-150. The present calculations were performed with the 2/15/71 trajectory. However, it appeared interesting to analyze the effect of the trajectory on the local heating rates. Here again, the MDAC/ESS configuration was used in this study.

The results obtained from the 15 February 1971 trajectory have been used and modified to account for the slight variation in flow properties following the analysis of Reference 3 for the laminar flow and that of Reference 4 for turbulent flow. Obviously, this analysis is based upon small perturbations and is only valid when the two flight conditions do not differ significantly.

- a. Laminar Boundary Layer Analysis. The film coefficient for the 2 March 1971 trajectory is then

$$h_2(x) = h_1(x) \frac{M_{\infty 2}}{M_{\infty 1}} \sqrt{\frac{p_{\infty 2}}{p_{\infty 1}} \frac{u_e 2}{u_e 1}}$$

The recovery temperature is given by the following relationship:

$$T_{ad} = T_{\infty} \left(1 + \frac{\gamma - 1}{2} r_{laminar} M_{\infty 2}^2 \right)$$

- b. Turbulent Boundary Layer Analysis. Applying the same small perturbation analysis for the turbulent flow as previously described for the laminar flow, the film coefficient for the 2 March 1971 trajectory is given by the following relationship:

$$h_2(x) = h_1(x) \left[\frac{M_{\infty 2}^2}{M_{\infty 1}^2} \frac{p_{\infty 2}}{p_{\infty 1}} \frac{u_e 2}{u_e 1} \right]^{0.2}$$



The recovery temperature is given by

$$T_{ad} = T \left(1 + \frac{\gamma - 1}{2} r_{turbulent} M_{\infty 2}^2 \right)$$

The film coefficients versus time for both the 15 February 1971 and the 2 March 1971 trajectories are given in Volume XII. However, on the semilog plot, it is difficult to accurately read and discriminate among the values for the two trajectories. During the analysis of the 15 February 1971 trajectory, the film coefficients were carefully computed and included in the thermal model. To take advantage of this previous setup, the ratio $h_2/h_1 = f(t)$ was also computed and is presented with the recovery temperature, in Volume XII.

A parametric thermal analysis was made for the two trajectories in order to analyze variation in peak wall temperature. The following parameters were investigated:

Wall thickness	$0.02 \leq 0 \text{ inch} \leq 0.16$
Radiation to space factor	$0.085 \leq \sigma_r \leq 0.8$
Solar absorption factor	yes/no

The difference between the two peak wall temperatures has been computed and is represented on Figure 5-153. It can be seen that the maximum difference is of the order of 13 degrees and that furthermore this result is obtained for a very low radiation-to-space factor, unlikely to occur on the present system.

The conclusion of the present analysis can be summarized as follows:

The Reynolds number is the most significant parameter influencing the local heating rates

The Mach number and angle of attack have almost no influence in the range investigated

The effect of the gap distance with M_{∞} and Re_{∞} must be investigated.

The results of the literature survey show that the aerodynamic simulation of the protuberances as a function of the boundary layer

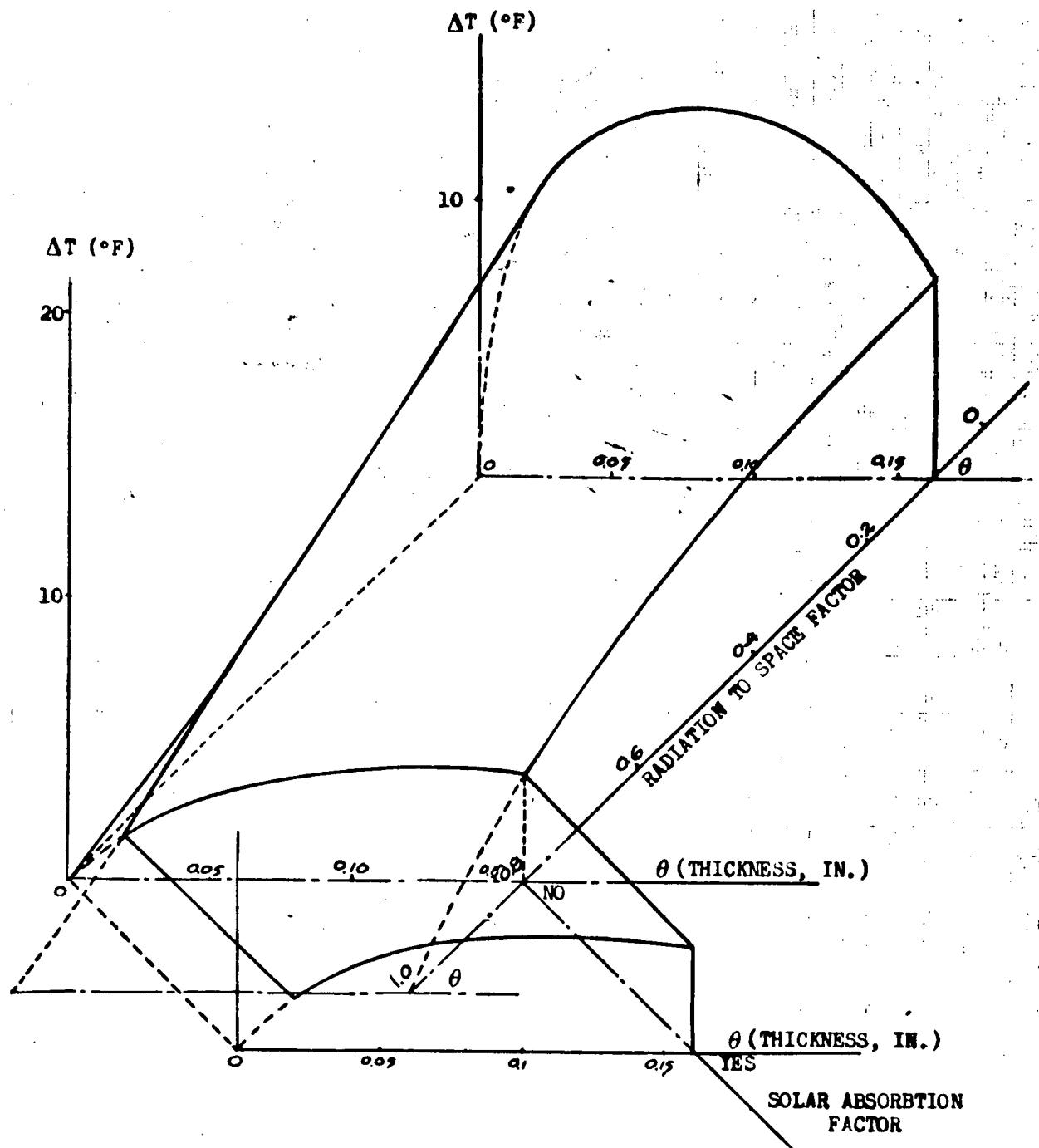


Figure 5-153. Peak Wall Temperature Difference Due to Change in Trajectory



thickness could create a serious problem when attempting to apply the wind tunnel results to actual flight cases.

2. Aerodynamic Heating on the GDC B9U Booster. From schlieren pictures, it can be seen that the payload nose shocks and the booster nose shock reflected from the payload back to the booster are of equal strength for all payloads, shuttle included.

The influence of the ESS payloads on the local heating rates on the booster are of two types:

- a. The influence of the close proximity of the ESS will increase the local heat transfer rates when compared with the booster-alone configuration. This problem exists also with the present shuttle-booster configuration. In this analysis, it has been assumed that by reason of symmetry the local heating rates on the booster at a given station were identical to those on the ESS at the same location. This was later substantiated by the aerodynamic test tunnel data on the booster provided by GDC on the shuttle-booster configuration.
- b. The space tug payload presents a conical interstage inducing a shock wave at its interaction with the cylindrical section that impinges on the booster upper surface. This shock impingement will create local overpressure and heating rates that are more severe than those existing for the other payloads, shuttle included. Also, since the impingement point on the booster is a function of the flight Mach number, it will vary during the ascent phase. An analysis of the phenomena has been made based upon the methods and assumptions described in Volume XII.

The influence on the booster of the impinging shock wave could be avoided by a better fairing design of the interstage, which would be developed for payloads such as space tug.

The following figures present an evaluation of the thermal compatibility of the baseline B-9U booster with the nuclear (RNS), space tug and space station expendable second stages. The ESS trajectories used for this analysis are low q trajectories subsequently derived to limit the aerodynamic forces imposed upon the expendable second stages. Figure 5-154 compares the three ESS ascent trajectories to the baseline T-B9U-1 trajectory. At each velocity, the ESS trajectories are at a higher altitude (and therefore lower air density) than the T-B9U-1 trajectory. Thus,

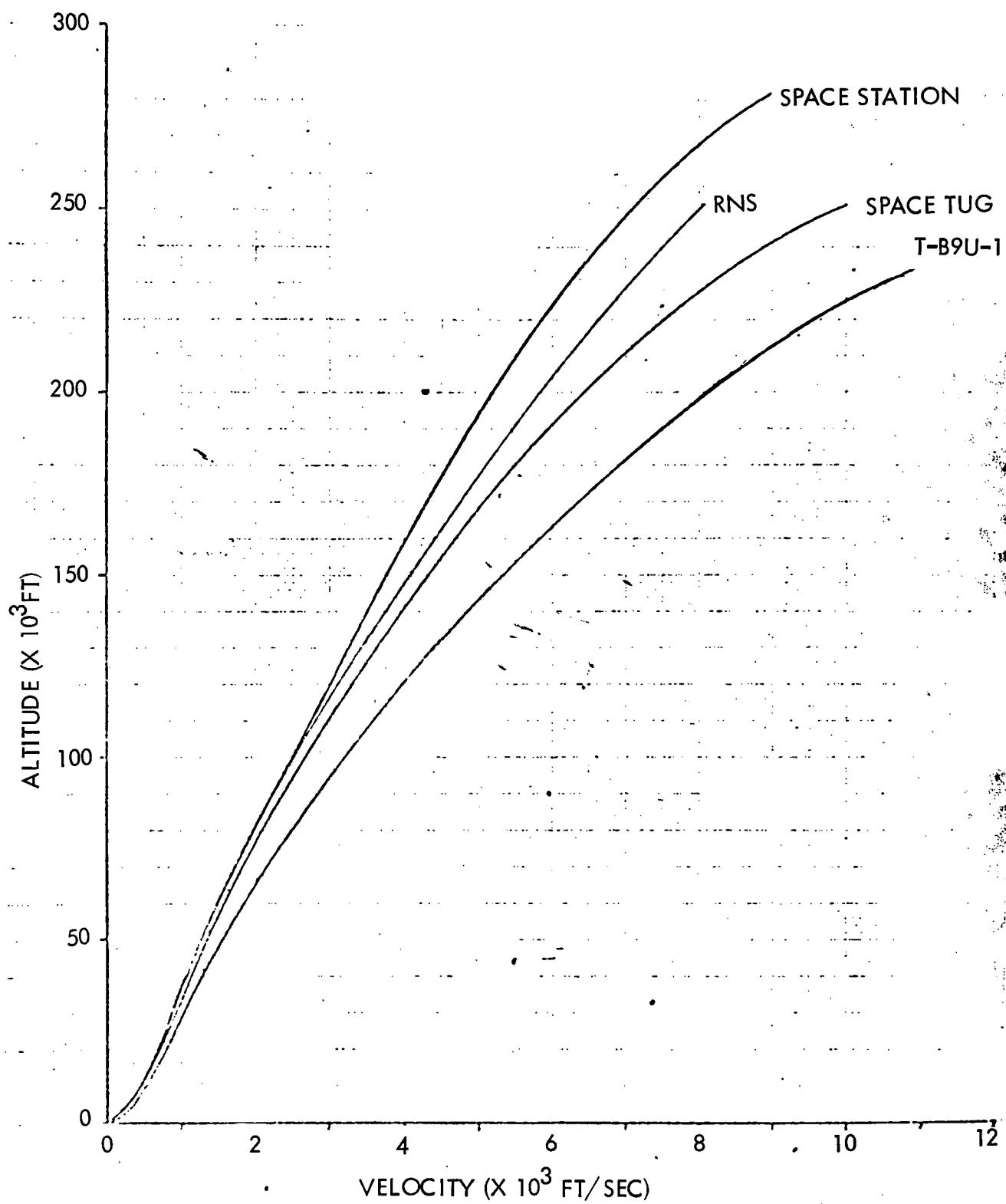


Figure 5-154. Comparison of Ascent Trajectories Studies



these low-q ESS trajectories will produce less severe aerodynamic heating during ascent than will the baseline T-B9U-1 trajectories.

Three points on the booster fuselage upper surface were investigated for the aerodynamic heating effect of the three ESS configurations and trajectories. These points are illustrated in Figure 5-155. Points A and B represent two areas on the booster forward section experiencing shock interference due to the second stage. Their locations vary according to the second stage configuration as illustrated in Figures 5-151 and 5-152. Based on shadowgraphs taken during Phase B space shuttle heat transfer tests, it can be seen that the location of the orbiter bow shock impingement point on the B-9U booster top surface is a strong function of free stream Mach number. Point C is located in the most severe interference heating region caused by the mated attachment struts. Points A and B were modeled as an 0.025-inch Rene-41 skin and point C as an 0.025-inch Rene-41 skin over the LO₂ tank.

Table 5-10 tabulates for each point and mated configuration the view factor to space (used for radiation cooling) and the aerodynamic heating factor. The heating factors are referenced to the stagnation point heating to a one-foot radius sphere. The heating factors for point C are shown in Figure 5-156. The heating factors were applied to the stagnation point heating of a one-foot radius sphere flown along the trajectory to obtain the aerodynamic heating to each point.

Figure 5-157 presents the temperature histories of the three forward points on the fuselage upper surface for each of the ESS configurations. Table 5-11 summarizes the maximum ascent temperatures of the three ESS configurations for comparison with the minimum ascent temperatures of the baseline orbiter configuration. From this figure it is seen that the booster ascent temperatures for the ESS configurations are significantly less than for the baseline orbiter, as anticipated from the trajectory comparison.

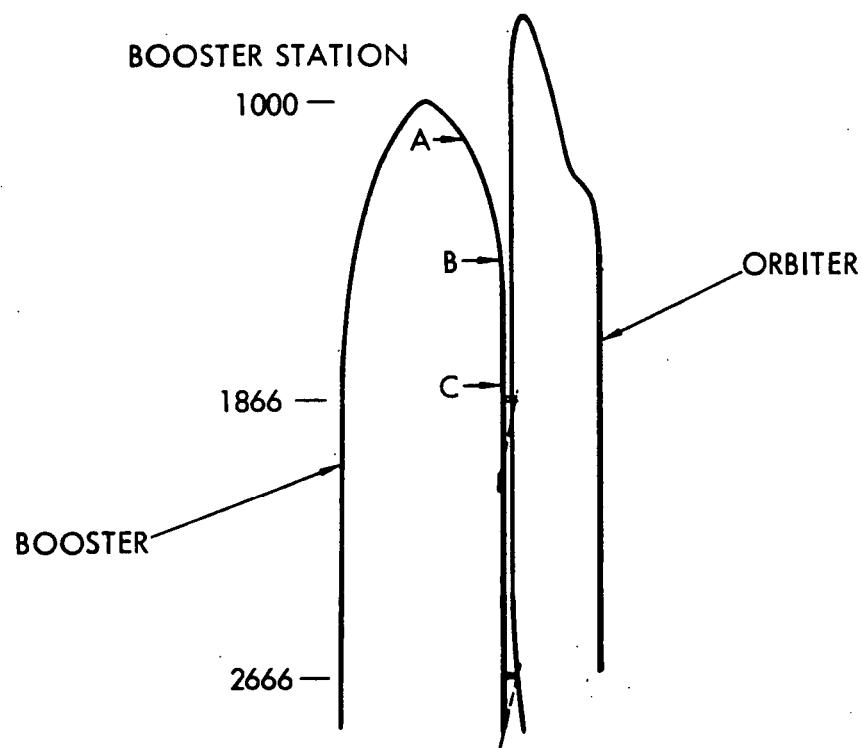


Figure 5-155. Booster Top Centerline Locations Investigated

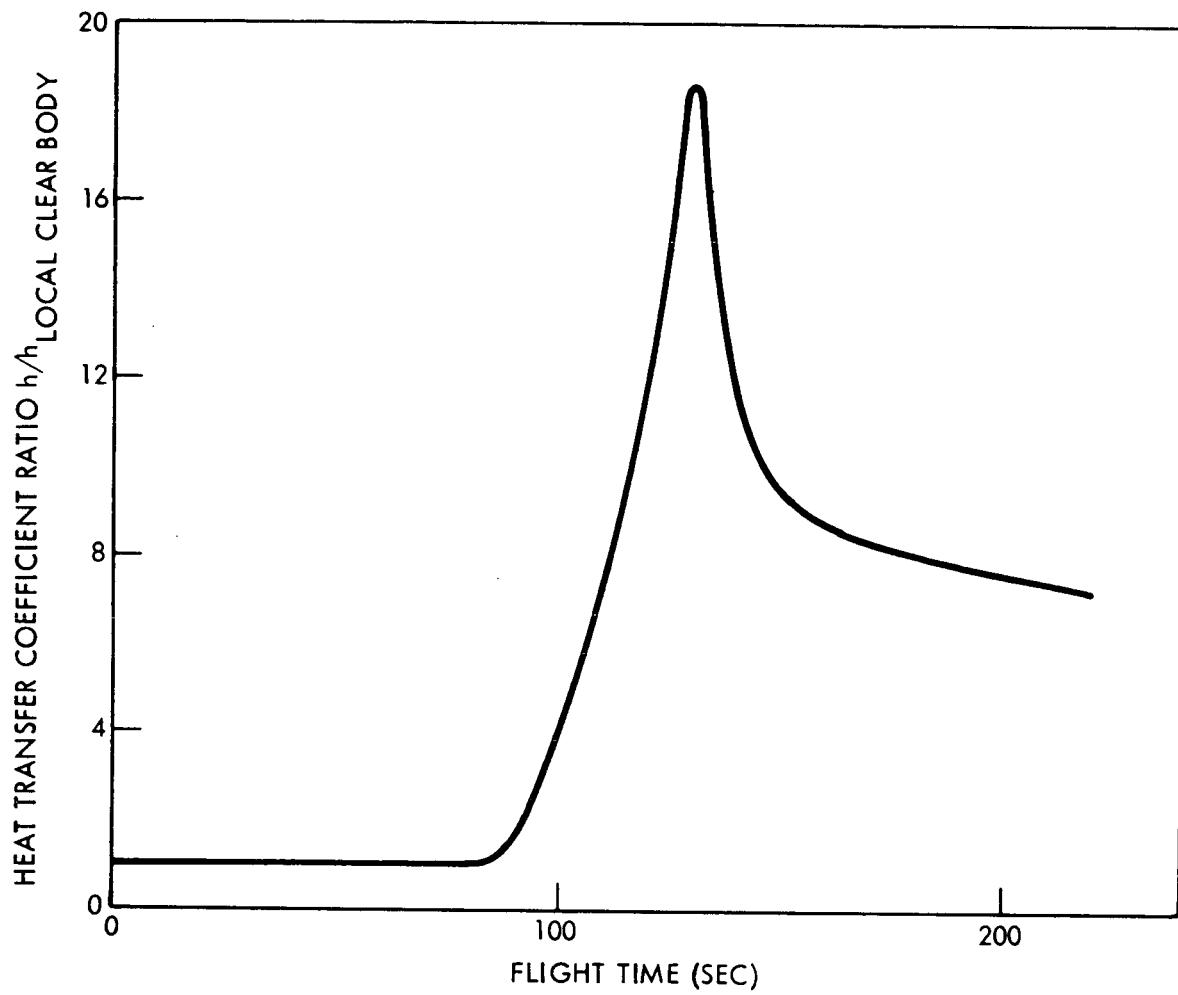


Figure 5-156. Aerodynamic Heating Factor for Area Around
Mated Attachment Strut



SPACE STATION SECOND STAGE AND TRAJECTORY

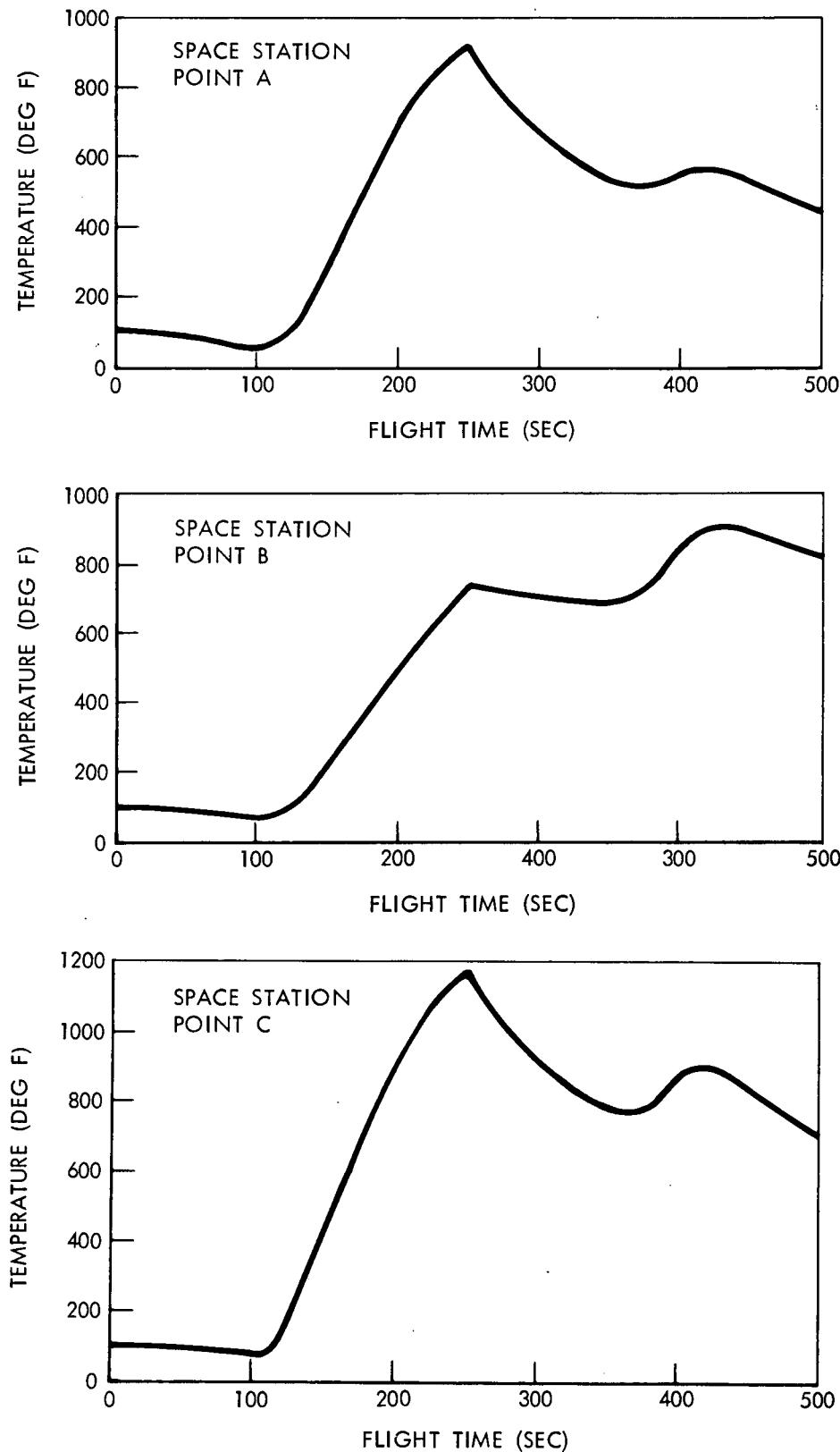


Figure 5-157. Booster Upper Surface Skin Temperature (Sheet 1 of 3)



RNS SECOND STAGE AND TRAJECTORY

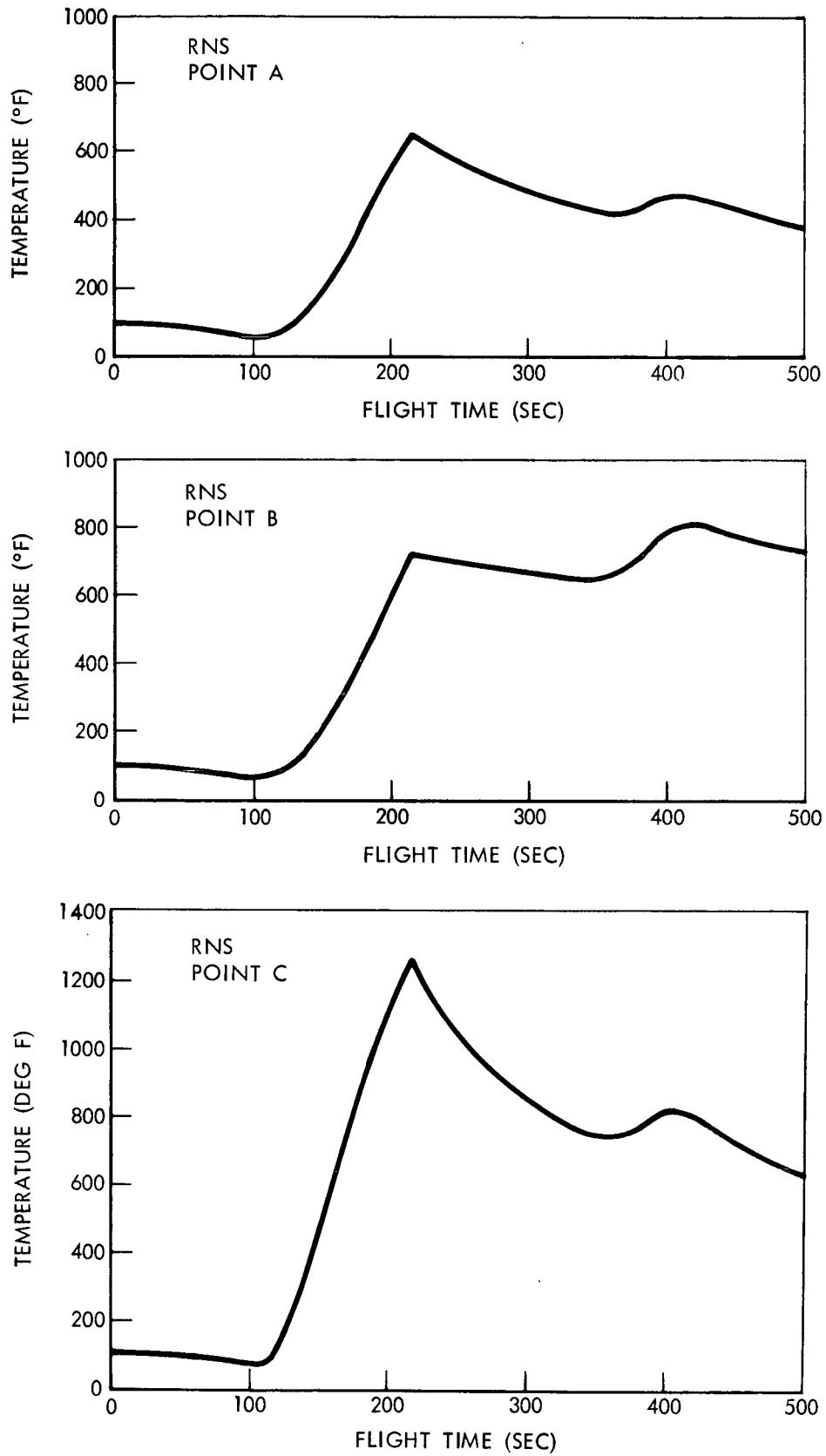


Figure 5-157. Booster Upper Surface Skin Temperature (Sheet 2 of 3)



SPACE TUG SECOND STAGE AND TRAJECTORY

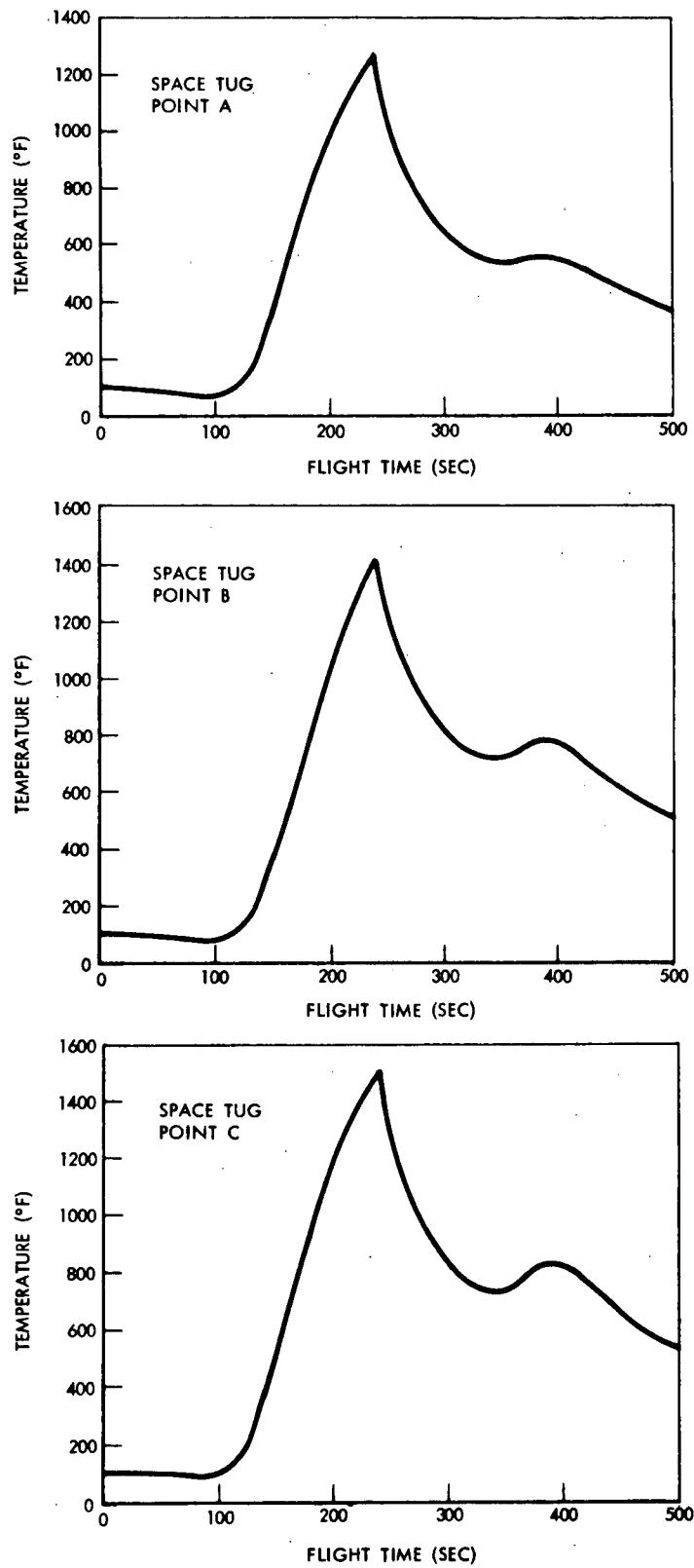


Figure 5-157. Booster Upper Surface Skin Temperature (Sheet 3 of 3)



Table 5-10. Heat Transfer Factors

	POINT A		POINT B		POINT C		POINT D		POINT E	
SECOND STAGE	VIEW FACTOR TO SPACE	HEATING FACTOR								
ORBITER	0.55	1.0	0.10	0.5	0.083	0.16 X •	0.02	0.008	0.02	0.008 X FIG. 4
NUCLEAR STAGE	0.54	0.5	0.10	0.5	0.10	0.16 X •	0.10	0.008	0.10	0.008 X FIG. 4
SPACE STATION	0.60	1.0	0.10	0.5	0.10	0.16 X •	0.10	0.008	0.10	0.008 X FIG. 4
SPACE TUG	0.87	1.0	0.55	1.0	0.35	0.16 X •	0.10	0.008	0.10	0.008 X FIG. 4

• h/h Local Clear Body

The preceding data was derived using the following references:

1. "SSV Launch Phase Testing in the NASA/Ames Research Center 3.5-Ft Hypersonic Wind Tunnel, Test 107." (to be published).
2. "SSV Launch Phase Testing in the NASA/Langley Research Center Unitary Plan Wind Tunnel, Test 945." (to be published).
3. N. Cohen and E. Reshoto. "Similar Solutions for Compressible Boundary Layer With Heat Transfer and Pressure Gradient." NACA TN-3325 (February 1955)
4. R. Michel. "Aérodynamique — Couches limites, Frottement et Transport de Chaleur." Ecole Nationale Supérieure de l'Aéronautique (1967)

Orbital Heating. An orbital heating analysis has been conducted to aid in the selection of the initial orbit altitude for the ESS vehicle. Convective and radiative heat transfer to the protuberances and side wall of the ESS were computed at orbital velocities and altitudes. Stagnation point theory was used to represent protuberance heating and flat plate theory to represent side wall heating. Radiative heat transfer was estimated and found to be negligible when compared to the convective heating. The results of this



Table 5-11. Peak Temperatures on Booster
Top Surface During Ascent

SECOND STAGE	TRAJECTORY	PEAK TEMPERATURE DURING ASCENT (DEG. F)		
		POINT A	POINT B	POINT C
ORBITER	B9U-1	1770	1780	2250
	ESS (3-2-71)	1870	2120	-
	ESS (2-15-71)	-	2380	-
	LOW Q	-	730	-
NUCLEAR STAGE	ESS (3-2-71)	1500	2140	2290
	ESS (2-15-71)	-	2380	-
	LOW Q	-	730	-
SPACE STATION	ESS (3-2-71)	1830	2140	2290
	ESS (2-15-71)	-	2380	-
	LOW Q	-	730	-
SPACE TUG	ESS (3-2-71)	1650	1870	1940



analysis are presented in Figure 5-158. When the calculated values of convective heating exceed the limiting free-molecular-flow heat transfer rate values, the free-molecular-flow values were used. Stagnation point and stagnation line heating, to a one-foot sphere and cylinder, respectively, is shown, as well as heating to a thirty-three-foot-diameter cylinder. This illustrates the impact of varying radii on stagnation heating. Similarly, heating to the 10-foot and 100-foot-long flat plates, which shows the effect of running length on side wall heating, are presented. Below 66 nautical miles, as indicated in Figure 5-158, the heat transfer rates increase rapidly. Therefore, an initial orbital altitude of 66 nautical miles has been selected for the ESS vehicle.

ESS Base Region Heating. Figure 5-159 shows the ESS base region configuration analyzed. The base region was assumed to be closed out by a rigid heat shield at station 41.0, except in the vicinity of the space shuttle orbiter engines where flexible curtains are attached to allow engine gimbaling.

Exhaust plume properties used in the analysis were computed by means of a method of characteristics computer program. Figures 5-160 and 5-161 show the exhaust plume iso-Mach lines for the nozzle retracted and extended respectively. The plumes correspond to the following conditions:

MR	= 6.05
Chamber Pressure	= 3000 psia
Chamber temperature	= 6520 R
Altitude	= 250,000 ft

Reverse flow gas recovery temperature was determined by extrapolating hot flow test results where nozzle Reynolds number effects on reverse flow gas recovery temperature were studied. For the space station orbiter engine nozzle extended case, the gas recovery temperature was found to be 4300 R. A small reduction is expected for the nozzle retracted position, but it was neglected in the present analysis.

The base region reverse flow field was established by means of methods based on heating rate data on the 1/10 scale GD/A Centaur two-engine model in conjunction with estimates of the reverse mass flow rates from the plume impingement regions. The heating rates to various base region components were then computed using stagnation region heating rates to various base region components were then computed using stagnation region heating rate equations.

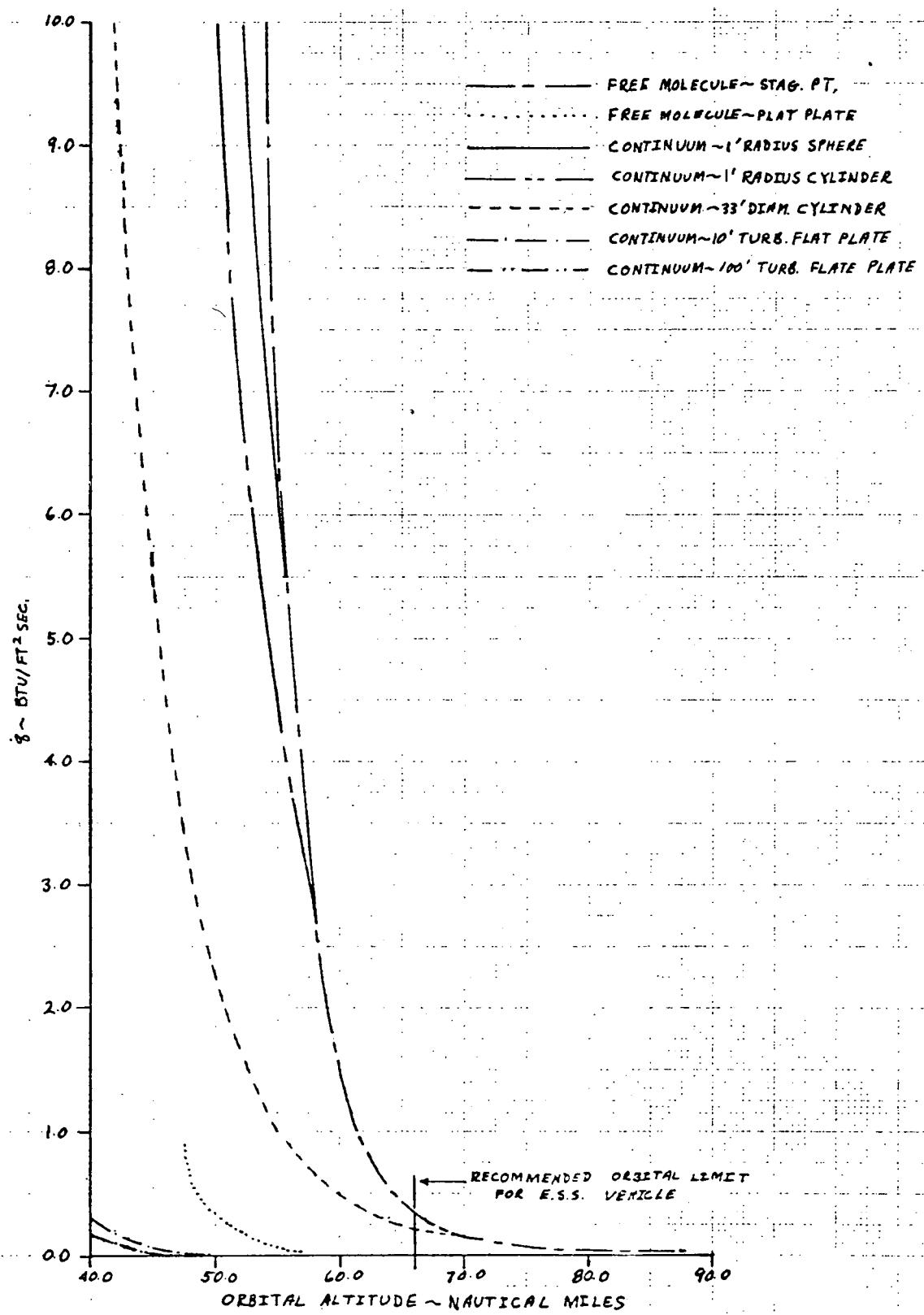


Figure 5-158. Orbital Heat Transfer

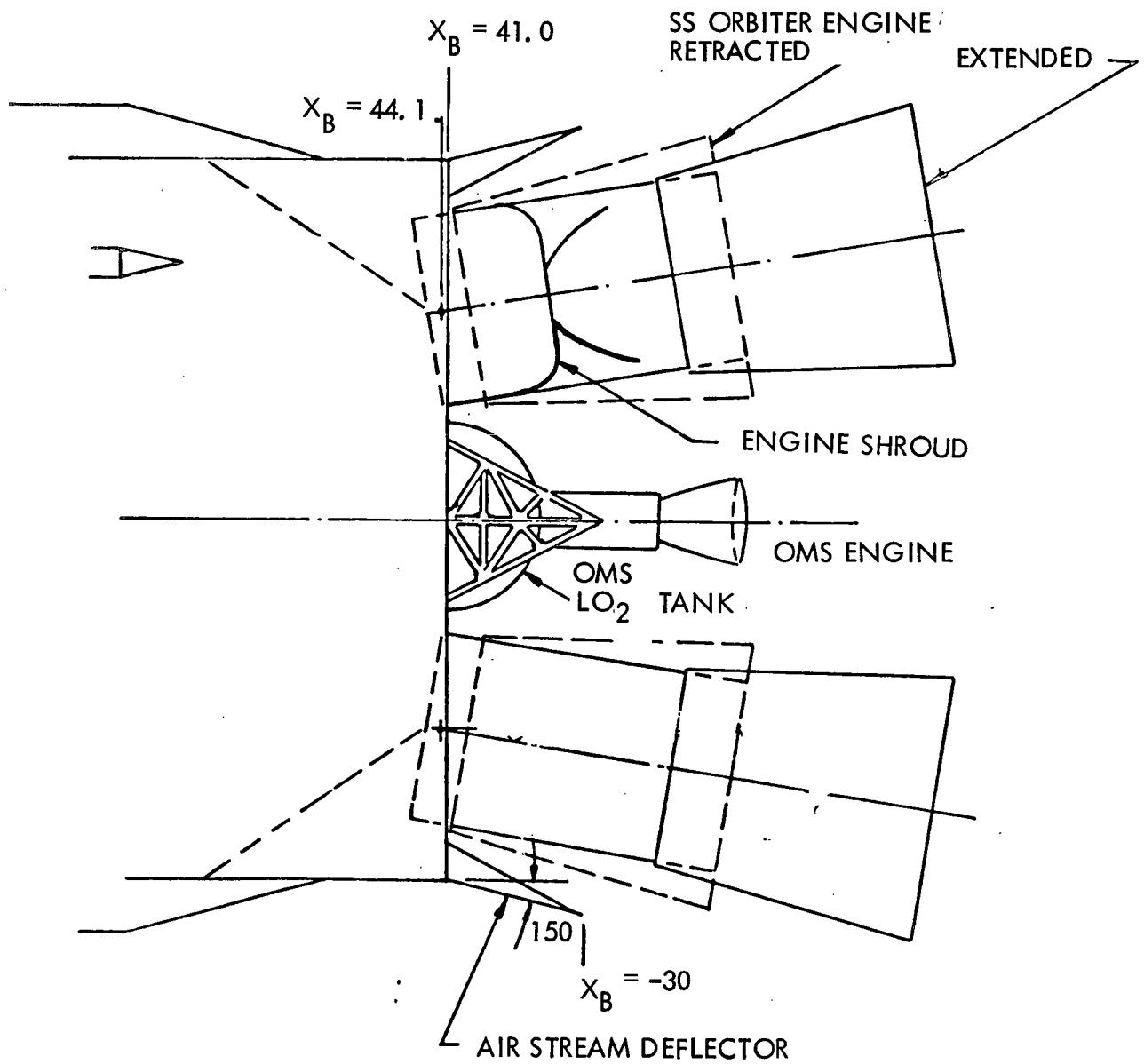


Figure 5-159. ESS Base Region Geometry

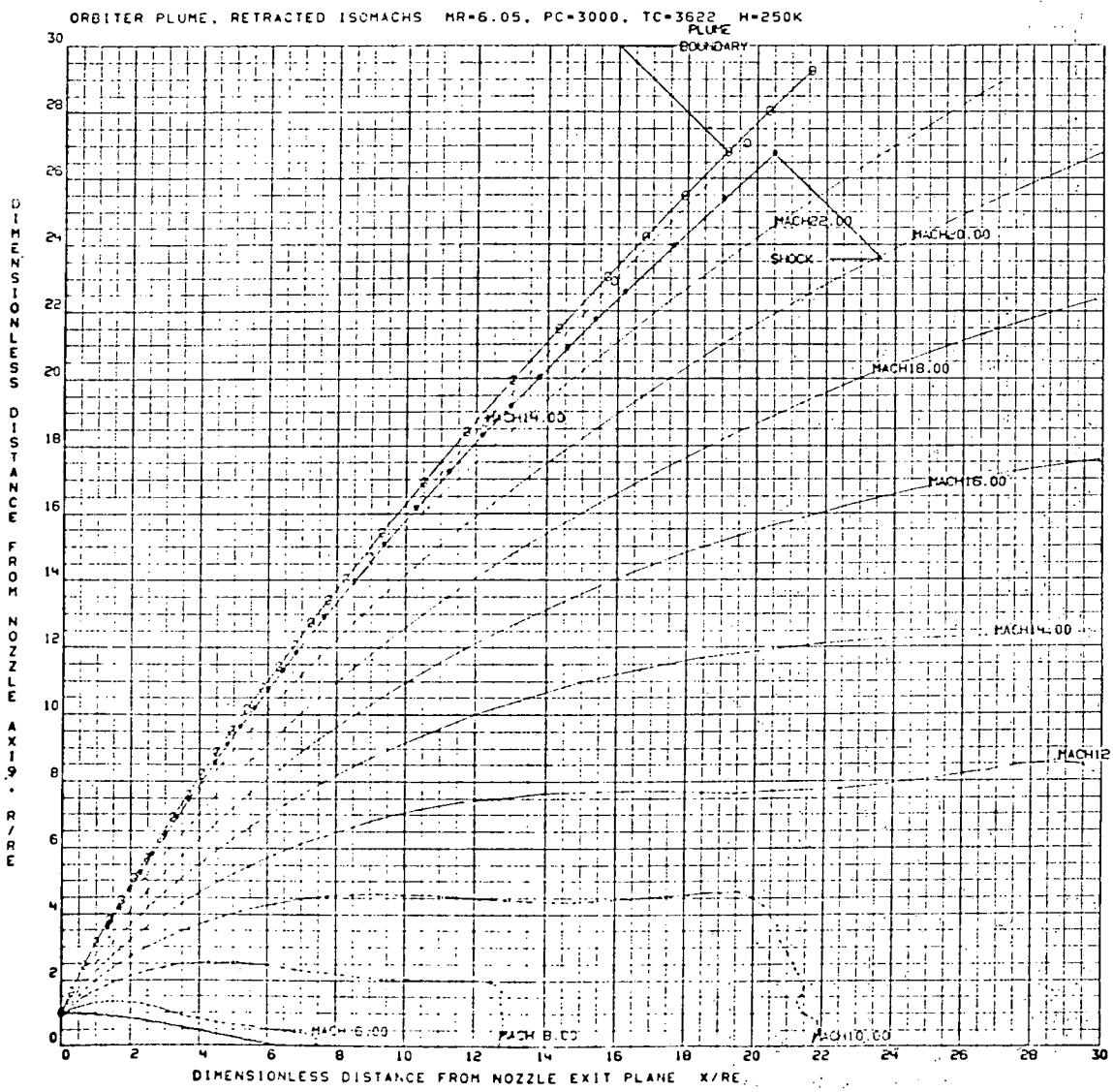


Figure 5-160. Isomach Times for Nozzle Retracted



ORBITER PLUME ISOMACHS MR=6.05, PC=3000, T=3622 H=250K

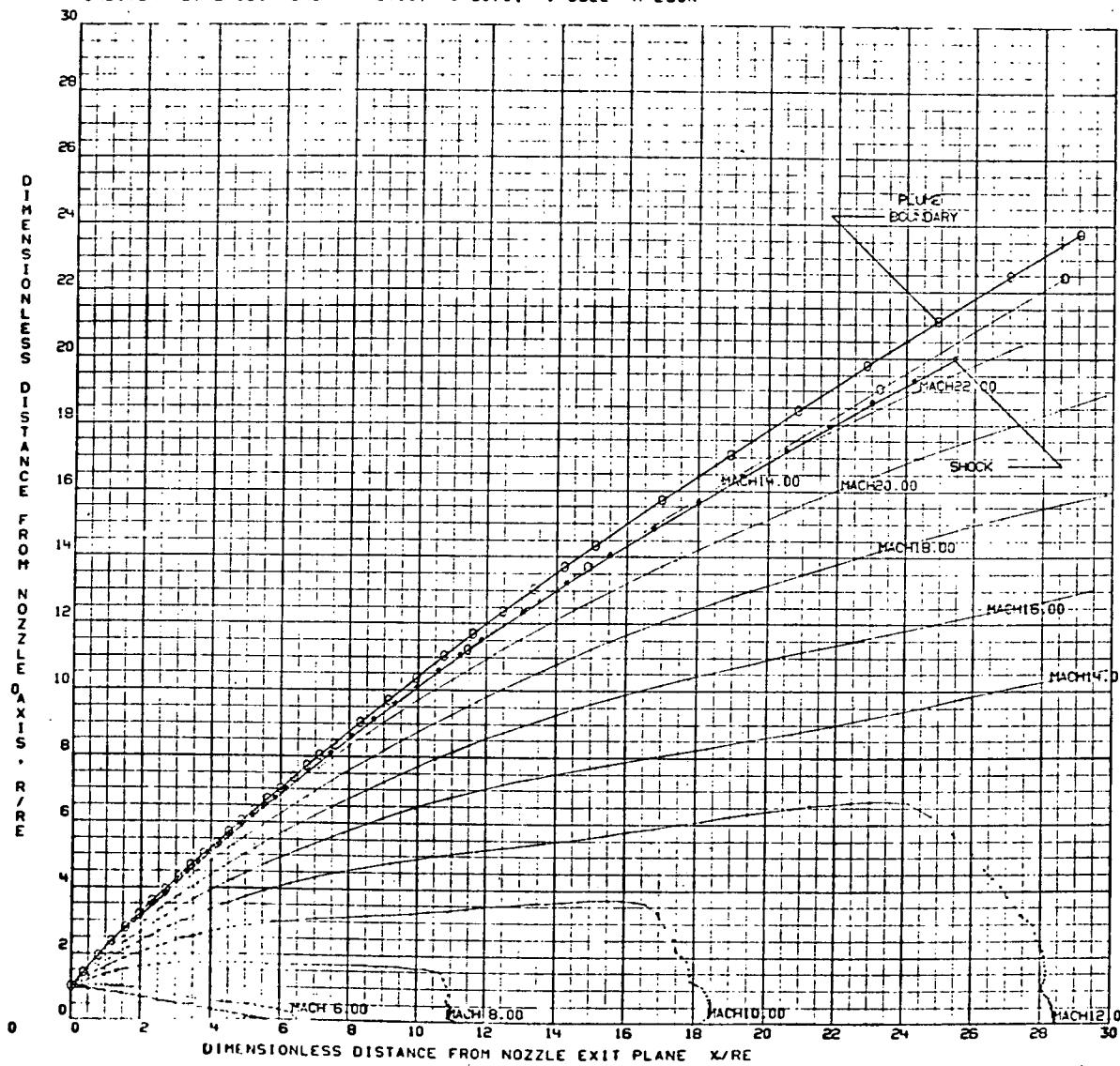


Figure 5-161. Isomach Times for Nozzle Extended



Figure 5-162 presents the heating rates to the APS LO₂ tank for both orbiter engines extended and retracted. It is seen that the heating rates are approximately doubled for the engine-retracted case compared with the corresponding values when the engines are extended. The heating rate analysis was carried out for the condition where the orbiter engines are trailing, since this condition is expected to produce the maximum heat rates. Figure 5-163 shows the rigid base heat shield convective-heating rate variation with radial distance from the center and Figure 5-164 shows the convective heating rate to the orbiter engines shroud for the nozzle-extended case. With the nozzle retracted, the heating rates for the engine shroud will be considerably lower than the corresponding nozzle-extended values; therefore, the latter establish the design thermal environment for the engine shroud. Figure 5-165 shows typical stagnation line heating rate values for the OMS engine support structure cylindrical members. These heating rates were computed by assuming spherical expansion from the impingement region origin to ambient pressure and using yawed cylinder relationships to compute the heat flux.

The variation of incident radiative heat flux to an aft facing surface located along the vehicle axis is presented in Figure 5-166 for both the retracted- and extended-nozzle positions.

The incident radiative heat flux values were obtained by means of the computer program using the appropriate exhaust plume and interaction region properties.

The results are approximate, since the radiation program used does not describe correctly the engine spacing or base region geometry.

Figure 5-166 shows that the incident radiative heat flux with the nozzle retracted is an order of magnitude higher than the corresponding nozzle extended values.

ESS/ACPS Plume Impingement Pressures and Heating Rates. A layout of the proposed ESS/ACPS engine locations is shown in Figure 5-167. It is seen that there are three typical engine installations with respect to plume impingement pressure and heating rates analysis, i.e., station 30, station 386, and any one of the yaw engines at stations 67, 77, 87 and 97. The boundary region of the station 107 pitch engine plume will most probably impinge on the LH₂ feed line and the ACPS yaw engines. However, since the impinging portions of the plume are highly expanded, the resulting impingement pressures and heating rates will be very low, and therefore have not been analyzed.

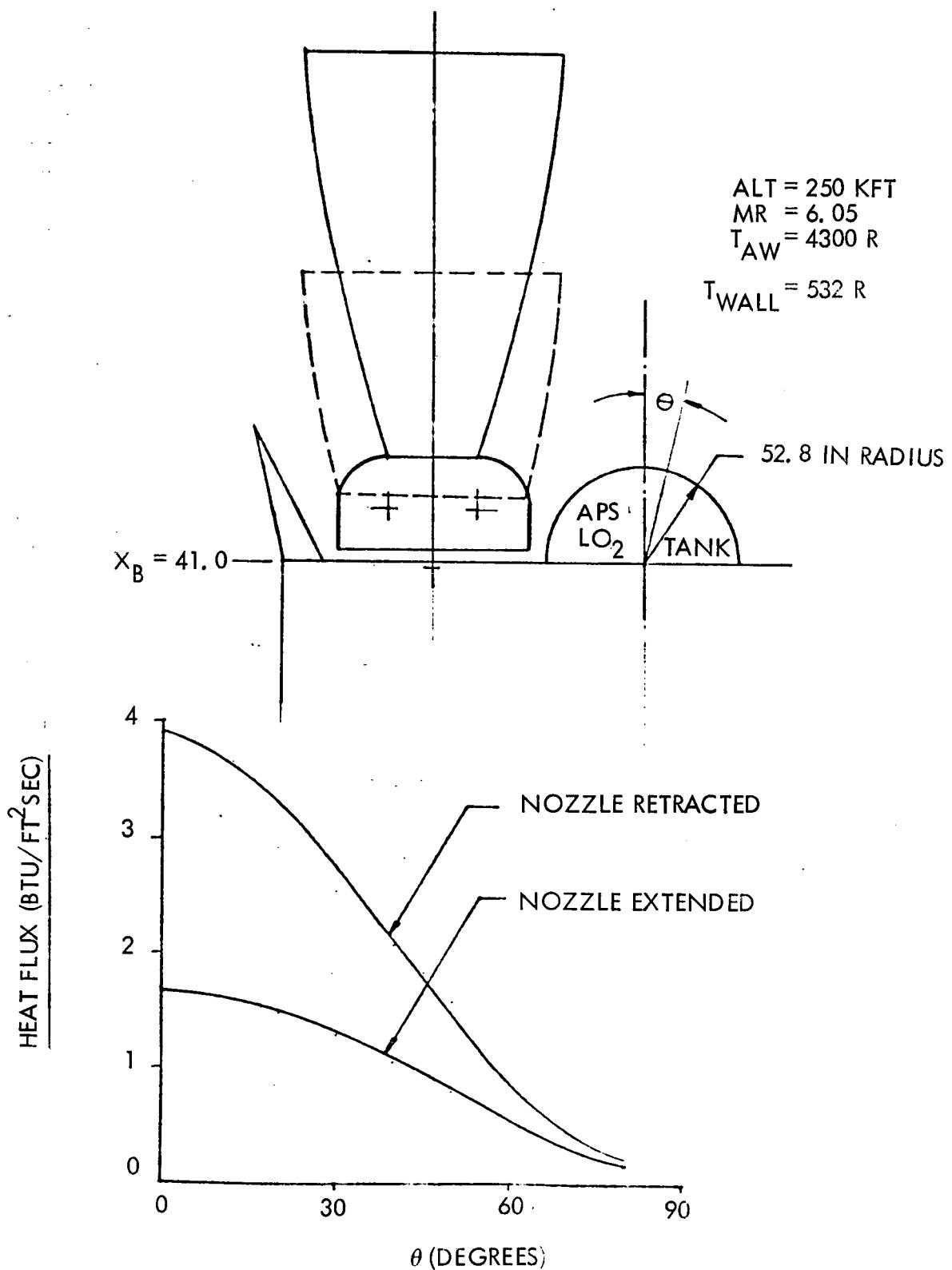


Figure 5-162. ESS Base Region Convective Heating Rates, APS LO₂ Tank

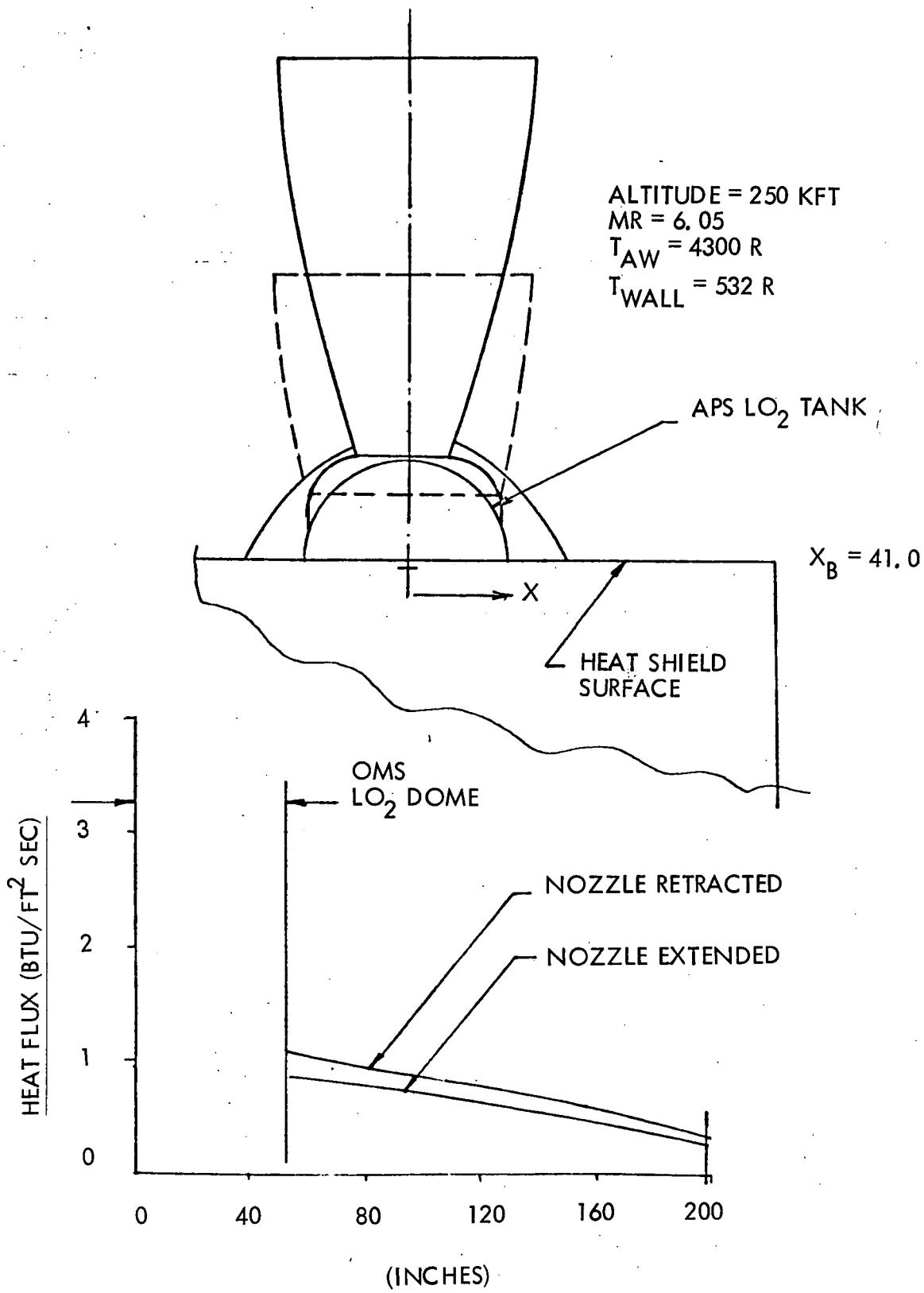


Figure 5-163. ESS Base Region Convective Heating Rates, Base Heat Shield

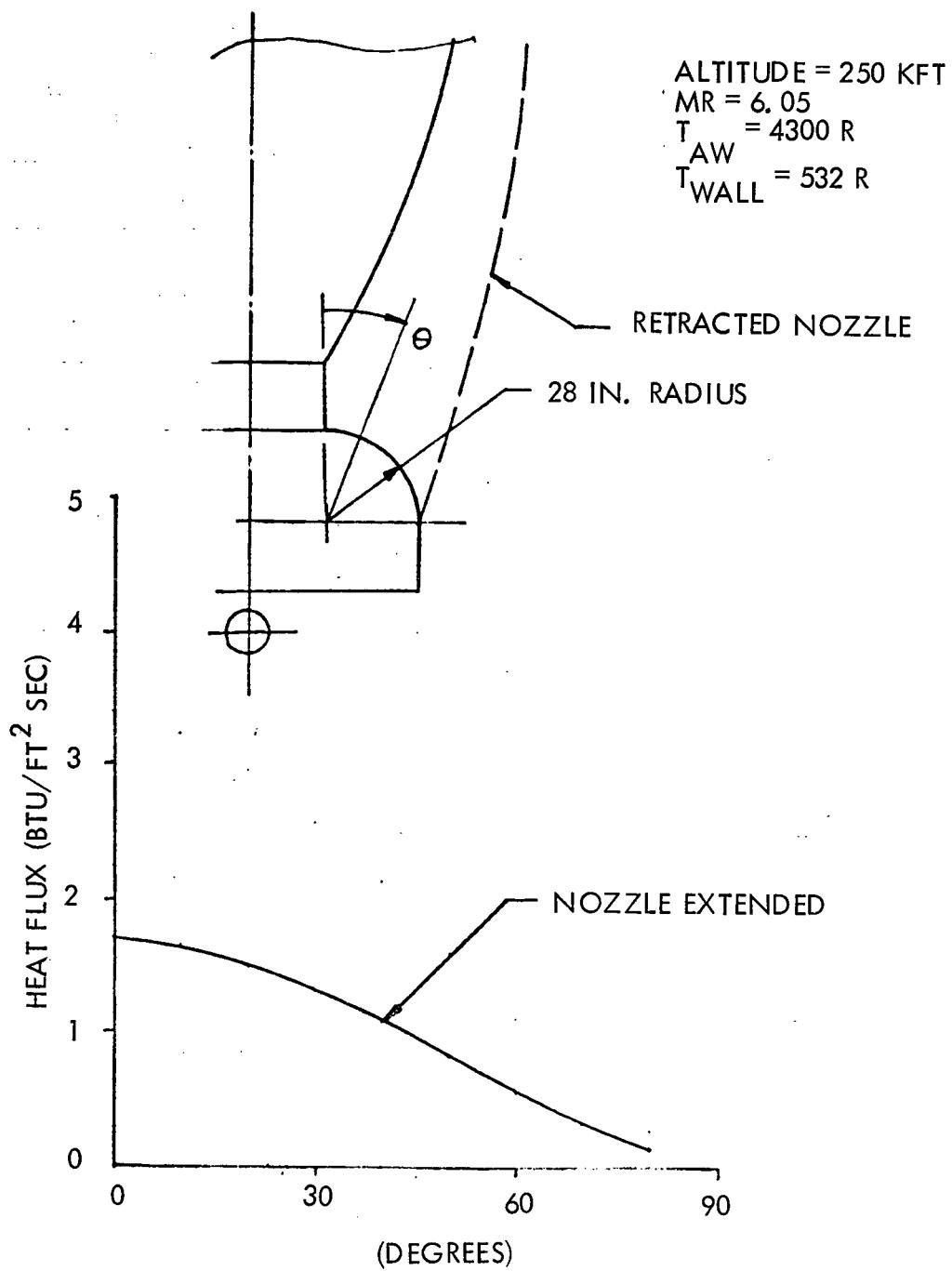
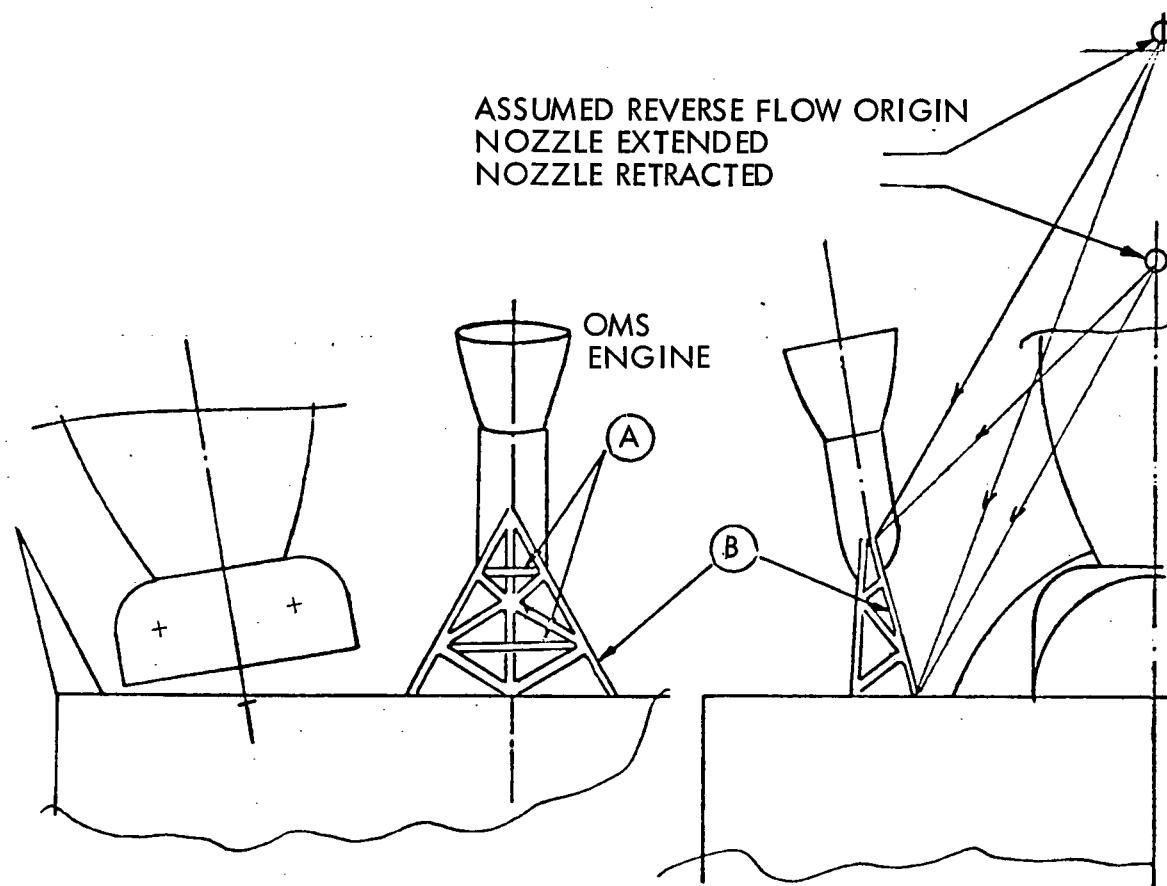


Figure 5-164. ESS Base Region Convective Heating Rates, Shuttle Orbiter Engine Shroud



OMS ENGINE SUPPORT STRUCTURE COMPONENT	STAGNATION LINE HEATING RATES [*] (BTU/FT ² SEC)	
	NOZZLE RETRACTED,	NOZZLE EXTENDED
A	5.4	4.8
B	2.6 + 3.5	1.8 + 2.2

$$T_{AW} = 4300 \text{ R}$$

$$T_W = 532 \text{ R}$$

$$ALT = 250 \text{ KFT}$$

$$MR = 6.05$$

$$P_C = 3000 \text{ PSIA}$$

$$T_C = 6520.0 \text{ R}$$

*TO 6-INCH-DIAMETER CYLINDER

Figure 5-165. ESS Base Region Convective Heating Rates,
OMS Engine Support Structure

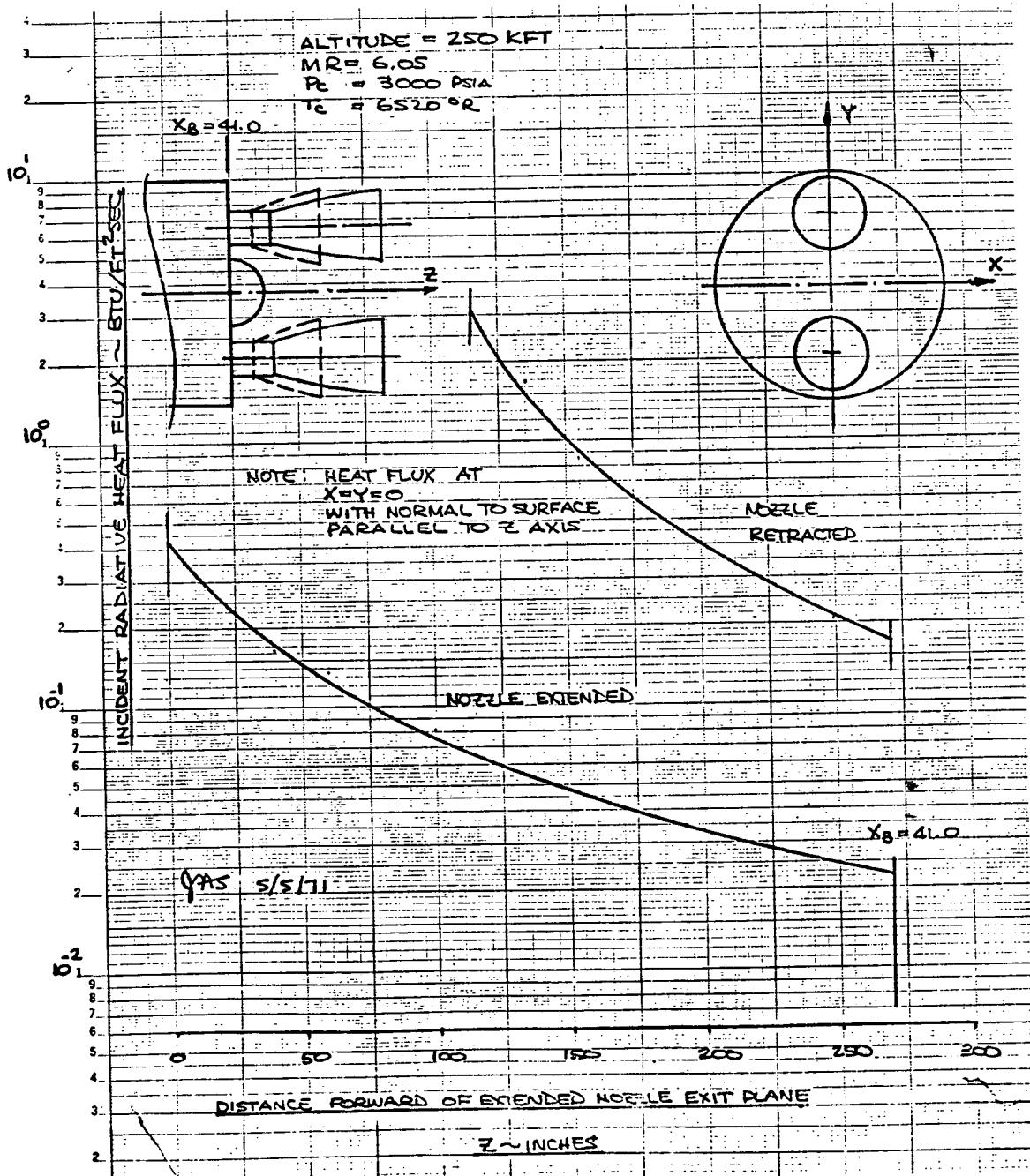


Figure 5-166. ESS Base Region Radiative Heat Rates

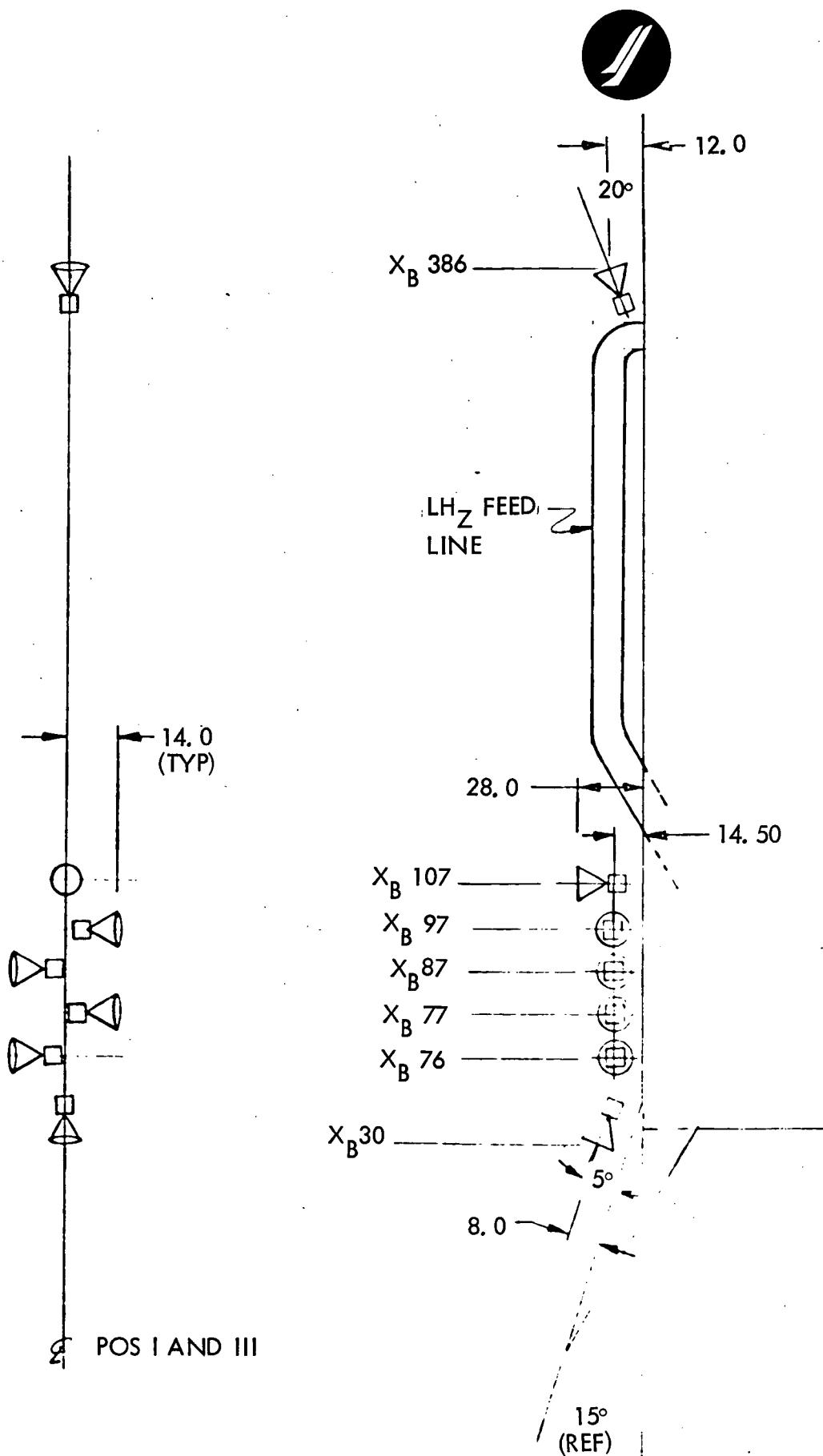


Figure 5-167. ACPS/ESS Schematic



Figure 5-168 shows the ESS/ACPS engine iso-Mach lines which were obtained by means of the method-of-characteristics computer program. The ACPS engine has the following characteristics:

Area ratio = 20

Nozzle exit diameter = 10.07 in.

Nozzle lip angle = 11.5°

Mixture ratio = $4.0 (\text{GO}_2/\text{GH}_2)$

Chamber pressure = 300 psia

Chamber temperature = 5500°R

ACPS engine plume impingement pressure is shown in Figures 5-169 through 5-171. These pressures were computed from the local undisturbed plume properties using oblique shock relationships. In the vicinity of the nozzle exit plane, the flow angles are too large for attached oblique shock to exist; therefore, in this region, the impingement properties were computed by means of nominal shock equations.

Impingement convective heating rates were computed using laminar and turbulent heat transfer relationships for flow with varying external flow properties. Figures 5-172 through 5-174 present the resulting convective heating rates to the ESS. The heating rates to the cylindrical ESS surface, due to the roll engine plume impingement, Figure 5-175, have been computed neglecting the relief effect of the cylindrical surface; therefore, the far region heating rates are slightly too high.

In all cases, the heating rates computed are to a smooth surface; i.e., the effect of the longitudinal stringers or the convective heating rates have not been accounted for. Therefore, local heating rates could be appreciably higher.

Booster Entry and Flyback Heating. Three points on the booster fuselage lower surface centerline and one point on the wing leading edge were also evaluated for the aerodynamic heating effect of the three ESS trajectories. Figure 5-175 shows the maximum temperatures at these four points for each ESS trajectory along with the corresponding baseline T-B9U-1 trajectory temperatures. At these four points, the maximum aerodynamic heating occurs during the entry portion of the flight. For the three ESS trajectories the booster temperatures are less than the corresponding baseline booster temperatures.



MR = 4.0, P_C = 300 PSIA, T_C = 5500°R, $\gamma = 1.290B$

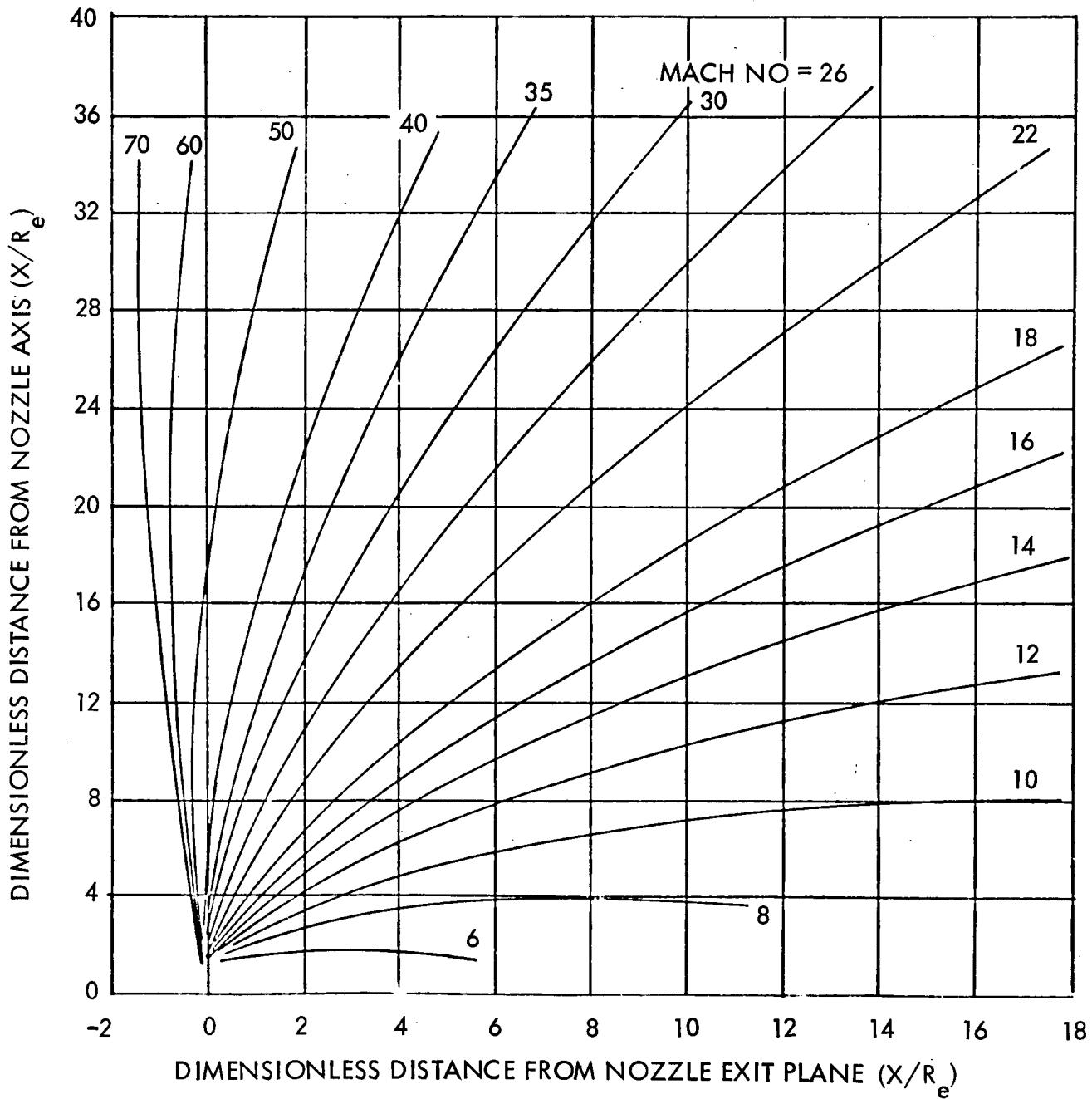


Figure 5-168. ESS/ACPS Engine Exhaust Plume Isomachs



ALT = SPACE
MR = 4.0
 P_C = 300 PSIA
 T_C = 5500 R
 γ = 1.290B

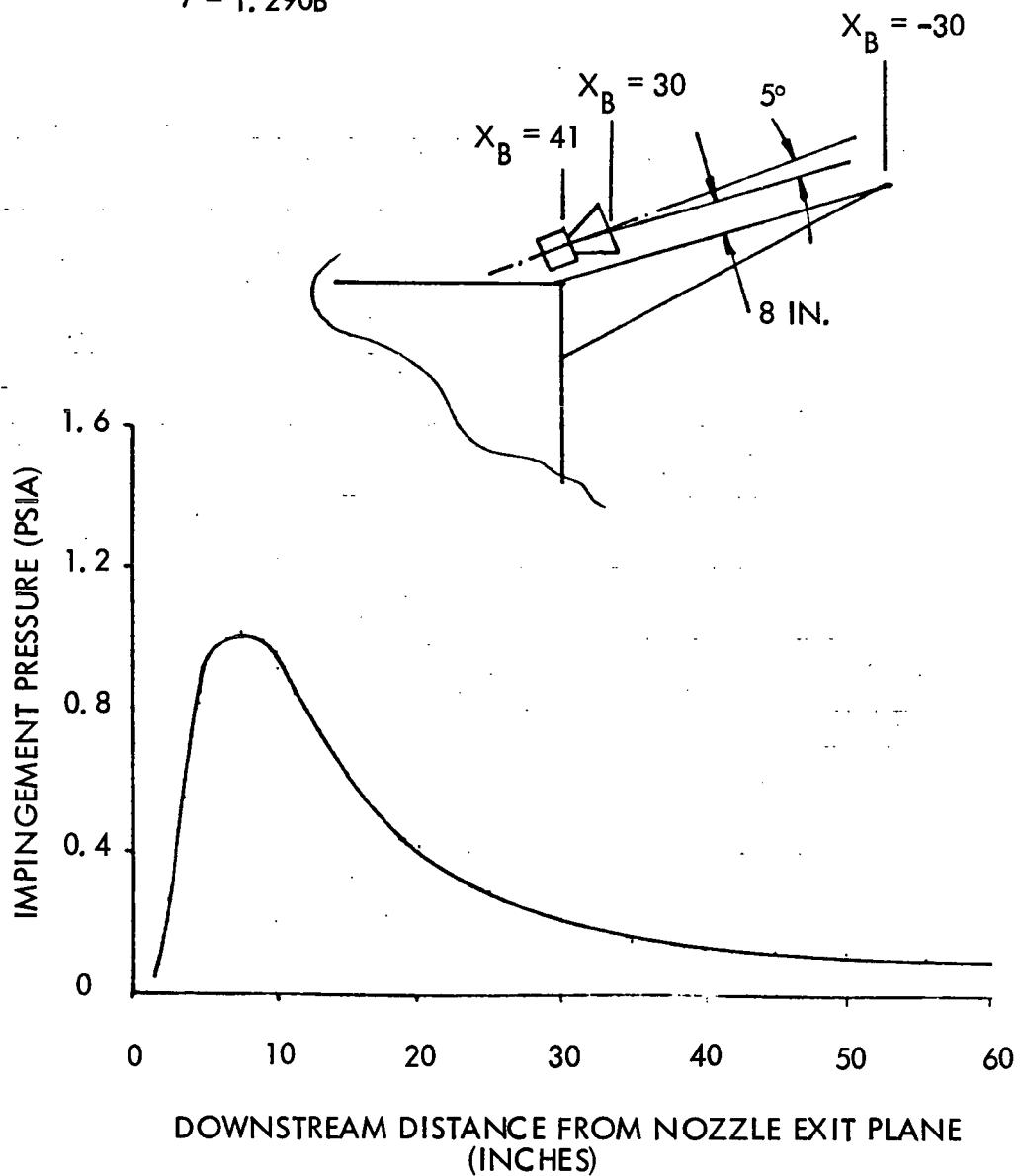


Figure 5-169. ACPS Plume Impingement Pressures,
Air Stream Deflector

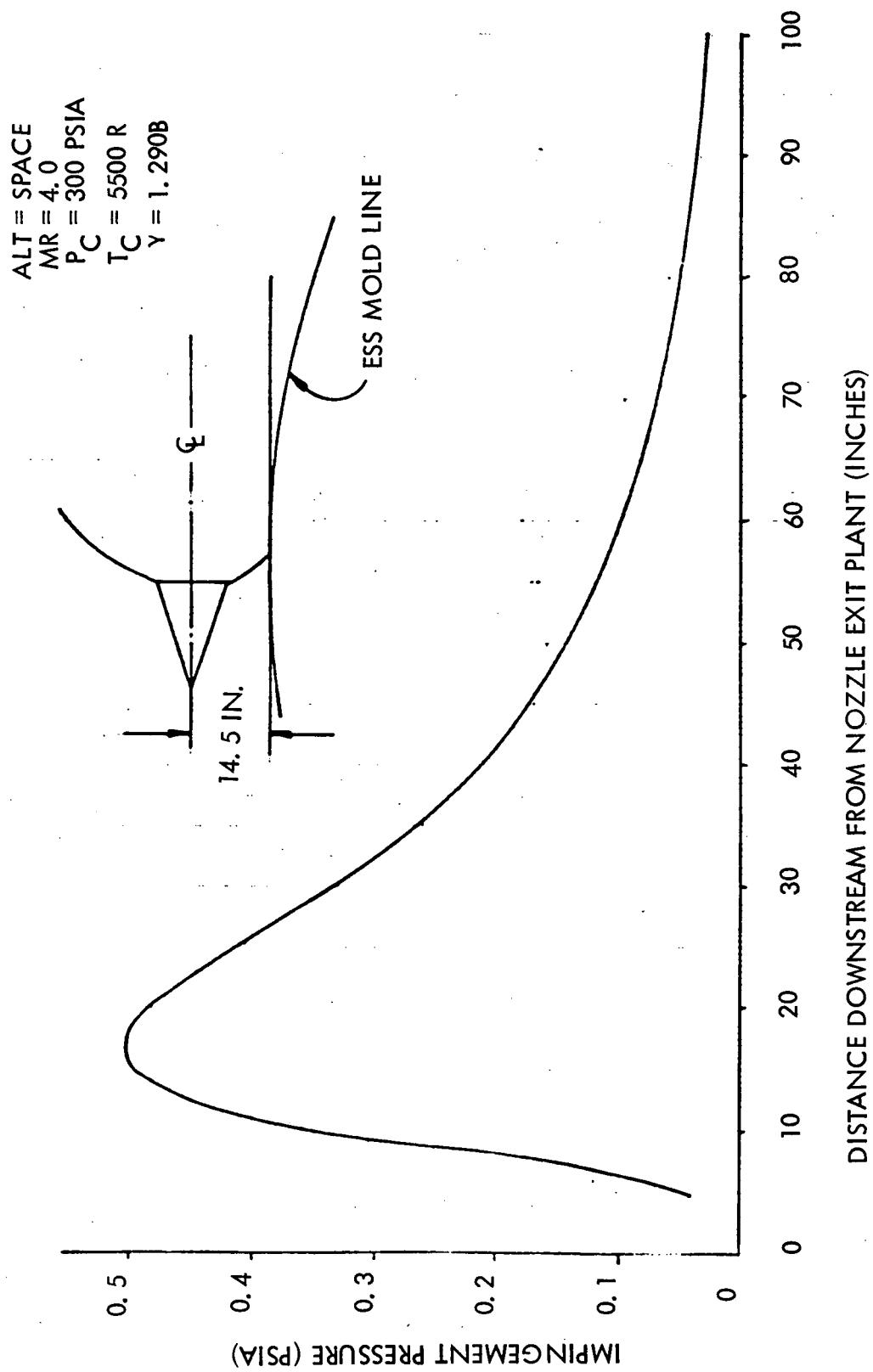


Figure 5-170. ACPS Plume Impingement Pressures, Roll Engine / ESS Surface

$ALT = \text{SPACE}$
 $MQ = 4.0$
 $P_c = 300 \text{ PSIA}$
 $T_c = 5500 \text{ R}$
 $\gamma = 1.2908$

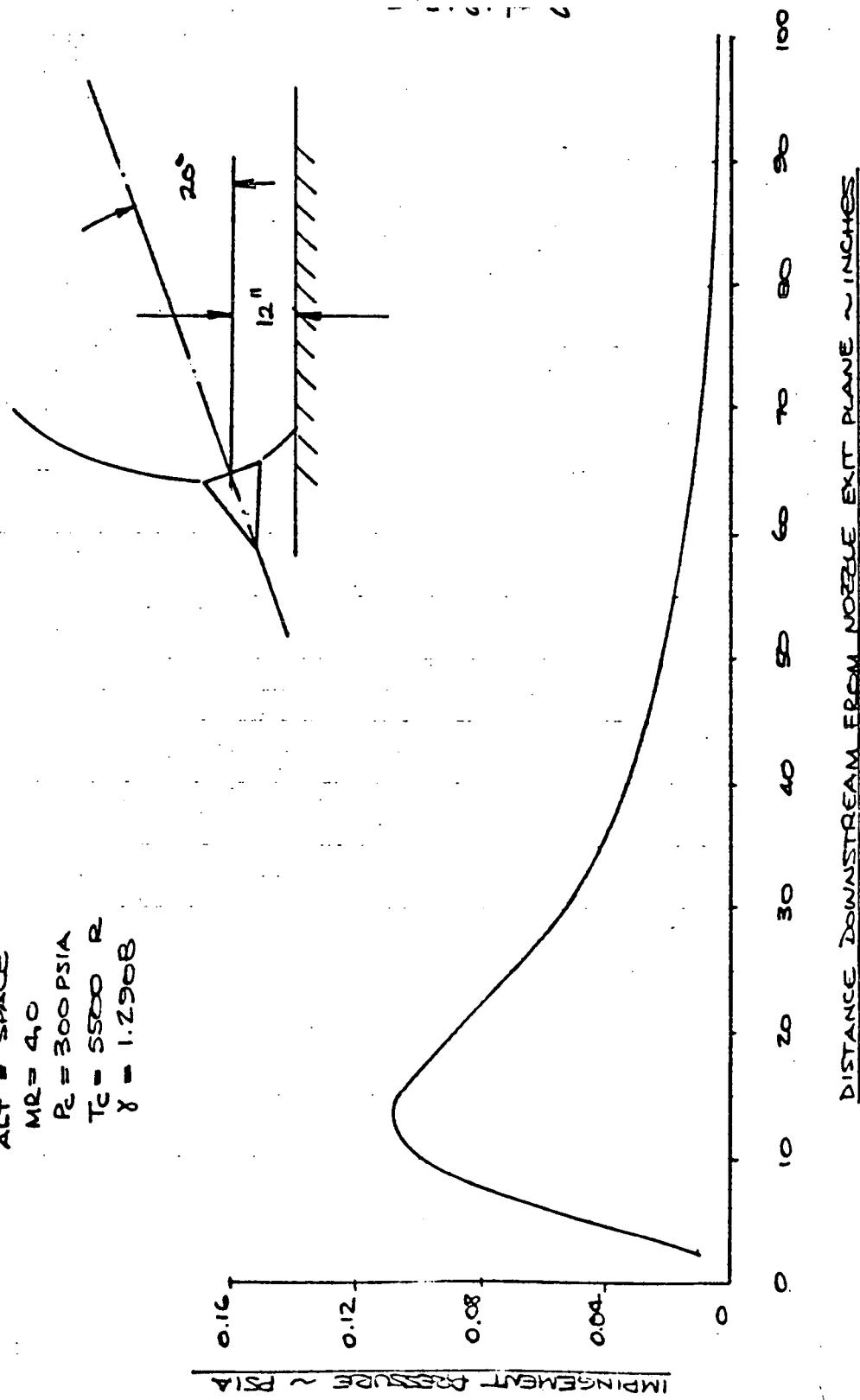


Figure 5-171. ACPS Plume Impingement Pressures to ESS Surface

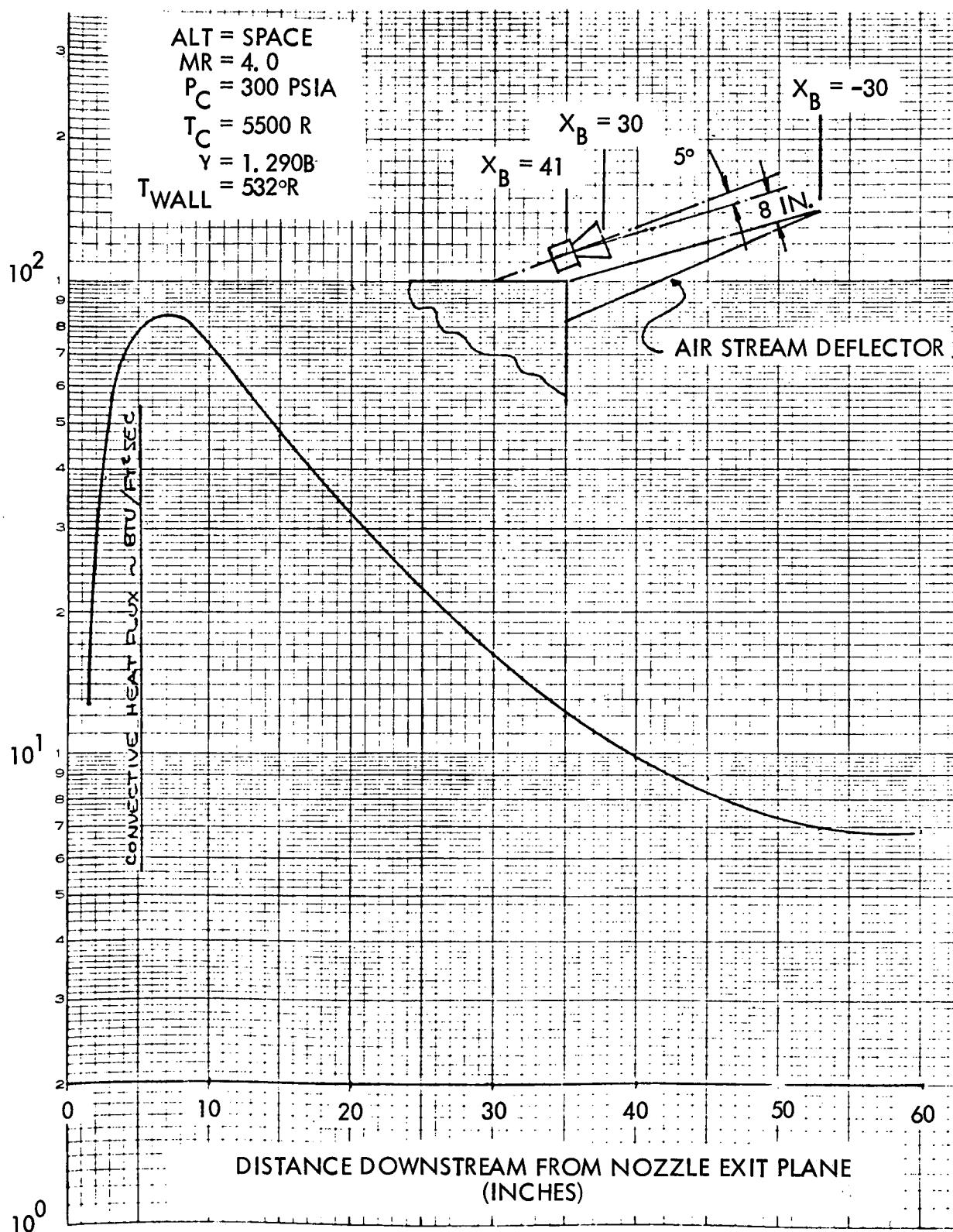


Figure 5-172. ACPS Plume Impingement Heating,
Air Stream Deflector

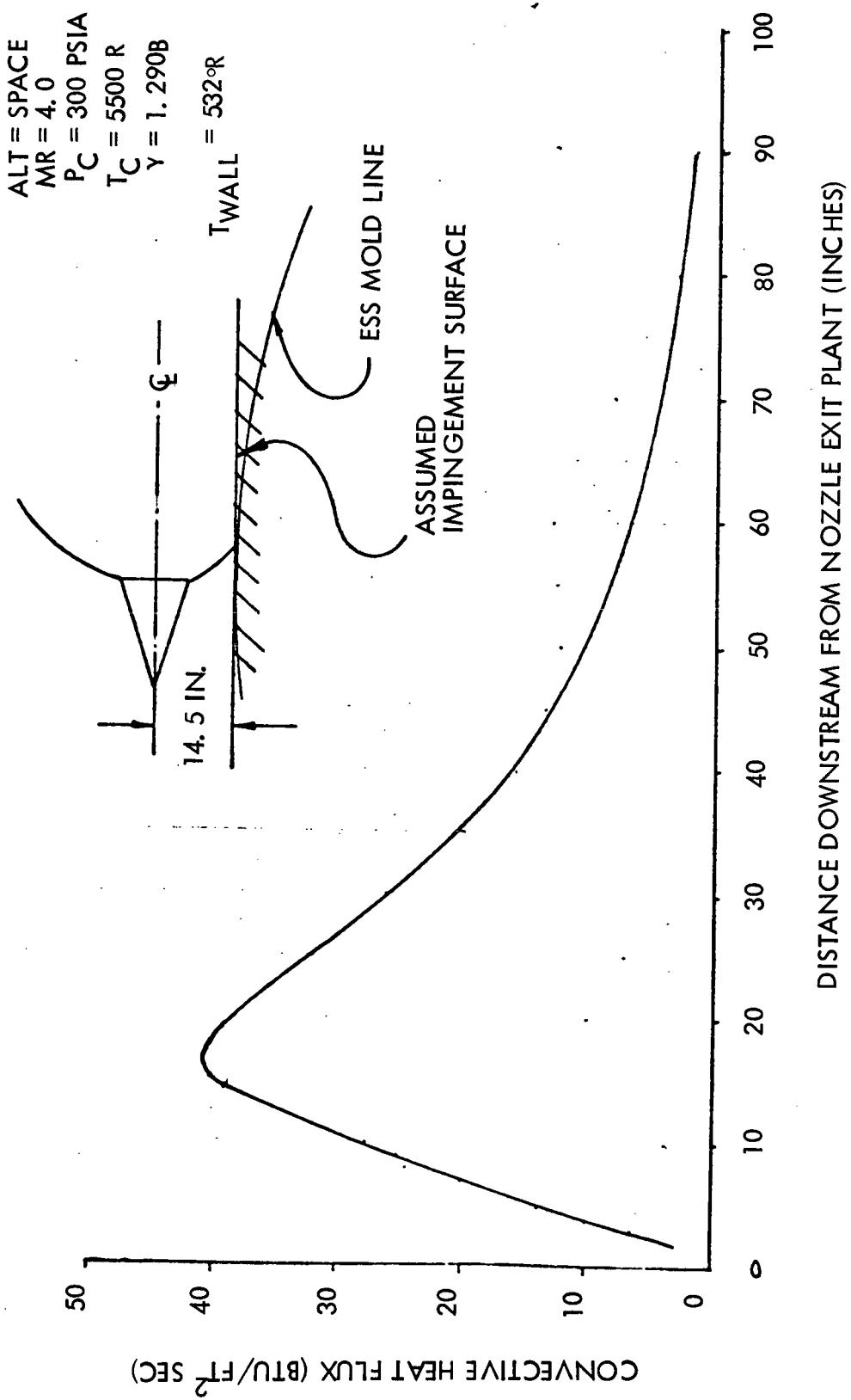


Figure 5-173. ACPS Plume Impingement Heating to ESS Surface

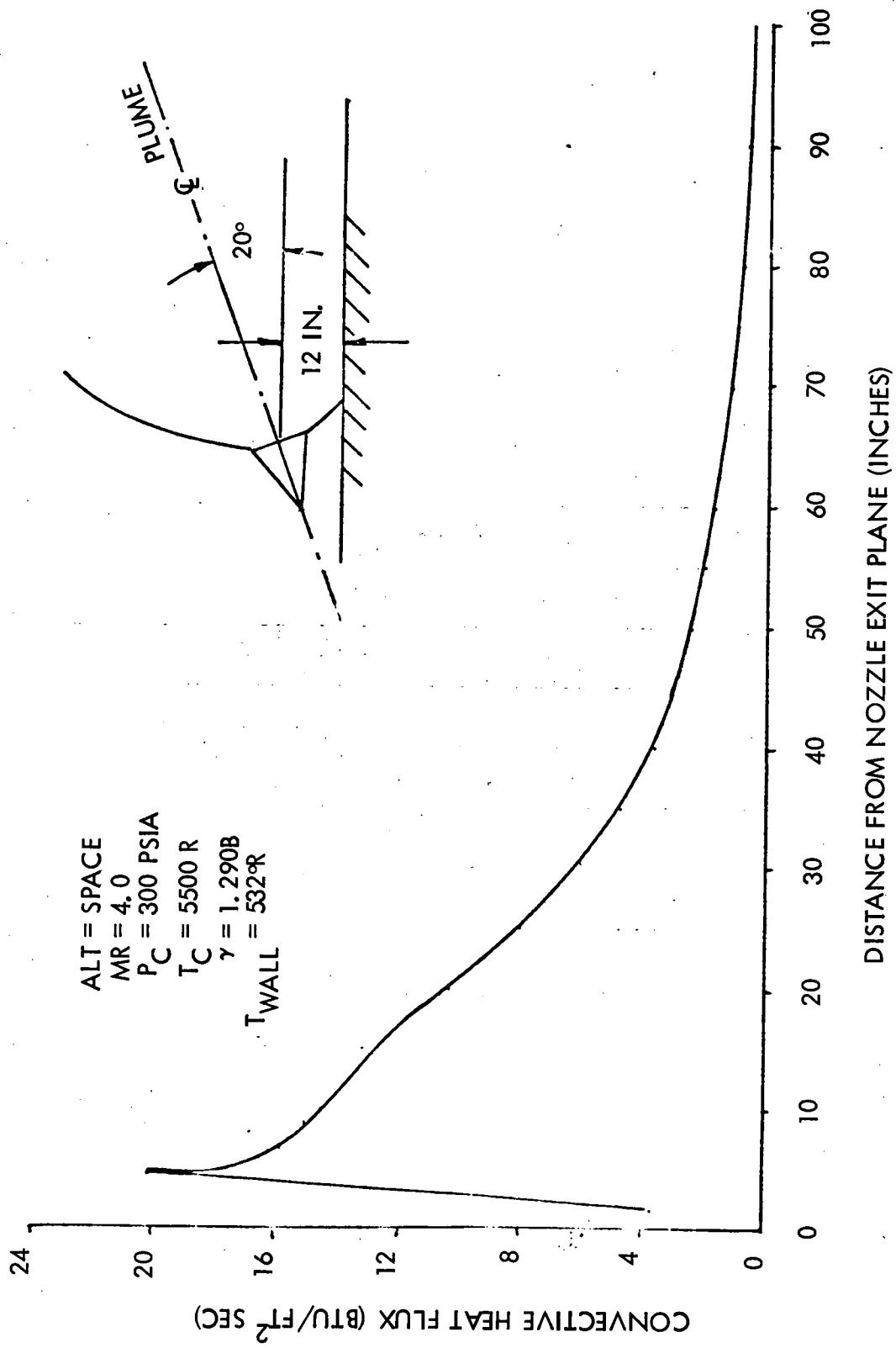


Figure 5-174. ACPS Plume Impingement Heating to ESS Surface

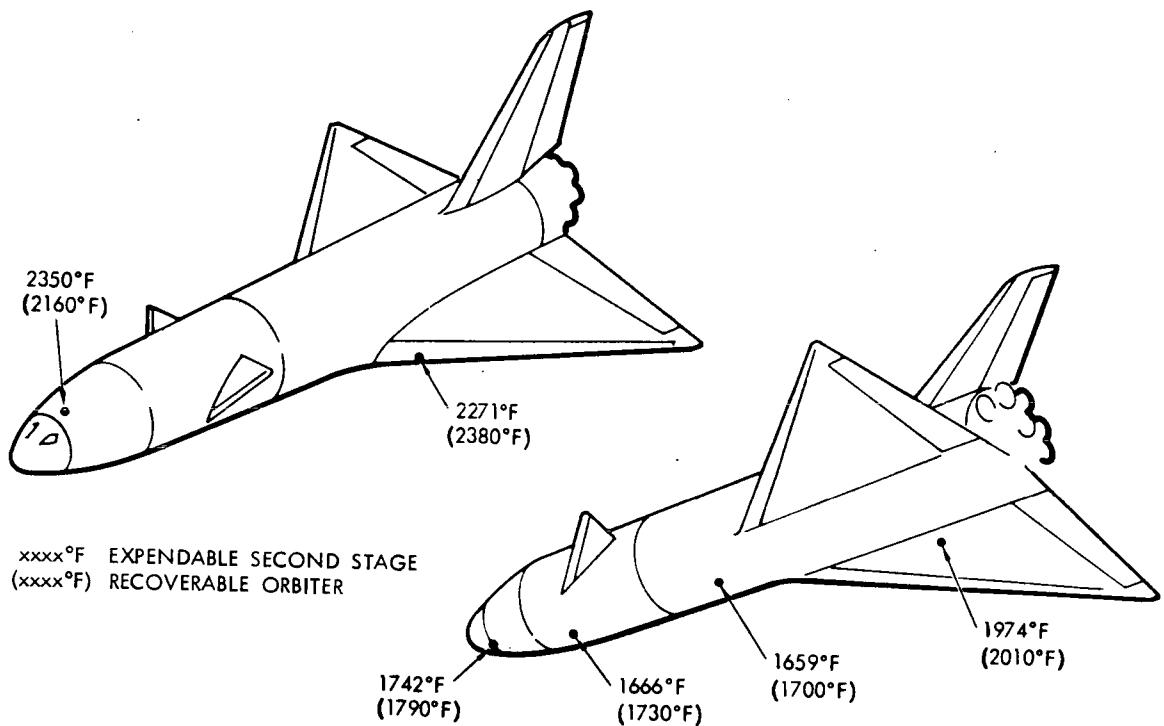


Figure 5-175. Booster Temperature When Used With the ESS



Acoustic Environment and Effects

Booster Environment. The data herein represent the latest, updated estimate of the booster acoustic environment through ascent. Noise sources include the rocket engines and various aerodynamic sources such as boundary layer turbulence, oscillating shocks, boundary layer shock interaction and separated flow. Transient effects due to staging or abort conditions are not included herein.

Acoustic estimates shown herein relate to Configuration B-9U which employs 12 rocket engines of 550,000 lb thrust each, for a total thrust of 6.6×10^6 lb. Figure 5-176 is a plot of overall sound pressure level (OASPL) at launch as a function of vehicle station, measured from the exit plane of the rocket nozzles. Figure 5-177 comprises a plot for various vehicle stations of 1/3 octave band sound pressure levels (1/3 OBSPS's). The effects of launch pad geometry (Kennedy Space Center Launch Pad No. 39B) and vehicle surface reflection are included in the data. In addition to the references included herein which provided the primary basis for the estimates of rocket noise at launch, consideration has also been given to the results of discussions between Space Shuttle contractors and personnel of S&E-ASTN-ADV, held at MSFC on 28 April and 20 May 1971.

The launch noise levels shown in Figures 5-176 and 5-177 will be valid for approximately 8 to 10 seconds after liftoff, at which time they will have decreased by about 3 db due to the fact that the exhaust plumes (considered as an array of acoustic sources) will be free of the flame deflectors and will be trailing aft of the vehicle. At about 15 seconds, the noise levels will have decreased another 3 db since the vehicle will be at an altitude above 1000 feet and the noise radiation may be considered as effectively spherical rather than hemispherical as is the case on or near the ground plane. After 15 seconds, the rocket noise on the vehicle will decrease with altitude as a function of the reduction in the characteristic impedance of the atmosphere; i.e., density times speed of sound. When the local flow velocity reaches Mach 1, rocket noise will not be propagated forward on the vehicle.

Figure 5-178 shows aerodynamically induced pseudo-noise during ascent of the vehicle at maximum dynamic pressure. For boundary layer noise the overall levels are essentially independent of location on the vehicle. However, the frequency at which the maximum acoustic pressure occurs is directly related to the thickness of the local boundary layer. Thus, at the front of the vehicle where the boundary layer is thin the characteristic frequency is high; moving aft, the characteristic frequency decreases with an increase in boundary layer thickness. As a result of shock-boundary layer interaction between the mated booster and ESS, the pressure level increases significantly while the characteristic frequency decreases to a

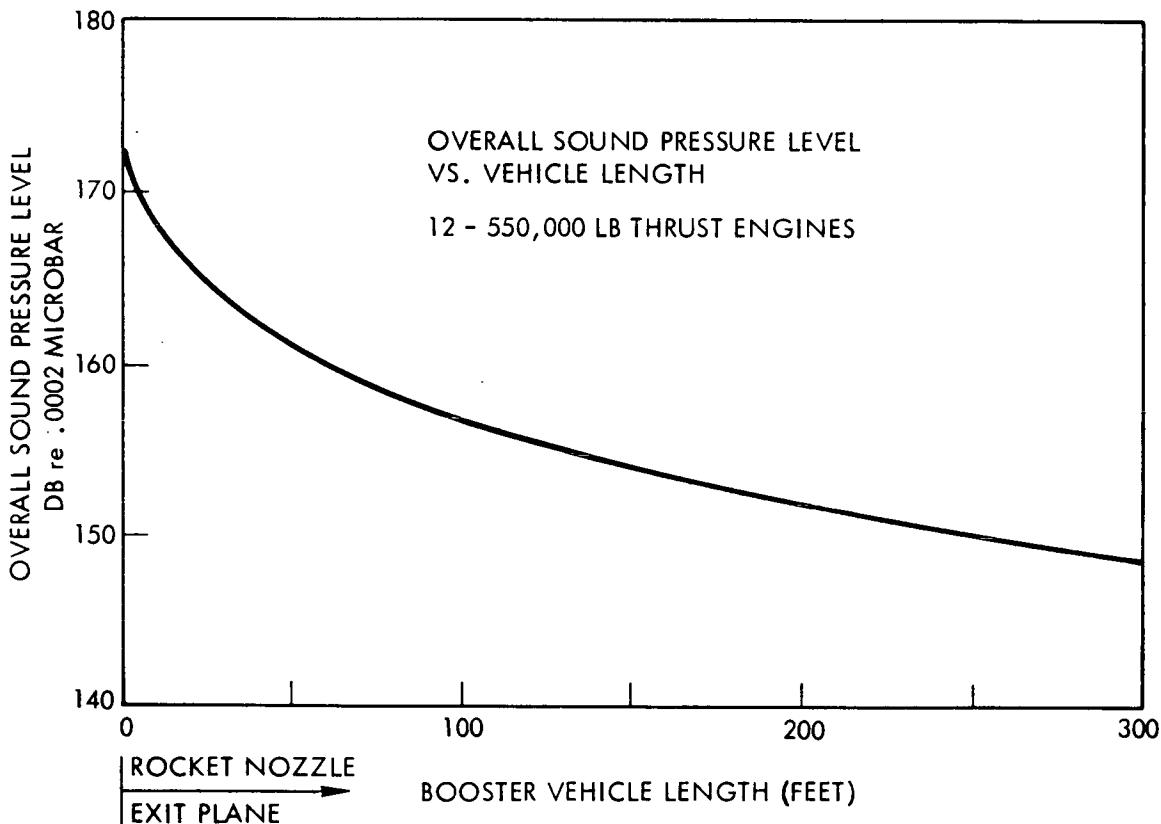


Figure 5-176. Launch Acoustic Environment (on Pad)

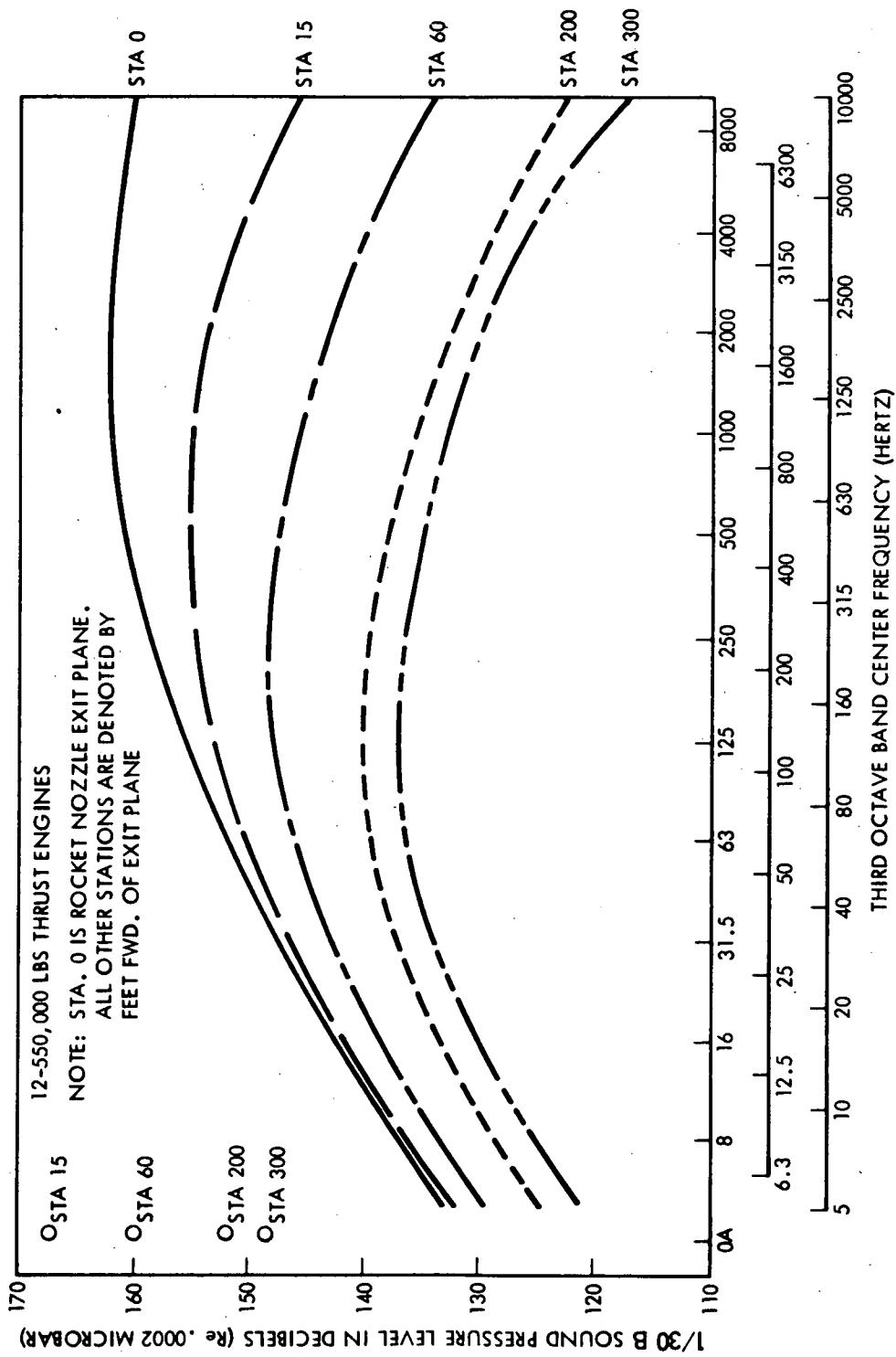


Figure 5-177. Launch Acoustic Environment (on Pad),
1/3-Octave Band Sound Pressure Levels

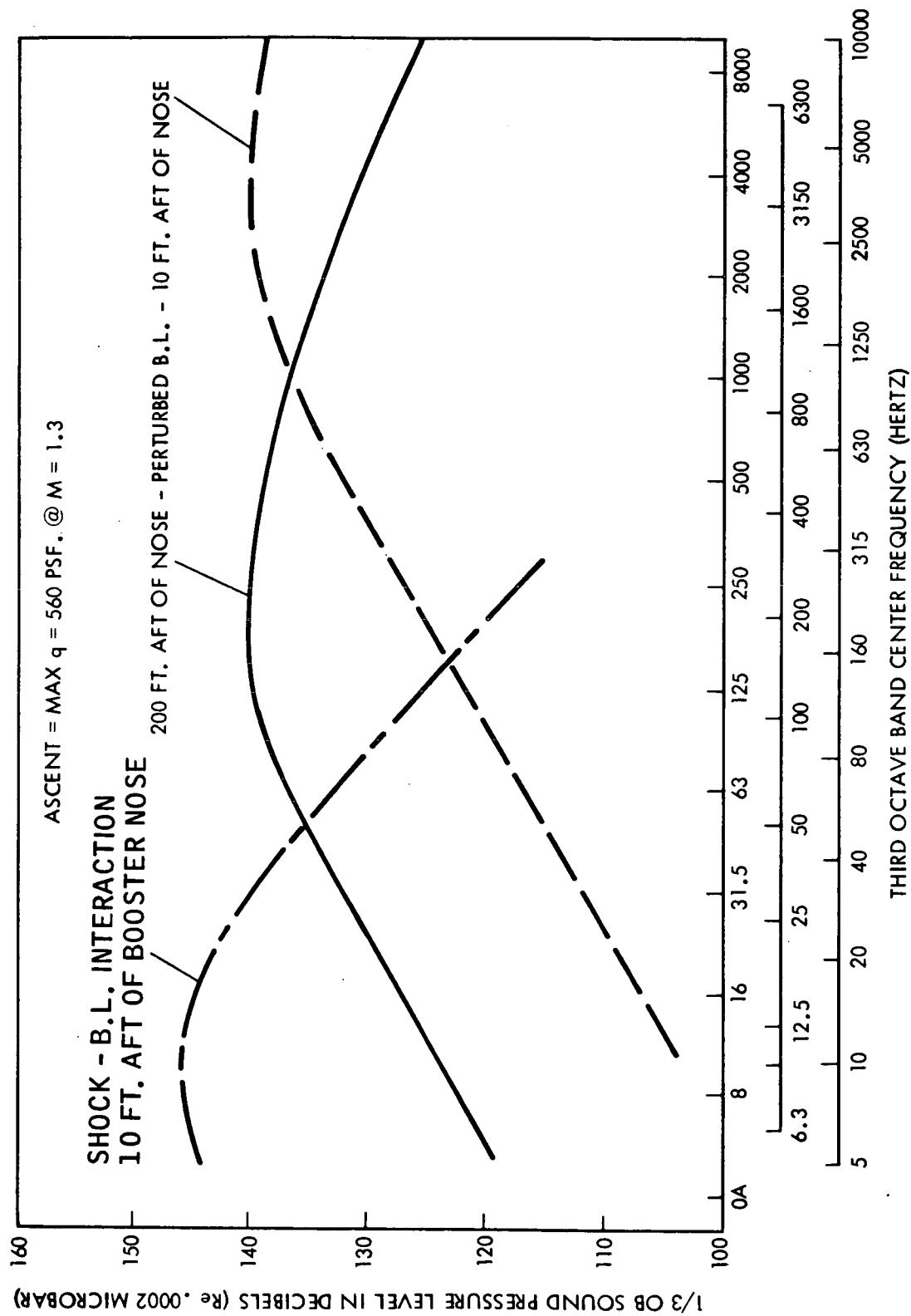


Figure 5-178. Aerodynamic Pseudo-Noise



very low value. This results from concurrent detachment and reattachment of the local boundary layer and shock oscillation.

To summarize, rocket engine noise at launch is well correlated over large areas of the structure. Hence, large structural elements tend to respond in their fundamental modes with higher modes being only weakly excited.

Acoustic Environment Effects on the ESS. The acoustic noise applied by the rocket engines of the shuttle booster to the external surface of the ESS was investigated for lift-off from the launch pad. The sound pressure levels were converted into the vibration spectra shown in Figure 5-179. The levels are for unloaded ring frames with the assumption that the structure is unchanged from the Saturn S-II structure. Saturn S-II static firing, Saturn V launch, and S-II high force test data were utilized in the conversion of the sound pressure levels to vibration responses. Information accumulated on the Saturn S-II program shows that the structural response to acoustic excitation is generally the greatest in the radial direction, i.e., normal to ring-frame caps, and significantly attenuated in the tangential and longitudinal directions. Therefore, only the levels in the radial direction were studied.

5.2.3 Aborts and Contingency Missions

The ESS design incorporates considerable redundancy to meet FO/FS failure criteria. These criteria are not met, however, by the main propulsion system as its design incorporates only two engines.

For light payloads, it is possible to provide capability to complete the nominal mission after incurring an engine failure at staging as indicated in Figure 5-3. Providing this capability implies providing larger propellant reserves as indicated in Figure 5-180. In most launches, these reserves will not be used, thereby necessitating a propellant dump system capable of accommodating them. As indicated in Book 2, the ESS design permits dumping of the quantities indicated. It is seen from Figure 5-180, that mission completion can be provided for payloads up to about 120,000 pounds. For heavier payloads, Figure 5-181 shows the tolerance of the system to engine failure. If engine failure occurs later than 50 seconds after nominal ignition, the MDAC space station can be maneuvered to a safe orbit by use of the OMS as well as the remaining major engine. If the failure occurs later than 100 seconds after staging, the DRM can be achieved. Every effort during Phase B was directed at producing a minimal structural effect on the reusable booster. Hence, the "low-loads" trajectories were devised and these incur performance penalties which otherwise could be avoided. If somewhat higher loads were permitted on the booster by the MDAC Space Station/ESS combination, abort to orbit with one engine out from staging would be possible.



PREDICTED LIFTOFF VIBRATION LEVELS - S-II THRUST
STRUCTURE - RING FRAMES - RADIAL AXIS

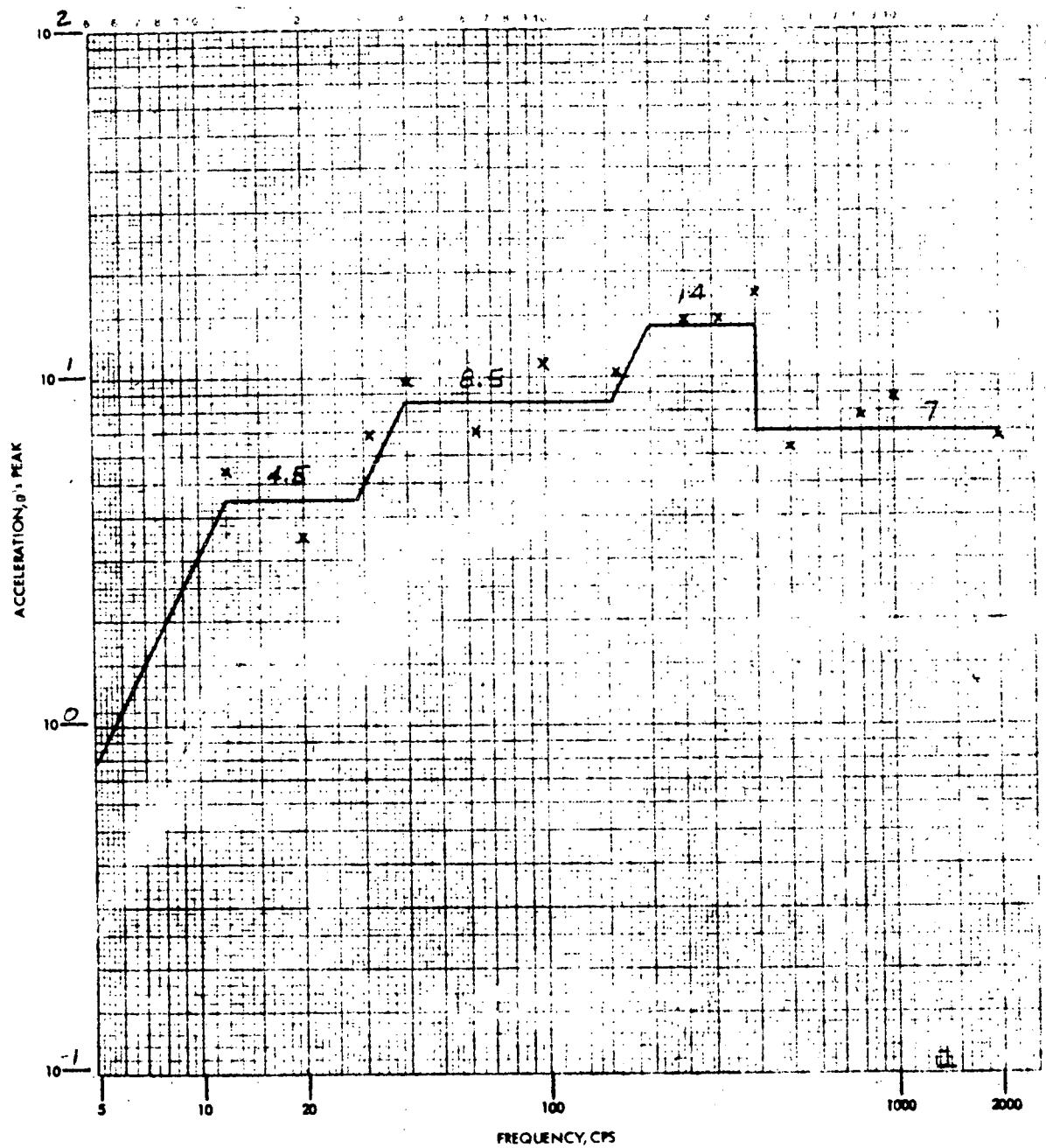


Figure 5-179. Vibration Spectra (Sheet 1 of 6)



PREDICTED LIFTOFF VIBRATION LEVELS - S-II THRUST
STRUCTURE - RING FRAMES - RADIAL AXIS

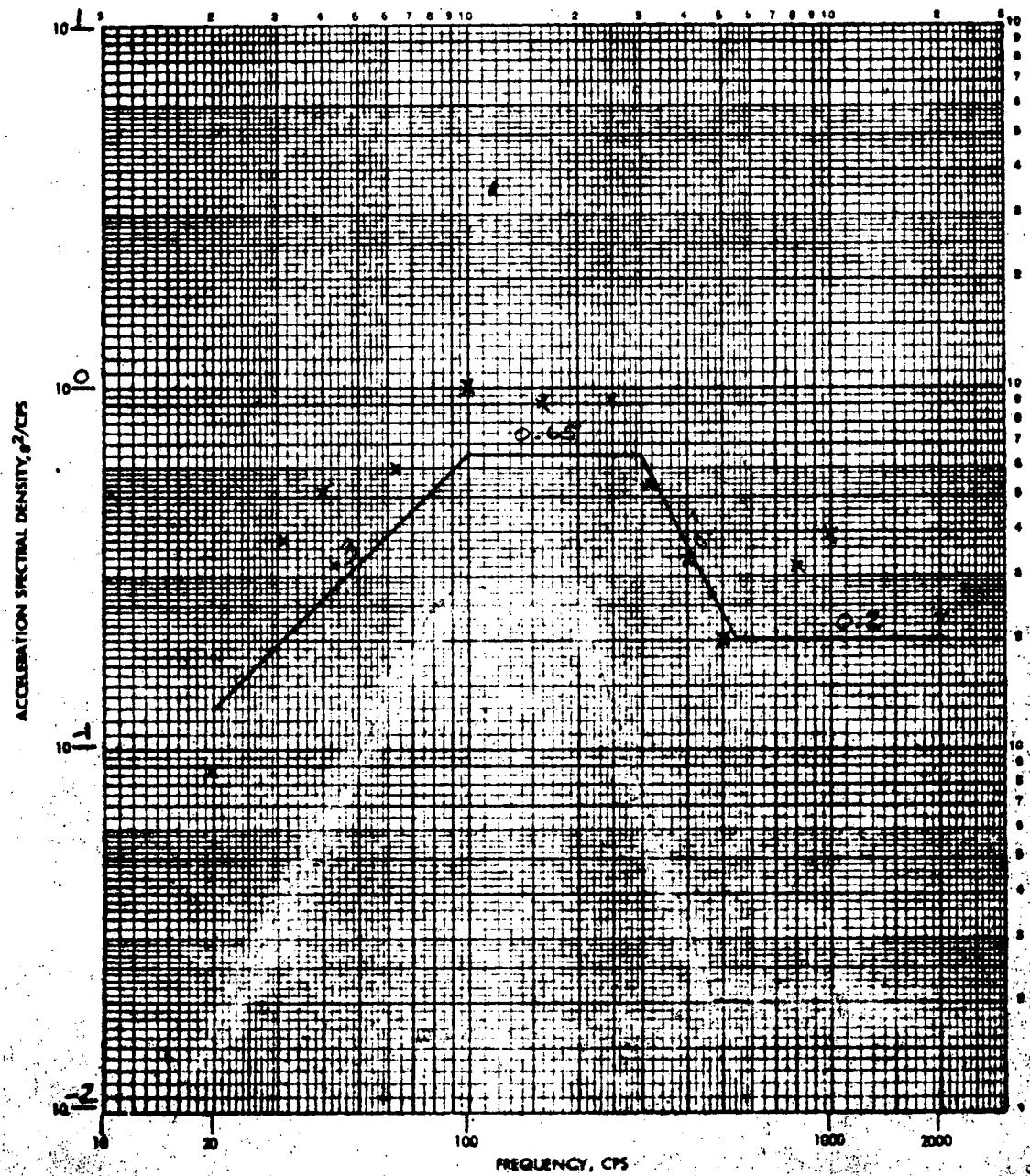


Figure 5-179. Vibration Spectra (Sheet 2 of 6)



PREDICTED LIFTOFF VIBRATION LEVELS - S-II THRUST
STRUCTURE - RING FRAMES - RADIAL AXIS

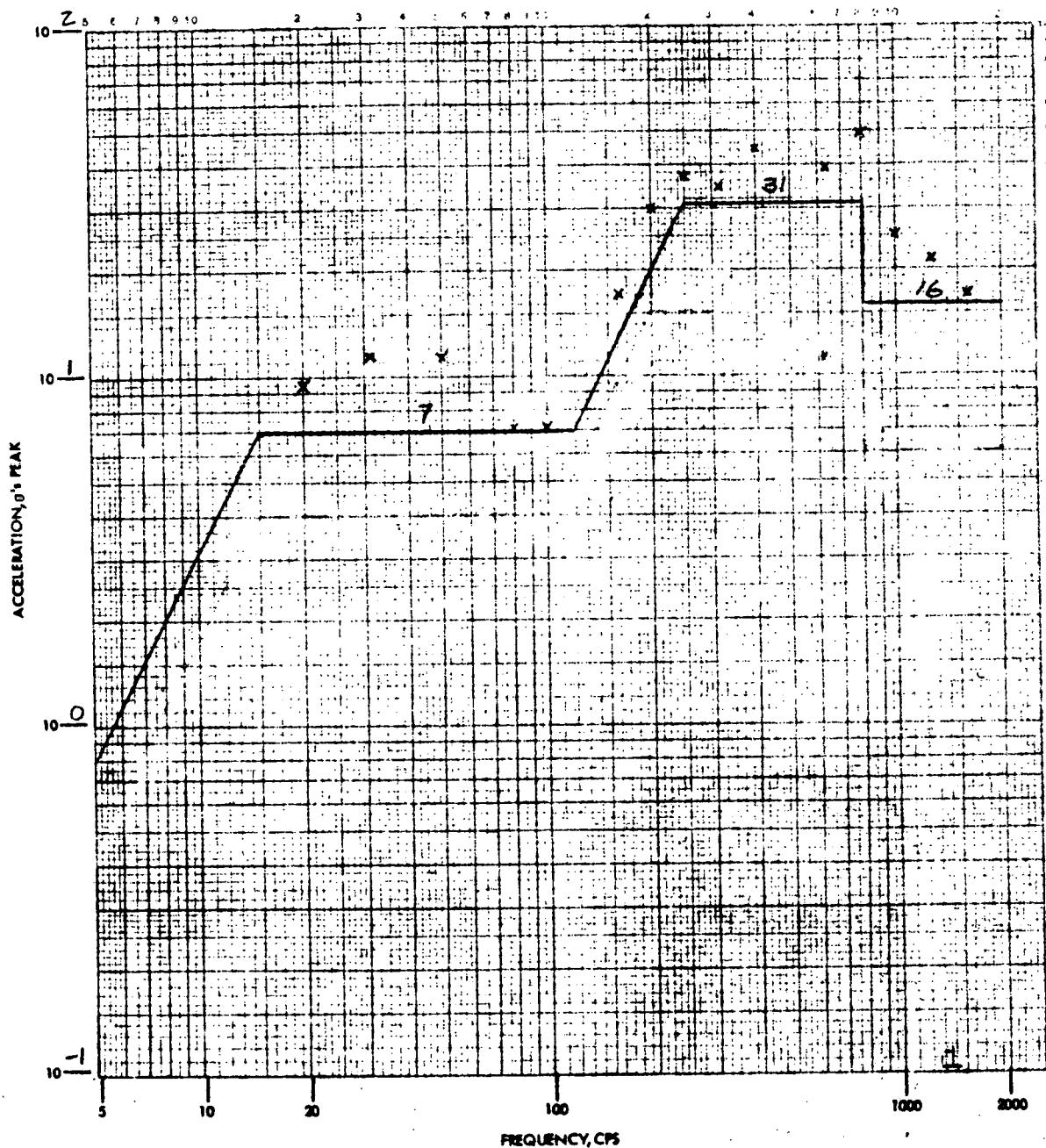


Figure 5-179. Vibration Spectra (Sheet 3 of 6)



PREDICTED LIFTOFF VIBRATION LEVELS - S-II THRUST
STRUCTURE - RING FRAMES - RADIAL AXIS

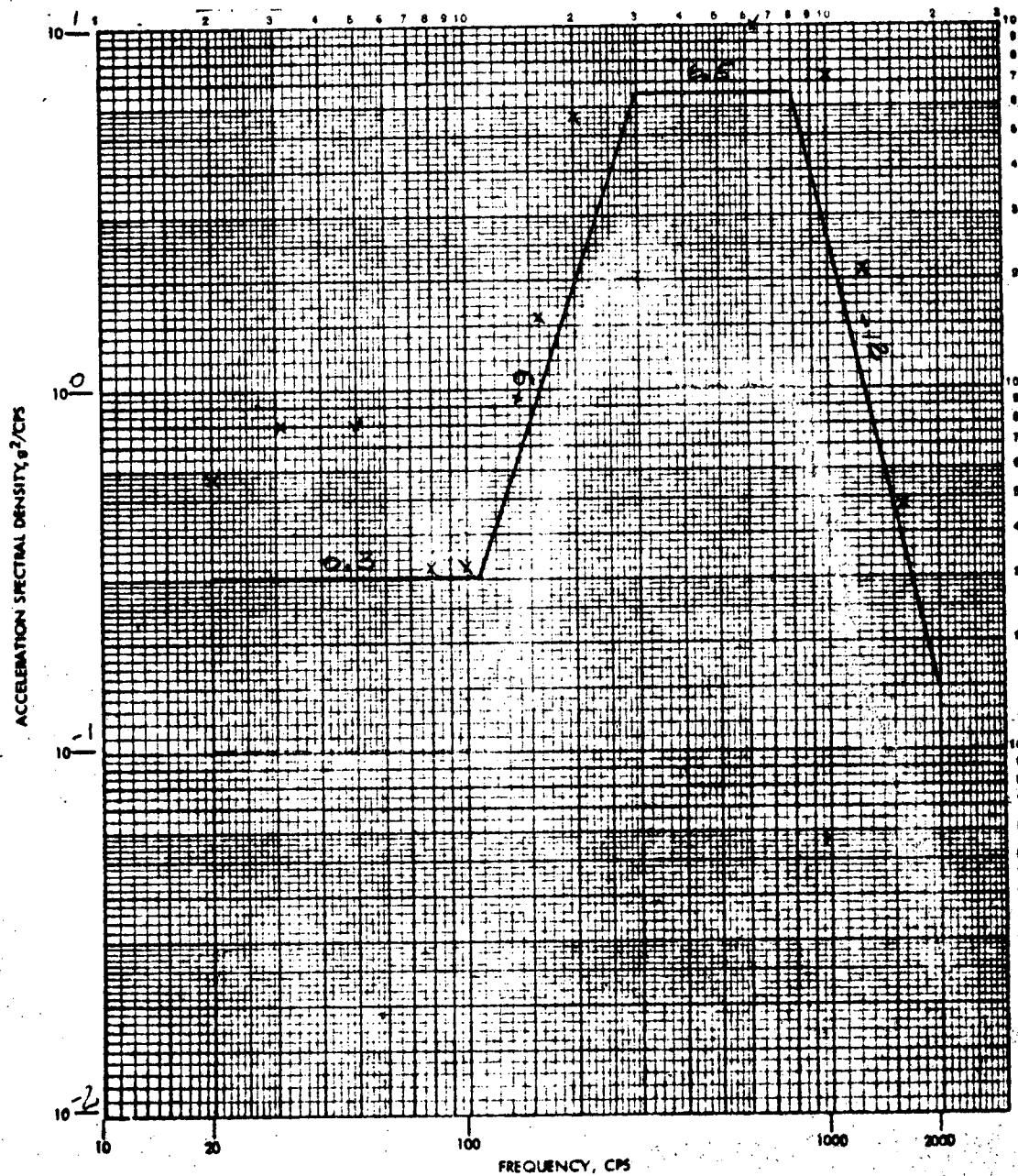


Figure 5-179. Vibration Spectra (Sheet 4 of 6)



PREDICTED LIFTOFF VIBRATION LEVELS - S-II THRUST
STRUCTURE - RING FRAMES - RADIAL AXIS

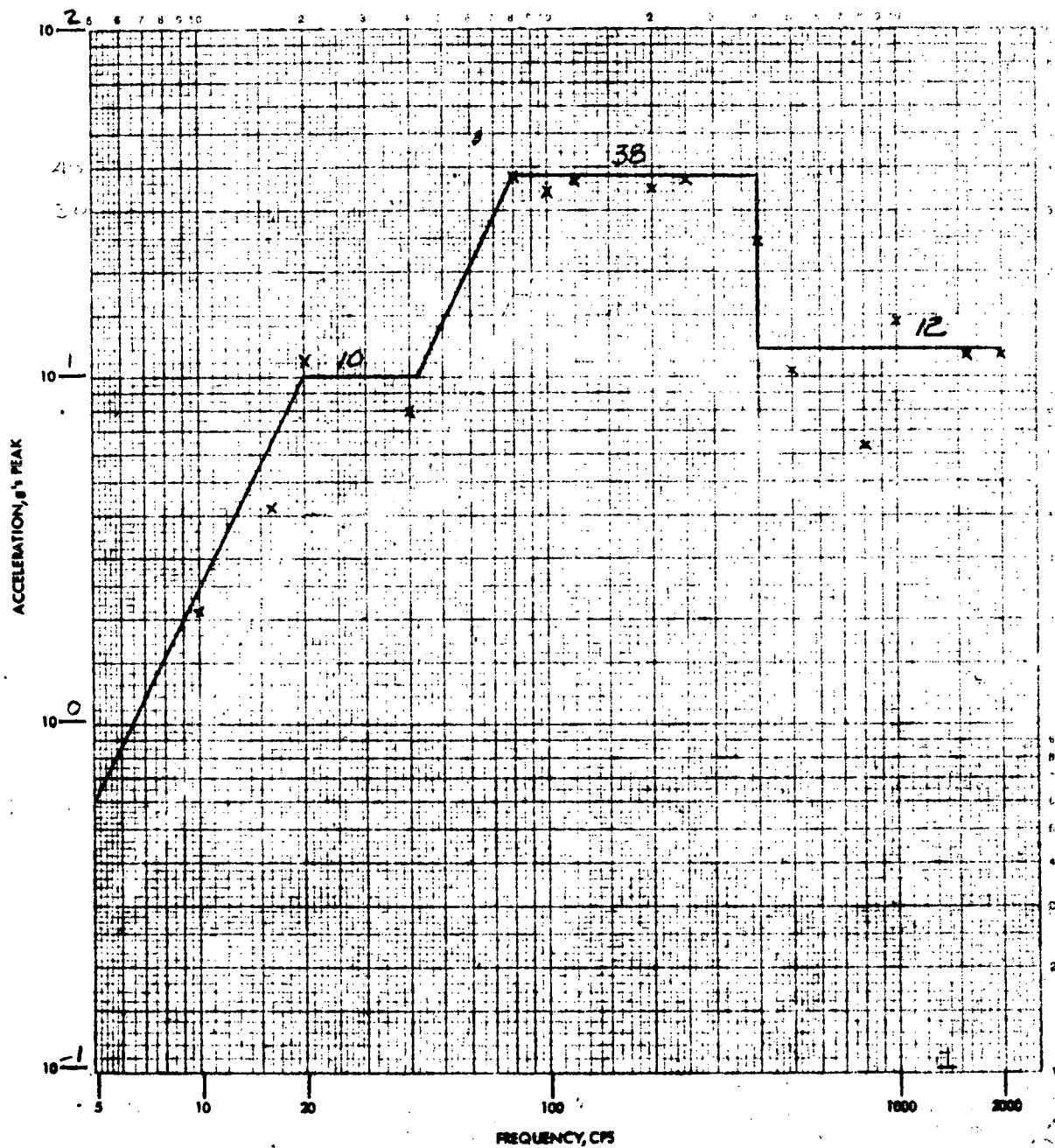


Figure 5-179. Vibration Spectra (Sheet 5 of 6)



PREDICTED LIFTOFF VIBRATION LEVELS - S-II THRUST
STRUCTURE - RING FRAMES - RADIAL AXIS

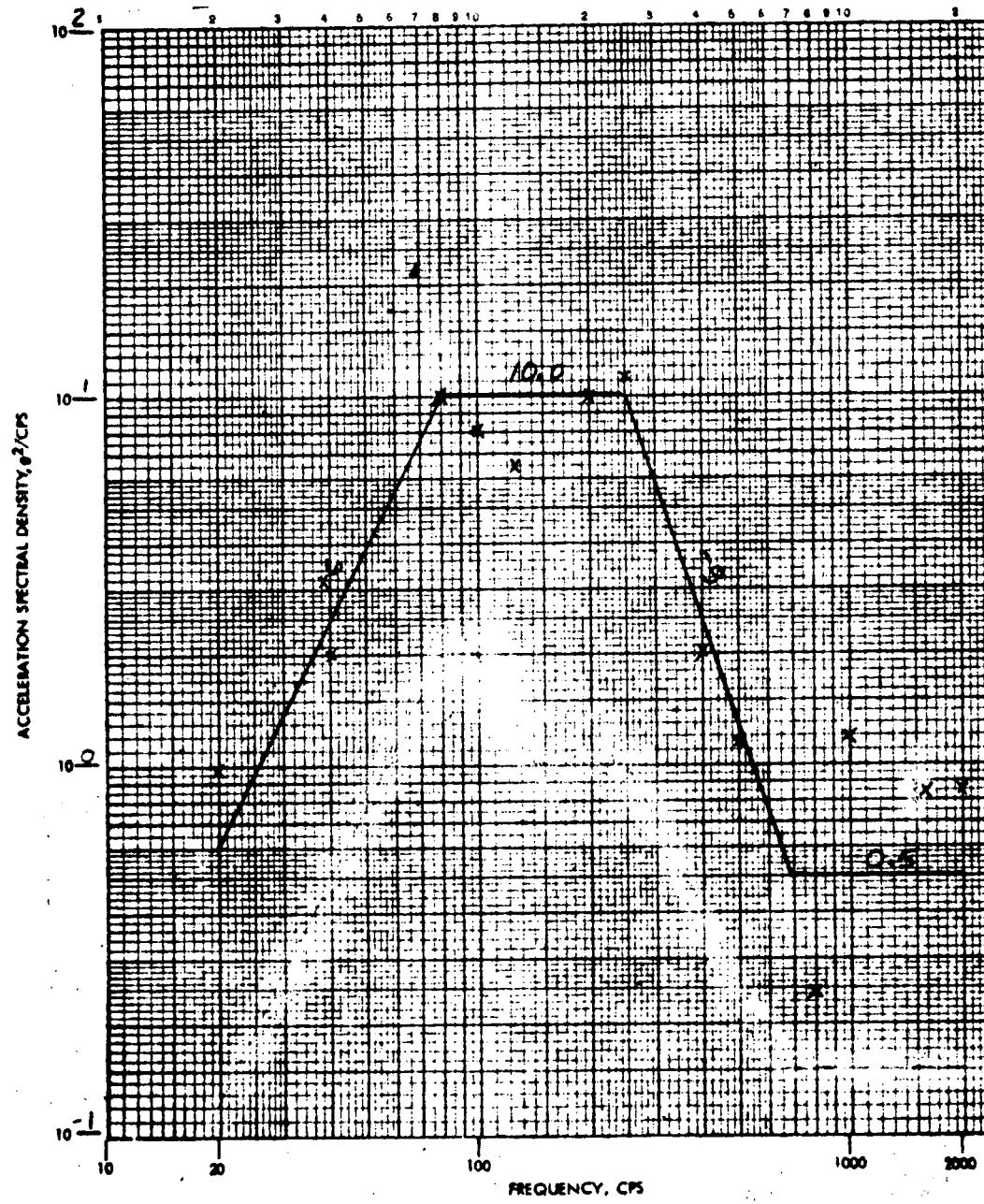


Figure 5-179. Vibration Spectra (Sheet 6 of 6)

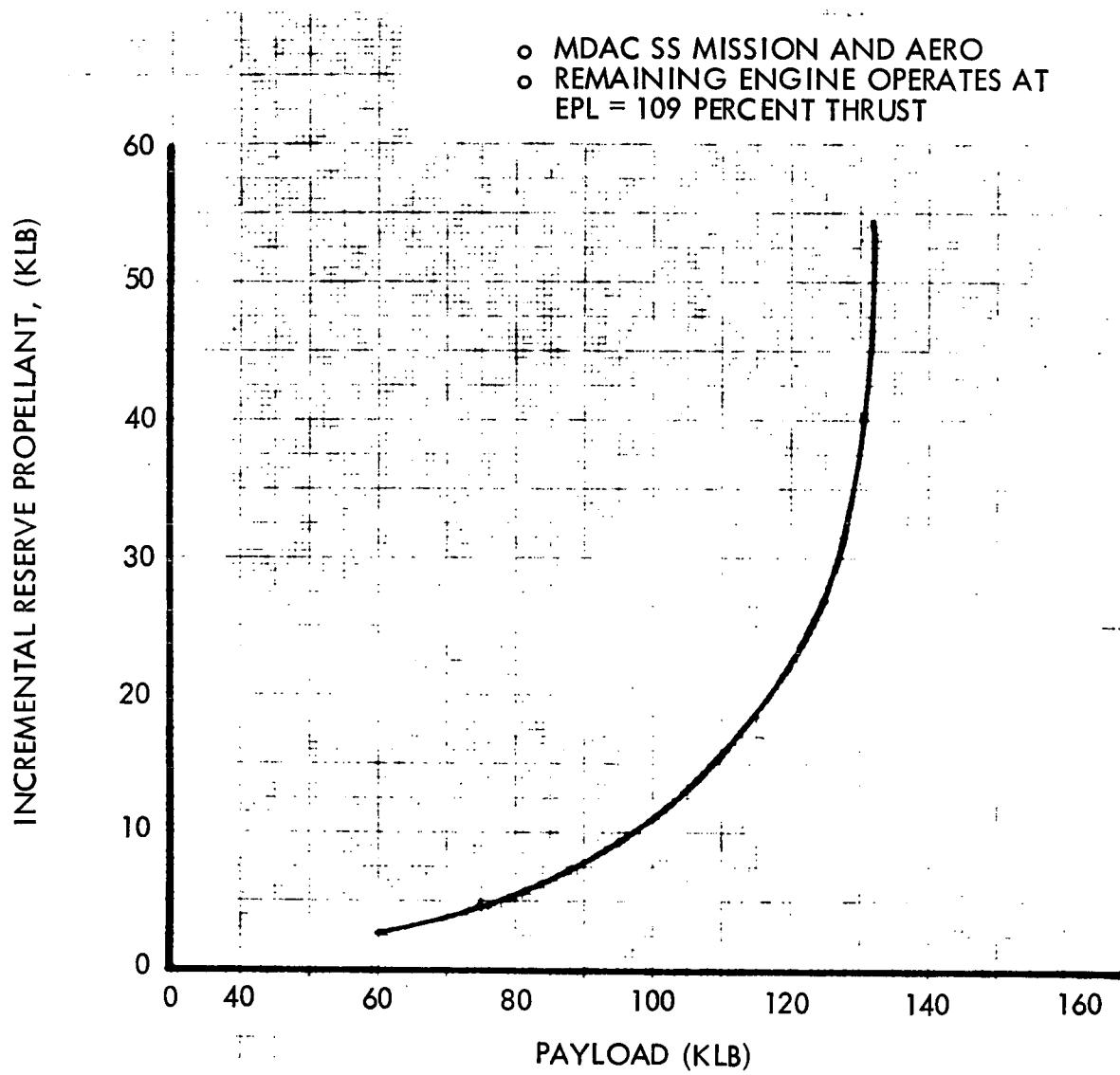


Figure 5-180. Variation in Reserve Propellant Requirements for Mission Completion with One Engine Failed at Ignition

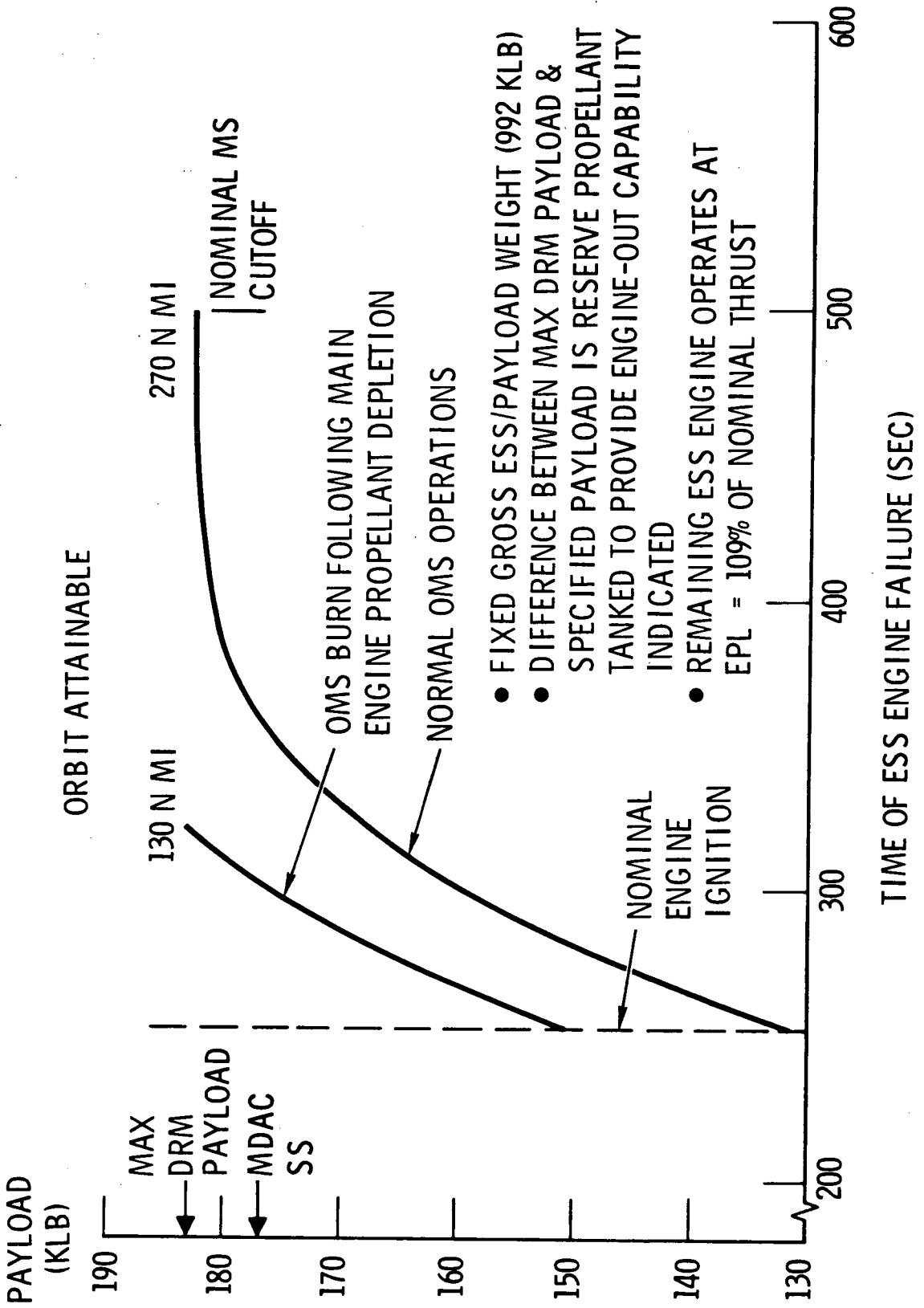


Figure 5-181. One Engine-In/Out Performance for Baseline



5.3 ORBITAL OPERATIONS AND DEORBIT

5.3.1 Rendezvous/Safing

To effect the recovery of high-value components from the spent ESS vehicle, it has been assumed that the mission plan will provide an orbiter at the location of the ESS. The orbiter will have performed its primary mission and thus will be available to recover components from the ESS before returning to earth. To accomplish this task, the orbiter must perform a rendezvous with a passive ESS, hard-docking at a docking port or structure provided on the ESS. All ESS systems not needed for docking will have been rendered safe before the docking operation. After docking, the entire vehicle will be safed.

5.3.2 Recovery of Components

ESS Effects

The effects on ESS of component recovery are in two categories: hardware changes required for recovery and procedural changes required to support recovery. The hardware changes to support recovery include the following:

1. Provision of linear-shaped charges to separate electrical equipment containers and aft closeout.
2. Provision of separable nuts to separate the engine interfaces.
3. Support hardware changes, such as providing separation disconnects at the electrical containers, provision of handling points for manipulator arm attach, heat shield removal provisions, and repackaging of electrical equipment.
4. Provision of a deorbit avionics package.
5. Addition of a docking port at Postition III, with resultant redesign of the fairing.

Procedural changes include:

1. Addition of the propellant dump to remove residual liquid propellants from the main tanks before safing.
2. Software changes to power down for component removal and power up for deorbit.



Orbiter Effects

The recovery of high-cost ESS hardware components depends on the availability of the orbiter on orbit with the ESS and the prompt retrieval and storage of these items in the cargo compartment of the orbiter. The structural compatibility of the orbiter for the successful storage of the recovered hardware components is shown in Figure 5-182 (NR Drawing VA70-3201). Sheets 1 and 2 of the drawing show the details of the orbiter structure with which to attach recovered hardware support structure for the return to earth. Figure 5-183 (NR Drawing 5080-5002) illustrates the positioning of ESS-recovered hardware components in the orbiter cargo compartment.

Orbiter manipulator details are shown in Figure 5-184 (NR Drawing VA70-5510, Manipulator Assembly); Figure 5-185 (NR Drawing VA70-5530, Cargo Retention System Installation); and Figure 5-186 (NR Drawing VA70-5540 Cargo Transfer Tunnel Installation). Recovery of the ESS hardware components will require that a special mechanical adapter hand (TBD) be available on the orbiter. This "hand" will handle the ESS hardware and secure the items within the orbiter cargo compartment. This unit will be one of the many special adapters carried by the orbiter to permit successful fulfillment of the orbiters many missions while on orbit.

Recovery of the ESS hardware, stowage within the orbiter, securing for entry, and landing will require specific cargo-handling pallets and/or cradles, which must be included in the orbiter payload capability. Table 5-12 is a breakdown of weights for the items impacting the orbiter. As noted, recovery of the high-cost hardware components from the ESS vehicle is within the capacity and capability of the present design of the NR orbiter vehicle (NR Configuration 161C).

5.3.3 Deorbit

Introduction

Debris in space is never particularly desirable but it can be unusually hazardous if it is left orbiting in the vicinity of a manned spacecraft. Collisions with the payload are a worrisome possibility and rendezvous vehicles must carefully skirt the debris. Once it has delivered its payload into orbit, the ESS stage can become hazardous space debris unless it performs evasive maneuvers. Although a variety of disposal techniques are available (see SD70-683 "Saturn INT-21 Launch Vehicle Task 9 separation and disposal") controlled deorbit of the stage is the most desirable technique



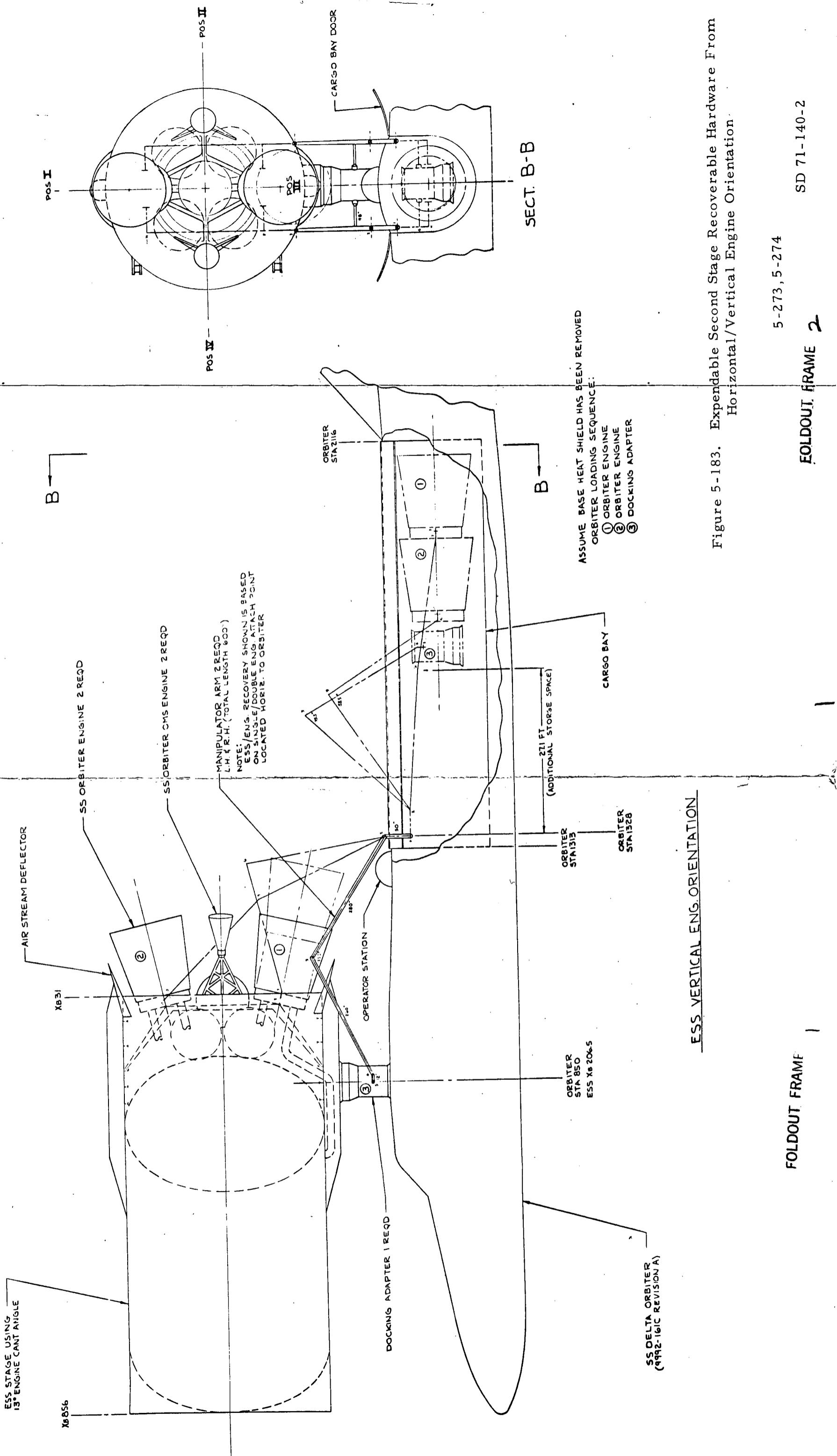
Table 5-12. Shuttle Payload Assessment for Recovery

Item	Up	Down
Shuttle Provisions		
Passenger provisions	180	180
Consumables	220	-
2 passengers	440	
Cargo Module		
Module dry weight	9,500	9,500
Consumables	1,320	-
Cargo (passengers and bulk)	10,550	-
Growth		
25 percent dry weight	<u>2,830</u>	<u>2,830</u>
Required Payload	25,000	12,510
Estimated Δ Weight — Recovery		
Deorbit propellant (OMS)	8,500	-
Handling gear	1,830	1,830
Recovered items, ESS	-	22,540
EVA suits (2)	355	-
	<u>35,685</u>	<u>36,880</u>

that provides a permanent solution to the debris problem. This method has the additional advantage of allowing the spent stage to be dropped into an unpopulated ocean rather than from a random point along its orbit.

The major purpose of this study phase was to determine the most desirable ESS deorbit conditions (ΔV , firing angle, and deorbit time) and the expected footprint dimensions. In addition, the most favorable deorbit opportunities were pinpointed, and the potentially adverse effects of engine failures were evaluated. Finally, solar orbit disposal was briefly examined as a possible alternative to controlled deorbit, and a set of specific conclusions and recommendations concerning the proper deorbit techniques were developed.

Page intentionally left blank



Page intentionally left blank

Page intentionally left blank

Page intentionally left blank



Available Ocean Impact Areas

A spacecraft encircling the earth in a low altitude circular orbit traces out a sinusoidal ground track, as shown in Figure 5-187. This ground track corresponds to a typical 270-nm ESS orbit with an orbital inclination of 55 degrees. Because of the earth's rotation, the track drifts westward about 22 degrees per orbit.

Several sparsely inhabited ocean areas are available for deorbit, most of them spanning several thousand miles of open ocean. The Pacific and Indian Oceans off the east and west coasts of Australia provide particularly attractive impact regions. A careful examination of Figure 5-187 reveals that there will be one or two deorbit opportunities per orbit, provided the deorbit footprint can be kept fairly small (i. e., 2000 nautical miles or so in length) The desirable impact regions can be reached by proper choice of the deorbit firing time. The deorbit ΔV and the firing angle will also be free variables open to optimization but these parameters would most likely be chosen before lift-off. Only the exact deorbit time will be chosen in real time, and its choice would be made in such a way as to allow the vehicle to splash down in one of the large open ocean areas.

Deorbit ΔV and Optimal Firing Angle

The weight of the deorbit propellants must be deducted from the allowable payload weight. Thus, it is desirable to plan the deorbit maneuver so that it requires the minimum possible deorbit ΔV . (It costs about 7 pounds of propellants for each foot per second change in the velocity of the ESS stage.) Theoretically, a retro maneuver that drops the spent stage into the ocean after it encircles half the earth would represent the minimum deorbit ΔV Unfortunately, the resultant reentry trajectory barely grazes the earth and thus is inordinately sensitive to small perturbations in the initial conditions. Therefore, a 180-degree entry range angle yields a rather large impact footprint. The footprint size can be decreased, however, by reducing the entry range angle. A practical range angle is about 135 degrees. This corresponds to a travel distance of about 8000 nautical miles between retro ignition and impact, (Figure 5-188). Shortening the travel arc requires a larger deorbit ΔV but results in a smaller footprint size and provides a small performance pad to cover for rocket ignition failures.

Figure 5-189 is a clearer illustration of the effect the nominal ΔV selection has on the length of the footprint. Note that as the velocity drops below 450 ft/sec, the footprint length increases rapidly. This results from the fact that the entry range angle begins to approach 180 degrees, and

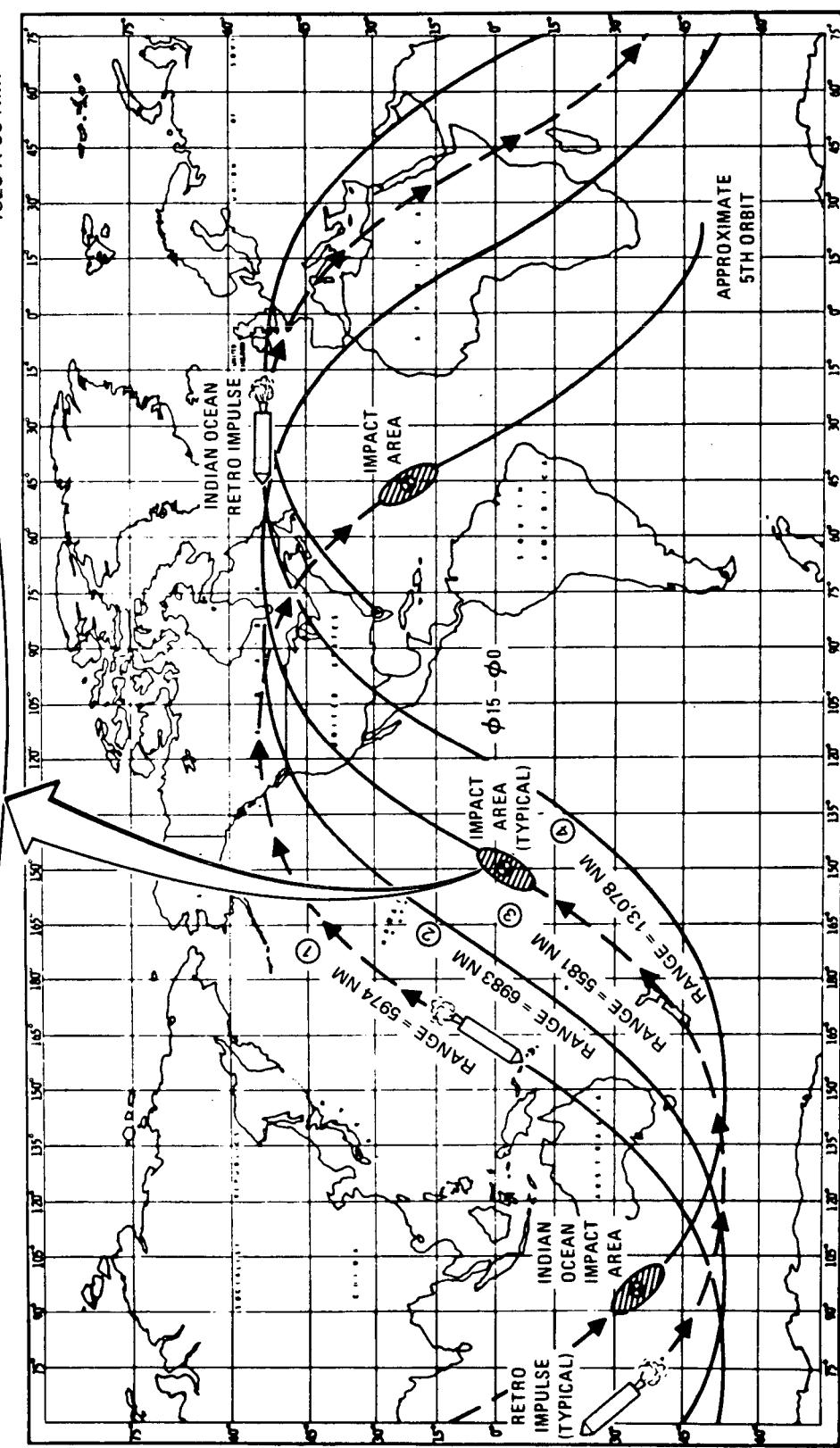
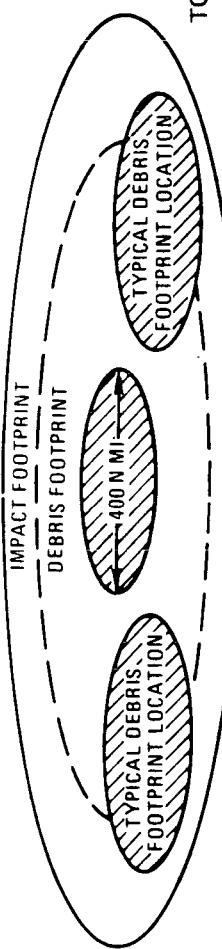


Figure 5-187. Orbit Trace for 55-Degree, 270-NM Orbit

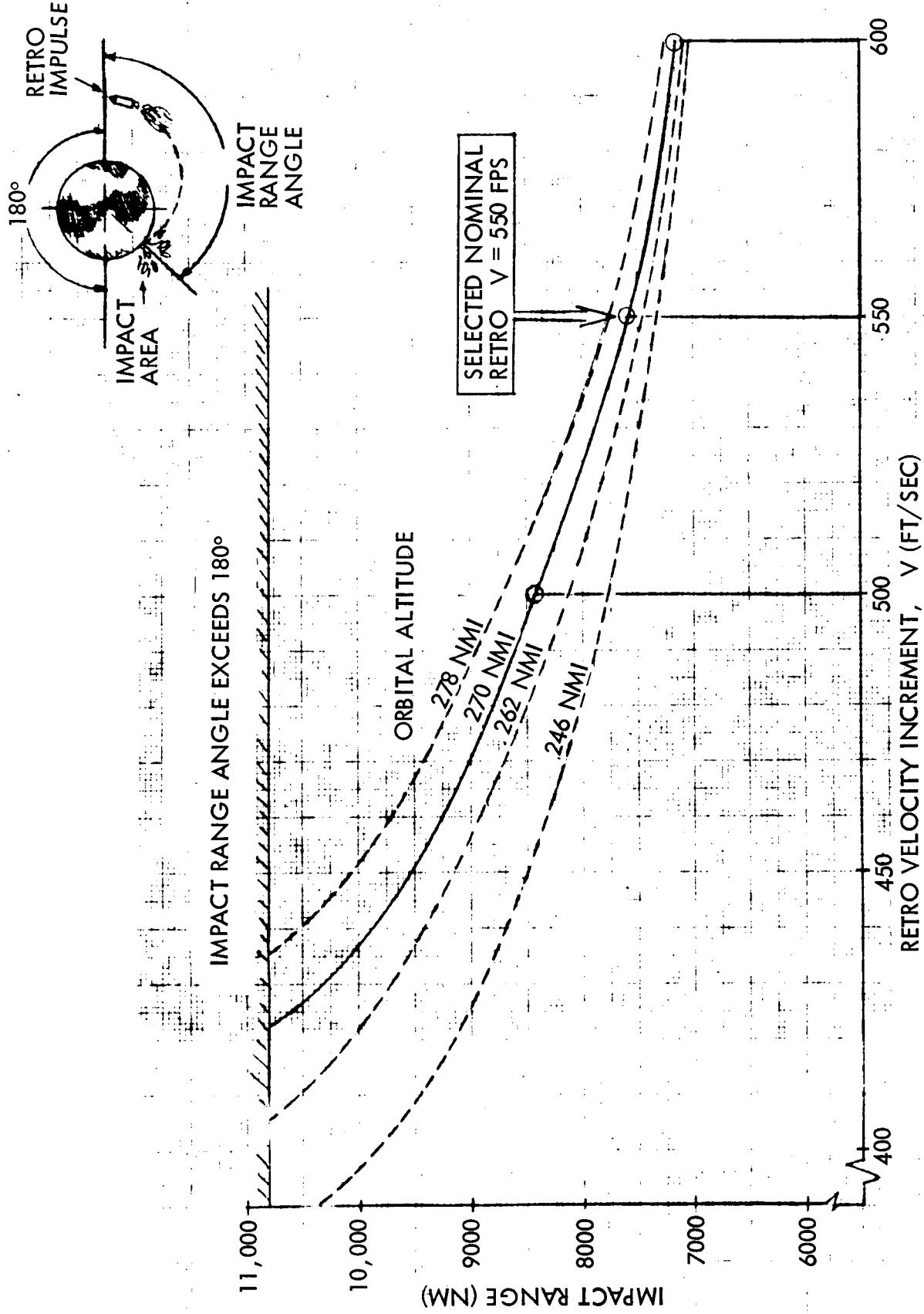


Figure 5-188. ESS Impact for Various Velocity Increments and Orbital Altitudes

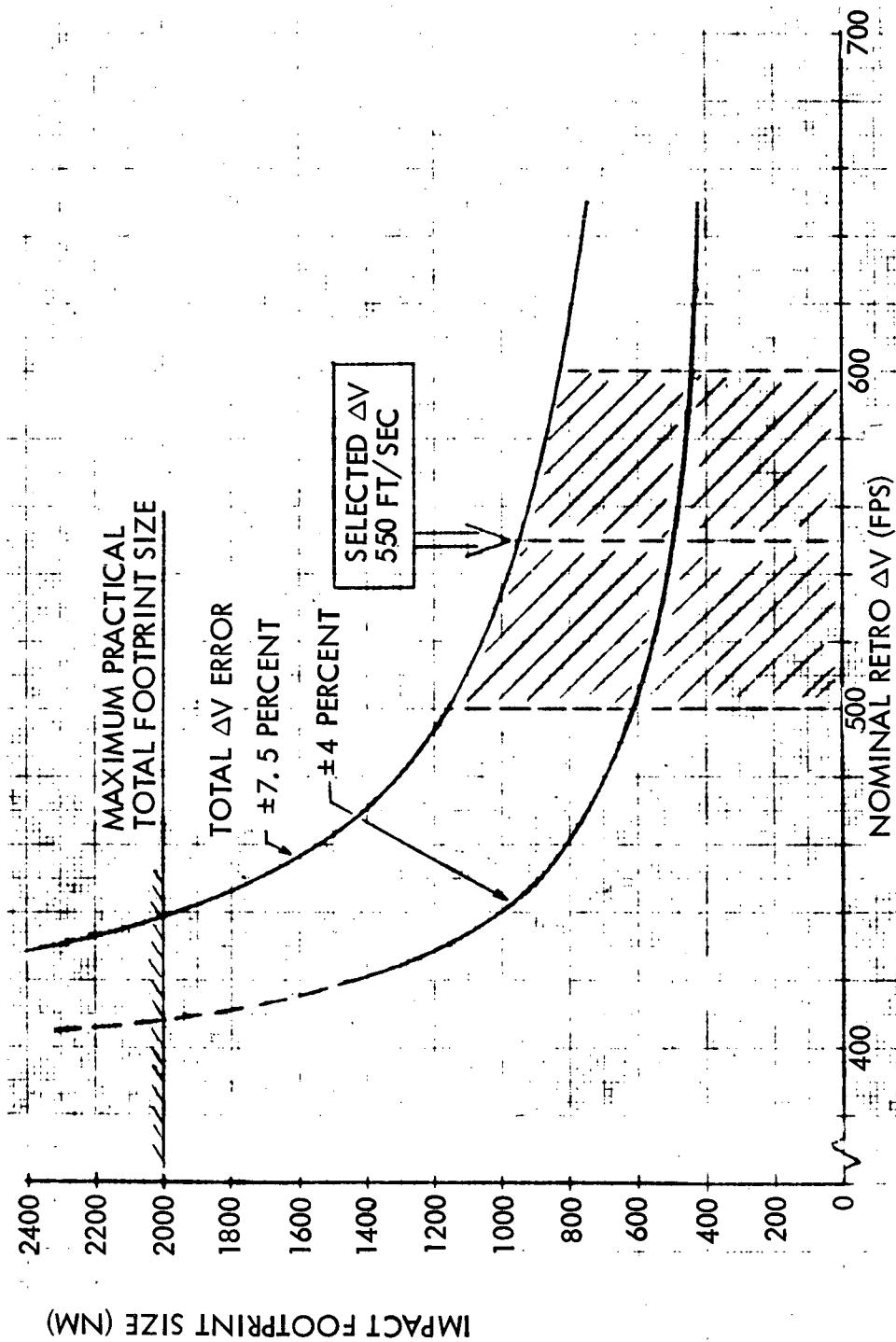


Figure 5-189. Locus of Footprint Length Due to ΔV Perturbation



the impact occurs at an ever more shallow angle. In order to stay away from the knee of the curve, a nominal velocity increment of 550 ft/sec was selected for the ESS deorbit operations. A slightly smaller ΔV would possibly suffice, but a small pad is desirable to help hold down the effect of other statistical perturbations.

The deorbit firing angle is also a free variable available for optimization. The optimal firing angle for an entry range distance of 10,820 nautical miles is zero degree. In other words, if a 180-degree entry range angle is desired, a pure retro maneuver would yield minimum propellant consumption. However, if the entry range is to be less than half the circumference of the earth (which is desirable), a nose-down firing angle would minimize the entry range for a given deorbit velocity increment.

Figure 5-190 illustrates the effect of firing-angle variations on entry range. A 17-degree nose-down attitude yields minimum entry range for the 550 ft/sec deorbit ΔV . The entry range for $\alpha = 17$ degrees, however, is only about 250 nautical miles shorter than the range for $\alpha = 0$ degree. This small range reduction is of no particular importance, but using an optimal firing angle is desirable for a different reason. If the optimal 17-degree value of α is utilized, variations in α have a smaller effect on the entry range. Thus, optimizing α minimizes the length of the footprint. For this reason, it is recommended that the optimal 17-degree firing angle be utilized for ESS applications.

Figure 5-191 shows the entry profiles (range versus altitude) for a fan of firing angles. Note that, for a 25-degree firing angle, the stage swings downward initially, but the trajectory for the 17-degree firing eventually crosses it. This results from the fact that in the 25-degree case, too much of the velocity increment is used to turn the velocity vector and not enough of it is used to reduce the vehicle's orbital energy. Thus, the 17-degree value is more efficient.

Debris Footprint

When a body plunges into the sensible atmosphere, it begins to undergo intense heating effects and high dynamic loads, which usually result in structural breakup before earth impact. The ESS vehicle will, most likely, disintegrate at an altitude of two or three hundred thousand feet. The particles will follow different entry trajectories, spraying over a fairly large region of the ocean.

(The ballistic parameter of a body has a direct influence on its entry profile. This parameter is defined by the ratio $W/C_D A$, where W is the body's weight, C_D is its drag coefficient, and A is its reference area.)

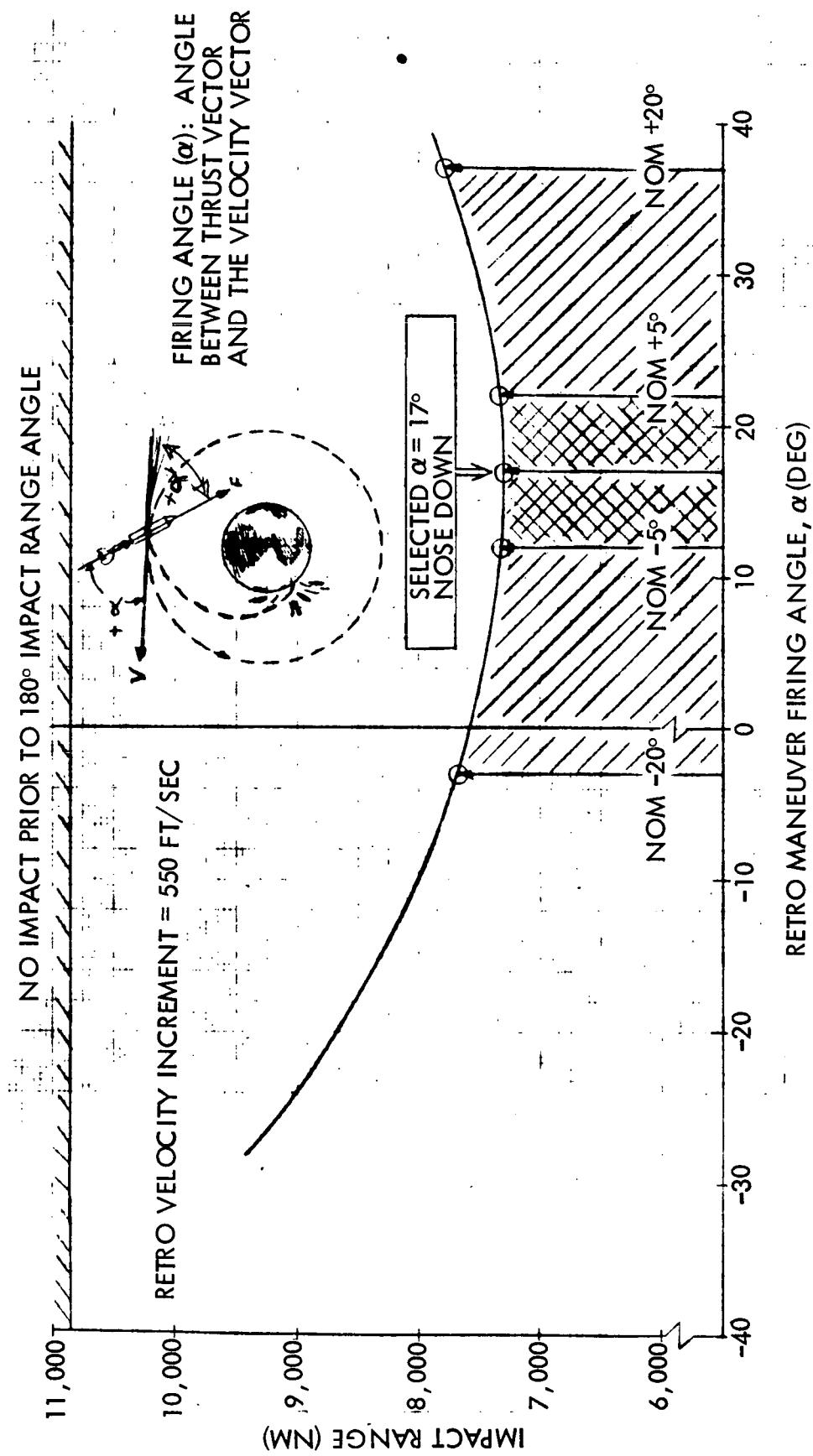


Figure 5-190. Effect of Angle of Attack on ESS Impact Range

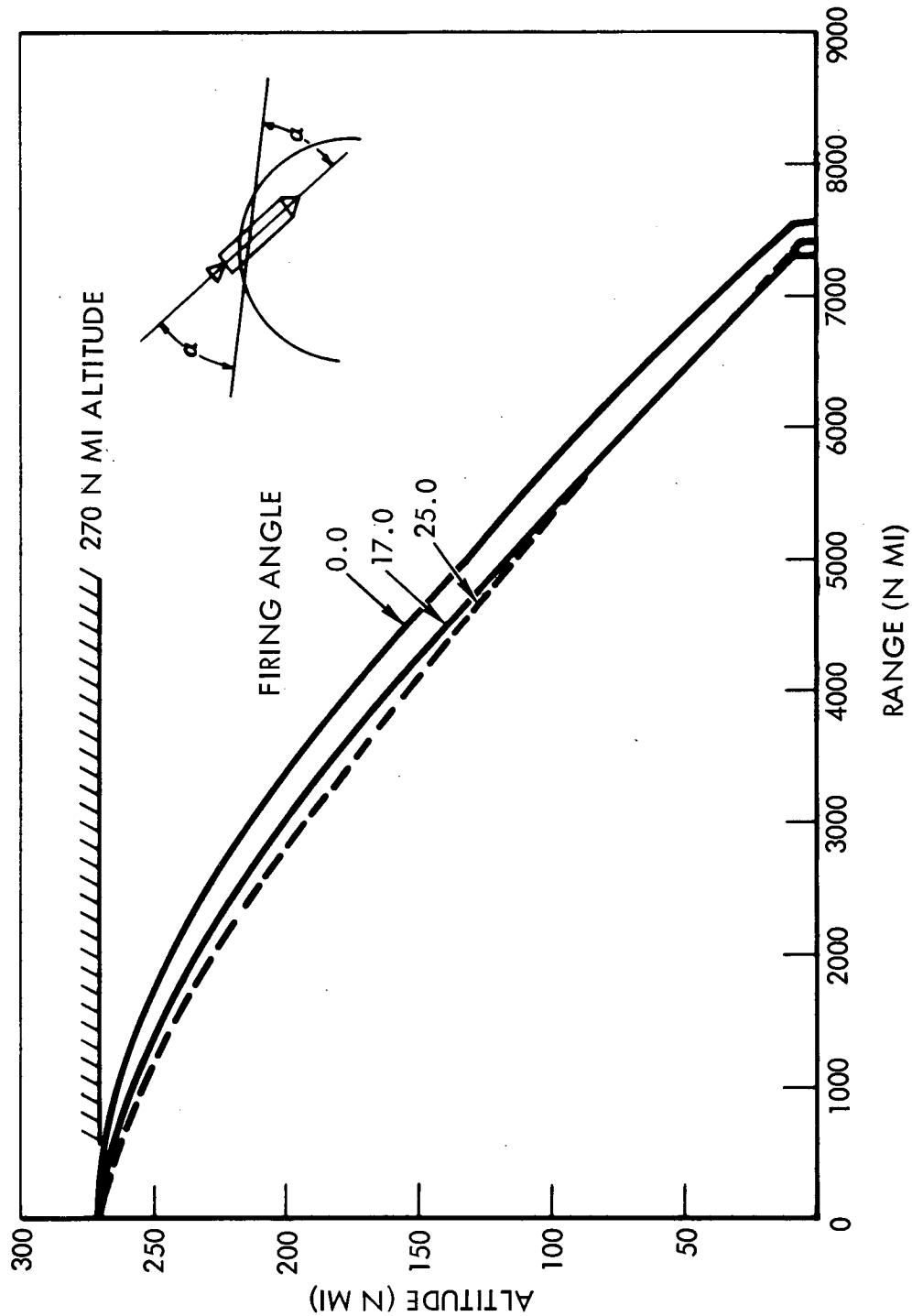


Figure 5-191. ESS Deorbit Profiles



At breakup, the fragments will have various sizes, shapes, and compositions — thus they will have various ballistic parameter values. Figure 5-192 shows the ballistic parameter values for spherical bodies composed of various materials. A variation in ballistic parameters of 10 to 1000 lb/ft² following vehicle breakup seems to be a rather large span. A recent study conducted at Lockheed Aircraft Corporation, Retro Velocity Requirements for Controlled Reentry of the S-II Stage From Various Orbits (TM 54/30-232), led a team of independent researchers to a similar conclusion.

Figures 5-193 and 5-194 show how the fragments will fan out after vehicle breakup. Note that the region covered with debris, assuming vehicle disintegration at 300,000 feet, is 400 nautical miles long. The width of the debris footprint has not actually been determined by simulations but it is estimated to be only a few nautical miles. Figure 5-192 more clearly illustrates the effect of ballistic parameter variations on the impact ellipse.

Impact Footprint

The debris footprint is the area of ocean that will be covered with vehicle fragments after breakup. The location of the center of the debris footprint is a statistical variable characterized as the impact footprint, whose size depends on the magnitude of the expected variations in the deorbit conditions.

Table 5-13 lists the statistical perturbations which affect the impact footprint. The perturbations are broken into two classifications: best-case conditions and worst-case conditions. The best-case conditions will occur when the primary deorbit propulsion system (OMS) is used to power the deorbit maneuvers, and a velocity sensing system is used to shut down the engines once the desired deorbit velocity is reached. Use of the OMS propulsion system will yield a relatively short maximum deorbit burn of 92.5 seconds. During this interval, it will be possible to control the vehicle's attitude to within ± 5 degrees. On the other hand, if the two OMS engines should both fail, the ACPS system would be used as the backup and the maximum burn duration would be lengthened to 467 seconds. The longer burn for the ACPS system results from three factors:

1. Lower thrust.
2. Lower specific impulse.
3. The two ACPS engines are canted 20 degrees to the vehicle centerline.

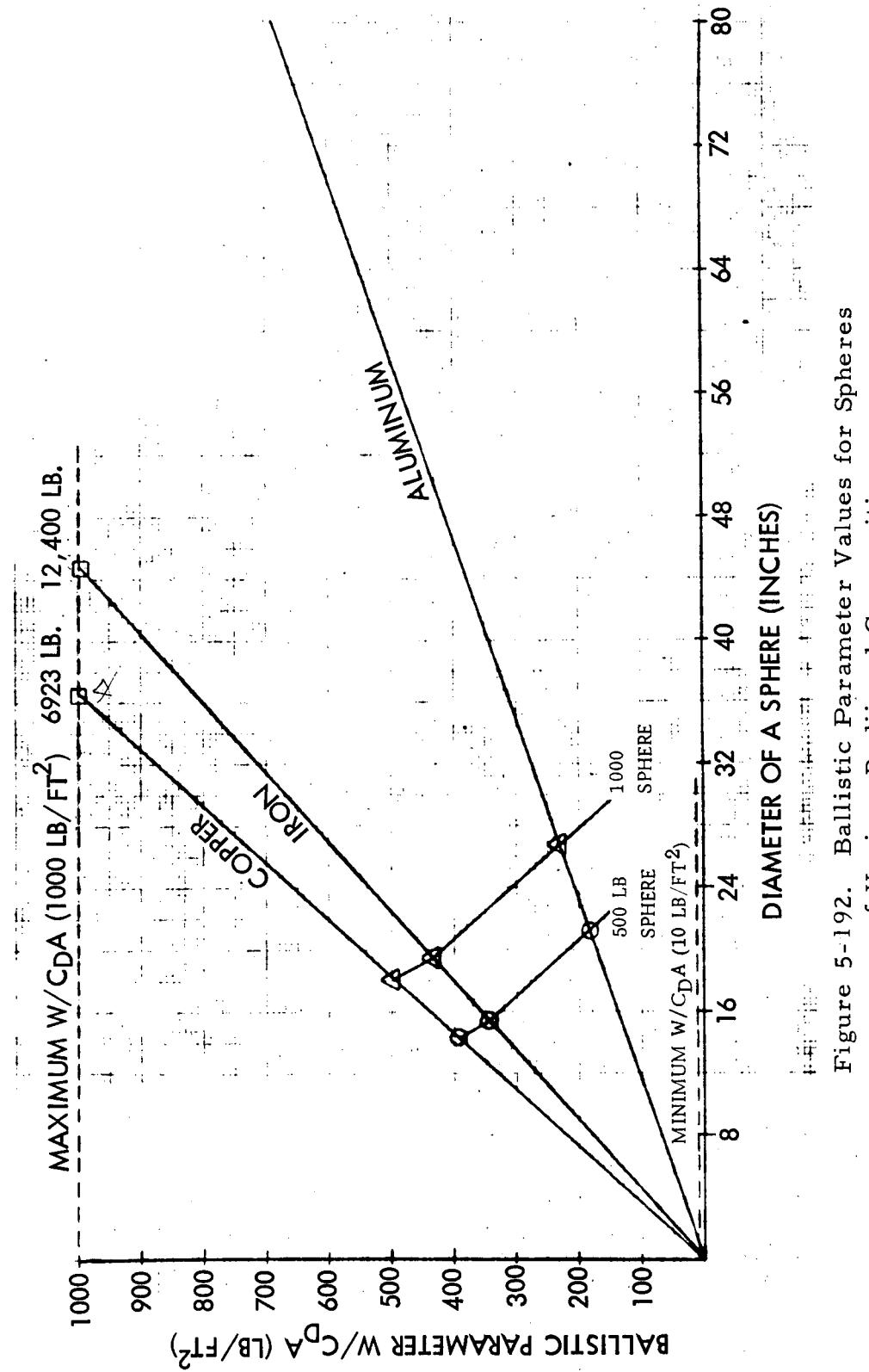


Figure 5-192. Ballistic Parameter Values for Spheres
of Various Radii and Composition

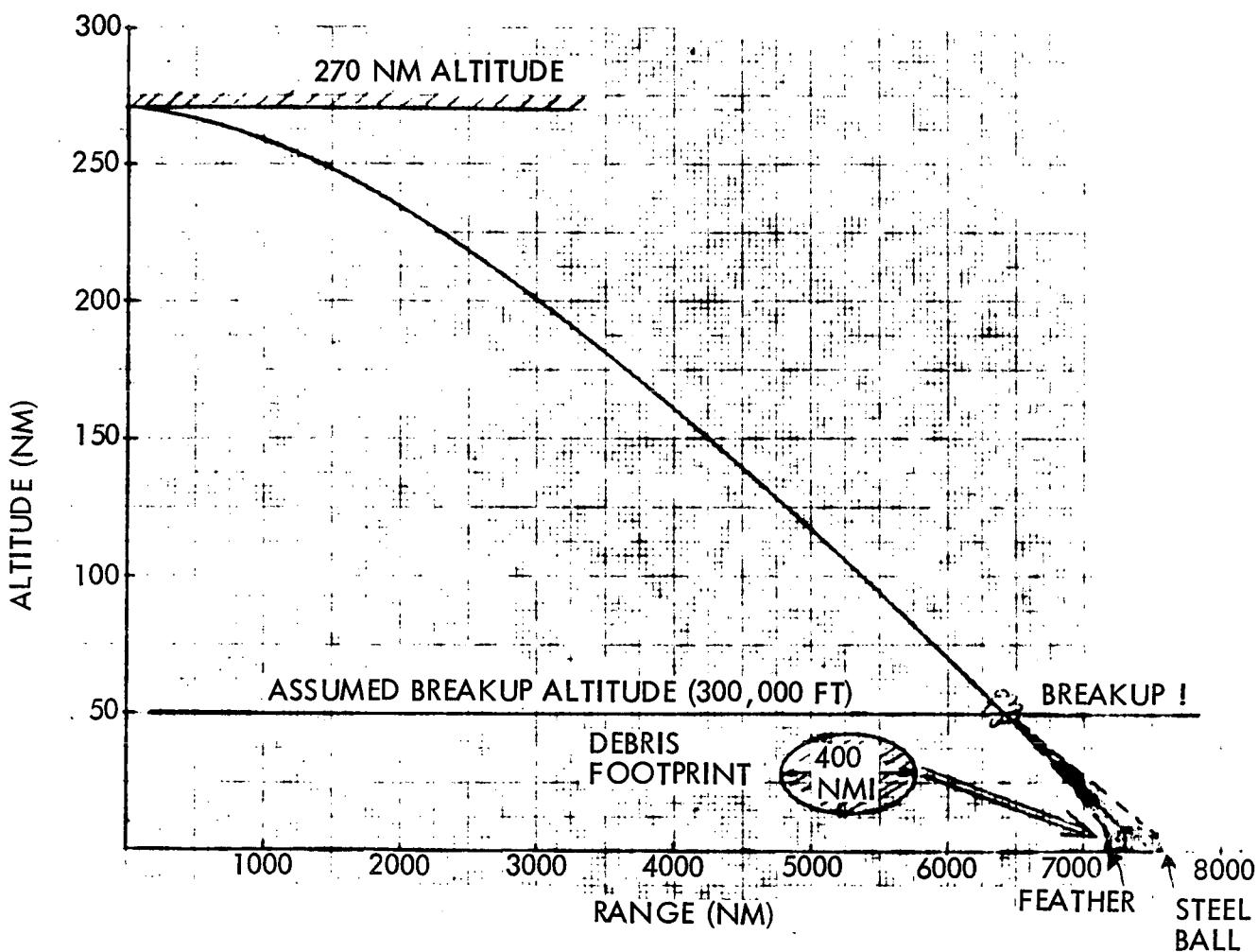


Figure 5-193. Debris Footprint Resulting From ESS Vehicle Breakup

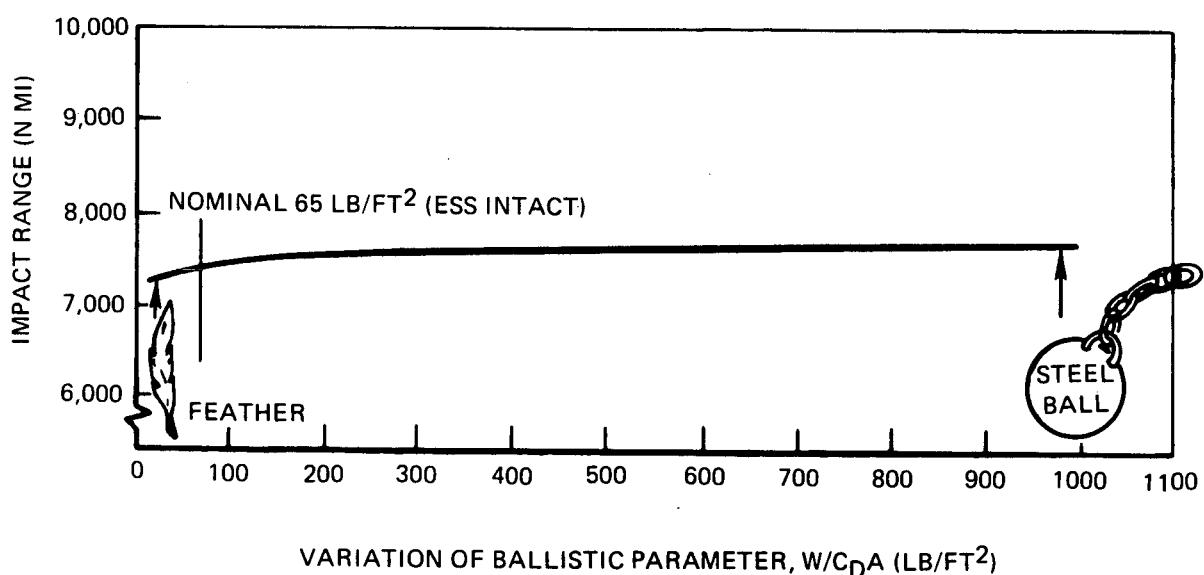


Figure 5-194. Impact Range Versus Ballistic Parameter



This long burn time will reduce the accuracy of the deorbit control system due to vibration effects and the lack of cross-product steering, and it is estimated that the resultant average attitude error might be as high as ± 20 degrees.

Under the best-case conditions, shutdown will be controlled by velocity cutoff rather than by a sequencer. Velocity cutoff will allow shutdown to within ± 1 percent of the desired value. Removal of the inertial measurement unit (IMU) before deorbit will result in economic savings, but without the IMU the OMS velocity error will be larger (approximately ± 3 percent). In addition, an error of about ± 1 percent will be caused by variations in the OMS residual propellant weight. The overall ΔV error for the worst case is therefore equal to ± 4 percent of the total deorbit velocity increment.

The reentry range variations tabulated in Table 5-13 were obtained by making a series of computer simulations of the various reentry trajectories. Under best-case conditions, note that the largest share of the footprint length results from vehicle breakup. On the other hand, for worst-case conditions, the largest contributor is the ΔV error.

The total footprint was obtained by algebraically summing the effect of the various perturbations. The resultant maximum total footprint is 1520 nautical miles long (including the effects of vehicle breakup), and the minimum footprint length is 790 nautical miles. The maximum width of the footprint is estimated to be about 60 nautical miles. The main contributors to the crossrange dispersion are the yaw attitude error and the effects of winds on the descending fragments.

Algebraically summing the effects yields an overly generous footprint size, because the various perturbative influences will not occur simultaneously at their maximum level. The perturbations are actually statistically independent effects, and thus it is more appropriate to combine them by root-sum-squaring in accordance with the laws of statistics. The maximum and minimum root-sum-square values are tabulated in Table 5-13.

Deorbit Opportunities

The largest footprint obtained in the previous discussion has a length of 1520 nautical miles and a width of 60 nautical miles (assuming breakup at 300,000 feet). As shown in Figure 5-195, this footprint fits comfortably into many open ocean areas. Sketches of three typical deorbits are shown in the figure. Note that the deorbit burn (550 ft/sec at 17 degrees) must be scheduled about 135 degrees short of the desired impact point.

Table 5-13. ESS Deorbit Footprint

Variables	Nominal Value	Best Conditions		Worst Conditions	
		Perturbation	Total Range Variation (nm)	Perturbation	Total Range Variation (nm)
Vehicle Breakup	Breakup at 300,000 feet assumed	W/CDA varies from 1.0 to 1000 lb/ft ²	400 400	W/CDA varies from 10 to 1000 lb/ft ²	400 400
Retro ΔV	500 ft/sec	±1%	130	±4%	510
Firing Angle	17 deg	±5 deg	100	±20 deg	450
Altitude	270 nm	±1 nm	60	±1 nm	60
Other (winds, ignition time error, error, atmospheric density)	-	-	100	-	100
Total Footprint (algebraic sum)	-	-	breakup $390 + \frac{400}{400} =$ 790 nm	-	$1120 + \frac{400}{400} =$ 1520 nm
Total Footprint (root-sum-square)	-	-	breakup $201 + \frac{400}{400} =$ 601 nm	-	$690 + \frac{400}{400} =$ 1090 nm



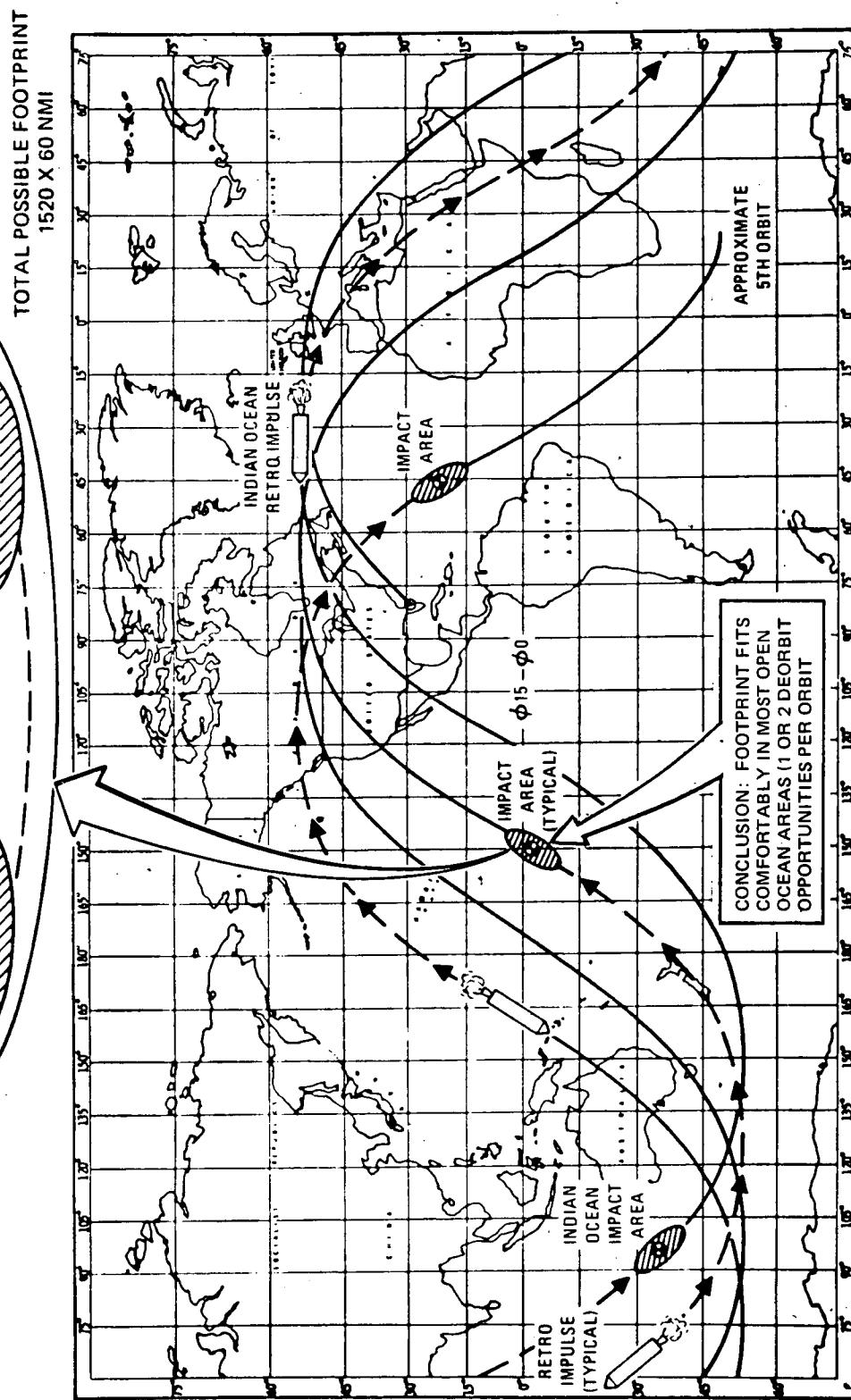
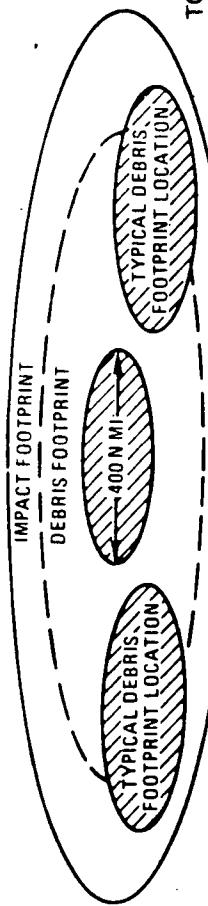


Figure 5-195. ESS 1520-NM Impact Areas



To minimize computer time, the deorbit range values obtained were simulated with the tacit assumption of an impulsive deorbit burn (i.e., of zero duration). In reality, however, the nominal burn time will be about 92.5 seconds, during which the spent stage will travel several hundred nautical miles. Numerical integration of the nominal deorbit case with a finite burn shows that the nominal impact point is 167 nautical miles farther downrange than in the case of an impulsive burn. The extra range results from the fact that when a finite burn is employed, the vehicle gradually reaches the deorbit velocity, and during this interval it is hurtling downrange.

The difference between impulsive and finite burn deorbit simulations is not large enough to change any of the conclusions of this study. However, in the actual preflight deorbit trajectory simulations, a finite burn should be used for determining the predicted nominal impact point.

Effects of Lift

The effects of lift on debris fragments was not considered in this study because it was felt that the fragments will tumble randomly and the net lift will be zero. (A similar assumption was made in the analysis documented in Lockheed TM 54/30-232, Retro Velocity Requirements for Controlled Reentry of the S-II Stage From Various Orbits.) If, on the other hand, some of the fragments should undergo lift, the debris footprint would be significantly enlarged. The impact range for a fragment with a lift-to-drag ratio of 0.5, for example, would be 1400 nautical miles greater than that of the same fragment with a lift-to-drag ratio of zero.

Engine Failure Effects

Engine failure would lengthen the burning interval. Ignition failure of one OMS engine, for example, would double the deorbit burn time, and, as a result, the nominal impact point would be 168 nautical miles farther down range. Should both OMS engines fail to ignite, the ACPS system would be used to generate the required deorbit ΔV , and the impact point would be about 693 nautical miles farther down range than if the OMS engines had burned successfully. This value was determined with the assumption that the ACPS would be ignited within a fraction of a second of OMS failure. Theoretically, this could be accomplished by igniting both the OMS and the ACPS engines simultaneously or by having a self-monitoring system that would sense ignition failures and automatically fire the backup system. If these approaches prove to be impractical, an alternative approach would be to have the vehicle coast to the next desirable deorbit point where the backup system would be ignited. Table 5-14 presents the important performance parameters for firing the various engine combinations. The ACPS system



Table 5-14. Effect of Engine Failures on ESS Deorbit
($\Delta V = 550$ ft/sec, $\alpha = 17^\circ$)

Engines Operating	Thrust (lb)	Burn Time (sec)	Specific Impulse (sec)	Range to Impact (nm)	Range to Impact (nm)	Propellants Consumed (lb)	Guidance Accuracy (degrees)
Impulsive ΔV	-	0	451.4	7300	(-167)	4100	5
Two OMS	20,000	88	451.4	7467	0	4100	5
One OMS	10,000	135 to 185	451.4	7635	168	4100	5
Two ACPS	4,200 * C. L. Thrust = 3946	-	370.0	8160	693	5300	20

*Engines Canted 20°



requires a larger propellant supply by 900 to 1200 pounds than the OMS system. The extra range resulting from the ACPS system's longer burning interval can be tolerated by planning the nominal splashdown in an ocean area large enough to absorb both the impact ellipse and the extra 693 nautical miles that would result from a failure of both OMS engines.

Solar Orbit Disposal

Driving the spent stage into a solar orbit is sometimes suggested as a practical alternative to earth deorbit. Like deorbit, this technique eliminates all recontact hazards once and for all and has the added advantage of eliminating all hazards to personnel. Unfortunately, the velocity increment required to reach the energy of escape is more than 10,000 fps and the corresponding propellant supply amounts to more than 100,000 pounds. These values were computed with the assumption that the vehicle starts in a 270-nautical-mile orbit. At higher orbital altitudes, however, the deorbit ΔV increases and the escape ΔV decreases. It therefore seems plausible that at some altitude it is equally easy to drive the vehicle up to escape velocity or to deorbit it into the ocean. As is shown in Figure 5-196, this altitude is 13,000 nautical miles and the accompanying minimum ΔV is about 5000 fps. Solar orbit disposal is therefore, of only theoretical interest.

Conclusions

The analysis presented above leads to the following specific conclusions:

1. Controlled deorbit of the ESS stage is feasible using the OMS as the primary propulsion system and the ACPS as a backup.
2. The nominal velocity increment is equal to 550 fps at a nose-down firing angle of 17 degrees. (Maximum nominal propellant consumption is 4100 pounds with 5300 pounds required if both OMS engines fail.)
3. Assuming vehicle breakup occurs at 300,000 feet, the resulting fragments will cover a 400-nautical-mile impact region a few nautical miles in width.
4. The maximum impact footprint dispersions will result from an ACPS system deorbit controlled by a sequencer. Under these conditions, the total footprint will span at most 1520 nautical miles of ocean.

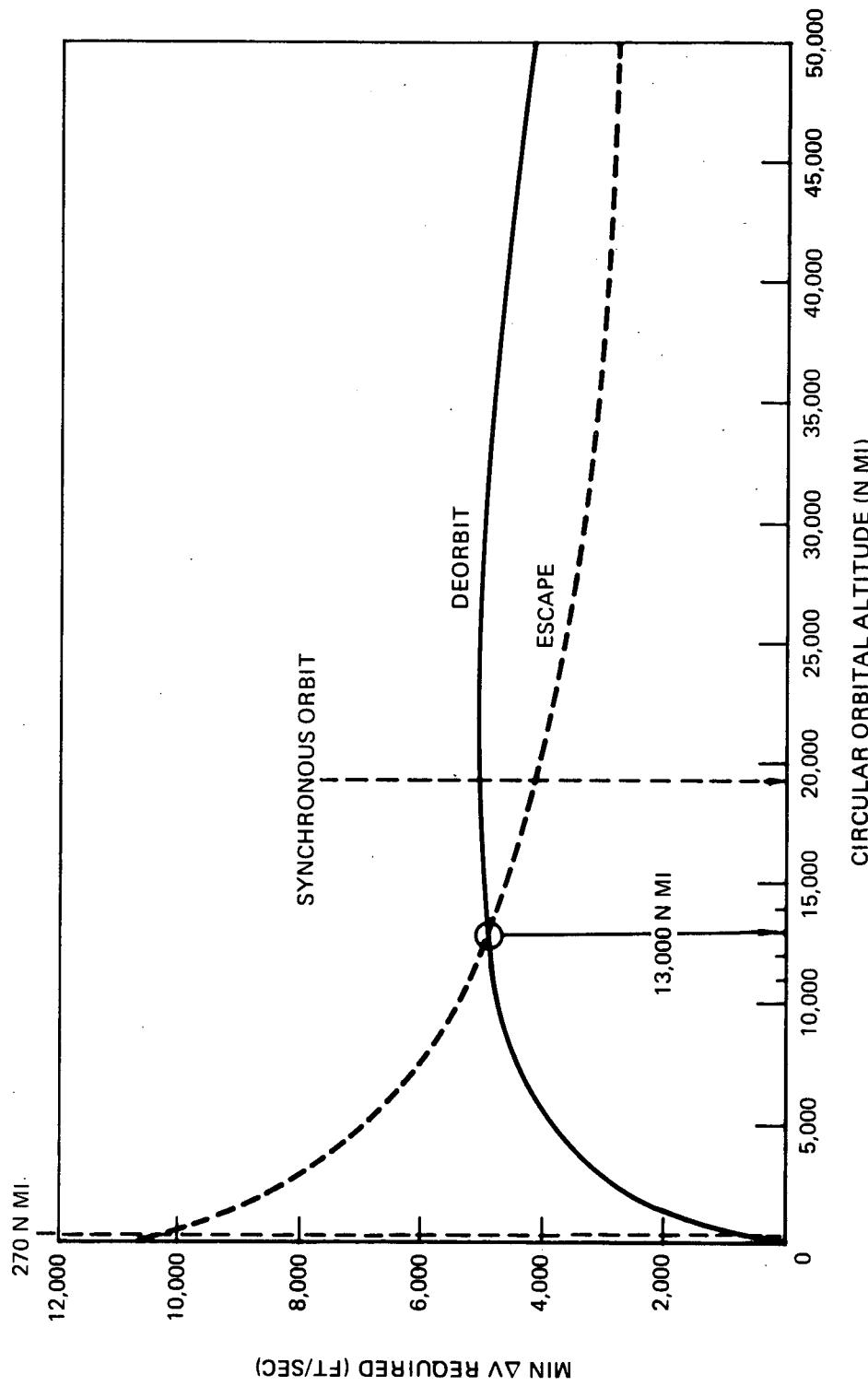
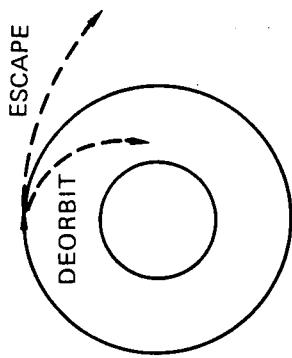


Figure 5-196. Minimum Velocity Required to Deorbit and Escape From a Circular Orbit



5. Footprints in the 1500-nautical-mile range fit comfortably into many open ocean areas and, in general, the vehicle will have one or two deorbit opportunities per orbit.
6. Control of the deorbit maneuver firing time will allow the vehicle to be dropped into one of the safe ocean areas. The burn should be performed about 135 degrees short of the desired impact point.
7. Ignition failure of one OMS engine would result in the nominal impact point being displaced downrange 168 nautical miles.
8. Provisions for using the ACPS engines as a backup in case of a failure of both OMS engines could be made by scheduling instantaneous ignition of the ACPS engines upon OMS failure or by firing them at a subsequent deorbit opportunity. In either case, the entry range will be 693 nautical miles greater than the case of successful ignition of the OMS engines.
9. Disposal of the ESS stage by driving it into a solar orbit is completely impractical (the required ΔV amounts to more than 10,000 fps).



5.4 SYSTEM SAFETY

The prime system safety consideration is the elimination, minimization, and/or control of potential hazards associated with the reusable booster - expendable second stage (ESS) conceptual configuration. The emphasis of the safety effort for this study was, therefore, upon defining measures which would tend to prevent, or reduce the probability of, occurrence of an emergency or hazardous condition.

The safety measures defined are integrated with, and expressed as safety, reliability, and quality criteria for the ESS. The criteria may be used as a checklist to evaluate the safety considerations included in, or omitted from, vehicle design. A more valuable application, however, is to use the criteria to provide a safety baseline against which other desirable ESS vehicle features or aspects of vehicle development could be compared for vehicle optimization.

The safety study revealed that an acceptable level of system safety could be achieved within the current technological base. There are some areas, however, in which uncertainties exist or assumptions were made which indicate the necessity of further consideration. The areas that require further consideration are the separation mechanism system and the separation signal system to be utilized by the ESS-shuttle booster configuration.

5.4.1 Methods of Approach and Assumptions

The safety effort of the study accomplished, so far as possible, the identification of hazard potentials that would affect vehicle safety. This assumption was necessary in order to scope the safety effort. The techniques utilized involved a review of shuttle - orbiter data, the identification of potential hazards and relevant safety guidelines, and the generation of applicable safety criteria.

A logic analysis was initiated to represent conditions which, taken singly or in combination, could result in the development of specific undesired events. This analysis resulted in gross, top-level conditions describing only major components of functions Figure 5-197. Three specific hazardous potentials were analyzed as extensions of the statement contained in Figure 5-197: explosion and/or fire, contamination, and radiation. The analysis consists of describing the basic undesired condition; subdividing the condition into numerous subsidiary undesired events by several different, but appropriate, categories; indicating the events which would cause each subsidiary undesired event; and reiterating the process to establish basic identifiable causal events.

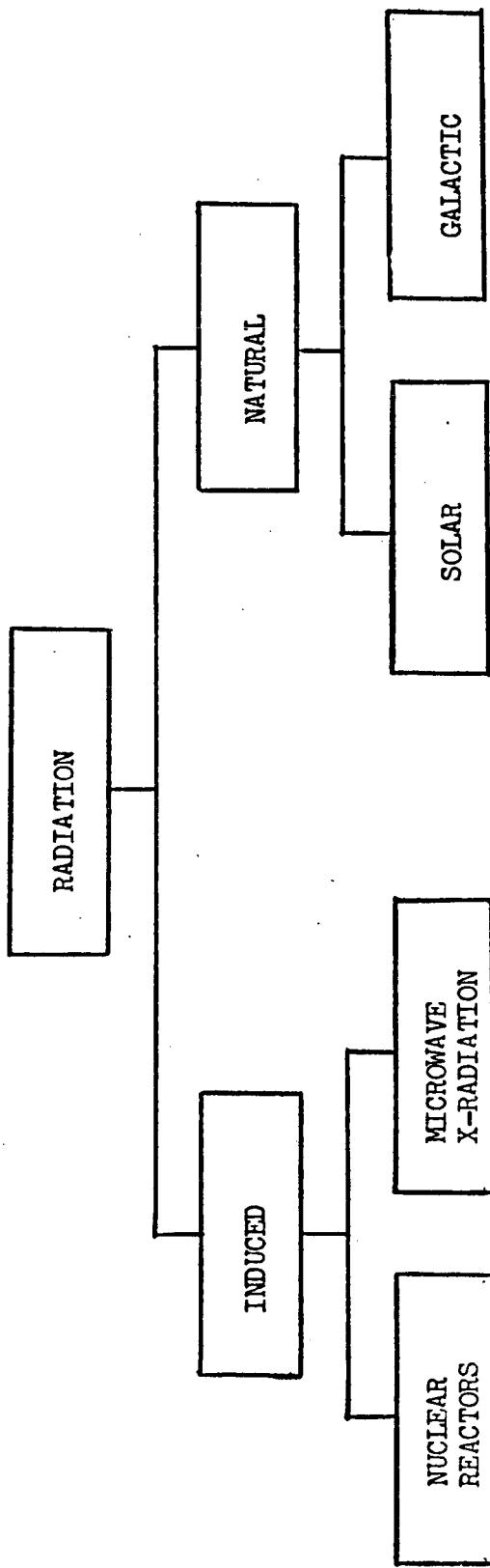


Figure 5-197. Gross Hazards Analysis (Sheet 1 of 4)

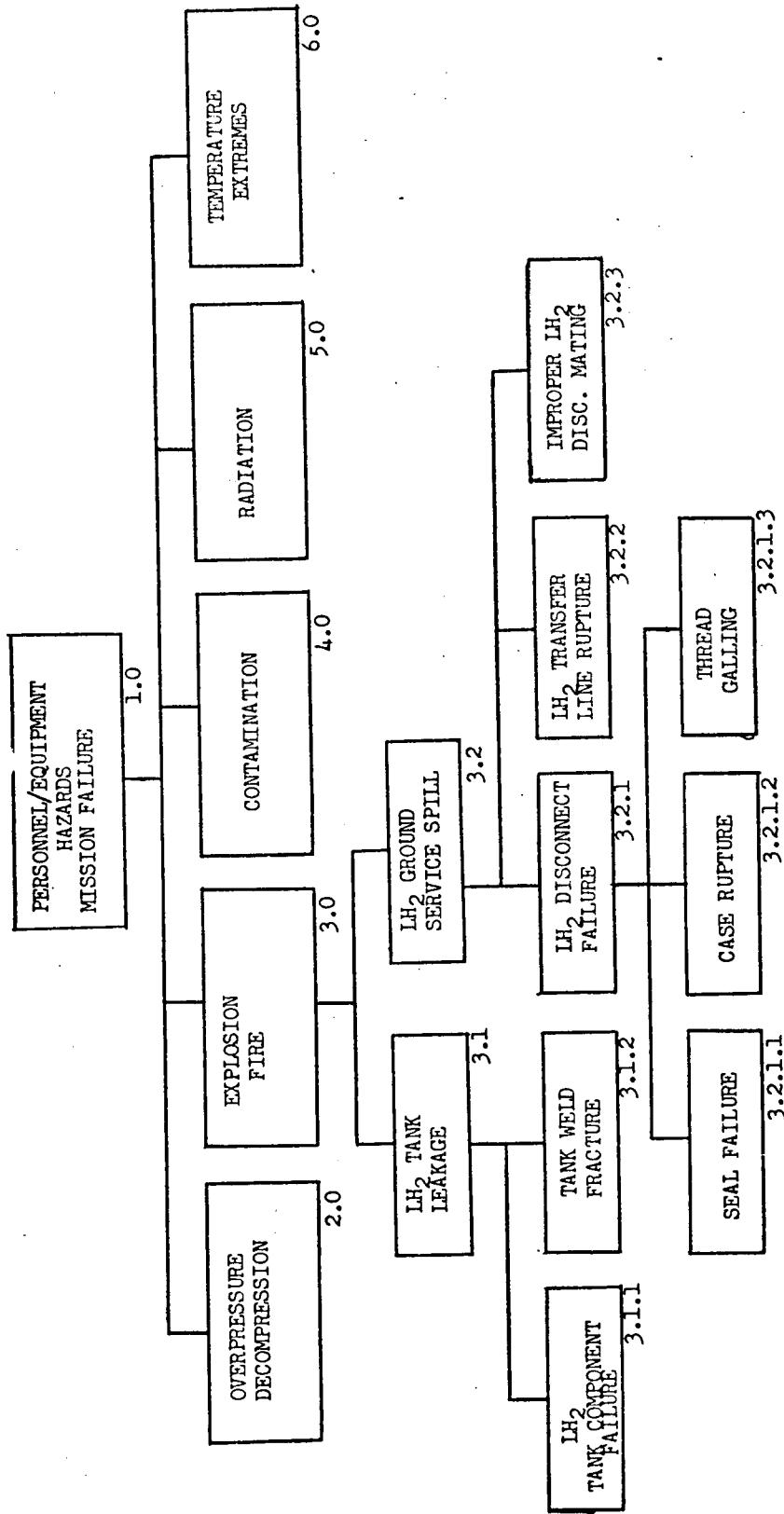


Figure 5-197. Gross Hazards Analysis (Sheet 2 of 4)

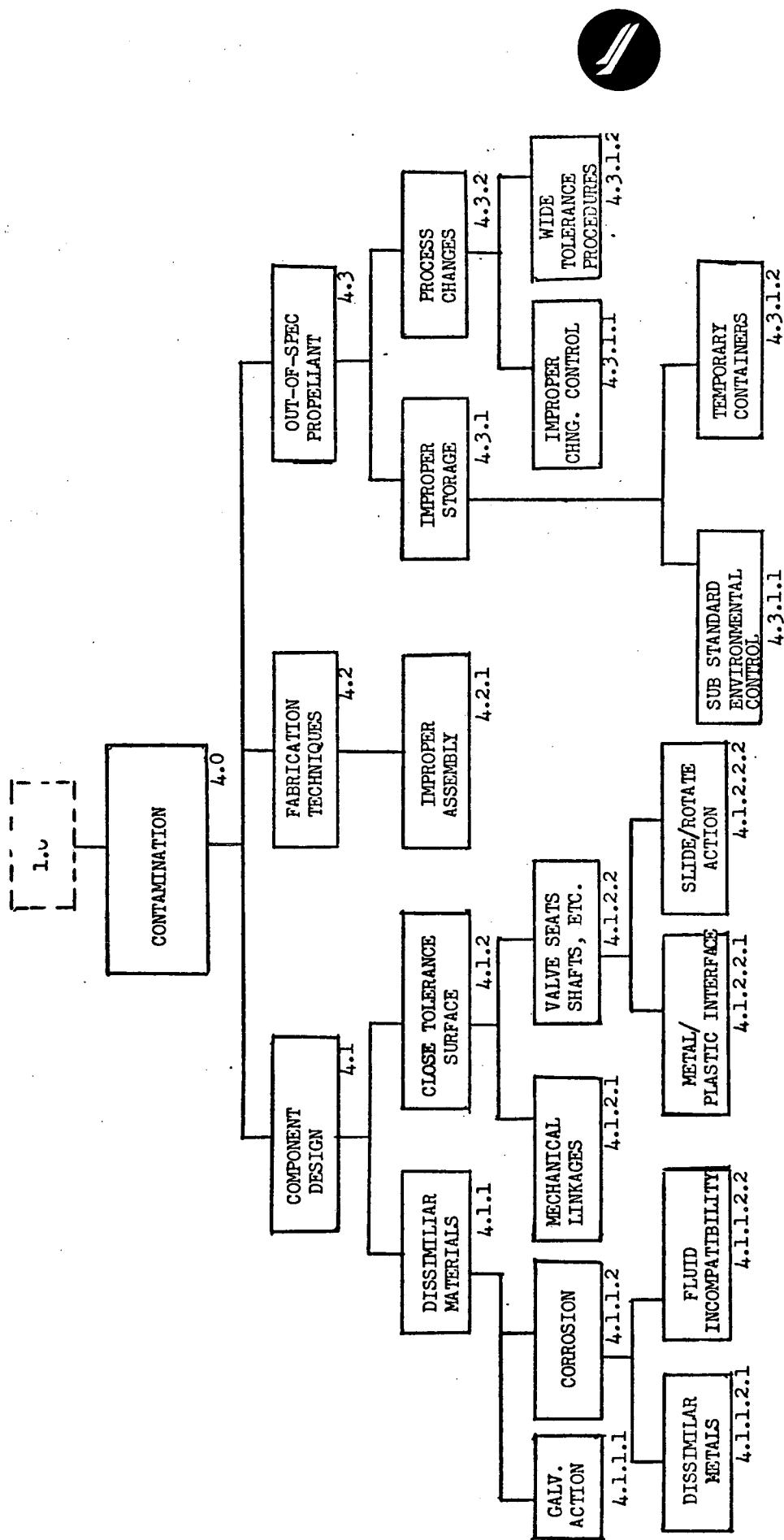


Figure 5-197. Gross Hazards Analysis (Sheet 3 of 4)

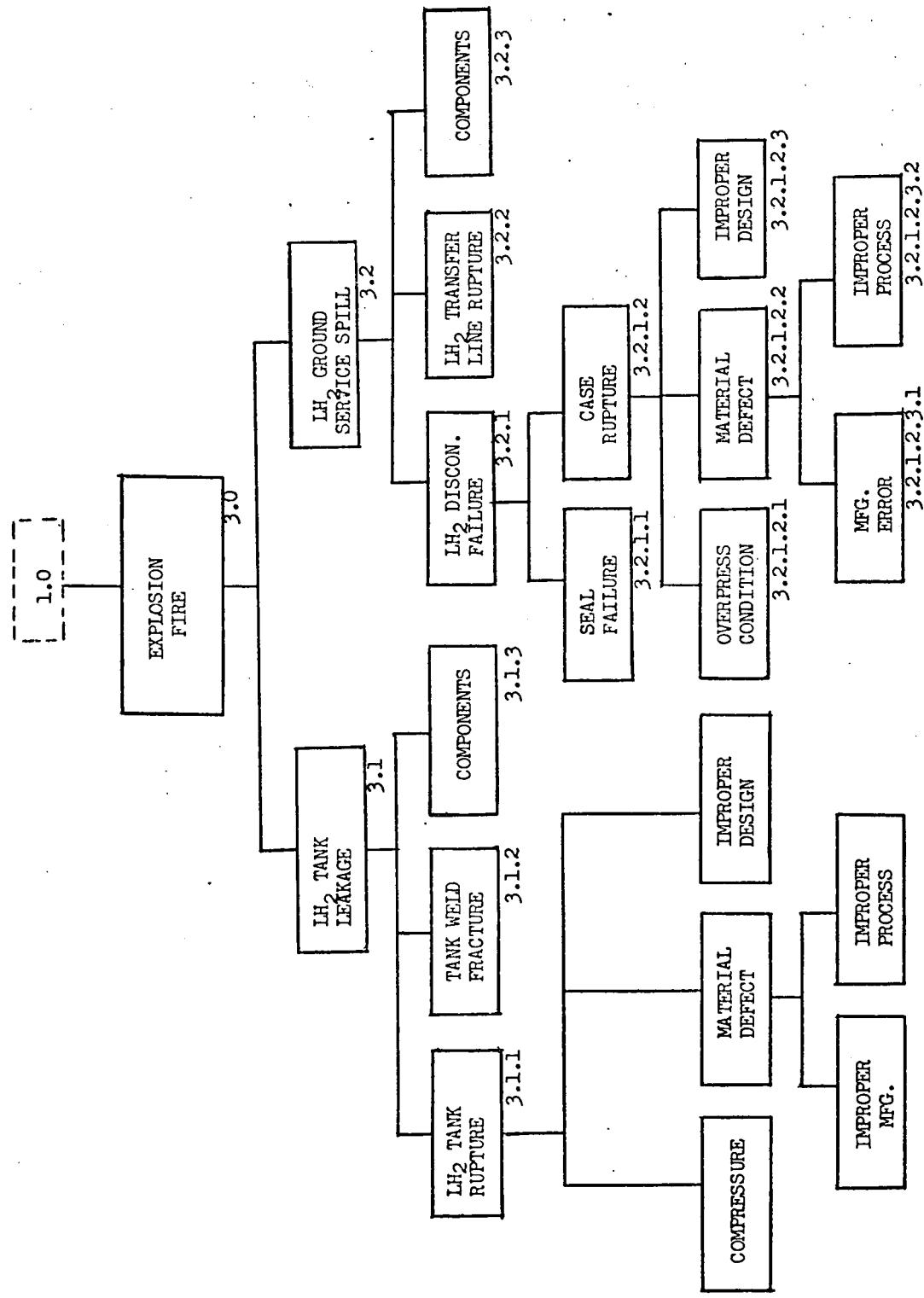


Figure 5-197. Gross Hazards Analysis (Sheet 4 of 4)



5.4.2 Areas Requiring Further Effort — Separation System

The separation signal system used with the orbiter is basically the same as that used with the ESS, based on the computers of each vehicle and associated controls. This in turn requires no modification to the booster separation system. A final backup severing system is required on the separation links to meet the FO/FS requirement.

In the event of an abort separation, in an atmospheric environment, a potential catastrophic hazard exists due to the absence of aerodynamic stability in the second stage. This stage will probably begin to tumble and may disintegrate (explode) before the booster is a safe distance away. Based on the FO/FS of the booster and the safe-landing requirement of fuel depletion in the booster, the incidence of such an atmospheric separation probability is considered to be very low.

Identification of Hazard Potentials

The identification of gross hazard potentials reflect these conditions that are inherent to ESS design, such as the vehicle requirement to contain extremely large quantities of high energy propellants. The hazard identification data in Table 5-15 include the description of the hazard, the hazard group code, and safety guidelines that are intended as preventive measures rather than remedial. Individually, each guideline expresses or suggests some measure which will lessen the probability of occurrence of an undesired event or alleviate a hazard to some finite degree. In the aggregate, they represent a list of measures which should be taken to enhance vehicle safety.



Table 5-15. ESS Preliminary (Gross) Hazard Identification

Page 1 of 8

Date Feb. 1971

<u>HAZARD GROUP</u>	<u>HAZ. GR. CODE</u>
EXPLOSION/FIRE	B,M
<u>HAZARD DESCRIPTION</u>	
This group includes violent disruption of the expendable second stage, sectors of the stage, or components within or attached to the stage. The disruption may result from over-pressure, chemical, electrical and/or physical conditions.	
<u>SAFETY GUIDELINE</u>	
All relays including motor start relays, switches, commutators, etc., which can produce an electrical arc, should be hermetically sealed. This seal should continue to provide full protection during and after being subjected to deep space vacuum.	
Design of overboard vent/dump mechanism should preclude the possibility of accumulation of flammable/explosive material near the stage.	
The stage subsystem design should provide the capability of returning to a safe condition at anytime during separation, test, or maintenance.	
Propellant tanks should have enough separation or adequate shielding, to minimize damage to other tanks in the event one tank ruptures.	
Stage pressure systems should be capable of withstanding all structural, acceleration, or other loads which are not of hydraulic/pneumatic origin, without sustaining damage.	



Table 5-15. ESS Preliminary (Gross) Hazard Identification (Cont)

Page 2 of 8

Date Feb. 1971

<u>HAZARD GROUP</u>	<u>CONTAMINATION</u>	<u>HAZ. GR. CODE</u>	<u>K</u>
<u>HAZARD DESCRIPTION</u>			
This group includes hazards which are related to or caused by stage contamination. The sources of contamination vary and include by-products produced through outgassing and interreactions among various combinations of chemicals and/or hardware. In many cases, contaminants will be present in trace amounts only, but in some cases a potential contaminant will be on-board the stage in significant quantities.			
<u>SAFETY GUIDELINE</u>			
Equipment, including electrical wiring, that could become contaminated or damaged by leaking propellants should be located to preclude coming in contact with possible leakage or should be provided suitable protection.			
All orifices, close tolerance valves and contamination - sensitive equipment in fluid systems should be adequately protected from contamination.			
Filter design should take into consideration the increased demand imposed by zero-g operation to remove contaminants which, under one-g operation, would naturally separate out.			



Table 5-15. ESS Preliminary (Gross) Hazard Identification (Cont)

Page 3 of 8

Date Feb. 1971

<u>HAZARD GROUP</u>	<u>HAZ. GR. CODE</u>
IMPACT, VIBRATION & ACCELERATION	D
<u>HAZARD DESCRIPTION</u>	
This group includes hazards associated with all planned or unplanned motions of the stage without regard to the cause of or reason for the motion.	
<u>SAFETY GUIDELINE</u>	
Materials used for insulation or filler of stage walls should be noncombustible.	
The flight path selection required during the mission should be such that the probability of collision with man-made debris and other space items is sufficiently low to provide adequate confidence to proceed with the mission.	



Table 5-15. ESS Preliminary (Gross) Hazard Identification (Cont)

Page 4 of 8

Date Feb. 1971

<u>HAZARD GROUP</u>	<u>RADIATION</u>	<u>HAZ. GR. CODE</u>	A
<u>HAZARD DESCRIPTION</u>			
Hazards in the group are defined as those which are associated with any or all of the following: alpha particles, beta particles, gamma rays, x-rays, cosmic rays, neutrons, high-speed electrons, high-speed protons, and other atomic particles. Also associated with this group of hazards are RF energies emitted by electrical equipments.			
<u>SAFETY GUIDELINE</u>			
Should radar and/or communications equipment exist on-board sufficient to present a hazard for equipment to the produced RF or x-radiation, then positive protective measures should be incorporated.			
The stage radiation protection provisions should be consistent with the flight path type orbital height, and inclination selected.			
Radiation effects upon stage electronic materials, Microelectronic circuit elements, electrical systems, metals, ceramics, polymers, and other organic and inorganic materials should be thoroughly investigated for radiation-induced transient and permanent effects in terms of false signals, degradation, catastrophic failures and contamination.			



Table 5-15. ESS Preliminary (Gross) Hazard Identification (Cont)

Page 5 of 8

Date Feb. 1971

<u>HAZARD GROUP</u>	<u>TEMPERATURE EXTREMES</u>	<u>HAZ. GR. CODE</u>	C
<u>HAZARD DESCRIPTION</u>			
This group includes those hazards associated with the departure of temperatures from normal, including temperature increases, decreases, or fluctuations. It also includes extreme heat, such as that generated by fire, and extreme cold, such as that associated with cryogenics and the space environment itself.			
<u>SAFETY GUIDELINE</u>			
Adequate cooling capability should be provided to prevent overheating of electrical power sources even during worst-case conditions.			
Current limiting devices or techniques should be used to preclude hazardous over-currents. They should provide protection both to the current source and to the "using" equipment.			
Design provisions should be made which assure that no heated surfaces would provide a source of ignition.			
The stage thermal protection provisions should be consistent with the flight path type, orbital height, and inclination selected.			



Table 5-15. ESS Preliminary (Gross) Hazard Identification (Cont)

Page 6 of 8

Date Feb. 1971

<u>HAZARD GROUP</u>	<u>DECOMPRESSION/OVERPRESSURE</u>	<u>HAZ. GR. CODE</u>	L
<u>HAZARD DESCRIPTION</u>			
This hazard group includes those systems utilizing pressurized fluids that could result in overpressures and subsequent rupture or explosion, or leakage and contamination, or decompression that may affect vehicle safety.			
<u>SAFETY GUIDELINE</u>			
Any pressurizable volume that can be confined or isolated by any means, such as by valves, should include some means for automatic protection from over-pressure.			
Any pressurizable volume where decompression is a critical condition; positive means shall be incorporated to prevent volume collapse or degradation of structural integrity.			



Table 5-15. ESS Preliminary (Gross) Hazard Identification (Cont)

Page 7 of 8

Date Feb. 1971

<u>HAZARD GROUP</u>	<u>PREMATURE ARMING OR DELAYED DISARMING</u>	<u>HAZ. GR. CODE</u> <u>GENERAL</u>
<u>HAZARD DESCRIPTION</u>		
Premature arming (separation devices, squibs, etc.) creates the risk of inadvertent and possible undesirable operation of that equipment, by increasing exposure time to the possibility of stray currents or transient voltages.		
<u>SAFETY GUIDELINE</u>		
Stage subsystems should be armed only when they are to be used, and immediately disarmed when their function is no longer required or subsequent use will not be for a prolonged period.		



Table 5-15. ESS Preliminary (Gross) Hazard Identification (Cont)

Page 8 of 8

Date Feb. 1971

<u>HAZARD GROUP</u>	<u>HAZ. GR. CODE</u>
ABNORMAL PROPULSION PERFORMANCE	GENERAL
<u>HAZARD DESCRIPTION</u>	<u>GENERAL</u>
<p>1. Inability to achieve thruster cut-off - excessive thruster burn time could result in an angular rate detrimental to stage structure, equipment, and/or payload.</p> <p>2. Premature engine cut-off and/or inadequate thrust conditions - these conditions could result in mission/vehicle loss by failing to achieve required flight trajectories.</p>	
<u>SAFETY GUIDELINE</u>	
1. Provision should be incorporated for sensing build-up toward excessive angular rates with automatic thrust termination mechanisms.	
2. Provisions should be incorporated to provide the necessary mechanisms to preclude inadvertant and/or premature thruster cutoff.	

APPENDIXES

APPENDIXES



APPENDIX A. COST/DESIGN PERFORMANCE MANAGEMENT PLAN FOR ESS PHASE B STUDY

1.0 INTRODUCTION

1.1 PURPOSE AND OBJECTIVES

Consideration of cost in all design activities was a primary requirement of the ESS in the reusable shuttle booster Phase B effort. A management plan was established that provided management with the timely information of cost/design performance so that management control could be exercised over the system design to meet the low cost, economical, space transportation system objectives.

This document describes the plan by which the above objectives were accomplished. It fulfills the requirements set forth in the following sections of Contract NAS9-10960, Exhibit B, MSC-JC421-M67-1-1P, "Phase A/B Study for an Expendable Second Stage on a Reusable Shuttle Booster," July, 1970, and revised August 26, 1970:

Paragraph 5.8 of the Statement of Work, "Cost Consideration in Design."

Section VI of the Study Control Document, "Cost Control and Design Performance Management System."

1.2 SCOPE

This plan describes the Phase B study of the Expendable Second Stage on a Reusable Shuttle Booster Program. The plan includes all program phases (DDT&E, recurring production, and recurring operations) and includes the hardware, software, personnel, and consumables required, per the WBS, to provide and operate a complete system to meet the program objectives. Identification of specific items which were excluded from the systems/program costs are shown in Section 4.3. Although there were system/program elements not under the direct control of North American Rockwell, these elements were considered in the trade study efforts.



1.3 REQUIREMENTS

This plan was to provide management with the depth of visibility into the design of the system necessary to direct and control the design. The visibility requirement was relative to cost and performance, since cost was one of NASA's defined controlling criteria.

In this plan, management was represented by the Engineering Review Board (ERB) which reviewed the alternatives (trade studies) for the subsystem designs. Alternatives that could not be resolved by the ERB were taken to the next higher management group called Program Review Board (PRB). All engineering activities were directed through the ERB (approval to conduct trade studies, the approval to proceed on particular designs, etc.). This ERB/PRB action was appropriate to WBS Levels 2, 3, 4, and 5.

Subsystem Management was responsible for design decisions for items of WBS Levels 6, 7, etc., except where those decisions resulted in changing the ERB/PRB directed items of WBS Level 2, 3, 4, or 5.

Figure A-1 presents the logic diagram for the flow of data and activities. It also shows the activity responsibility.

Basically, the plan required:

1. Establishment of the baseline system/program and its cost effectiveness
2. Establishment of alternative systems (based on the baseline system)
3. Definition of cost effectiveness requirements for each alternative system/program
4. Comparison of each alternative system/program with the baseline system/program and selections made from those various alternatives.
5. An updated or revised baseline system was defined, composed of the selected subsystems and operations, then reevaluated and compared with the original baseline.
6. When the comparison noted in Step 5 above showed that the cost effectiveness of the new baseline system was not superior to that of the previous baseline, the reasons were analyzed and a new baseline was defined. Steps 5 and 6 were repeated until the most cost effective system was defined.

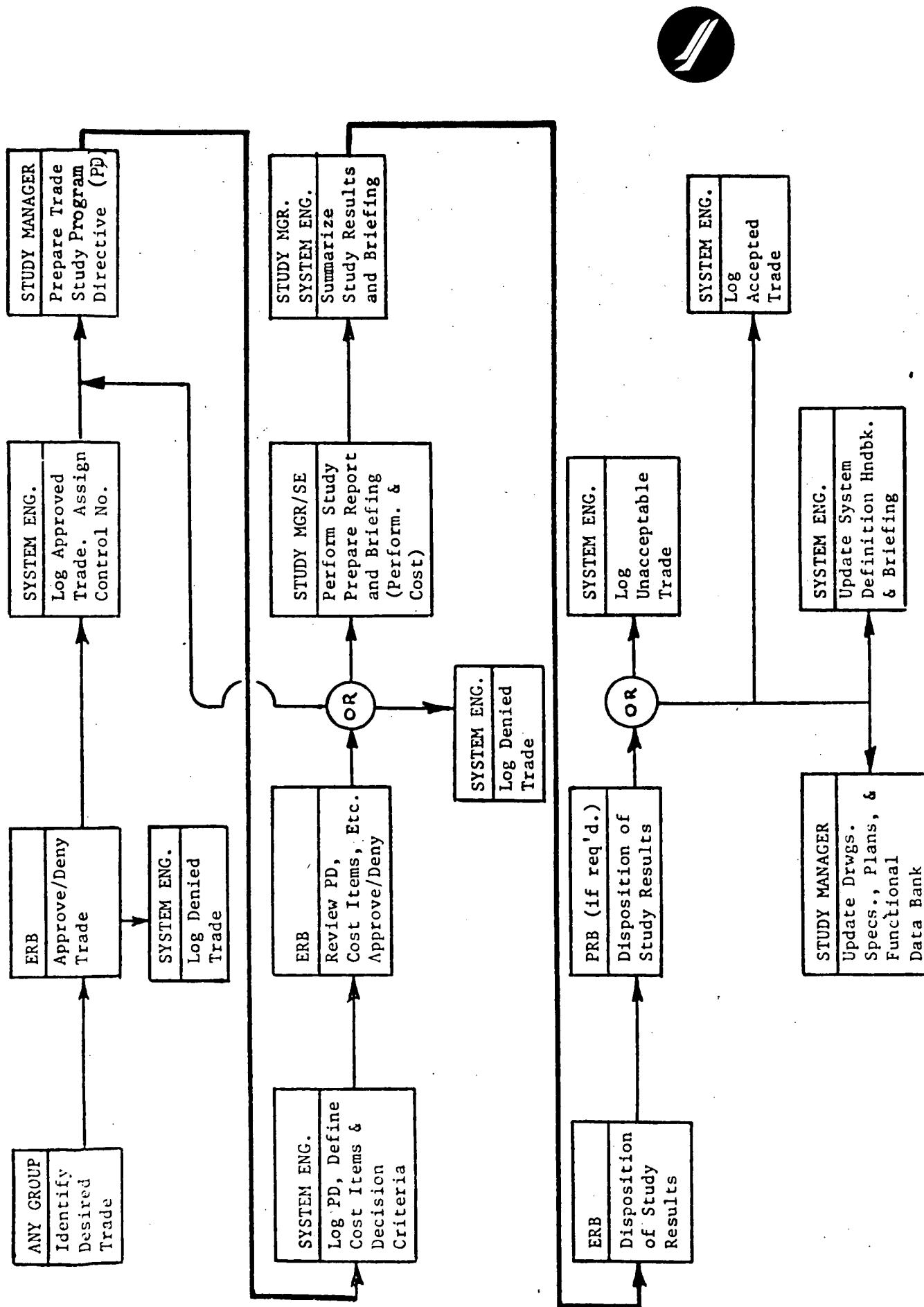


Figure A-1. Cost and Performance Considerations



1.4 SCHEDULE OF MILESTONES

Figure A-2 shows the milestone schedule of the events accomplished during the Phase B study program to meet the requirements of, and maintain the cost/design performance management plan.

	MARCH	APRIL	MAY	JUNE
Mgmt. Plan Defined	▲			
First ERB Action	▲			
Choice System/ Program Reevaluated		▲ ▲	▲	
Final ERB Review				▲
Final Report & Briefing				▲

Figure A-2. Milestone Schedule



2.0 WORK BREAKDOWN STRUCTURE

The work breakdown structure (WBS) upon which this plan was based is shown in Figures A-3 and A-4. All estimated costs and the cost/ performance evaluation of trade studies (Section 4.0) were structured using this document as a guideline. The trade studies were conducted at levels appropriate to the defined WBS details.

The initial baseline cost/performance is shown in Section 4.1 at the WBS Level 4. As design details were defined, the costs were estimated at levels consistent with that information. The final report contains cost estimates to Level 5. A dictionary of WBS terms is shown in Volume XI, Appendix A. The WBS conforms to suggestions in Section VIII of the Study Control Document and is similar to the WBS used for the basic space shuttle study.

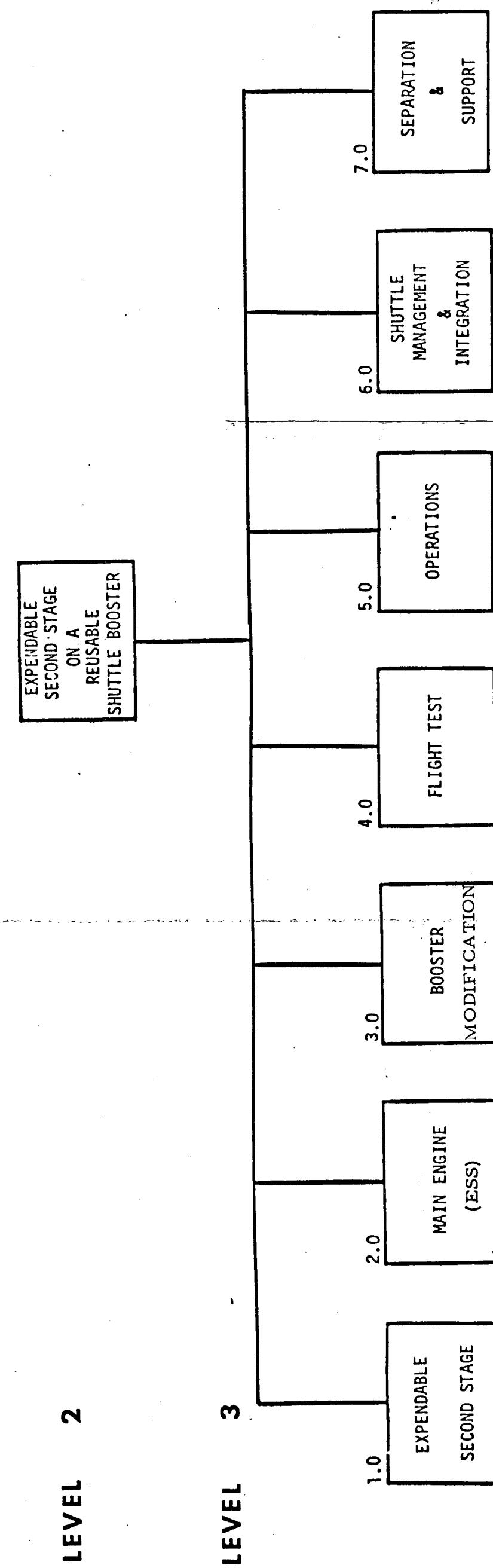


Figure A-3. Work Breakdown Structure Summary

PRECEDING PAGE BLANK NOT FILMED

Preceding Page blank

FOLDOUT FRAME 1

A-7, A-8
FOLDOUT FRAME 2
SD 71-140-2

Page intentionally left blank

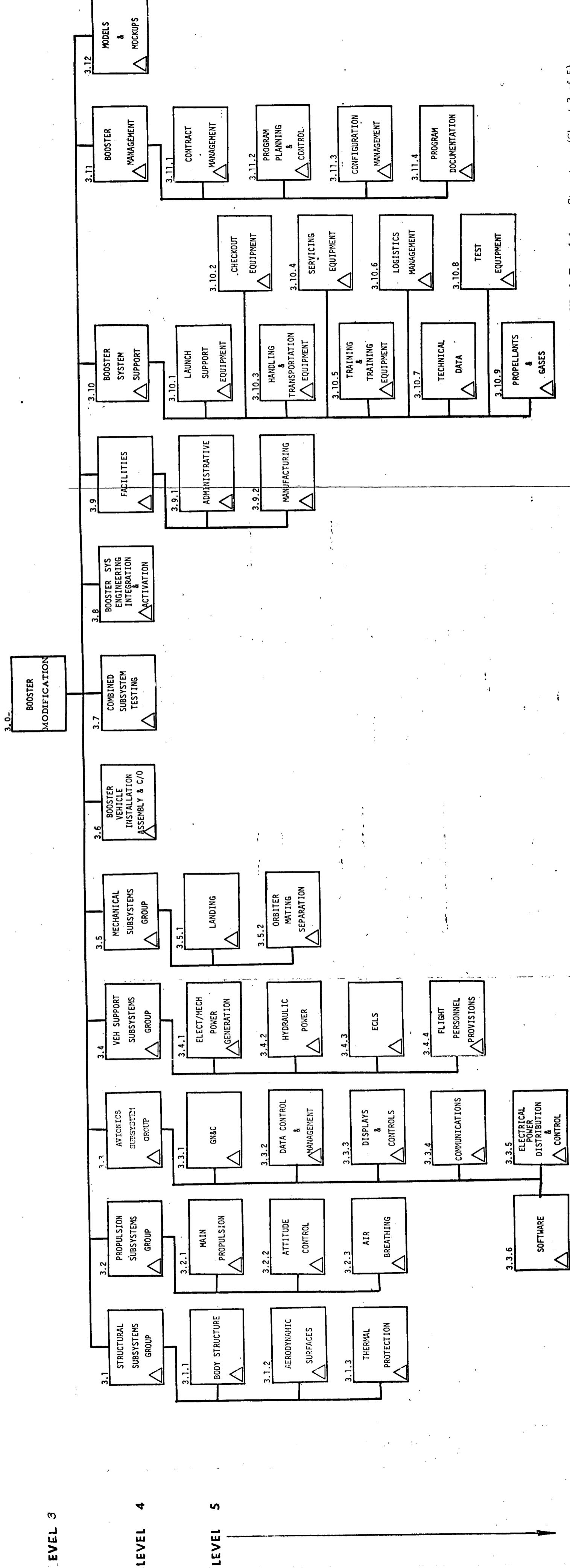


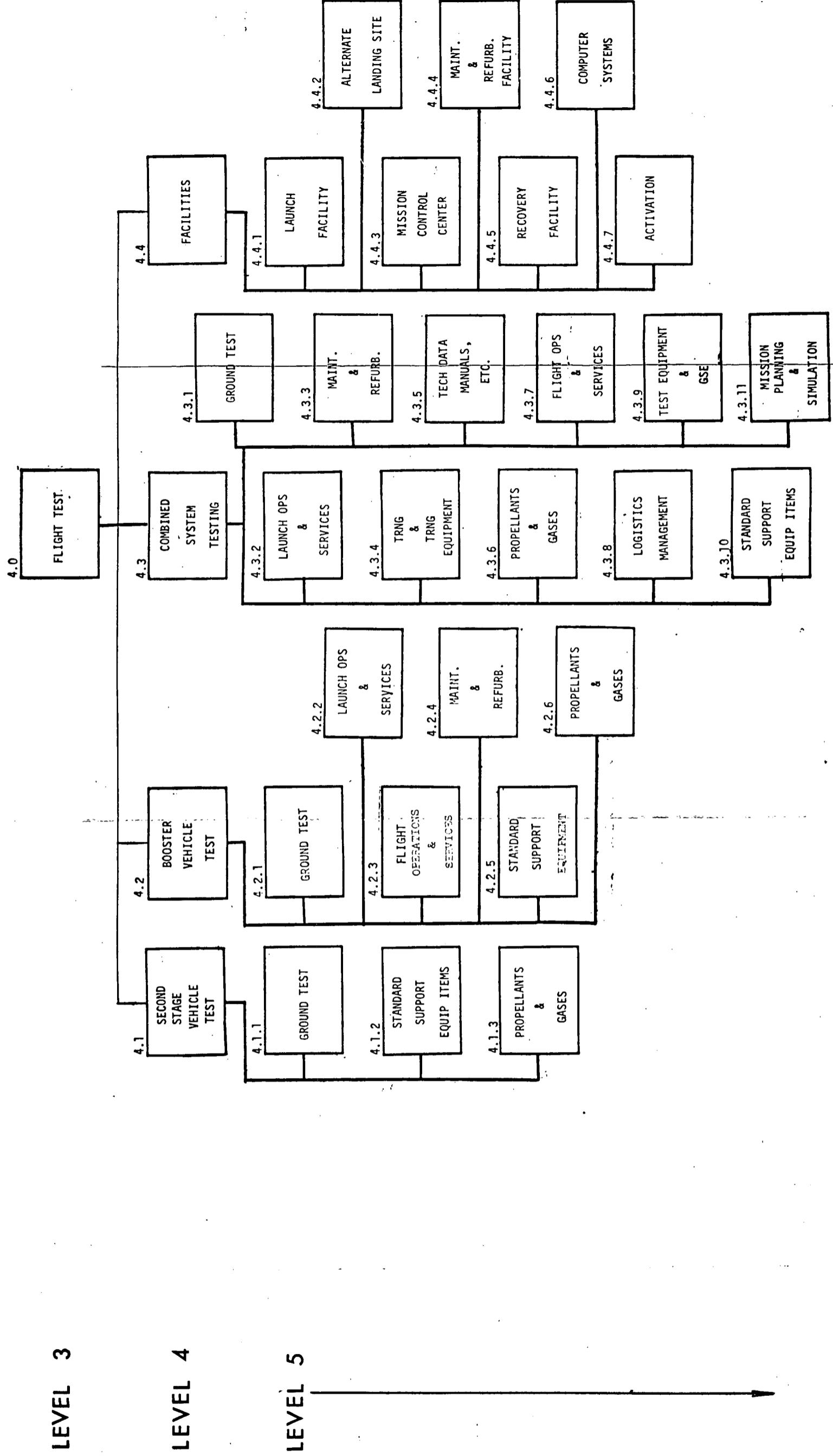
Figure A-4. Work Breakdown Structure (Sheet 2 of 5)

A-11, A-12

SD 71-140-2

FOLDOUT FRAME 2

FOLDOUT FRAME 1



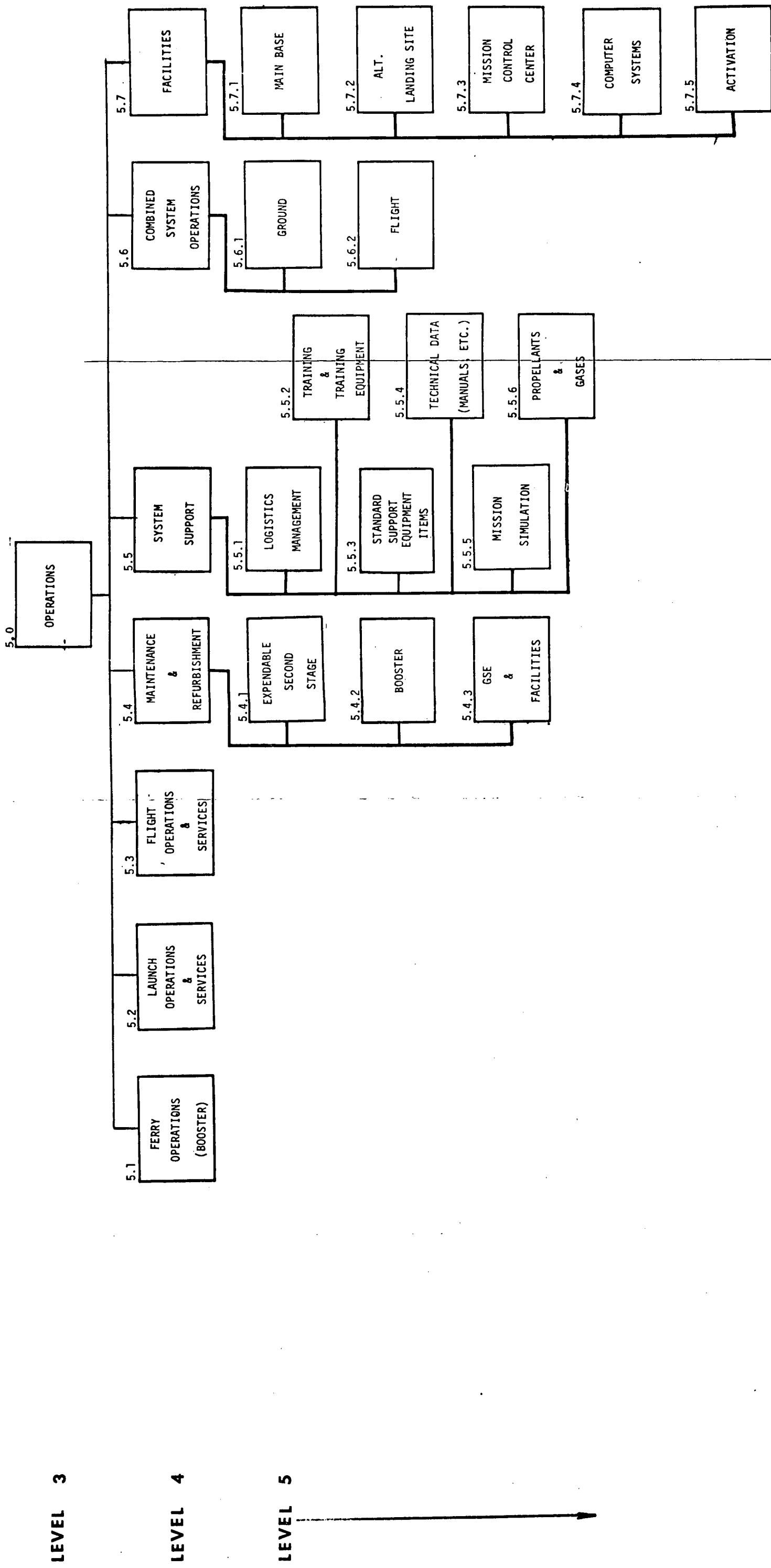


Figure A-4. Work Breakdown Structure (Sheet 4 of 5)

FOLDOUT FRAME 1

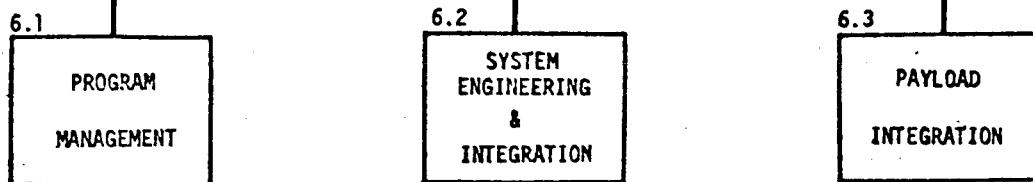
A-15, A-16 SD 71-140-2
FOLDOUT FRAME 2



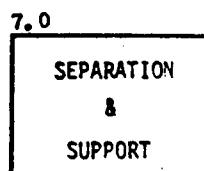
LEVEL 3



LEVEL 4



LEVEL 3



LEVEL 4

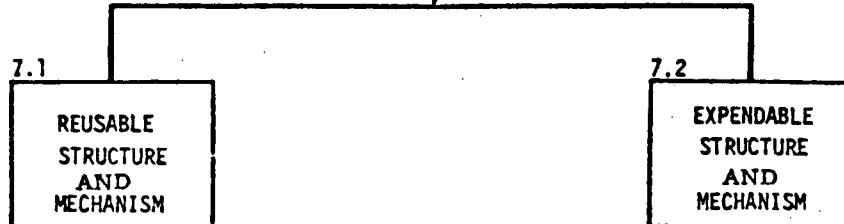


Figure A-4. Work Breakdown Structure (Sheet 5 of 5)



3.0 TRAFFIC AND MISSION MODEL

The traffic model consists of 20 launches over 10 years (2 per year) following the first launch in 1979. This traffic model was a NASA study ground rule.

The mission model used for the evaluation of systems was stated in the Study Control Document; the payload is to be delivered to 270 nautical miles altitude (circular) in a 55-degree inclination, an accuracy of ± 10 nautical miles (11 nautical miles from the orbiting body that is the subject of the rendezvous) and a 24-hour lifetime (launch-to completion of deorbit burn). Additional details of the mission/traffic/system/program requirements are provided in the contract Study Control Document; and each alternative system studied met those requirements.

The mission model also assumes that the space shuttle orbiter will rendezvous with the ESS, remove high cost elements (e.g., main engines and avionics), and return them for reuse in subsequent ESS missions. The performance of the ESS used in the cost effectiveness evaluation, was based on the maximum payload capability to the design reference mission (270 nautical miles and 55-degree inclination).



4.0 COST BASELINE

4.1 COST

Table A-1 reflects the baseline system/program costs versus the WBS as functions of nonrecurring (DDT&E), recurring (production plus operations), and total (nonrecurring plus recurring) costs. Estimated costs of the baseline Expendable Second Stage (ESS) are provided through WBS Level 4 (Table A-2). The baseline costs represent the estimates which were updated to 15 March 1971 (based on quantity and operational procedural changes) available at the date of Phase B go-ahead (February 1971).

Table A-1. Estimated Baseline System/Program Cost

WBS	Nonrecurring (\$ millions)	Recurring (\$ millions)	Total (\$ millions)
1.0 Expendable 2nd stage	77.88	518.40	596.28
2.0 Main engines (ESS)	0	24.60	24.60
3.0 Booster mod's. (B-9U)	0	0	0
4.0 Flight test	0	0	0
5.0 Operations	0	87.44	87.44
6.0 Management and integration	5.11	38.03	43.14
7.0 Separation and support structure	7.27	3.44	10.71
Total	90.26	671.91	762.17
Recurring cost per flight	\$33.59 million		
Total cost per flight	\$38.11 million		
Payload (270 nautical miles x 55 degrees = 177,300 pounds			
Recurring cost per pound payload = 189 (dollars/pound)			



Table A-2. Estimated ESS Cost (Levels 3 and 4)

WBS	Nonrecurring Cost Estimates (\$ million)	Recurring Cost Estimates (\$ million)
1.0 Expendable Second Stage	77.88	518.4
1.1 Structural subsystem group	9.20	111.5
1.2 Propulsion subsystem group	13.92	88.0
1.3 Avionics subsystem group	10.44	117.8
1.4 Vehicle support subsystem	1.30	11.4
1.5 Mechanical subsystem	0	0
1.6 Vehicle assembly installation and checkout	5.71	59.0
1.7 Combined subsystem testing	6.91	6.0
1.8 System engineering integration and activities	13.88	44.2
1.9 Facilities	1.40	17.1
1.10 System support	14.22	44.3
1.11 Vehicle management	0.40	5.1
1.12 Models and mockups	0.50	0
1.13 Payload integration	0	0
1.14 Transportation	0	14.0

4.2 GROUND RULES AND ASSUMPTIONS

NR/GD estimates of cost were based on the following:

1. The ESS (modified S-II) initial baseline was recommended in the Study Interim Final Report (SD 70-607), modified for removal, recovery, and reuse of the stage's expensive elements. This baseline ESS was structurally an S-II with the length of the LH₂ tank reduced by removal of one 99-inch section, using space shuttle orbiter engines (2) for main propulsion, S-IVB attitude control propulsion subsystem (ACPS), lunar module descent engine (LM-DE) for orbital maneuvering propulsion system (OMS), and partial avionics from the space shuttle orbiter
2. The booster for the baseline ESS system was defined as the General Dynamics Convair booster designated B-9U
3. Phase C/D Contract go-ahead will be received in the first quarter of CY 1972, with the first ESS flight in CY 1979



4. Flight program as described in Section 3.0
5. Fleet size of 20 stages (no spare stage) for the 20 flights
6. Estimates for nonrecurring (design, development, test and evaluation, DDT&E), and recurring (production plus operations) costs
7. Performance defined as the payload weight ahead of the stage that is delivered to the design reference mission orbit (270 nautical miles attitude circular and 55-degree inclination)
8. Hardware developed for other programs and used by the ESS, will have that nonrecurring cost charged to that other program
9. Production rate was defined as the minimum cost rate that is adequate to meet the flight rate (2 per year). For the initial baseline cost estimates, this was assumed to be a production rate of 3 per year (the cost of a storage facility and the cost of stage storage maintenance was not included. During Phase B, storage cost was included, and three per year was still cost optimum).
10. It is assumed that the orbiters (space shuttle) performing the recovery of ESS components were launched for other specific shuttle missions and were thus available for the recovery operations at no cost to the ESS program

4.3 EXCLUSIONS

The baseline costs exclude those costs related to the following items.

1. Office of Manned Space Flight (OMSF) operating base
2. Other program peculiar support not included in operating base
3. Shuttle technology program
4. Phase A and B study effort
5. Payloads (experiments) definition, development, production, and integration
6. Development costs of all ESS subsystems that are, were, or will be developed for other programs



7. Contractor's fee
8. Allowance for major program problems identified beyond the start of the Phase C shuttle efforts. It is expected that the contractors will retain an allowance for normal change activity
9. Inflation factors



5.0 MASTER SCHEDULE

The master schedule is shown in Figure A-5. The objectives, ground rules, and conditions for achieving the objectives are described in the following paragraphs.

5.1 OBJECTIVES

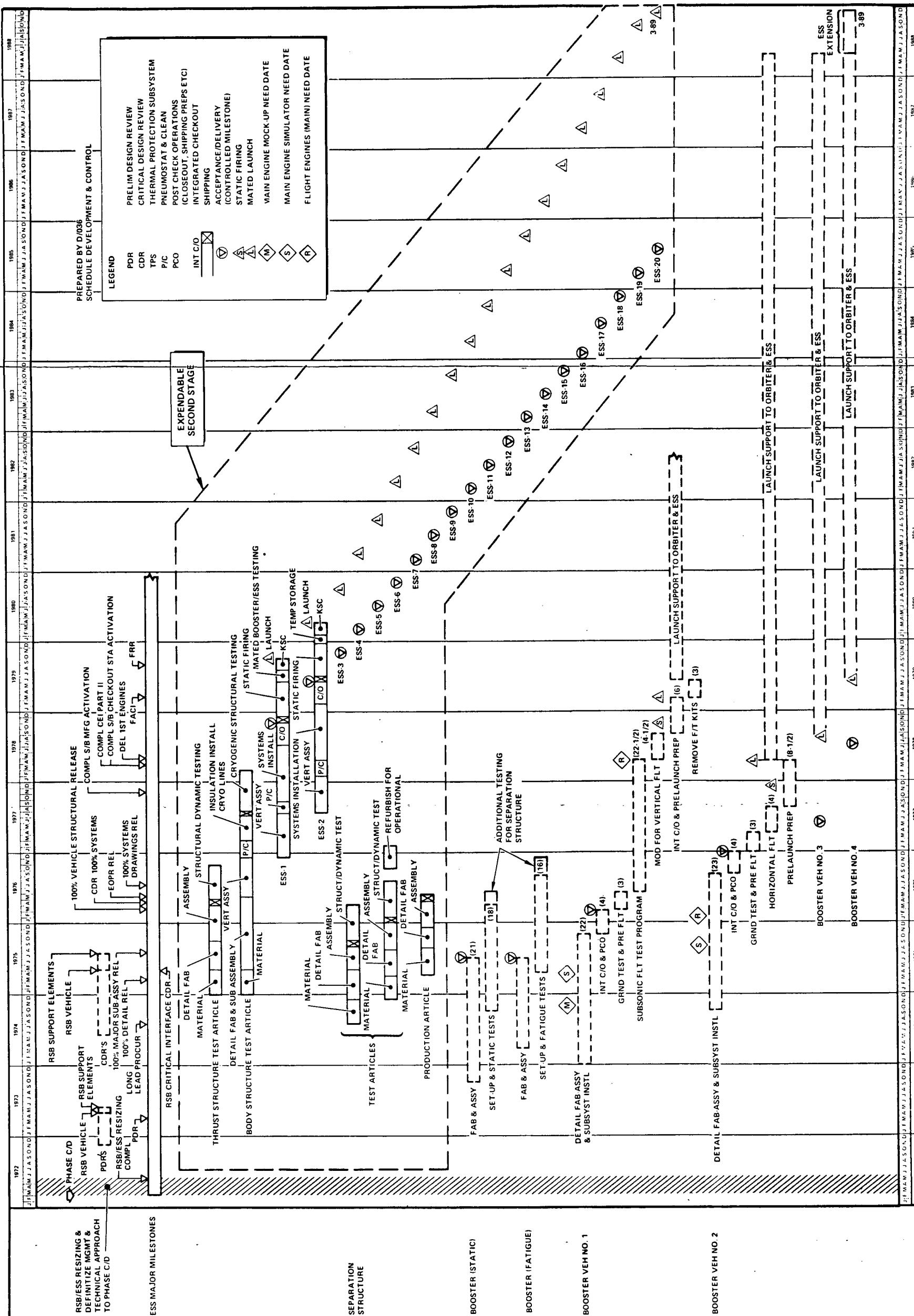
The first orbital flight is planned for 1979. Phase C is to start March 1, 1972.

5.2 SCHEDULE GROUND RULES AND CONDITIONS

The first mated ESS orbital flight will be in 1979. Phase C is to start March 1, 1972. The Phase D cost proposal effort will be started three months after Phase C go-ahead and will be submitted within four weeks after the final PDR (April 1, 1973). The award of Phase D go-ahead (July 1, 1973) is to be three months after final PDR.

At the start of Phase C, approval is expected for the release of Engineering Order Purchase Requests (EOPR's) for critical long lead-time ESS material and components. These components support final mockups and test hardware; e. g., structural test elements and test development hardware, and certain long lead facility commitments.

The PDR completion for all other elements (e. g., GSE, facilities, systems) will be contingent upon completion of the ESS/booster PDR.



Ernesto A. Montaner, S. J. - 1 -

PRECEDING PAGE BLANK NOT FILMED



6.0 COSTS IN DESIGN DECISIONS

It was recognized that there are two major concerns in regard to the shuttle program costs, namely, (1) a requirement for a major reduction in the cost of placing payloads in orbit over the cost of using current, expendable launch systems, and (2) a requirement that development costs for the shuttle be within the limits of potentially available funds for the DDT&E phase. These considerations led to what NR/GD defines as the resource/evaluation criteria. Cost criteria were constructed which reflect the program cost goals. These criteria were integrated into the total trade study decision process.

Trade studies (Section 6.4) are identified by the Work Breakdown Structure (WBS) most affected by the change. This does not imply that a particular WBS item is the only item to be changed. All WBS items are considered and changes are identified as a function of the change to the basic WBS item, e.g., changes in WBS 1.2.3 from LEM-D OMS to the shuttle 10,000 OMS requires changes also in 1.1 structures (due to different mounting and weights); 1.3 avionics (due to different data and control requirements); 1.4 vehicle support subsystems (due to different power requirements); 1.6 vehicle assembly, integration, and checkout; 1.7 combined subsystem testing; 1.10 system support (due to the required services and checkout of NTO/UDMH versus LO₂/LH₂, etc.); and 5.0 operations (due to change in operational facilities and the quantity of operational crew personnel).

By definition, trade studies were evaluated (cost effectiveness) based on the total program level. Total program is defined as that combination of hardware (boosters, ESS's, support equipment, etc.), software, operational personnel, and consumables required to perform the mission/traffic model. In WBS terms, the total program level is 2; wherein, the ESS is Level 3.

This approach minimized the Level 2 recurring cost per pound of payload to orbit. It was possible that if only the ESS (WBS 1.0, Level 3) recurring cost was minimized, other Level 3 WBS items (2.0 through 7.0) would increase such that the Level 2 cost would not be minimum. Similarly, the effectiveness parameter requires the total system (ESS without the booster has zero effectiveness) be considered. Thus, the objective function of the trade studies was to establish the Level 2 recurring cost per pound of payload to orbit (payload to orbit was based on the maximum capability) of the system to deliver a payload to the design reference orbit (270 nautical



miles circular altitude and 55-degree inclination). In the case of similar Level 2 recurring costs per pound, the second objective function total program cost was used.

6.1 TRADE STUDY PROCESS

Figure A-1 reflected the processes used for assuring consideration of cost in all shuttle program decisions. Three types of reviews were exercised by the Engineering Review Board (ERB). This procedure required that the responsible study manager obtain approval to (1) proceed with the study, (2) investigate specific alternatives and criteria, and (3) incorporate specific recommendations into the appropriate control documents. Cost considerations were taken into account in all phases of this activity. Decisions to proceed with the study were based upon cost effectiveness considerations.

6.2 COST DECISION CRITERIA

As in all optimization procedures, a single objective quantity and a series of constraints were identified. NASA/NR identified the recurring cost per pound of payload in orbit as the objective quantity to be minimized.

Total program cost was used as the objective quantity to resolve ties in the basic selection.

6.3 COST MODEL

The existing cost model was updated for the purpose of study program decisions, and reporting requirements at WBS Level 5 (subsystem). It was oriented to the lowest level of available design information for each of the trade studies. As detailed design information evolved, supplier costs, manufacturing and operational man-hours and materials data, test and support equipment data, etc., were utilized in the cost model. "Technical Characteristics Data Form C," of DRD MF003M, was used throughout the study.

6.4 TRADE STUDIES

The following trade studies were considered during the study. The defined baseline program was the basis for all trade studies and was changed only on March 28, April 15, and May 15 by direction of the engineering review board. Some of the items in the following WBS list were the subjects of analysis only.

1.0 Expendable Second Stage

1.1 Structures



- 1.1.1 Body
 - 1.1.2 Aero surfaces (considered only - not required)
 - 1.1.3 Thermal protection
- 1.2 Propulsion
- 1.2.1 Main engines (no trades-use shuttle orbiter engines)
 - 1.2.2 Attitude control
 - 1.2.3 Orbital maneuver (LEM-D vs. RL-10 vs. Shuttle OMS)
- 1.3 Avionics (ground and flight system optimization), primarily a trade of combinations of 1.2, 1.3, 1.4, 1.7, 1.10, and 5.0)
- 1.3.1 GN&C (shuttle GN&C vs. IU) (removable, deorbit kit)
 - 1.3.2 Data control and management (removable, deorbit kit)
 - 1.3.3 Communication (removable)
 - 1.3.4 Electrical power distribution and control (S-II - ESS IA vs. data bus)
 - 1.3.5 Software (no trade - new = (1.2, 1.3, 1.4, and 1.10)
- 1.4 Vehicle support subsystems
- 1.4.1 Electrical/mechanical power generator (batteries) (changed to part of 1.3.4)
 - 1.4.2 Hydraulic power (engine driven vs. electric vs. pneumatic) (changed to part of 1.2.1)
 - 1.4.3 Environmental control (purging subsystem) (changed to part of 1.3)
- 1.5 Mechanical subsystems (no trades)
- 1.6 Vehicle assembly, installation, and checkout (no trades)
- 1.7 Combined subsystem testing (no trades)
- 1.8 System engineering (no trades)



1. 9 Facilities (design, development, and manufacturing)
1. 10 System support (refer to 1. 3)
 1. 10. 1 Launch support equipment
 1. 10. 2 Checkout equipment
 1. 10. 3 Handling and transportation equipment
 1. 10. 4 Servicing equipment
 1. 10. 5 Training equipment
 1. 10. 6 Logistics management
 1. 10. 7 Technical data
 1. 10. 8 Test equipment
 1. 10. 9 Propellants and gases
1. 11 Vehicle management (no trades)
1. 12 Models and mockups (no trades)
1. 13 Payload integration (no trades)
1. 14 Transportation and delivery (no trades)
2. 0 Main Engines (ESS) (no trades - use shuttle orbiter engines)
3. 0 Booster Modifications (kept to a minimum for the shuttle program)
4. 0 Flight Test (none planned)
5. 0 Operations (refer to 1. 3, also consider various flight trajectories, recovery of ESS elements, etc.)
5. 1 Ferry operations (booster) (none assumed - booster returns to operational site)
5. 2 Launch operations and services (consider sharing personnel with shuttle)



- 5.3 Flight operations and services (shuttle personnel are adequate)
- 5.4 Maintenance and refurbishment (personnel should be shared with shuttle)
- 5.5 System support (only changes required to support other trades)
- 5.6 Facilities (where is ESS preparation area?, what modifications to launch pad are required?, LUT, etc., and GAFSO)
- 6.0 Management and Integration (no trades)
- 7.0 Separation/Support Structure (tension link vs. movable platform vs. fixed platform)



7.0 DATA CONTROL AND REPORTING

7.1 DATA CONTROL

An informal data control system was utilized during the Phase B study to track and consolidate technical, cost, and schedule data of design and trade studies. This system provided the data base from which periodic reviews on the status of costs, schedule, and technical data were prepared.

7.2 REPORTING

At the reviews, data was presented concerning the trade studies and decisions by management. The technical and cost results determined for each reporting period were provided to the appropriate WBS levels. Cumulative costs were structured and compared to those shown in Table A-1. Data was reported in a format similar to that used in Tables A-1 and A-2.



8.0 TRADE STUDY RESULTS

The charts that were used in the trade studies (Tables A-3 through A-7) were presented to the ERB and in the customer briefings. Technical backup data for these trades can be found in Volume II for the selected subsystem and Appendixes for the unselected subsystems.

Table A-3 presents information for the orbital maneuver subsystem (OMS) trade of LEM-D (in the baseline system) versus RL-10 versus the 10,000-pound thrust nozzles used by the space shuttle orbiter. Each alternative OMS was required to supply 1196 feet per second (ΔV). Based on the differences in I_{sp} , mixture ratios, etc., the differences in weight were defined. The propulsion subsystems (OMS) were costed, as were other WBS elements that changed under investigation. The identical recurring cost (\$86.5 million) for the 1.2 propulsion subsystem group under both RL-10 and 10K SS Orbiter OMS is purely coincidental and explainable. The recurring cost per pound of payload (\$/lb) for the RL-10 and the 10,000-pounds thrust SS engines (\$181/lb) and (\$180/lb, respectively) indicated that the choice should be the 10,000-pound thrust engine equipped subsystem. However, the difference of 1 in 180 (a little more than 1/2 of 1 percent may be questioned in terms of the accuracy of each of the numbers; thus the secondary objective function (total program cost) was used to confirm the choice of the OMS equipped with the 10,000-pound thrust engine.

Table A-4 presents the trade of the conventional (S-II) electrical subsystem (in the baseline system) with the data bus approach also used in the basic space shuttle orbiter. The data bus approach is, in a sense, a hybrid cross of hardwire and multiplex (see the description in Book 2). The selection of the data bus saves \$10/pound.

Table A-5 presents the trade of the initial baseline system versus a system (System A) that is the baseline but with the 10,000-pound thrust engine OMS (from Table A-3) and with the Data Bus (from Table A-4). System A was clearly the choice over the initial baseline system, and was immediately adapted as the new baseline system (System A).

Table A-6 considers the power source for gimbaling the main propulsion subsystem engines. The ICD for the space shuttle orbiter engines does not provide for an engine actuation subsystem (EAS) since the orbiter will have auxiliary power units (APU) driving hydraulic pumps to gimbal engines, operate control surfaces, extend air-breathing engines,



Table A-3. Orbital Maneuvering Subsystem
Engine Trades*

PROGRAM: 2/YR FOR 10 YRS
*MILLIONS OF DOLLARS

	OMS							
	BASELINE SYSTEM (LEM-D)		ALTER NO. 1 RL-10 OMS		ALTER NO. 2 10K SHUTTLE OMS		ALTER NO. 4	
	\$NR	\$R	\$NR	\$R	\$NR	\$R	\$NR	\$R
1.0 EXPENDABLE SECOND STAGE	77.9	518.4	105.6	815.4	73.2	515.4		
1.1 STRUCTURE	9.2	111.5	-	-	-	-		
1.2 PROPULSION	13.9	88.0	39.4	86.5	11.9	86.5		
1.3 AVIONICS	10.5	117.8	-	-	-	-		
1.4 VEHICLE SUPPORT	1.3	11.4	1.4	-	1.2	-		
1.5 MECHANICAL	-	-	-	-	-	-		
1.6 VEH ASSEM INTEG & C/O	5.7	59.0	6.9	58.4	5.2	58.4		
1.7 COMBINED SUBSYSTEM TESTING	6.9	6.0	-	-	-	-		
1.8 SYS ENGRG	13.9	44.2	14.0	43.9	13.0	43.9		
1.9 FACILITIES	1.4	17.1	-	-	-	-		
1.10 SYSTEM SUPPORT	14.2	44.3	14.9	43.8	13.0	43.8		
1.11 VEHICLE MGMT	0.4	5.1	0.5	5.0	-	5.0		
1.12 MODELS & MOCKUPS	0.5	-	-	-	-	-		
1.13 PAYLOAD INTEG	-	-	-	-	-	-		
1.14 TRANSPORTATION	-	14.0	-	-	-	-		
2.0 MAIN ENGINES (ESS)	-	24.60	-	-	-	-		
3.0 BOOSTER MODIFICATIONS	-	-	-	-	-	-		
4.0 FLIGHT TEST	-	-	-	-	-	-		
5.0 OPERATIONS	-	87.44	-	87.3	-	87.0		
6.0 MANAGEMENT & INTEG	5.11	38.03	6.77	37.84	4.82	37.83		
7.0 SEP/SUPPORT STRUCTURE	7.27	3.44	-	-	-	-		
SUB-TOTAL	90.28	671.91	119.84	688.58	85.29	688.27		
TOTAL	762.19		788.22		753.56			
PERFORMANCE (270 X 56 ³) LB	177,300		188,045		188,905			
RECURRING COST/POUND PAYLOAD \$/LB	189		181		180			
RECURRING COST/FLIGHT	33.6		33.4		33.4			

Table A-4. Electrical Power Distribution and Control Subsystem Trades*

NO.	WBS ELEMENT	BASIC SYSTEM		DATA BUS		NO. WBS ELEMENT	BASIC SYSTEM		DATA BUS	
		\$NR	\$R	\$NR	\$R		\$NR	\$R	\$NR	\$R
1.1 STRUCTURES	9.2	111.5				1.0 EXPENDABLE SECOND STAGE	77.9	518.4	76.4	493.0
1.2 PROPULSION	13.9	88.0				2.0 MAIN ENGINES (ESS)	0	24.6		
1.3 AVIONICS	10.5	117.8	9.8	98.9		3.0 BOOSTER MODIFICATIONS	0	0		
1.4 VEHICLE SUP	1.3	11.4				4.0 FLIGHT TEST	0	0		
1.5 MECHANICAL	0	0				5.0 OPERATIONS	0	87.44		87.0
1.6 ASSEM, INTEG & C/O	5.7	59.0	5.5	56.4		6.0 MANAGEMENT & INTEGRATION	5.1	38.0	5.0	36.5
1.7 COMB SUBSYS	6.9	6.0				7.0 SEPARATION/ SUPPORT STRUC	7.27	3.44		
1.8 SYST ENGRG	13.9	44.2	13.6	42.4						
1.9 FACILITIES	1.4	17.1								
1.10 SYSTEM SUP	14.2	44.3	13.9	42.2						
1.11 VEHIC MGT	0.4	5.1								
1.12 MODELS & MOCKUPS	0.5	0								
1.13 PAYLOAD INTEG	0	0								
1.14 TRANSPORTATION	0	14.0								
SUB-TOTAL	77.9	518.4	76.4	493.0		SUB-TOTAL	90.3	671.9	88.7	644.5
20 FLIGHTS RECOVER ELEMENTS						TOTAL	762.2		733.2	
*MILLIONS OF DOLLARS						PERFORMANCE (DRM)	177,300 LB		179,880 LB	
						RECUR COST/POUND PAYLOAD \$/LB	189		179	
						RECUR COST/FLIGHT	33.6		32.2	



Table A-5. Initial Baseline System Versus System A Trades*

NO.	WBS ELEMENT	BASIC SYSTEM		SYSTEM A **		NO. WBS ELEMENT	BASIC SYSTEM		SYSTEM A	
		\$NR	\$R	\$NR	\$R		\$NR	\$R	\$NR	\$R
1.1	STRUCTURES	9.2	111.5			1.0 EXPENDABLE SECOND STAGE	77.9	518.4	72.2	490.2
1.2	PROPULSION	13.9	88.0	11.9	86.5	2.0 MAIN ENGINES (ESS)	0	24.6		
1.3	AVIONICS	10.5	117.8	9.8	98.9	3.0 BOOSTER MODIFICATIONS	0	0		
1.4	VEHICLE SUP	1.3	11.4	1.2		4.0 FLIGHT TEST	0	0		
1.5	MECHANICAL	0	0			5.0 OPERATIONS	0	87.44		
1.6	ASSEM, INTEG, & C/O	5.7	59.0	5.1	55.8	6.0 MANAGEMENT & INTEGRATION	5.1	38.0	4.8	36.3
1.7	COMB SUBSYS TEST	6.9	6.0			7.0 SEPARATION/SUPPORT STRUC	7.27	3.44		
1.8	SYST ENRG	13.9	44.2	12.9	42.1					
1.9	FACILITIES	1.4	17.1							
1.10	SYSTEM SUP	14.2	44.3	12.9	41.9					
1.11	VEHIC MGT	0.4	5.1							
1.12	MODULES/MOCKUPS	0.5	0							
1.13	PAYOUT INTEG	0	0							
1.14	TRANSPORTATION	0	14.0							
SUB-TOTAL		77.9	518.4	72.2	490.2	SUB-TOTAL	90.3	671.9	84.3	641.1
						TOTAL	762.2		725.4	
20 FLIGHTS RECOVER ELEMENTS						PERFORMANCE (DRM)	177,300 LB		188,450 LB	
*MILLIONS OF DOLLARS						RECUR COST/POUND	189		170	
**BASELINE SYSTEM WITH 10,000 POUNDS THRUST SHUTTLE OMS AND DELTA BUS						PAYOUT \$/LB				
						RECUR COST/FLIGHT	33.6		32.1	

Table A-6. Main Propulsion Engine Actuation Subsystem Trades*

NO.	WBS ELEMENT	SYSTEM A (MILLIONS OF DOLLARS)				ENG DRIVE HYDRAULIC	ELEC DRIVE HYDRAULIC	PNEUMATIC ACTUATOR	PNEU/MYDR CONVERSION	APU DRIVE HYDRAULIC
		NR	R	NR	R					
1.1	STRUCTURES	9.2	111.5	9.2	111.5	9.2	111.5	9.2	111.5	9.2
1.2	PROPULSION	11.9	86.5	12.4	86.7	13.9	86.7	12.4	87.6	11.9
1.3	AVIONICS	9.8	98.9	10.8	100.1	9.8	98.9	9.8	98.9	9.8
1.4	VEHICLE SUP	1.2	11.4	1.7	12.8	1.7	12.8	1.7	12.8	13.2
1.5	MECHANICAL	0	0	0	0	0	0	0	0	0
1.6	ASSEM, INTEG & C/O	5.1	55.8	5.1	56.2	5.3	55.7	5.2	55.9	5.6
1.7	COMB SUBSYS TEST	6.9	6.0	7.0	6.0	8.1	6.0	7.3	6.0	13.8
1.8	SYST ENRG	12.9	42.1	13.2	42.3	13.8	42.1	13.2	42.1	13.8
1.9	FACILITIES	1.4	17.1	1.4	17.1	1.4	17.1	1.4	17.1	1.4
1.10	SYSTEM SUP	12.9	41.9	13.2	41.9	13.7	41.9	13.2	41.9	14.6
1.11	VEHIC MGT	0.4	5.0	0.4	5.0	0.4	5.0	0.4	5.0	0.4
1.12	MODULES/MOCKUP	0.5	0	0.5	0	0.5	0	0.5	0	0
1.13	PAYOUT INTEGRATION	0	0	0	0	0	0	0	0	0
1.14	TRANSPORTATION	0	14.0	0	14.0	0	14.0	0	14.0	0
1.0 SUBTOTAL ESS		72.2	490.2	74.9	493.6	77.8	491.7	74.3	492.8	94.2
2.0	MAIN ENGINES	* 0	* 24.6	0	24.6	0	24.6	0	24.6	0
3.0	BOOSTER MOD	0	0	0	0	0	0	0	0	0
4.0	FLIGHT TEST	0	0	0	0	0	0	0	0	0
5.0	OPERATIONS	0	86.6	0	86.6	0	86.6	0	86.6	0
6.0	MANAGEMENT & INTEGRATION	4.8	36.3	4.8	36.3	4.8	36.3	4.8	36.3	4.8
7.0	SEPARATION/SUPPLY STRUCT	7.3	3.4	7.3	3.4	7.3	3.4	7.3	3.4	3.4
	TOTAL	* 84.3	* 641.1	87.0	644.5	89.8	642.6	86.4	643.7	108.3
	PERFORMANCE (DRM)	183,000		182,130		182,885		182,750		182,685
	RECUR COST \$/LB PAYLOAD TO DRM	*175.16		178.83		175.76		178.11		178.83
	RECUR COST PER FLIGHT	*32,055		32,225		32,130		32,185		32,270

(*DOES NOT INCLUDE POTENTIAL ENGINE ACOST)



extend landing gear, etc. Thus, the orbiter requires hydraulic power even when the main propulsion engines are not operating. Initial indication at the beginning of Phase B was that the preferred approach for the ESS would be a power takeoff from the main engine for hydraulic power. Other candidates are shown in Table A-6. This table was presented to NASA at the May 21 briefing. NR requested direction on whether engine power takeoff could be considered.

NASA indicated that consideration was being given to this approach. Hence, the preferred approach for this report is that discussed above. However, if the engine power takeoff is not approved, the alternative approach recommended would be a pneumatic-driven hydraulic actuator design.

Table A-7 is a trade of deorbit propulsion sources; i.e., the OMS, ground installed solids, or orbiter delivered (space) and installed solids. System A provides for deorbit by the OMS. The choice is the OMS.

Figure A-6 presents the trades of (1) no recovery of the avionics, (2) recovery of a small part of the avionics, or (3) recovery of all major removable avionics. This figure presents the information parametrically since there is a major unanswered question affecting this choice. "What is

Table A-7. Deorbit Propulsion (OMS Versus Solids) Trades

NO.	WBS ELEMENT	BASIC SYSTEM "A"		SPACE DELIVERED SOLIDS		GR'D INSTAL SOLIDS		NO.	WBS ELEMENT	BASIC SYSTEM "A"		SPACE DELIVERED SOLIDS		GR'D INSTAL SOLIDS	
		\$NR	\$R	\$NR	\$R	\$NR	\$R			\$NR	\$R	\$NR	\$R	\$NR	\$R
1.1	STRUCTURES	9.2	111.5	9.7	115.8	9.5	114.4	1.0	EXPENDABLE SECOND STAGE	72.2	490.2	74.8	491.3	74.6	490.8
1.2	PROPULSION	11.9	86.5	13.3	80.7	13.3	80.7	2.0	MAIN ENGINES (ESS)	0	24.6				
1.3	AVIONICS	9.8	98.9	9.9	99.5	9.9	99.5	3.0	BOOSTER MODIFICATIONS	0	0				
1.4	VEHICLE SUP	1.2	11.4					4.0	FLIGHT TEST	0	0				
1.5	MECHANICAL	0	0					5.0	OPERATIONS	0	86.6				
1.6	ASSEM, INTEG & C/O	5.1	55.8	5.3	56.8	5.3	57.8	6.0	MANAGEMENT & INTEGRATION	4.8	36.3	4.9	36.5	4.9	36.5
1.7	COMB SUBSYS	6.9	6.0					7.0	SEPARATION/ SUPPORT STRUC	7.3	3.4				
1.8	SYST ENRG	12.9	42.1	13.1	42.5	13.1	42.5								
1.9	FACILITIES	1.4	17.1												
1.10	SYSTEM SUP	12.9	41.9	13.1	42.4	13.1	42.4								
1.11	VEHIC MGT	0.4	5.0												
1.12	MODELS & MOCKUPS	0.5	0												
1.13	PAYOUT INTEG	0	0												
1.14	TRANSPORTATION	0	14.0												
SUB TOTAL		72.2	490.2	74.8	991.3	14.6	490.8	SUB-TOTAL		84.3	641.1	87.0	644.8	86.8	644.3
SYSTEM "A" - OMS FOR DEORBIT								TOTAL		725.4		731.8		731.1	
20 FLIGHTS RECOVER ELEMENTS								PERFORMANCE (DRM)		183,000		182,700		166,200	
* MILLIONS OF DOLLARS								RECUR COST/POUND PAYLOAD \$/B		175		177		194	
(A) OMS ENGINES RECOVERED (3 SETS)								RECUR COST/FLIGHT		32.1		32.2		32.2	



the effect of the space environment on nonoperating and nonenvironmentally controlled avionics?" The answer to this basic question can have two effects; (1) the cost of refurbishing the avionics, and (2) the number of exposures limiting the useful life, thus effecting the quantity required. As can be seen in the figure, Option III (maximum recovery of parts) shows a greater potential saving than does Option II (partial recovery of parts); and, as one might suspect, the fewer sets required at the start results in greater savings. If the refurbishment costs exceed approximately 55 percent, there should be no attempt to recover any part of the avionics. Since the effect of the space environment on avionics is unknown, additional discussion and details are included in Book 2. It was decided that the ESS Phase B Study would be finished with recoverable avionics.

Tables A-8 and A-9 present tradeoff information for the launch operations facility requirements. The vehicle assembly building (VAB) will be used for the ESS and SS booster in a manner similar to the basic space shuttle. However, the prelaunch servicing and checkout of the ESS require

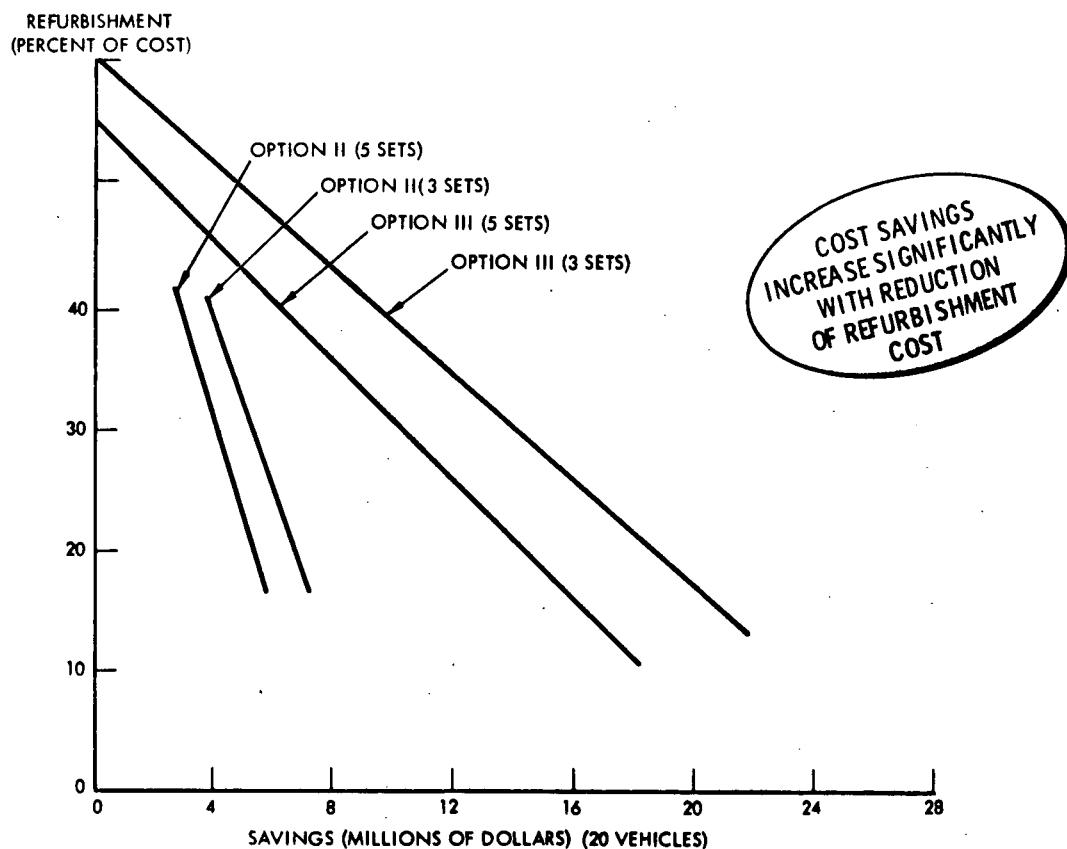


Figure A-6. Recoverable Avionics Cost Savings



different accessibility areas than the SS orbiter. The column labeled "LUT Swing Arms" assumes that swing arms from the launch umbilical tower (LUT) would be provided at the necessary elevations. These swing arms are quite long, they reach across the aerodynamic surfaces of the booster and therefore have to be disconnected and swung out of the way prior to booster engine start, and would require a rapid, automatic reconnect in the event of pad abort.

Table A-8. Launch Facility Trades*

COST ELEMENT	CONFIGURATION								
	LUT SWING ARMS			RISE-OFF PYLONS			PAD SERVICE TOWER		
	NR	R	TOT.	NR	R	TOT.	NR	R	TOT.
SERVICE CONNECTIONS	4.4	-	4.4	1.9	-	1.9	4.4	-	4.4
VAB MODIFICATIONS	.1	-	.1	.1	-	.1	.1	-	.1
SWING ARMS	17.2	-	17.2	-	-	-	11.5	-	11.5
RISEOFF PYLON MODS	-	-	-	5.7	.2	5.9	-	-	-
LAUNCH TOWER	-	-	-	-	-	-	16.5	-	16.5
SPECIAL FLUID/GAS/ELECT. ROUTING	3.0	-	3.0	3.0	-	3.0	3.0	-	3.0
ESS MODIFICATIONS	-	-	-	15.9	24.1	40.0	-	-	-
TOTAL	24.7	-	24.7	26.6	24.3	50.9	35.5	-	35.5

*COSTS (IN MILLIONS OF DOLLARS) REPRESENT DELTA TO BASELINE LAUNCH FACILITY

Table A-9. Launch Pad Configuration Concept Trades

ALTERNATE CONCEPT			
EVALUATION FACTORS	LUT SWING ARMS	RISEOFF PYLONS	PAD SERVICE TOWER
TOTAL COST (STAGE II & FAC)	24.7	50.9	35.5
ADDED ENVIRONMENT EXPOSURE	NONE	NONE	1 DAY LONGER THAN SHUTTLE
DEVELOPMENT RISK	HIGHEST	2ND HIGHEST	LOWEST
SAFETY ASSESSMENT	LOWEST	2ND PREFERRED	PREFERRED
LIFTOFF CLEARANCE	LOWEST	2ND HIGHEST	HIGHEST
COMPATIBILITY WITH SHUTTLE BASELINE	2ND HIGHEST	LOWEST	HIGHEST

* MILLIONS OF DOLLARS



The second column, "Rise-Off Pylons," is an adaptation of the pylons used for the orbiter. This requires a two-axis rotatable extension arm and extensive redesign of the plumbing of the ESS.

The last column in Tables A-8 and A-9, "Pad Service Tower," is for a tower to be erected on one launch pad that would provide swing arms for the services required by the ESS. The service disconnects would be the same as those presently used by the S-II in the Saturn V stack. Only one modified launch pad is required to meet the launch rate of two launches per year.

These facility trade studies were put in the form shown in these tables and figures, rather than the more standard form, because operational facility costs were not included in the initial baseline or in System A. Facility cost is primarily a nonrecurring cost and would not change the selection in the prior trades, however since the information was available, it was added. The rise-off pylons increase the recurring cost per pound of payload in orbit due to the additional stage plumbing, and the LUT swing arms are not considered acceptably safe due to the disconnect timing problem. The choice was the pad service tower.

While the handling, servicing, and checkout of the payloads for the ESS were not a contractual responsibility, it was pointed out that the pad service tower approach is probably the only acceptable approach of those listed. That tower could have additional swing arms for servicing, checking-out, and manned access to the different payloads that may mount the ESS. It could also provide similar functions for the payloads in the orbiter cargo bay.



APPENDIX B. IMPACT OF UTILIZING ESS ON BOOSTER FOR EXTERNAL HYDROGEN TANK STUDY

1.0 COMPARISON B-17E AND B-9U BOOSTER

The analyses conducted in this study and described in the other sections of this report were based on the shuttle B-9U booster as defined for the 270-day data report, and described in Volume II, Book 3. A second shuttle booster, designated B-17E and shown in Figure B-1 is currently in the process of definition. The B-17E booster is designed for use with an orbiter incorporating external hydrogen fuel tanks for the main propulsion system. The more significant physical and performance differences between the B-17E and the B-9U booster are summarized in Table B-1 and the differences in the mating/attachment loads are shown in Figure B-2.

The following sections describe the results of a study conducted to determine the shuttle/ESS program implications if a decision were made to use the B-17E instead of the B-9U as the shuttle booster. Since the basic study results using the B-9U booster have shown that the RNS and space tug payloads are not the critical payloads for booster design, the results discussed below consider only the space station payload. The space station weight (with a performance margin) was kept constant at 183,000 pounds for both boosters. However, the ESS velocity at separation is lower when used with the B-17E booster, resulting in an ESS/payload weight at separation of 1.223M pounds compared to 0.992M pounds when used with the B-9U booster.

1.1 MASS PROPERTIES

Table B-2 contains the weight statement for the B-17E booster for the ESS-space station mission and Table B-3 is the sequence mass property statement for the same mission.

1.2 TRAJECTORY

Table B-4 presents the trajectory for the ESS with the B-17E booster. The payload considered in this trajectory study was the MDAC space station.



Figure B-3 shows the variation in payload capability of the system with propellant loading and number of engines employed on the ESS and is based on maximum performance trajectories, i.e., zero alpha steering and throttling employed only to keep the mated ascent load factor to 3 g's. (These data are based on the B-17D booster which differed slightly from the B-17E.) Based on these results, it was concluded that (1) a three-engine ESS configuration was required, (2) attachment load reduction techniques similar to those employed on the B-9U were required, (3) it was desirable to retain the present overall dimensions of the ESS, and (4) a fully loaded ESS should be employed to permit implementation of load reduction techniques while still retaining capability to launch the MDAC space station.

Based on the above conclusions, a series of trajectories was calculated as shown in Figure B-4. The maximum performance capability is 209,500 pounds and results in maximum dynamic pressure of 600 psf. Employing throttling and steering as indicated, the maximum dynamic pressure can be reduced to 410 psf while having the same performance capability (183,000 pounds) as currently estimated for the baseline B-9U system.

It should be noted that the aerodynamics used are for the B-9U/ESS/MDAC SS with the reference area corresponding to the smaller B-17E. Therefore, some uncertainty in the performance is likely.

1.3 AIRLOADS

Airload distributions of the B-17E/MDAC configuration are presented in Figures B-5 and B-6 for the maximum " βq " pitch and yaw plane conditions, respectively. A comparison of these loads with those obtained for the B-9U/MDAC configuration shows the MDAC loads ($C_{N_0(B)}$ and $C_{A_0(B)}$) to act further forward on the nose of the B-17E booster than on the B-9U. The magnitude of these loads, in pounds, is the same.

1.4 LOADS AND STRUCTURES

The loads imposed by the ESS/MDAC stage on the B-17E booster structure were compared to those imposed by the NR orbiter VB70-0500, which represents the present structural capability. The three loading conditions that proved to be critical in the previous ESS/MDAC/B-9U analyses were used in this study since these conditions would probably produce the most critical effects on the B-17E/ESS/MDAC configuration. The three critical loading conditions were maximum "beta q," 2-g maximum acceleration, and one-hour ground sidewinds.

Page intentionally left blank

Table B-1. Comparison - B-9U and B-17E Boosters

BOOSTER	
	B-9U
WEIGHTS	
BOOSTER AT LIFTOFF (LBS)	4,188,223
TOTAL VEHICLE AT LIFTOFF (LBS)	5,047,430
STAGING	
ALTITUDE (FT)	242,074
VELOCITY (FPS)	10,832
FLIGHT PATH ANGLE (DEG)	6
BOOSTER ENGINES	
THRUST-SEA LEVEL (LBS)	550,000
CANT ANGLE (DEG)	3
NUMBER OF ENGINES	12
FLYBACK DISTANCE (N. MI.)	399
MAXIMUM BODY DIMENSIONS	
LENGTH (FT)	255.6
WIDTH (FT)	36
DEPTH (FT)	41
BODY STRUCTURE - TYPE	AL. ALLOY PROTECTED BY HEAT SHIELDS
	AL. ALLOY HEAT SINK



CONDITION	B-9U						B-17E			
	F _x	F _y	F _z	A _y	A _z	F _x	F _y	F _z	A _y	A _z
ONE HOUR GROUND WINDS FUELED UNPRESSURIZED	859	+33.2	84.5	±10.3	137	1122	±27.7	99.6	±11.5	178
DYNAMIC LIFTOFF + ONE HOUR GROUND WINDS	1296	±21.1	118	±2.24	177	1746	±1.64	118	±13.1	254
MAX $\alpha-q$	1676	0	127	0	-254 +842	2342	0	-190 +283	0	-590 +873
MAX $\beta-q$	1796	±50.5	139	±225	119	2356	±126	36.5	±279	20.3
3G MAX THRUST	2825	±54.9	195	±31.0	358	3697	0	32.1	0	430
BOOSTER BURNOUT	2817	±54.9	118	±31.0	408	3685	0	32.1 -50.8	0	430 -423

LOADS IN KIPS

Figure B-2. Booster (Limit) Loads Comparison (Orbiter Induced)



Table B-2. Summary Weight Statement
(Launch Condition)

B-17E DELTA WING BOOSTER

SYSTEM	Reusable Orbiter	Space Station
Wing Group	49453	49453
Tail Group	15487	15487
Body Group*	141247	144362
Induced Environ Protect	38371	38371
Landing, Docking	19856	19856
Propulsion, Ascent	99012	99012
Propulsion, Cruise	30498	30498
Propulsion, Auxiliary	6596	6596
Prime Power/Electrical	3011	3011
Hydraulic Conv. & Dist	2395	2395
Surface Controls	5702	5702
Avionics	4214	4214
Personnel Provision/ECS	2935	2935
Contingency/Growth	32617	32617
Subtotal (Dry Wt)	451395	454309
Personnel	476	476
Residual Fluids	11534	11534
Subtotal (Inert Wt)	463404	466519
Inflight Losses/ACS	16050	16050
Propellant - Ascent	2322205	2322205
Propellant - Cruise	58615	58615
Total Booster Weight	2860274	2863389
Second Stage	1123449	1222625
Total Vehicle Weight	3983723	4086014

* The Space Station requires a special separation mechanism (+200 lbs) and some beef-up to the separation system bulkheads and skins (+2915 lbs).



Table B-3. Spacecraft Sequence Mass Properties Statement

SPACECRAFT SEQUENCE MASS PROPERTIES STATEMENT										Of	
Configuration B-17E + MDAC SPACE STATION			By							Date	6/17/71
No.	Mission Event	Weight (lb)	Center of Gravity (inches)			Moment of Inertia (slug- $\text{ft}^2 \times 10^6$)			Product of Inertia (slug- $\text{ft}^2 \times 10^6$)		
Booster			x	y	z	I_{x-x}	I_{y-y}	I_{z-z}	I_{xy}	I_{xz}	I_{yz}
Liftoff		28633889	1947	0	383	7.898	266.10	265.70	0	-9.09	0
Max Q		1789680	2184	0	373	7.029	186.30	186.00	0	-6.64	0
Max Q (2 g)		1450614	2320	0	367	6.723	158.00	157.70	0	-5.22	0
Burnout (Entry)		541184	2727	0	348	5.045	64.04	63.91	0	-1.62	0
Start Cruise		525134	2724	0	348	4.946	62.65	62.59	0	-1.44	0
Landing		466519	2758	0	361	4.670	55.78	55.91	0	-1.20	0
<u>MDAC Space Station</u>											
Liftoff		1222625	1815	0	817	1.571	46.95	46.97	0	0	0
<u>Combined Vehicle</u>											
Liftoff		4086014	1908	0	513	44.270	351.10	315.90	0	-19.70	0
Max Q		3012305	2034	0	533	39.500	285.50	254.20	0	-32.30	0
Max Q (2 g)		2673239	2089	0	573	37.320	270.50	241.20	0	-37.80	0
Burnout		1763899	2095	0	673	24.440	196.10	178.10	0	-36.20	0

1

All e.g.s in Booster coordinate system:

Booster nose = 1000, + aft

Propellant tank Q = 400

Propellant tank $Q_L = 400$

Table B-4. Trajectory for ESS With B-17E Booster

NR TRAJECTORY/WEIGHT SIZING PROGRAM

DATE - 05/26/71	HOUR - 12
FIRST ATTEMPT AT B-17E BOOSTER FOR ESS APPLICATION (SIMILAR TO B170 EXCEPT DIMENSIONS)	
13.415K SL THRUST ENGINES	
DERIVED BASED ON 3-ENGINE EXTERNAL LH2 TANK ORBITER	
B-9U/ESS/MAC SS AERO WITH B17E REF AREA	
XAC DATA SCALED FROM B-9U TO REFLECT REDUCED BOOSTER LENGTH	
BOOSTER CG DATA FROM L HASSEMAN DATA OF 17 MAY 1971	
HAS ISP DEGRADATION WITH THROTTLING FOR BOOSTER (-3 SEC PER -50%)	
ALPHA PROFILE AS BELOW EXCEPT WHEN O*ALPHA WOULD BE EXCEEDED	
AND AT LIFTOFF WHERE ALPHA IS COMPUTED TO GIVE VERTICAL RISE	
SAME AS FOR 3-9U/ESS LOADS TRAJECTORIES	
TIME	20 30 40 7C 90 120+
ALPHA-2	0 0 -2 -2 -8
O*ALPHA LIMIT	= -600 PSF-DEG
T/W BO	= 2.0 G'S
FIXED FLYBACK RANGE = 241+1 NM	
FLYBACK RANGE CALCULATIONS BASED ON EXTRAPOLATION	
OF B-9U DATA TO LOW VELOCITIES WITH BIAS OF -20 NM	
TO AGREE WITH TWISP VEHICLE SIZING RUN	
GUESSED ESS WEIGHT BASED ON 3X415 K THRUST ENGINE	
FULLY LOADED ESS (91000 LBS MS PROPELLANT)	
2 DEG/SEC PITCH RATE AT ESS IGNITION	
OMS AND RCS AS REQUIRED TO FLY MISSION AND PROVIDE	
ENGINE OUT ROLL CONTROL	
6 DEGREE ENGINE CAN FOR ESS MS ENGINES OPERATING NORMALLY	
RETAIN ESS INTERSTAGE TO ORBIT AND DEORBIT WITH STAGE	
740 FPS OMS DV BUDGET---67G + 10 PERCENT	
DRA---27CNM---55 DEG INCL	
OAS ISP = 450.3 SEC = COS 4 (NOM ISP - 4)	
OMS LOSSES (BOILOFF AND CHILLDOWN) = 83 POUNDS OF LH2	
T/W LO = 1.21	

Table B-4. Trajectory for ESS With B-17E Booster (Cont)

PRELIMINARY TRAJECTORY FOR ANALYSIS OF ESS ON B-17E BOOSTER

VEHICLE CHARACTERISTICS	DATE - 05/26/71	CASE 19	PAGE 1 OF 9
STAGE	1	2	3
GROSS STAGE WEIGHT, (LBS)	4113505.0	1232625.0	<u>1222625.0</u>
GROSS STAGE THRUST/WEIGHT	1.312	0.0	1.164
THRUST, (LBS)	5915000.0	0.0	1423177.0
ISP, (SEC)	439.000	2.500	456.480
INERT WEIGHT, (LBS)	482361.0	10000.0	106200.0
PROPELLANT, (LBS)	2342024.0	0.0	<u>910422.3</u>
PERF. FRAC., (NU)	0.5693	0.0	0.7446
PROPELLANT FRAC., (NU)	0.8292	0.0	0.3955
BURNOUT TIME, (SEC)	205.763	208.263	499.795
BURNOUT VELOCITY, (FT/SEC)	6858.902	6332.352	25762.500
BURNOUT GAMMA, (DEGREES)	20.040	19.465	-0.000
BURNOUT ALTITUDE, (FT)	265154.3	270912.0	397994.0
BURNOUT RANGE, (NM)	52.9	55.1	666.3
IDEAL VELOCITY, (FT/SFC)	11535.9	* * * * *	19736.4
* * * * *	* * * * *	* * * * *	* * * * *
INJECTION VELOCITY, (FT/SEC)	313.2	FLYBACK RANGE(NM)	239.9
INJECTION PROPELLANT, (LBS)	6729.8	FLYBACK PROP(LBS)	56495.0
ORBIT MANEUVERING REQUIREMENTS	RENDEZVOUS	DEORBIT	*LOSSES
DELTA V, (FT/SEC)	740.0	550.0	0.0
SPECIFIC IMPULSE, (SEC)	450.3	450.3	0.0
PROPELLANT, (LBS)	15545.9	3056.7	32.0
RCS PROPULSION, (LBS)	4060.0	TOTAL RCS+GMS PROP, (LBS)	18685.5
MDAC SS	MARGIN	6297	176,960 LBS

Table B-4. Trajectory for ESS With B-17E Booster (Cont)

ATMOSPHERIC TRAJECTORY

TIME W	VREL VDT	ALT CDT	GAMMA VGRAV	QBAR VDRG	LOAD FACTOR
ALPHA	MACH	LIFT XCG (IN)	RANGE	DRAG	THRUST
ATTITUDE	TVC DEFL	XCG (IN)	ZCG (IN)	PITCH AC (IN)	THROTTLE RATIO
FLOW RATE	2*J*V	AERO HEAT	Q*ALPHA	AERO MOM (IN-LB)	NORMAL LF
0.0	0.0	0.0	0.0	0.0	0.121000E 01
0.411351E 07	0.67503CE 01	0.0	0.0	0.0	0.502734E 07
-0.487973E 01	0.0	0.0	0.0	0.500000E 05	0.931851E 00
0.851203E 02	0.487973E 01	0.192353E 04	0.515052E 03	0.265000E 04	0.103962E 00
0.125579E 05	0.0	0.0	0.0	0.0	0.120552E 01
0.100000E 02	0.7344615E 02	0.357793E 03	0.900002E 02	0.613669E 01	0.124693E 01
0.398193F 07	0.793961E 01	0.129975E -04	0.322165E 03	0.424709E 01	0.503334E 07
-0.502740E 01	0.646436E -01	-0.257504E 03	-0.125609E -06	0.606772E 05	0.931851E 00
0.849727E 02	0.502156E 01	0.192932E 04	0.518809E 03	0.265000E 04	0.109079E 00
0.125579E 05	0.901620E 03	0.22512CF 04	-0.308516E 02	-0.279572E 07	0.124215E 01
0.200000E 02	0.153692E 03	0.160328E 04	0.900002E 02	0.277392E 02	0.128284E 01
0.386235E 07	0.904967E 01	0.154972E -05	0.644305E 03	0.105495E 02	0.505228E 07
-0.510484E 01	0.140240E 00	-0.171177E 05	-0.721840E -06	0.974607E 05	0.931851E 00
0.848953E 02	0.528077E 01	0.193415E 04	0.522831E 03	0.265000E 04	0.113732E 00
0.125579E 05	0.830400E 04	0.413531E 05	-0.141604E 03	0.832273E 07	0.127779E 01
0.200000E 02	0.153692E 03	0.150928E 04	0.863925E 02	0.277392E 02	0.128284E 01
0.386235E 07	0.916244E 01	-0.730959E 00	0.644306E 03	0.105495E 02	0.505228E 07
-0.510484E 01	0.140240E 00	-0.171177E 05	-0.721840E -06	0.974607E 05	0.931851E 00
0.812877E 02	0.528077E 01	0.193416E 04	0.522831E 03	0.265000E 04	0.113732E 00
0.125579F 05	0.830400E 04	0.413531E 05	-0.141604E 03	0.832273E 07	0.127779E 01
0.300000E 02	0.256211E 03	0.356293E 04	0.817475E 02	0.685493E 02	0.131851E 01
0.373677E 07	0.103844E 02	-0.104616E 00	0.964271E 03	0.212423E 02	0.508453E 07
0.0	0.228629E 00	0.222319E 05	0.437145E -01	0.160365E 06	0.931851E 00
0.317475E 02	0.515531E 01	0.19407E 04	0.527036E 03	0.265477E 04	0.128251E 00
0.125579E 05	0.352222E 05	0.241180E 06	0.0	-0.321290E 08	0.131225E 01

Table B-4. Trajectory for ESS With B-17E Booster (Cont)

ATMOSPHERIC TRAJECTORY										CASE 19	PAGE 3 OF 9
TIME W	VREL	ALT GDT	GAMMA	QBAR VDRG	LOAD FACTOR						
ALPHA	VDT	LIFT	VGRAV	DRAG	THRUST						
ATTITUDE	TVC DEFL	XCG(IN)	ZCG(IN)	PITCH AC(IN)	NORMAL LF						
FLOW RATE	2*Q*V	AERO HEAT	Q*ALPHA	AERO MOM(IN-LB)	AXIAL LF						
0.40000E 02	0.366650E 03	0.663418E 04	0.906318E 02	0.127406E 03	0.135455E 01						
0.36119E 07	0.115111E 02	-0.1C3208E 00	0.128250E 04	0.390085E 02	0.512926E 07						
0.0	0.329405E 00	0.414130E 05	0.125770E 00	0.242883E 06	0.931851E 00						
0.806318E 02	0.519338E 01	0.194352E 04	0.531515E 03	0.267157E 04	0.140161E 00						
0.125579E 05	0.934295E 05	0.853677E 26	9.0	-0.534323E 08	0.134728E 01						
0.50000E 02	0.489939E 03	0.108401E 05	0.72055E 02	0.199207E 03	0.139608E 01						
0.344561E 07	0.131340E 02	-0.197009E 00	0.159953E 04	0.643223E 02	0.518410E 07						
-0.666667E 00	0.445798E 00	0.346583E 05	0.253234E 00	0.322284E 06	0.931851E 00						
0.785389E 02	0.542356E 01	0.195629E 04	0.536309E 03	0.269097E 04	0.149583E 00						
0.125579E 05	0.195904E 06	0.226064E 07	-0.13271E 03	-0.521877E 08	0.138805E 01						
0.60000E 02	0.630291E 03	0.163041E 05	0.757186E 02	0.278699E 03	0.144314E 01						
0.336003E 07	0.149844E 02	-0.298078E 00	0.191428E 04	0.987703E 02	0.524542E 07						
-0.133333E 01	0.583793E 00	0.108362E 05	0.453238E 00	0.398699E 06	0.931851E 00						
0.753153E 02	0.583405E 01	0.196736E 04	0.541471E 03	0.270332E 04	0.159147E 00						
0.125579E 05	0.351324E 06	0.495334E 07	-0.31599E 03	-0.317744E 08	0.143433E 01						
0.70000E 02	0.790599E 03	0.231497E 05	0.733185E 02	0.352950E 03	0.149326E 01						
0.323445E 07	0.171239E 02	-0.38058CE 01	0.222496E 04	0.141462E 03	0.530870E 07						
-0.200000E 01	0.752365E 00	-0.322401E 05	0.769013E 00	0.477775E 06	0.931851E 00						
0.713195E 02	0.657336E 01	0.201631E 04	0.546735E 03	0.271094E 04	0.172778E 00						
0.125579E 05	0.558148E 06	0.946463F 97	-0.705900E 03	0.905408E 07	0.148323E 01						
0.30000E 02	0.963183E 03	0.314721E 05	0.693436E 02	0.402360E 03	0.149911E 01						
0.310887E 07	0.180370E 02	-0.421394E 00	0.252938E 04	0.199774E 03	0.536897E 07						
-0.199827E 01	0.957733E 00	-0.547033E 05	0.124997E 01	0.705336E 06	0.931851E 00						
0.673553E 02	0.680287E 01	0.206224F 04	0.552525E 03	0.271221E 04	0.179190E 00						
0.125579E 05	0.779116E 06	0.161794E 08	-0.800000E 03	-0.206219E 08	0.148836E 01						

Table B-4. Trajectory for ESS With B-17E Booster (Cont)

ATMOSPHERIC TRAJECTORY							CASE 19 PAGE 4 OF 9						
TIME W	VREL VROT	ALT GDT	GAMMA VGRAV	QBAR VDRG	LOAD FACTOR	THRUST	ATTITUDE	TVC DEFL	LIFT XCG(IN)	DRAG	THROTTLE RATIO	NORMAL LF	AXIAL LF
ALPHA	MACH	W	RANGE	W	W	W	W	W	W	W	W	W	W
0.900000E 02	0.115995E 04	0.412497E 05	0.650622E 02	0.403844E 03	0.157257E 01								
0.293329E 07	0.213007E 02	-0.42317CE 09	0.232528E 04	0.280402E 03	0.542083E 07								
-0.193096E 01	0.120197E 01	-0.251808E 05	0.195164E 01	0.730129E 06	0.931851E 00								
0.630912E 02	0.699083E 01	0.21C477E 04	0.558339E 03	0.268618E 04	0.203945E 00								
0.125579E 05	0.93648CE 06	0.248144E 03	-0.800000E 03	-0.608782E 08	0.155929E 01								
0.100000E 03	0.140268E 04	0.526090E 05	0.608907E 02	0.355245E 03	0.173162E 01								
0.285771E 07	0.274332E 02	-0.411779E 09	0.311090E 04	0.349703E 03	0.546021E 07								
-0.225197E C1	0.147683E 01	0.402599E 04	0.293779E 01	0.514226E 06	0.931851E 00								
0.586397E 02	0.718559E 01	C. 208441E 04	C. 565802E 03	0.267512E 04	0.233337E 00								
0.125579E 05	C. 996591E 06	0.345973E 08	-0.800000E 03	-0.592535E 08	0.171583E 01								
0.110000E 03	C. 171172E 04	0.658669E 05	C. 557122E 02	0.261392E 03	0.190207E 01								
0.273213E 07	0.342395E 02	-0.424226E 00	C. 338489E 04	0.374916E 03	0.548540E 07								
-0.306053E 01	0.179358E 01	-0.660138E 05	0.430136E 01	0.284337E 06	0.931851E 00								
0.536517E 02	0.783066E 01	0.205787E 04	0.573454E 03	0.263243E 04	0.245806E 00								
0.125579E 05	0.894361E 06	0.441491E 08	-0.800000E 03	0.795405E 07	0.188612E 01								
0.120000E 03	0.208404E 04	0.812829E 05	0.524010E 02	0.176348E 03	0.200061E 01								
0.250724E 07	0.389337E 02	-0.441874E 00	0.364551E 04	0.418730E 03	0.534435E 07								
-0.453543E 01	0.212994E 01	-0.112114E 06	0.615917E 01	0.121950E 06	0.905604E 00								
0.478545E 02	0.844251E 01	0.203164E 04	0.581945E 03	0.258366E 04	0.254381E 00								
0.122058E 05	0.735032E 06	0.523359E 08	-0.800000E 03	0.536826E 08	0.198437E 01								
0.130700E 03	0.248252E 04	0.937739E 05	0.478062E 02	0.107820E 03	0.200015E 01								
0.248929E 07	0.407332E 02	-0.481091E 07	0.359060E 04	0.427026E 03	0.500198E 07								
-0.741980E 01	0.248330E 01	-0.132977E 06	0.862366E 01	0.209324E 05	0.846519E 00								
0.403864E 02	0.908579E 01	0.205051E 04	0.5920579E 03	0.2533242E 04	0.263253E 00								
0.114144E 05	0.5332329E 06	0.537052E 08	-0.300000E 03	0.702110E 08	0.198275E 01								



Table B-4. Trajectory for ESS With B-17E Booster (Cont)

ATMOSPHERIC TRAJECTORY				CASE 19 PAGE 5 OF 9			
TIME	VREL VOUT	ALT GDT	GAMMA VGRAV	QBAR VORG	LOAD FACTOR		
ALPHA	MACH	LIFT	RANGE	DRAG	THRUST		
ATTITUDE	TVC DEFL	XCG(IN) AERO HEAT	ZCG(IN)	PITCH AC(IN)	ACUM(IN-LB)	NORMAL LF	ROTATE RATE
ELON RATE	2**J*V	Q*ALPHA	AERO MUM(IN-LB)	ACUM(IN-LB)	ACUM(IN-LB)	AXIAL LF	
0.140000E 03	C. 239920E 04	0.117907E 06	0.431450E 02	0.606152E 02	0.200006E 01		
0.23739E 07	0.425385E 02	-0.438836E 00	0.411771E 04	0.425895E 03	0.472452E 07		
-0.930000E 01	0.281690E 01	-0.858745E 05	0.117892E 02	-0.338336E 05	0.799056E 00		
0.351450E 02	0.946302E 01	0.208176E 04	0.539546E 03	0.247930E 04	0.293022E 00		
0.107350E 05	0.351472E 06	0.631032E 08	-0.434922E 03	0.434301E 08	0.197848E 01		
0.150000E 03	0.3333392E 04	0.138335E 06	0.390173E 02	0.328182E 02	0.199989E 01		
0.227335E 07	0.443337E 02	-0.387969E 00	0.432662E 04	0.419009E 03	0.448616E 07		
-0.300000E 01	0.313959E 01	-0.513737E 05	0.157120E 02	-0.617497E 05	0.758588E 00		
0.310173E 02	C. 992390E 01	0.210583E 04	0.609045E 03	0.242767E 04	0.321661E 00		
0.102335E 05	0.213327E 06	0.659116E 08	-0.262546E 03	0.287102E 08	0.197385E 01		
0.160000E 03	0.378550E 04	0.159801E 06	0.353606E 02	0.178135E 02	0.199977E 01		
0.217346E 07	0.459010E 02	-0.344417E 00	0.451841E 04	0.408787E 03	0.427004E 07		
-C. 800000E 01	C. 3491155E 01	-0.333722E 05	0.204239E 02	-0.777164E 05	0.721963E 00		
0.273606E 02	0.134694E 02	0.212312E 04	0.619120E 03	0.237135E 04	0.346462E 00		
0.974029E 04	0.134866E 06	0.676465E 08	-0.142503E 03	0.236146E 08	0.196953E 01		
0.170000E 03	0.425276E 04	0.182072E 06	0.320985E 02	0.100199E 02	0.199972E 01		
0.207323E 07	0.474731E 02	-0.308744E 00	0.459424E 04	0.396395E 03	0.407189E 07		
-0.300000E 01	0.401300E 01	-0.240143E 05	0.259705E 02	-0.851950E 05	0.688425E 00		
0.240735E 02	0.108774E 02	0.212613E 04	0.626285E 03	0.228956E 04	0.363999E 00		
0.920136E 04	0.852241E 05	0.687328E 03	-0.301589E 02	0.219602E 08	0.196631E 01		
0.180000E 03	0.473455E 04	0.204926E 06	0.291719E 02	0.528144E 01	0.199966E 01		
0.193734E 07	0.483691E 02	-0.277173E 00	0.495527E 04	0.382494E 03	0.388523E 07		
-0.802000E 01	C. 464952E 01	-0.190415E 05	0.323625E 02	-0.899577E 05	0.656853E 00		
C. 211719E 02	C. 113137E 02	0.212387E 04	0.638330E 03	0.226889E 04	0.380344E 00		
0.33777CE 04	C. 500105E 05	0.693989E 03	-0.422515E 02	0.227997E 08	0.196316E 01		



Table B-4. Trajectory for ESS With B-17E Booster (Cont)

ATMOSPHERIC TRAJECTORY										CASE 19 PAGE 6 OF 9		
TIME W	VREL V00T	ALT G0T	GAMMA VGRAV	LOAD FACTOR QBAR	THRUST VDRG	THROTTLE RATIO	ZCG (IN) XCG (IN)	PITCH AC (IN) Q*ALPHA	NORMAL LF	AERO MOM (IN-LB)	AXIAL LF	
0.190000E 03	0.5222973E 04	0.228163E 06	0.265427E 02	0.251686E 01	0.19963E 01							
0.190055E 07	0.501512E 02	-0.249194E 00	0.500260E 04	0.367350E 03	0.370889E 07							
-0.300000E 01	0.538236E 01	-0.161037E 05	0.396263E 02	-0.926336E 05	0.627035E 00							
0.185427E 02	0.117449E 02	0.211639E 04	0.649303E 03	0.224507E 04	0.395631E 00							
0.949143E 04	0.263250E 05	0.697721E 38	-0.201348E 02	0.238554E 08	0.196010E 01							
0.200000E 03	0.573719E 04	0.251699E 06	0.241773E 02	0.106026E 01	0.19960E 01							
0.181764E 07	0.512239E 02	-0.224357E 00	0.513736E 04	0.351168E 03	0.354170E 07							
-0.800000E 01	0.619692E 01	-0.145309E 05	0.477787E 02	-0.940836E 05	0.598767E 00							
0.161773E 02	0.121661E 02	0.210374E 04	0.661230E 03	0.221614E 04	0.40932E 00							
0.810379E 04	0.121658E 05	0.669579E 08	-0.848206E 01	0.250297E 08	0.195713E 01							
0.205763E 03	0.603479E 04	0.265154E 06	0.229222E 02	0.608746E 00	0.19963E 01							
0.177154E 07	0.519539E 02	-0.211369E 00	0.520971E 04	0.341422E 03	0.344921E 07							
-0.800000E 01	0.671177E 01	-0.140356E 05	0.528942E 02	-0.945061E 05	0.593129E 00							
0.149222E 02	0.124028E 02	0.209410E 04	0.668545E 03	0.219297E 04	0.417763E 00							
0.789483E 04	0.734730E 04	0.700132E 08	-0.486997E 01	0.257441E 08	0.195550E 01							

Table B-4. Trajectory for ESS With B-17E Booster (Cont)

ATMOSPHERIC TRAJECTORY

FOLLOWING PRINT POINTS REPRESENT CLOSEST POINTS TO 33000 FOOT ALTITUDE, MAX Q
AND INITIAL MAX LOAD FACTOR CONSIDERING INTEGRATION INTERVAL OF 2.00 SECONDS

TIME W	VREL VOOT	ALT GOT	GAMMA VGRAV	QBAR VDRG	LOAD FACTOR	
					LIFT RANGE	THRUST DRAg
0.82000E 02	0.100438E 04	0.333125E 05	0.694928E 02	0.406356E 03	0.149766E 01	
0.308375E 07	0.181543E 02	-0.429399E 00	0.258931E 04	0.215009E 03	0.538017E 07	
-0.136372E 01	0.1CC260E 01	-0.580334E 05	0.137098E 01	0.759557E 06	0.931851E 00	
0.665241E 02	0.680937E 01	0.207103E 04	0.53752E 03	0.271143E 04	0.179591E 00	
0.125579E 05	0.816275E 06	0.177748E 08	-0.800000E 03	-0.323843E 08	0.148686E 01	
0.86000E 02	0.107904E 04	0.371643E 05	0.667715E 02	0.408767E 03	0.151805E 01	
0.303352E 07	0.191752E 02	-0.431091E 09	0.270308E 04	0.247750E 03	0.540141E 07	
-0.195710E 01	0.109778E 01	-0.435366E 05	0.164101E 01	0.795609E 06	0.931851E 00	
0.648144E 02	0.684136E 01	0.2049319E 04	0.556230E 03	0.269049E 04	0.188803E 00	
0.125579E 05	0.882149E 06	0.211739E 08	-0.300000E 03	-0.530688E 08	0.150627E 01	
0.11800E 03	0.200637E 04	0.780235E 05	0.532790E 02	0.192186E 03	0.200068E 01	
0.263193E 07	0.386698E 02	-0.436106E 00	0.359455E 04	0.415397E 03	0.542136E 07	
-0.416264E 01	0.2C5967E 01	-0.105057E 06	0.574226E 01	0.149488E 06	0.919004E 00	
0.491163E 02	0.834053E 01	0.203679E 04	0.530198E 03	0.259385E 04	0.254863E 00	
0.123855E 05	0.771192E 06	0.508297E 08	-0.300000E 03	0.464447E 08	0.198438E 01	

Table B-4. Trajectory for ESS With B-17E Booster (Cont)

EXO-ATMOSPHERIC TRAJECTORY				CASE 19 PAGE 8 OF 9			
TIME W	V(R) V(L)	GAM(R) GAM(I)	ALT THETAIR	RANGE	T/W		
0.205763E 03	0.603479E 04	0.229222E 02	0.265154E 06	0.528842E 02	0.0		
0.123268E 07	0.685990E 04	0.200405E 02	0.149222E 02				
0.208263E 03	0.600462E 04	0.222824E 02	0.270912E 06	0.551418E 02	0.0		
0.123268E 07	0.683235E 04	0.194653E 02	0.149658E 02				
0.2092263E 03	0.600492E 04	0.222824E 02	0.270912E 06	0.551418E 02	0.116398E 01		
0.122268E 07	0.683235E 04	0.194653E 02	0.149658E 02				
0.210370E 03	0.605871E 04	0.216784E 02	0.275648E 06	0.570567E 02	0.117027E 01		
0.121611E 07	0.688964E 04	0.189562E 02	0.192177E 02				
0.25037CE 03	0.728439E 04	0.124714E 02	0.351728E 06	0.982723E 02	0.130399E 01		
0.109140E 07	0.815436E 04	0.111223E 02	0.170016E 02				
0.290370E 03	0.885595E 04	0.62258CE 01	0.402208E 06	0.149603E 03	0.147221E 01		
0.966692E 06	0.974227E 04	0.565746E 01	0.148604E 02				
0.330370E 03	0.107677E 05	0.221852E 01	0.429520E 06	0.212577E 03	0.169026E 01		
0.841983E 06	0.116593E 05	0.204879E 01	0.128339E 02				
0.37037CE 03	0.130600E 05	-0.132385E 00	0.436848E 06	0.289172E 03	0.198413E 01		
0.717275E 06	0.139525E 05	-0.123917E 00	0.109720E 02				
0.410370E 03	0.158321E 05	-0.121062E 01	0.428944E 06	0.382034E 03	0.240170E 01		
0.592567E 06	0.167242E 05	-0.114604E 01	0.933802E 01				

Table B-4. Trajectory for ESS With B-17E Booster (Cont)

EXOATMOSPHERIC TRAJECTORY				CASE 19 PAGE 9 OF 9
TIME W	V(R) V(I)	GAM(R) GAM(I)	ALT THETA(R)	RANGE T/W
0.450370E 03	0.192301E 05	-0.123587E 01	0.412992E 06	0.494859E 03
0.467859E 06	0.201715E 05	-0.118125E 01	0.801434E 01	0.304187E 01
0.486314E 03	0.232766E 05	-0.434204E 00	0.401168E 06	0.617795E 03
0.355798E 06	0.241076E 05	-0.418196E 00	0.718286E 01	0.399993E 01
0.499795E 03	0.248715E 05	-0.810027E-04	0.399984E 06	0.666323E 03
0.318936E 06	0.257625E 05	-0.782013E-04	0.699416E 01	0.399993E 01

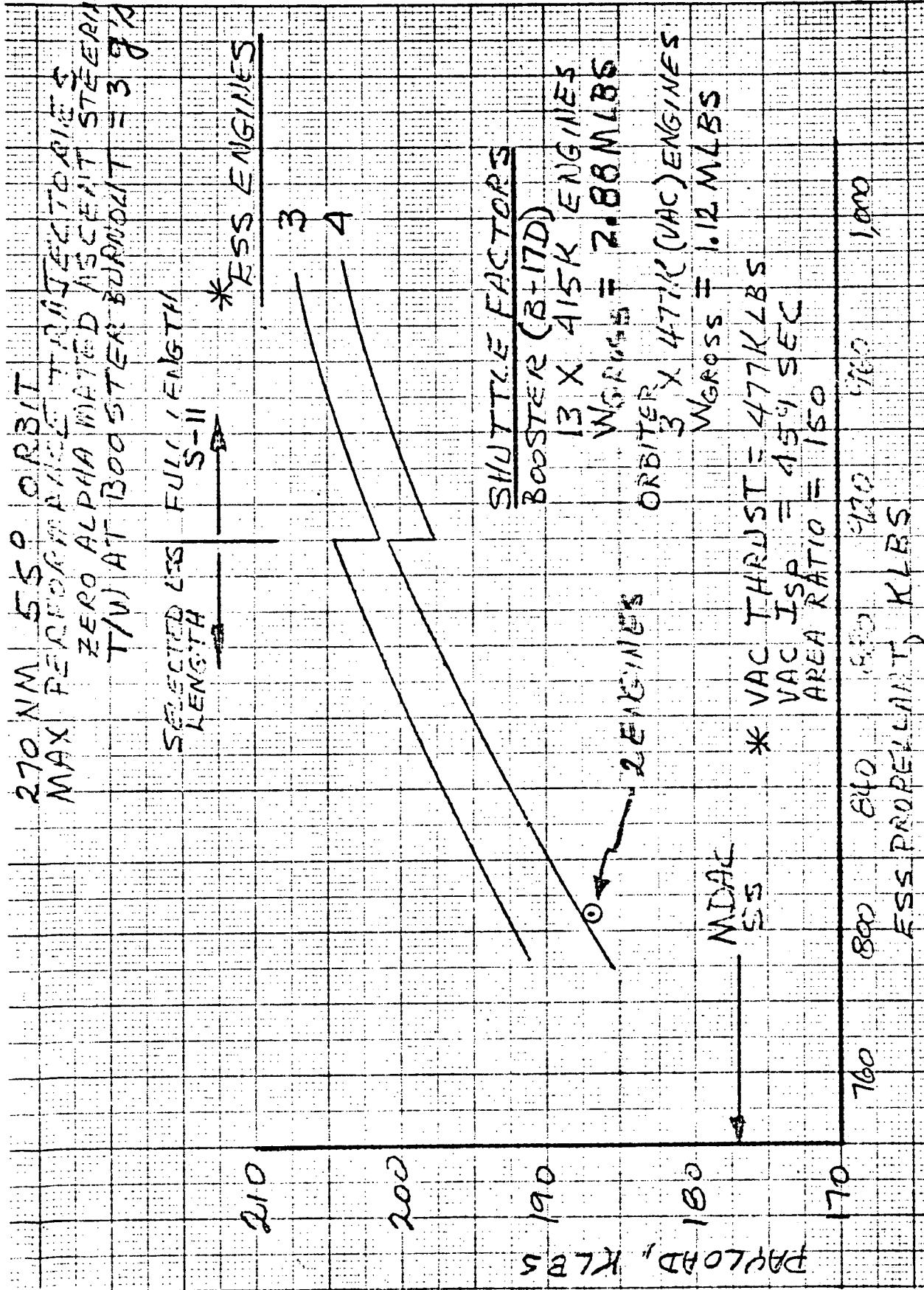


Figure B-3. Preliminary ESS Performance
B-17D Booster

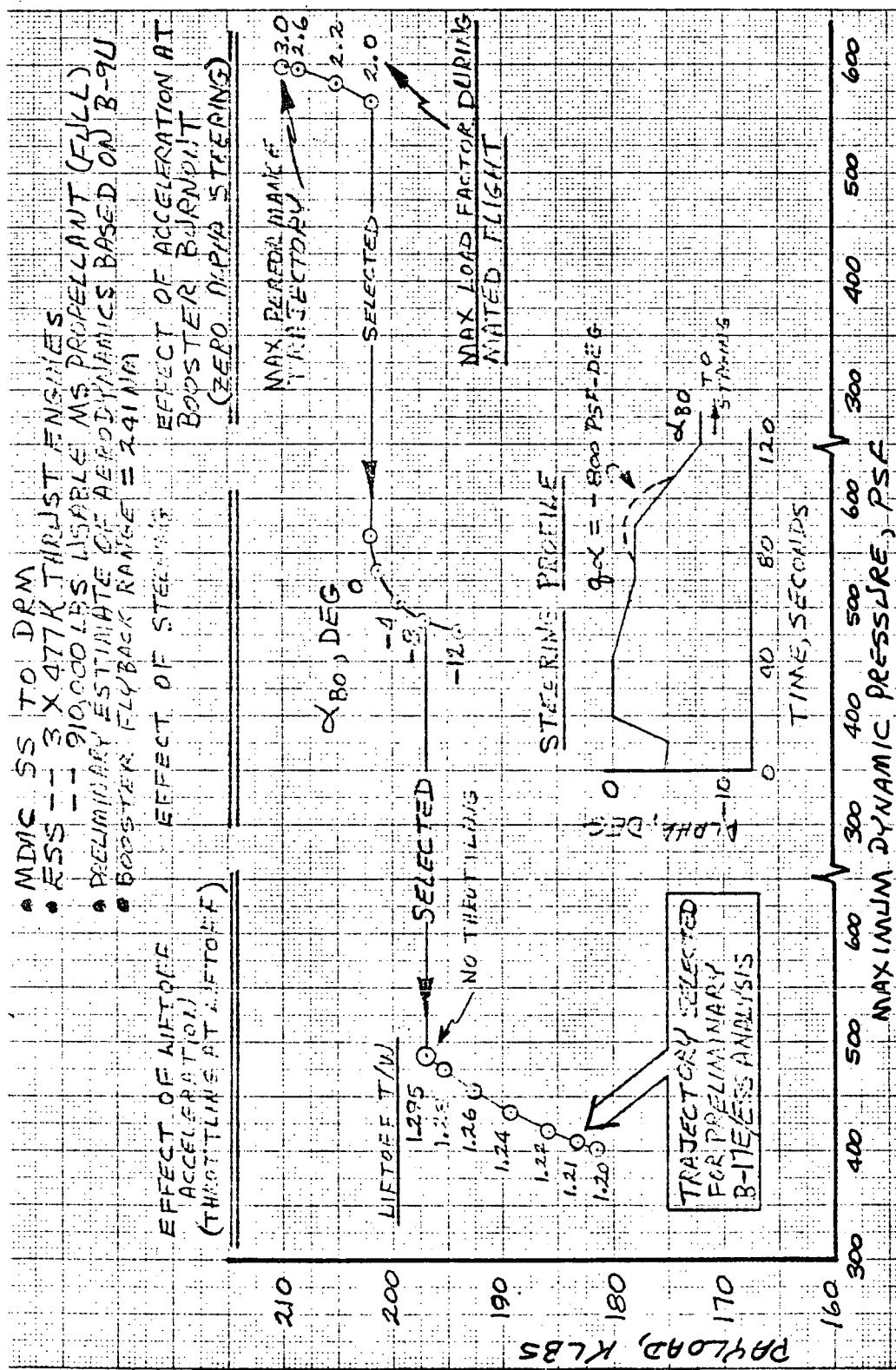


Figure B-4. B-17E/ESS Trajectory Shaping Effects

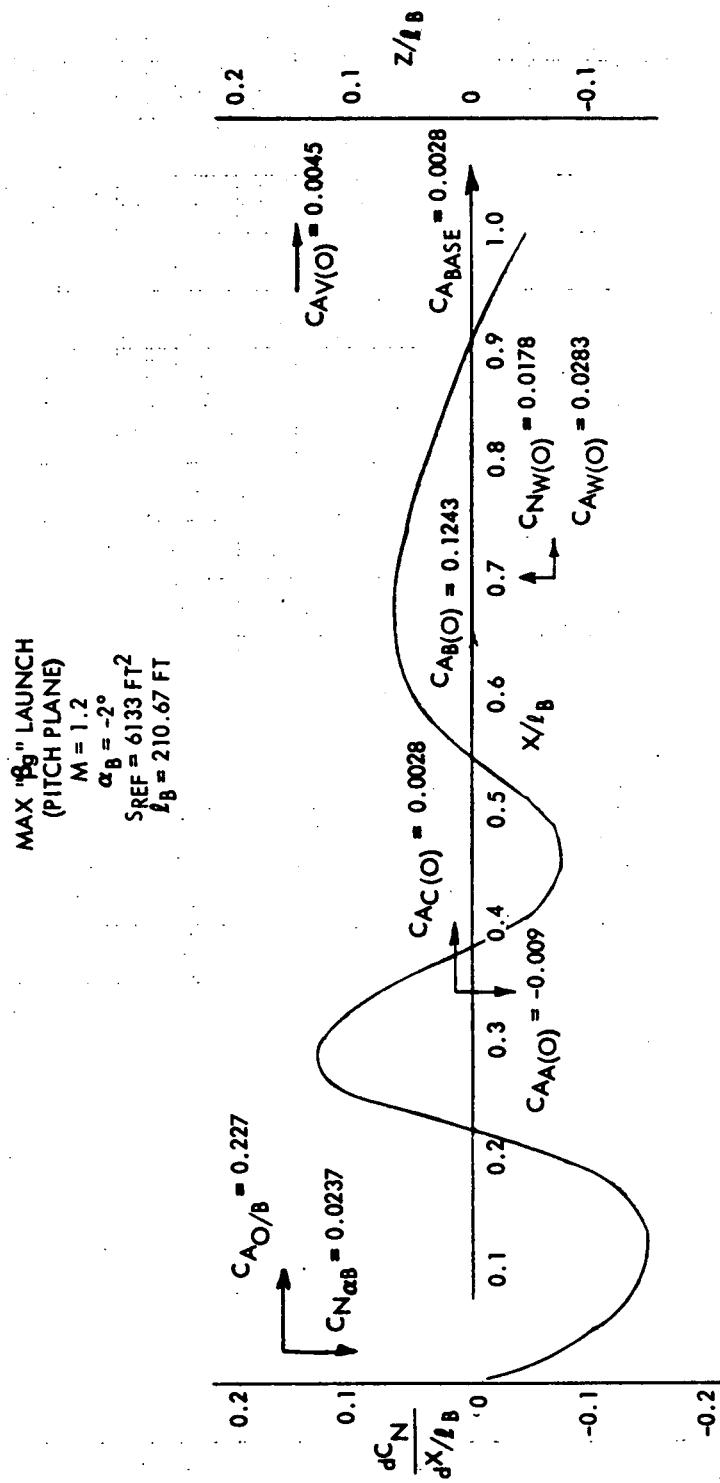


Figure B-5. Air-Load Distribution, Maximum "β_q" Launch-Pitch Plane

MAXIMUM "B_g" LAUNCH
 (YAW PLANE)
 $M = 1.2$
 $B = 4 \text{ DEG}^\circ$
 $S_{REF} = 6133 \text{ FT}^2$
 $\ell_B = 210.67 \text{ FT}$

$$C_{Y_O(B)} = -0.0683$$

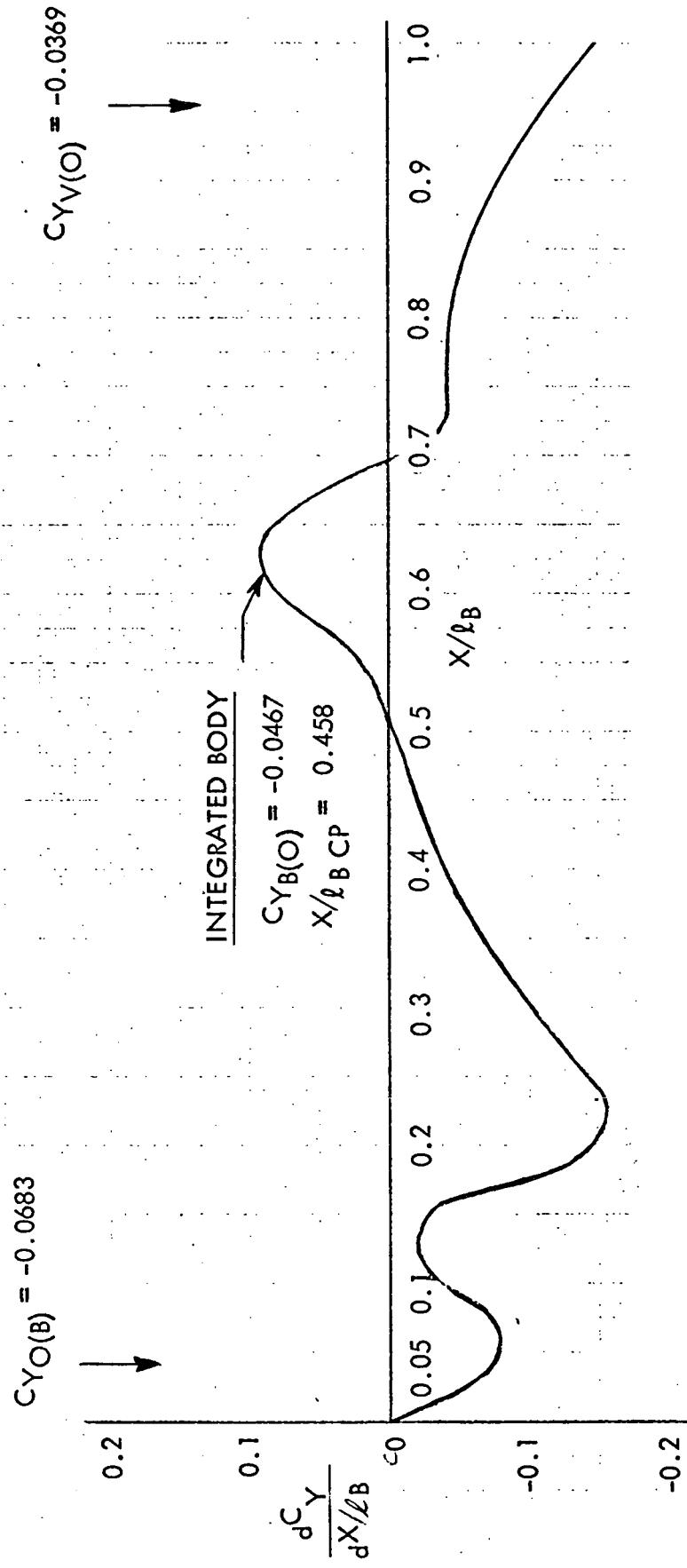


Figure B-6. Air-Load Distribution, Maximum "B_g" Launch-Yaw Plane



Table B-5 lists the loading conditions used to develop the current design load envelope for the B-17E booster. Tables B-6 and B-7 give the peak tension and compression ultimate loads versus booster station for the B-17E/NR orbiter VB70-0500 as of 9 June 1971.

Table B-8 lists the loading conditions investigated for the ESS/MDAC stage. Tables B-9 and B-10 give the peak tension and compression ultimate loads versus booster station for the ESS/MDAC stage. Figures B-7, B-8, and B-9 are plots of the loads shown in Tables B-6 through B-9. The areas on the booster where the ESS/MDAC load intensities exceed the baseline are shown on these plots along with the loading condition which caused the overload.

Figure B-10 gives the design limit attachment loads that are applied to the B-17E/ESS/MDAC fixed-platform separation system from the ESS/MDAC stage.

The effects of the ESS/MDAC stage on the structural weight of the B-17E booster have been evaluated and the results are presented in Figure B-11. The critical flight condition is at maximum thrust—the point in the trajectory where the axial acceleration initially reaches 2.0 g and throttling is initiated. The critical component is the B-17E hydrogen tank bulkhead at Station 2398. This station is comparable to B-9U Station 2866 shown in Figure B-12, except that the distance between this bulkhead and the adjacent bulkhead has been decreased by 65 inches, increasing the angle of the diagonal link. A drag support is required, as shown in Figure B-12, to transfer the longitudinal loads from the aft ESS structure to the forward booster structure. This arrangement, as explained in Volume II, Book 3, provides the maximum structural compatibility between the ESS and the booster, but it induces a vertical load component in the aft booster bulkhead as shown. This vertical load component establishes the requirement for the additional 2530 pounds of bulkhead weight and 150 pounds of additional weight to the adjacent skins as shown in Table B-9.

A comparison of the loads defined in Figure B-10 with the ESS/B-9U booster loads shown in Volume II shows an increase for the B-17E configuration. This increased load would require additional structural modifications to the ESS forward and aft skirt structure. These modifications are considered minor with respect to the modifications defined for the basic ESS configurations.

Table B-5. Booster B-17E Ultimate Internal Loads

COND 1	BOOSTER	3-17E/NR	ORBITER	V870-05J0	1HR GROUND HEADWINDS	TANKED	UNPRESS
COND 2	1300 BOOSTER	3-17E/NR	ORBITER	V870-05J0	1HR GROUND TAILWINDS	TANKED	UNPRESS
COND 3	300 BOOSTER	3-17E/NR	ORBITER	V870-05J0	1HR GROUND SIDEWINDS	TANKED	UNPRESS
COND 4	900 BOOSTER	3-17E/NR	ORBITER	V870-05J0	LIFT OFF +1HR GROUND HEADWINDS		
COND 5	800 BOOSTER	3-17E/NR	ORBITER	V870-05J0	LIFT OFF +1HR GROUND TAILWINDS		
COND 6	900 BOOSTER	3-17E/NR	ORBITER	V870-05J0	LIFT OFF +1HR GROUND SIDEWINDS		
COND 7	900 BOOSTER	3-17E/NR	ORBITER	V870-05J0	NAX ALPHA Q HEADWINDS		
COND 8	300 BOOSTER	3-17E/NR	ORBITER	V870-05J0	NAX ALPHA Q TAILWINDS		
COND 9	900 BOOSTER	3-17E/NR	ORBITER	V870-05J0	NAX DELTA Q		
COND 10	900 BOOSTER	3-17E/NR	ORBITER	V870-05J0	3.0 G MAX THRUST		
COND 11	900 BOOSTER	3-17E/NR	ORBITER	V870-05J0	3 G NOSE UP BURNOUT		
COND 12	900 BOOSTER	3-17E/NR	ORBITER	V870-05J0	4G RECOVERY		

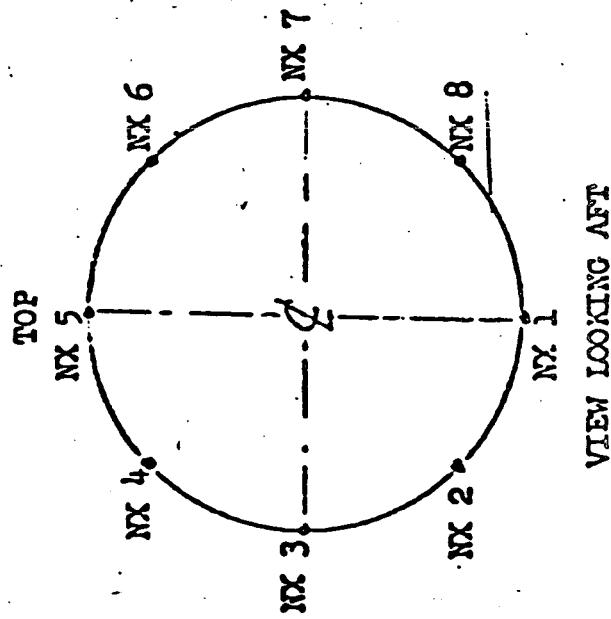


Table B-6. Booster B-17E Peak Ultimate Axial Tension
Load Intensities

STATION (IN)	NX1 (LB/IN)	NX2 (LB/IN)	NX3 (LB/IN)	NX4 (LB/IN)	NX5 (LB/IN)	NX6 (LB/IN)	NX7 (LB/IN)	NX8 (LB/IN)
1000	0 (12)	0 (12)	0 (12)	0 (12)	0 (12)	0 (12)	0 (12)	0 (12)
1143	21 (12)	16 (12)	5 (12)	-1 (8)	14 (3)	-1 (9)	5 (12)	16 (12)
1294	54 (12)	59 (12)	3 (12)	29 (8)	73 (8)	29 (9)	3 (12)	39 (12)
1296	55 (12)	40 (12)	3 (12)	33 (8)	72 (8)	30 (8)	3 (12)	40 (12)
1288	56 (12)	40 (12)	3 (12)	31 (8)	73 (8)	31 (8)	3 (12)	46 (12)
1414	147 (12)	75 (12)	-2 (12)	87 (6)	159 (-3)	78 (-8)	-2 (12)	75 (12)
1416	2354 (12)	2322 (12)	2243 (12)	2194 (11)	2228 (11)	2194 (11)	2243 (12)	2322 (12)
1418	2355 (12)	2323 (12)	2243 (12)	2153 (11)	2227 (11)	2193 (11)	2243 (12)	2323 (12)
1461	2382 (12)	2341 (12)	2242 (12)	2194 (11)	2226 (11)	2184 (11)	2242 (12)	2341 (12)
1463	2383 (12)	2342 (12)	2242 (12)	2184 (10)	2226 (11)	2184 (11)	2242 (12)	2342 (12)
1465	2394 (12)	2343 (12)	2242 (12)	2172 (11)	2210 (11)	2172 (11)	2242 (12)	2343 (12)
1579	2732 (10)	2525 (11)	2235 (12)	2089 (12)	2027 (12)	2039 (12)	2235 (12)	2525 (10)
1591	3254 (10)	3098 (11)	2219 (12)	2014 (12)	1929 (12)	2014 (12)	2219 (12)	3698 (10)
1592	3311 (11)	2926 (11)	2219 (12)	2014 (12)	1929 (12)	2014 (12)	2219 (12)	2926 (11)
1593	1469 (11)	684 (11)	-26 (12)	-232 (12)	-317 (12)	-232 (12)	-26 (12)	684 (11)
1595	1493 (11)	691 (11)	-27 (12)	-234 (12)	-320 (12)	-234 (12)	-27 (12)	691 (11)
1939	2790 (11)	1165 (11)	-41 (12)	-339 (12)	-463 (12)	-339 (12)	-41 (12)	1155 (11)
1844	2720 (11)	1170 (11)	-52 (12)	-353 (12)	-479 (12)	-353 (12)	-52 (12)	1170 (11)
1942	2740 (11)	1174 (11)	-52 (12)	-355 (12)	-480 (12)	-355 (12)	-52 (12)	1174 (11)
1996	4341 (11)	1542 (11)	-69 (12)	-342 (12)	-455 (12)	-342 (12)	-69 (12)	1642 (11)
1989	7225 (11)	4510 (11)	2330 (12)	2060 (12)	1948 (12)	2060 (12)	2330 (12)	4510 (11)
1990	7227 (11)	4510 (11)	2330 (12)	2062 (12)	1951 (12)	2062 (12)	2330 (12)	4510 (11)
2002	7236 (11)	4494 (11)	2329 (12)	2075 (12)	1970 (12)	2075 (12)	2328 (12)	4494 (11)
2261	6718 (11)	4123 (11)	2310 (12)	2280 (12)	2268 (12)	2280 (12)	2310 (12)	4123 (11)
2263	6714 (11)	4120 (11)	2310 (12)	2281 (12)	2270 (12)	2281 (12)	2310 (12)	4124 (11)
2265	6699 (11)	4168 (11)	2310 (12)	2293 (12)	2271 (12)	2293 (12)	2310 (12)	4108 (11)





Table B-6. Booster B-17E Peak Ultimate Axial Tension
Load Intensities (Cont)

STATION (IN)	NX1 (LB/IN)	NX2 (LB/IN)	NX3 (LB/IN)	NX4 (LB/IN)	NX5 (LB/IN)	NX6 (LB/IN)	NX7 (LB/IN)	NX8 (LB/IN)
2336	5681(11)	3372(11)	2315(12)	2353(12)	2309(12)	2353(12)	2315(12)	3372(11)
2398	5066(11)	3361(11)	2315(12)	2354(12)	2370(12)	2315(12)	3361(11)	3361(11)
2433	5650(11)	3349(11)	2315(12)	2355(12)	2371(12)	2315(12)	3349(11)	3349(11)
2538	4423(11)	2464(11)	2319(12)	2407(12)	2644(12)	2407(12)	2319(12)	2464(11)
2748	2929(11)	2223(12)	2323(12)	2423(12)	2454(12)	2423(12)	2323(12)	2223(12)
2898	2121(12)	2186(12)	2345(12)	2533(12)	2569(12)	2533(12)	2345(12)	2186(12)
2934	1936(12)	2074(12)	2286(12)	2493(12)	2587(12)	2439(12)	2286(12)	2074(12)
2902	1993(12)	2172(12)	2287(12)	2531(12)	2590(12)	2531(12)	2287(12)	2072(12)
3173	1617(12)	1731(12)	2247(12)	2763(12)	2976(12)	2763(12)	2247(12)	1731(12)
3166	1320(12)	1595(12)	2258(12)	2921(12)	3196(12)	2921(12)	2258(12)	1596(12)
3168	1357(12)	1673(12)	2300(12)	2967(12)	3244(12)	2967(12)	2330(12)	1633(12)
3179	-1147(12)	-769(12)	-99(12)	572(12)	85(12)	572(12)	-99(12)	-769(12)
3255	-1337(12)	-967(12)	-74(12)	619(12)	1189(12)	619(12)	-74(12)	-957(12)
3392	-389(12)	-285(12)	-34(12)	216(12)	329(12)	216(12)	-34(12)	-285(12)
3395	132(1)	124(1)	110(3)	207(12)	317(12)	217(12)	103(2)	124(1)
3397	129(1)	121(1)	108(3)	201(12)	298(12)	201(12)	101(2)	121(1)
3430	514(10)	458(10)	323(10)	232(7)	285(12)	270(9)	323(10)	458(10)
3402	503(10)	448(10)	316(10)	229(7)	276(12)	263(3)	316(10)	448(10)
3423	409(10)	364(10)	256(10)	164(11)	138(12)	164(11)	256(10)	364(10)
3528	6(4)	0(4)	0(6)	0(5)	0(5)	0(5)	0(5)	0(4)
3573	0(12)	0(12)	0(12)	0(12)	0(12)	0(12)	0(12)	0(12)
3773	0(12)	0(12)	0(12)	0(12)	0(12)	0(12)	0(12)	0(12)

Table B-7. Booster B-17E Peak Ultimate Axial Compression
Load Intensities

STATION (IN)	NX1 (LB/IN)	NX2 (LB/IN)	NX3 (LB/IN)	NX4 (LB/IN)	NX5 (LB/IN)	NX6 (LB/IN)	NX7 (LB/IN)	NX8 (LB/IN)
1 JJJ	-0 (10)	-J (10)	-0 (10)	-0 (6)	-0 (5)	-0 (5)	-0 (11)	-0 (10)
1143	-116 (10)	-98 (10)	-56 (9)	-48 (7)	-53 (7)	-48 (7)	-55 (10)	-96 (10)
1284	-211 (8)	-170 (8)	-131 (9)	-94 (9)	-93 (7)	-93 (7)	-93 (10)	-170 (8)
1286	-214 (8)	-173 (8)	-132 (9)	-95 (9)	-94 (7)	-94 (7)	-91 (10)	-173 (8)
1288	-218 (8)	-175 (8)	-134 (9)	-97 (9)	-95 (7)	-95 (7)	-93 (10)	-175 (8)
1414	-339 (8)	-309 (8)	-217 (9)	-157 (9)	-138 (7)	-133 (7)	-132 (10)	-309 (8)
1416	-140 (6)	-170 (5)	333 (4)	403 (1)	441 (1)	459 (1)	299 (6)	157 (6)
1418	-145 (6)	-167 (5)	308 (4)	410 (1)	443 (1)	410 (1)	299 (6)	154 (6)
1461	-245 (6)	-152 (6)	296 (4)	437 (1)	435 (1)	437 (1)	289 (6)	163 (6)
1463	-250 (6)	-156 (6)	295 (4)	439 (1)	437 (1)	439 (1)	208 (6)	167 (6)
1465	-244 (6)	-152 (6)	295 (4)	435 (1)	482 (1)	435 (1)	247 (6)	163 (6)
1578	259 (2)	264 (4)	267 (6)	236 (1)	248 (1)	229 (3)	221 (3)	262 (3)
1591	363 (2)	344 (2)	236 (6)	-262 (1)	-359 (1)	-277 (3)	-177 (3)	336 (3)
1592	-3274 (4)	-3338 (4)	-3508 (6)	-3713 (5)	-3816 (5)	-3713 (5)	-3491 (4)	-3338 (4)
1593	-3412 (4)	-3465 (4)	-3637 (6)	-3942 (5)	-3935 (5)	-3842 (5)	-3619 (4)	-3462 (4)
1595	-3333 (4)	-3464 (4)	-3652 (6)	-3874 (5)	-3975 (5)	-3874 (5)	-3634 (4)	-3464 (4)
1938	-2330 (7)	-3356 (4)	-4760 (6)	-6785 (10)	-8232 (11)	-6785 (10)	-4706 (4)	-3356 (4)
1840	-2363 (7)	-3344 (4)	-4776 (6)	-6957 (10)	-9419 (10)	-6857 (10)	-4722 (4)	-3344 (4)
1942	-2958 (7)	-3352 (4)	-4792 (6)	-6929 (10)	-8517 (10)	-6928 (10)	-4737 (4)	-3352 (4)
1996	-3309 (7)	-3869 (7)	-5901 (6)	-11374 (10)	-14744 (10)	-11974 (10)	-5964 (9)	-3869 (7)
1988	-1792 (7)	-2744 (4)	-5495 (6)	-10275 (10)	-13018 (10)	-10275 (10)	-5444 (4)	-2744 (4)
1390	-1810 (7)	-2745 (4)	-5493 (6)	-10288 (10)	-13034 (10)	-10288 (10)	-5408 (4)	-2743 (4)
2002	-1933 (7)	-2757 (4)	-5503 (6)	-10292 (10)	-13023 (10)	-10292 (10)	-5409 (4)	-2757 (4)
2261	-4748 (7)	-4484 (7)	-5597 (6)	-10131 (10)	-12773 (10)	-10131 (10)	-5451 (4)	-4483 (7)
2265	-4776 (7)	-4504 (7)	-5598 (6)	-10120 (10)	-12757 (10)	-10120 (10)	-5452 (4)	-4499 (7)

Table B-7. Booster B-17E Peak Ultimate Axial Compression
Load Intensities (Cont)

STATION (IN)	NX1 (LB/IN)	NX2 (LB/IN)	NX3 (LB/IN)	NX4 (LB/IN)	NX5 (LB/IN)	NX6 (LB/IN)	NX7 (LB/IN)	NX8 (LB/IN)
2396	-5186(7)	-4816(7)	-5622(6)	-9505(10)	-11864(11)	-9506(10)	-5480(4)	-4806(7)
2398	-5192(7)	-4810(7)	-5623(6)	-9495(10)	-11850(11)	-9496(10)	-5480(4)	-4810(7)
2400	-5198(7)	-4915(7)	-5623(6)	-9437(10)	-11837(11)	-9437(10)	-5480(4)	-4815(7)
2558	-5052(7)	-5148(7)	-5643(6)	-9725(10)	-10734(11)	-6725(11)	-509(4)	-5148(7)
2748	-6210(7)	-5551(7)	-5658(6)	-7790(10)	-9391(11)	-7790(11)	-544(4)	-5551(7)
2999	-6498(7)	-5102(7)	-5825(6)	-794(10)	-8375(11)	-7194(10)	-731(4)	-6102(7)
2916	-7039(7)	-3220(7)	-5826(6)	-7184(10)	-8260(11)	-7184(10)	-732(4)	-6220(7)
2332	-7446(7)	-3225(7)	-5827(6)	-7174(10)	-8345(11)	-7174(11)	-733(4)	-6225(7)
3370	-7743(7)	-6760(7)	-5871(6)	-6300(10)	-747(11)	-6300(10)	-833(4)	-6760(7)
3166	-7310(7)	-6468(7)	-5895(6)	-6103(5)	-6212(11)	-6009(5)	-844(4)	-6468(7)
3163	-7909(7)	-7069(7)	-6781(6)	-6389(5)	-6955(5)	-6839(5)	-6731(4)	-7069(7)
3170	-9432(7)	-9595(7)	-7294(6)	-8205(10)	-8670(11)	-8205(10)	-7155(4)	-8595(7)
3255	-9130(7)	-9465(7)	-7262(6)	-7752(10)	-7962(11)	-7752(11)	-7243(10)	-8405(7)
5392	-8216(5)	-7993(10)	-7519(10)	-7045(10)	-6848(11)	-7045(10)	-7519(10)	-7993(10)
3395	-8234(10)	-8028(10)	-7530(10)	-7032(10)	-6825(11)	-7032(11)	-7530(10)	-8028(10)
5397	-8263(10)	-8050(10)	-7537(10)	-7023(10)	-6810(11)	-7023(10)	-7537(10)	-8050(10)
3400	-344(12)	-252(12)	-30(12)	79(-1)	71(-1)	79(-1)	-30(12)	-252(12)
3402	-333(12)	-244(12)	-29(12)	77(-1)	69(-1)	77(-1)	-29(12)	-244(12)
3420	-221(12)	-168(12)	-41(12)	63(-1)	56(-1)	63(-1)	-41(12)	-168(12)
3528	-6(5)	-1(5)	-0(5)	-0(-4)	-0(-4)	-0(-4)	-0(-4)	-0(-4)
3670	0(12)	0(12)	0(12)	0(12)	0(12)	0(12)	0(12)	0(12)
3770	0(12)	0(12)	0(12)	0(12)	0(12)	0(12)	0(12)	0(12)



Table B-8. ESS/MDAC/B-17E Booster Ultimate
Internal Loads

CCNO 1 BOOSTER B-17E/FSS-MDAC MAX BET₀ Q
CCNO 2 BOOSTER B-17E/FSS-MDAC 2.0G MAX THRUST
CCNO 3 BOOSTER B-17E/FSS-MDAC 1HR GROUND STANDING TANKED UNPRESS

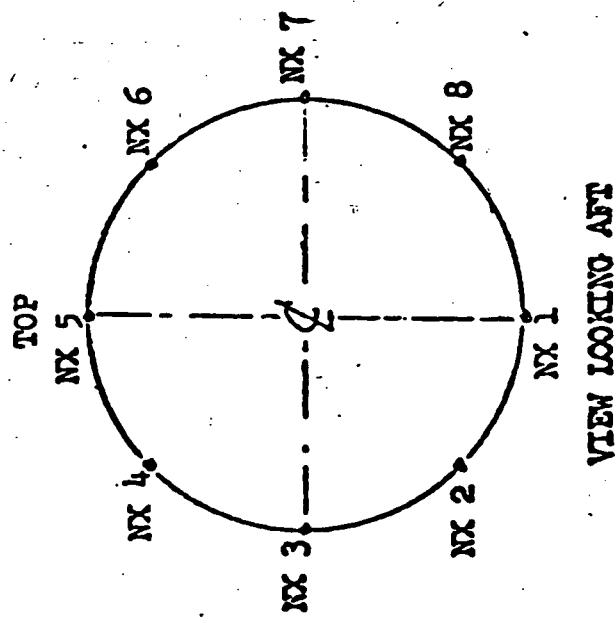


Table B-9. ESS/MDAC/B-17E Booster Peak Ultimate
Axial Tension Load Intensities

STATION (IN)	NX1 (LB/IN)	NX2 (LB/IN)	NX3 (LB/IN)	NX4 (LB/IN)	NX5 (LB/IN)	NX6 (LB/IN)	NX7 (LB/IN)	NX8 (LB/IN)
1000	-0 (3)	-0 (3)	-0 (3)	-0 (3)	-0 (3)	-0 (3)	-0 (3)	-0 (3)
1143	-23 (3)	-19 (3)	-14 (3)	-11 (3)	-4 (1)	-4 (1)	-19 (3)	-22 (3)
1284	-36 (3)	-28 (3)	-19 (3)	-15 (3)	6 (1)	12 (1)	-28 (1)	-40 (3)
1286	-37 (3)	-28 (3)	-19 (3)	-15 (3)	8 (1)	12 (1)	-29 (1)	-40 (2)
1288	-37 (3)	-28 (3)	-19 (3)	-15 (3)	9 (1)	12 (1)	-29 (1)	-41 (3)
1414	-147 (2)	-125 (3)	-22 (3)	71 (3)	99 (7)	45 (3)	-46 (1)	-127 (2)
1416	2101 (2)	2117 (2)	2157 (2)	2197 (2)	2213 (2)	2197 (2)	2157 (2)	2117 (2)
1418	2190 (2)	2116 (2)	2156 (2)	2196 (2)	2213 (2)	2106 (2)	2156 (2)	2116 (2)
1461	2069 (2)	2090 (2)	2139 (2)	2188 (2)	2258 (2)	2188 (2)	2139 (2)	2090 (2)
1463	2068 (2)	2088 (2)	2138 (2)	2187 (2)	2208 (2)	2187 (2)	2138 (2)	2088 (2)
1465	2175 (2)	2093 (2)	2137 (2)	2181 (2)	2199 (2)	2181 (2)	2137 (2)	2093 (2)
1578	2487 (2)	2373 (2)	2099 (2)	1826 (2)	1712 (2)	1956 (1)	2111 (1)	2377 (2)
1691	2799 (2)	2592 (2)	2091 (2)	1581 (2)	1672 (1)	2141 (1)	2333 (1)	2592 (2)
1692	1086 (2)	879 (2)	-440 (2)	-399 (2)	-678 (1)	472 (1)	664 (1)	879 (2)
1693	-1160 (2)	-1367 (2)	-1866 (2)	-2031 (3)	-1897 (1)	-1426 (1)	-1234 (1)	-1367 (2)
1695	-1134 (2)	-1355 (2)	-1881 (2)	-2056 (3)	-1959 (1)	-1473 (1)	-1251 (1)	-1355 (2)
1832	597 (2)	-611 (2)	-2560 (3)	-3816 (3)	-4639 (3)	-4549 (3)	-2592 (1)	-589 (1)
1840	615 (2)	-603 (2)	-2568 (3)	-3841 (3)	-4674 (3)	-4578 (3)	-2529 (1)	-578 (1)
1842	647 (2)	-590 (2)	-2576 (3)	-3967 (3)	-4708 (3)	-4608 (3)	-2547 (1)	-566 (1)
1986	2706 (2)	790 (2)	-3121 (3)	-5667 (3)	-7147 (3)	-6695 (3)	-3817 (1)	390 (2)
1988	5598 (2)	7266 (2)	-3092 (3)	-5646 (3)	-7135 (3)	-6678 (3)	-2300 (1)	3266 (2)
1990	5604 (2)	3270 (2)	-3081 (3)	-5650 (3)	-7143 (3)	-6686 (3)	-2302 (1)	3269 (2)
2102	5614 (2)	3276 (2)	-3065 (3)	-5642 (3)	-7149 (3)	-6703 (3)	-2288 (1)	3276 (2)
2261	5797 (2)	3308 (2)	-2705 (3)	-5465 (3)	-7274 (3)	-6955 (1)	-1977 (1)	3388 (2)
2263	5798 (2)	7389 (2)	-2703 (3)	-5464 (3)	-7275 (3)	-6953 (1)	-1975 (1)	3389 (2)
2265	5799 (2)	33A9 (2)	-2700 (3)	-5463 (3)	-7276 (3)	-6956 (1)	-1977 (1)	3389 (2)

Table B-9. ESS/MDAC/B-17E Booster Peak Ultimate
Axial Tension Load Intensities (Cont)

STATION (IN)	NX1 (LP/IN)	NX2 (LB/IN)	NX3 (LB/IN)	NX4 (LR/IN)	NX5 (LR/IN)	NX6 (LP/IN)	NX7 (LB/IN)	NX8 (LR/IN)
2396	5829(2)	3400(2)	-2551(3)	-5421(3)	-7377(3)	-7116(1)	-2116(1)	3400(2)
2398	5830(2)	3400(2)	-2549(3)	-5420(3)	-7378(3)	-7118(1)	-2118(1)	3400(2)
2400	5830(2)	3400(2)	-2546(3)	-5420(3)	-7380(3)	-7121(1)	-2120(1)	3400(2)
2558	5010(2)	2801(2)	-2354(3)	-5076(3)	-7097(3)	-6782(1)	-2302(1)	2811(2)
2748	3294(2)	1581(2)	-2112(3)	-4424(3)	-6430(3)	-5974(1)	-2585(1)	1581(2)
2998	1598(2)	-780(2)	-2013(3)	-3977(3)	-5968(3)	-5469(1)	-3004(1)	-788(2)
2900	1577(?)	-803(2)	-2010(3)	-3971(3)	-5961(3)	-5465(1)	-3051(1)	-803(2)
2902	1556(2)	-818(2)	-2008(3)	-3964(3)	-5954(3)	-5458(1)	-3056(1)	-818(2)
3070	-1288(2)	-1560(3)	-1799(3)	-3365(3)	-5344(3)	-4797(1)	-3462(1)	-2046(2)
3166	-2723(2)	-1750(3)	-1673(3)	-3014(3)	-4988(3)	-4474(1)	-3676(1)	-2834(2)
3168	-3052(?)	-2223(3)	-2240(3)	-3576(3)	-5549(3)	-5027(1)	-4241(1)	-3558(2)
3170	-3032(3)	-2373(3)	-2283(3)	-3615(3)	-5588(3)	-6551(1)	-5777(1)	-5218(1)
3255	-4228(3)	-2571(3)	-2196(3)	-3322(3)	-5290(3)	-6297(1)	-6066(1)	-5841(1)
3192	-4676(3)	-2892(3)	-2051(3)	-2845(3)	-4809(3)	-5840(1)	-6383(1)	-6840(3)
3305	110(3)	110(3)	110(3)	97(3)	88(3)	87(3)	96(3)	109(3)
2397	1116(3)	1117(3)	108(3)	95(3)	86(3)	86(3)	95(3)	107(3)
3400	273(2)	256(2)	214(2)	172(2)	202(1)	220(1)	214(2)	256(2)
3402	268(2)	250(2)	209(2)	168(2)	200(1)	215(1)	209(2)	250(2)
3420	219(2)	204(2)	169(2)	134(2)	120(2)	134(2)	169(2)	204(2)
3528	0(3)	0(3)	0(3)	0(3)	0(3)	0(2)	0(2)	0(2)
3670	0(3)	0(3)	0(3)	0(3)	0(3)	0(3)	0(3)	0(3)
3770	0(3)	0(3)	0(3)	0(3)	0(3)	0(3)	0(3)	0(3)



Table B-10. ESS/MDAC/B-17E Booster Peak Ultimate
Axial Compression Load Intensities

STATION (IN)	NX1 (LB/IN)	NX2 (LB/IN)	NX3 (LB/IN)	NX4 (LP/IN)	NX5 (LP/IN)	NX6 (LB/IN)	NX7 (LB/IN)	NX8 (LB/IN)
1000	-0 (2)	-0 (2)	-0 (2)	-0 (2)	-0 (2)	-0 (2)	-0 (2)	-0 (2)
1143	-62 (2)	-61 (1)	-44 (1)	-21 (1)	-11 (2)	-19 (2)	-36 (2)	-54 (2)
1284	-134 (1)	-138 (1)	-93 (1)	-37 (1)	-23 (2)	-34 (2)	-60 (2)	-89 (1)
1286	-176 (1)	-140 (1)	-59 (1)	-38 (1)	-24 (2)	-34 (2)	-61 (2)	-90 (1)
1288	-178 (1)	-142 (1)	-100 (1)	-38 (1)	-24 (2)	-35 (2)	-61 (2)	-91 (1)
1414	-239 (1)	-239 (1)	-159 (1)	-48 (2)	-32 (2)	-48 (2)	-88 (2)	-159 (1)
1416	190 (3)	245 (3)	350 (3)	445 (3)	473 (3)	419 (3)	313 (3)	219 (3)
1418	187 (7)	242 (3)	350 (3)	446 (3)	476 (3)	420 (3)	313 (3)	216 (3)
1461	-211 (3)	193 (3)	347 (3)	487 (3)	531 (3)	453 (3)	300 (3)	-167 (3)
1463	-214 (3)	191 (3)	347 (3)	489 (3)	534 (3)	455 (3)	299 (3)	-170 (3)
1465	-213 (3)	192 (3)	349 (3)	489 (3)	532 (3)	452 (3)	296 (3)	-170 (3)
1578	190 (3)	337 (3)	475 (3)	514 (3)	431 (3)	274 (3)	-191 (3)	-230 (3)
16c1	207 (3)	450 (3)	615 (3)	586 (3)	387 (3)	-191 (3)	-348 (3)	-318 (3)
1692	-2356 (2)	-2113 (2)	-1956 (3)	-1986 (3)	-2186 (3)	-2439 (3)	-2596 (3)	-2566 (3)
16c3	-2412 (3)	-2280 (1)	-2572 (1)	-2372 (1)	-2572 (2)	-2485 (2)	-2643 (3)	-2612 (3)
1695	-2799 (3)	-2374 (1)	-2596 (1)	-2424 (1)	-2642 (2)	-2513 (3)	-2656 (3)	-2608 (3)
1878	-1517 (3)	-1960 (1)	-4299 (1)	-6422 (2)	-7624 (2)	-6422 (2)	-3596 (3)	-2341 (3)
1940	-1504 (3)	-1853 (1)	-4372 (1)	-6482 (2)	-7700 (2)	-6482 (2)	-3619 (3)	-2337 (3)
1842	-1491 (3)	-1845 (1)	-4356 (1)	-6542 (2)	-7775 (2)	-6542 (2)	-3624 (3)	-2333 (3)
1986	-547 (3)	-1260 (1)	-6059 (1)	-10790 (2)	-13105 (2)	-10790 (2)	-5200 (2)	-2028 (3)
1988	1711 (3)	1254 (3)	-4552 (1)	-9080 (2)	-11410 (2)	-9080 (2)	-4542 (3)	-1978 (-3)
1993	1716 (2)	1258 (3)	-4560 (1)	-9093 (2)	-11427 (2)	-9093 (2)	-4547 (3)	-1978 (3)
2002	1719 (3)	1267 (1)	-4585 (1)	-9104 (2)	-11442 (2)	-9104 (2)	-4566 (3)	-1988 (3)
2261	1789 (7)	884 (1)	-5090 (1)	-9335 (2)	-11743 (2)	-9335 (2)	-4979 (3)	-2219 (3)
2263	1790 (3)	881 (1)	-5094 (1)	-9336 (2)	-11746 (2)	-9336 (2)	-4982 (3)	-2221 (3)
2265	1791 (3)	882 (1)	-5093 (1)	-9338 (2)	-11747 (2)	-9338 (2)	-4985 (3)	-2222 (3)

Table B-10. ESS/MDAC/B-17E Booster Peak Ultimate
Axial Compression Load Intensities (Cont)

STATION (IN)	NX1 (LR/IN)	NX2 (LR/IN)	NX3 (LR/IN)	NX4 (LR/IN)	NX5 (LR/IN)	NX6 (LR/IN)	NX7 (LR/IN)	NX8 (LR/IN)
2396	1956(3)	971(1)	-5026(1)	-9425(2)	-11054(2)	-9425(2)	-5170(3)	-2299(3)
2398	1957(3)	977(1)	-5025(1)	-9426(2)	-11056(2)	-9426(2)	-5172(3)	-2311(3)
2400	1958(3)	974(1)	-5024(1)	-9427(2)	-11058(2)	-9427(2)	-5175(3)	-2312(3)
2558	1530(3)	550(1)	-4918(1)	-8919(2)	-11106(2)	-8909(2)	-5404(3)	-2602(3)
2748	-1372(3)	-1340(1)	-4728(1)	-7786(2)	-9500(2)	-7786(2)	-5691(3)	-3379(3)
2898	-2075(3)	-2218(1)	-4682(1)	-7034(2)	-8327(2)	-7034(2)	-6030(3)	-4065(3)
2900	-2182(3)	-2708(1)	-4722(1)	-7021(2)	-8309(2)	-7021(2)	-6034(3)	-4077(3)
2902	-2091(3)	-2318(1)	-4720(1)	-7009(2)	-8291(2)	-7009(2)	-6037(3)	-4082(3)
3070	-2791(3)	-3217(1)	-4552(1)	-5938(2)	-6736(2)	-6575(3)	-6337(3)	-4770(3)
3166	-1700(3)	-7630(1)	-4428(1)	-5305(2)	-5817(2)	-6438(3)	-6515(3)	-5174(3)
3168	-3778(3)	-4199(1)	-4995(1)	-6000(2)	-6505(2)	-7003(3)	-7087(3)	-5751(3)
3170	-5207(1)	-5739(1)	-6550(2)	-7756(2)	-8255(2)	-7756(2)	-7137(3)	-5806(3)
3255	-5910(1)	-6147(1)	-6656(2)	-7224(2)	-7460(2)	-7224(2)	-7322(3)	-6195(3)
3392	-7544(2)	-7337(2)	-6839(2)	-6341(2)	-6134(2)	-6792(3)	-7634(3)	-7337(2)
3395	-7585(2)	-7368(2)	-6846(2)	-6324(2)	-6107(2)	-6324(2)	-6846(2)	-7358(2)
3397	-7612(2)	-7389(2)	-6851(2)	-6313(2)	-6090(2)	-6313(2)	-6851(2)	-7389(2)
3460	113(3)	112(3)	104(3)	92(3)	83(3)	83(3)	92(3)	104(3)
3462	110(3)	110(7)	102(3)	90(3)	81(3)	81(3)	90(3)	102(3)
3470	90(3)	89(3)	82(3)	72(3)	65(3)	65(3)	72(3)	83(3)
3528	0(3)	0(2)	0(2)	0(2)	0(3)	0(3)	-0(3)	-0(3)
3670	0(3)	0(3)	0(3)	0(3)	0(3)	0(3)	0(3)	0(3)
3770	0(3)	0(3)	0(3)	0(3)	0(3)	0(3)	0(3)	0(3)

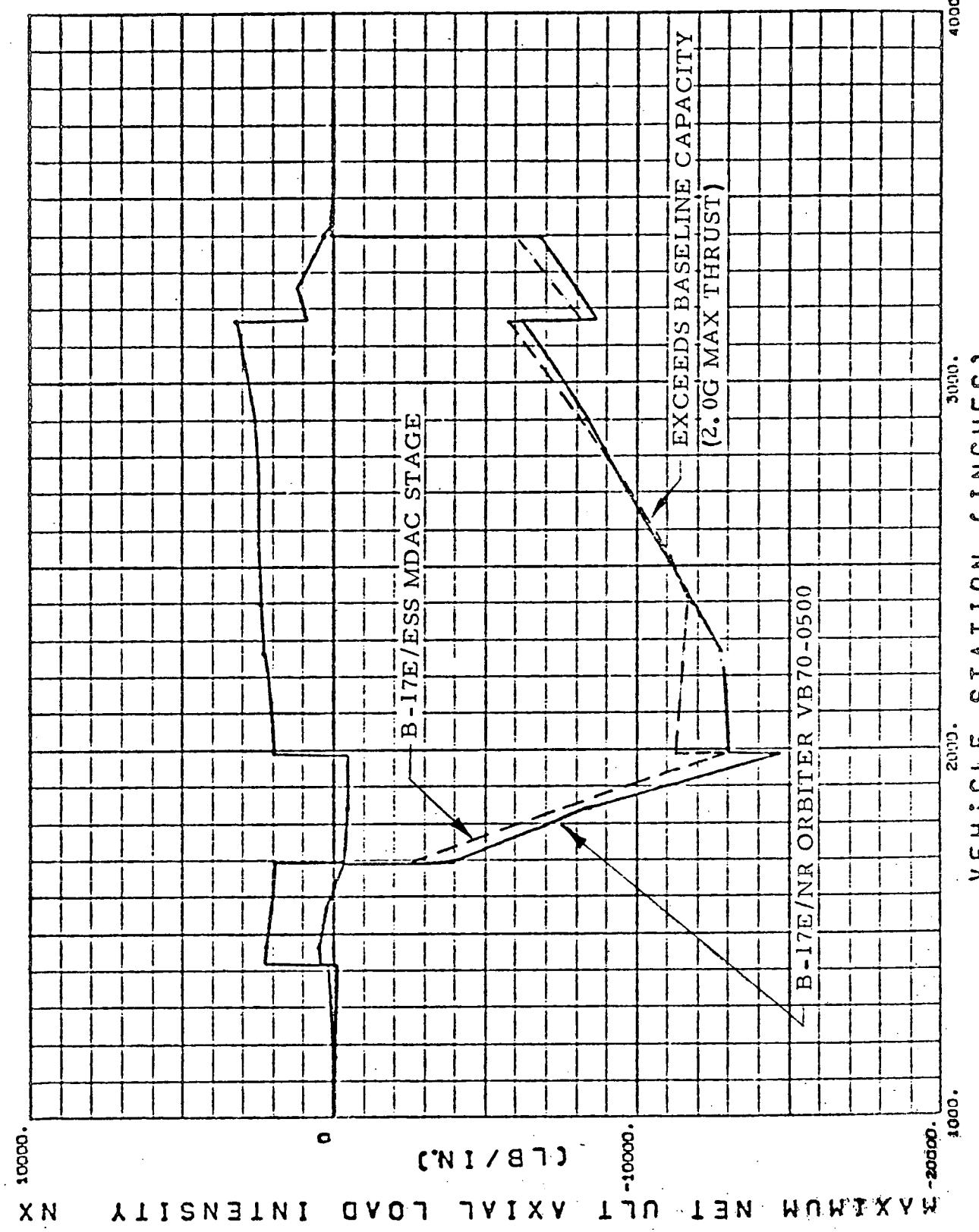


Figure B-7. GDC/B-17E Internal Loads at Top Centerline

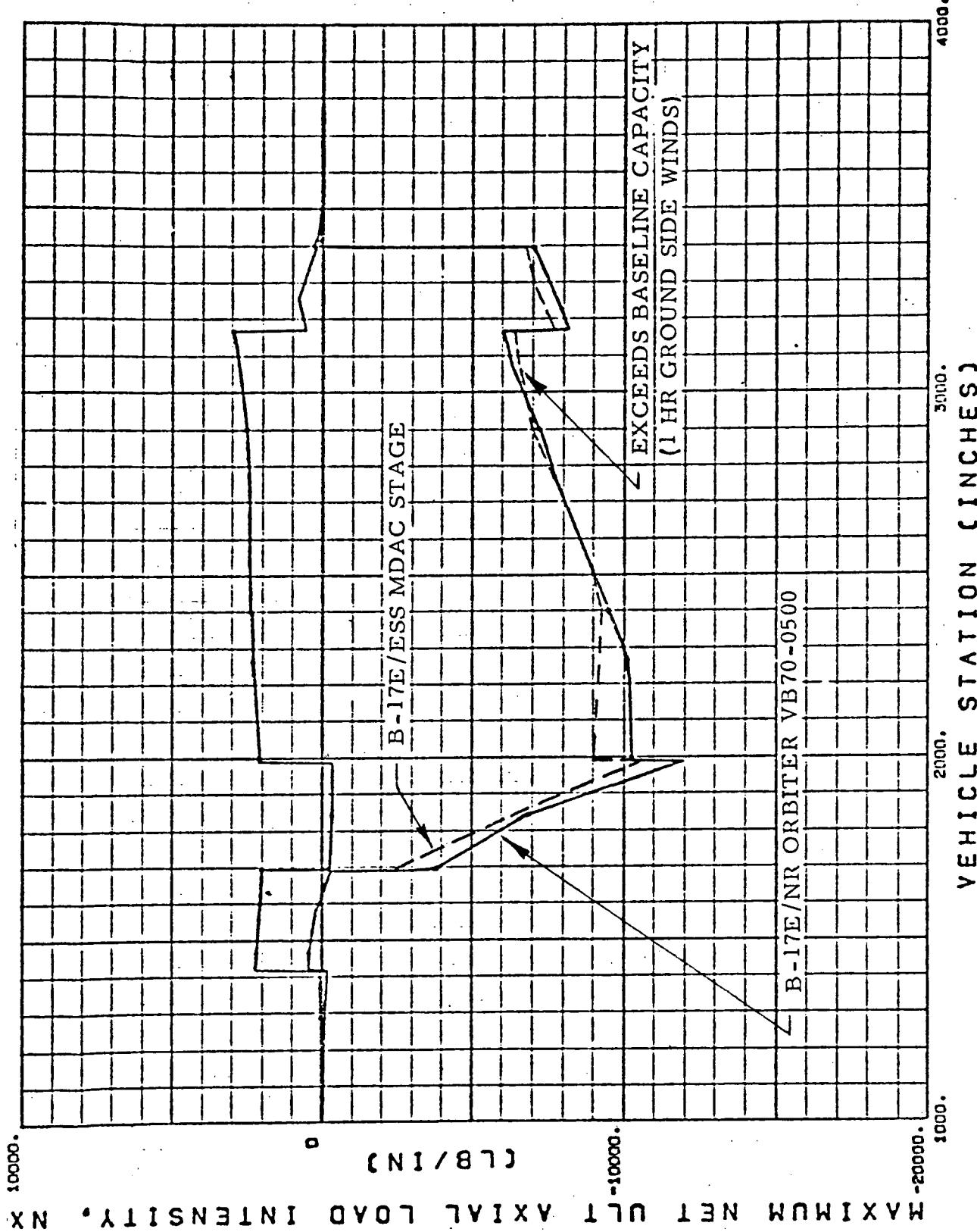


Figure B-8. GDC/B-17E Internal Loads 45 Degrees From Top

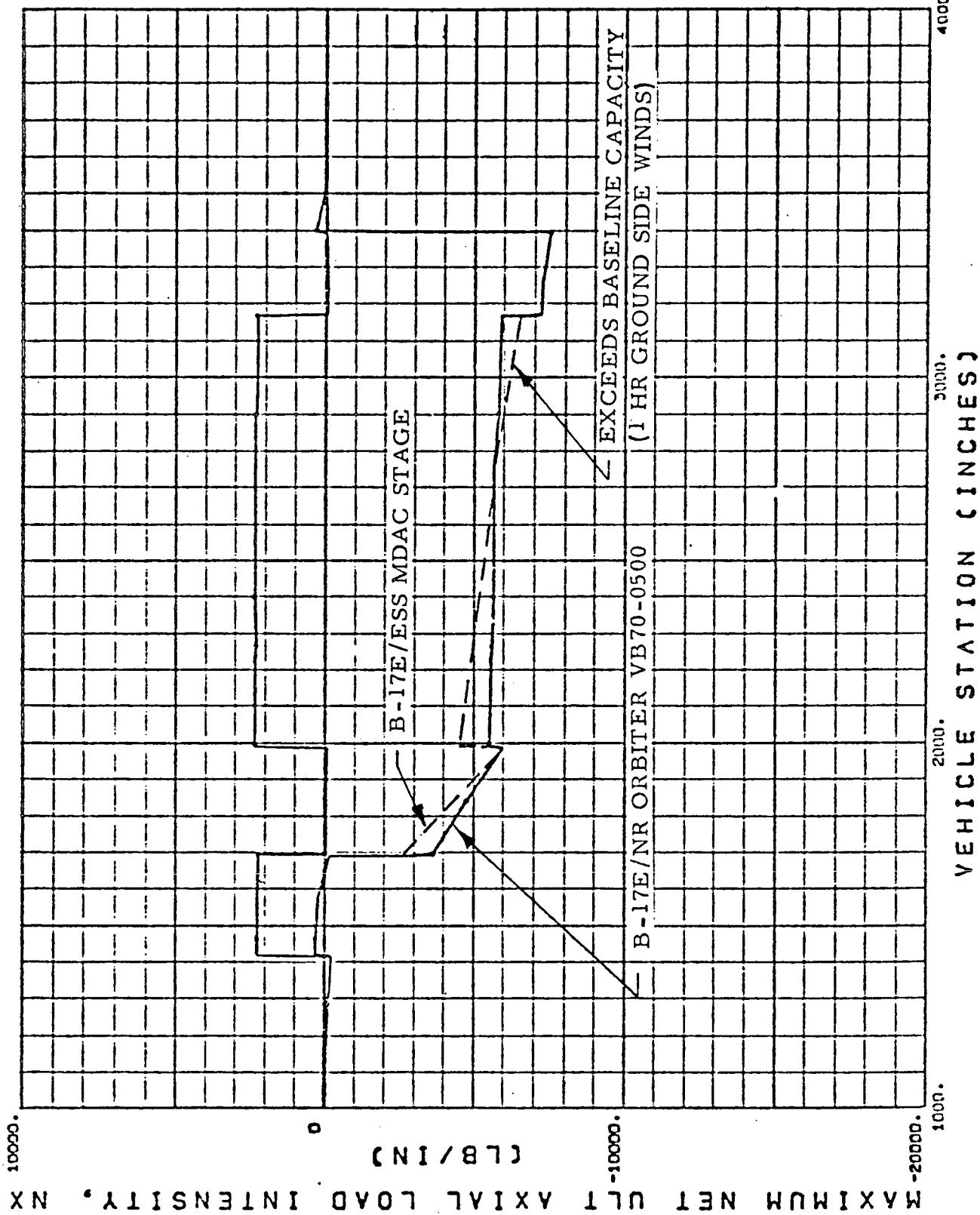


Figure B-9. GDC/B-17E Internal Loads at Side



B-17E/ESS MDAC STAGE LIMIT LOADS)		$F'X$ ($\times 10^3$ LB)	$F'Y$ ($\times 10^3$ LB)	$F'Z$ ($\times 10^3$ LB)	A^Y ($\times 10^3$ LB)	A^Z ($\times 10^3$ LB)	M_X (10^6 IN./LB)
CONDITION	WIND						
TWO WEEK GROUND WINDS UNFUELED	HEAD TAIL SIDE						
1 HOUR GROUND WINDS FUELED UNPRESSURIZED	HEAD TAIL SIDE	1219	± 84.9	192	± 21.5	285	± 14.4
DYNAMIC LIFT OFF + 1 HOUR GROUND WINDS	HEAD TAIL SIDE						
MAX -Q	HEAD TAIL						
MAX -Q	SIDE	2354	± 186.0	258	± 175.0	541	± 11.06
2 g MAX THRUST	-	2664		324		697	
BOOSTER BURNOUT	-						

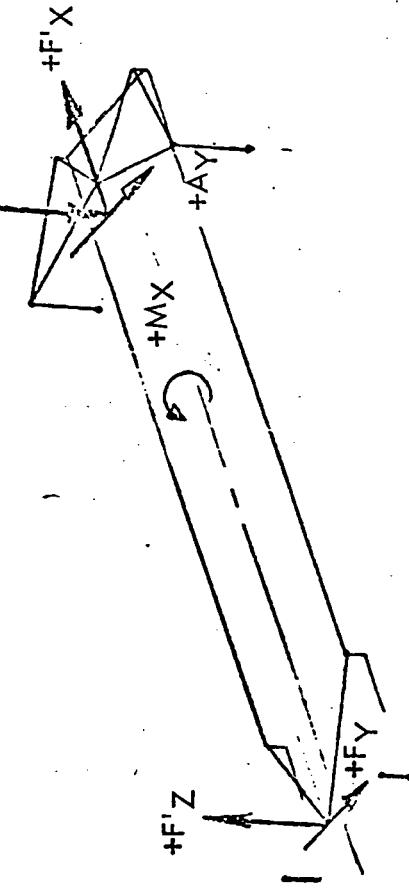


Figure B-10. B-17E/ESS Fixed-Platform Separation System Attachment Loads



AFFECTED COMPONENT	CRITICAL CONDITION	ADDED WEIGHT (LBS)	
		GROUND CONDITIONS	FLIGHT CONDITIONS
STA 1463 BULK'D	MAX. β_q	0	94
STA 1693 BULK'D	—	0	0
STA 2263 BULK'D	—	0	0
STA 2398 BULK'D ADJACENT SKIN	2.0 MAX g	0	2821
LH ₂ TANK THRUST STRUCT.	—	0	0
TOTALS		.	2915
		2915	

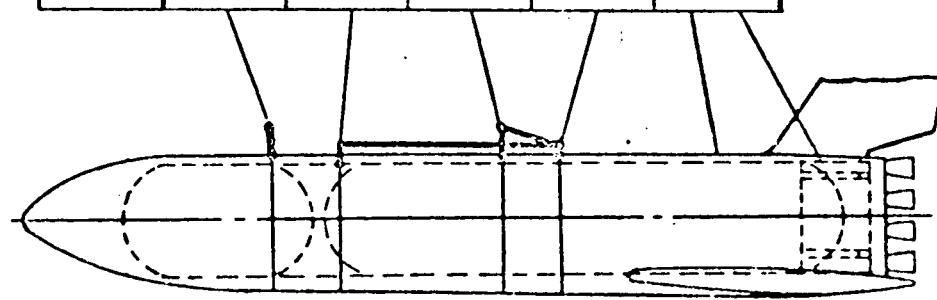


Figure B-11. ESS/Space Station Effect on Structure Weight of B-17E Booster

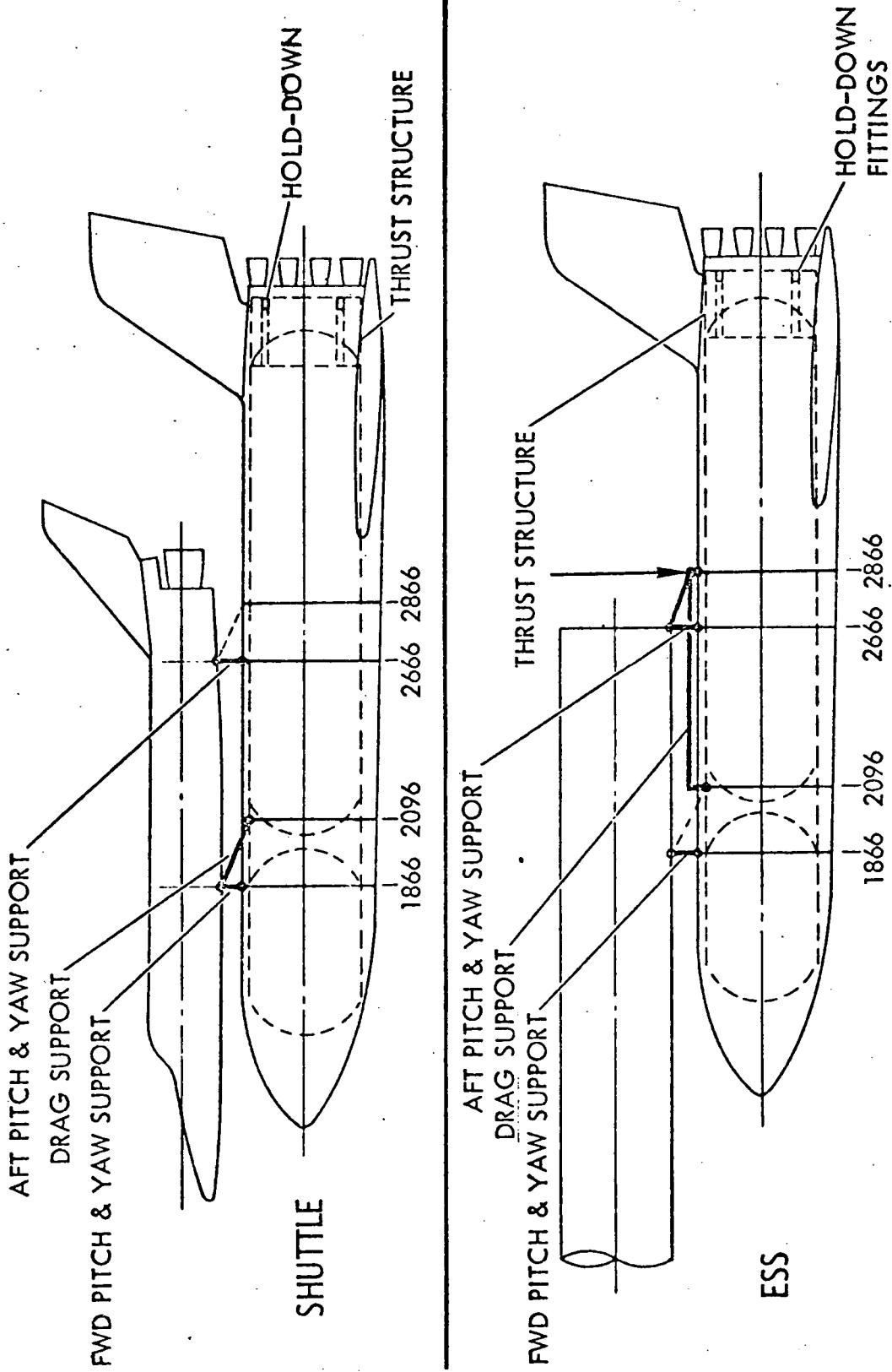


Figure B-12. Mating/Separation System Structure Schematic



1.5 AERODYNAMIC HEATING

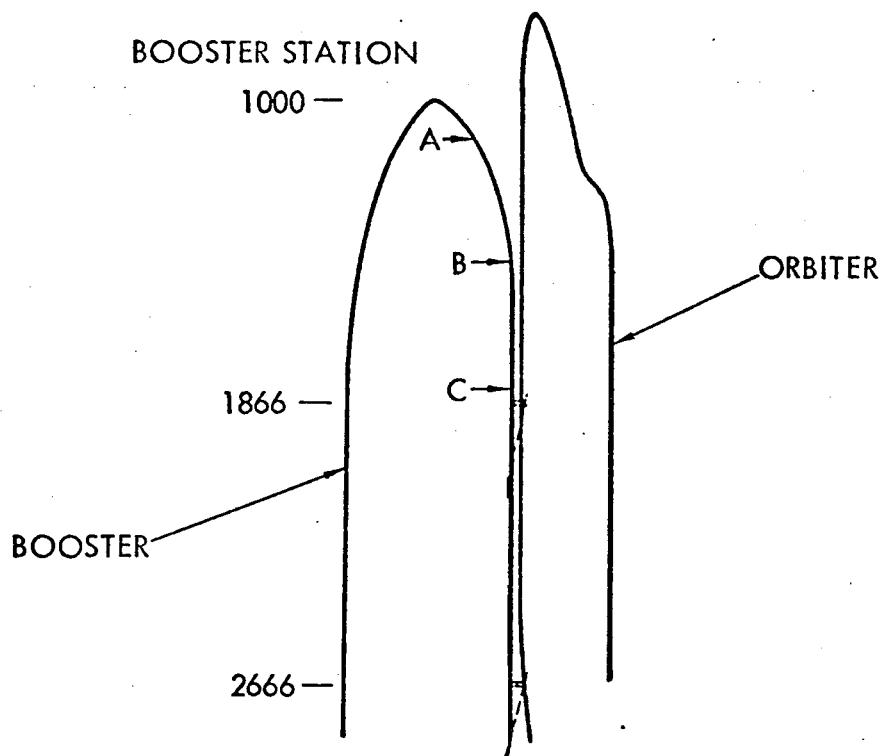
The B-9U booster entered from a staging velocity of 10,800 fps, and the aluminum alloy liquid hydrogen and liquid oxygen propellant tank structure was protected by a heat shield. The B-17E booster enters from a staging velocity of 7,720 fps with the aluminum alloy liquid hydrogen and liquid oxygen tank structure exposed to the entry environment and sized to provide an adequate heat sink. Material thicknesses for the B-17E body have been selected to prevent temperatures from exceeding 300 F.

The effects of the ESS missions on B-9U booster temperatures during ascent, including shock impingement effects, and during entry are shown in Figures B-13 and B-14 and compared to peak booster temperatures encountered during a shuttle mission. The results clearly show that "low q" trajectories selected for the ESS missions significantly reduce the temperatures when compared to the shuttle booster temperatures encountered along its maximum performance or "high q" trajectory. There is a corresponding reduction in heat transfer rates.

A time history of dynamic pressure for the B-9U and B-17E boosters during ascent on an ESS/space station mission is shown in Figure B-15 and compared to a shuttle mission. Since there is a similar reduction in ascent dynamic pressure for the B-17E booster when used for the ESS mission, there would be comparable reduction in booster temperatures and heating rates encountered during ascent.

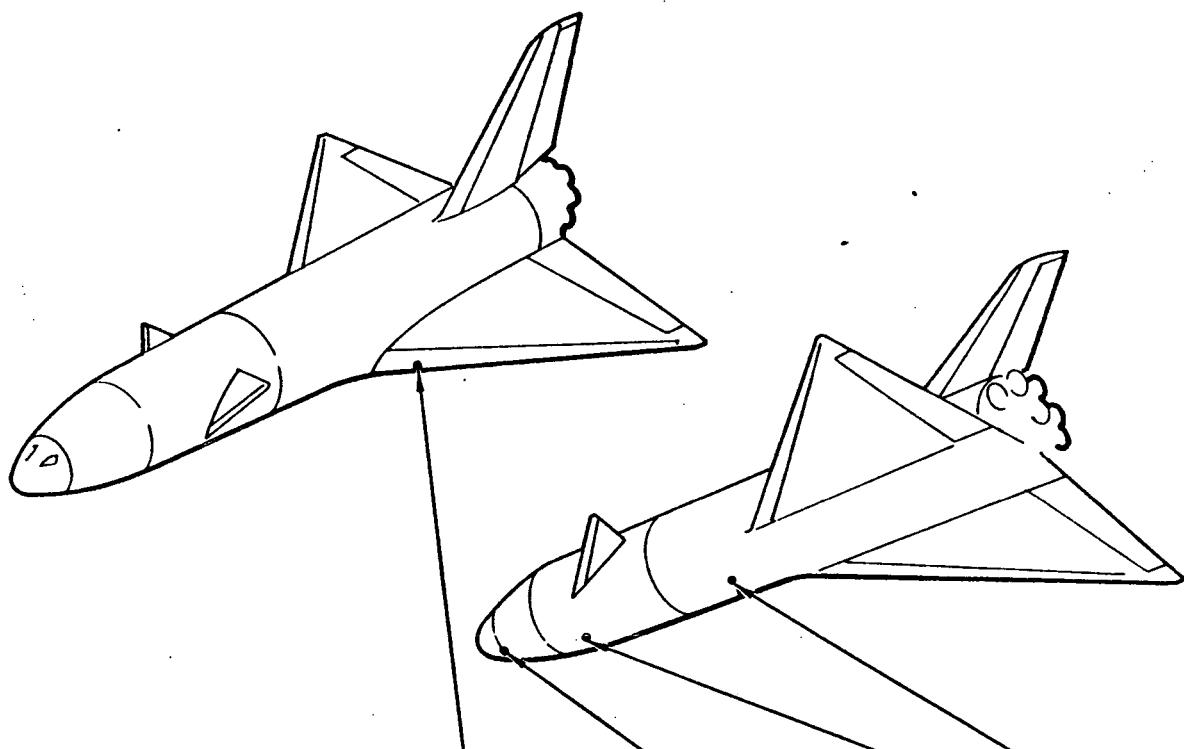
Figure B-16 shows the B-9U thermostructural limits as a function of booster apogee velocity and altitude. The B-9U apogee velocity and altitude are shown in this figure for the shuttle mission and ESS-space station mission. Since the slope of the limit line is generally consistent for variations in temperature limits the line was translated, as shown in Figure B-16, through the B-17E apogee conditions. Two ESS-space station mission apogee points are also identified, representing two trajectory runs that resulted in payloads of 183,000 pounds and 187,000 pounds (alternate trajectory). These data indicate that the space station mission can be accomplished without exceeding the B-17E heating limitations. If the B-17E displays the same characteristic heating trends as the B-9U booster for the other ESS missions, the RNS payload would result in less severe and the space tug would result in slightly more severe heating environments.

It is reasonable to conclude, in the absence of detailed aerodynamic heating analyses, that the use of the B-17E heat sink booster for the ESS missions should present no severe structural heating problems. In addition, since the ESS missions do not force the use of maximum performance trajectories, it would be possible to use trajectory shaping if required to alleviate any marginal conditions.



SECOND STAGE	TRAJECTORY	PEAK TEMPERATURE DURING ASCENT (DEG F)		
		POINT A	POINT B	POINT C
ORBITER	B-9U-1	1770	1780	2250
NUCLEAR STAGE	ESS/RNS	650	720	1280
SPACE STATION	ESS/SPACE STATION	930	740	1180
SPACE TUG	ESS/SPACE TUG	1270	1430	1510

Figure B-13. Peak Temperatures on Booster Top Surface During Ascent



SPACE TUG	2150	1630	1555	1540
NUCLEAR STAGE	1855	1340	1285	1245
SPACE STATION	2070	1530	1480	1440
ORBITER	2380	1790	1730	1700
SECOND STAGE	PEAK TEMPERATURE DURING ENTRY (DEG F)			

Figure B-14. Maximum Booster Entry Temperatures

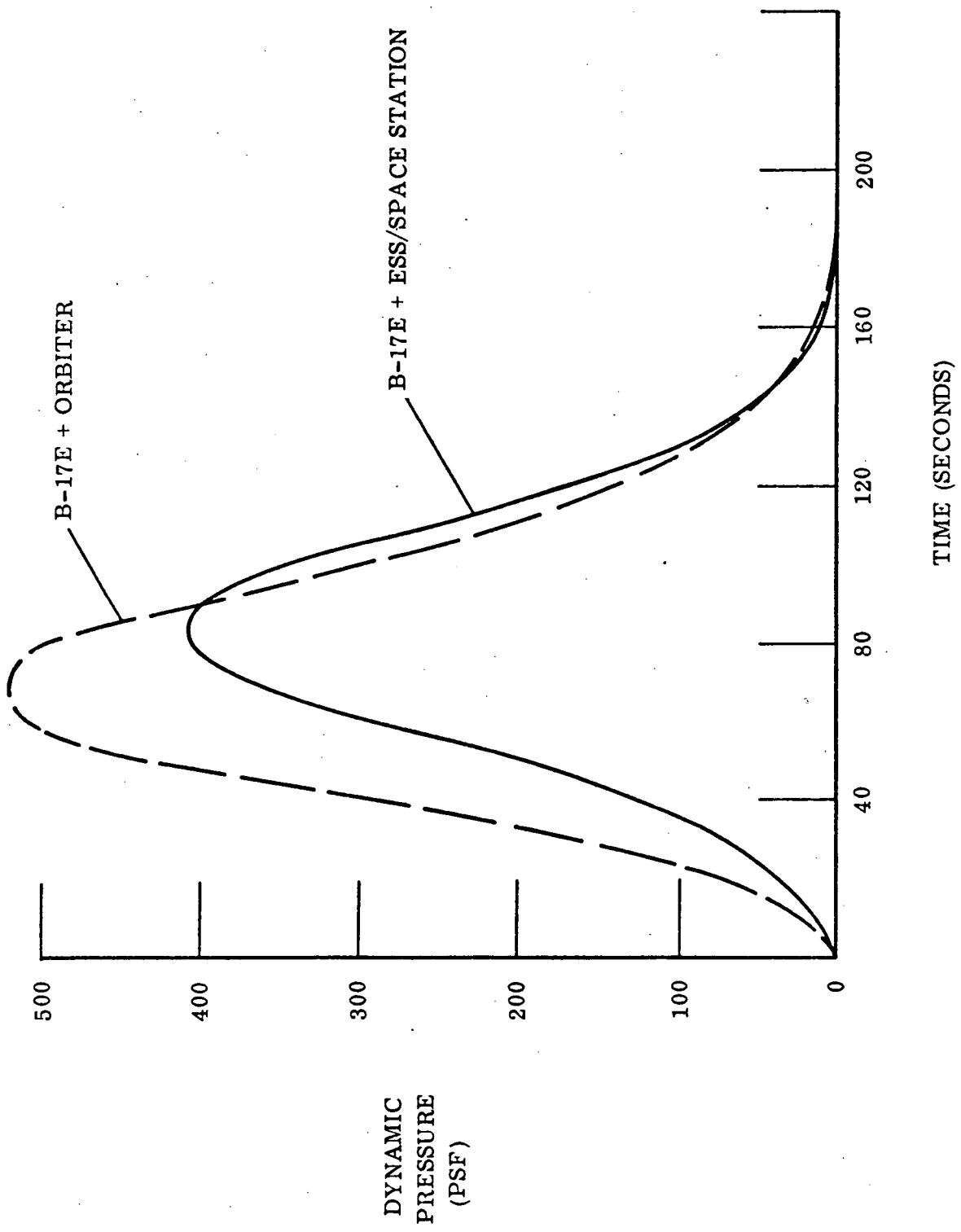


Figure B-15. Comparison of Ascent Dynamic Pressures

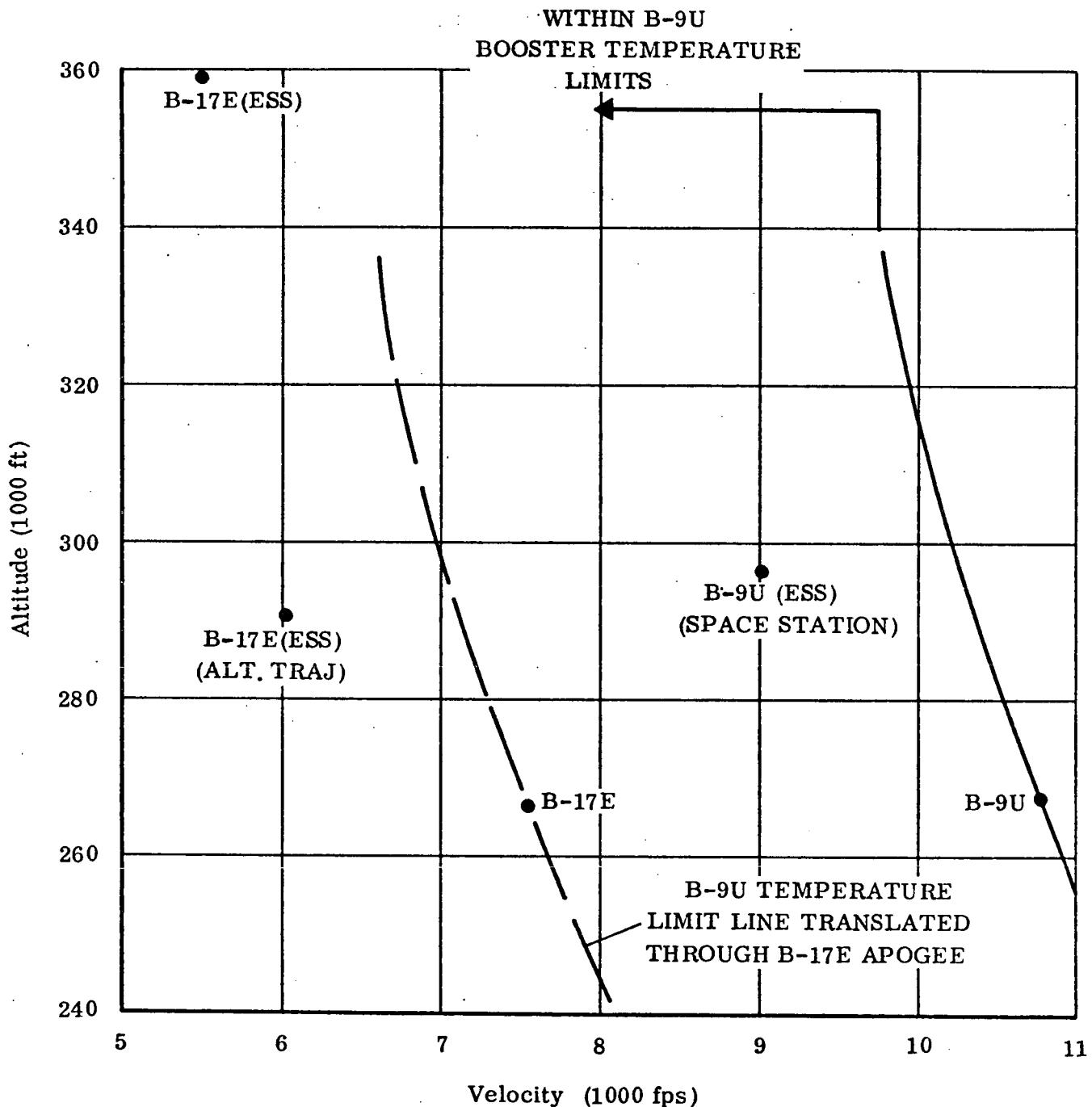


Figure B-16. Shuttle Booster Thermostructural Apogee Limits



1.6 ASCENT CONTROLS

The main rocket engines on the B-9U booster were canted at an angle of three degrees relative to a booster water-line plane. This cant angle was also shown to be satisfactory when the booster was used for ESS missions. On the B-17E booster the engine centerlines are parallel to a water line plane, that is, at zero cant angle. Figure B-17 shows the gimbal angles required on the B-17E to track the vehicle center of gravity. If the zero cant angle were retained, a gimbal angle of 11.80 degrees in a negative direction would be required to track the center of gravity for the composite vehicle at booster burnout. This exceeds the engine capability of ± 10 degrees. To remain within the engine capability the engines should be installed in a canted position of approximately 4 degrees as shown in Figure A-1. This would require the installation of tapered plates at the engine attachment surface to prepare the booster for an ESS mission. This also affects the propellant feed lines. Detailed studies will need to be conducted to determine whether or not the propellant feed lines can be designed to permit attachment to the engine when installed with a cant angle between zero and four degrees.

The application of load relief as described in Volume II, Book 1, for the B-17U booster is also applicable to the B-17E. The gimbal angle limits defined for the B-9U in the region of maximum dynamic regions would differ for the B-17E. Determination of the actual required gimbal limits would require detailed analyses using the six-degree-of-freedom digital simulation program.

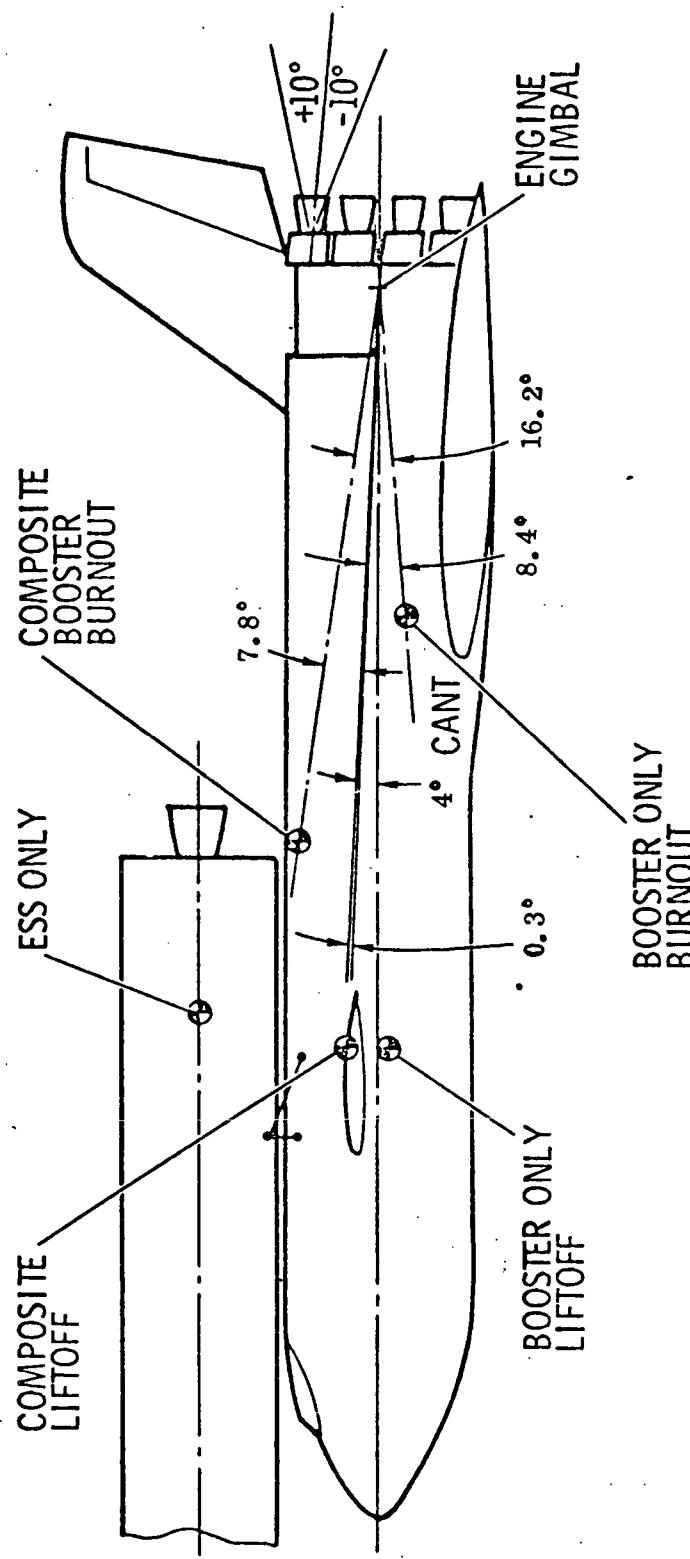


Figure B-17. B-17E Booster/ESS Space Station Gimbal Requirements
Due to CG Travel, Nominal



2.0 CONCLUSIONS

The NR orbiter for the Orbiter External Hydrogen Tank Study employs three space shuttle engines at an altitude thrust of 477,000 pounds each. By employing three identical engines on the short S-II expendable second stage, filling the propellant tanks, and launching on the 2.9-million-pound (B-17E) booster, a total payload potential with the MDAC space station to design reference orbit (270 nm, 55 degrees) is nearly 210,000 pounds. The MDAC space station weight is 176,960 pounds. By trading payload margin for reduced loads (booster engine throttling and a low-q trajectory), the MDAC space station can be easily placed in the required orbit. For the same payload capability (183,000 pounds) as estimated for the baseline ESS on the B-9U shuttle baseline booster, a weight penalty on the B-17E booster is 2915 pounds. This constitutes a very small percentage of the estimated dry weight of the B-17E booster of 451,400 pounds.

To the extent feasible in this cursory investigation, analyses have indicated that the selected ESS vehicle (short S-II stage) can serve on either the shuttle baseline booster (B-9U) or the booster for the Orbiter External Hydrogen Tank Study (B-17E). In each case, more than adequate payload performance is available to meet the specified payload requirements. In each case, the effect on the reusable booster is a small structural weight increase of approximately 3000 pounds, including both flight and one-hour ground wind effects.

The selected ESS is an adaptable vehicle. It provides a large-lift capability to supplement the space shuttle.



APPENDIX C. DELIVERY OF PROPELLANTS TO ORBIT

A limited investigation was performed to determine the maximum LH₂ or LO₂ that could be delivered to orbit with the ESS booster. Three concepts were evaluated for this mission;

1. LO₂ on-loaded in the ESS with a nose cone closeout on the ESS forward skirt
2. LH₂ tanker using the MDAC space station configuration
3. RNS payload with LH₂ in the tank

These concepts were evaluated to determine the system controllability and the effect on the booster fitting loads. Total gross weight for the ESS plus payload was held constant at 992,000 pounds, permitting essentially the same trajectory during mated flight.

Tables C-1 and C-2 present the summary weight statement and mass properties for the LO₂ loaded ESS. Figure C-1 defines the c. g. travel for this configuration.

Weight summary, mass properties and c. g. travel for the LH₂ tanker, with the MDAC space station shape used, are shown in Tables C-3 and C-4 and Figure C-2.

Reusable nuclear shuttle (RNS) mass property data and c. g. travel are shown in Tables C-5 and C-6 and Figure C-3.

A limited loads analysis was performed to establish a rough order of magnitude fitting load comparison. Table C-7 presents results of this analysis for the maximum Q_a and end boost conditions with a MDAC space station -2° trajectory. Results of this analysis are approximately the same as those for the ESS/MDAC configuration in the same -2° trajectory.

From the standpoint of performance of the system, the ESS has the capability to place substantial quantities of propellants in orbit, with loads and control factors probably acceptable. Other factors have not been evaluated.



Table C-1. Summary Weight Statement (Launch Condition)

CONFIGURATION B-9U/ESS - LO ₂ TANKER (ESS O ₂ TANK)				BY			DATE								
CODE	SYSTEM	BOOSTER	EST	CALC	ACT	ESS	EST	CALC	ACT						
1.0	WING GROUP	61990													
2.0	TAIL GROUP	19230													
3.0	BODY GROUP	182772				57847	42	21	37						
4.0	INDUCED ENVIR PROTECT	82644													
5.0	LANDING, DOCKING	27361													
6.0	PROPULSION, ASCENT	130186				25328	90	10							
7.0	PROPULSION, CRUISE	50413													
8.0	PROPULSION, AUXILIARY	10557				4710	100								
9.0	PRIME POWER	1801				3400	100								
10.0	ELECTRICAL CONV & DISTR	1438				1190	100								
11.0	HYDR & PNEU DISTR	1862				406	10	90							
12.0	SURFACE CONTROLS	7889													
13.0	AVIONICS	5468				2955	100								
14.0	ENVIRONMENTAL CONTROL	1650				1100	100								
15.0	PERSONNEL PROVISION	1600													
16.0	RANGE SAFETY														
17.0	BALLAST														
18.0	GROWTH	46486													
19.0	ESS PLATFORM	9770													
	SUBTOTAL (DRY WT)	643117				96936	63	15	22						
20.0	PERSONNEL	476													
21.0	*PAYLOAD					176960	100								
22.0	ORDNANCE														
23.0	RESIDUAL FLUIDS	11476				5965	100								
24.0	PAYOUT MARGIN					5330	100								
	SUBTOTAL (INERT WT)	655069				285191	88	5	7						
25.0	RESERVE FLUIDS					6659	100								
26.0	INFILIGHT LOSSES	20802				83	100								
27.0	PROPELLANT-ASCENT	3382307				677150	100								
28.0	PROPELLANT-CRUISE	143786													
29.0	PROPELLANT-MANEUV/ACS	1500				29917	100								
30.0															
	TOTAL (GROSS WT) LB	4203464	100			992000	98	1	1						
DESIGNATIONS:				NOTES & SKETCHES:											
EST	% ESTIMATED WEIGHT	*PAYLOAD IS NOSECONE + LO ₂ IN ESS O ₂ TANK. NOSECONE FAIRING (6000 LB) IN LIEU OF MDAC SS.													
CALC	% CALCULATED WEIGHT														
ACT	% ACTUAL WEIGHT														



Table C-2. Sequence Mass Properties Statement

CONFIGURATION B-9U/+ESS LO ₂ TANKER (NO EXTERNAL PAYLOAD)				BY		DATE		PAGE OF			
NO.	MISSION EVENT	CENTER OF GRAVITY INCHES			MOMENT OF INERTIA SLUG FT ² X 10 ⁻³			PRODUCT OF INERTIA SLUG FT ² X 10 ⁻³			
		WEIGHT LB.	X	Y	Z	I _{x-x}	I _{y-y}	I _{z-z}	I _{xy}	I _{xz}	I _{yz}
Liftoff	5195464 -1412842	2195	0.0	471.3	49.8	604.9	567.1				
Booster Ascent Prop											
Max q Flight Condition	3782622 -612441	2388	0.0	498.0	47.7	446.9	411.1				
Booster Ascent Prop											
Flight Condition	3170181 -1351264	2484	0.0	516.9	46.2	377.3	343.1				
Booster Ascent Prop											
Booster Thrust Decay	-5760										
Booster Burnout	1813157 -920000	2703	0.0	616.8	36.3	205.3	180.1				
Orbiter Separation											
Booster Vent Residuals	-17571 -1500										
Booster ACS Prop											
Booster Start Cruise	802086 -3231	3049	0.0	332.0	9.99	129.5	130.7				
Booster APU Prop											
Cruise Fuel (JP)	-143786										
Booster Landing (Gear Down)	655069	3146	0.0	344.0	9.63	103.9	105.3				

NOTES:

COMBINED SYSTEM C.G. TRAVEL

B-9U + ESS/ALTERNATE PAYLOAD

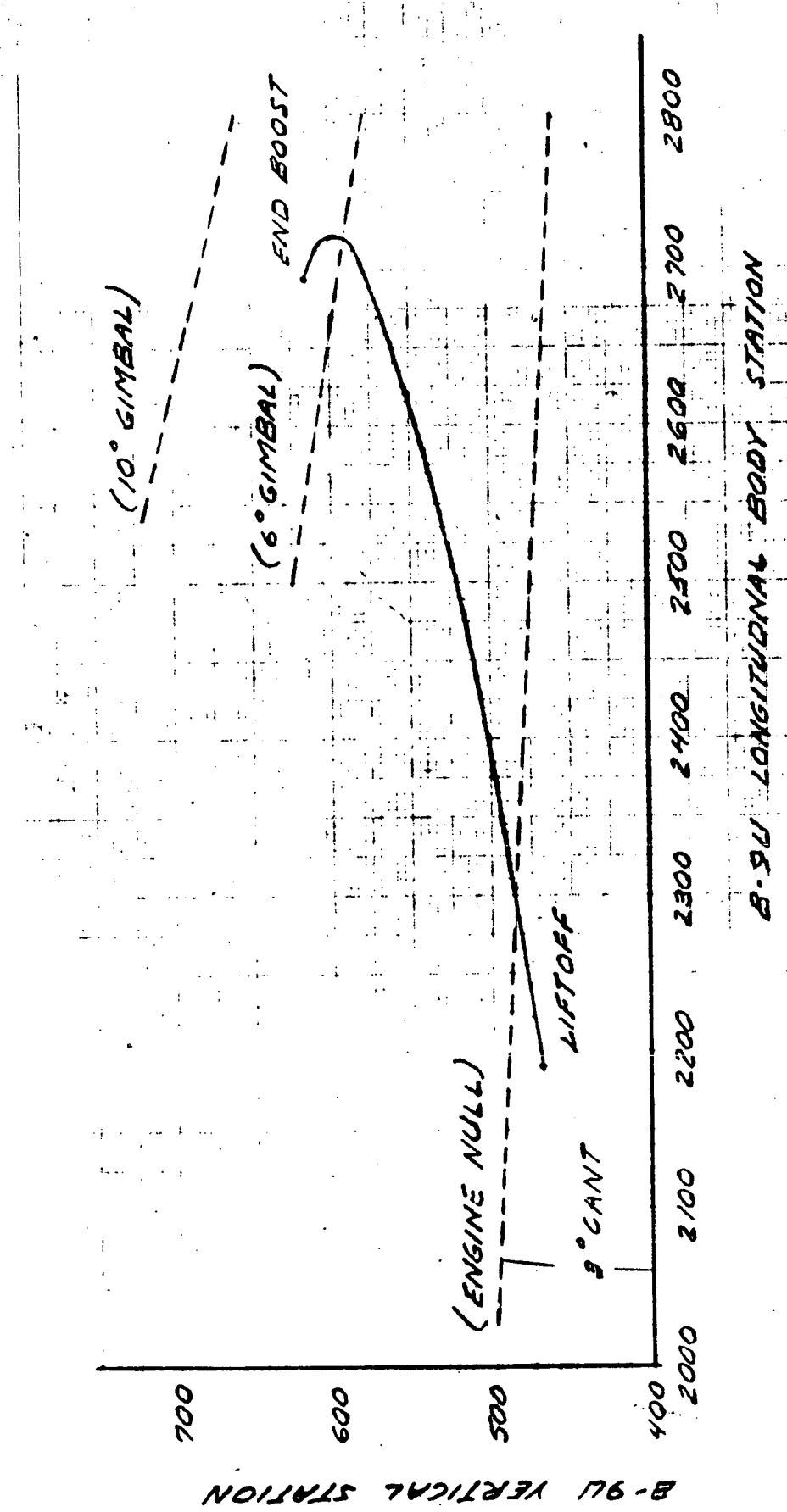


Figure C-1. LO₂ Tanker Nosecone Fairing (992,000 Gross Weight)



Table C-3. Summary Weight Statement (Launch Condition)

CONFIGURATION B-9U/ESS - LH ₂ TANKER (MDAC)			BY			DATE			
CODE	SYSTEM	BOOSTER	EST	CALC	ACT	ESS	EST	CALC	ACT
1.0	WING GROUP	61990							
2.0	TAIL GROUP	19230							
3.0	BODY GROUP	182772				57847	42	21	37
4.0	INDUCED ENVIR PROTECT	82644							
5.0	LANDING, DOCKING	27361							
6.0	PROPULSION, ASCENT	130186				25328	90	10	
7.0	PROPULSION, CRUISE	50413							
8.0	PROPULSION, AUXILIARY	10557				4710	100		
9.0	PRIME POWER	1801				3400	100		
10.0	ELECTRICAL CONV & DISTR	1438				1190	100		
11.0	HYDR & PNEU DISTR	1862				406	10	90	
12.0	SURFACE CONTROLS	7889							
13.0	AVIONICS	5468				2955	100		
14.0	ENVIRONMENTAL CONTROL	1650				1100	100		
15.0	PERSONNEL PROVISION	1600							
16.0	RANGE SAFETY								
17.0	BALLAST								
18.0	GROWTH	46486							
19.0	ESS PLATFORM	9770							
	SUBTOTAL (DRY WT)	643117				96936	63	15	22
20.0	PERSONNEL	476							
21.0	*PAYLOAD					176960	100		
22.0	ORDNANCE								
23.0	RESIDUAL FLUIDS	11476				5965	100		
24.0	PAYOUT MARGIN					5330	100		
	SUBTOTAL (INERT WT)	655069				285191	88	5	7
25.0	RESERVE FLUIDS					6659	100		
26.0	INFLIGHT LOSSES	20802				83	100		
27.0	PROPELLANT-ASCENT	3382307				677150	100		
28.0	PROPELLANT-CRUISE	143786							
29.0	PROPELLANT-MANEUV/ACS	1500				22917	100		
30.0									
	TOTAL (GROSS WT) LB	4203464	100			992000	98	1	1
DESIGNATIONS:			NOTES & SKETCHES: *PAYLOAD IS LH ₂ + TANKAGE (176960 LBS) MDAC CONFIG						
EST	% ESTIMATED WEIGHT								
CALC	% CALCULATED WEIGHT								
ACT	% ACTUAL WEIGHT								

Table C-4. Sequence Mass Properties Statement

CONFIGURATION B-9U + ESS/LH ₂ TANKER (MDAC SHAPE)				BY			DATE			PAGE OF		
NO.	MISSION EVENT	CENTER OF GRAVITY			MOIMENT OF INERTIA			PRODUCT OF INERTIA			SLUG FT ² X 10 ⁻³	SLUG FT ² X 10 ⁻³
		WEIGHT LB	X	Y	Z	I _{xx}	I _{yy}	I _{zz}	I _{xy}	I _{xz}	I _{yz}	
Liftoff	5195464	2161	0.0	471.3		50.0	632.8	594.9				
Booster Ascent Prop	-1412842											
Max q Flight Condition	3782622	2341	0.0	498.0	47.9	489.1	453.3					
Booster Ascent Prop	-612441											
Flight Condition	3170181	2428	0.0	516.9	46.4	426.6	392.3					
Booster Ascent Prop	-1351264											
Booster Thrust Decay	-5760											
Booster Burnout	1813157	2604	0.0	616.8	36.4	269.8	245.4					
Orbiter Separation	-992000											
Booster Vent Residuals	-17571											
Booster ACS Prop	-1500											
Booster Start Cruise	802086	3049	0.0	332.0	9.99	129.5	130.7					
Booster APU Prop	-3231											
Cruise Fuel (JP)	-143786											
Booster Landing (Gear Down)	655069	3146	0.0	344.0	9.63	103.9	105.3					
NOTES:												

COMBINED SYSTEM C.G. TRAVEL
B-9U + ESS/ALTERNATE PAYLOAD

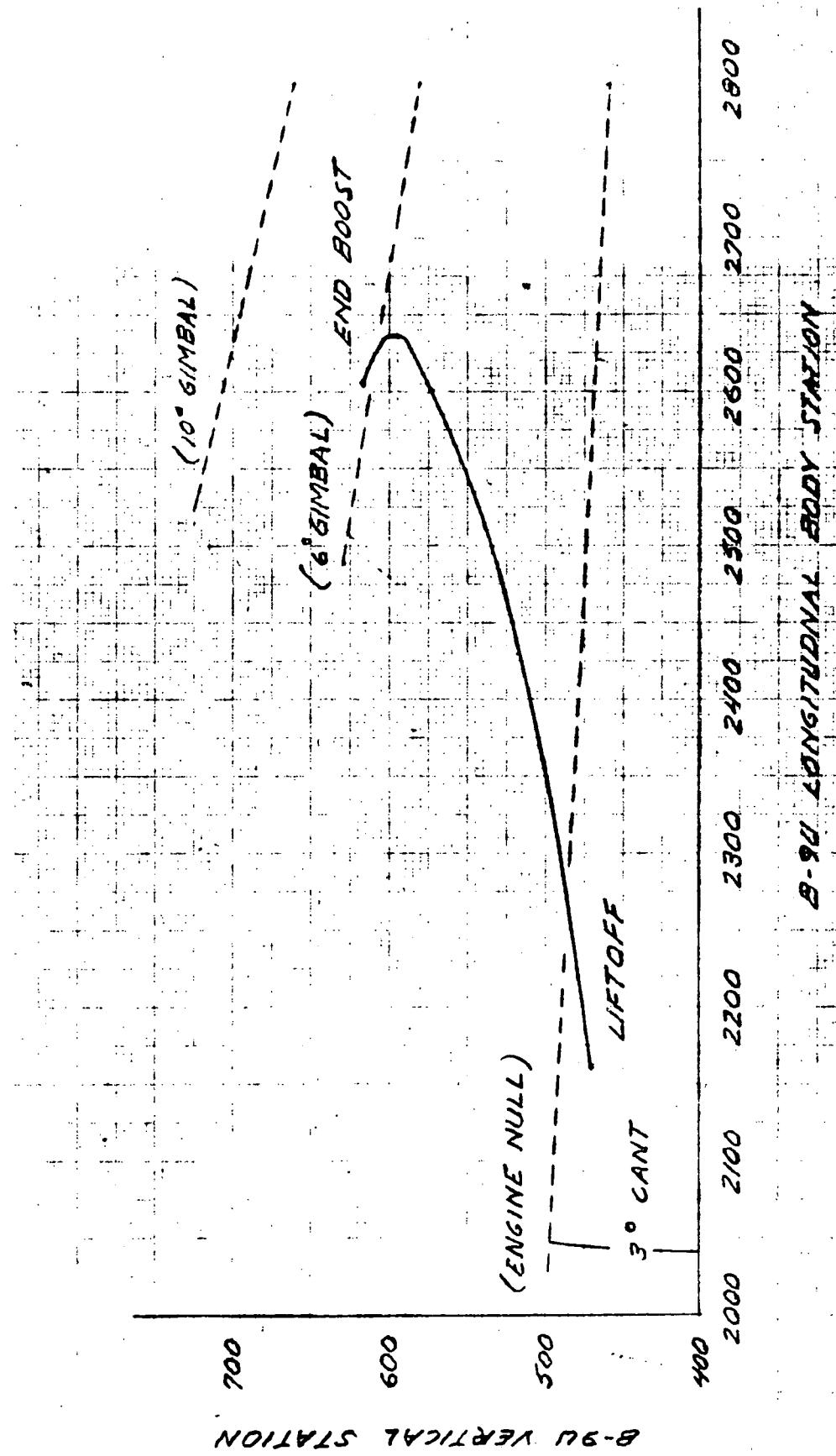


Figure C-2. LH₂ Tanker MDAC Payload Shape (992,000 Gross Weight)



Table C-5. Summary Weight Statement (Launch Condition)

CONFIGURATION B-9U/ESS - RNS WITH LH ₂ IN TANK			BY			DATE			
CODE	SYSTEM	BOOSTER	EST	CALC	ACT	ORBITER	EST	CALC	ACT
1.0	WING GROUP	61990							
2.0	TAIL GROUP	19230							
3.0	BODY GROUP	182772				57847	42	21	37
4.0	INDUCED ENVIR PROTECT	82644							
5.0	LANDING, DOCKING	27361							
6.0	PROPULSION, ASCENT	130186				25328	90	10	
7.0	PROPULSION, CRUISE	50413							
8.0	PROPULSION, AUXILIARY	10557				4710	100		
9.0	PRIME POWER	1801				3400	100		
10.0	ELECTRICAL CONV & DISTR	1438				1190	100		
11.0	HYDR & PNEU DISTR	1862				406	10	90	
12.0	SURFACE CONTROLS	7889							
13.0	AVIONICS	5468				2955	100		
14.0	ENVIRONMENTAL CONTROL	1650				1100	100		
15.0	PERSONNEL PROVISION	1700							
16.0	RANGE SAFETY								
17.0	BALLAST								
18.0	GROWTH	46486							
19.0	ESS PLATFORM	9770							
	SUBTOTAL (DRY WT)	643117				96936	63	15	22
20.0	PERSONNEL	476							
21.0	*PAYLOAD					176960	100		
22.0	ORDNANCE								
23.0	RESIDUAL FLUIDS	11476				5965	100		
24.0	PAYLOAD MARGIN					5330	100		
	SUBTOTAL (INERT WT)	655069				285191	88	5	7
25.0	RESERVE FLUIDS					6659	100		
26.0	INFLIGHT LOSSES	20802				83	100		
27.0	PROPELLANT-ASCENT	3382307				677150	100		
28.0	PROPELLANT-CRUISE	143786							
29.0	PROPELLANT-MANEUV/ACS	1500				22917	100		
30.0									
	TOTAL (GROSS WT) LB	4203464	100			992000	98	1	1
DESIGNATIONS:			NOTES & SKETCHES:						
EST	% ESTIMATED WEIGHT		*PAYLOAD CONSISTS OF RNS (83,000 LB) WITH 93,960 LB OF LH ₂ LOADED IN RNS TANK						
CALC	% CALCULATED WEIGHT								
ACT	% ACTUAL WEIGHT								



Table C-6. Sequence Mass Properties Statement

CONFIGURATION B-9U + ESS/RNS WITH LH ₂ LOAD			CENTER OF GRAVITY INCHES			MOMENT OF INERTIA SLUG FT ² X 10 ⁻³			PRODUCT OF INERTIA SLUG FT ² X 10 ⁻³			PAGE OF
NO.	MISSION EVENT	WEIGHT LB.	X	Y	Z	I _{x-x}	I _{y-y}	I _{z-z}	I _{xy}	I _{xz}	I _{yz}	
	Liftoff	5195464	2155	0.0	471.3							
	Booster Ascent Prop	-1412842										
	Max q Flight Condition	3782622	2332	0.0	498.0							
	Booster Ascent Prop	-612441										
	Flight Condition	3170181	2416	0.0	516.9							
	Booster Ascent Prop	-1351264										
	Booster Thrust Decay	-5760										
	Booster Burnout	1813157	2585	0.0	616.8							
	Orbiter Separation	-992000										
	Booster Vent Residuals	-17571										
	Booster ACS Prop	-1500										
	Booster Start Cruise	802086	3049	0.0	332.0	9.99	129.5	130.7				
	Booster APU Prop	-3231										
	Cruise Fuel (JP)	-143786										
	Booster Landing (Gear Down)	655069	3146	0.0	344.0	9.63	103.9	105.3				

NOTES:

COMBINED SYSTEM C.G. TRAVEL

B-9U + ESS/*ALTERNATE PAYLOAD

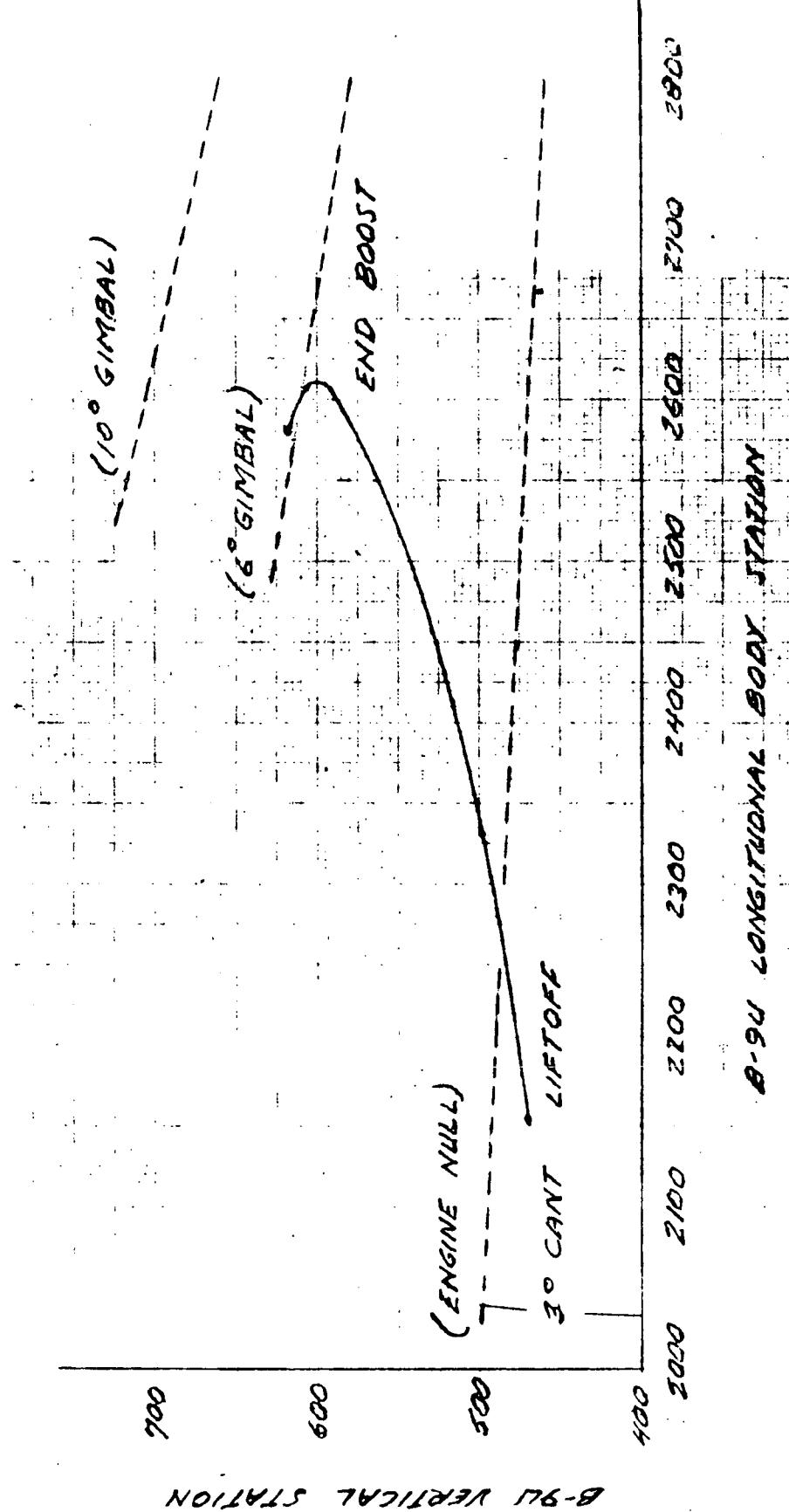


Figure C-3. RNS Payload + LH₂ in Tank (992,000 Gross Weight)



Table C-7. ESS/RNS Limit Fitting Loads (Partially Loaded RNS
With a -2° MDAC Trajectory)

Load Condition		Forward Fitting (lb x 10 ⁻³)			Aft Fitting (lb x 10 ⁻³)	
Description	Wind Direction	Axial F _x	Normal F _z	Lateral F _y	Normal F _z	Lateral F _y
Max Q Q = 484 psf $\alpha = 3.1^\circ$	Head	2088	-614.6	0	838.8	0
Max Q Q = 346 psf $\alpha = -8.37$	Tail	2026	-182.1	0	270.5	0
End Boost $N_{total} = 2.06$ $N_x = -2.03$ $N_z = 0.34$	No wind	2231	-344.8	0	716.6	0

NOTES:

1. Normal (F_z) fitting loads are negative in tension and positive in compression.
2. The aft fitting axial load = 0 pound..
3. Dynamic factors:

	Max Q	End Boost
F _x	1.1	1.1
F _z	1.2	1.1
4. The forward fitting axial (F_x) load is positive toward the nose nose of the payload.



APPENDIX D. SINGLE-ENGINE ESS PERFORMANCE ANALYSIS

At the informal request of NASA, performance data were developed for an ESS powered by a single space shuttle orbiter engine. The engine was assumed to operate at its emergency power level (EPL) of 109 percent of nominal thrust. A layout of this configuration is included in Volume VII.

Figure D-1 shows the performance capability of the single-engine ESS. It is seen that only maximum performance trajectories provide performance capable of launching the MDAC space station. The booster attachment loads associated with these trajectories will be higher than those of comparable twin-engine ESS trajectories. This is because loads for the twin-engine case can be reduced by throttling and steering. These techniques cause considerable performance degradation but they can be compensated for by increasing the ESS propellant load. This is not possible with the single-engine design, as illustrated in Figure D-1. Therefore, the following comparisons are based on maximum performance single-engine trajectories versus minimum loads twin-engine trajectories.

Typical values of maximum dynamic pressure are 380 psf and 575 psf, respectively, for the twin-engine low-loads cases and the single-engine maximum performance cases. This represents approximately a 50 percent increase. Axial attachment loads at booster burnout are shown in Figure D-2. Loads for the single-engine cases are approximately 40 percent higher. Based on these factors, it is considered that the twin-engine design would be likely to cause the least effect on the shuttle booster. Table D-1 depicts characteristics of the vehicle assuming a 10,000-pound payload margin. Other characteristics of a single-engine design are:

1. The ability to accommodate different booster sizes and designs is compromised. That is, the vehicle at maximum performance with the present booster is seen to be capable of launching the MDAC space station. With lower performing boosters (e.g., booster for the Orbiter External Hydrogen-Tank Study), it is questionable whether the required performance could be obtained.
2. Separation from the booster with the engine failed is likely to be a problem with the present separation linkage design.



3. Abort capability at low altitude will be compromised due to the low T/W.
4. The engine-out capability is trivial. (There would be a short time prior to nominal shutdown when OMS propulsion could be used to attain a safe orbit.)
5. All-azimuth launch capability is lost because of the inability to steer toward and reach a safe impact zone if the engine fails.

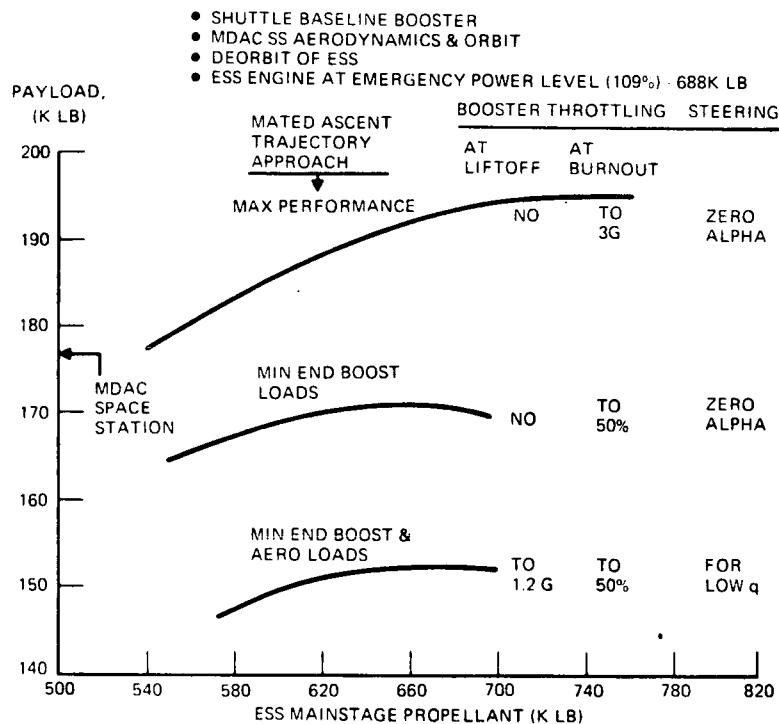


Figure D-1. Performance of ESS (One SSE₀ Design)

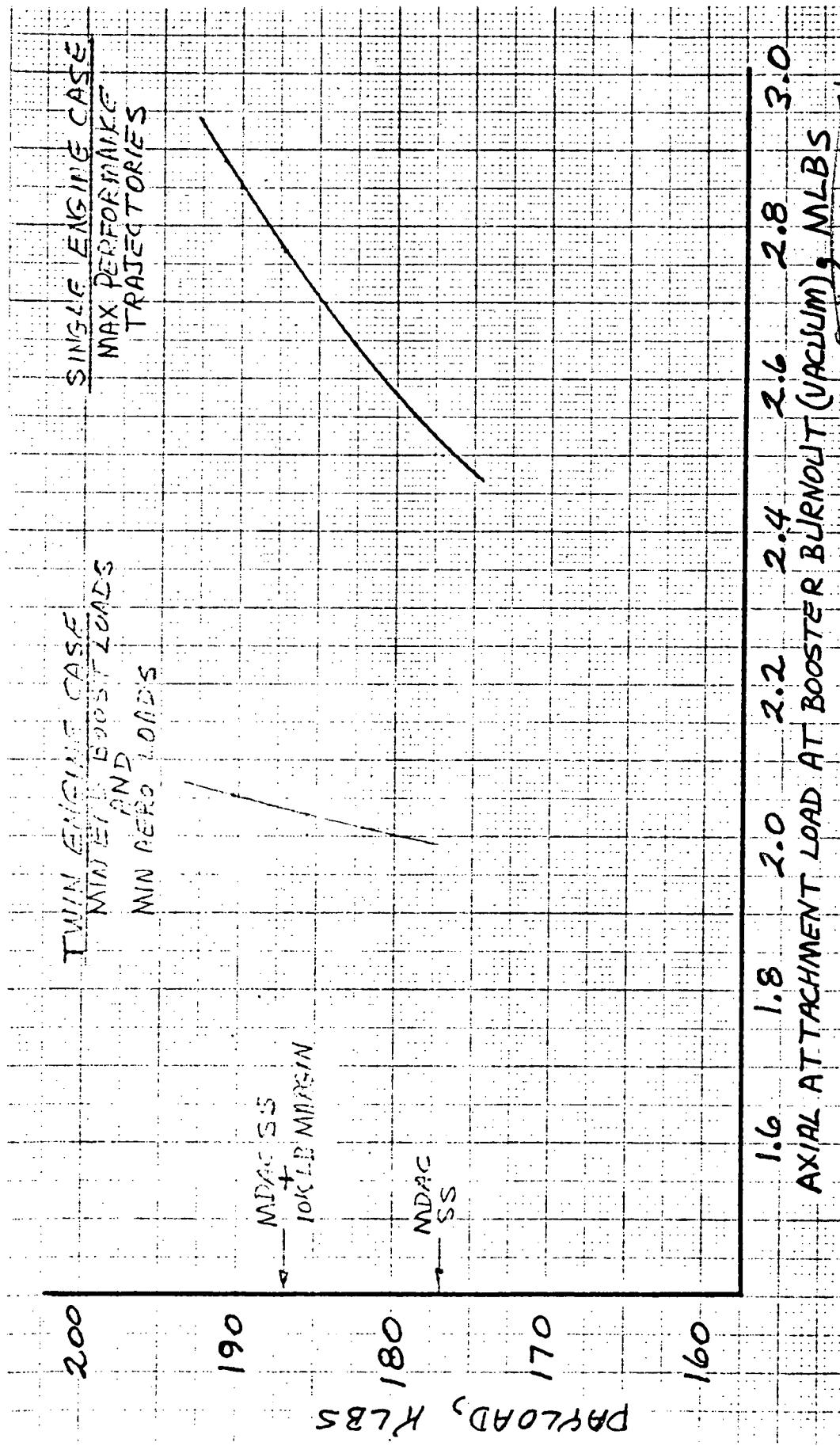


Figure D-2. Comparison of Axial Attachment Load at End Boost

Table D-1. Single Engine ESS Launch of MDAC SS, Maximum Performance Trajectory



D - 4

SD 71-140-2



APPENDIX E. EFFECTS OF FIXED EXPANSION RATIO NOZZLE

At the informal request of NASA-MSFC, a brief evaluation was made of the selected ESS/B-9U booster. The ESS was equipped with two space shuttle orbiter engines, each with a fixed expansion ratio nozzle. Data on such an engine were informally received from NASA-MSFC.

The data are:

Length: 218 inches

Exit dia: 115 inches

Expansion ratio, ϵ : 90:1

Actuator loads per ICD, Paragraph 7.2

Sea level (SL) engine excursion angle side loads per ICD, $\pm 0.6^\circ$ to $\pm 10^\circ$

I_{sp} (vac) minimum: 450.2 sec

I_{sp} (vac) nominal: 453.2 sec

I_{sp} (SL) minimum: 342 sec

I_{sp} (SL) nominal: 345 sec

Thrust (vac): 624.5 K lbs

Thrust (SL): 473.5 K lb

Engine dry weight: 8465 lb

Engine wet weight: 9088 lb

Cost delta DDT&E (objective 1): \$-15.1M

Cost delta operational, including DDT&E and facilities

(Objective 2): \$-27.2M

Figure E-1 summarizes the brief evaluation of the fixed expansion ratio nozzle compared with the two-position nozzle (per ICD). For the same gross weight attached to the reusable booster as the selected ESS with the MDAC space station payload (992,000 pounds), the fixed nozzle shows a DRM payload reduction of 5950 pounds from the nominal 183,000 pounds of the selected system. The specified weight of the MDAC space station is 176,960 pounds, which is less than the 179,050-pound capability. If the propellant load on the ESS is fixed, 178,200 pounds of capability remains, still more than required. If the same payload capability as the selected system is desired (183,000 pounds), the ESS/payload gross weight required is 1,019,200 pounds, or 27,200 pounds more than the selected ESS. This could have a minor additional effect on the booster.



For the selected ESS/B-9U booster combination, the use of a fixed expansion ratio nozzle with characteristics as listed would be acceptable to the ESS and it can be accommodated from a performance standpoint. Design requirements, installation, test requirements, and related factors have not been evaluated.

PERFORMANCE FACTORS ($\epsilon = 90:1$)

- I_{SP} REDUCED BY 5.8 SECONDS
- THRUST REDUCED BY 7400 POUNDS
- STAGE INERT WEIGHT REDUCED BY 700 POUNDS

CONCLUSION
SELECTED ESS
COULD ACCOMMODATE
FIXED EXPANSION
RATIO NOZZLE
ENGINE DESIGN

PERFORMANCE EFFECTS, MACDAC SS TO DRM

RATIONALE	ESS / PAYLOAD GROSS WEIGHT LB	ESS MS PROPELLANT LB	PAYOUT ' LB
2-POSITION NOZZLE REFERENCE	992,000	683,800	183,000
FIXED ESS / PAYLOAD GROSS	992,000	688,710	179,050
FIXED ESS PROPELLANT	886,200	683,800	178,200
FIXED PAYLOAD	1,019,200	711,600	183,000

Figure E-1. Effects of Fixed Expansion Ratio Nozzle



APPENDIX F. TRAJECTORY DATA - SELECTED SYSTEM

The following trajectory data represent the final iteration of the Phase B Study and the basic for performance quotations for the selected system. Each of the three specified payloads is treated individually, as indicated.

Other trajectory data, which reflect earlier iterations, are given in Volume XII.

REVISED BASELINE ASCENT TRAJECTORY

For MDAC space station launch (5-6-71), this trajectory represents the revised baseline trajectory. It reflects an ESS gross weight of 992,000 pounds and is consistent with the space station trajectory dated 4-13-71 upon which analyses for the current study phase were conducted.

REVISED BASELINE ASCENT TRAJECTORY FOR MDAC SPACE STATION LAUNCH

DATE - 05/05/71

CASE 1 PAGE 1 OF 9

STAGE	1	2	3	
GROSS STAGE WEIGHT, (LBS)	5190223.0	1002000.0	<u>992000.0</u>	ESS/PAYLOAD GROSS WEIGHT
GROSS STAGE THRUST/WIGHT	1.272	0.0	1.267	
THRUST, (LBS)	7243500.0	0.0	<u>1256858.0</u>	
ISP, (SFC)	439.000	2.500	456.480	
INERT WEIGHT, (LBS)	663531.0	<u>10000.0</u>	<u>102190.0</u>	BOOSTER ATTACHMENT
PROPELLANT, (LBS)	3376547.0	0.0	<u>683809.1</u>	ESS MAINSTAGE PROPELLANT
PERF. FRAC., (%)	0.6506	0.0	0.6893	
PROPELLANT FRAC., (%)	0.9358	0.0	<u>0.8700</u>	
BURNOUT TIME, (SEC)	249.781	252.281	498.238	
BURNOUT VELOCITY, (FT/SEC)	9834.523	9828.711	25763.105	
BURNOUT GAMMA,(DEGREES)	4.447	4.053	-0.000	
BURNOUT ALTITUDE, (NM)	281749.4	282552.0	399984.0	
BURNOUT RANGE, (NM)	108.9	112.6	714.2	
FINAL VELOCITY, (FT/SEC)	14539.8	0.0	16855.9	
INJECTION VELOCITY, (FT/SEC)	314.0	<u>FLYBACK RANGE(NM)</u>	<u>392.7</u>	
INJECTION PROPELLANT, (LBS)	6658.9	FLYBACK PROP(LBS)	148145.0	
ORBIT MANEUVERING REQUIREMENTS	Rendezvous	DEORBIT	*LOSSES	TOTALS *LOSSES = 83.0
DELTA V, (FT/SEC)	740.0	550.0	0.0	1290.0 LBS ♦ 0.0 PERCENT
SPECIFIC IMPULSE, (SEC)	450.3	450.3	0.0	0.0 OF USEABLE PROPELLANT
PROPELLANT, (LBS)	15346.1	3056.7	83.0	18485.8
RCSS PROPELLANT, (LBS)	4514.2	TOTAL RCS+OMS PROP, (LBS)	23000.0	MARGIN MDAC SS
PAYOUTLOAD, (LBS)	183000.9 - 6,041	= 176,960		

NR TRAJECTORY/WEIGHT SIZING PROGRAM

DATE - 05/05/71

HOUR - 20

BASELINE ESS---5 MAY 1971

PAYOUT = MDAC SPACE STATION + ABOUT 6000 LBS MARGIN
ESS GROSS WEIGHT = 992000 LBS CONSISTENT WITH LOADS WORK

CONDUCTED BY GD AND SLV DURING THIS STUDY PHASE
MIN LOADS BOOST TRAJECTORY--LOW Q AND LOW END BOOST

T/W IN = 1.2 AND 50 % THROTTLING AT END BOOST
ALPHA PROFILE TO GIVE NEGATIVE ALPHA IN MAX Q REGIME

ALPHA PROFILE AS FOLLOWS

TIME	20	30	40	70	90	120+
ALPHA-2	0	0	-2	-2	-8	
Q*ALPHA LIMIT	= -800	PSF-DEG				

ALPHA AT MAX Q EQUAL -2 DEG

COMPLETE PITCH AERO FOR B-9U/ESS/MDAC SPACE STATION---3-24-71--

BOoster WEIGHT DATA FROM GD STATUS REPORT OF 24 MARCH

BOoster CG DATA ABOUT THE SLV CALCULATIONS OF 3-16-71

BOOSTER ATTACHMENT MECHANISM = 10000 LBS

ESS WEIGHTS FROM SLV---3 MAY 1971

FLY BACK RANGE LIMITED TO 383 NM

BOOSTER FLYBACK TANKS FULL

6 DEGREE ENGINE CANT FOR ESS MS ENGINES OPERATING NORMALLY

DEMI---270NM---55 DEG INCL

RETAIN ESS INTERSTAGE TO ORBIT AND DECORIT WITH STAGE

740 FPS OMS DV BUDGET---670 + 10 PERCENT

DECORIT ESS WITH DELTA V OF 550 FPS

ENTRY WEIGHT = 79000 LBS---MS ENGINES HAVE BEEN REMOVED

OMS ISP = 450.3 SFC = 0.04 (NOM ISP = 4)

OMS LOSSES (BOLLOFF AND CHILDDOWN) = 93 POUNDS OF LH2

FULL OMS TANKS---23000 LBS-

RCS PROPELLANT = 23000 - OMS PROP REQUIRED

ATMOSPHERIC TRAJECTORY

CASE 1 PAGE 2 OF 9

TIME H	VRFL VDDT	ALT GDI	GAMMA VGRAV	LOAD FACTOR		
				THRUST	THROTTLE RATIO	THROTTLE LF
ALPHA	MACH	LIFT	RANGE			
ATTITUDE	TVC DEFL	XCG(LIN)	PITCH ACC(IN)	NORMAL LF		
FLOW PATH	2*0*V	AERO HFAT	Q*ALPHA	AERO MM(LIN-LBR)	AXIAL LF	
0.0	0.0	0.0	0.900000E 02	0.0	0.120000E 01	
0.519027E 07	0.642859F 01	0.0	0.0	0.0	0.627827E 07	
-0.236825E 01	0.0	0.0	0.0	0.500000E 05	0.951252E 00	
0.876317E 02	0.236825F 01	0.217362E 04	0.472350E 03	0.300900E 04	0.499843E-01	
0.156974F 05	0.0	0.0	0.0	0.0	0.11996F 01	
0.100000E 02	0.701431F 02	0.341393E 03	0.900003E 02	0.560049E 01	0.123656F 01	
0.503325E 07	0.760600F 01	0.268221E-05	0.322165E 03	0.38908E 01	0.628551E 07	
-0.246728F 01	0.617373F-01	0.488771E 03	-0.266033E-06	0.615782E 05	0.951252E 00	
F	0.875330F 02	0.245425F 01	0.219292E 04	0.474513E 03	0.300900E 04	0.530460F-01
-0.156074E 05	0.785995F 03	0.195879E 04	-0.138180E 02	-0.226187E 07	0.123542F 01	
0.200000E 02	0.152105E 03	0.144335E 04	0.900003E 02	0.255313E 02	0.127291E 01	
0.497627F 07	0.8778P3F 01	0.506639E-06	0.644307E 03	0.852349F 01	0.630942E 07	
-0.255184F 01	0.134387E 00	-0.608138F 04	-0.114812E-05	0.101362E 06	0.951252E 00	
0.874484F 02	0.258936F 01	0.221194E 04	0.476869E 03	0.300900F 04	0.562746F-01	
0.156974E 05	0.776685F 04	0.363148E 05	-0.651517E 02	0.322488E 07	0.127166F 01	
0.200000E 02	0.152105E 03	0.144335E 04	0.882029E 02	0.255313E 02	0.127291E 01	
0.497627E 07	0.879467F 01	-0.380136E 00	0.644307E 03	0.852349E 01	0.630942F 07	
-0.255184F 01	0.134387F 00	-0.608138F 04	-0.114812E-05	0.101362E 06	0.951252F 00	
0.856510E 02	0.258936E 01	0.221194E 04	0.476869E 03	0.300900E 04	0.562746F-01	
0.156974F 05	0.776685F 04	0.363148E 05	-0.651517E 02	0.322488E 07	0.127166F 01	
0.300000E 02	0.246063E 03	0.342109E 04	0.857087E 02	0.631428E 02	0.130949E 01	
0.471930E 07	0.996735E 01	-0.659452E-01	0.965841E 03	0.175732E 02	0.634778E 07	
0.0	0.218873E 00	0.28281RE 05	0.215936E-01	0.174138E 06	0.951252F 00	
0.857087E 02	0.252997E 01	0.223065E 04	0.479435E 03	0.301284E 04	0.653669F-01	
0.156974F 05	0.310741E 05	0.212575E 06	0.0	-0.295432E 08	0.130688E 01	

ATMOSPHERIC TRAJECTORY

CASE 1 PAGE 3 OF 9

TIME	VRFI	VRDT	ALT	GDI	GAMMA	ORAR	LNDN FACTR
W	MACH	RANGE	SDT	VGRAV	VDRG	THRUST	
ALPHA	TVC DFL	XCG (IN)	LIFT	PITCH AC (IN)	DRAG	THRSTTLF PATTN	
ATTITUDE	2*3*V	AERO HFACT	Q*ALPHA	AERO MOM (IN-LR)	DITCH AC (IN)	NORMAL LF	
FLW RATE					AERO MOM (IN-LR)	AXIAL LF	

0.40000E 02	0.351466E .03	0.638958E .04	0.850728E .02	0.117942E .03	0.134446E .01	0.640271E .07	
0.456232E 07	0.111497E .02	-0.582386E -01	0.128681E .04	0.310889E .02	0.310889E .02	0.640271E .07	
0.0	0.315531E 00	0.528266E 05	0.631350E -01	0.271799E .06	0.951252E .00	0.951252E .00	
* 0.850728E 02	0.254198E 01	0.225032E 04	0.482176E 03	0.393249E .04	0.738211E -01	0.738211E -01	
0.156974E 05	0.829054E 05	0.754813E 06	0.0	-0.506415E 08	0.134243E 01	0.134243E 01	
0.50000E 02	0.4629556E .03	0.104659E .05	0.840254E .02	0.185810E .03	0.138498E .01	0.647050E .07	
0.440535E 07	0.125409E .02	-0.156110E 00	0.160731E 04	0.552661E .02	0.647050E .07	0.647050E .07	
-0.666667E 00	0.426912E 00	0.440907E 05	0.129597E 00	0.371287E 06	0.951252E .00	0.951252E .00	
0.833597E 02	0.273329E 01	0.227223E 04	0.485056E 03	0.305512E 04	0.706988E -01	0.706988E -01	
F 0.156974E 05	0.174533E 06	0.200655E 07	-0.123873E 03	-0.403707E 08	0.138272E 01	0.138272E 01	
0.60000E 02	0.603171E 03	0.157767E 05	0.818711E 02	0.259508E 03	0.142050E .01	0.654685E .07	
0.444837E 07	0.141886E 02	-0.275301E 00	0.192669E 04	0.874871E 02	0.654685E .07	0.654685E .07	
-0.133333E 01	0.557640E 00	0.102623E 05	0.242896E 00	0.470139E 06	0.951252E .00	0.951252E .00	
-0.805378E 02	0.308387E 01	0.229363E 04	0.488227E 03	0.307307E 04	0.827435E -01	0.827435E -01	
0.156974F 05	0.313055F 06	0.440633E 07	-0.346010E 03	-0.289561E 07	0.142810F 01	0.142810F 01	
0.70000E 02	0.754248E .03	0.224493E .05	0.785092E .02	0.328448E .03	0.147763E .01	0.662630E .07	
0.409140F 07	0.160612F 02	-0.397204E 00	0.224361E '04	0.127923E 03	0.181935E 03	0.670269E .07	
-0.200000E 01	0.715537F 00	-0.459006E 05	0.442686E 00	0.579727E 06	0.951252E .00	0.951252E .00	
0.765092E 02	0.360611F 01	0.231446E 04	0.491720E 03	0.308150E 04	0.857087E -01	0.857087E -01	
0.156974E 05	0.495462F 06	0.841870F 07	-0.656896E 03	0.638318E 08	0.147514E 01	0.147514E 01	
0.80000E 02	0.922515E .03	0.305862E .05	0.742453E 02	0.376463E 03	0.149362E .01	0.670269E .07	
0.393442F 07	0.171615F 02	-0.464467E 00	0.255592E 04	0.181935E 03	0.181935E 03	0.670269E .07	
-0.200000E 01	0.908667F 00	-0.639973E 05	0.783844F 00	0.824710E 06	0.951252E .00	0.951252E .00	
0.722453F 02	0.374471E 01	0.2333663E 04	0.495380E 03	0.308546E 04	0.876924E -01	0.876924E -01	
0.156974F 05	0.694585F 06	0.143850E 08	-0.752925E 03	0.565122E 08	0.149105E 01	0.149105E 01	

ATMOSPHERIC TRAJECTORY

CASE 1

PAGE 4 OF 6

TIME W	VREL VDDT	MACH	ALPHA	ATTITUDE FLOW RATE	TVC DFFL 2*Q*V	ALT GDT	GAMMA VGRAV RANGE	QBAR VDRG DRAG	THROTTLE RATIO NORMAI LF	LOAD FACTOR THRUST
0.90000E 02	0.110013F 04				0.401706F 05	0.692452F 02	0.379080F 03	0.152087F 01		
0.77745F 07	0.192307F 02	-0.522653F 00	0.286082E 04	0.261751E 03	0.676925F 07					
-0.20000E 01	0.113476E 01	-0.545228E 05	0.132710F 01	0.989133F 06	0.951252F 00					
0.672452F 02	0.366610E 01	0.235994E 04	0.499262E 03	0.305370F 04	0.910214F 01					
0.156074F 05	0.834077F 06	0.220909E 08	-0.758160F 03	0.600029F 07	0.152716F 01					
0.100000E 03	0.132147E 04	0.512218F 05	-0.638111E 02	0.337495F 03	0.167075F 01					
0.362047F 07	0.252950F 02	-0.553135F 00	0.315497F 04	0.337623F 03	0.682032F 07					
-0.237040F 01	0.140831F 01	-0.353878E 05	0.214948E 01	0.738173F 06	0.951252F 00					
0.614406F 02	0.382857F 01	0.238232E 04	-0.503617E 03	0.304344F 04	0.107597E 00					
0.156074F 05	0.891983F 06	0.308037E 08	-0.800000F 03	-0.3489921E 07	0.167630F 01					
0.110000E 03	0.160970E 04	0.639741E 05	0.581722F 02	0.255593E 03	0.184990E 01					
0.346350F 07	0.323424F 02	-0.577228F 00	0.343512E 04	0.393701E 03	0.685363F 07					
-0.312998F 01	0.169267F 01	-0.913079F 05	0.335735F 01	0.445262E 06	0.951252F 00					
0.550422F 02	0.429980F 01	0.240364E 04	0.508509E 03	0.300532E 04	0.114985F 00					
0.156074E 05	0.922853F 06	0.394656E 08	-0.800000F 03	0.389632F 08	0.184632F 01					
0.120000E 03	0.196792F 04	0.786011E 05	0.523135F 02	0.179628E 03	0.200756F 01					
0.330652F 07	0.393061F 02	-0.592710F 00	0.369793E 04	0.422431E 03	0.687227F 07					
-0.445364F 01	0.201853E 01	-0.150903E 06	0.508590E 01	0.235109F 06	0.951252F 00					
0.478599E 02	0.476121F 01	0.242998E 04	0.513640E 03	0.294666E 04	0.121402F 00					
0.156074F 05	0.706990F 06	0.471334E 08	-0.800000E 03	0.733788E 09	0.200388F 01					
0.130000E 03	0.238304F 04	0.950488E 05	0.663202E 02	0.118687E 03	0.205020E 01					
0.315238F 07	0.427977F 02	-0.608817E 00	0.394015E 04	0.438212F 03	0.654026F 07					
-0.674043E 01	0.239675F 01	-0.176283E 06	0.748304E 01	0.937403F 05	0.905275F 00					
0.395798E 02	0.512419E 01	0.245702E 04	0.519214F 03	0.287858E 04	0.126532F 00					
0.149418E 05	0.565671F 06	0.535282F 08	-0.800000E 03	0.798765E 08	0.2044629F 01					

H-6

SD 71-140-2

ATMOSPHERIC TRAJECTORY

CASE 1 PAGE 5 OF 6

TIME W	VREF VDOT	ALT GDT	GAMMA VGRAV	DRAP VDRG.	LOAD FACTOR THUST
ALPHA MACH	TVC DEFL	LIFT	RANGE	DRAG	THRUST/FRAFT
ATTITUDE FLOW RATE	?*Q*V	XCG (IN)	ZCG (IN)	PITCH AC (IN)	NORMAL LF
0.140000E 03	0.292272F .04	0.112837F .06	0.402850E .02	0.723559F .02	0.205003F .01

TIME W	VREF VDOT	ALT GDT	GAMMA VGRAV	DRAP VDRG.	LOAD FACTOR THUST
ALPHA MACH	TVC DEFL	LIFT	RANGE	DRAG	THRUST/FRAFT
ATTITUDE FLOW RATE	?*Q*V	XCG (IN)	ZCG (IN)	PITCH AC (IN)	NORMAL LF
0.140000E 03	0.292272F .04	0.112837F .06	0.402850E .02	0.723559F .02	0.205003F .01
0.300744E 07	0.452163F .02	-0.574667E 00	0.415869E 04	0.443451E 03	0.617050F .07
-0.800000E 01	0.276443F .01	-0.132225E 06	0.106704F 02	0.128777F 05	0.852350F 00
0.322850E 02	0.527602F .01	0.248085F 04	0.525141E 03	0.280883E 04	0.144532F 00
0.140736E 05	0.408480F 06	0.593837E 08	-0.578846E 03	0.493688F 08	0.204493F 01
0.150000E 03	0.328726F .04	0.131395E 06	0.348713E 02	0.429141E 02	0.204985F 01
0.287048E 07	0.474705F .02	-0.509410F 00	0.435257E 04	0.442009E 03	0.584596F 07
-0.900000E 01	0.312726E 01	-0.917843F 05	0.147230F 02	-0.39347E 05	0.807275F 00
0.269713E 02	0.543374F 01	0.250579F 04	0.530434E 03	0.273873E 04	0.166284F 00
0.133351E 05	0.282139F 06	0.618058E 08	-0.343313E 03	0.254585E 08	0.204310F 01
0.160000E 03	0.377561F .04	0.150283F 06	0.300693E 02	0.257510F 02	0.204973F 01
0.274046E 07	0.499741F .02	-0.452208E 00	0.452295E 04	0.436543E 03	0.55535F 07
-0.800000E 01	0.350487F 01	-0.530351F 05	0.196880F 02	-0.595587E 05	0.767039F 00
0.220593E 02	0.569280F 01	0.252733E 04	0.536296E 03	0.266573E 04	0.184943E 00
0.126764E 05	0.194452E 06	0.641595E 08	-0.206008E 03	0.156603E 08	0.204137E 01
0.170000E 03	0.428615F .04	0.169099F 06	0.258029E 02	0.162824E 02	0.204965F 01
0.261676E 07	0.521066F 02	-0.402126E 00	0.467136E 04	0.428418E 03	0.528815F 07
-0.800000E 01	0.397968E 01	-0.374021E 05	0.256013F 02	-0.739441E 05	0.730090F 00
0.178022E 02	0.601007E 01	0.254562F 04	0.542744E 03	0.257393E 04	0.201370E 00
0.120720F 05	0.139578F 06	0.658053E 08	-0.130259E 03	0.119312E 08	0.203974F 01
0.180000E 03	0.481714F .04	0.187479E 06	0.220081E 02	0.105460E 02	0.204963F 01
0.249986F 07	0.540632F 02	-0.357693F 00	0.479950E 04	0.418656E 03	0.503092F 07
-0.800000E 01	0.458451E 01	-0.289731E 05	0.324905E 02	-0.809846E 05	0.605800F 00
0.140081E 02	0.639576E 01	0.257106F 04	0.549110E 03	0.254662E 04	0.217700F 00
0.115111E 05	0.101603E 06	0.670034E 08	-0.843677E 02	0.121850E 08	0.203804F 01



ATMOSPHERIC TRAJECTORY

TIME

VRFL
YDNT
MACH
TVC DEFL
2#0#VALT
GDT
LIFT
XCG(IN)
AFRO HEATGAMMA
VGRAV
RANGE
ZCG(IN)
Q*ALPHAQRAP
VDRG
DRAG
PITCH AC (IN)
AFRO MOM(MIN-LB)LOAD FACTOR
THRUST
THROTTLE RATIO
NORMAL IF
AXIAL IF

TIME	VRFL	YDNT	MACH	TVC DEFL	2#0#V	ALT	GDT	LIFT	XCG(IN)	AFRO HEAT	Q*ALPHA	QRAP	VDRG	DRAG	PITCH AC (IN)	AFRO MOM(MIN-LB)	LOAD FACTOR	THRUST	THROTTLE RATIO	NORMAL IF	AXIAL IF
0.100000E 03	0.536679F 04	-	0.205100E 06	-	-	0.186316E 02	-	-	-	-	-	0.674064E 01	-	-	-	-	0.204050F 01	-	-	-	-
0.238643E 07	0.558409F 02	-	0.318376F 00	-	-	0.490912E 04	-	-	-	-	-	0.407611E 03	-	-	-	-	0.480445F 07	-	-	-	-
-0.900000E 01	0.527219E 01	-	-0.234639E 05	-	-	0.403762F 02	-	-	-	-	-	0.862458F 05	-	-	-	-	0.663288F 00	-	-	-	-
0.106316E 02	0.681080F 01	-	0.259254F 04	-	-	0.556153E 03	-	-	-	-	-	0.251911E 04	-	-	-	-	0.234045F 00	-	-	-	-
0.109793F 05	0.723512F 05	-	0.678658F 08	-	-	-0.539251E 02	-	-	-	-	-	0.131139F 08	-	-	-	-	0.203618F 01	-	-	-	-
0.200000E 03	0.593335E 04	-	0.221692F 06	-	-	0.156251E 02	-	-	-	-	-	0.424062F 01	-	-	-	-	0.204056F 01	-	-	-	-
0.227918F 07	0.574469F 02	-	0.283600F 00	-	-	0.500193E 04	-	-	-	-	-	0.395459F 03	-	-	-	-	0.458140F 07	-	-	-	-
-0.800000F 01	0.602593F 01	-	-0.198145E 05	-	-	0.492739E 02	-	-	-	-	-	0.896276F 05	-	-	-	-	0.632449F 00	-	-	-	-
F-8	0.762509F 01	-	0.724933E 01	-	-	0.260984E 04	-	-	-	-	-	0.248858F 04	-	-	-	-	0.250514F 00	-	-	-	-
0.104756F 05	0.504239F 05	-	0.684752F 08	-	-	-0.399969E 02	-	-	-	-	-	0.142364F 08	-	-	-	-	0.203410F 01	-	-	-	-
0.210000E 03	0.651516E 04	-	0.236986E 06	-	-	0.129458E 02	-	-	-	-	-	0.266544E 01	-	-	-	-	0.204954F 01	-	-	-	-
0.217683F 07	0.589009F 02	-	0.252910F 00	-	-	0.507956E 04	-	-	-	-	-	0.382348E 03	-	-	-	-	0.436968F 07	-	-	-	-
-0.800000F 01	0.682806F 01	-	-0.174373E 05	-	-	0.591950E 02	-	-	-	-	-	0.916964E 05	-	-	-	-	0.603258F 00	-	-	-	-
0.494580F 01	0.769756F 01	-	0.262698E 04	-	-	0.571643E 03	-	-	-	-	-	0.244446E 04	-	-	-	-	0.266804F 00	-	-	-	-
0.909727E 04	0.347316E 05	-	0.688965F 08	-	-	-0.213235E 02	-	-	-	-	-	0.152847E 08	-	-	-	-	0.201210F 01	-	-	-	-
0.220000E 23	0.711064E 04	-	0.250810F 06	-	-	0.105549E 02	-	-	-	-	-	0.169102E 01	-	-	-	-	0.204952E 01	-	-	-	-
0.27915F 07	0.601858E 02	-	-0.225772F 00	-	-	0.514354E 04	-	-	-	-	-	0.368375E 03	-	-	-	-	0.416811F 07	-	-	-	-
-0.900000E 01	0.766766F 01	-	-0.159660E 05	-	-	0.701485F 02	-	-	-	-	-	0.929558E 05	-	-	-	-	0.575457F 00	-	-	-	-
0.255489E 01	0.815277E 01	-	0.264602E 04	-	-	0.579002E 03	-	-	-	-	-	0.239828E 04	-	-	-	-	0.282927F 00	-	-	-	-
0.954247E 04	0.240485E 05	-	0.691968E 08	-	-	-0.135282E 02	-	-	-	-	-	0.162573E 08	-	-	-	-	0.202090F 01	-	-	-	-
0.230000E 03	0.771838E 04	-	0.262985E 06	-	-	0.842134E 01	-	-	-	-	-	0.110865E 01	-	-	-	-	0.204951F 01	-	-	-	-
0.198590E 07	0.613425F 02	-	0.201026F 00	-	-	0.519525E 04	-	-	-	-	-	0.353590E 03	-	-	-	-	0.397658F 07	-	-	-	-
-0.900000F 01	0.854252F 01	-	-0.150817F 05	-	-	0.821412E 02	-	-	-	-	-	0.937013E 05	-	-	-	-	0.548087F 00	-	-	-	-
0.421341F 00	0.869352F 01	-	0.266379E 04	-	-	0.588130E 03	-	-	-	-	-	0.235016E 04	-	-	-	-	0.301707F 00	-	-	-	-
0.910908E 04	0.171140F 05	-	0.693901E 08	-	-	-0.886919E 01	-	-	-	-	-	0.173389E 08	-	-	-	-	0.202718F 01	-	-	-	-

ATMOSPHERIC TRAJECTORY

TIME	VREF	ALT	GAMMA	QBAR	LOAD FACTOR
	VDDT	GDT	VGRAV	VDRG	THRUST
ALPHA	MACH	LIFT	RANGE	DRAG	THRUST/LIFT RATIO
ATTITUDE	TVC_DFL	XCG(IN)	ZCG(IN)	PITCH AC(IN)	NORMAL LIFT
FLOW RATE	2*0*V	AERO HEAT	Q*ALPHA	AERO MOM(MIN-LR)	AXIAL LIFT
0.240000F 03	0.833700F 04	0.273383E 06	0.652886F 01	0.763499F 00	0.206949F 01
0.139689F 07	0.623630F 02	-0.178103F 00	0.523599E 04	0.338016E 03	0.379296F 07
-0.900000F 01	0.943105F 01	-0.145550E 05	0.951733E 02	-0.941393F 05	0.523761F 00
-0.147114F 01	0.935625F 01	0.267474E 04	0.600675E 03	0.230129E 04	0.324460F 00
0.959589F 04	0.127306F 05	0.695379E 08	-0.610799E 01	0.186951E 08	0.202364F 01
0.249781E 03	0.835139F 04	0.281749F 06	0.488129F 01	0.550682F 00	0.204951E 01
0.121374F 07	0.632497E 02	-0.159141E 00	0.525641E 04	0.322017F 03	0.352334F 07
-0.600000F 01	0.101261F 02	-0.142263F 05	0.108943F 03	-0.944035E 05	0.500220F 00
-0.311371F 01	0.986076F 01	0.264273E 04	0.616824E 03	0.227000E 04	0.341595E 00
0.831009F 04	0.985973E 04	0.696469F 08	-0.440545E 01	0.204033E 08	0.202084E 01

0.240000F 03	0.833700F 04	0.273383E 06	0.652886F 01	0.763499F 00	0.206949F 01
0.139689F 07	0.623630F 02	-0.178103F 00	0.523599E 04	0.338016E 03	0.379296F 07
-0.900000F 01	0.943105F 01	-0.145550E 05	0.951733E 02	-0.941393F 05	0.523761F 00
-0.147114F 01	0.935625F 01	0.267474E 04	0.600675E 03	0.230129E 04	0.324460F 00
0.959589F 04	0.127306F 05	0.695379E 08	-0.610799E 01	0.186951E 08	0.202364F 01
0.249781E 03	0.835139F 04	0.281749F 06	0.488129F 01	0.550682F 00	0.204951E 01
0.121374F 07	0.632497E 02	-0.159141E 00	0.525641E 04	0.322017F 03	0.352334F 07
-0.600000F 01	0.101261F 02	-0.142263F 05	0.108943F 03	-0.944035E 05	0.500220F 00
-0.311371F 01	0.986076F 01	0.264273E 04	0.616824E 03	0.227000E 04	0.341595E 00
0.831009F 04	0.985973E 04	0.696469F 08	-0.440545E 01	0.204033E 08	0.202084E 01



FY0-ATMOSPHERIC TRAJECTORY

CASE 1 PAGE A NF 9

TIME M S	V(P) V(I)	GAM(P) GAM(I)	ALT THETAIR	PANGE	T/W
0.249781F 03 0.100206E 07	0.895130F 04 0.983452E 04	0.498129F 01 0.444202E 01	0.281749F 06 0.369620E 02	0.108943E 03	0.0
0.252281F 03 0.100206E 07	0.994500F 04 0.982871F 04	0.445370E 01 0.405257E 01	0.293552F 06 0.370283E 02	0.112563F 03	0.0
0.252281F 03 0.992061F 06	0.994500E 04 0.992871F 04	0.445370E 01 0.405257E 01	0.293552E 06 0.370283E 02	0.112563E 03	0.176602E 01
0.292281F 03 0.891926F 04	0.103497F 05 0.112254F 05	0.344778E 01 0.317569E 01	0.309728E 06 0.316258E 02	0.174896E 03	0.142513E 01
0.332281F 03 0.771792E 06	0.120518F 05 0.129390E 05	0.275405F 01 0.256506E 01	0.333696E 06 0.253844E 02	0.247230E 03	0.162849E 01
0.372281F 03 0.661657E 06	0.141307F 05 0.150193F 05	0.218102F 01 0.205193E 01	0.356064E 06 0.184092E 02	0.331706E 03	0.180956E 01
0.412281F 03 0.551523F 06	0.166974F 05 0.175871E 05	0.158899E 01 0.150850E 01	0.376256E 06 0.109905E 02	0.431078E 03	0.227888E 01
0.452281F 03 0.441388E 06	0.199239E 05 0.208145E 05	0.904647F 00 0.865938E 00	0.392096E 06 0.360618E 01	0.548996E 03	0.284750E 01
0.492281F 03 0.331254E 06	0.241280E 05 0.250190E 05	0.172667E 00 0.18299E 00	0.399840E 06 -0.316141E 01	0.690633E 03	0.379622E 01





EXO-ATMOSPHERIC TRAJECTORY

T/W	V(R)	V(I)	GAM(R)	GAM(I)	ALT	RANGE	CASE	PAGE	OF	OF
0.408239E 03	0.249721E 05	-0.257631E 05	-0.424771E-04	-0.410080E-04	0.399984E 06	0.714201E 03	0.399180E 01			
0.314951E 06	0.257631E 05	-0.410080E-04	-0.408080E 01							



REVISED TRAJECTORIES FOR RNS AND TUG LAUNCHES (5-11-71)

The following trajectories update previous trajectories for ESS launch of the space tug and the RNS. They represent the final Phase B Study system. They reflect the following rationale:

1. Capability for mission completion with one ESS engine failed at nominal ignition
2. 10,000-pound-payload weight margin
3. Propellant offloaded from both booster and ESS with distribution to yield nominal staging conditions (fixed booster ΔV)
4. Low q trajectories

Also, ESS weight and engine performance data have been updated to reflect current systems design.

Listed in Table F-1 are some critical parameters compared to those of the previous iteration.

The printouts for both the engine-out trajectory and the nominal trajectory are included for the ESS powered phase.

Table F-1. Critical Parameters

Parameter	Space Tug		RNS	
	Tug (4-15-71)	Current (5-11-71)	RNS (4-8-71)	Current (5-11-71)
Liftoff T/W, Lb/Lb	1.2	1.2	1.2	1.2
Glow, MLb	4.536	4.512	3.975	4.217
q_{max} (psi)	407	405	370	393
σ at q_{max} (deg)	-2	-2	-4	-2
Booster propellant (MLb)	3.030	2.936	2.480	2.744
Booster burnout				
Booster throttling (%)	50	50	50	50
Load factor (g's)	2.468	2.358	2.487	2.523
ESS/payload weight (lb)	691,523	754,885	680,000	651,701
ESS mainstage propellant (lb)	(449,690)	(514,907)	(467,340)	(438,678)
Nominal boost	444,694	496,422	462,946	428,191
Flight perf reserve	4,996	5,275	4,394	4,557
Increment for engine out at staging	0	13,210	0	5,930
Payload capability (lb)	(128,467)	(127,304)	(91,458)	(93,025)
Specified payload	107,180	107,180	83,000	83,000
Adapter	10,000	10,000	0	0
Payload margin	11,287	10,124	8,458	10,025

ATMOSPHERIC TRAJECTORY

TIME W.	VREL DDOT	ALT GDT	GAMMA	LOAD FACTOR
ALPHA	MACH	LIFT	VGRAV	THRUST
ATTITUDE	TVC DEFL	XCG (IN)	RANGE	THROTTLE RATIO
FLOW RATE	2*Q*V	AERO HEAT	ZCG (IN)	NORMAL LF
0.0	0.0	0.0	-	0.120000E 01
0.451220E 07	0.647785E 01	0.0	0.0	0.546463E 07
-0.201474E 01	0.0	3.0	0.0	0.827975E 00
0.879853E 02	0.201474E 01	0.223368E 04	0.459427E 03	0.425775E-01
0.136741E 05	0.0	0.0	0.0	0.119924E 01

TIME W.	VREL DDOT	ALT GDT	GAMMA	LOAD FACTOR
ALPHA	MACH	LIFT	VGRAV	THRUST
ATTITUDE	TVC DEFL	XCG (IN)	RANGE	THROTTLE RATIO
FLOW RATE	2*Q*V	AERO HEAT	ZCG (IN)	NORMAL LF
0.0	0.0	0.0	-	0.120000E 01
0.437545E 07	0.766558E 01	0.145286E-05	0.0	0.547099E 07
-0.210947E 01	0.622042E-01	0.458720E 03	0.0	0.827975E 00
0.878905E 02	0.209176E 01	0.225087E 04	0.461331E 03	0.452469E-01
0.136741E 05	0.303731E 03	0.200324E 04	-0.119924E 02	0.123606E 01

TIME W.	VREL DDOT	ALT GDT	GAMMA	LOAD FACTOR
ALPHA	MACH	LIFT	VGRAV	THRUST
ATTITUDE	TVC DEFL	XCG (IN)	RANGE	THROTTLE RATIO
FLOW RATE	2*Q*V	AERO HEAT	ZCG (IN)	NORMAL LF
0.0	0.0	0.0	-	0.120000E 01
0.423871E 07	0.897164E 01	0.498965E-04	0.644307E 03	0.926329E 01
-0.219692E 01	0.135515E 00	-0.521509E 04	-0.872775E-06	0.898544E 05
0.878035E 02	0.222418E 01	0.227143E 04	0.463240E 03	0.309200E 04
0.136741E 05	0.796050E 04	0.371849E 05	-0.570126E 02	0.496604E 07

TIME W.	VREL DDOT	ALT GDT	GAMMA	LOAD FACTOR
ALPHA	MACH	LIFT	VGRAV	THRUST
ATTITUDE	TVC DEFL	XCG (IN)	RANGE	THROTTLE RATIO
FLOW RATE	2*Q*V	AERO HEAT	ZCG (IN)	NORMAL LF
0.0	0.0	0.0	-	0.120000E 01
0.423871E 07	0.888450E 01	-0.339502E 00	0.644307E 03	0.926329E 01
-0.219692E 01	0.135515E 00	-0.521509E 04	-0.872775E-06	0.898544E 05
0.861822E 02	0.222418E 01	0.227143E 04	0.463240E 03	0.309200E 04
0.136741E 05	0.796050E 04	0.371849E 05	-0.570126E 02	0.496604E 07

TIME W.	VREL DDOT	ALT GDT	GAMMA	LOAD FACTOR
ALPHA	MACH	LIFT	VGRAV	THRUST
ATTITUDE	TVC DEFL	XCG (IN)	RANGE	THROTTLE RATIO
FLOW RATE	2*Q*V	AERO HEAT	ZCG (IN)	NORMAL LF
0.300000E 02	0.248437E 03	0.345101E 04	-0.860914E 02	0.643370E 02
0.419196E 07	0.101185E 02	-0.714219E-01	0.965942E 03	0.181957E 02
0.0	0.221051E 00	0.297134E 05	0.197365E-01	0.146177E 06
0.860914E 02	0.213493E 01	0.229170E 04	0.465337E 03	0.309305E 04
0.136741E 05	0.319738E 05	0.218238E 06	0.0	-0.249805E 08

F-14

ATMOSPHERIC TRAJECTORY

CASE 2 PAGE 3 OF 9

	TIME	VREL	ALT	GAMMA	QBAR	LOAD FACTOR
	W	VDT	GDT	VGRAV	VDRG	THRUST
ALPHA	MACH	TVC DEFL	LIFT	RANGE	DRAG	THROTTLE RATIO
ATTITUDE		2*Q*V	XCG(IN)	ZCG(IN)	PITCH AC (IN)	NORMAL LF
FLOW RATE			AERO HEAT	Q*ALPHA	AERO MOM (IN-LB)	AXIAL LF
0.400000E 02	0.355858E 03	0.645405E 04	0.853738E 02	0.120672E 03	0.135080E 01	
0.396522E 07	0.114029E 02	-0.698954E-01	0.128706E 04	0.329084E 02	0.557394E 07	
0.0	0.319536E 00	0.540574E 05	0.587518E-01	0.220252E 06	0.827975E 00	
0.853738E 02	0.211742E 01	0.231164E 04	0.467642E 03	0.309798E 04	0.655704E-01	
0.136741E 05	0.358843E 05	0.778271E 06	0.0	-0.449232E 03	0.134920E 01	
0.500000E 02	0.477268E 03	0.105904E 05	0.841349E 02	0.191141E 03	0.139570E 01	
0.382347E 07	0.129435E 02	-0.184461E 00	0.160766E 04	0.541820E 02	0.563364E 07	
-0.65667E 00	0.433893E 00	0.387970E 05	0.123817E 00	0.291687E 06	0.927975E 00	
0.334682E 02	0.230631E 01	0.233121E 04	0.470176E 03	0.310369E 04	0.684783E-01	
0.136741E 05	0.182451E 06	0.208146E 07	-0.127427E 03	-0.340618E 08	0.139402E 01	
0.600000E 02	0.615875E 03	0.159988E 05	0.815710E 02	0.268669E 03	0.144864E 01	
0.369173E 07	0.148611E 02	-0.330689E 00	0.192698E 04	0.819274E 02	0.570095E 07	
-0.133333E 01	0.569827E 00	-0.512446E 04	0.241255E 00	0.352959E 06	0.827975E 00	
0.902377E 02	0.261476E 01	0.235261E 04	0.472742E 03	0.310909E 04	0.668368E-01	
0.136741E 05	0.330934E 06	0.460485E 07	-0.358226E 03	-0.584103E 07	0.144709E 01	
0.700000E 02	0.776118E 23	0.228233E 05	0.774778E 02	0.343635E 03	0.150895E 01	
0.355498E 07	0.172503E C2	-0.488781E 00	0.224325E 04	0.115578E 03	0.577102E 07	
-0.200000E 01	0.737461E 00	-0.778472E 05	0.460697E 00	0.405886E 06	0.827975E 00	
0.754786E 02	0.301891E 01	0.237497E 04	0.475461E 03	0.311412E 04	0.596258E-01	
0.136741E 05	0.533403E 06	0.888599E 07	-0.687271E 03	0.356447E 08	0.150777E 01	
0.800000E 02	0.957428E 03	0.311768E 05	0.723249E 02	0.397451E 03	0.152620E 01	
0.341424E 07	0.185749E 02	-0.527006E 00	0.255343E 04	0.160591E 03	0.583822E 07	
-0.200000E 01	0.945777E 00	-0.644741E 05	0.853013E 00	0.620116E 06	0.927975E 00	
0.703249E 02	0.345034E 01	0.239655E 04	0.478507E 03	0.312256E 04	0.776094E-01	
0.136741E 05	0.761052E 06	0.153754E 03	-0.794903E 03	0.788287E 08	0.152422E 01	

F-15



ATMOSPHERIC TRAJECTORY

CASE 2 PAGE 4 OFF 9

TIME	VREL	ALT	GAMMA	QBAR	LOAD FACTOR
W	VDT	GDT	VGRAV	VDRG	THRUST
ALPHA	MACH	LIFT	RANGE	DRAG	THROTTLE RATIO
ATTITUDE	TVC DEFL	XCG (IN)	ZCG (IN)	PITCH AC (IN)	NORMAL LF
FLOW RATE	2*Q*V	AERO HEAT	Q*ALPHA	AERO MOM (IN-LB)	AXIAL LF
0.90000E 02	0.114445E 04	0.410142E 05	0.668807E 02	0.396825E 03	0.153894E 01
0.328149E 07	0.200675E 02	-0.566033E 00	0.285431E 04	0.236994E 03	0.599616E 07
-0.200000E 01	0.114474E 01	-0.432073E 05	0.148155E 01	0.845206E 06	0.327975E 00
0.548807E 02	0.354416E 01	0.241755E 04	0.481921E 03	0.312861E 04	0.375282E-01
0.136741E 05	0.908291E 06	0.238214E 03	-0.793651E 03	0.672421E 08	0.153645E 01
0.120000E 03	0.137772E 04	0.522945E 05	0.610933E 02	0.348034E 03	0.170133E 01
0.314475E 07	0.257401E 02	-0.537019E 00	0.314247E 04	0.309428E 03	0.593966E 07
-0.229362E 01	0.146935E 01	-0.138135E 05	0.242341E 01	0.589236E 06	0.327975E 00
0.587952E 02	0.349048E 01	0.243982E 04	0.435631E 03	0.311723E 04	0.103087E 00
0.136741E 05	0.953678E 06	0.332451E 08	-0.300000E 03	0.286781E 08	0.169821E 01
0.110000E 03	0.168099E 04	0.651971E 05	0.550824E 02	0.261219E 03	0.186941E 01
0.300300E 07	0.339541E 02	-0.614056E 00	0.341435E 04	0.357333E 03	0.596731E 07
-0.306255E 01	0.176360E 01	-0.930529E 05	0.379600E 01	0.343362E 06	0.327975E 00
0.520108E 02	0.397604E 01	0.246770E 04	0.489425E 03	0.308700E 04	0.989068E-01
0.136741E 05	0.878215E 06	0.425087E 08	-0.800000E 03	0.698199E 08	0.196679E 01
0.120000E 03	0.205624E 04	0.798452E 05	0.488904E 02	0.184334E 03	0.202431E 01
0.287126E 07	0.410824E 02	-0.621763E 00	0.366632E 04	0.384938E 03	0.598255E 07
-0.433995E 01	0.210550E 01	-0.159339E 06	0.574489E 01	0.172314E 06	0.827975E 00
0.445504E 02	0.437468E 01	0.249432E 04	0.493776E 03	0.304939E 04	0.990570E-01
0.136741E 05	0.753068E 06	0.507061E 08	-0.800000E 03	0.925797E 08	0.202189E 01
0.130000E 03	0.250254E 04	0.961013E 05	0.426706E 02	0.124450E 03	0.217157E 01
0.273451E 07	0.481539E 02	-0.623366E 00	0.389516E 04	0.397694E 03	0.599037E 07
-0.642827E 01	0.251309E 01	-0.133366E 06	0.842715E 01	0.608364E 05	0.827975E 00
0.362423E 02	0.463835E 01	0.252172E 04	0.498388E 03	0.3003380E 04	0.108024E 00
0.136741E 05	0.622382E 06	0.576254F 08	-0.800000E 03	0.916930E 08	0.216889E 01



ATMOSPHERIC TRAJECTORY

CASE 2 PAGE 5 OF 9

TIME W	VREL VDT	ALT GDT	GAMMA VGRAV	LOAD FACTOR	
				VDRG	THRUST
ATTITUDE FLOW RATE	TVC DEFL 2*Q*V	XCG (IN) AERO HEAT	ZCG (IN) Q*ALPHA	PITCH AC (IN)	NORMAL LF
0.140000E 03	0.30194CE 04	0.113597E 06	C.364949E 02	0.799110E 02	0.230931E 01
0.259777E 07	0.551427E 02	-0.537569E 00	0.409818E 04	0.401741E 03	0.539415E 07
-0.800000E 01	0.295258E 01	-0.151024E 06	0.120046E 02	0.569908E 04	0.827975E 00
0.294949E 02	0.470442E 01	0.254933E 04	C.502923E 03	0.292997E 04	0.131368E 00
0.136741E 05	0.452407E 06	0.631398E 03	-0.639238E 03	0.604578E 08	0.230557E 01
0.150000E 03	0.359562E 04	0.131881E 06	0.310438E 02	0.502801E 02	0.235803E 01
0.246277E 07	0.593116E 02	-0.503818E 00	0.427479E 04	0.399653E 03	0.576690E 07
-0.800000E 01	0.341327E 01	-0.949071E 05	0.166112E 02	-0.344405E 05	0.796353E 00
0.230439E 02	0.431705E 01	0.257515E 04	0.508303E 03	0.285173E 04	0.160421E 00
0.131562E 05	0.361536E 06	0.673444E 09	-0.402241E 03	0.303608E 08	0.235257E 01
0.160000E 03	0.420034E 04	0.150518E 06	0.263693E 02	0.315787E 02	0.235794E 01
0.233491E 07	0.616529E 02	-0.433296E 00	0.442713E 04	0.393328E 03	0.544378E 07
-0.800000E 01	0.389873E 01	-0.612394E 05	0.223139E 02	-0.584288E 05	0.751634E 00
0.183693E 02	0.506705E 01	0.260152E 04	0.514088E 03	0.277101E 04	0.183430E 00
0.124243E 05	0.265314E 06	0.704553E 08	-0.252630E 03	0.167310E 08	0.235079E 01
0.170000E 03	0.43280CE 04	0.169053E 06	0.223356E 02	0.206938E 02	0.235788E 01
0.221406E 07	0.637415E 02	-0.375215E 00	0.455770E 04	0.384015E 03	0.514704E 07
-0.800000E 01	0.448258E 01	-0.445041E 05	0.291463E 02	-0.713690E 05	0.710618E 00
0.143356E 02	0.541323E 01	0.263183E 04	0.520054E 03	0.270478E 04	0.204091E 00
0.117534F 05	0.195819E 06	0.727547E 08	-0.165550E 03	0.123622E 08	0.234903E 01
0.180000E 03	0.547487E 04	0.187090E 06	C.188339E 02	0.138186E 02	0.235783E 01
0.209968E 07	0.655977E 02	-0.326379E 00	0.46684E 04	0.372760E 03	0.487011E 07
-0.800000E 01	0.520720E 01	-0.343709E 05	0.371327E 02	-0.792427E 05	0.672363E 00
0.109339E 02	0.582222E 01	0.265732E 04	0.526814E 03	0.263087E 04	0.224332E 00
0.111277E 05	0.15131CE 06	0.745030E 08	-0.110549E 03	0.108778E 08	0.234714E 01



ATMOSPHERIC TRAJECTORY

CASE 2 PAGE 6 OF 9

TIME W	VREL DDT	ALT GDT	GAMMA VGRAV	LOAD FACTOR	
				ALPHA	MACH
ATTITUDE	TVC DEFL	LIFT	ZCG (IN)	PITCH AC (IN)	THROTTLE RATIO
FLOW RATE	2*Q*V	XCG (IN)	Q*ALPHA	AERO MOM (IN-LB)	NORMAL LF AXIAL LF
0.190000E 03	0.513922E 04	0.204298E 06	0.157835E 02	0.909791E 01	0.235779E 01
0.199133E 07	0.572413E 02	-0.284732E 00	0.476273E 04	0.359785E 03	0.460924E 07
-0.80000CE 01	0.602166E 01	-0.274231E 05	0.462899E 02	-0.851727E 05	0.636337E 00
0.778342E 01	0.625901E 01	0.257910E 04	0.534384E 03	0.254932E 04	0.245062E 00
0.105335E 05	0.111708E 06	0.758110E 08	-0.727833E 02	0.108682E 08	0.234502E 01
0.200000CE 03	0.691392E 04	0.220403E 06	0.131177E 02	0.591632E C1	0.235776E 01
0.199337E 07	0.686907E 02	-0.249304E 00	0.484135E 04	0.345338E 03	0.436407E 07
-0.8000200E 01	0.690721E 01	-0.225710E 05	0.566301E 02	-0.887014E 05	0.502495E 00
0.511770E 01	0.671749E 01	0.270471E 04	0.540828E 03	0.252165E 04	0.264972E 00
0.399473E 04	0.805399E 05	0.767663E 08	-0.473306E 02	0.115543E 08	0.234282E 01
0.210000E 03	0.751243E 04	0.235182E 06	0.107817E 02	0.383677E 01	0.235773E 01
0.179157E 07	0.699679E 02	-0.218574E 00	0.490648E 04	0.329605E 03	0.413276E 07
-0.800000E 01	0.784407E 01	-0.193786E 05	0.681621E 02	-0.909859E 05	0.570549E 00
0.278165E 01	0.720193E 01	0.272726E 04	0.548066E 03	0.249237E 04	0.285549E 00
0.346210E 04	0.576470E 05	0.774519E 08	-0.306942E 02	0.125337E 08	0.234037E 01
0.220000CE 03	0.821733E 04	0.248461E 06	0.874103E 01	0.252072E 01	0.235770E 01
0.169944E 07	0.710872E 02	-0.189379E 07	0.495972E 04	0.312683E 03	0.391430E 07
-0.800000E 01	0.381346E 01	-0.173451E 05	0.808924E 02	-0.924176E 05	0.540339E 00
0.741030E 00	0.792150E 01	0.275614E 04	0.558794E 03	0.246192E 04	0.314391E 00
0.836323E 04	0.414237E 05	0.779423E 08	-0.201658E 02	0.138300E 08	0.233658E 00
0.230000E 03	0.393363E 04	0.260130E 06	0.696344E 01	0.170840E 01	0.235763E 01
0.161211E 07	0.720522E 02	-0.165426E 00	0.500258E 04	0.294623E 03	0.375743E 01
-0.800000E 01	0.982572E 01	-0.160826E 05	0.948252E 02	-0.932936E 05	0.511674E 00
-0.103156E 01	0.858113E 01	0.273811E 04	0.574512E 03	0.243045E 04	0.341342E 00
0.850024E 04	0.305244E 05	0.782984E 08	-0.136672E 02	0.157121E 08	0.232684E 00





ATMOSPHERIC TRAJECTORY

TIME	VREL	ALT	GAMMA	LOAD FACTOR
W	VROT	GDT	VGRAV	THRUST
ALPHA	MACH	LIFT	RANGE	THROTTLE RATIO
ATTITUDE	TVC DEFL	XCG (IN)	PITCH AC (IN)	NORMAL LF
FLOW RATE	2*Q*V	AERO HEAT	AERO MOM (IN-LB)	AXIAL LF
0.234229E 03	0.923914E 04	0.264562E 06	0.628845E 01	0.146938E 01
0.157656E 07	0.724331E 02	-0.156207E 00	0.501791E 04	0.286648E 03
-0.900000E 01	0.102618E 02	-0.157050E 05	0.101078E 03	-0.935449E 05
-0.171155E 01	0.883667E 01	0.272495E 04	0.581763E 03	0.242500E 04
0.831225E 04	C.271517E 05	0.734202E 03	-0.117551E 02	C.165645E 03

EXO-ATMOSPHERIC TRAJECTORY (ONE ESS ENGINE FAILED AT STAGING)

CASE 2 PAGE 8 OF 9

TIME W	V(R) V(I)	GAM(R) GAM(I)	ALT THETAR(R)	RANGE	T/W
0.234229E 03 0.764886E 06	0.923914E 04 0.105835E 05	0.6238845E 01 0.548443E 01	0.264562E 06 0.437433E 02	0.101078E 03	0.0
0.236729E 03 0.754886E 06	0.923082E 04 0.105812E 05	0.588570E 01 0.513239E 01	0.266992E 06 0.438146E 02	0.104809E 03	0.0
0.236729E 03 0.754886E 06	0.923032E 04 0.105812E 05	0.598570E 01 0.513239E 01	0.266992E 06 0.438146E 02	0.104809E 03	0.912424E 00
0.276729E 03 0.594862E 06	0.100934E 05 0.114540E 05	0.418145E 01 0.368585E 01	0.300464E 06 0.402278E 02	0.167265E 03	0.991241E 00
0.316729E 03 0.634939E 06	0.111196E 05 0.124784E 05	0.296892E 01 0.264538E 01	0.326544E 06 0.360019E 02	0.235853E 03	0.108496E 01
0.356729E 03 0.574314E 06	0.123216E 05 0.136925E 05	0.213091E 01 0.191937E 01	0.347098E 06 0.310947E 02	0.311607E 03	0.119825E 01
0.396729E 03 0.514790E 06	0.137398E 05 0.151022E 05	0.155089E 01 0.141095E 01	0.363600E 06 0.255273E 02	0.395786E 03	0.133797E 01
0.436729E 03 0.454766E 06	0.154188E 05 0.167922E 05	0.112306E 01 0.103181E 01	0.377024E 06 0.194217E 02	0.489915E 03	0.151456E 01
0.476729E 03 0.394743E 06	0.174153E 05 0.187796E 05	0.765993E 00 0.710343E 00	0.387744E 06 0.130256E 02	0.595847E 03	0.174486E 01



EXO-ATMOSPHERIC TRAJECTORY

TIME W	V(R) V(I)	GAM(R) GAM(I)	ALT THETAIR	RANGE	T/W
0.516729E 03 0.334719F 06	0.193070E 05 0.211719E 05	0.435494E 00 0.407420F 00	0.395440E 06 0.569806E 01	0.715869E 03	0.205776E 01
0.556729E 03 0.274695F 06	0.227146E 05 0.240797E 05	0.130727E 00 0.123316E 00	0.399504E 06 0.848443E 00	0.852897E 03	0.250740E 01
0.576454E 03 0.245097E 05	0.243975E 05 0.257627E 05	0.303113E-03 0.237056E-03	0.400000E 06 -0.174095E 01	0.927882E 03	0.281020E 01

NOMINAL ESS POWERED TRAJECTORY
EXO-ATMOSPHERIC TRAJECTORY

TIME W	V(R) V(I)		GAM(R) GAM(I)		ALT THETA(R)	RANGE	T/W	CASE 3 PAGE 3 OF 8
	V(R)	V(I)	GAM(R)	GAM(I)				
0.234229E 03	0.923985E 04	0.627643E 01	0.264448E 06	0.101093E 03	0.0			
0.764996E 06	0.1053392E 05	0.547400E 01	0.292359E 02					
0.236729E 03	0.923155E 04	0.587371E 01	0.266848E 06	0.104824E 03	0.0			
0.764385E 06	0.1053320E 05	0.512199E 01	0.293672E 02					
0.236729F 03	0.923155E C4	0.587371E 01	0.266848E 06	0.104824E 03	0.0			
0.754386E 06	0.1053200E 05	0.512199E 01	0.293672E 02					
0.276729E 03	0.112866E 05	0.478550E 01	0.304656E 06	0.170919E 03	0.0			
0.644751E 06	0.126414E 05	0.427163E 01	0.219744E 02					
0.316729E 03	0.138679E 05	0.368329E 01	0.341568E 06	0.251908E 03	0.0			
0.534617E 06	0.152268E 05	0.335420E 01	0.137318E 02					
0.356729E 03	0.171684E 05	0.240169E 01	0.374320E 06	0.351741E 03	0.0			
0.424432E 06	0.185308E 05	0.222502E 01	0.512730E 01					
0.396729E 03	0.215427E 05	0.883611E 00	0.396240E 06	0.476069E 03	0.0			
0.314347E 06	0.229074E 05	0.930964E 00	-0.310225E 01					
0.396777E 03	0.215488E 05	0.881711E 00	0.396240E 06	0.476237E 03	0.0			
0.314215E 06	0.229136E 05	0.829191E 00	-0.311155E 01					
0.419066E 03	0.243982E 05	-0.111781E-03	0.400032E 06	0.558935E 03	0.0			
0.258465E 06	0.257634E 05	-0.105858E-03	-0.723888E 01					

H-22

SD 71-140-2



REVISED TRAJECTORY FOR RNS LAUNCH
VEHICLE CHARACTERISTICS

DATE - 05/07/71

CASE 5 PAGE 1 OF 8

STAGE

1

2

3

GROSS STAGE WEIGHT, (LBS) 4216877.0

661701.0

651701.0

GROSS STAGE THRUST/WEIGHT

1.565

0.0

1.057

THRUST, (LBS)

7243500.0

0.0

688775.9

ISP, (SEC)

439.000

2.500

459.000

INERT WEIGHT, (LBS)

663531.0

10000.0

102190.0

PROPELLANT, (LBS)

2743500.0

0.0

438678.4

LOADING REQUIREMENT FOR ESS ENGINE-OUT
AT STAGING

PERF. FRAC., (NU)

0.6506

0.0

0.6731

IF NO ENGINE FAILED, NOMINAL USABLE
RESIDUALS ARE (LBS)

PROPELLANT FRAC., (NU)

0.8052

0.0

0.8111

BURNOUT TIME, (SEC)

223.466

230.966

520.318

FLIGHT PERFORMANCE RESERVE
INCREMENT FOR ENGINE-OUT

4,557

5,930

10,487

25763.805

25763.805

BURNOUT GAMMA, (DEGREES)

6.220

5.866

0.000

BURNOUT ALTITUDE, (FT)

259342.7

262030.0

400048.0

BURNOUT RANGE, (NM)

94.7

98.5

307.4

IDEAL VELOCITY, (FT/SEC)

* * * * *

14533.7

* * * * *

16205.9

INJECTION VELOCITY, (FT/SEC)

* * * * *

307.4

FLYBACK RANGE(NM)

383.7

INJECTION PROPELLANT, (LB)

4480.6

FLYBACK PROP(LBS)

148145.0

ORBIT MANEUVERING REQUIREMENTS

RENDEZVOUS

740.0

550.0

0.0

TOTAL LOSSES = 83.0
LBS

DELTA V, (FT/SEC)

450.3

450.3

0.0

SPECIFIC IMPULSE, (SEC)

10607.3

3056.7

83.0

OF USABLE PROPELLANT

PROPELLANT, (LBS)

4060.0

TOTAL RCS+OMS PROP, (LBS)

13747.0

RCS PROPELLANT, (LBS)

MARGIN

$\frac{RMS}{10,025} = \frac{83,000}{10,025}$ LBS

PAYOUT, (LBS)



ATMOSPHERIC TRAJECTORY

CASE 5 PAGE 2 OF 8

TIME W	VREL VDOT	ALT GDT	GAMMA VGRAV	LOAD FACTOR THRUST
ALPHA	MACH	LIFT	RANGE	THROTTLE RATIO
ATTITUDE	TVC DEFL	XCG(IN)	ZCG(IN)	NORMAL LF
FLOW RATE	2*Q*V	AERO HEAT	Q*ALPHA	AXIAL LF
0.0	0.0	0.0	0.90000E 02	0.120000E 01
0.42169E 07	0.647290E 01	0.0	0.0	0.511025E 07
-0.131061E 01	0.0	0.0	0.500000E 05	0.774280E 00
0.381394E 02	0.181051E 01	0.225935E 04	0.452590E 03	0.382896E-01
0.127949E 05	0.0	0.0	0.0	0.119939E 01
0.102000E 02	0.706106E 02	0.343631E 03	0.300000E 02	0.567183E 01
0.408893F 07	0.765009E 01	-0.920147E-06	0.322165E 03	0.413163E 01
-0.189168E 01	0.621317E-01	0.899261E 03	0.307416E-07	0.599841E 05
0.881083E 02	0.135715E 01	0.227999E 04	0.454190E 03	0.294800E 04
0.127949E 05	0.800932E 03	0.199703E 04	-0.107293E 02	0.405470E-01
0.200000E 02	0.1523961E 03	0.145216E 04	0.899999E 02	0.258130E 02
0.396094E 07	0.881517E 01	-0.249594E-06	0.644307E 03	0.101220E 02
-0.195430E 01	0.135148E 00	-0.227867E 04	0.284160E-06	0.939498E 05
0.880456E 02	0.195366E 01	0.229837E 04	0.455948E 03	0.294800E 04
0.127949E 05	0.789677E 04	0.369570E 05	-0.504465E 02	0.428114E-01
0.200000E 02	0.152961E 03	0.145216E 04	0.885724E 02	0.258130E 02
0.396093E 07	0.882515E 01	-0.299826E 00	0.644307E 03	0.101220E 02
-0.195430E 01	0.135148E 00	-0.227867E 04	0.284160E-06	0.939488E 05
0.866181E 02	0.195366E 01	0.229837E 04	0.455948E 03	0.294800E 04
0.127949E 05	0.789677E 04	0.369570E 05	-0.504465E 02	0.272167E 07
0.300000E 02	0.247054E 03	0.344072E 04	0.865941E 02	0.636163E 02
0.383303E 07	0.997049E 01	-0.535830E-01	0.966047E 03	0.202525E 02
0.0	0.219769E 00	0.295692E 05	0.172481E-01	0.156174E 06
0.965841E 02	0.185497E 01	0.231748E 04	0.457880E 03	0.295103E 04
0.127949E 05	0.314333E 05	0.215613E 06	0.0	0.303828E 08



ATMOSPHERIC TRAJECTORY

CASE 5 PAGE 3 OF 8

TIME W	VREL VDT	ALT GDT	GAMMA VGRAV	LOAD FACTOR THRUST
ALPHA	MACH	LIFT	RANGE	THROTTLE RATIO
ATTITUDE	TVC DEFL	XCG (IN)	ZCG (IN)	NORMAL LF
FLOW RATE	2*J*V	AERO HEAT	Q*ALPHA	AXIAL LF
0.400000E 02	0.352350E 03	0.642232E 04	0.860990E 02	0.118419E 03
0.370508E 07	0.111332E 02	-0.405498E-01	0.128740E 04	0.371584E 02
0.0	0.316356E 00	0.550416E 05	0.503598E-01	0.237554E 06
0.860390E 02	0.178756E 01	0.233630E 04	0.460005E 03	0.296584E 04
0.127949E 05	0.834496E 05	0.762500E 06	0.0	0.543353E 08
0.500000E 02	0.470349E 03	0.105132E 05	0.951964E 02	0.186085E 03
0.357713E 07	0.125274E 02	-0.146983E 00	0.160842E 04	0.617904E 02
-0.666667E 00	0.427503E 00	0.464001E 05	0.103383E 00	0.316568E 06
0.3452293E 02	0.188221E 01	0.235739E 04	0.462081E 03	0.298288E 04
0.127949E 05	0.175050E 06	0.201974E 07	-0.124057E 03	-0.559677E 08
0.600000E 02	0.6033947E 03	0.158431E 05	0.830358E 02	0.259632E 03
0.344918E 07	0.142510E 02	-0.287942E 00	0.192853E 04	0.940912E 02
-0.133333E 01	0.558437E 00	0.113732E 05	0.198286E 00	0.386844E 06
0.817025F 02	C.210792E 01	0.237892E 04	0.464313E 03	0.299634E 04
0.127949E 05	C.3136308E 06	0.442433E 07	-0.346176E 03	-0.398426E 08
0.700000E 02	0.756659E 03	0.225494E 05	0.793822E 02	0.329495E 03
0.332123F 07	C.163402E 02	-0.444682E 00	0.224638E 04	0.134001E 03
-0.200000E 01	C.713130E 00	-0.527922E 05	0.378676E 00	0.453999E 06
0.773322E 02	C.249145E 01	0.239998E 04	0.466816E 03	0.300273E 04
0.127949F 05	C.493631E 06	0.845190E 07	-0.658990E 03	-0.294805E 07
0.800000E 02	C.930504E 03	0.307497E 05	0.745308E 02	0.380897E 03
0.319328E 07	C.182297E 02	-0.529377E 00	0.255943E 04	0.183939E 03
-0.200000E 01	C.917267E 00	-0.442959E 05	0.709343E 00	0.582537E 06
0.725308E 02	C.227966E 01	0.242050E 04	0.469622E 03	0.300248E 04
0.127949E 05	C.708953E 06	0.144915E 08	-0.761794E 03	-0.534853E 08



ATMOSPHERIC TRAJECTORY

TIME	VREL W	VDDT	ALT GDT	GAMMA VGRAY	LOAD FACTOR THRUST
0.90000E 02	0.112093E 04	0.404664E 05	0.687929E 02	0.389010E 03	0.156515E 01
0.306533E 07	0.205113E 02	-0.608249E 00	0.286419E 04	0.253563E 03	0.551127E 07
-0.200000E 01	0.115769E 01	-0.416560E 05	0.126512E 01	0.713787E 06	0.774280E 00
0.657329E 02	0.195672E 01	0.244095E 04	0.472737E 03	0.299039E 04	0.396820E-01
0.127949E 05	0.672103E 06	0.2246688E 03	-0.778020E 03	-0.121747E 09	0.156465E 01

TIME	VREL W	VDDT	ALT GDT	GAMMA VGRAY	LOAD FACTOR THRUST
ALPHA	MACH	LIFT XCG(IN)	RANGE ZCG(IN)	PITCH AC(IN)	THROTTLE RATIO
ATTITUDE	TVC DEFL	AERO HEAT	Q*ALPHA	AERO MOM(IN-LB)	NORMAL LF
FLOW RATE	2*Q*V				AXIAL LF
0.90000E 02	0.112093E 04	0.404664E 05	0.687929E 02	0.389010E 03	0.156515E 01
0.306533E 07	0.205113E 02	-0.608249E 00	0.286419E 04	0.253563E 03	0.551127E 07
-0.200000E 01	0.115769E 01	-0.416560E 05	0.126512E 01	0.713787E 06	0.774280E 00
0.657329E 02	0.195672E 01	0.244095E 04	0.472737E 03	0.299039E 04	0.396820E-01
0.127949E 05	0.672103E 06	0.2246688E 03	-0.778020E 03	-0.121747E 09	0.156465E 01

TIME	VREL W	VDDT	ALT GDT	GAMMA VGRAY	LOAD FACTOR THRUST
ALPHA	MACH	LIFT XCG(IN)	RANGE ZCG(IN)	PITCH AC(IN)	THROTTLE RATIO
ATTITUDE	TVC DEFL	AERO HEAT	Q*ALPHA	AERO MOM(IN-LB)	NORMAL LF
FLOW RATE	2*Q*V				AXIAL LF
0.100000E 03	0.135554E 04	0.516935E 05	0.625517E 02	0.347625E 03	0.171785E 01
0.293739E 07	0.263913E 02	-0.630963E 00	0.315634E 04	0.319696E 03	0.555291E 07
-0.230133E 01	0.144654E 01	-0.159139E 05	0.213826E 01	0.506937E 06	0.774280E 00
0.602504E 02	0.208002E 01	0.246845E 04	0.475774E 03	0.297234E 04	0.562692E-01
0.127949E 05	0.943202E 06	0.316376E 08	-0.900000E 03	-0.127329E 09	0.171693E 01
0.110000E 03	0.166146E 04	0.6466059E 05	0.561484E 02	0.263308E 03	0.188273E 01
0.280943E 07	0.340367E 02	-0.650134E 00	0.343197E 04	0.363541E 03	0.557950E 07
-0.303827E 01	0.174504E 01	-0.919937E 05	0.344818E 01	0.291337E 06	0.774280E 00
0.531102E 02	0.277966E 01	0.249495E 04	0.479262E 03	0.292832E 04	0.581162E-01
0.127949E 05	0.874953E 06	0.408200E 08	-0.800000E 03	-0.553221E 08	0.188183E 01
0.120000E 03	0.203711E 04	0.792759E 05	-0.496225E 02	0.186114E 03	0.203459E 01
0.268148E 07	0.411003E 02	-0.652526E 00	0.368688E 04	0.388443E 03	0.559421E 07
-0.429844E 01	0.208754E 01	-0.154026E 06	0.534118E 01	0.143206E 06	0.774280E 00
0.453241E 02	0.338277E 01	0.252032E 04	0.493267E 03	0.287147E 04	0.618189E-01
0.127949E 05	0.758270E 06	0.490050E 08	-0.800000E 03	-0.198600E 07	0.203366E 01
0.130000E 03	0.248349E 04	0.955532E 05	0.431159E 02	0.125822E 03	0.218001E 01
0.255353E 07	0.481645E 02	-0.649674E 00	0.391799E 04	0.399527E 03	0.560173E 07
-0.635818E 01	0.249595E 01	-0.178200E 06	0.797555E 01	0.460461E 05	0.774280E 00
0.367577E 02	0.376491E 01	0.254883E 04	0.486755E 03	0.280367E 04	0.726924E-01
0.127949E 05	0.624956E 06	0.557356E 08	-0.800000E 03	0.205254E 08	0.217890E 01

ATMOSPHERIC TRAJECTORY

CASE 5 PAGE 5 OF 8

TIME	VREL	ALT	GAMMA	QBAR	LOAD FACTOR
W	VDDT	GDT	VGRAV	VDRG	THRUST
ALPHA	MACH	LIFT	RANGE	DRAG	THROTTLE RATIO
ATTITUDE	TVC DEFL	XCG (IN)	ZCG (IN)	PITCH AC (IN)	NORMAL LF
FLOW RATE	2*Q*V	AERO HEAT	Q*ALPHA	AERO MOM (IN-LB)	AXIAL LF
0.140000E 03	0.299972E 04	0.113042E 06	0.366840E 02	0.809512E 02	0.231760E 01
0.242558E 07	0.552225E 02	-0.611583E 00	0.412236E 04	0.402307E 03	0.560535E 07
-0.800000E 01	0.293634E C1	-0.149683E 06	0.115145E 02	-0.360739E 04	0.774280E 00
0.286940E 02	0.394578E 01	0.257595E 04	0.490398E 03	0.271214E 04	C.981184E-01
0.127949E 05	0.485663E 06	0.614765E 08	-0.647610E 03	0.112709E 08	0.231552E 01

TIME	VREL	ALT	GAMMA	QBAR	LOAD FACTOR
W	VDDT	GDT	VGRAV	VDRG	THRUST
ALPHA	MACH	LIFT	RANGE	DRAG	THROTTLE RATIO
ATTITUDE	TVC DEFL	XCG (IN)	ZCG (IN)	PITCH AC (IN)	NORMAL LF
FLOW RATE	2*Q*V	AERO HEAT	Q*ALPHA	AERO MOM (IN-LB)	AXIAL LF
0.150000E 03	0.3583361E 24	0.131273E 06	0.310154E 02	0.514117E 02	0.246079E 01
0.229763E 07	0.625478E 02	-0.523808E 00	0.429933E 04	0.399073E 03	0.560702E 07
-0.800000E 01	0.341457E 01	-0.950445E 05	0.160986E 02	-0.399442E 05	0.774280E 00
0.230154E 02	0.415587E 01	0.260111E 04	0.495895E 03	0.261277E 04	0.138733E 00
0.127949E 05	0.3684992E 06	0.657275E 08	-0.411293E 03	0.216311E 07	0.245688E 01
0.160000E 03	0.424227E 04	0.149913E 06	0.261762E 02	0.330001E 02	0.252301E 01
0.217099E 07	0.669910E 02	-0.445335E 00	0.445111E 04	0.391701E 03	0.541209E 07
-0.300000E 01	0.393948E 01	-0.622765E 05	0.218383E 02	-0.613182E 05	0.747260E 00
0.131762E 02	0.448630E 01	0.263441E 04	0.501117E 03	0.250359E 04	0.170522E 00
0.123528E 05	0.279990E 06	0.689533E 09	-0.264000E 03	-0.711101E 05	0.251724E 01
0.170000E 03	0.492314E 04	0.168545E 06	0.220571E 02	0.219152E 02	0.252297E 01
0.205103E 07	0.691397E 02	-0.380730E 00	0.458047E 04	0.381393E 03	0.509983E 07
-0.300000E 01	0.456858E 01	-0.456177E 05	0.287943E 02	-0.723172E 05	0.704100E 00
0.140571E 02	0.496722E 01	0.266529E 04	0.507016E 03	0.244722E 04	0.193938E 00
0.116468E 05	0.215793E 06	0.714093E 09	-0.175322E 03	0.649140E 06	0.251550E 01
0.180000E 03	0.562416E 04	0.186751E 06	0.185231E 02	0.147655E 02	0.252293E 01
0.193789E 07	0.710277E 02	-0.327612E 00	0.469006E 04	0.369156E 03	0.480823E 07
-0.800000E 01	0.534528E 01	-0.351164E 05	0.369919E 02	-0.792013E 05	0.663826E 00
0.105231E 02	0.529631E 01	0.269111E 04	0.513759E 03	0.238734E 04	0.216795E 00
0.109981E 05	0.166037E 06	0.733121E 08	-0.118124E 03	0.215923E 07	0.251359E 01



ATMOSPHERIC TRAJECTORY

CASE 5 PAGE 6 OF 8

TIME W	VREL VDT	ALT GFT	GAMMA VGRAV	LOAD FACTOR THRUST
ALPHA	MACH	LIFT XCG(IN)	RANGE	THROTTLE RATIO
ATTITUDE	TVC DEFL	ZCG(IN)	PITCH AC(IN)	NORMAL LF
FLW RATE	2*J*V	AERO HEAT	Q*ALPHA	AXIAL LF

0.190000E 03	0.634288E 04	0.204170E 06	0.154751E 02	0.975980E 01
0.183113E 07	0.726817E 02	-0.283336E 00	0.479231E 04	0.355119E 03
-0.800000E 01	0.621989E 01	-0.277668E 05	0.464485E 02	-0.847348E 05
0.747511E 01	0.574697E 01	0.271738E 04	0.520355E 03	0.233178E 04
0.103684E 05	0.123310E 06	0.747552E 08	-0.780784E 02	0.442435E 07
0.200000E 03	0.707770E 04	0.220510E 06	0.128331E 02	0.634486E 01
0.173039E 07	0.741293E 02	-0.246093E 00	0.485934E 04	0.339441E 03
-0.800000E 01	0.717101E 01	-0.225962E 05	0.571758E 02	-0.884321E 05
0.483309E 01	0.621451E 01	0.274567E 04	0.526548E 03	0.230921E 04
0.978657E 04	0.898061E 03	0.758164E 08	-0.507589E 02	0.702678E 07
0.210000E 03	0.782482E 04	0.235538E 06	0.105394E 02	0.409792E 01
0.163528E 07	0.753970E 02	-0.212877E 00	0.492304E 04	0.322275E 03
-0.800000F 01	0.817625E 01	-0.192367E 05	0.691823E 02	-0.908378E 05
0.253942E 01	0.682799E 01	0.277440E 04	0.535197E 03	0.228531E 04
0.923946E 04	0.641310E 05	0.765796E 08	-0.327833E 02	0.935134E 07
0.220000E 03	0.858439E 04	0.249094E 06	0.856367E 01	0.267076E 01
0.154548E 07	0.764897E 02	-0.193203E 00	0.497513E 04	0.303721E 03
-0.800000F 01	0.922390E 01	-0.171300E 05	0.824734E 02	-0.923485E 05
0.563671E 00	0.758529E 01	0.278558E 04	0.548356E 03	0.226043E 04
0.872427E 04	0.458537E 05	0.771242E 08	-0.213661E 02	0.117381E 03
0.228466E 03	0.923540E 04	0.259343E 06	0.710425E 01	0.189715E 01
0.147338E 07	0.773025E 02	-0.162003E 00	0.501134E 04	0.286971E 03
-0.800000F 01	0.101403E 02	-0.160065E 05	0.947283E 02	-0.931558E 05
-0.895746E 00	0.814357E 01	0.275697E 04	0.562983E 03	0.224200E 04
0.931251E 04	0.350419E 05	0.774641E 08	-0.151772E 02	0.138962F 08



EXO-ATMOSPHERIC TRAJECTORY (ONE ESS ENGINE FAILED AT STAGING)

TIME W	V(R) V(I)	GAM(R) GAM(I)	ALT THETA(R)	CASE 5 PAGE 7 OF 8	
				RANGE	T/W
0.228465E 03	0.923540E 04	0.710425E 01	0.259343E 06	0.947283E 02	0.0
0.661705E 06	0.105423E 05	0.621983E 01	0.366505E 02		
0.230366E 03	0.922597E 04	0.67C109E 01	0.262080E 06	0.984523E 02	0.0
0.661705E 06	0.105340E 05	0.586595E 01	0.367215E 02		
0.230966E 03	0.922577E 04	0.670108E 01	0.262080E 06	0.984523E 02	0.105699E 01
0.651705E 06	0.105340E 05	0.586595E 01	0.367215E 02		
0.270965E 03	0.103510E 05	0.476169E 01	0.300640E 06	0.161617E 03	0.116410E 01
0.591681E 06	0.116652E 05	0.422418E 01	0.324509E 02		
F-29	0.110966E 03	0.116332E 05	0.334465E 01	0.331328E 06	0.232766E 03
0.531657E 06	0.130015E 05	0.300521E 01	0.276026E 02		0.129552E 01
0.350966E 03	0.132617E 05	0.230620E 01	0.355536E 06	0.313304E 03	0.146040E 01
0.471633E 06	0.145824E 05	0.209723E 01	0.222235E 02		
0.390966E 03	0.151389E 05	0.152564E 01	0.374240E 06	0.404954E 03	0.167337E 01
0.411609E 06	0.164613E 05	0.140305E 01	0.164479E 02		
0.430966E 03	0.173879E 05	0.915925E 00	0.387840E 06	0.509853E 03	0.195905E 01
0.351585E 06	0.187115E 05	0.851038E 00	0.105109E 02		
0.470966E 03	0.201185E 05	0.430634E 00	0.396416E 06	0.630727E 03	0.236236E 01
0.291561E 06	0.214429E 05	0.404039E 00	0.473175E 01		





EXO-ATMOSPHERIC TRAJECTORY

CASE	5	PAGE	8 OF 8		
TIME W	V(R) V(I)	GAM(R) GAM(I)	ALT THETA(R)	RANGE	T/W
0.510366E 03 0.231538E 05	0.235163E 05 0.248408E 05	0.655255E-01 0.620317E-01	C.399936E 06 -0.531594E 00	0.771239E 03	0.297477E 01
0.520319E 03 0.217504E 05	0.244393E 05 0.257638E 05	0.168900E-03 0.160217E-03	0.400048E 06 -0.164988E 01	0.807444E 03	0.316670E 01

NOMINAL ESS POWERED TRAJECTORY
EXO-ATMOSPHERIC TRAJECTORY

CASE 6 PAGE 7 OF 7

TIME W	V(R) V(I)	GAM(R) GAM(I)	ALT THETA(R)	RANGE	T/W
0.229466E 03	0.923609E 04	0.709187E 01	0.259233E 06	0.947420E 02	0.0
0.661705E 06	0.105430E 05	0.620905E 01	0.265220E 02		
0.230966E 03	0.922668E 04	0.668872E 01	0.261984E 06	0.984664E 02	0.0
0.661705E 06	0.105349E 05	0.585510E 01	0.265930E 02		
0.230966E 03	0.922668E 04	0.668872E 01	0.261984E 06	0.984664E 02	0.192857E 01
0.651705E 06	0.105348E 05	0.585510E 01	0.265930E 02		
0.270966E 03	0.117033E 05	0.542504E 01	0.305840E 06	0.165731E 03	0.232077E 01
0.541570E 06	0.130166E 05	0.487628E 01	0.181239E 02		
0.310966E 03	0.149005E 05	0.393399E 01	0.348976E 06	0.251199E 03	0.291320E 01
0.431436E 06	0.162189E 05	0.361374E 01	0.885985E 01		
0.350966E 03	0.191613E 05	0.209011E 01	0.384448E 06	0.360508E 03	0.391177E 01
0.321301E 06	0.204340E 05	0.195509E 01	-0.446472E 00		
0.353539E 03	0.194956E 05	0.195922E 01	0.386176E 06	0.368540E 03	0.399999E 01
0.314215E 06	0.203085E 05	0.193462E 01	-0.102387E 01		
0.392412E 03	0.244388E 05	-0.115616E-03	0.400016E 06	0.506425E 03	0.399999E 01
0.223507E 06	0.257633E 05	-0.109673E-03	-0.912172E 01		



APPENDIX G. LOW-LOAD TRAJECTORY/PERFORMANCE EFFECTS

To reduce structural effects on the reusable booster to a minimum, low-load trajectory characteristics have been formulated. The trajectory shaping and acceleration control techniques used to provide mated ascent trajectories yielding low ESS attachment loads result in lower booster thrusting efficiency. Therefore, in order to provide the same performance (payload) to orbit, it is necessary to add propellant to the ESS (which is off-loaded). In the range investigated, it was possible to launch the MDAC space station to the DRM by this method. Therefore, the performance effect can be defined as the change in ESS propellant necessary to accommodate the fixed mission.

Figure G-1 shows this effect as a function of the maximum dynamic pressure (q_{max}) incurred during boost— q_{max} being a qualitative measure of maximum attachment loads due to aerodynamic effects. The maximum performance trajectory (E) requires 561,000 pounds of ESS propellant and results in q_{max} of 550 psf. The graph shows the cumulative effects of (D) throttling the booster engines to 50 percent at end boost, (C) introducing an angle-of-attack of -2 degrees for 30 seconds in the q_{max} region—to relieve a loading problem caused by positive angle-of-attack incurred due to headwinds, (B) throttling the booster engines by 5 percent immediately after clearing the launch tower, and (A) introducing an angle-of-attack of -8 degrees from the q_{max} region to staging. (A) represents the selected approach documented in Volume II, Book 1. It requires 683,000 pounds of ESS propellant and results in q_{max} of 384 psf. Compared to this trajectory, the maximum performance trajectory (E) requires 18 percent less ESS propellant but incurs 43 percent higher maximum dynamic pressure. Also, the maximum axial attachment load at end boost would be increased by 28 percent if the maximum performance approach were followed. The selected trajectory (A) has been used in the final evaluation of ESS effect on the reusable booster. These results are given in Volume II, Book 3.

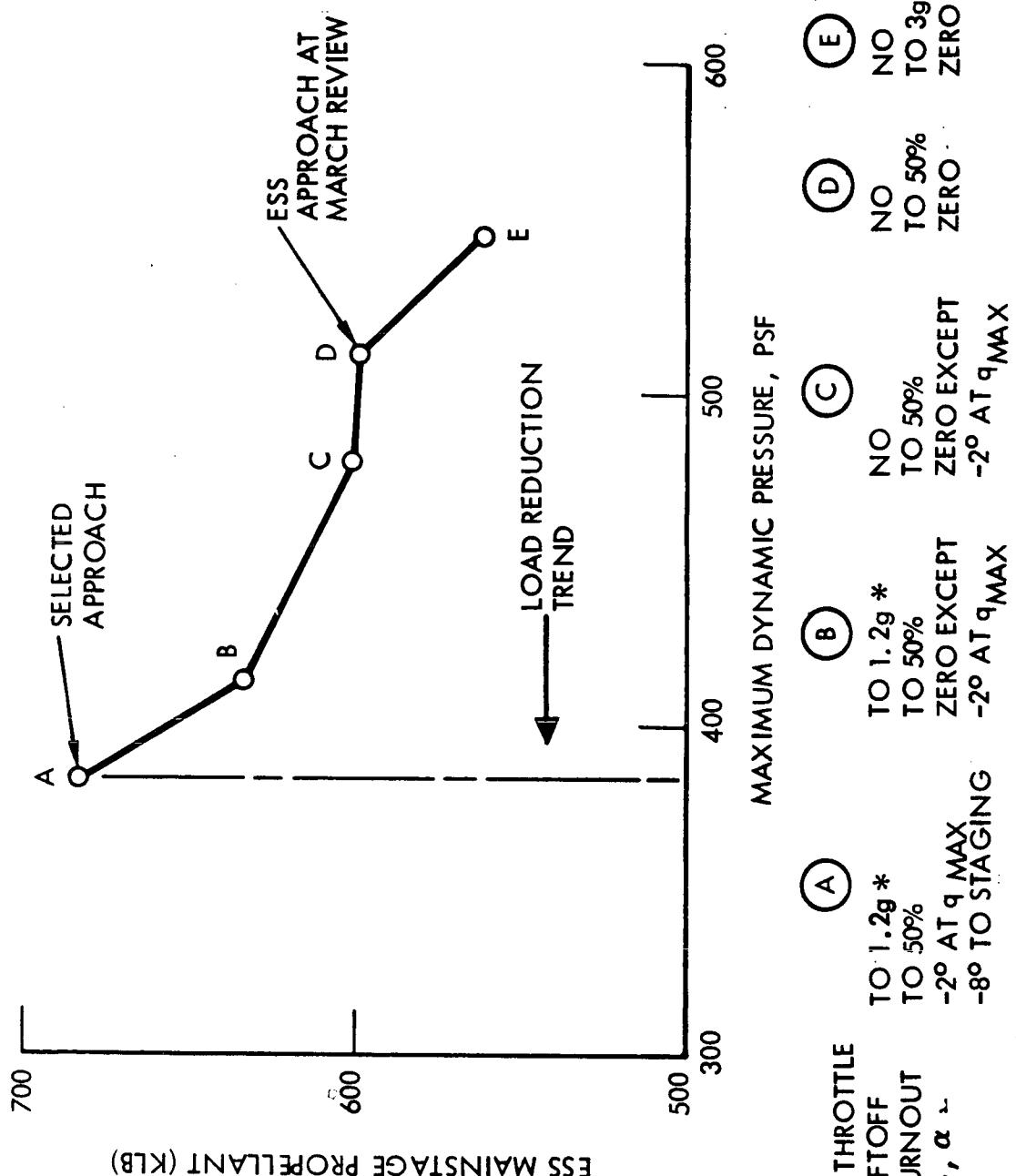


Figure G-1. Booster Throttling and Steering for Low-Load Trajectories,
MDAC SS Launch ($W_{PL} = 176,960 \text{ lb} + 6,000\text{-lb Margin}$)